PB87-177515

Reburning Application to Firetube Package Boilers

Acurex Corp., Mountain View, CA

Prepared for

Environmental Protection Agency
Research Triangle Park, NC

Mar 87

U.S. Department of Commerce
National Technical Information Service
NTIS

PB87-177515

EPA/600/7-87/011
March 1987

REBURNING APPLICATION TO FIRETUBE PACKAGE BOILERS

By:

James A. Mulholland, E. Eugene Stephenson,
Charles Pendergraph, and Jeffrey V. Ryan
Acurex Corporation
P. O. Box 13109
Research Triangle Park, NC 27709

EPA Contract No. 68-02-3648
Task No. 49

EPA Project Officer: Robert E. Hall
Air and Energy Engineering Research Laboratory
U. S. Environmental Protection Agency
Research Triangle Park, NC 27711

AIR AND ENERGY ENGINEERING RESEARCH LABORATORY
OFFICE OF RESEARCH AND DEVELOPMENT
U.S. ENVIRONMENTAL PROTECTION AGENCY
RESEARCH TRIANGLE PARK, NC 27711

REPRODUCED BY
U.S. DEPARTMENT OF COMMERCE
NATIONAL TECHNICAL
INFORMATION SERVICE
SPRINGFIELD, VA 22161

TECHNICAL REPORT DATA

(Please read Instructions on the reverse before completing)

1. REPORT NO. EPA/600/7-87/011	2.	3. RECIPIENT'S ACCESSION NO. PB87 177515/AS
4. TITLE AND SUBTITLE Reburning Application to Firetube Package Boilers		5. REPORT DATE March 1987 6. PERFORMING ORGANIZATION CODE
7. AUTHOR(S) James A. Mulholland, E. Eugene Stephenson, Charles Pendergraph, and Jeffrey V. Ryan		8. PERFORMING ORGANIZATION REPORT NO.
9. PERFORMING ORGANIZATION NAME AND ADDRESS Acurex Corporation P.O. Box 13109 Research Triangle Park, North Carolina 27709		10. PROGRAM ELEMENT NO. 11. CONTRACT/GRANT NO. 68-02-3648, Task 49
12. SPONSORING AGENCY NAME AND ADDRESS **EPA, Office of Research and Development** **Air and Energy Engineering Research Laboratory** **Research Triangle Park, NC 27711**		13. TYPE OF REPORT AND PERIOD COVERED Task Final; 5/83 - 9/85 14. SPONSORING AGENCY CODE **EPA/600/13**

15. SUPPLEMENTARY NOTES AEERL project officer is Robert E. Hall, Mail Drop 65, 919/541-2477.

16. ABSTRACT The report gives results of pilot-scale experimental research that examined the physical and chemical phenomena associated with the NOx control technology of reburning applied to gas- and liquid-fired firetube package boilers. Reburning (staged fuel combustion) diverts some of the fuel and combustion air from the main burner(s) for injection into the post-flame gases, resulting in three distinct zones in the boiler radiant section: a fuel-lean primary zone, a fuel-rich reburning zone, and a fuel-lean burnout zone. NOx is reduced both by reduction of NOx formation and by destruction of primary flame NOx by secondary fuel radicals. The research showed that, with minimal facility modification, NOx emissions from a firetube package boiler can be reduced by 50% or more from an initial level of 200 ppm (measured dry, at zero % O_2). Several hypotheses were evaluated in the study. Results indicate that the overall NOx reduction via reburning has a reaction rate order of about 1.5 with respect to primary NOx. Secondary fuel-bound nitrogen is found to reduce reburning effectiveness. An overall gas-phase reaction time constant of 50 ms is observed for the reburn zone nitrogenous species; the characteristic time constant is greater for liquid fuel reburning due to droplet vaporization requirements. Increased temperature increases N_2 formation in the fuel-rich zone, but decreases it in the burnout.

17. KEY WORDS AND DOCUMENT ANALYSIS

a. DESCRIPTORS		b. IDENTIFIERS/OPEN ENDED TERMS	c. COSATI Field/Group	
Pollution	Fuel Oil	Pollution Control	13B	21D
Afterburning	Natural Gas	Stationary Sources	21B	
Fire Tube Boilers		Reburning	13A	
Unitizing		Package Boilers	15E	
Nitrogen Oxides		Staged Combustion	07B	
Combustion				

18. DISTRIBUTION STATEMENT **Release to Public**	19. SECURITY CLASS *(This Report)* **Unclassified**	21. NO. OF PAGES 447
	20. SECURITY CLASS *(This page)* **Unclassified**	22. PRICE

EPA Form 2220-1 (9-73)

NOTICE

This document has been reviewed in accordance with U.S. Environmental Protection Agency policy and approved for publication. Mention of trade names or commercial products does not constitute endorsement or recommendation for use.

ABSTRACT

A pilot-scale experimental research program has been conducted to examine the physical and chemical phenomena associated with the NO_x control technology of reburning applied to gaseous and liquid-fired firetube package boilers. Reburning, or staged fuel combustion, involves diverting a portion of the fuel and combustion air from the main burner(s) for injection into the post-flame gases, resulting in three distinct zones in the boiler radiant section: a fuel-lean primary zone, a fuel-rich reburning zone, and a fuel-lean burnout zone. NO_x is reduced both by a reduction in NO_x formation and by a destruction of primary flame NO_x by secondary fuel radicals.

Several hypotheses were evaluated in this study. Results indicate that the overall NO_x reduction via reburning has a reaction rate order of approximately 1.5 with respect to primary NO_x. Secondary fuel-bound nitrogen is found to reduce reburning effectiveness. An overall gas phase reaction time constant of 50 ms is observed for the reburn zone nitrogenous species; the characteristic time constant is greater for liquid fuel reburning due to droplet vaporization requirements. Increased temperature increases N_2 formation in the fuel-rich zone, but decreases N_2 formation in the burnout zone. Secondary fuel injector design does not significantly influence reburning effectiveness in the firetube package boiler class due to the existence of large scale turbulent structures in the reacting flow that dominate secondary fuel jet parameters. Nitrogen-free fuel oil yields slightly greater NO_x reductions than natural gas in reburning application. These results were obtained on a 1.0 MW (3.5×10^6 Btu/hr) research boiler simulator and verified on a commercial Scotch type package boiler (2.5×10^6 Btu/hr).

It is shown that with minimal facility modification, NO_x emissions from a firetube package boiler can be reduced by 50 percent and more from an initial level of 200 ppm (measured dry, at zero percent O_2).

ACKNOWLEDGMENT

This report entitled "Reburning Application to Firetube Package Boilers" summarizes the results from a pilot-scale EPA in-house reburning study. The program was initiated by W. S. Lanier, original project officer for this contract, who was involved in every technical aspect of the program. Review of this report was provided by R. E. Hall of EPA and R. K. Srivastava of Acurex. Finally, D. Kattaron's preparation of this report is acknowledged.

NOMENCLATURE

Abbreviations:

Symbol	Definition
D	Detailed (test)
EA	Excess Air
FGD	Flue Gas Recirculation
FR	Firing Rate
GM	Gas mingling
k	Reaction rate constant
I/O	Input/Output (test)
K	Equilibrium constant
NSPS	New Source Performance Standard
OFA	Over Fire Air
P	Pressure
PBS	Package Boiler Simulator
ppm	parts per million
R	universal gas constant
SR	Stoichiometric Ratio
T	Temperature
t	time
TFN	Total Fixed Nitrogen
τ	residence time
y	mole fraction

Subscripts:

Symbol	Definition
b	bulk
BO	Burn Out
EX	Exhaust (stack)
init	initial
PRI	PRImary
R	Reburn
TOT	TOTal
1	PBS precombustion chamber zone
2	PBS primary zone
3	PBS reburn zone
4	PBS burnout zone

Chemical Species:

Symbol	Common Name
C	Carbon atom
H	Hydrogen atom
O	Oxygen atom
N	Nitrogen atom
H_2	Molecular hydrogen
O_2	Molecular oxygen
N_2	Molecular nitrogen
NO	Nitric oxide
NO_2	Nitrite
NO_3	Nitrate
NO_x	Nitrogen oxides
N_2O	Nitrous oxide
HCN	Hydrogen cyanide
NH_3	**Ammonia**
CO	Carbon monoxide
CO_2	Carbon dioxide
CH_4	Methane
C_2H_2	Acetylene
CH	Methylidyne radical
C_5H_5N	Pyridine
H_2O	Water
OH	Hydroxyl radical

TABLE OF CONTENTS

SECTION PAGE

ABSTRACT iii

ACKNOWLEDGMENT iv

NOMENCLATURE v

LIST OF FIGURES xi

LIST OF TABLES xix

1 INTRODUCTION AND BACKGROUND 1-1

1.1 Definition 1-1

1.2 NO_x Chemistry Overview 1-3

1.3 Reburn Technology Review 1-12

1.4 Program Objectives 1-19

2 EXPERIMENTAL FACILITIES 2-1

2.1 Firetube Package Boiler Simulator 2-1

2.2 Reburning Hardware Design and Modification 2-15

2.3 North American Boiler 2-21

3 EXPERIMENTAL METHODS 3-1

3.1 Temperature Measurement 3-1

3.2 Velocity Measurement 3-3

3.3 Stack Gas Speciation Measurement 3-7

3.4 In-Flame Gas Speciation Measurement 3-11

4 BASELINE TEST RESULTS 4-1

4.1 Precombustion Chamber Zone Characterization 4-3

4.2 Primary Zone Characterization 4-6

4.3 Secondary Fuel Injection Definition 4-16

TABLE OF CONTENTS

SECTION PAGE

5 PBS NATURAL GAS REBURNING TEST RESULTS 5-1

5.1 Input/Ouput Trials 5-4

5.1.1 Primary NO_x and Reburn Zone Stoichiometry. 5-4

5.1.2 Ammonia-Doped Secondary Fuel 5-15

5.1.3 Reburn Zone Residence Time 5-19

5.1.4 Primary Zone Stoichiometry 5-24

5.1.5 Burnout Zone Stoichiometry 5-26

5.1.6 Primary Fuel 5-26

5.2 Detailed Trials 5-29

5.2.1 Temperature and Velocity Profiles 5-29

5.2.2 Uniform Secondary Fuel Injection Validation 5-35

5.2.3 Chemical Species Profiles 5-37

5.3 Secondary Fuel Injection Method Studies 5-68

5.3.1 Spoked Secondary Fuel Injection 5-69

5.3.2 Unspoked Secondary Fuel Injection 5-77

5.3.3 Turbulent Eddy Size 5-80

5.3.4 Conclusions 5-82

5.4 Reburn Zone Thermal Environment Studies 5-84

5.4.1 Primary Load Variation 5-84

5.4.2 Insulated Reburning Zone 5-86

5.4.3 Insulated Primary Zone 5-90

5.4.4 Secondary Fuel Injection Location 5-98

5.4.5 Conclusions 5-107

TABLE OF CONTENTS
(continued)

SECTION PAGE

5.5 Staged Air Jet Studies 5-107

5.5.1 Observed Phenomenon 5-108

5.5.2 Key Parameters 5-114

5.5.3 Possible Mechanisms 5-120

5.5.4 Conclusions 5-128

5.6 Alternative Staging Strategies 5-129

5.6.1 Air Staging 5-129

5.6.2 Biased Reburning 5-133

5.6.3 Optimum Reburn Zone Stoichiometries . . . 5-136

5.6.4 Conclusions 5-140

5.7 High Primary NO_x Trials 5-143

6 PBS FUEL OIL REBURNING TEST RESULTS 6-1

6.1 Input/Ouput Trials 6-1

6.1.1 Primary NO_x and Reburn Zone Stoichiometry. 6-4

6.1.2 Pyridine-Doped Secondary Fuel 6-11

6.1.3 Reburn Zone Residence Time 6-12

6.1.4 Primary Zone Stoichiometry 6-18

6.1.5 Burnout Zone Stoichiometry 6-23

6.1.6 Primary Fuel 6-23

6.1.7 Secondary Fuel Atomization 6-25

6.1.8 Reburn Zone Thermal Environment 6-28

6.2 Detailed Tests 6-32

TABLE OF CONTENTS

SECTION PAGE

7 NORTH AMERICAN BOILER REBURNING APPLICATION TEST RESULTS 7-1

7.1 Baseline Tests 7-1

7.2 Natural Gas Reburning Tests 7-7

7.3 Fuel Oil Reburning Tests 7-17

8 CONCLUSIONS 8-1

REFERENCES R-1

APPENDIX A: QUALITY ASSURANCE/QUALITY CONTROL REPORT . A-1

APPENDIX B: DATA SUMMARY B-1

LIST OF FIGURES

No.	Title	Page
1	Reburning Cartoon	2
2	Package Boiler Simulator Schematic	5
3	Reburning Effectiveness	7
4	Reburning Zone Residence Time Effect	8
5	Reburning Zone Nitrogen Species Profiles	10
6	Reburning Application Test Results	11
1-1	Reburning Schematic	1-2
1-2	Adiabatic Flame Temperature Versus Stoichiometry	1-5
1-3	Equilibrium Fixed Nitrogen Species Versus Stoichiometry	1-6
1-4	Equilibrium NO_x Versus Temperature for Fuel-Lean Combustion . .	1-7
1-5	Equilibrium TFN Versus Temperature for Fuel-Rich Combustion . .	1-9
1-6	Proposed NO_x Destruction Mechanism by Hydrocarbons	1-13
1-7	MACT Application for Gas Firing	1-15
1-8	MACT Application for Oil Firing	1-15
1-9	MACT Application for Coal Firing	1-15
1-10	NO_x Destruction via Reburning -- Chen's Data [12]	1-18
2-1	Firetube Package Boiler Simulator	2-2
2-2	Low-NO_x Prechamber Burner	2-4
2-3	Burner/Boiler Transition Section	2-5
2-4	Combustion Air Supply System Diagram	2-7
2-5	Natural Gas Supply System Diagram	2-8
2-6	Fuel Oil Supply System Diagram	2-13
2-7	Ammonia Supply System Diagram	2-14
2-8	Burner Management System Logic Diagram	2-16

LIST OF FIGURES
(continued)

No. Title Page

2-9 Reburn Fuel and Air Booms 2-17

2-10 Second and Third Generation Fuel Booms 2-19

2-11 Secondary Fuel Oil Supply System Diagram 2-20

2-12 Modified Boiler Endplate 2-22

2-13 North American Boiler 2-23

3-1 Suction Pyrometer 3-2

3-2 Temperature Measurement Calibration Curve 3-4

3-3 Prandtl Probe 3-5

3-4 Velocity Measurement Calibration Curve 3-8

3-5 Continuous Emissions Monitoring System Diagram 3-9

3-6 Combustion Gas Sample Probe 3-10

3-7 Condensible Species Sample Train 3-13

4-1 PRS Baseline Operation Schematic 4-2

4-2 Baseline NO$_{EX}$ Versus SR$_1$ 4-4

4-3 Baseline NO$_{EX}$ Versus Percent Ammonia Dopant in Fuel 4-5

4-4 Effect of Secondary Air Injection Mode on Baseline NO$_{EX}$ 4-7

4-5 Baseline NO$_{EX}$ Versus SR$_2$ 4-9

4-6 Axial Temperature Profiles 4-10

4-7 Radial Temperature Profile 4-11

4-8 Radial Velocity Profile 4-13

4-9 Axial NO Profile 4-14

4-10 Radial NO and O$_2$ Profiles 4-18

5-1 PRS Natural Gas Reburning Schematic 5-2

5-2 Natural Gas Reburning Effectiveness 5-5

5-3 Ammonia-Doped Natural Gas Reburning Effectiveness 5-6

5-4 Comparison of NO Reduction and Net NO Destruction 5-8

LIST OF FIGURES
(continued)

No.	Title	Page
5-5	Hypothetical Effect of Nonuniform Secondary Fuel Injection . . .	5-10
5-6	Effect of NO_{PRI} for Natural Gas Reburning	5-12
5-7	Reaction Rate Order Determination for $SR_R = 0.78$	5-13
5-8	Reaction Rate Order Determination for $SR_R = 0.87$	5-14
5-9	Effect of NO_{PRI} for Ammonia-Doped Natural Gas Reburning	5-16
5-10	Comparison of Undoped and Ammonia-Doped Natural Gas Reburning . .	5-17
5-11	Net Fractional Conversion of Ammonia to Exhaust NO	5-18
5-12	Effect of Ammonia Dopant for Natural Gas Reburning	5-20
5-13	Net Fractional Conversion of Ammonia to Exhaust NO	5-21
5-14	Effect of Reburn Zone Length for Natural Gas Reburning	5-23
5-15	Effect of Primary Zone Stoichiometry for Natural Gas Reburning . .	5-25
5-16	Effect of Burnout Zone Stoichiometry for Natural Gas Reburning . .	5-27
5-17	Effect of Primary Fuel Type for Natural Gas Reburning	5-28
5-18	Reburn Zone Axial Temperature Profiles	5-30
5-19	Reburn Zone Radial Temperature Profiles	5-33
5-20	Reburn Zone Radial Velocity Profile	5-34
5-21	Degree of Uniformity of Spoked Secondary Fuel Injection	5-36
5-22	Reburn Zone Carbon Species Profiles for Natural Gas Reburning . .	5-40
5-23	Calculated Reburn Zone UHC (as CH_4) and H_2 Profiles for Natural Gas Reburning	5-42
5-24	Water-Gas Equilibrium Constant	5-43
5-25	Reburn Zone Nitrogen Species Profiles for Natural Gas Reburning, $SR_R = 0.97$	5-46
5-26	Reburn Zone Nitrogen Species Profiles for Natural Gas Reburning, $SR_R = 0.86$	5-47
5-27	Reburn Zone Nitrogen Species Profiles for Natural Gas Reburning, $SR_R = 0.78$	5-48

LIST OF FIGURES
(continued)

No. Title Page

5-28 Reburn Zone Nitrogen Species Profiles for Natural Gas Reburning, NO_{PRI} = 122 PPM 5-49

5-29 Reburn Zone Nitrogen Species Profiles for Natural Gas Reburning, NO_{PRI} = 49 PPM 5-50

5-30 Reburn Zone Nitrogen Species Profiles for 0.5% Ammonia-Doped Natural Gas Reburning, SR_R = 0.95 5-51

5-31 Reburn Zone Nitrogen Species Profiles for 0.5% Ammonia-Doped Natural Gas Reburning, SR_R = 0.87 5-52

5-32 Reburn Zone Nitrogen Species Profiles for 0.5% Ammonia-Doped Natural Gas Reburning, SR_R = 0.78 5-53

5-33 Reburn Zone Nitrogen Species Profiles for 0.5% Ammonia-Doped Natural Gas Reburning, NO_{PRI} = 119 PPM 5-54

5-34 Reburn Zone Nitrogen Species Profiles for 0.5% Ammonia-Doped Natural Gas Reburning, NO_{PRI} = 69 PPM 5-55

5-35 Nitrogen Species Concentrations at the Reburn Zone Exit for Natural Gas Reburning 5-57

5-36 Reburn Zone NO Profiles for Natural Gas Reburning 5-58

5-37 TFN to NO Conversion Efficiency in the Burnout Zone for Natural Gas Reburning 5-60

5-38 Reburn Zone NO Profiles for Natural Gas Reburning 5-63

5-39 Reburn Zone NO Profiles for 0.5% Ammonia-Doped Natural Gas Reburning 5-65

5-40 Net Conversion of Ammonia to NO in the Reburn Zone 5-66

5-41 Secondary Fuel Injection Schematics 5-71

5-42 Effect of Secondary Fuel Injection Method 5-73

5-43 Reburn Zone CO Profiles with Nonuniform Spoke Injection 5-76

5-44 Comparison of Spoked and Unspoked Secondary Fuel Injection 5-78

5-45 Upstream Secondary Fuel Flow Effects 5-83

5-46 Baseline Temperature Profiles with Increased Primary Load 5-85

5-47 Reburning Effectiveness at Low Temperatures 5-87

5-48 Reburn Zone Temperature Profiles with Insulated Primary Zone and Insulated Reburn Zone 5-88

LIST OF FIGURES
(continued)

No.	Title	Page
5-49	Natural Gas Reburning Effectiveness with Insulated Reburning Zone	5-89
5-50	Baseline Temperature Profile with Insulated Primary Zone	5-91
5-51	Reburn Zone Radial Velocity Profile with Insulated Primary Zone .	5-92
5-52	Natural Gas Reburning Effectiveness with Insulated Primary Zone .	5-94
5-53	Reburn Zone Carbon Species Profiles for Natural Gas Reburning with Insulated Primary Zone	5-95
5-54	Reburn Zone Nitrogen Species Profiles for Natural Gas Reburning with Insulated Primary Zone	5-96
5-55	Reburn Zone Nitrogen Species Profiles for 0.5% Ammonia-Doped Natural Gas Reburning with Insulated Primary Zone	5-97
5-56	PRS Natural Gas Reburning Schematic with Secondary Fuel Room #3 .	5-99
5-57	Baseline Radial Temperature Profiles for SR_1 = 0.91 and SR_2 = 1.06	5-101
5-58	Thermal Effects for Natural Gas Reburning	5-102
5-59	Thermal Effects for 0.5% Ammonia-Doped Natural Gas Reburning . .	5-103
5-60	Baseline Radial Temperature Profiles for SR_1 = SR_2 = 1.10	5-104
5-61	Thermal Effects for Natural Gas Reburning, NO_{PRI} = 1050 PPM . . .	5-105
5-62	Thermal Effects for 0.5% Ammonia-Doped Natural Gas Reburning, NO_{PRI} = 1050 PPM	5-106
5-63	Axial NO and O_2 Profiles through the Burnout Air Jet	5-109
5-64	Circumferential NO and O_2 Profiles in the Burnout Air Jet	5-112
5-65	Effect of Reburn Zone Load on Burnout Air Jet NO Destruction . .	5-115
5-66	Effect of Burnout Air Jet Flow on NO Destruction	5-118
5-67	Effect of Temperature on Burnout Air Jet NO Destruction	5-119
5-68	Thermal De-NO_x in the PBS	5-122
5-69	Alternative PBS Firing Strategies	5-130
5-70	Staged Air NO Reduction on PBS	5-132

LIST OF FIGURES
(continued)

No.	Title	Page
5-71	Natural Gas Reburning Versus Biased Reburning	5-134
5-72	Natural Gas Reburning Versus Advanced Biased Reburning	5-135
5-73	Optimum Reburning Stoichiometry	5-138
5-74	Equilibrium TFN for Methane/Air Combustion at 1 Atmosphere . . .	5-141
5-75	Reburning Effectiveness for NO_{PRI} = 1016 ppm	5-144
6-1	PBS Fuel Oil Reburning Schematic	6-2
6-2	Distillate Fuel Oil Reburning Effectiveness	6-5
6-3	Heavy Fuel Oil Reburning Effectiveness	6-6
6-4	Effect of NO_{PRI} for Fuel Oil Reburning	6-7
6-5	Comparison of Natural Gas and Fuel Oil Reburning	6-9
6-6	Pyridine-Doped Distillate Fuel Oil Reburning Effectiveness . . .	6-10
6-7	Net Fractional Conversion of Pyridine to NO_{EX}	6-13
6-8	Effect of Reburn Zone Residence Time for Distillate Fuel Oil Reburning	6-14
6-9	Effect of Reburn Zone Residence Time for Heavy Fuel Oil Reburning	6-15
6-10	Comparison of Natural Gas and Fuel Oil Reburning with Residence Time	6-16
6-11	Effect of Reburn Zone Residence Time for Low NO_{PRI}	6-19
6-12	Effect of Reburn Zone Residence Time for Pyridine-Doped Distillate Fuel Oil Reburning	6-20
6-13	Effect of Primary Zone Stoichiometry for Distillate Fuel Oil Reburning	6-21
6-14	Effect of Primary Zone Stoichiometry for Heavy Fuel Oil Reburning	6-22
6-15	Effect of Burnout Zone Stoichiometry for Fuel Oil Reburning . . .	6-24
6-16	Effect of Primary Fuel Type for Distillate Fuel Oil Reburning . .	6-26
6-17	Effect of Primary zone Insulation for Distillate fuel Oil Reburning	6-30

LIST OF FIGURES
(continued)

No.	Title	Page
6-18	Baseline Centerline Temperature Profile for Fuel-Lean Prechamber Burner Operation	6-31
6-19	Thermal Effects for Fuel-Lean Distillate Fuel Oil Reburning	6-33
6-20	Reburn Zone Nitrogen Species Profiles for Distillate Fuel Oil Reburning, SR_R = 0.89	6-34
6-21	Reburn Zone Nitrogen Species Profiles for Distillate Fuel Oil Reburning, SR_R = 0.94	6-35
6-22	Reburn Zone Nitrogen Species Profiles for Distillate Fuel Oil Reburning, SR_R = 1.03	6-36
6-23	Reburn Zone Nitrogen Species Profiles for Distillate Fuel Oil Reburning, NO_{PRI} = 125 PPM	6-37
6-24	Reburn Zone Nitrogen Species Profiles for Distillate Fuel Oil Reburning, NO_{PRI} = 80 PPM	6-38
6-25	Reburn Zone Nitrogen Species Profiles for Heavy Fuel Oil Reburning, SR_R = 0.87	6-39
6-26	Reburn Zone Nitrogen Species Profiles for Heavy Fuel Oil Reburning, SR_R = 0.93	6-40
6-27	Reburn Zone Nitrogen Species Profiles for Heavy Fuel Oil Reburning, SR_R = 1.02	6-41
6-28	Reburn Zone Nitrogen Species Profiles for Heavy Fuel Oil Reburning, NO_{PRI} = 135 PPM	6-42
6-29	Reburn Zone Nitrogen Species Profiles for Heavy Fuel Oil Reburning, NO_{PRI} = 83 PPM	6-43
6-30	Reburn Zone Nitrogen Species Profiles for Heavy Fuel Oil Reburning, Long Reburn Zone Residence Time	6-44
6-31	Comparison of Reburn Zone NO Profiles for Natural Gas and Fuel Oil Reburning	6-47
7-1	Effect of Load on Baseline NO_{EX}	7-2
7-2	Effect of Load on Primary Flame Length	7-4
7-3	Baseline Axial Temperature Profiles	7-5
7-4	North American Boiler Reburning Application Schematic	7-6

LIST OF FIGURES
(continued)

No.	Title	Page
7-5	Natural Gas Reburning Effectiveness	7-8
7-6	Comparison of PBS and North American Boiler Natural Gas Reburning Results	7-10
7-7	Effect of Ammonia-Doping of Secondary Natural Gas	7-12
7-8	Effect of Secondary Natural Gas Injection Location	7-13
7-9	Natural Gas Reburning Application Example	7-15
7-10	Natural Gas Reburning Application Example Result Summary	7-16
7-11	Fuel Oil Reburning Effectiveness	7-18
7-12	Comparison of PBS and North American Boiler Fuel Oil Reburning Results	7-20
7-13	Effect of Secondary Fuel Oil Injection Location	7-21
7-14	Distillate Fuel Oil Reburning Application Example	7-22
7-15	Heavy Fuel Oil Reburning Application Example	7-23
8-1	HCN Reaction Pathways in the Reburn Zone	8-4
8-2	NH_3 Reaction Pathways in the Reburn Zone	8-5

LIST OF TABLES

No.	Title	Page
1-1	Summary of MACT Pilot-Scale Results	1-16
2-1	Fuel Analyses	2-9
3-1	Gaseous Emission Monitor Specifications	3-15
4-1	Secondary Natural Gas Uniform Injection Spoke Specifications	4-19
5-1	Input Parameters -- Natural Gas Reburning	5-3
5-2	Detailed Trial Test Matrix -- Natural Gas Reburning	5-31
5-3	Temperature, Velocity, and Speciation Entering Reburn Zone	5-38
5-4	Comparison of Measured and Calculated CO and CO_2 Equilibrium Concentration in the Reburn Zone	5-38
5-5	Molar Dilution Factors Between Boiler Zones	5-45
5-6	Effect of Secondary Natural Gas Fuel Nozzle	5-80
5-7	Radial NO and O_2 Variation in the Burnout Air Jet	5-110
5-8	Fixed Nitrogen Species in the Burnout Air Jet	5-113
5-9	Effect of Jet Composition on NO Destruction	5-116
5-10	Reburning with Ammonia Injection in the Burnout Air Jet	5-123
5-11	Zeldovich Reaction Rate Calculations	5-126
6-1	Input Parameters -- Fuel Oil Reburning	6-3
6-2	Effect of Secondary Fuel Oil Nozzle	6-27
6-3	Detailed Trial Test Matrix -- Fuel Oil Reburning	6-45
7-1	Comparison of PBS and North American Boiler Operating Parameters	7-7
8-1	Summary of PBS Test Results	8-2
8-2	Summary of North American Boiler Test Results	8-2

SECTION 1

INTRODUCTION AND BACKGROUND

The U.S. Environmental Protection Agency's Air and Energy Engineering Research Laboratory (AEERL) located in Research Triangle Park, North Carolina, has sponsored an in-house study of the application of a combustion technology known as reburning. Reburning is an in-furnace nitrogen oxides (NOx) control technology in which portions of the fuel and oxidizer streams are diverted downstream of the primary flame. Acurex Corporation has been contracted by EPA to modify two existing pilot-scale firetube package boiler research facilities, conduct reburning application tests, and report on the results. This comprehensive final report documents the experimental findings, covering the period of performance from March, 1983 to April, 1985. Much of this information has been, or will be, documented in various technical papers published outside the EPA; these publications are cited in this report. The entire scope of the two year reburning program is presented here.

In this section, reburning is defined, a cursory overview of NO_x chemistry in hydrocarbon fuel/air flames is presented, a review of reburn technology research and development is outlined, and the objectives of this program are defined. The material presented in this section provides a basis for understanding the reburning test results presented in later sections.

1.1 DEFINITION

Reburning is an in-furnace NO_x control technology in which portions of the fuel and combustion air streams are diverted downstream of the primary flame. In this way, the combustor has three distinct zones: a fuel-lean primary zone, a fuel-rich reburning zone, and a fuel-lean burnout zone. This is shown schematically in Figure 1-1.

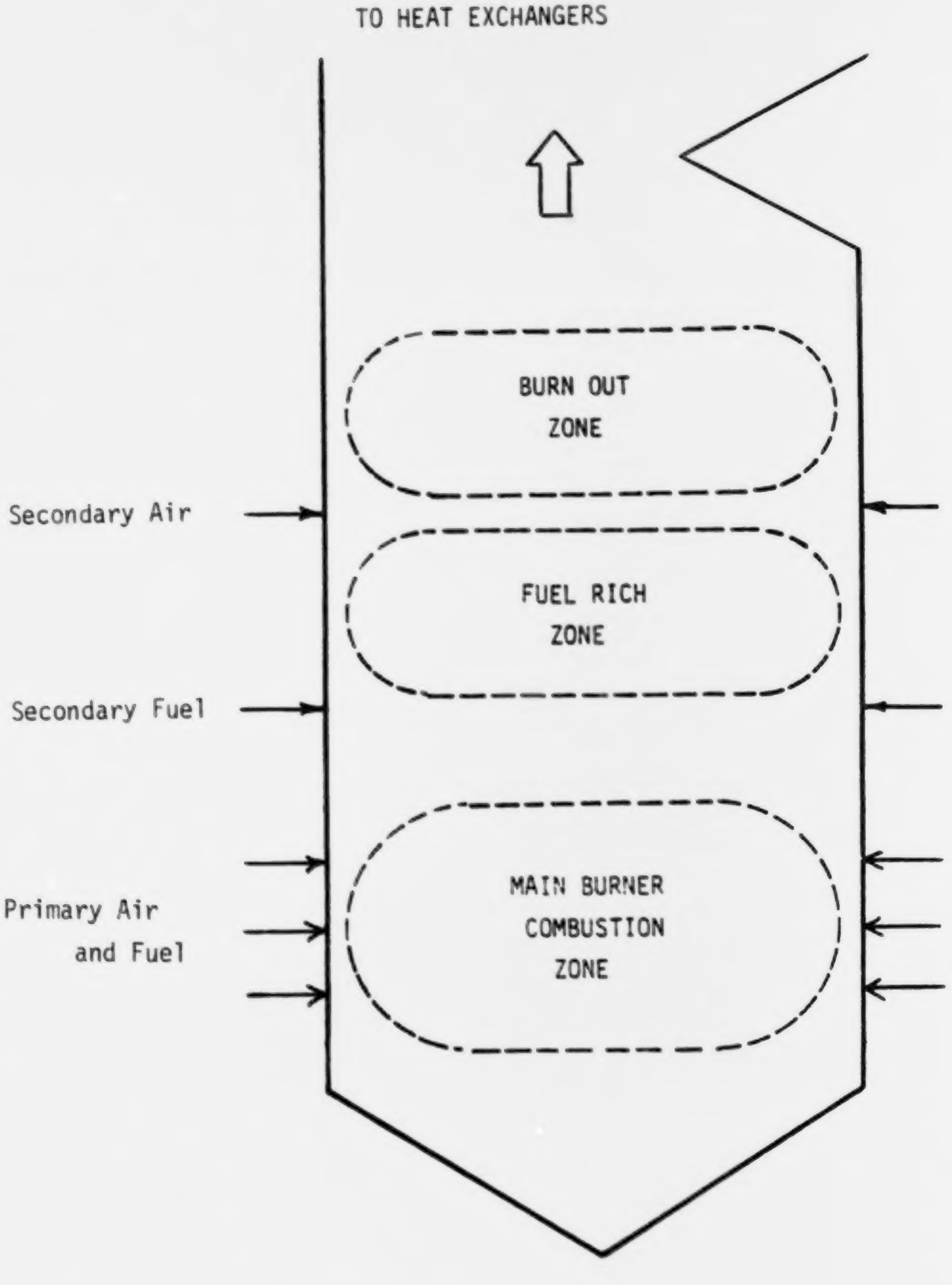
TO HEAT EXCHANGERS
BURN OUT ZONE
Secondary Air
FUEL RICH ZONE
Secondary Fuel
Primary Air and Fuel
MAIN BURNER COMBUSTION ZONE

Figure 1-1: Reburning Schematic

NO_x reduction via reburning occurs both by the combustion of a portion of the fuel at low flame temperatures and under fuel-rich stoichiometries (conditions not promoting NO_x formation), and by a chemical destruction mechanism involving secondary flame radical reactions with nitric oxide (NO), which results eventually in nitrogen molecule (N_2) formation. An advantage of reburning is that it is a technology that can be coupled with other NO_x control technologies to achieve very low NO_x emissions (less than 100 ppm at zero percent oxygen for natural gas and light fuel oil reburning). A disadvantage of reburning is that it necessitates hardware modification to the combustor. Before proceeding further, a review of well known NO_x chemistry principles is presented. This will prove useful in studying the reburning phenomenon, since reburning is a particular application of these principles.

1.2 NO_x CHEMISTRY OVERVIEW

To understand NO_x formation in a practical combustion facility, aerodynamic, thermodynamic, and kinetic effects must be considered. Aerodynamic effects in turbulent reacting flows are highly system, or hardware, dependent. These system effects will be discussed in Section 5.4 where results from mixing tests are presented. Chemical thermodynamics and chemical kinetics are process effects that provide a basis for understanding the NO_x chemistry of reburning.

Chemical Thermodynamics

All chemical reactions are either endothermic or exothermic; that is, they either absorb or release energy. This energy can be quantified from basic thermodynamic principles. Thus, given the temperature, pressure, and state of the reactants, the final temperature and product composition can be calculated for an isolated system.

The adiabatic flame temperature is a theoretical maximum combustion temperature (i.e., the flame temperature in a combustor with no heat extraction).

Plots of adiabatic flame temperature versus oxidizer-to-fuel ratio peak at approximately the stoichiometric mixture ratio. In Figure 1-2 the adiabatic flame temperature is shown as a function of stoichiometry (the inverse of equivalence ratio) for methane/air combustion at 1 atmosphere pressure. For this calculation, performed on a computer using the NASA thermodynamic equilibrium code [1], 67 possible products of the C, H, O, N system are considered. These products consist of the normal stable species CO_2, H_2O, N_2, and O_2, as well as various products of dissociation reactions, such as C, CO, H, H_2, H_2O_2, HO_2, O, OH, N, NO, NO_2 and N_2O. In a traditional combustor, fuel and air are introduced through a burner, typically at a 5 to 30 percent excess air stoichiometry. The resulting flame can reach temperatures on the order of 2500K (4040°F).

Equilibrium concentrations of significant fixed nitrogen species (species containing the nitrogen atom) are plotted versus stoichiometry in Figure 1-3 under adiabatic flame temperature and atmospheric pressure conditions for methane/air combustion. Under fuel-lean (SR>1) conditions, Total Fixed Nitrogen (TFN) is composed almost entirely of NO. Under fuel-rich conditions (SR<1), ammonia (NH_3) and hydrogen cyanide (HCN) concentrations become dominant. It is interesting to note that there is a minimum in the equilibrium TFN curve. For the adiabatic flame temperature condition, this minimum occurs at a stoichiometry of 0.6. As flame temperature decreases, this minimum shifts to the right, approaching a stoichiometry of 1.0 from the fuel-rich side. In Figure 1-4, equilibrium NO_x concentration is plotted against temperature for a 10 percent excess air condition. As heat is extracted from the combustion gases under typical excess air conditions, equilibrium NO_x concentration falls rapidly. At adiabatic flame temperatures, equilibrium NO_x concentrations can be several thousand parts per million (ppm); at typical combustor stack temperatures (e.g., 450K), equilibrium NO_x concentrations are less than 1 ppm.

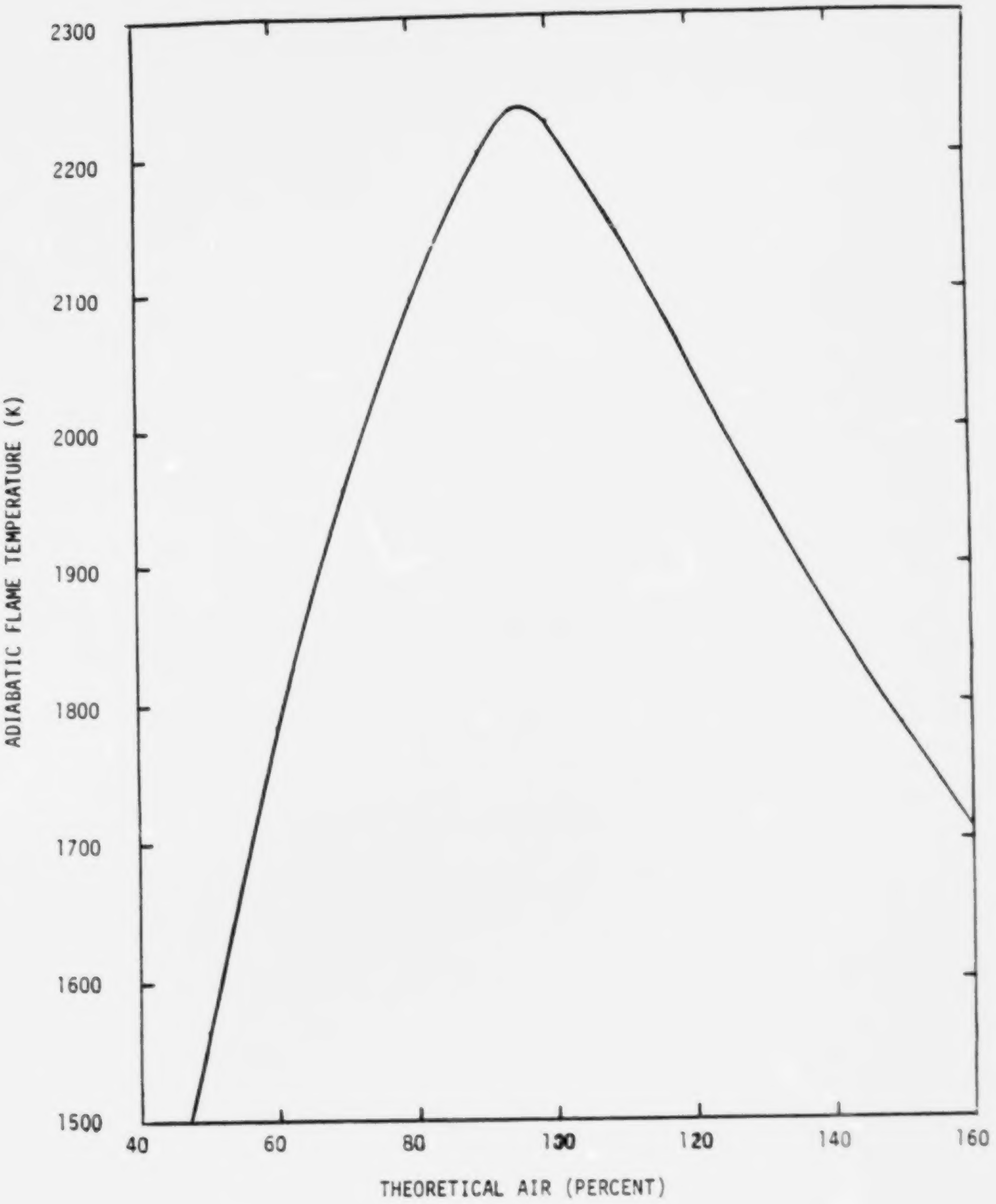

Figure 1-2: Adiabatic Flame Temperature Versus Stoichiometry for Methane/Air Combustion at 1 atm.

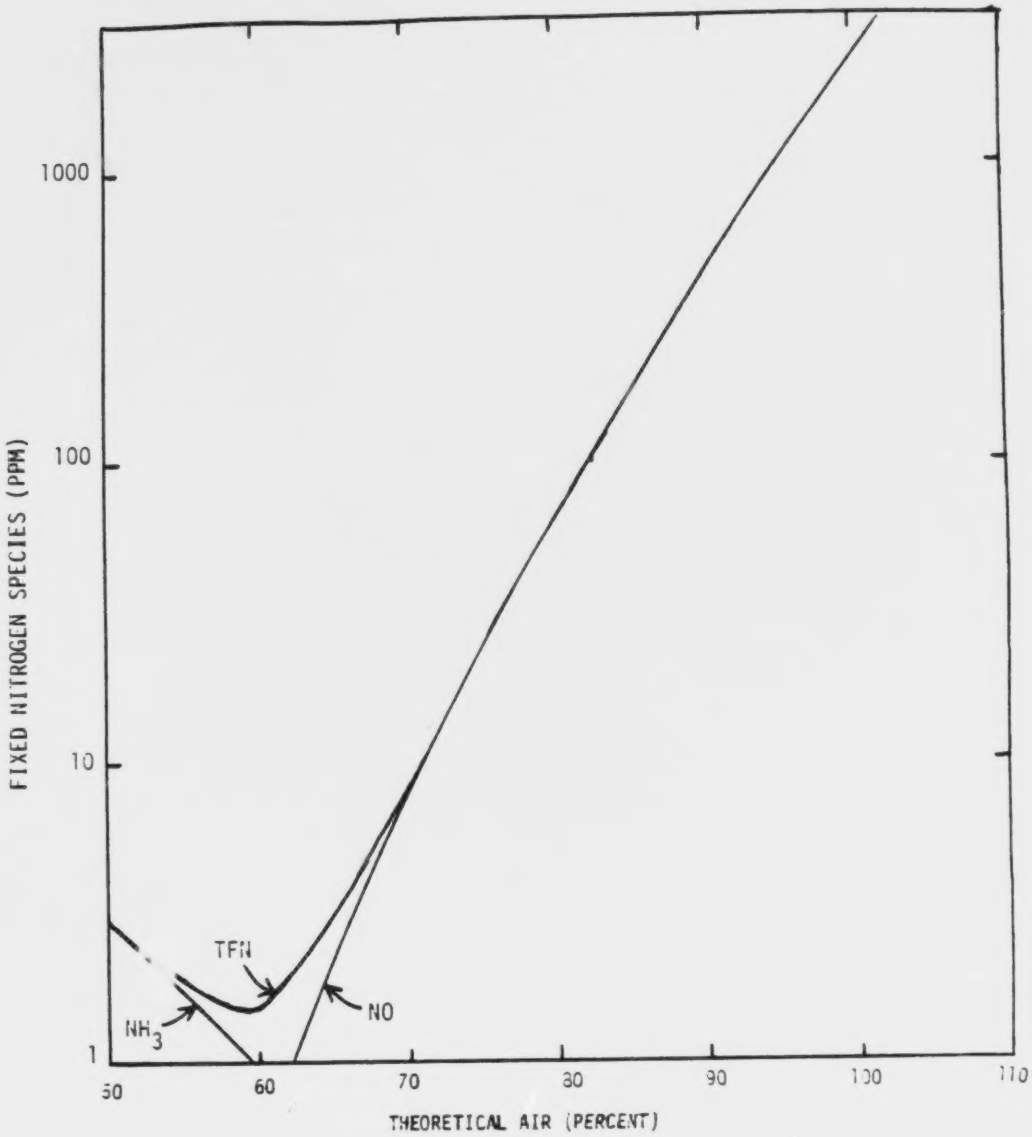

Figure 1-3: Equilibrium Fixed Nitrogen Species Versus Stoichiometry for Methane/Air Combustion at Adiabatic Flame Temperatures and 1 atm.

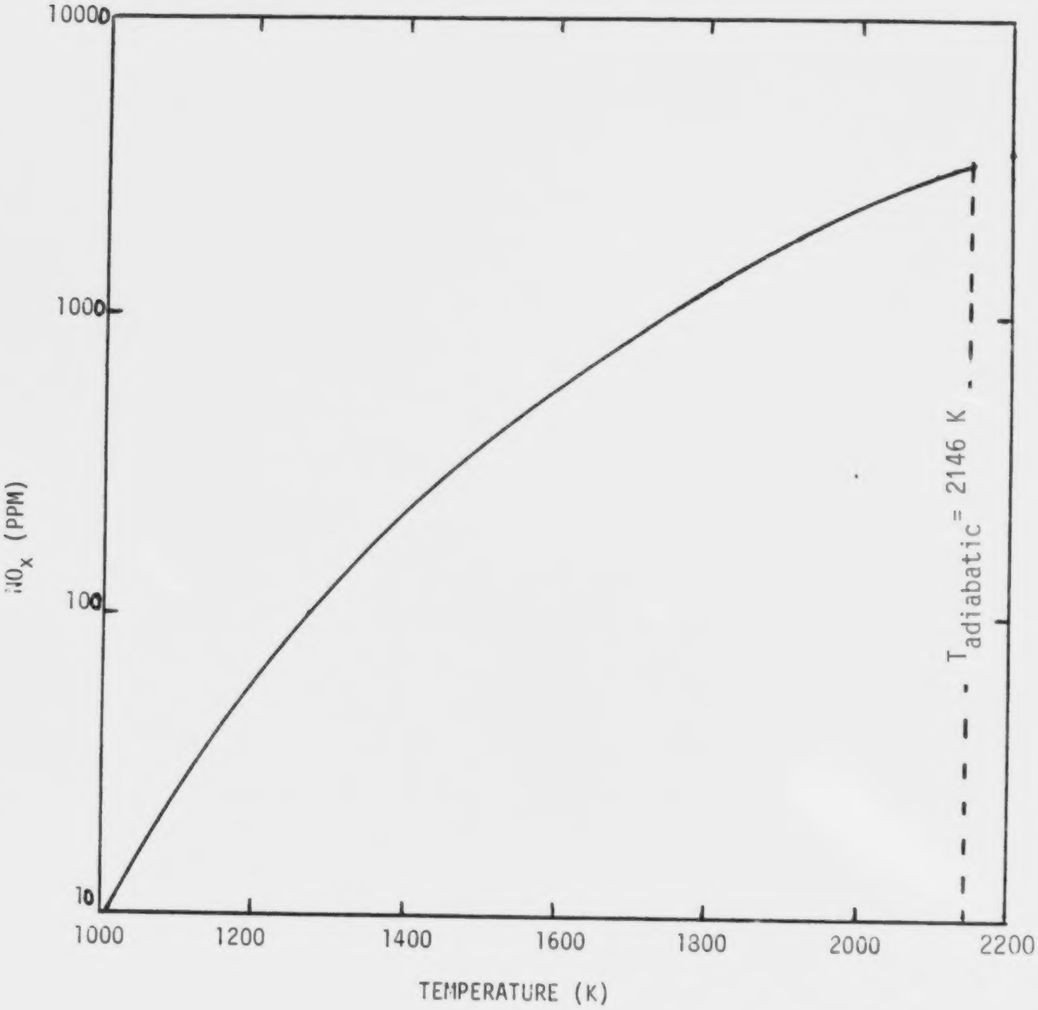

Figure 1-4: Equilibrium NO_x Versus Temperature for Fuel-Lean Combustion (110% Theoretical Air) of Methane/Air at 1 atm.

Under fuel-rich conditions, the trend of equilibrium TFN concentration with temperature is reversed (up to 1600 K). As shown in Figure 1-5, equilibrium TFN decreases with increasing temperature under a fuel-rich condition. It is also noted that the equilibrium TFN curve at 80 percent theoretical air is several orders of magnitude below the equilibrium NO_x curve at 110 percent theoretical air.

Results from equilibrium calculations indicate the thermodynamically favored speciation at specified temperature, pressure, and elemental constituency. These calculations suggest various NO_x control strategies, such as low excess air systems, low flame temperature burners, and staged combustion processes. In practical combustor devices, however, the kinetic rates for the dominant nitrogen reactions are too slow to allow for NO_x concentrations that can be predicted based only on equilibrium considerations. Typically, NO_x concentration is frozen at a high level produced in the active flame due to the consumption of free radicals that are necessary to maintain high reaction rates. Thus, while chemical thermodynamics can provide a simple and useful tool for understanding the direction of NO_x chemistry, chemical kinetics provides an understanding of mechanisms which limit the achievement of equilibrium.

Chemical Kinetics

NO_x formation in hydrocarbon/air flames can occur by three different mechanisms, referred to as thermal NO_x, prompt NO_x, and fuel NO_x. Thermal NO_x is formed from the oxidation of N_2 molecules in the combustion air. In 1946, Zeldovich [2] postulated that the dominant path for N_2 oxidation is by the following chain reactions:

$$O_2 + M \Longleftrightarrow 2O + M \qquad (1\text{-}1)$$

$$N_2 + O \longrightarrow NO + N,\ k_{1\text{-}2} = 8 \times 10^{13} \exp(-75{,}500/RT) \qquad (1\text{-}2)$$

$$N + O_2 \longrightarrow NO + O,\ k_{1\text{-}3} = 6.4 \times 10^{9} \exp(-6280/RT) \qquad (1\text{-}3)$$

Here, the rate constant, k, is written in units of $cm^3/g\text{-mole}\cdot K$, R is the universal gas constant (1.987 cal/g-mole•K), and T is the absolute temperature

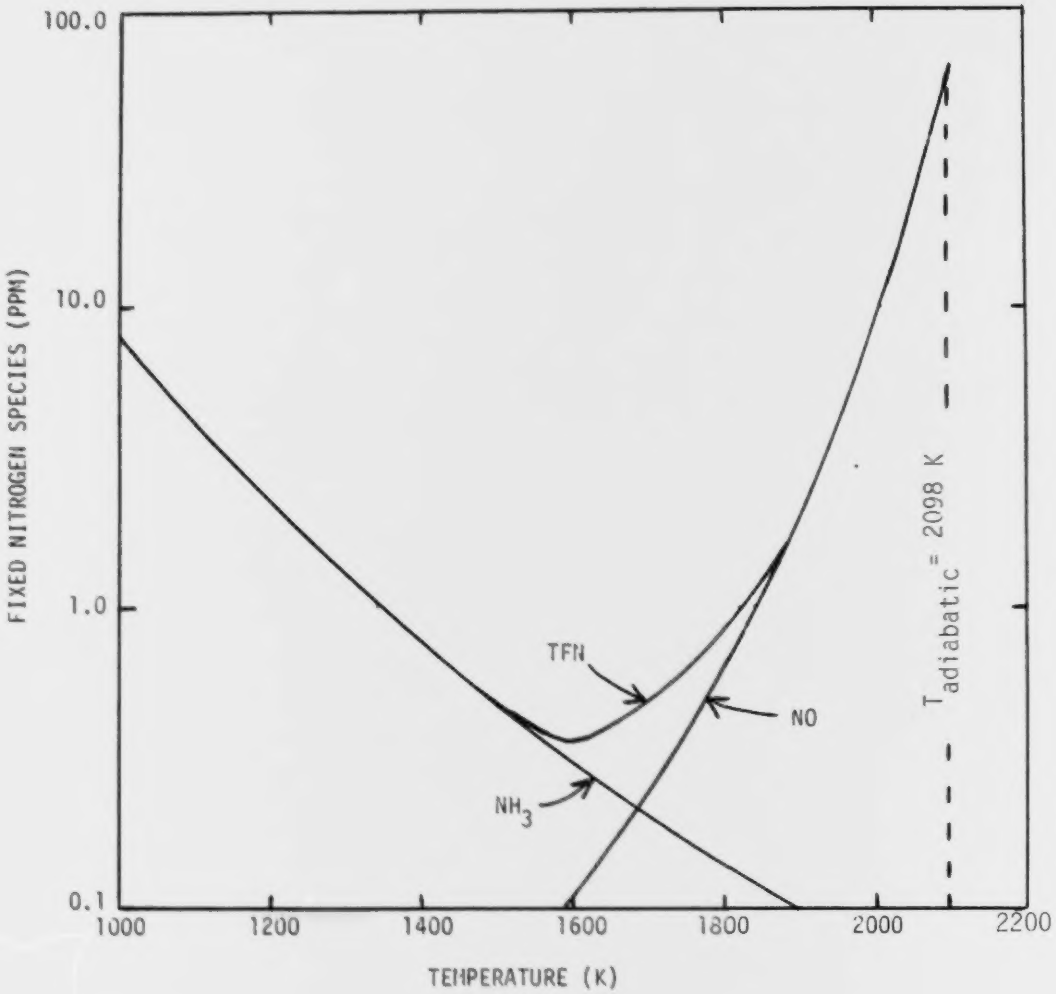

Figure 1-5: Equilibrium TFN Versus Temperature for Fuel-Rich Combustion (80% Theoretical Air) of Methane/Air at 1 atm.

(K). The rate constants were experimentally determined, with k_{1-2} cited in [3] and k_{1-3} cited in [4]. Because of its high activation energy, reaction 1-2 is much slower than reaction 1-3, and is, therefore, the rate-limiting step. Reaction 1-1 is, to a good approximation, equilibrated in the post-flame region (though within the active flame, peak O atom concentration may reach a super-equilibrium level).

Two characteristics of NO_x formation by the Zeldovich mechanism are observed. First, the rate of NO_x formation has a strong dependence on temperature; hence, it is referred to as "thermal NO_x". For peak flame temperatures less than 1800K (2780°F), very little thermal NO_x is produced. A second observation is that, the rate of NO_x formation by the Zeldovich mechanism being slow, thermal NO_x is formed primarily in the post-flame zone.

In 1971, Fenimore [4] argued that some NO_x was being formed in the flame region by reactions other than the Zeldovich mechanism. At local air/fuel ratios near stoichiometric or fuel-rich conditions, the availability of O_2 and O is low, and the concentration of fuel fragments, such as methyldyne (CH), is high. Under these conditions, alternate chemical pathways for attacking molecular nitrogen become significant. Fenimore postulated that "prompt NO_x" is formed in the flame zone primarily by the following step reaction:

$$CH + N_2 \longrightarrow HCN + N, \quad k_{1-4} = 1 \times 10^{11} \exp(-16{,}000/RT) \qquad (1\text{-}4)$$

The rate constant k_{1-4} is based on transition state theory, as cited in [3]. Its low activation energy implies that HCN and N atoms can be formed at relatively low temperatures. Thus, prompt NO_x formation may be important in reburning application.

A third chemical mechanism for NO_x formation is referred to as "fuel NO_x", as it represents the NO_x formed from fuel-bound nitrogen. Heavy residual fuel oils contain between 0.1 and 0.8 weight percent nitrogen; coal can contain up to 2 percent nitrogen [3]. The bound nitrogen compounds are thought to evolve from the parent fuel as low molecular weight compounds or radicals, such as HCN, CN, NH_3, and NH_2. There is much uncertainty concerning the oxidation paths of these nitrogen-containing compounds to NO, but it is apparent that the oxidation rate is rapid, occurring on the time scale of the energy release reactions in the combustor [4]. Further, it has been shown that for the high reaction rate and low activation energy characteristic of HCN oxidation, the fuel NO_x formation process lacks the strong temperature dependence characteristic of thermal NO_x formation [3].

NO_x can be destroyed as well as formed in combustion processes. In flames with normal excess air conditions, the primary path for NO decomposition is described by the reverse Zeldovich mechanism.

$$O + NO \longrightarrow N + O_2 \qquad (1\text{-}5)$$

$$N + NO \longrightarrow N_2 + O \qquad (1\text{-}6)$$

$$H + NO \longrightarrow N + OH \qquad (1\text{-}7)$$

These reactions have high activation energies resulting in kinetic rates too slow for significant NO decomposition. However, under fuel-rich conditions, high O, N or H atom concentrations may be sufficient to provide a significant NO_x destruction mechanism by reactions 1-5, 1-6 or 1-7.

In the application of reburning, another path for NO destruction exists:

$$CH + NO \longrightarrow HCN + O \qquad (1\text{-}8)$$

This reaction is exothermic by 70.2 kcal/g-mole and has a rate constant estimated to be 1×10^{13} cm^3/g-mole·sec (with zero activation energy) [3]. Once HCN is formed, it can be oxidized by the following reaction (or other oxidizing reactions) to form the amine radical (NH).

$$HCN + O \longrightarrow NH + CO \qquad (1\text{-}9)$$

NH may either form N_2 or regenerate NO. Under fuel-rich conditions, N_2 formation paths should dominate.

$$NH + OH \longrightarrow N + H_2O \qquad (1\text{-}10)$$

$$N + NO \longrightarrow N_2 + O \qquad (1\text{-}6)$$

$$NH + NO \longrightarrow N_2O + H \longrightarrow N_2 + OH \qquad (1\text{-}11)$$

An overall chemical mechanism for NO destruction by hydrocarbons is proposed in Figure 1-6.

It should be noted that the formation of N_2 by either the reverse Zeldovich mechanism or the proposed hydrocarbon mechanism involves the consumption of two NO molecules. That is, the overall N_2 formation reaction would appear to be second order in NO.

1.3 REBURNING TECHNOLOGY REVIEW

As much as 30 years ago, experimental results were available indicating that NO_x could be destroyed by reaction with hydrocarbon radicals [6,7]. Commercial utilization of this reaction path occurred in the late 1960's by the John Zink Corporation, which patented a NO_x control process for nitric acid plants based on secondary injection of natural gas [8]. Early fundamental studies of NO_x destruction by injection of secondary fuel into the flame zone were performed by Wendt et al. [9], who coined the name "reburning" to describe the process. Concerted effort to develop reburning for application to boilers occurred in Japan during the late 1970's and early 1980's. The first reporting of these efforts was by Takahashi et al. [10], documenting extensive laboratory-, pilot-, and full-scale evaluation of the process they refer to as Mitsubishi Advanced Combustion Technology, or MACT. Similar development was performed by Hatashi, who recently (1983) received a U.S. patent on the process. Related work has also been performed by Kelly et al. [11], who refer to the process as "fuel staging". It has also been referred to as "in-flame NO_x reduction" (IFNR). Thus, at least four different names are

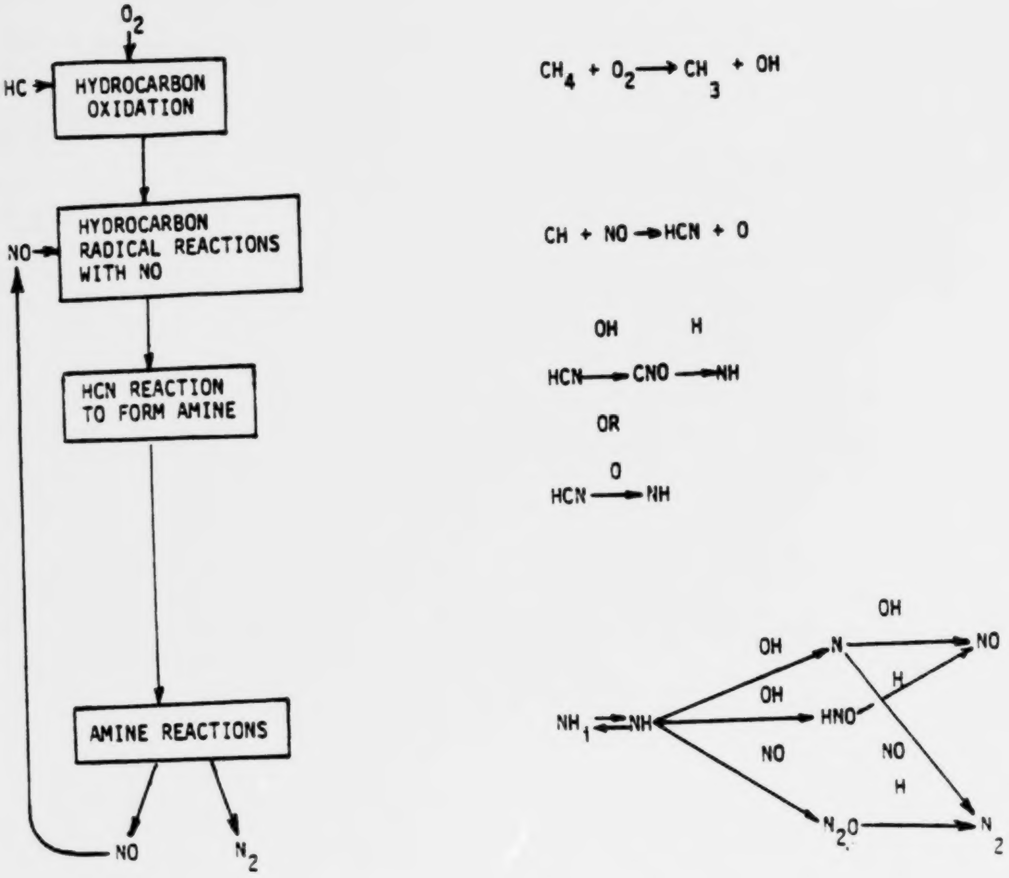
O2
HC
HYDROCARBON OXIDATION
NO
HYDROCARBON RADICAL REACTIONS WITH NO
HCN REACTION TO FORM AMINE
AMINE REACTIONS
NO
N2
CH4 + O2 → CH3 + OH
CH + NO → HCN + O
OH
H
HCN → CNO → NH
OR
O
HCN → NH
OH
OH
N
NO
H
OH
NH1 ⇌ NH
HNO
NO
NO
H
N2O
N2

Figure 1-6: Proposed NO_x Destruction Mechanism by Hydrocarbons

used to describe NO_x destruction by injection of a secondary stream of hydrocarbons. In deference to the earlier work by Wendt et al., the name reburning is used in this report.

Application of reburning requires that a portion of the fuel and combustion air be diverted from the main burner(s) for injection into the post-flame gases. A stable, fuel-lean flame is established in the main burner zone, but at slightly derated conditions (due to diverted fuel). The diverted fuel is injected near the end of the primary combustion flame in sufficient quantity to produce a local fuel-rich environment in the furnace. The diverted combustion air is injected at a location farther downstream, returning the system to an overall fuel-lean stoichiometry. Thus, reburning establishes a three-stage combustion process consisting of fuel-lean, fuel-rich, and fuel-lean zones. Heat release associated with combustion of the secondary fuel balances the main burner(s) derating to produce a zero net change in boiler heat release rate.

As described by Takahashi et al. [10], reburning is an extremely effective NO_x control technique. The MACT results indicate that NO_x emission rates are reduced by at least 50 percent from any initial NO_x level and that the technology is effective when firing gaseous, liquid, or solid fuels. The results from reburning application tests on a 20 MW (70 x 10^6 Btu/hr) boiler are presented in Figures 1-7, 1-8, and 1-9, and summarized in Table 1-1. Firing with propane, heavy oil, and coal, the Mitsubishi Heavy Industries (MHI) researchers varied initial NO_x concentration by: (1) varying the primary burner excess air level; and (2) applying overfire air (OFA) and flue gas recirculation (GM*) in series with reburning. As shown in the table, the NO_x emission level with reburning is approximately 50 percent below the baseline emission level, independent of initial NO_x concentration. This apparent first order rate dependence is surprising, since

---

*The MHI researchers refer to flue gas recirculation as gas mingling, or GM.

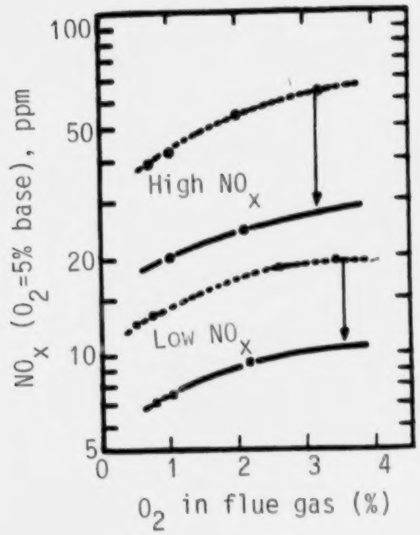

Figure 1-7: MACT Application for Gas Firing [10]

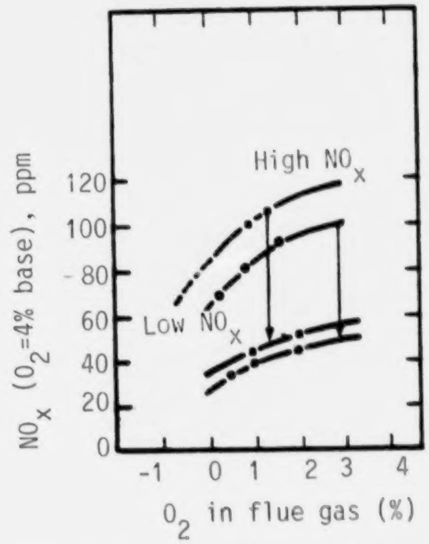

Figure 1-8: MACT Application for Oil Firing [10]

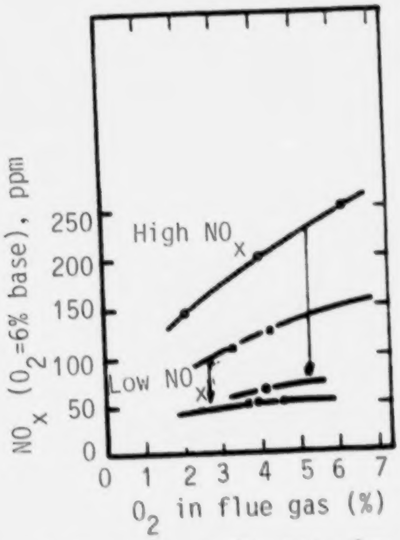

Figure 1-9: MACT Application for Coal Firing [10]

TABLE 1-1. SUMMARY OF MACT PILOT-SCALE RESULTS

Fuel-Combustion	NO_x Without MACT (ppm*)	NO_x With MACT (ppm*)	NO_x Reduction (percent)
Propane - Uncontrolled	80	35	56
- OFA + GM	25	13	48
Heavy Oil - Uncontrolled	142	65	54
- OFA + GM	123	59	52
Coal - Uncontrolled	245	84	66
- OFA	147	70	52

*at zero percent O_2

Test Condition: 10 MW load
15% excess air

the NO_x chemistry considerations presented in the previous section suggest a second order dependence. Also surprising is the apparent lack of influence of fuel-bound nitrogen on the reburning process. The MHI application tests are not well documented in the public literature (for proprietary reasons); therefore, close scrutiny of their data is not possible. It is probable that MHI optimized MACT by optimizing other system parameters as well as reburning process parameters. Therefore, their results may be system-specific, and not indicative of the fundamental reburning phenomenon. It is also suggested that MACT utilizes other NO_x control measures, including selective catalytic reduction, to achieve the low NO_x emissions that have been reported.

The promising, if somewhat puzzling, MHI full-scale results spurred U.S. interest in reburning. Further development is currently being sponsored by the U.S. Environmental Protection Agency (EPA), the Electric Power Research Institute (EPRI), the Gas Research Institute (GRI), and the U.S. Department of Energy (DOE). Chen et al. [12] have reported on bench-scale experiments, designed to verify the MHI results and better understand the influence of critical process parameters. Of particular interest was the finding that there is an optimum stoichiometry in the fuel-rich region for NO_x destruction. Figure 1-10, from the work of Chen et al., shows that NO_x destruction is maximized when the secondary fuel (propane) injection rate is sufficient to achieve a reburning zone stoichiometry of 90 percent theoretical air. This optimum is accentuated when the secondary fuel contains a significant quantity of fuel-bound nitrogen (0.86 percent nitrogen by weight, achieved here with ammonia dopant). Therefore, local variations of stoichiometry within the rich zone, governed by fuel injection techniques and mixing parameters, would appear to be important in optimizing reburning effectiveness in reducing NO_x emissions.

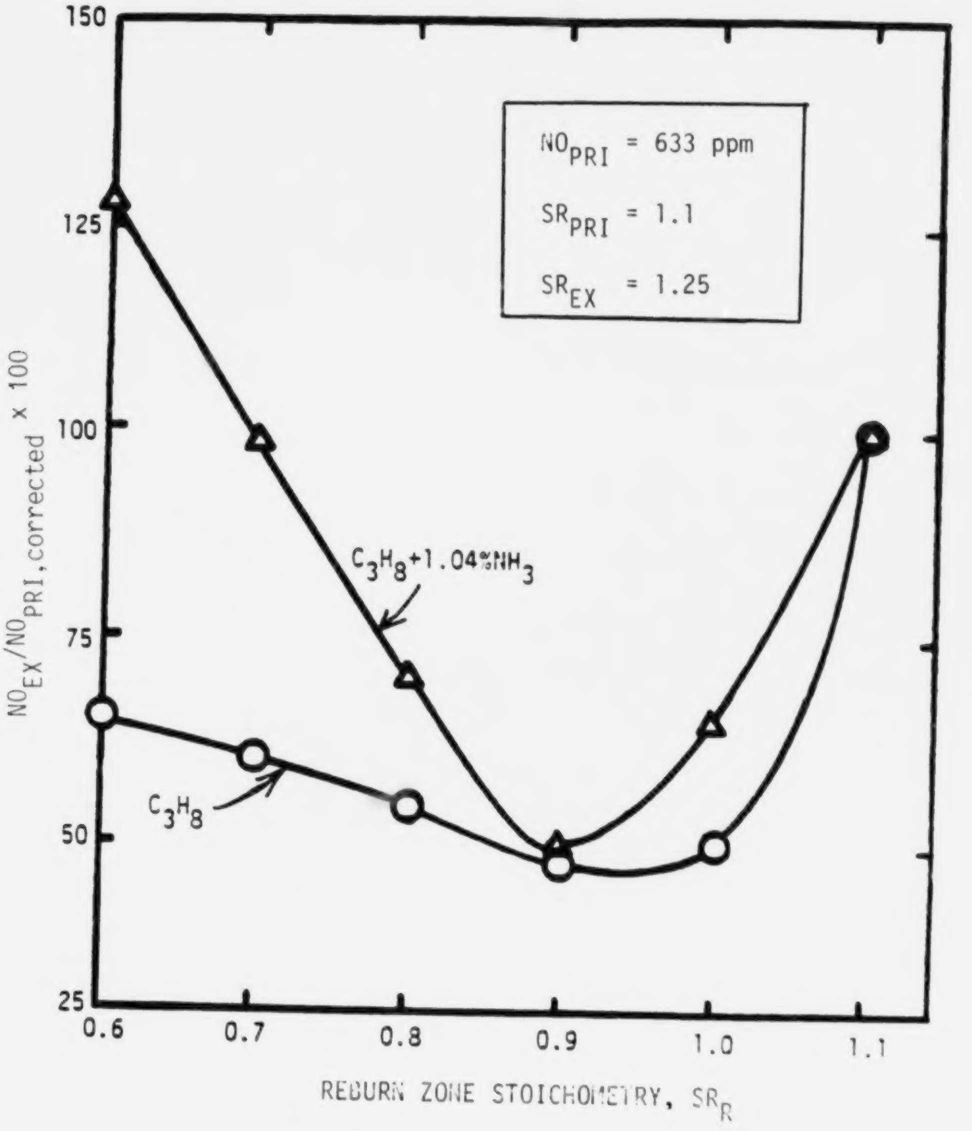

Figure 1-10: NOx Destruction Via Reburning--Chen's Data [12]

The experimental hardware and operating procedures employed by bench-scale researchers (e.g., Wendt et al., Chen et al., and Kelly et al.) facilitate understanding of the chemical processes controlling reburning, but remove important fluid mechanic and thermal gradient influences. In the full-scale work performed by MHI investigators, competing effects of a myriad of combustion phenomena make fundamental understanding difficult, if not impossible. To bridge the gap between hardware-specific full-scale results and oversimplified bench-scale fundamental results, detailed study of reburning application to a pilot-scale facility is required.

1.4 PROGRAM OBJECTIVES

As a part of a multi-scale research and development program to better understand the physical and chemical processes associated with reburning, the EPA has conducted in-house studies of the application of reburning to firetube package boilers.

The initial and primary phase of testing was designed to provide fundamental insight into the application of natural gas reburning to a package boiler by verifying or disproving the following 5 hypotheses:

1. Based on the fuel-rich nitrogen chemistry considerations presented in Section 1-2, it is hypothesized that overall NO_x destruction is second order in the level of NO_x produced by the primary flame.
2. Based on fuel-bound nitrogen chemistry, as described in Section 1-2, it is hypothesized that the presence of bound nitrogen (in the form of NH_3) in the secondary fuel stream will decrease the extent of NO_x reduction by reburning.
3. Based on the proposed mechanism of NO_x destruction described in Figure 1-6, it is hypothesized that characteristic times for NO_x,

HCN, and NH_3 reactions are significant to the overall reburning process, and that each of the time constants is influenced by such parameters as stoichiometry, temperature, and bound nitrogen content in the secondary fuel.

4. Based on the equilibrium calculations presented in Figure 1-5, it is hypothesized that, under fuel-rich conditions in the reburning zone, increasing temperature will decrease NO_x emissions.
5. Based on the observed dependence of reburning NO_x reduction effectiveness on reburn zone stoichiometry by various investigators (presented in Section 1-3), it is hypothesized that secondary fuel injector design will effect NO_x reduction.

From March, 1983 through February, 1984, a large quantity of natural gas reburning data was gathered in the first phase of the test program to evaluate these 5 hypotheses. This was followed by 6 months of fuel oil reburn testing, characterizing both distillate and heavy fuel oil reburning by evaluating the following 3 hypotheses:

6. The higher carbon-to-hydrogen ratio in fuel oils will produce higher concentrations of the methyldine radical (CH) in the reburning zone, thus enhancing NO_x destruction.
7. Fuel-bound nitrogen in the fuel oil will reduce NO_x reduction by reburning, similar to ammonia-doped natural gas results.
8. The characteristic time for NO_x reduction by reburning will increase to allow for droplet vaporization. Further, the increase in the characteristic time for NO_x reduction will be a function of the fuel oil volatility.

As will be discussed in Section 2, a research package boiler simulator was used in the first two test phases to obtain the fundamental insights necessary to prove or disprove the 8 hypotheses. In a third phase of the test program, reburning was applied to a commercial boiler to evaluate 2 final hypotheses:

9. Results obtained on the research simulator are applicable to a commercial system.
10. Reburn application can be optimized to result in at least 50 percent NO_x reduction.

Results from the natural gas reburning fundamental tests, the fuel oil reburning fundamental tests, and the reburning application tests are discussed in Sections 5, 6, and 7, respectively. Conclusions are drawn in Section 8. Before presenting the results and discussion, the experimental facilities are described (Section 2), the experimental methods are defined (Section 3), and baseline test results are presented (Section 4).

SECTION 2

EXPERIMENTAL FACILITIES

The principal experimental facility used to fulfill the reburning program objectives stated in Section 1.4 is a pilot-scale firetube Package Boiler Simulator (PBS), which was modified with the hardware necessary for reburning. To confirm PBS experimental results in a more realistic environment, a commercial North American firetube package boiler of similar size was used. Both facilities are located in the Wing G high bay area of EPA's Environmental Research Center in Research Triangle Park, North Carolina. Each facility is described in this section.

2.1 FIRETUBE PACKAGE BOILER SIMULATOR

The firetube package boiler simulator used in this study was manufactured by Dynamic Sciences, Inc., in 1972. The PBS has a nominal rated capacity of 1.0 MW (3.5 x 10^6 Btu/hr) and can be fired with natural gas, distillate oil, or residual oil. As seen in Figure 2-1, the radiant section is a double-walled circular cylinder of 2.3 m (7.5 ft) length and 0.6 m (2.0 ft) internal diameter. A 90 degree elbow section directs gas flow to the vertical stack. An induced draft fan can be used to pull gases through a horizontal convective section (shell and tube heat exchanger) and to return the gases to the stack. The convective section was not used in this study since all relevant chemistry is effectively frozen at the radiant section exit temperatures.

The radiant section is cooled with Dowtherm G® heat transfer fluid, with a heat extraction rate and wall temperatures similar to those found in commercial firetube package boilers. The Dowtherm system, which dumps its heat to a cooling tower through a house industrial water system, precludes problems associated with raising and disposing of steam. Wall penetrations (originally

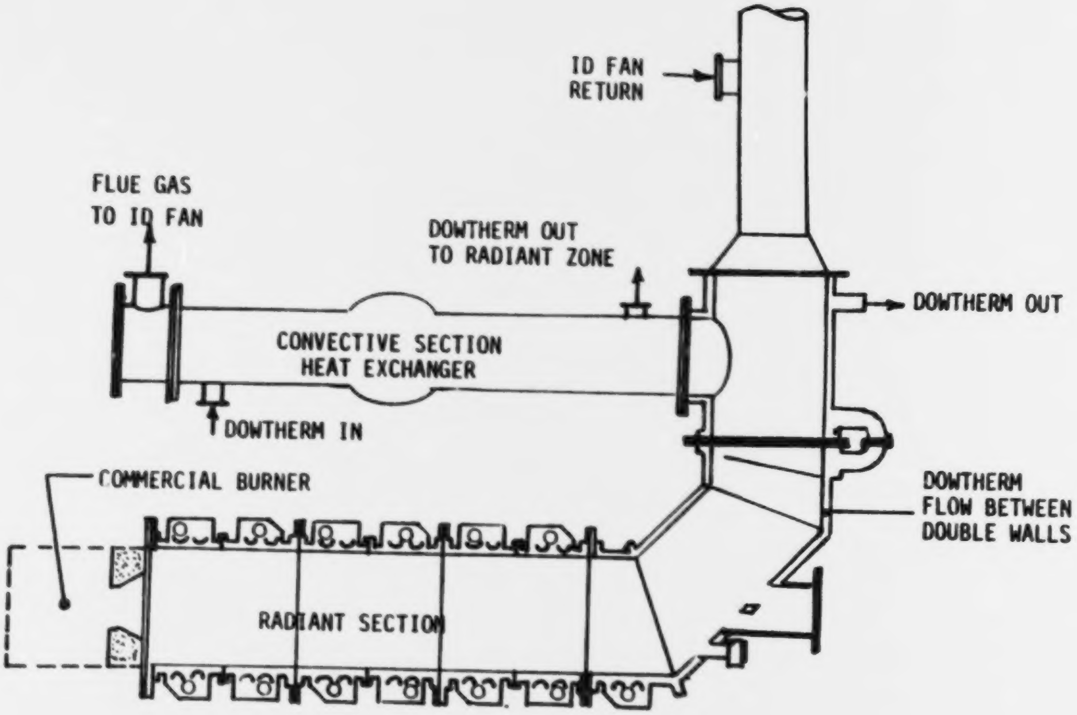
ID FAN RETURN
FLUE GAS TO ID FAN
DOWTHERM OUT TO RADIANT ZONE
DOWTHERM OUT
CONVECTIVE SECTION HEAT EXCHANGER
DOWTHERM IN
COMMERCIAL BURNER
DOWTHERM FLOW BETWEEN DOUBLE WALLS
RADIANT SECTION

Figure 2-1: Package Boiler Simulator

used in staged combustion studies) at 0.25 m (10 in.), 0.51 m (20 in.), 1.0 m (40 in.), and 1.3 m (50 in.) from the firetube front face were useful as test ports for the insertion of in-flame sampling probes and reburn fuel injectors.

With a standard commercial burner, it is impossible to vary NO_x concentration over a wide range of values without varying other process parameters, such as excess air. Yet, it was desired to vary primary NO_x concentration independent of other combustion parameters to evaluate the first program hypothesis. Therefore, it was decided to replace the commercial burner on the PBS with a more versatile burner system. This system, built by Energy and Environmental Research Corporation, is shown in Figure 2-2. It consists of a 0.51 m (20 in.) internal diameter layered refractory tube inside a steel shell. Fuel and primary combustion air enter through a fixed swirl vane premixing injector at the front end of the burner precombustion chamber. The precombustion chamber diameter is constricted to 0.25 m (10 in.) just before entering the PBS radiant section. This configuration helps maintain a nearly adiabatic environment in the precombustion chamber by reducing radiative heat transfer to the boiler. It also reduces air migration along the walls which aids in maintaining precise control of burner stoichiometry.

The burner is designed for substoichiometric (fuel-rich) operation, requiring secondary combustion air for complete burnout of primary fuel. This can be provided through either radial or axial injection ports in the burner/boiler water-cooled transition section, as shown in Figure 2-3. The portion of air introduced through each set of injectors can be varied to produce a continuous series of secondary flames, from a short, rapidly mixed flame (all-radial secondary air) to a long, axial flame (all-axial secondary air).

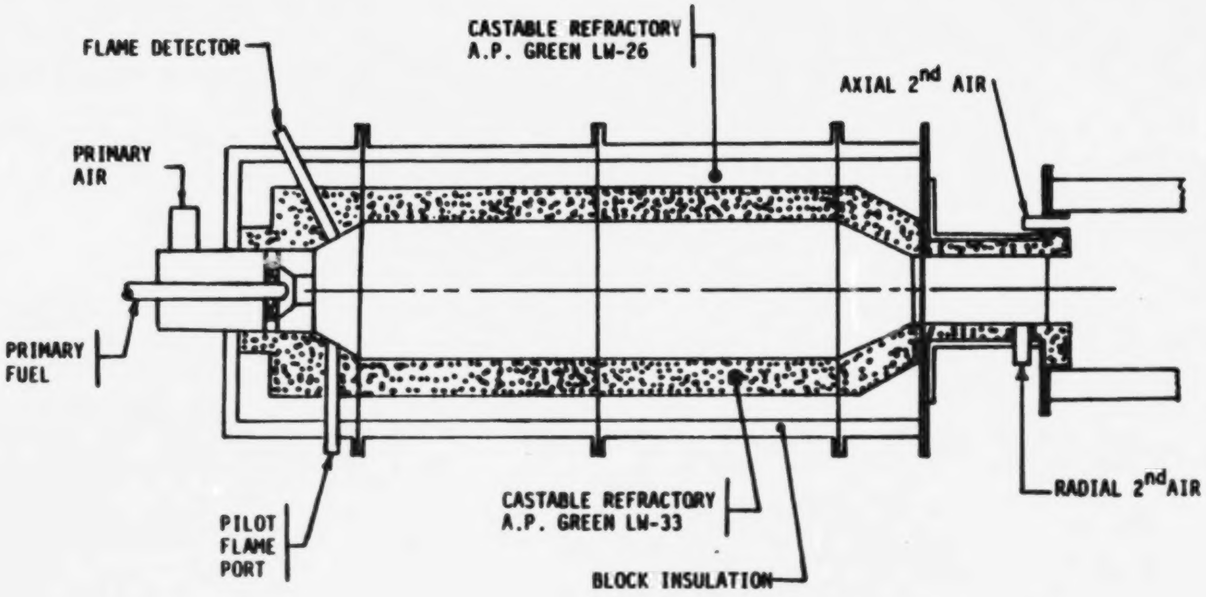
CASTABLE REFRACTORY
A.P. GREEN LW-26
FLAME DETECTOR
AXIAL 2nd AIR
PRIMARY AIR
PRIMARY FUEL
PILOT FLAME PORT
CASTABLE REFRACTORY
A.P. GREEN LW-33
BLOCK INSULATION
RADIAL 2nd AIR

Figure 2-2: Low NO_x Precombustion Chamber Burner

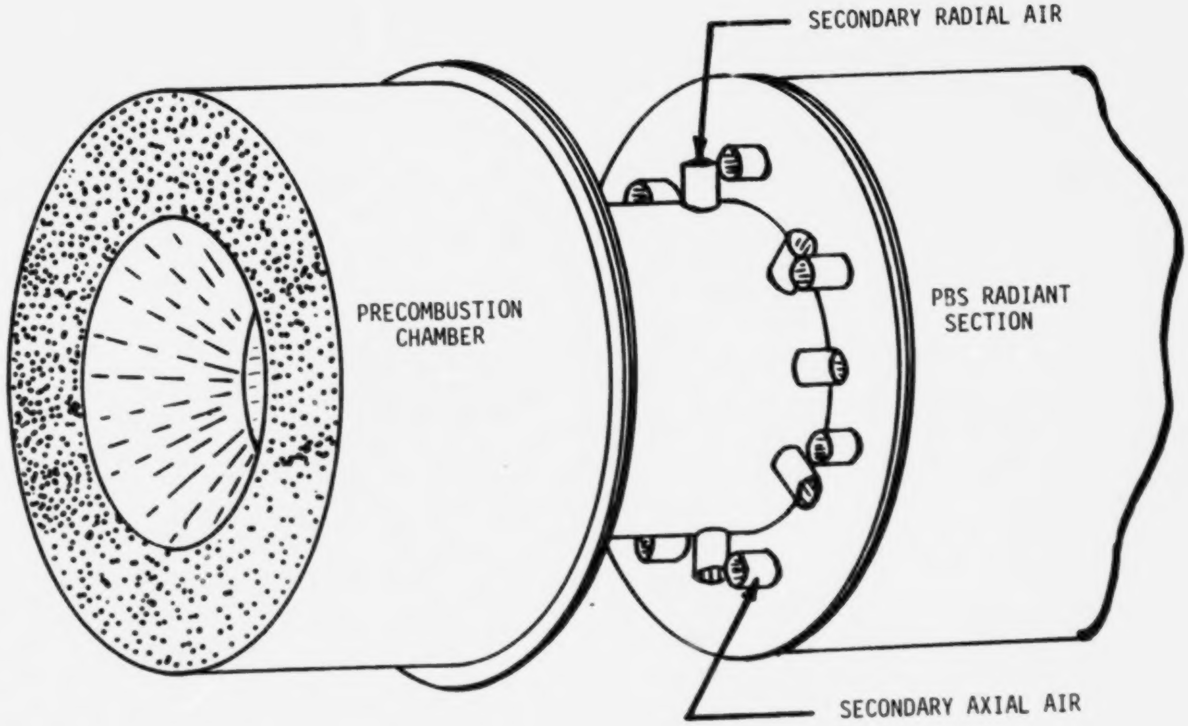
SECONDARY RADIAL AIR
PRECOMBUSTION CHAMBER
PBS RADIANT SECTION
SECONDARY AXIAL AIR

Figure 2-3: Burner/Boiler Transition Section

As seen in Figure 2-4, primary and secondary combustion airs are supplied by a single blower powered by an 11 kW (15 hp) electric motor. A Meriam laminar flow element (LFE) monitors total air flow. Primary air, secondary radial air and secondary axial air are monitored by venturi flow meters. All pressure differentials are measured with fluid manometers. A small amount of the primary combustion air is bled across the flame detector to prevent condensation on its lens. The inlet static pressures and temperatures of the flow devices are monitored with Magnehelic® pressure gauges and bi-metal thermometers to correct flows to standard conditions (1 atm, 70°F). All air flow devices were calibrated against a factory-calibrated standard LFE.

The refractory precombustion chamber burner can be fired on natural gas, distillate (#2) fuel oil, and a residual/distillate fuel oil mixture, or heavy fuel oil (with a net viscosity of a light #5 fuel oil). Table 2-1 presents results from fuel analyses performed on each of these fuels.

Figure 2-5 shows the natural gas supply system. The main burner natural gas flow is measured with an orifice plate and inclined manometer. House gas pressure is regulated to a nominal 5 psig. The gas flow splits after the orifice, with one leg going to the main burner and another to a pilot torch. Normally closed solenoid valves are electrically tied to the burner management/safety system, preventing fuel flow without a series of flame safeguards and limit switches being made. The primary burner gas pressure is further regulated before passing through a normally closed, motorized valve (actuated by the burner management/safety system) and a manual gascock. The gas cock, as well as the diameter of holes in the gas nozzle, regulates the gas flow. Six holes are drilled symmetrically around the gas nozzle centerline, at a 30 degree angle to the centerline axis. Several nozzles with varying diameter holes are used for flame stabilization at various loads during burner operation.

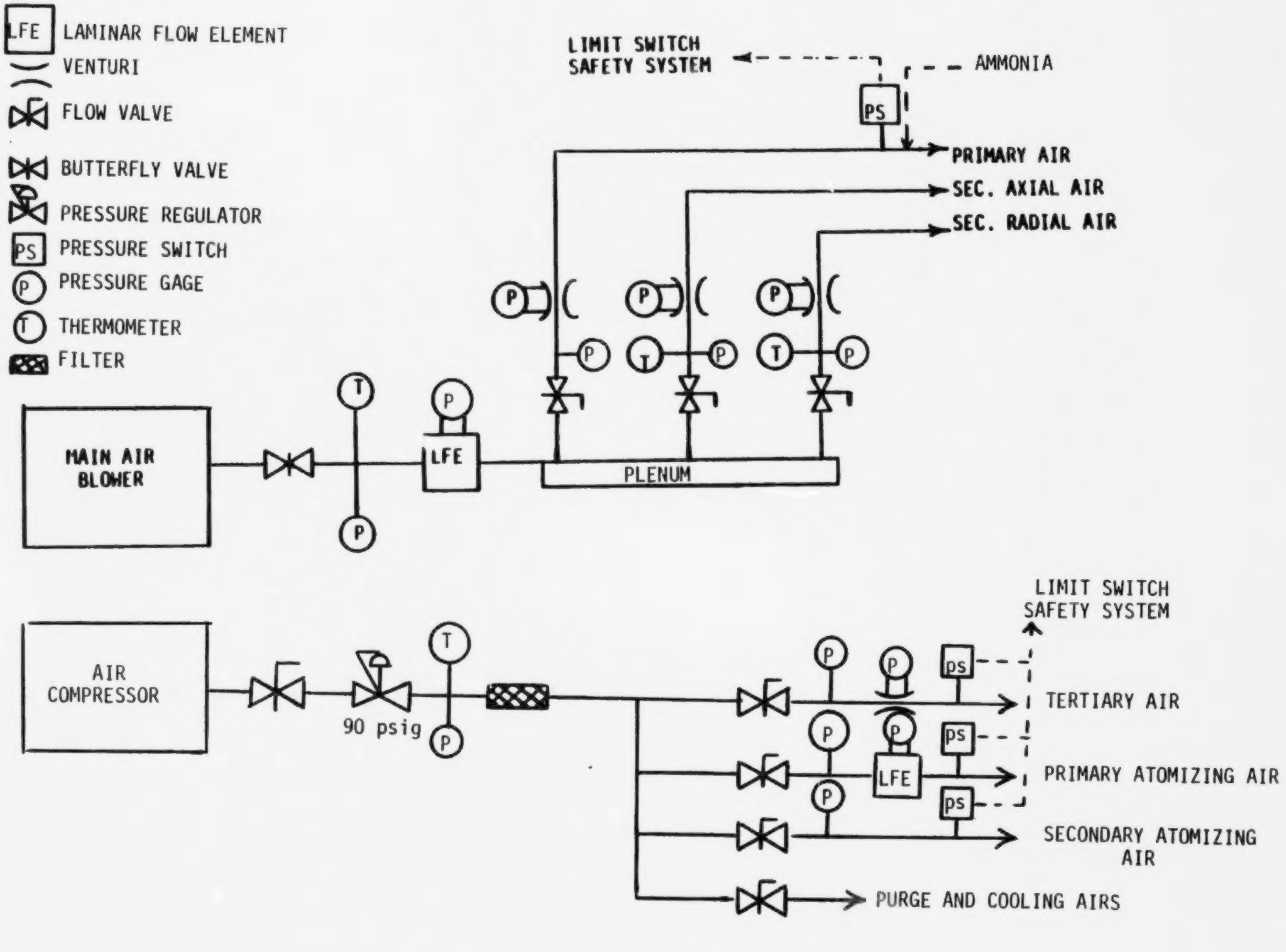
LFE LAMINAR FLOW ELEMENT
VENTURI
FLOW VALVE
BUTTERFLY VALVE
PRESSURE REGULATOR
PS PRESSURE SWITCH
P PRESSURE GAGE
T THERMOMETER
FILTER
LIMIT SWITCH SAFETY SYSTEM
AMMONIA
PS
PRIMARY AIR
SEC. AXIAL AIR
SEC. RADIAL AIR
P
T
MAIN AIR BLOWER
LFE
PLENUM
LIMIT SWITCH SAFETY SYSTEM
AIR COMPRESSOR
90 psig
ps
TERTIARY AIR
PRIMARY ATOMIZING AIR
SECONDARY ATOMIZING AIR
PURGE AND COOLING AIRS

Figure 2-4: Combustion Air Supply System Diagram

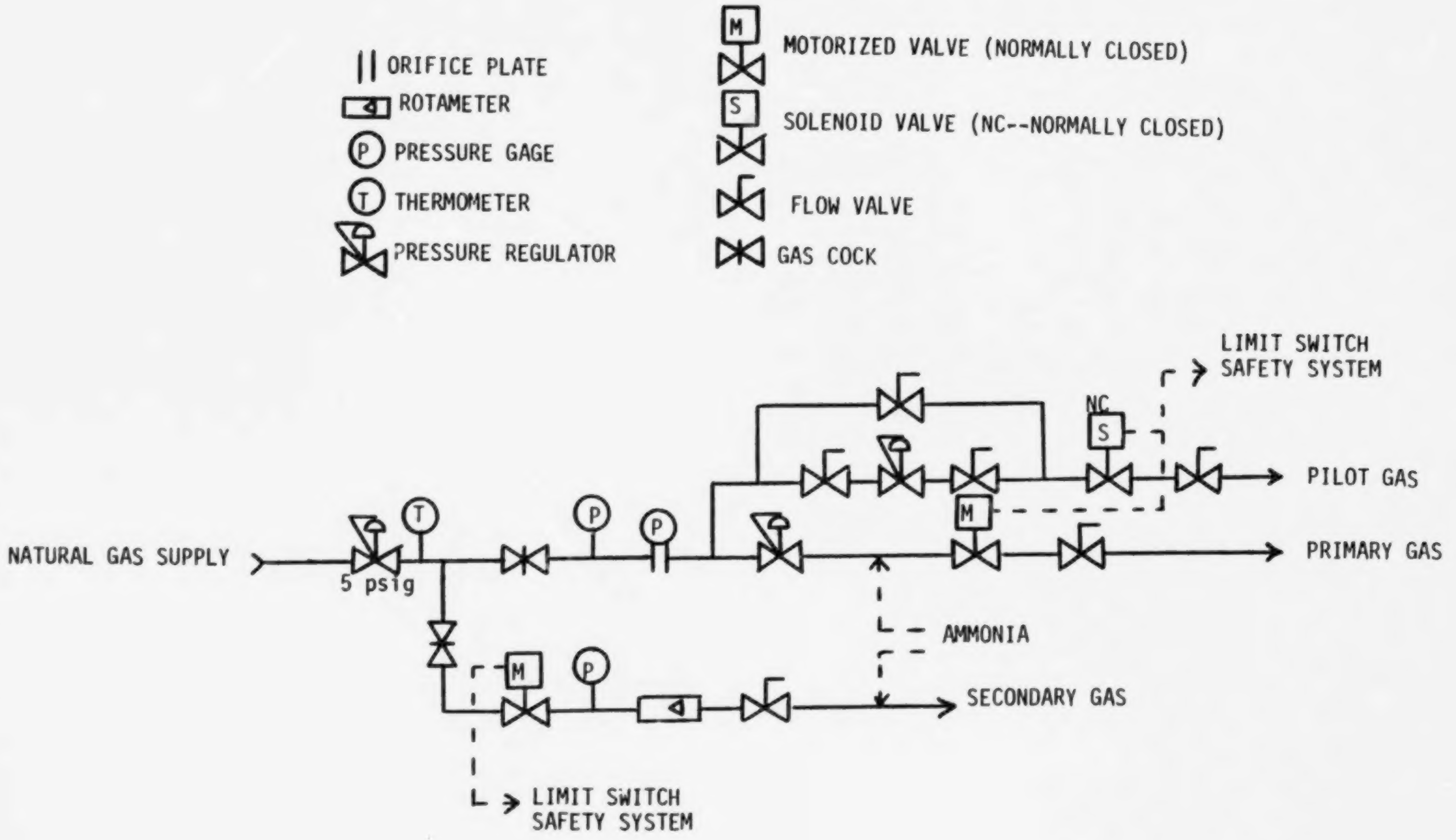
ORIFICE PLATE
ROTAMETER
PRESSURE GAGE
THERMOMETER
PRESSURE REGULATOR
M
MOTORIZED VALVE (NORMALLY CLOSED)
S
SOLENOID VALVE (NC--NORMALLY CLOSED)
FLOW VALVE
GAS COCK
LIMIT SWITCH
SAFETY SYSTEM
NC
S
PILOT GAS
NATURAL GAS SUPPLY
T
P
P
M
PRIMARY GAS
5 psig
AMMONIA
M
P
SECONDARY GAS
LIMIT SWITCH
SAFETY SYSTEM

Figure 2-5: Natural Gas Supply System Diagram

TABLE 2-1. FUEL ANALYSES

(a) Natural Gas

Analysis	Natural Gas
Heating Value (Btu/cubic ft, @ 60°F, 14.73 psia)	1031.6
(Btu/lb_f)	23,563
(kW-hr/kgf)	15.2
Encal Chromatograph Analysis (mol %)	
Nitrogen	0.35563
Carbon dioxide	0.91649
Methane	96.11870
Ethane	1.85666
Propane	0.38608
I-Butane	0.09849
N-Butane	0.10139
I-Pentane	0.04272
N-Pentane	0.02865
Hexanes Plus	0.09515
Specific Gravity (@ 60°F, 14.73 psia)	0.5848
Theoretical Air (mole air/mole fuel)	9.69
(lb_a/lb_f)	16.6
(lb_a/10,000 Btu)	7.04
(kga/kw-hr)	1.09

TABLE 2-1. FUEL ANALYSES
(continued)

(b) Fuel Oils

Analysis	Distillate Oil	Heavy Oil
Heating Value--Btu/lb$_f$ (kW-hr/kgf)		
Gross	19,382 (12.5)	18,734 (12.1)
Net	18,177 (11.7)	17,642 (11.4)
Ultimate Analysis (wt. %)		
Carbon	86.44	87.12
Hydrogen	13.21	11.97
Nitrogen	0.01	0.14
Sulfur	0.22	0.84
Ash	<0.01	0.02
Viscosity (cs)		
@ 100°F	2.58	26.76
@ 40°C	2.47	24.81
@ 210°F	1.08	4.68
@ 100°C	1.06	4.63
Density (g/cm^3)		
@ 100°F	0.8433	0.9213
@ 40°C	0.8417	0.9200
@ 210°F	0.8010	0.8813
@ 100°C	0.8001	0.8806
API Gravity (@ 60°F)	33.2	19.6
Cetane Index	43.0	(a)
Ramsbottom Carbon Residue (%)	--	4.87
Ramsbottom Carbon Residue on 10% Residuum (%)	0.22	--

TABLE 2-1. FUEL ANALYSES
(continued)

(b) Fuel Oils

Analysis	Distillate Oil		Heavy Oil	
Distillation	°F	°C	°F	°C
Initial Boiling Point	375	191	368	187
5%	414	213	440	227
10%	426	219	475	246
20%	451	233	521	272
30%	468	243	557	292
40%	485	252	579(b)	304(b)
50%	501	261		
60%	518	270		
70%	537	281		
80%	559	293		
90%	591	311		
95%	622	328		
End Point	633	334		
Recovery (%)	98.0			
Residue (%)	1.9			
Loss (%)	0.1			
Theoretical Air (lb_a/lb_f)	14.5		14.2	
(lb_a/10,000 Btu)	7.48		7.58	
(kga/kW-hr)	1.16		1.17	

---

[a] Cetane index is not possible on fuels which are not completely distillable
[b] Cracking at 39%

Figure 2-6 shows the primary fuel oil feed system. Two 38,000 l (10,000 gal) reservoirs supply distillate and heavy fuel oils to pumps, which continuously recirculate the oil back to the reservoirs. A portion of the recirculating flow is diverted to the PBS burner, via a second circulation pump, where it is filtered before passing through a heater (used on heavy oil only) and a flow totalizer. At the outlet of the flow totalizer, fuel can be drawn off for analysis. Two solenoid valves, controlled by the burner management/safety system, route the fuel oil either through a bypass line back to the burner pump inlet or to the fuel gun. The oil gun tip accepts a Sonicore air-atomizing fuel nozzle. Atomizing air, supplied by the house pressurized air system, is measured by a laminar flow element and inclined manometer.

Ammonia can be supplied to the precombustion chamber burner fuel or air flow to regulate primary NO_x concentration independent of other primary burner parameters. The supply system is shown in Figure 2-7. The ammonia flow, which is supplied from a cylinder regulated to nominal pressure of 10 psig, is controlled by a precision needle valve and monitored by a rotameter designed for ammonia service. For natural gas firing, ammonia is doped into the fuel line sufficiently upstream to ensure complete mixing prior to injection. For oil firing, ammonia is doped into the primary combustion air supply line.

A burner management/safety system built by the North American Manufacturing Company, is utilized to permit safe and consistent operation without operator attendance. The central feature of the system is a cam-driven programmer tied to an ultraviolet flame detector. Depending on which fuel is being fired, a series of safety interlocks must be made to initiate the starter sequence. These include initial and continuous checks on primary combustion air flow, atomizing air flow (oil firing only), Dowtherm temperature and flow, and water coolant flow (to burner head, transition

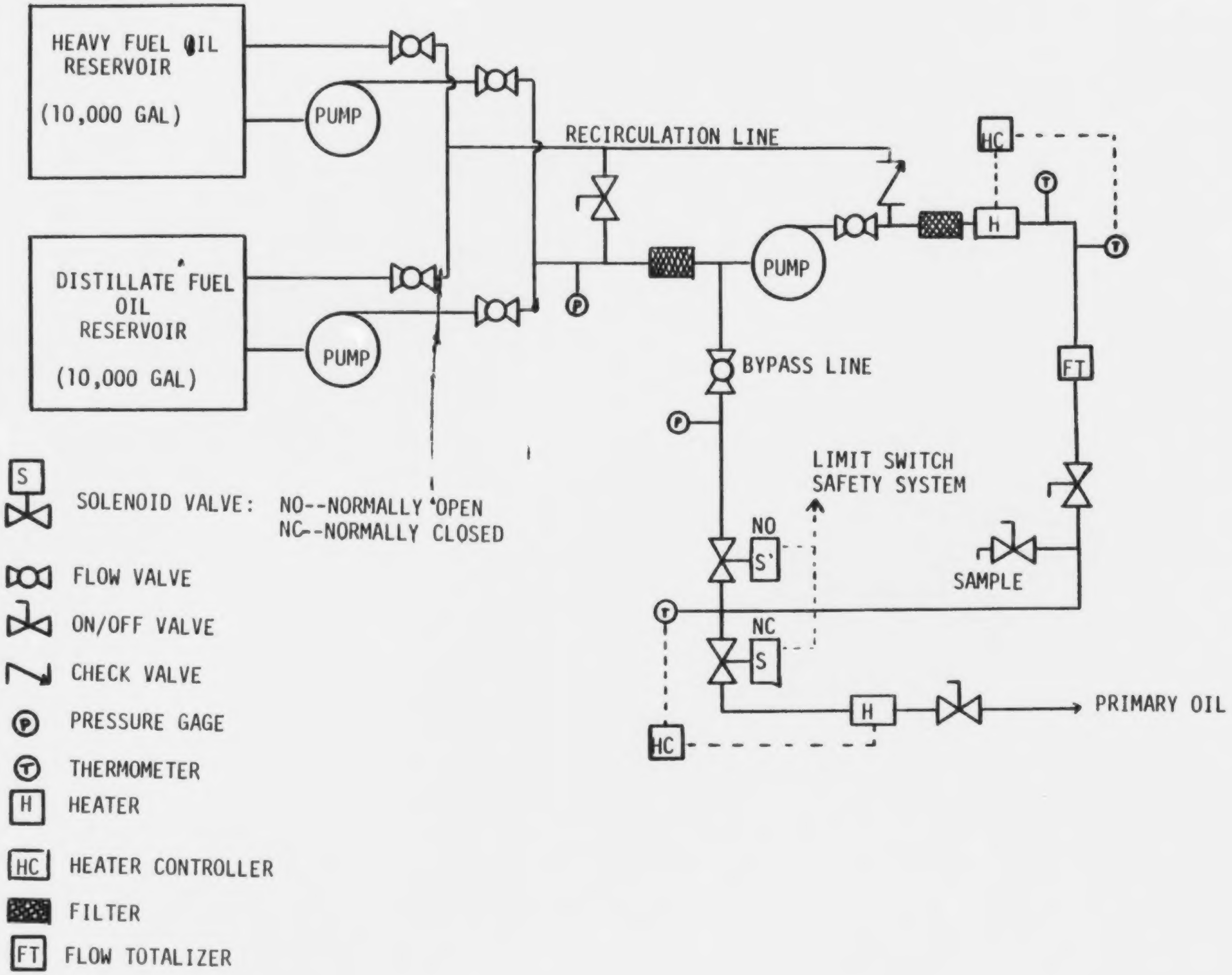
HEAVY FUEL OIL RESERVOIR
(10,000 GAL)
DISTILLATE FUEL OIL RESERVOIR
(10,000 GAL)
PUMP
PUMP
PUMP
RECIRCULATION LINE
BYPASS LINE
LIMIT SWITCH SAFETY SYSTEM
NO
NC
S'
S
HC
h
T
FT
SAMPLE
H
HC
PRIMARY OIL
S
SOLENOID VALVE: NO--NORMALLY OPEN
NC--NORMALLY CLOSED
FLOW VALVE
ON/OFF VALVE
CHECK VALVE
P PRESSURE GAGE
T THERMOMETER
H HEATER
HC HEATER CONTROLLER
FILTER
FT FLOW TOTALIZER

Figure 2-6: Fuel Oil Supply System Diagram

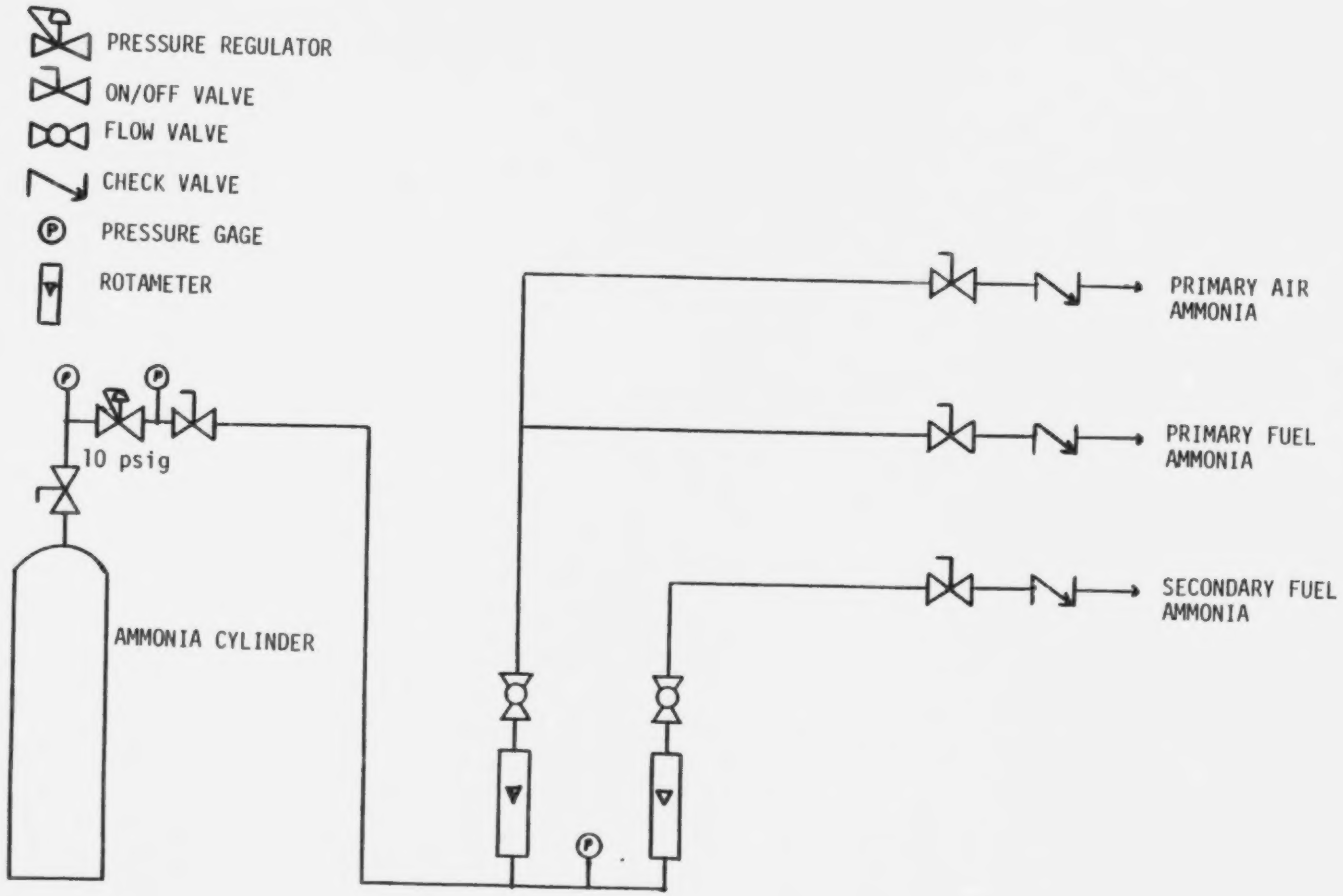
PRESSURE REGULATOR
ON/OFF VALVE
FLOW VALVE
CHECK VALVE
PRESSURE GAGE
ROTAMETER
10 psig
AMMONIA CYLINDER
PRIMARY AIR AMMONIA
PRIMARY FUEL AMMONIA
SECONDARY FUEL AMMONIA

Figure 2-7: Ammonia Supply System Diagram

section, and PBS end plate). A control system logic diagram is shown in Figure 2-8. With all interlocks made, the combustion air blower will prepurge the combustor for 1 minute. After this prepurge period, the pilot torch solenoid valve is actuated for 15 seconds, during which time the pilot torch is manually lit, inserted into the combustor, and detected by the UV flame detector. Then, the main fuel valves are automatically actuated. The pilot flame remains on for 5 seconds during which time the main flame must be lit. If it is not lit, the main fuel valves are de-energized and the combustor is purged for 30 seconds. A facility operation manual is located at the facility, as is a project safety manual.

The PBS stack contains both a thermocouple probe and a sampling probe. The sampling probe draws a sample through a porous metal filter, pulling from the entire cross-section of the stack. Stack gas analysis is performed by various analyzers, as discussed in Section 3.

2.2 REBURNING HARDWARE DESIGN AND MODIFICATION

To meet program objectives, the locations of reburn fuel injection and final air injection must be variable. The PBS (as with most commercial firetube package boilers) has a large opening at the end of the radiant section for maintenance access. It was decided to modify this access to insert concentric fuel and air booms down the firetube centerline. The original assembly that was used for natural gas reburning is shown in Figure 2-9. The telescoping booms are constructed of water-cooled stainless steel tubes. Radial spokes at the end of the fuel boom were designed with small ports directed circumferentially to distribute natural gas uniformly. These spokes are interchangeable with spokes of different hole pattern designs, or with caps for radial gas injection. The holes in the air boom were sized to

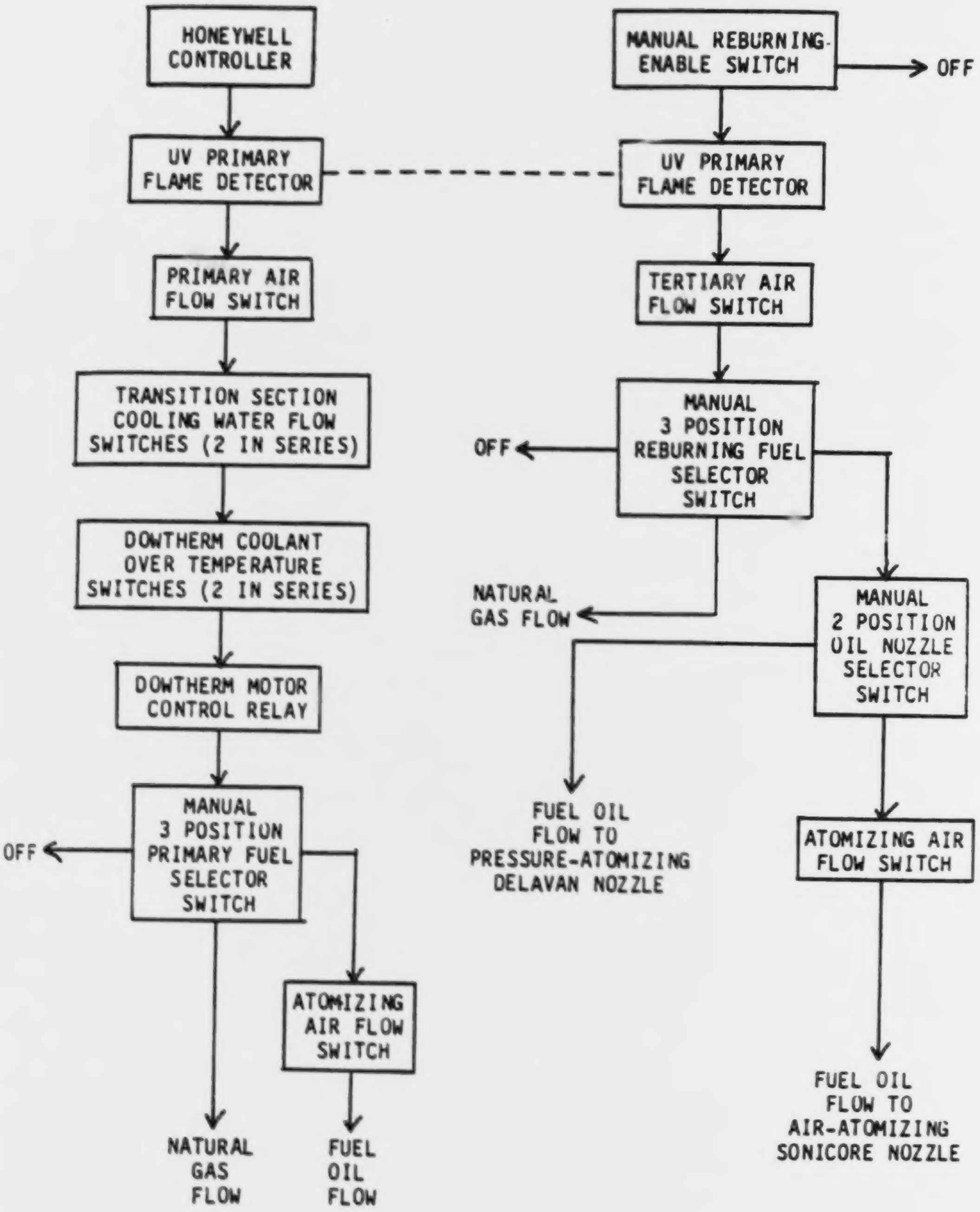
HONEYWELL CONTROLLER
UV PRIMARY FLAME DETECTOR
PRIMARY AIR FLOW SWITCH
TRANSITION SECTION COOLING WATER FLOW SWITCHES (2 IN SERIES)
DOWTHERM COOLANT OVER TEMPERATURE SWITCHES (2 IN SERIES)
DOWTHERM MOTOR CONTROL RELAY
MANUAL 3 POSITION PRIMARY FUEL SELECTOR SWITCH
OFF
ATOMIZING AIR FLOW SWITCH
NATURAL GAS FLOW
FUEL OIL FLOW
MANUAL REBURNING ENABLE SWITCH
OFF
UV PRIMARY FLAME DETECTOR
TERTIARY AIR FLOW SWITCH
MANUAL 3 POSITION REBURNING FUEL SELECTOR SWITCH
OFF
NATURAL GAS FLOW
MANUAL 2 POSITION OIL NOZZLE SELECTOR SWITCH
FUEL OIL FLOW TO PRESSURE-ATOMIZING DELAVAN NOZZLE
ATOMIZING AIR FLOW SWITCH
FUEL OIL FLOW TO AIR-ATOMIZING SONICORE NOZZLE

Figure 2-8: Burner Management System Logic Diagram

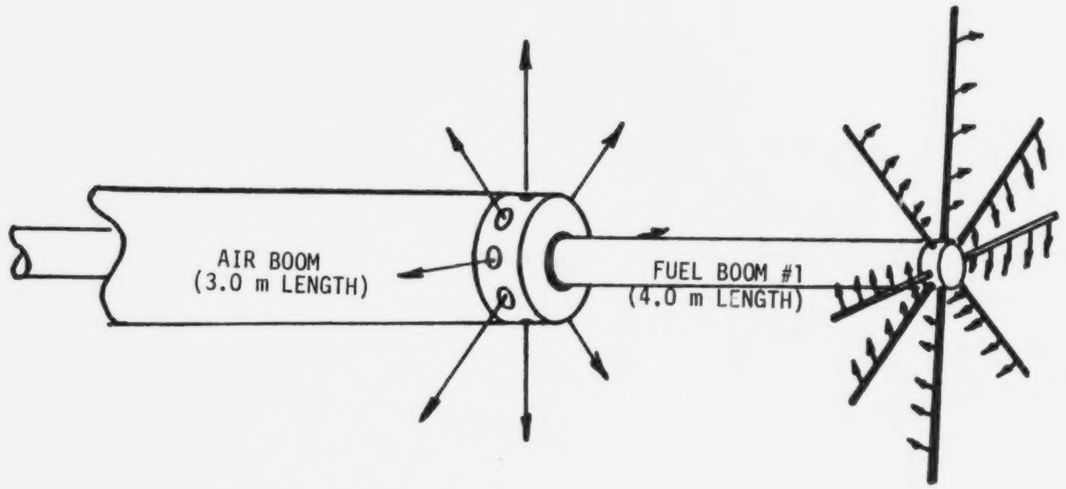
AIR BOOM
(3.0 m LENGTH)
FUEL BOOM #1
(4.0 m LENGTH)

Figure 2-9: Reburn Fuel and Air Booms

produce an injection velocity that ensures good mixing of the final air with the reburn zone effluent and prevents air impingement on the walls of the firetube.

A second generation fuel injection boom is shown in Figure 2-10(a). This water-cooled fuel boom is constructed to slide within the air boom in the same manner as the first fuel boom. The major difference between the two booms is the replacement of the spoked head with a threaded end that accepts various natural gas and fuel oil nozzles. For natural gas reburning, nozzles with eight radially oriented holes were designed. For fuel oil reburning, Delavan pressure-atomizing and Sonicore air-atomizing nozzles were used to inject fuel countercurrent to the combustion gas flow. A third generation water-cooled fuel boom was constructed for side-port insertion into the boiler, as shown in Figure 2-10(b). This boom allows secondary fuel to be injected in the same direction as the combustion gas stream.

The natural gas secondary fuel supply is tapped from the house natural gas supply system, as was shown in Figure 2-5. The fuel flow is metered by a rotameter designed for natural gas service. Ammonia can be doped into the secondary natural gas to simulate fuel-bound nitrogen. This flow is metered, as shown in Figure 2-7.

The secondary fuel oil supply system, shown in Figure 2-11, is separate from the house oil system. A variable speed, positive displacement metering pump circulates the fuel oil. A 208 l (55 gal) drum is used as a fuel oil reservoir. To simulate fuel-bound nitrogen, pyridine (C_5H_5N), or other liquid dopants, can be mixed with the fuel oil in the reservoir prior to testing. Temperature-controlled band drum heaters are used for heavy fuel oil reburning. The insulated fuel oil lines have heat tracing that is controlled manually by a variable voltage device.

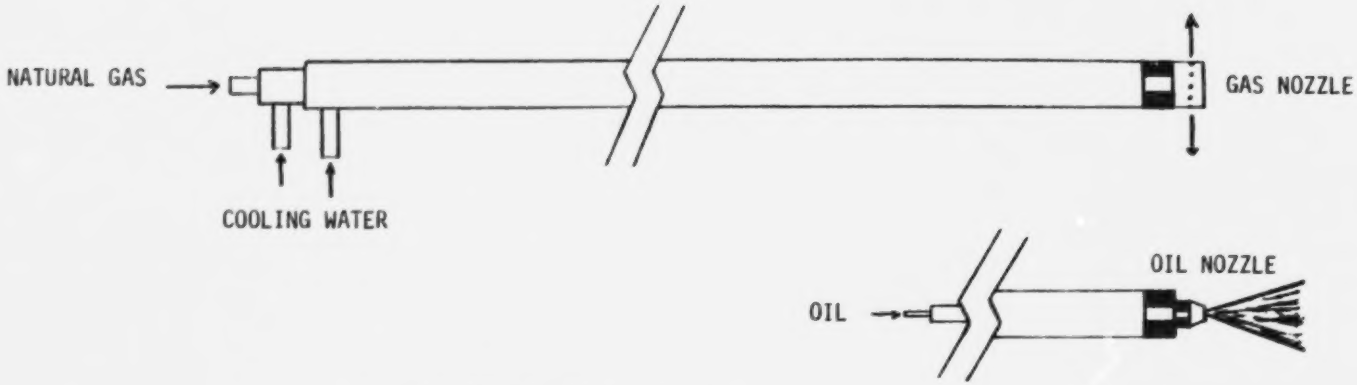
NATURAL GAS
GAS NOZZLE
COOLING WATER
OIL NOZZLE
OIL

(a) Fuel Boom #2 (5.0 m length)

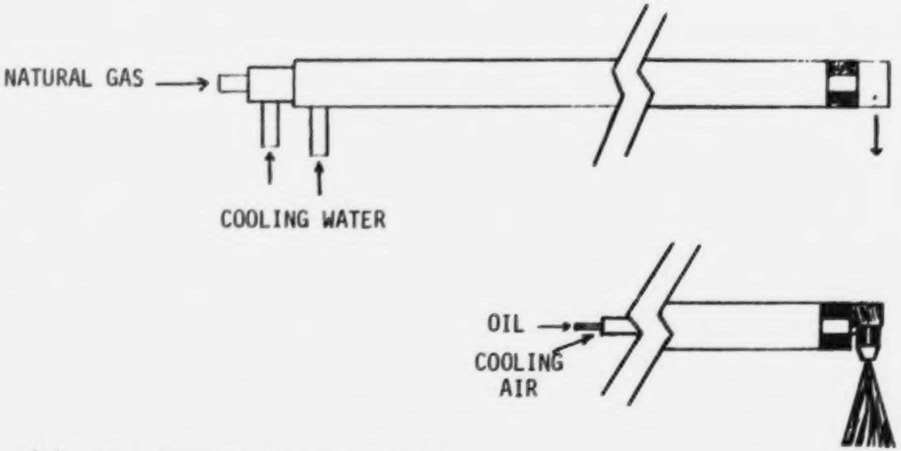
NATURAL GAS
COOLING WATER
OIL
COOLING AIR

(b) Fuel Boom #3 (1.0 m length)

Figure 2-10: Second and Third Generation Fuel Booms

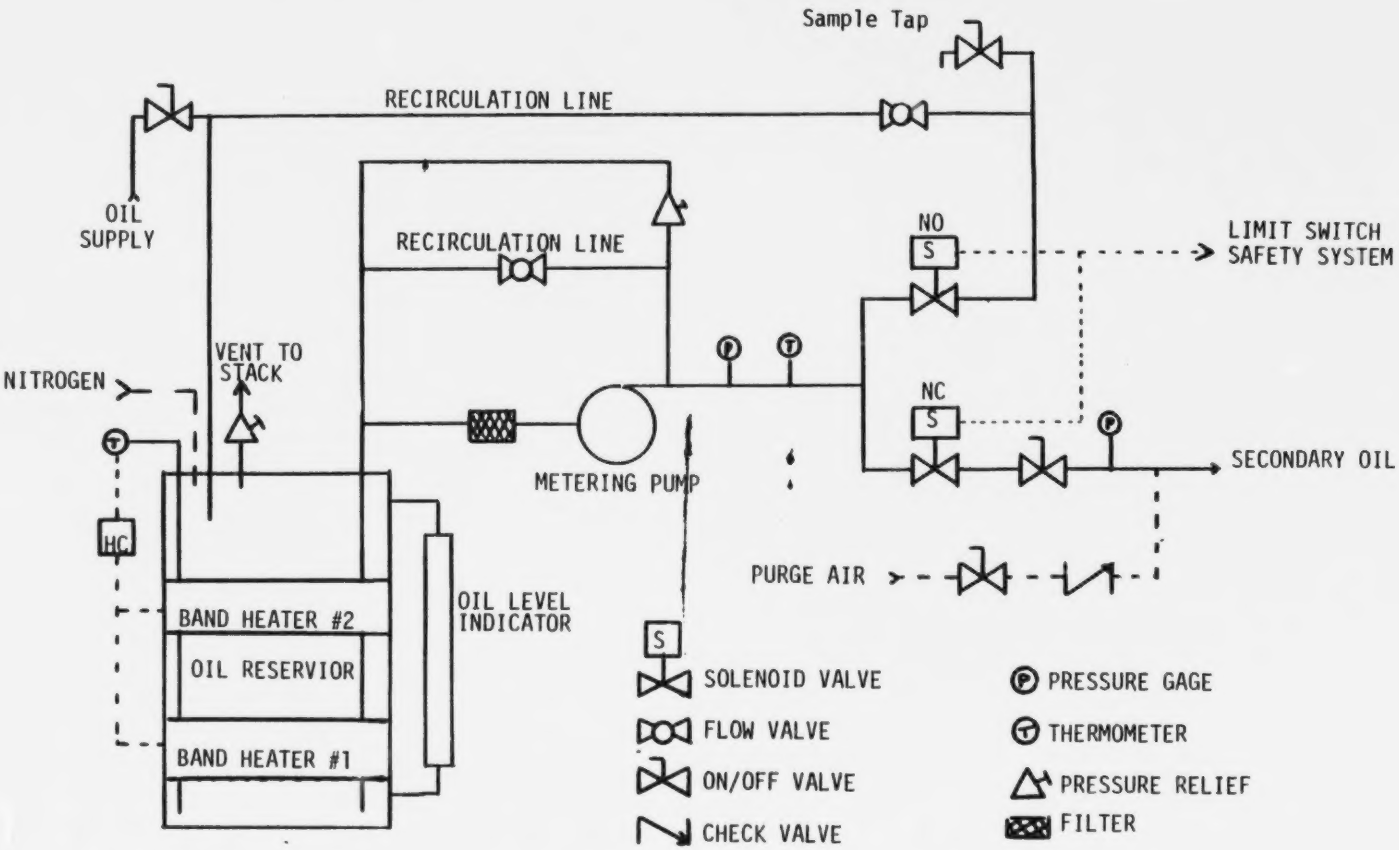
Sample Tap
RECIRCULATION LINE
OIL SUPPLY
RECIRCULATION LINE
NO
S
LIMIT SWITCH SAFETY SYSTEM
NC
S
SECONDARY OIL
NITROGEN
VENT TO STACK
METERING PUMP
PURGE AIR
HC
BAND HEATER #2
OIL RESERVIOR
BAND HEATER #1
OIL LEVEL INDICATOR
S
SOLENOID VALVE
FLOW VALVE
ON/OFF VALVE
CHECK VALVE
P PRESSURE GAGE
T THERMOMETER
PRESSURE RELIEF
FILTER

Figure 2-11: Secondary Fuel Oil Supply System Diagram

Final (burnout) combustion air is supplied by the house compressed air system, as was shown in Figure 2-4. The compressor output is regulated to a pressure of approximately 100 psig. The air flow is measured by a venturi meter with a U-tube manometer.

Reburn control/safety system modifications to the primary burner management/safety system are shown in Figure 2-8. The system provides for automatic shutdown in the event of a safety system upset. The facility operation and safety manuals [13,14] have been modified to include the new operating procedures and safety considerations.

To allow for the insertion of the reburning fuel and air booms and in-flame test probes (as described in Section 3), the 90 degree elbow section at the end of the PBS radiant section was modified. It was essentially converted from an elbow to a "tee" by the addition of a 0.60 M (2.0 ft) diameter steel extension of the firetube. The extension is cooled by an external copper coil connected to the municipal water supply. The end of the extension is flanged and studded to accept the new endplate, shown in Figure 2-12. The endplate is made of steel and is insulated inside with Fiberfrax® refractory board. A centerline port provides access for the reburning booms while the three smaller ports, located at 13.3, 18.4 and 23.5 cm (5.25, 7.25 and 9.25 in.), accept any of several in-flame test probes.

2.3 NORTH AMERICAN BOILER

A North American scotch-type package boiler, located next to the PBS facility at the EPA research laboratory, was used to verify PBS experimental results in an environment more representative of general industrial application. As shown in Figure 2-13, it is a three-pass, full wet-back boiler with a continuous service rating of 1089 kg (2400 lb) of steam per hour. The North American swirl burner can fire gas, distillate oil, or

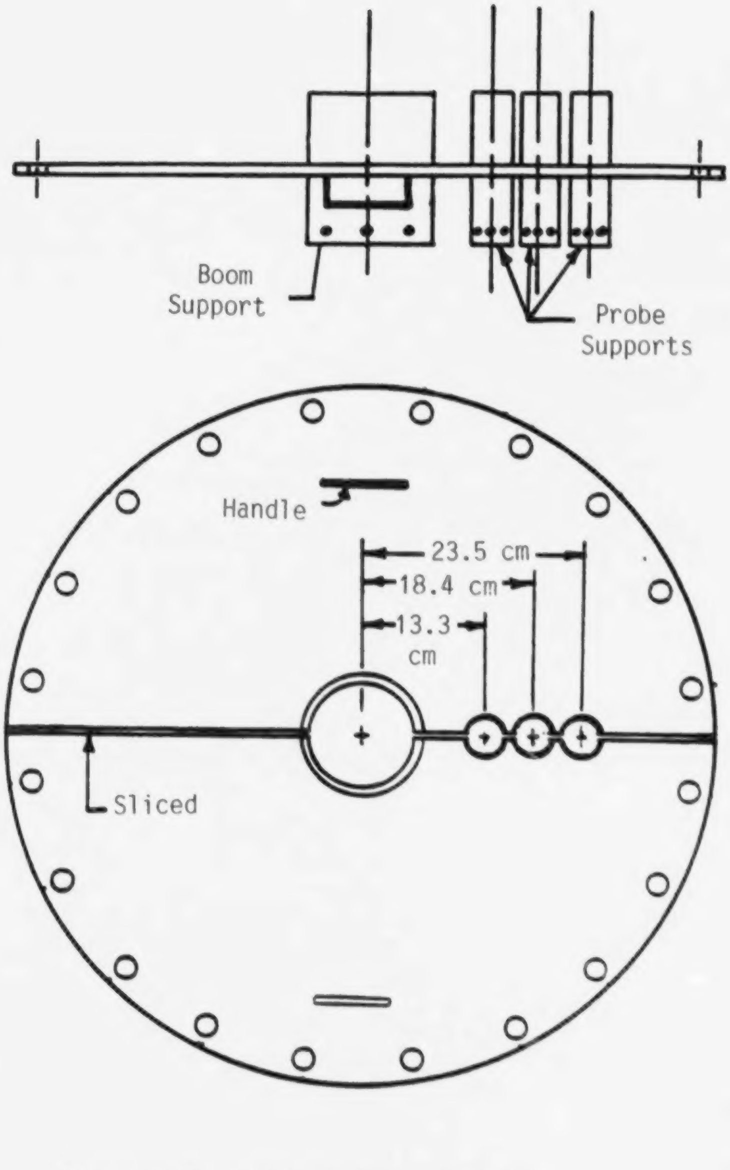
Boom Support
Probe Supports
Handle
23.5 cm
18.4 cm
13.3 cm
Sliced

Figure 2-12: Modified Boiler Endplate

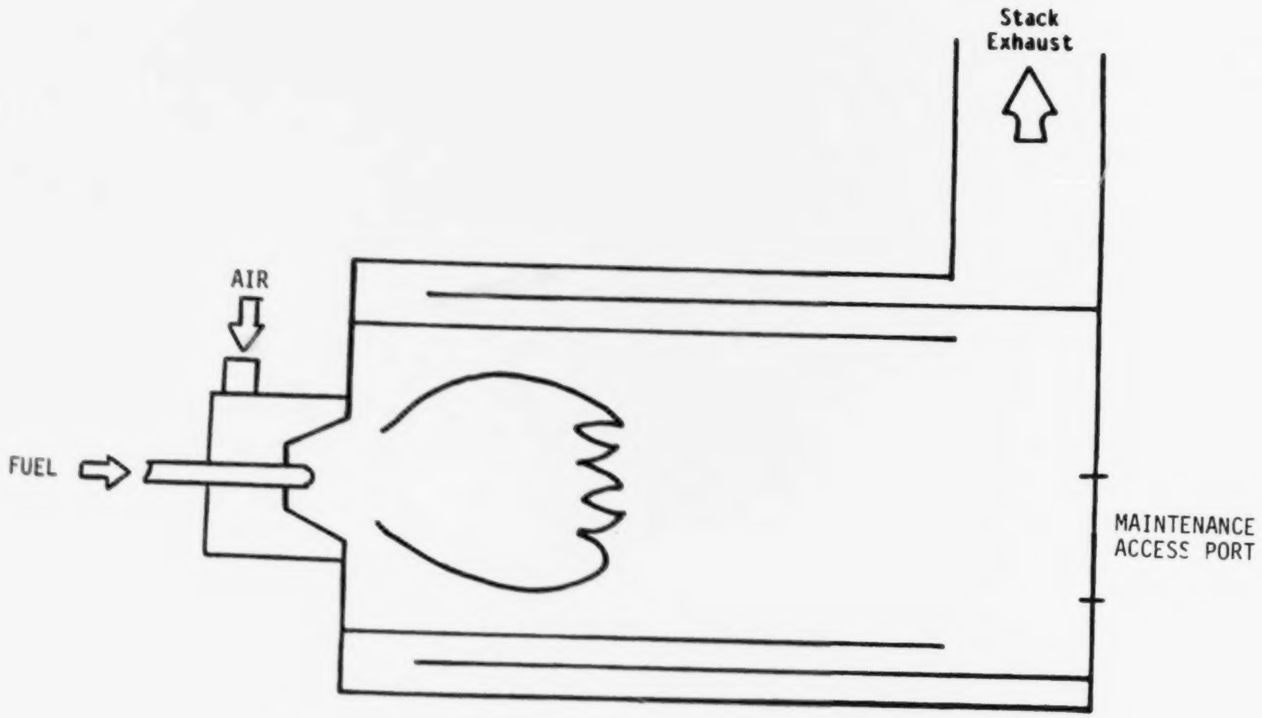
Stack
Exhaust
AIR
FUEL
MAINTENANCE
ACCESS PORT

Figure 2-13: North American Boiler

residual oil at a maximum firing rate of 0.73 MW (2.5 x 10^6 Btu/hr). The mechanical linkage for automatic control of air/fuel ratio with variation in load was disconnected. It is replaced with a manual adjustment that permits independent control of primary flame excess air at any desired load. The access plate on the boiler back wall was replaced with a plate containing ports for reburning boom insertion. Since the PBS is very near this facility, the same reburning fuel/air booms and supply systems were used on both.

SECTION 3

EXPERIMENTAL METHODS

To fulfill the reburning program objectives stated in Section 1.4, it was necessary to fabricate hardware, gather instrumentation and other equipment, and design experimental procedures to collect test data to monitor process parameters and operating conditions. Data measurements included the determination of: (1) radial and axial temperature profiles in the boiler radiant section; (2) radial and axial velocity profiles in the boiler radiant section; (3) stack gas chemical composition; and (4) radial and axial chemical composition throughout the boiler radiant section. These measurements were made as described below. A Quality Assurance/Quality Control (QA/QC) plan was prepared under this contract to establish data quality goals. A discussion of the data quality appears in Appendix A.

3.1 TEMPERATURE MEASUREMENT

Two suction pyrometers were designed for in-flame temperature measurement in the PBS: a 3.0 m (10 ft) long probe for axial traverses and a 1.0 m (3.3 ft) long probe for radial traverses. The basic design of the suction pyrometers is shown in Figure 3-1. Platinum and platinum/13% rhodium 10 mil (0.254 mm diameter) thermocouple wire is fed through a two-hole alumina tube and welded to form an R-type thermocouple junction. The thermocouple is slipped inside a 0.635 cm (0.25 in.) diameter alumina tube with a closed end for radiation shielding. To complete the suction pyrometer, the shielded R-type thermocouple is slipped into a water-cooled probe assembly. The thermocouple tip extends 15 cm (6 in.) past the end of the water-cooled probe, inside a closed-end alumina nosepiece with a 0.635 cm (0.25 in.) hole near its tip (see Figure 3-1).

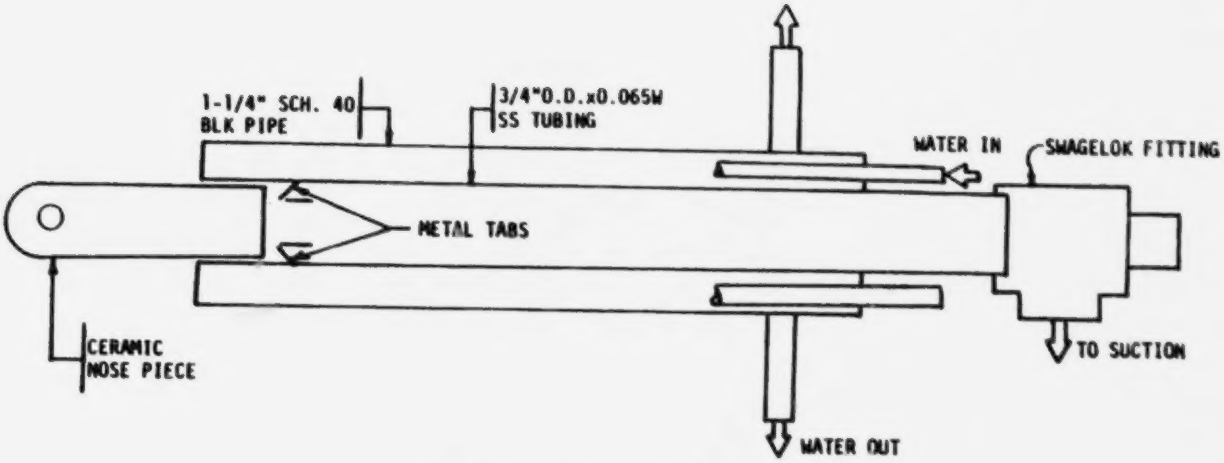
1-1/4" SCH. 40
BLK PIPE
3/4"O.D.x0.065W
SS TUBING
WATER IN
SWAGELOK FITTING
METAL TABS
CERAMIC
NOSE PIECE
TO SUCTION
WATER OUT

PART B- WATER COOLED PROBE ASSEMBLY

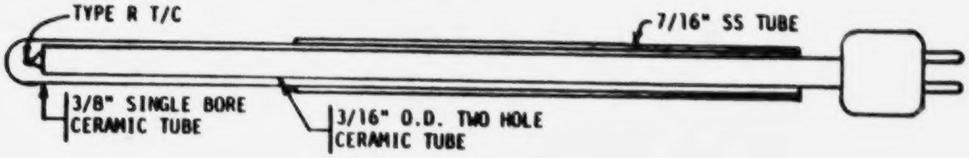
TYPE R T/C
7/16" SS TUBE
3/8" SINGLE BORE
CERAMIC TUBE
3/16" O.D. TWO HOLE
CERAMIC TUBE

PART A- SHIELDED THERMOCOUPLE

Figure 3-1: Suction Pyrometer

Suction for the pyrometer is provided by a carbon vane pump; the flow rate is monitored by a dry gas meter. The pump and meter are protected from moisture by an EPA Method 5 condensation train consisting of two impingers and a silica gel trap in an ice bath. Thermocouple output is read by an Omega Model 2166A digital thermometer.

When in operation, hot combustion gases are pulled at a high velocity through the nosepiece port and down the annulus between the nosepiece and the shielded thermocouple. As the gas flow rate across the shielded thermocouple increases, convective heat transfer to the thermocouple tip predominates radiative transfer to the cold boiler walls, and the actual gas temperature is approached. Figure 3-2 shows a suction pyrometer calibration curve, demonstrating that asymptotic operation (and, therefore, actual gas temperature indication) is achieved at suction flow rates exceeding 85 l/min (3.0 scfm). The pyrometer is operated at higher suction flow rates during the test program. As constructed, the pyrometer can measure a range of gas temperatures up to approximately 2000K (3140°F).

3.2 VELOCITY MEASUREMENT

Velocity measurements are made with a Prandtl probe, shown in Figure 3-3. The design of the probe is a copy of that used by the International Flame Research Foundation in IJmuiden, the Netherlands. The probe is water-cooled, with the exception of the stainless steel tip which allows any soot entering the stagnation pressure port to burn off. The static pressure line is attached to a thin cavity around which 8 pressure taps are drilled 3 probe diameters behind the tip.

Two Prandtl probes were constructed: a 2.5 m (8.3 ft) long probe for axial traverses and a probe with a 90 degree turn for radial traverses (shown in Figure 3-3). The 25 cm (10 in.) leg of the elbow-shaped probe is necessary

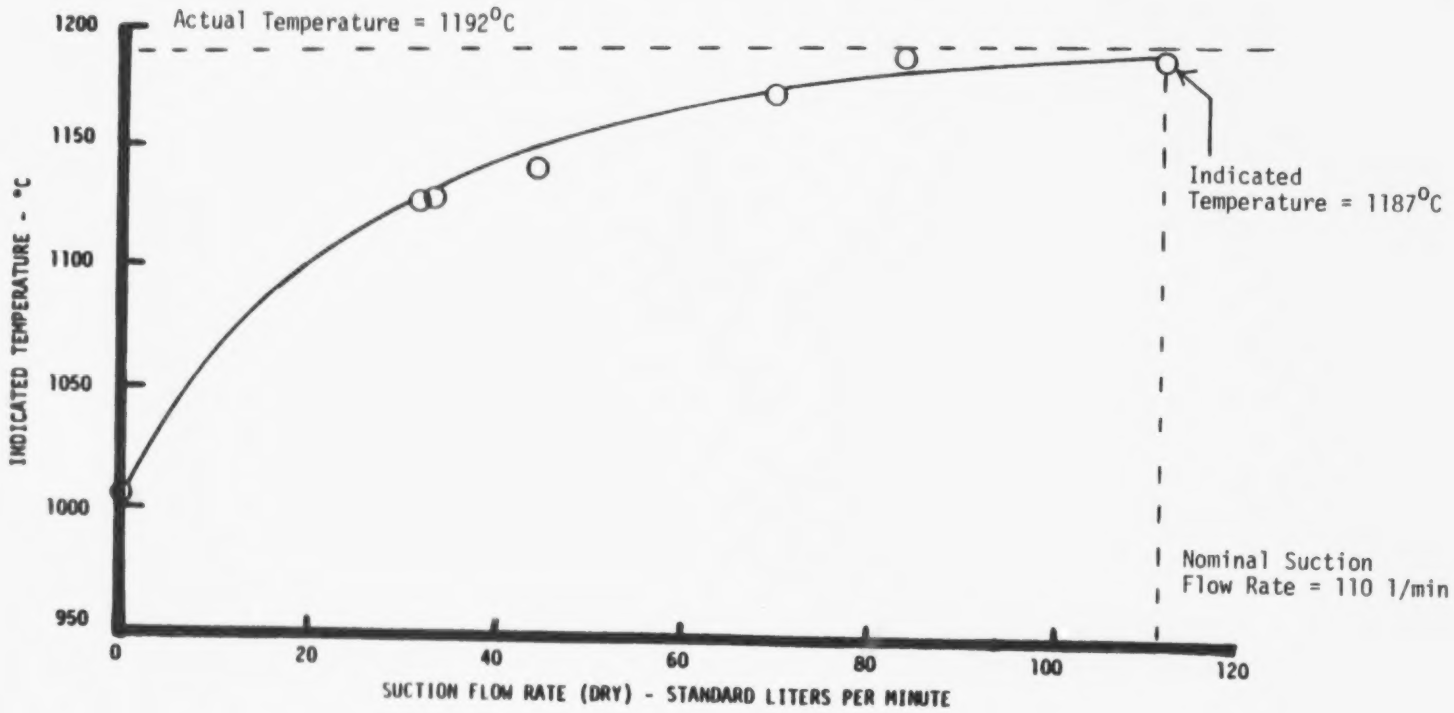

Figure 3-2: Temperature Measurement Calibration Curve

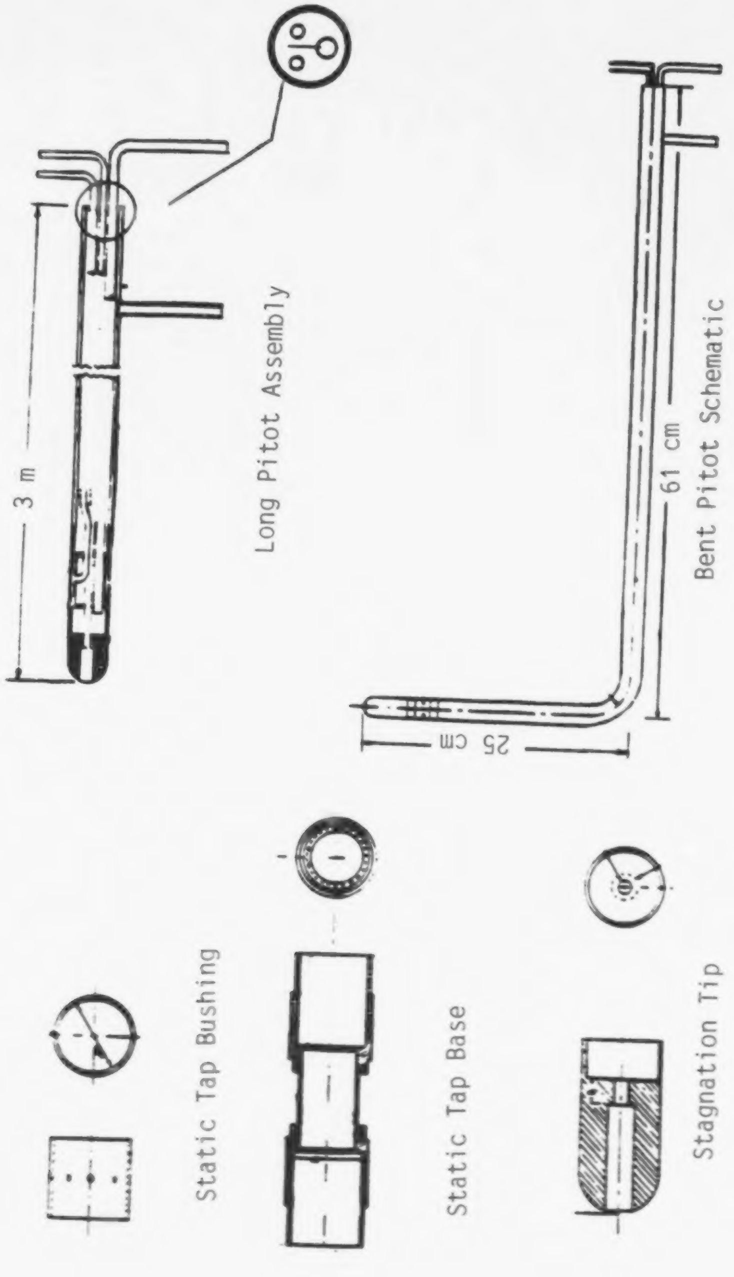
3 m
Long Pitot Assembly
61 cm
25 cm
Bent Pitot Schematic
Static Tap Bushing
Static Tap Base
Stagnation Tip

Figure 3-3: Prandtl Probe

to measure velocities and temperatures at the same axial location in the PBS. The temperature measurement ports are 25 cm (10 in.) upstream of the sight glass openings, through which the velocity probe is inserted. The Prandtl probe positioner, also shown in Figure 3-3, is bolted to the sightglass flange plate, allowing the probe to radially traverse the firetube by adjustment of a screw feed and counter.

To measure the small differential pressure between the stagnation and static ports in flows with a nominal velocity of 3 to 15 m/sec (10 to 50 fps), a high sensitivity pressure transducer/electronic manometer (Barocel Model 1173) system, made by Datametrics, was used. The system can detect pressure differentials ranging from 0.013 to 133 Pa (0.0001 to 1 torr). An analog meter indicates percent of full scale and a porportional electrical output from zero to 1000 volts DC is provided.

Significant pressure fluctuations caused by turbulence in the reacting flow make accurate velocity determination with the analog meter impossible. This problem is circumvented by sampling the electrical output with a microcomputer (Apple IIE) at an approximate rate of 15 Hz. The square root of each of 250 instantaneous readings is taken for each velocity measurement. With this technique, it is possible to obtain accurate measurements (with the mean and standard deviation repeatable to at least two significant digits) for boiler radiant section velocities greater than 3.0 m/sec (9.8 ft/sec). It is significant to note that the ratio of the standard deviation to the mean is often in excess of 50 percent, increasing with decreasing velocity. Dry air is used to purge the static and stagnation lines of moisture prior to each data reading. A check on the velocity measurement accuracy is made by making a complete radial traverse of the boiler and, assuming radial symmetry, integrating to obtain the total flow rate across the measurement plane (see

Figure 3-4). This flow is then compared to the measured input flow rate, with agreement typically within 10 percent.

3.3 STACK GAS SPECIATION MEASUREMENT

A schematic of the continuous emissions monitoring system (CEMS) is shown in Figure 3-5. The combustion gas sample is extracted through a porous metal filter inserted across the stack cross-section. Transported in stainless steel and teflon tubing, the sample gas passes through a Hankerson dryer and a particulate filter. The sample gas is then split such that a portion of the flow passes through a Dryrite® canister for further drying before going to the individual analyzers for oxygen, total unburned hydrocarbon, carbon dioxide, and carbon monoxide analyses. The rest of the sample goes directly to the NO_x analyzer, bypassing the NO_x absorbing Dryrite® material.

The NO_x meter is a Thermo-Electron Model 10A analyzer which operates via chemiluminescence. A small portion of the sample flow to the instrument is metered into a vacuum (reaction) chamber where it is allowed to come into contact with an excess of ozone from an integral ozonator. Nitric oxide (NO) and ozone (O_3) react to form N_2O, a portion (approximately 10% at room temperature) of which is elevated to an excited state. The excited molecules return to ground state and give off light of a characteristic frequency. This light is detected by a photomultiplier tube. The output is amplified and scaled to read directly in parts per million. High purity N_2 and a gas of known NO concentration are used to calibrate the instrument, whose range is zero to 10,000 ppm.

For the reburn tests, the NO_x analyzer is operated in the NO measurement mode. In this way, sample transport lines can be unheated. For the conditions sampled in the firetube package boiler, nearly all of the NO_x is in the form of NO. This is important since NO_2 is very soluble and NO in the presence of NO_2 will condense in water. When total NO_x measurements are

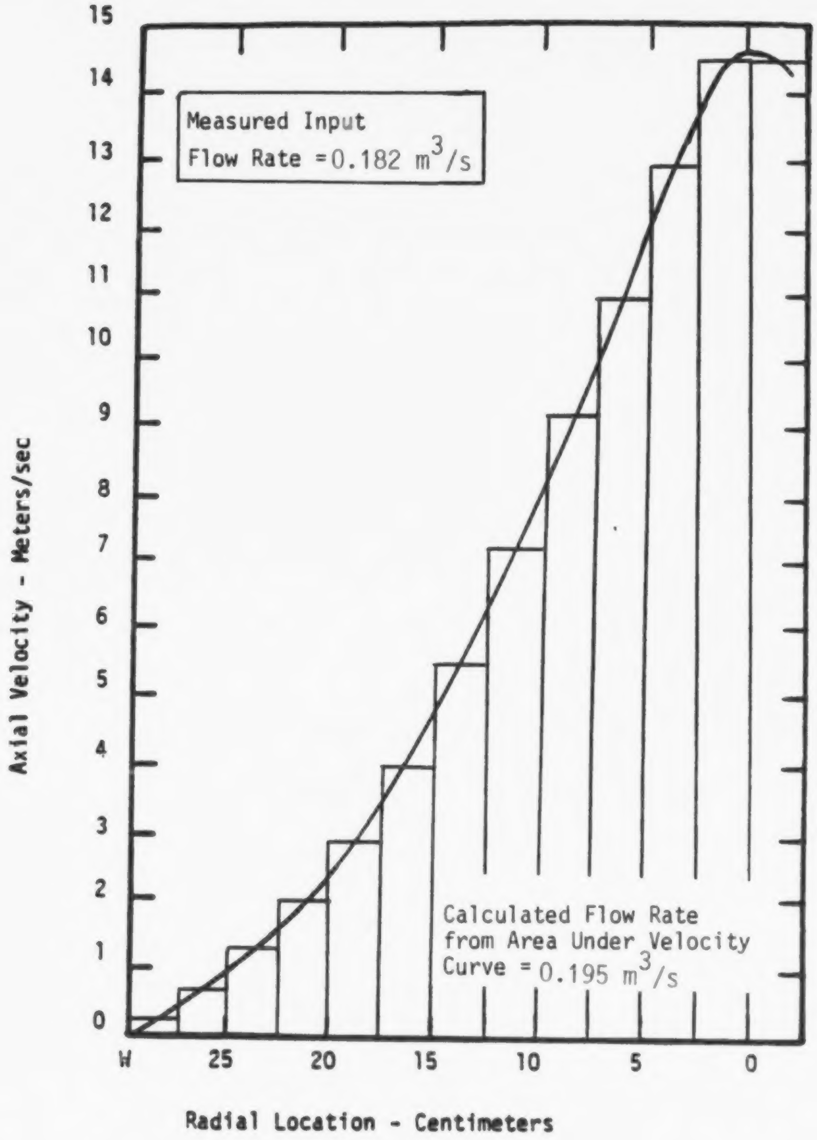

Figure 3-4: Velocity Measurement Calibration Curve

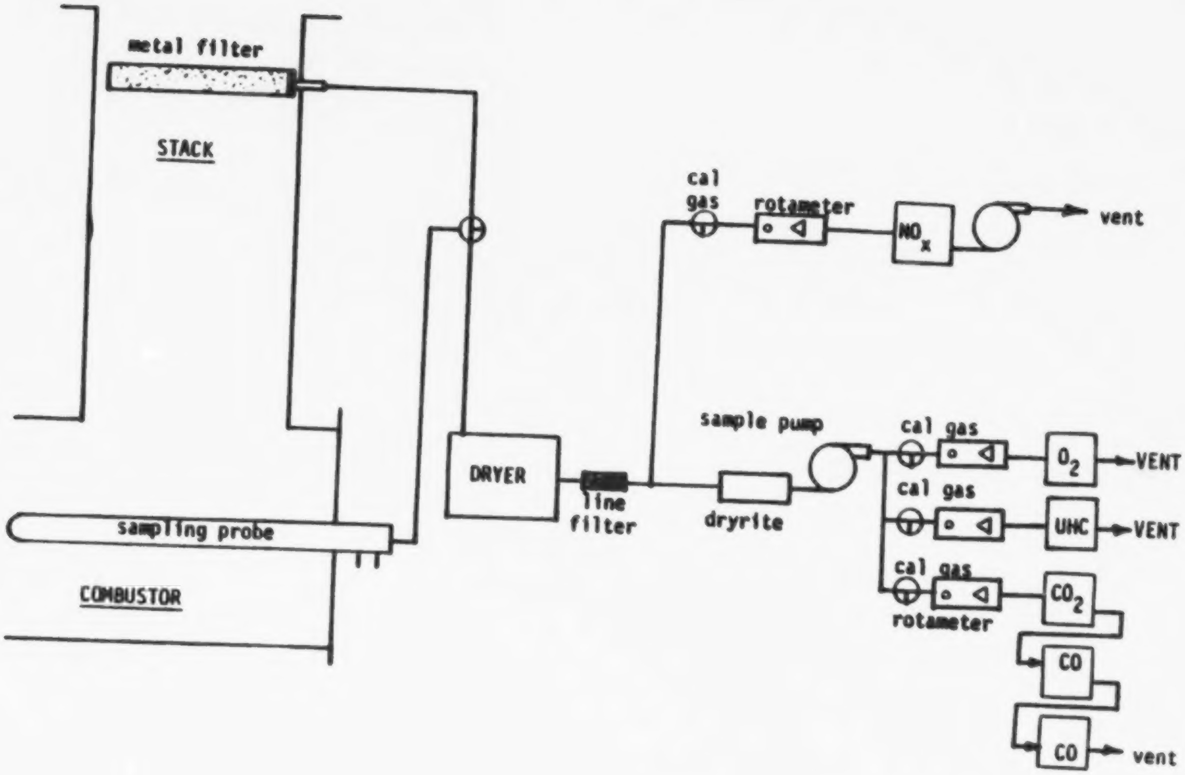
metal filter
STACK
cal gas
rotameter
NO$_x$
vent
sample pump
cal gas
O$_2$
VENT
DRYER
line filter
dryrite
cal gas
UHC
VENT
sampling probe
cal gas
CO$_2$
rotameter
COMBUSTOR
CO
CO
vent

Figure 3-5: Continous Emmissions Monitoring System (CEMS) Diagram

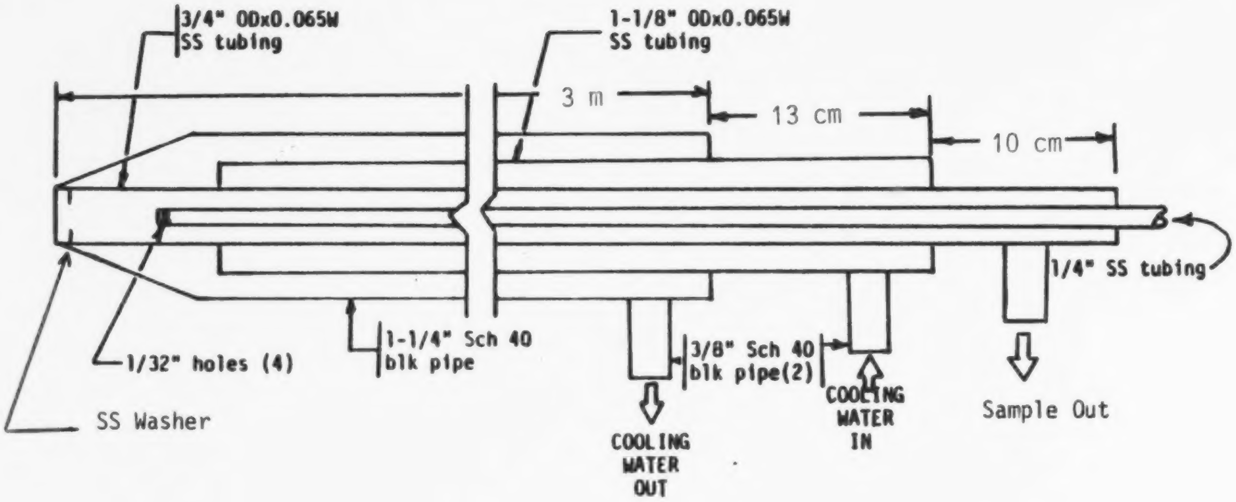
3/4" ODx0.065W SS tubing
1-1/8" ODx0.065W SS tubing
3 m
13 cm
10 cm
1/4" SS tubing
1-1/4" Sch 40 blk pipe
3/8" Sch 40 blk pipe(2)
1/32" holes (4)
SS Washer
COOLING WATER OUT
COOLING WATER IN
Sample Out

Figure 3-6: Combustion Gas Sample Probe

desired, wet samples are taken using a water-quench sample probe and SASS impinger bottles. These samples are analyzed on a Dionex System 14 ion chromatograph for NO_2 and NO_3. The exhaust gas from the sample train is analyzed for NO by the NO_x analyzer.

The O_2 meter is a Beckman Model F3 Oxygen Analyzer, which operates by utilizing the paramagnetic property of oxygen. Other gases present in significant concentration in the stack effluent do not exhibit this property. The instrument is calibrated with high purity N_2 and room air. Its measurement range is zero to 25 percent.

A Beckman Model 400 hydrocarbon analyzer, which uses a flame ionization detection method, is used to measure unburned total hydrocarbons on selected data points. The instrument range is zero to 50,000 ppm.

The CO_2 and CO monitors used are Beckman Series 864/865 Infrared Analyzers. They operate by directing identical infrared beams through a sample cell and a sealed reference cell. The difference between the strength of the beams, as measured by a detector at the opposite end of the cell, is proportional to the concentration of the target compound in the sample. Calibration is accomplished with a high purity N_2 gas and a known concentration sample of the target gas. The range of the CO_2 analyzer is zero to 20 percent. The range of the first of two CO monitors, used for stack gas measurement, is zero to 2000 ppm. The second CO monitor, used for in-flame measurements, has a range from zero to 5 percent.

3.4 IN-FLAME GAS SPECIATION MEASUREMENT

In-flame gas combustion samples are withdrawn with a 3.0 m (10 ft) sampling probe, shown in Figure 3-6. The probe is inserted into the PBS radiant section through one of the three boiler endplate ports. The probe is a water-cooled assembly with a stainless steel inner sample passage. A 0.63 cm (0.25 in.) diameter capped stainless steel tube is inserted down the probe centerline to inject a radial spray of deionized water at the sampling point. This spray quenches any continuing reactions in the sample gas at the sampling point.

For NO, O_2, CO_2, and CO measurements, the sample gas is transported directly to the CEMS, as described previously. The in-flame gas sample is also analyzed for hydrogen cyanide (HCN) and ammonia (NH_3). Both HCN and NH_3 are easily adsorbed by hot stainless steel surfaces; therefore, many probes used to collect these species are constructed of quartz. With the sample probe used in this study, however, HCN and NH_3 are condensed in the quench water spray, which cools the stainless steel lining quenching wall reactions.

HCN and NH_3 present in the sample gas are collected in solution with the sampling train shown in Figure 3-7. Vacuum and flow measurements are provided by a RAC Model 201091 "Staksamplr". The impinger bottle is initially filled with 500 ml of deionized water. At the start of the 5 minute sampling period, the sample flow and the water spray flow are begun simultaneously, at rates of 170 l/min and 200 ml/min, respectively. At the end of the sampling period, a 100 ml aliquot is transferred to a tinted glass sample jar containing 1 ml of 10 molar NaOH solution. The NaOH solution is added to stabilize the cyano and amine species in solution and to provide a proper ionic background strength for analysis.

The sample solutions are analyzed by specific ion electrode. A micro-processor, Orion Analyzer Model 901, gives a direct digital readout of target ion concentrations. The cyanide ion (CN^-) electrode, Orion Model 94-06, has a solid membrane tip in which inorganic silver compounds are bonded. When immersed in a cyanide solution, silver ions dissolve from the surface of the tip and are replaced by ions from within the membrane. This sets up a potential which is measured by the ionalyzer against a reference potential provided by an Orion Model 90-01 reference electrode. Calibration

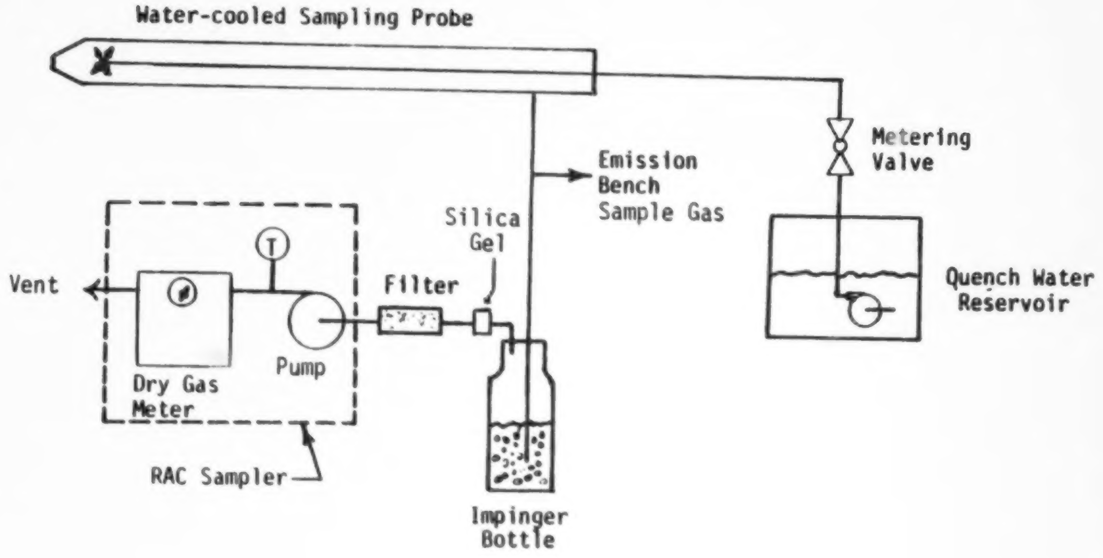
Water-cooled Sampling Probe
Metering Valve
Emission Bench Sample Gas
Silica Gel
Vent
Filter
Quench Water Reservoir
Dry Gas Meter
Pump
RAC Sampler
Impinger Bottle

Figure 3-7: Condensible Species Sample Train

is accomplished by the use of standard cyanide solutions of known concentration.

To measure the NH_3 concentration in the samples, an Orion Model 95-10 ammonia electrode with an internal reference element is used. The tip of the electrode has a hydrophobic, gas-permeable membrane which separates the electrode internal filling solution and the sample solution. Dissolved NH_3 diffuses through the membrane until the partial pressure of NH_3 on each side is the same. The NH_3 dissociates in the internal filling solution to the ammonia ion and the hydroxide ion. The potential difference between the internal filling solution and the internal reference element is proportional to NH_3 concentration in the solution. Calibration of the electrode is done with standard solutions of known NH_3 concentration.

The final in-flame gas constituent to be determined is nitrous oxide (N_2O), measured by gas chromatography. A Varian model 1400 gas chromatograph equipped with a ^{63}Ni electron capture detector (ecd) is used. Combustion gas samples are injected into a 3.66 m (12 ft) long stainless steel column packed with Porapak Q®. The packing material of the column separates the gaseous constituents and causes them to enter the ecd at different times, depending on their molecular weight. Nitrous oxide elutes approximately 4 minutes after injection (at the tail end of the CO_2 spike), for the system used in this study. Column and ecd temperatures are chosen to increase separation and enhance N_2O sensitivity. Calibration is done with standard gases of known N_2O concentration.

The gaseous emission monitor specifications are summarized in Table 3-1.

TABLE 3-1. GASEOUS EMISSION MONITOR SPECIFICATIONS

Gas	Sample Type	Instrument Type	Manufacturer/ Model	Range
O_2	Continuous	Paramagnetic	Beckman/F3	0 to 5, 10, 25%
CO_2	Continuous	Infrared	Beckman/864	0 to 5, 10, 20%
CO	Continuous	Infrared	Beckman/865	0 to 500, 1000, 2000 ppm
NO	Continuous	Chemiluminescence	Teco/10A	0 to 2.5, 10, 25, 100, 250, 1000, 2500, 10000 ppm
NO_2	Batch-wet	Ion Chromatograph	Dionex/System 14	1 to 1000 ppm
NO_3	Batch-wet	Ion Chromatograph	Dionex/System 14	1 to 1000 ppm
THC	Continuous	Flame ionization	Beckman/400	0 to 10, 100, 1000, 10000 ppm
NH_3	Batch-wet	Specific ion electrode	Orion/95-10	0.1 to 100 ppm
HCN	Batch-wet	Specific ion electrode	Orion/94-06	0.1 to 100 ppm
N_2O	Batch	Gas Chromatograph	Varian/1400	1 to 1000 ppm

SECTION 4

BASELINE TEST RESULTS

Baseline tests (conventional boiler operation) were performed at each test condition prior to reburning application. These tests included natural gas, distillate (#2) fuel oil, and heavy (#2 and residual mix) fuel oil fired in both the PBS and the North American boiler primary burners. By far, the bulk of data collected in this program were from tests performed on the PBS, operated with natural gas as the primary burner fuel. Detailed characterization of the PBS natural gas primary flame was made prior to the start of reburn testing. Baseline data from these tests are discussed in this section.

Characterization of the fuel oil primary flames in the PBS was less detailed than natural gas flame characterization, and is described in Section 5.1.6 with the reburning test results. Baseline test results from the North American boiler reburning application tests are described in Section 7.1.

In a typical reburning application, the boiler radiant section is divided into 3 zones: (1) primary combustion zone, (2) reburning zone and (3) burnout zone. This is shown in Figure 1-1. For the PBS tests, an additional zone, the precombustion chamber zone, is present. The four zones characteristic of PBS reburning tests are referred to as zone 1 through zone 4, with the designations used as subscripts to define zone parameters.

During baseline operation of the PBS, no reburning was applied, as shown in Figure 4-1. The purpose of the baseline tests was to characterize zones 1 (precombustion chamber zone) and 2 (primary zone) to establish: (1) an optimum SR_1 (stoichiometric ratio in zone 1) with a minimum NO; (2) a nominal axial location for secondary fuel injection; and (3) a secondary fuel injector design that would produce a uniform distribution of stoichiometry in the reburning zone.

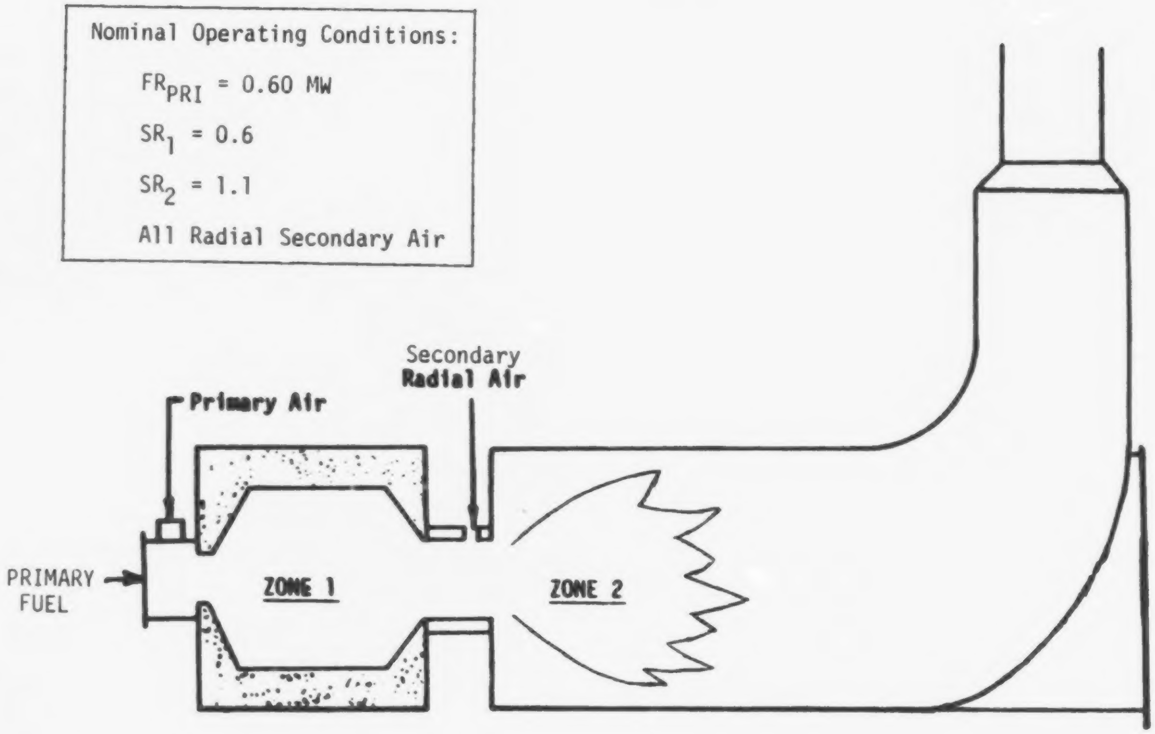
Secondary
Radial Air
Primary Air
PRIMARY
FUEL
ZONE 1
ZONE 2

Nominal Operating Conditions:

FR_{PRI} = 0.60 MW

SR_1 = 0.6

SR_2 = 1.1

All Radial Secondary Air

Figure 4-1: PBS Baseline Operation Schematic

To obtain fundamental insight into the reburning process (as described by program objectives defined in Section 1), it was decided, prior to the start of the experimental program, to hold primary load constant in the PBS. This would ensure that constant aerodynamic, thermal, and chemical properties would be maintained at the entrance to the reburning zone. Therefore, the primary burner firing rate (FR_{PRI}) was held constant at 0.60 MW (2.0×10^6 Btu/hr) during baseline testing. For the PBS reburning tests described in Sections 5 and 6, FR_{PRI} was held constant, and FR_{TOT} was allowed to vary.

The PBS primary burner is operated continuously to minimize daily warmup time. From a cold start, 24 hours are required to achieve sufficient thermal equilibrium and good data repeatability (as defined by QAQC goals).

4.1 PRECOMBUSTION CHAMBER ZONE CHARACTERIZATION

Baseline tests were performed to determine the influence of the precombustion chamber zone (zone 1) stoichiometry (SR_1) on stack NO (NO_{EX}) concentration, while holding primary zone (zone 2) stoichiometry (SR_2) constant at 10 percent excess air (EA). Both natural gas and ammonia -doped natural gas were fired. Figure 4-2 shows that for firing with both natural gas and natural gas doped with 0.75 percent (by weight) NH_3, NO_{EX} has a clear minimum at an SR_1 of approximately 0.70. Note that at the minimum, NO_{EX} is relatively insensitive to fuel nitrogen content. This feature, characteristic of this low-NO_x burner design [13], is shown in Figure 4-3 as well.

Two parameters considered important to choosing an operating SR_1 for the reburning tests were precombustion chamber temperature and primary NO_x variability. To prolong the life of the burner refractory, it was desirable to define a burner operating condition with a precombustion chamber temperature of less than 1920K (3000°F). Bare tip thermocouple measurements provide a good estimate of actual burner temperatures since the inner

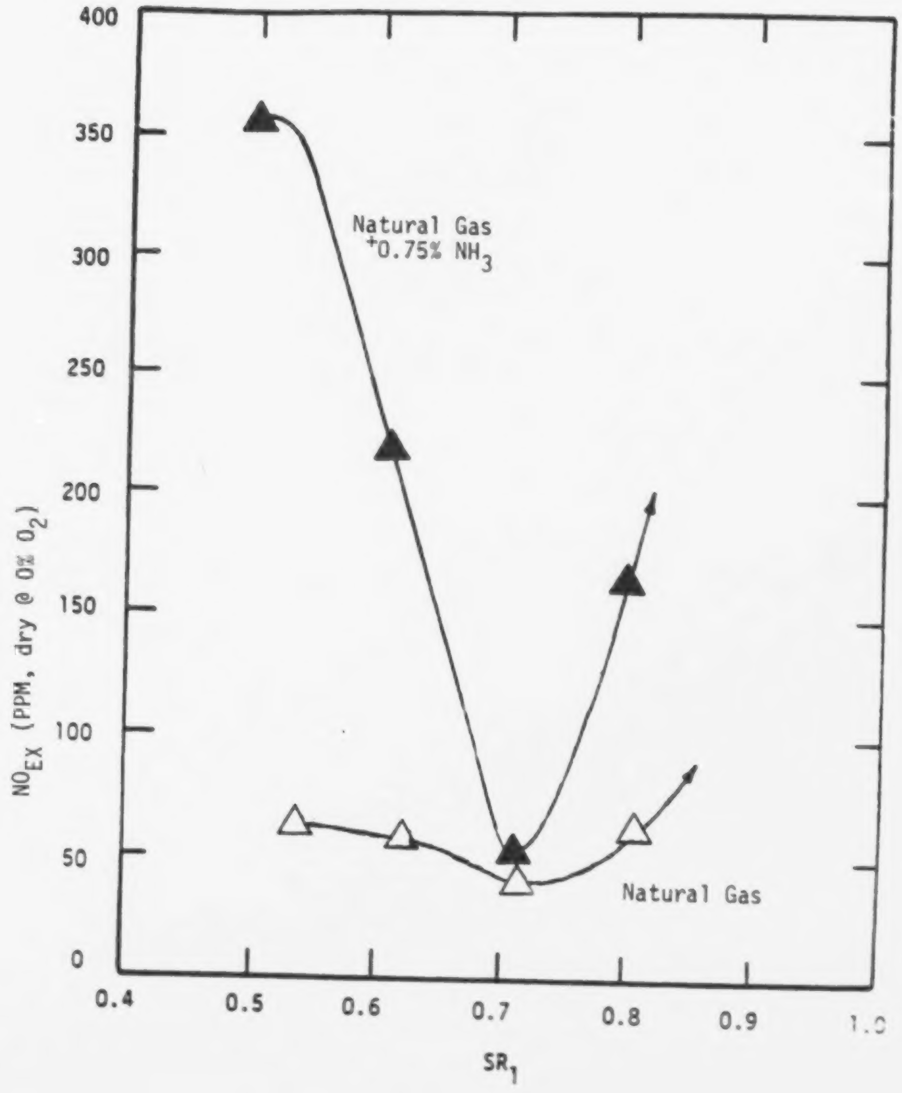

Figure 4-2: Baseline NO_{EX} Versus SR_1

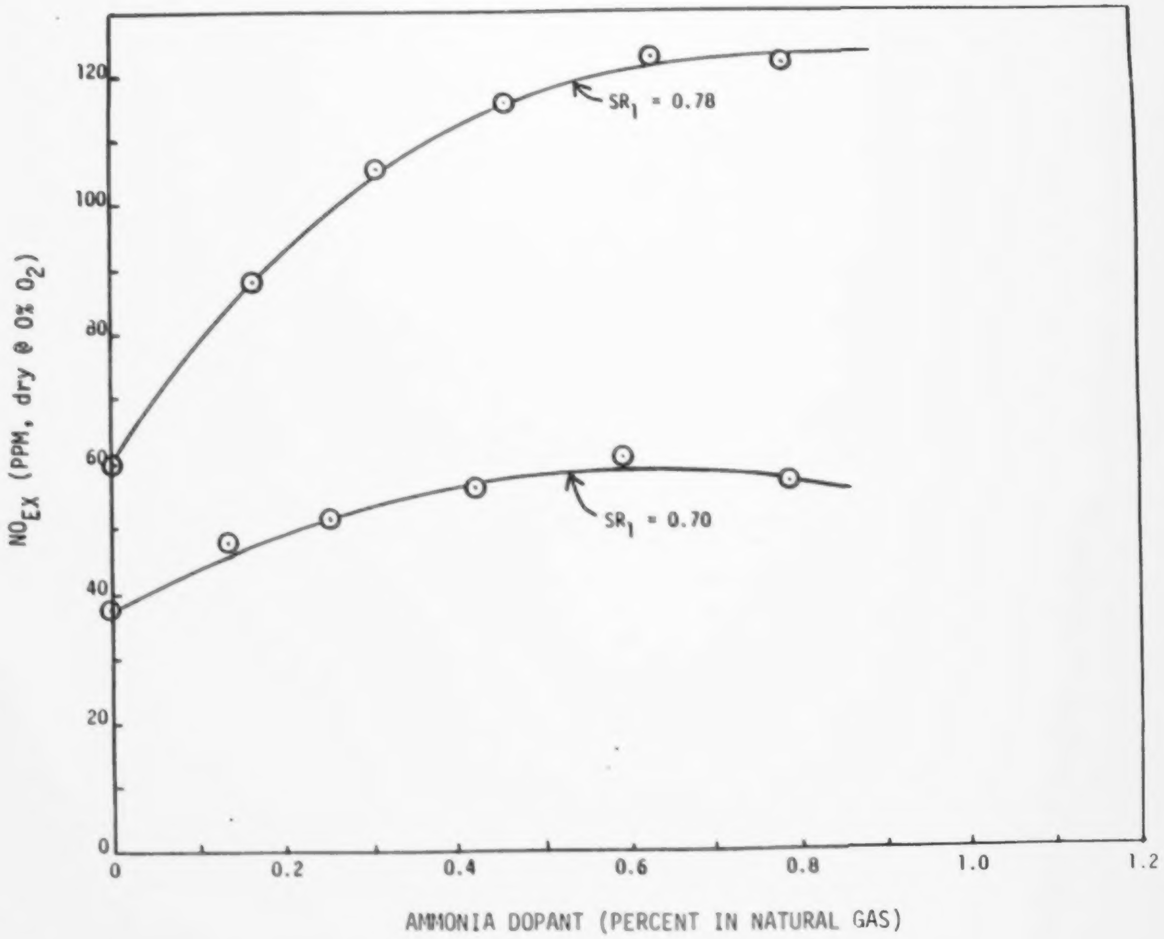

Figure 4-3: Baseline NO_{EX} Versus Percent Ammonia Dopant in Fuel

refractory wall is nearly the same temperature as the combustion gas. These measurements demonstrate zone 1 to be nearly adiabatic, with temperatures approaching adiabatic flame temperatures to within 38°C (100°F). Based on the adiabatic flame temperature calculations for methane/air combustion (presented in Figure 1-2), an SR_1 of less than 0.68 or greater than 1.32 is required to ensure burner temperatures of less than 1920K.

As stated in Section 1, it is desired to investigate reburning under conditions of low primary NO_x concentration. To achieve an operating range of 50 to 200 ppm (dry, at zero percent O_2), an SR_1 of 0.64 was chosen as a nominal operating condition. Operating on the rich side of the optimum SR_1 results in lower precombustion chamber temperatures than operating on the lean side, thus extending the burner refractory lifetime. At this SR_1, the primary NO_x could be varied over the aforementioned operating range by varying the amount of NH_3 dopant, up to 0.75 percent in the fuel gas.

4.2 PRIMARY ZONE CHARACTERIZATION

The primary zone (zone 2) is characterized by the method of secondary combustion air injection (axial or radial), the amount of excess air (defined by SR_2), and the detailed temperature, velocity, and chemical composition of the post-flame combustion gas.

Secondary Combustion Air Injection Mode

Baseline tests were performed to determine the effect of 3 different modes of secondary combustion air addition on NO_{EX}. As described in Section 2, secondary combustion air can be injected through axial or radial ports at the boiler entry. The three modes of injection investigated were: all-axial injection (axial/radial $= \infty$), all-radial injection (axial/radial = 0), and an equal split of axial and radial injection (axial/radial = 1). Figure 4-4 shows that, at the nominal SR_1 of 0.64, the variation of NO_{EX} is less than 5 ppm for the three test conditions. Radial temperature, velocity, and species

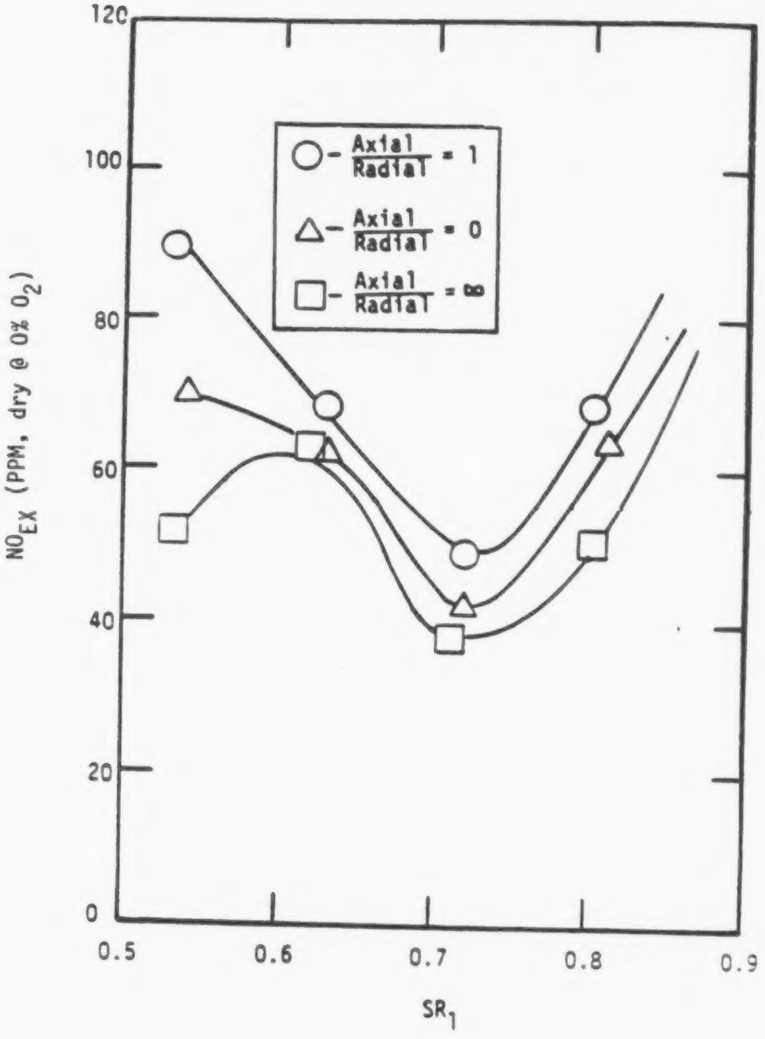

Figure 4-4: Effect of Secondary Air Injection Mode on Baseline NO_{EX}

profiles in the boiler radiant section did vary, however. Profiles for all-radial injection tests were much flatter (indicating faster mixing) than for all-axial injection tests. Primary zone flame length was considerably shorter for the all-radial mode (about 0.9 m) than for the all-axial mode (1.5 m). To allow maximum boiler length for reburning, and to provide maximum uniformity of speciation in the boiler, an all-radial secondary air addition mode was selected as the nominal operating condition. This mode provides most nearly a flat primary flame.

Primary Zone Stoichiometry

Under nominal operating conditions (FR_{PRI} = 0.62 MW; SR_1 = 0.64; axial/radial = 0), baseline tests were performed to determine the influence of primary zone stoichiometry (SR_2) on NO_{EX}. The results, plotted in Figure 4-5, indicate that NO_{EX} rises with increasing excess air, but at a less pronounced rate than typical of conventional burners. This reduced influence of SR_2 is probably due to lower primary flame temperatures for this burner.

Under nominal conditions (FR_{PRI} = 0.62 MW; SR_1 = 0.64; SR_2 = 1.1; axial/radial = 0) detailed measurements were made of primary zone temperature, velocity, and species concentration to define conditions entering the reburning zone.

Primary Zone Temperature

Boiler radiant section axial and radial profiles of combustion gas temperature were obtained via suction pyrometry. Figure 4-6 shows axial profiles at 3 radii: 13.3, 18.4, and 23.5 cm. The zero origin of axial location is the front face of the boiler. Figure 4-7 shows a radial temperature profile at a 1.0 m (40 in.) axial location. Here, zero refers to the boiler centerline. At the end of the visible flame (1.0 m axial location), the peak gas temperature (at centerline) is 1450 K (2150°F). As will be shown later (in Section 5.3), this represents a minimum temperature at

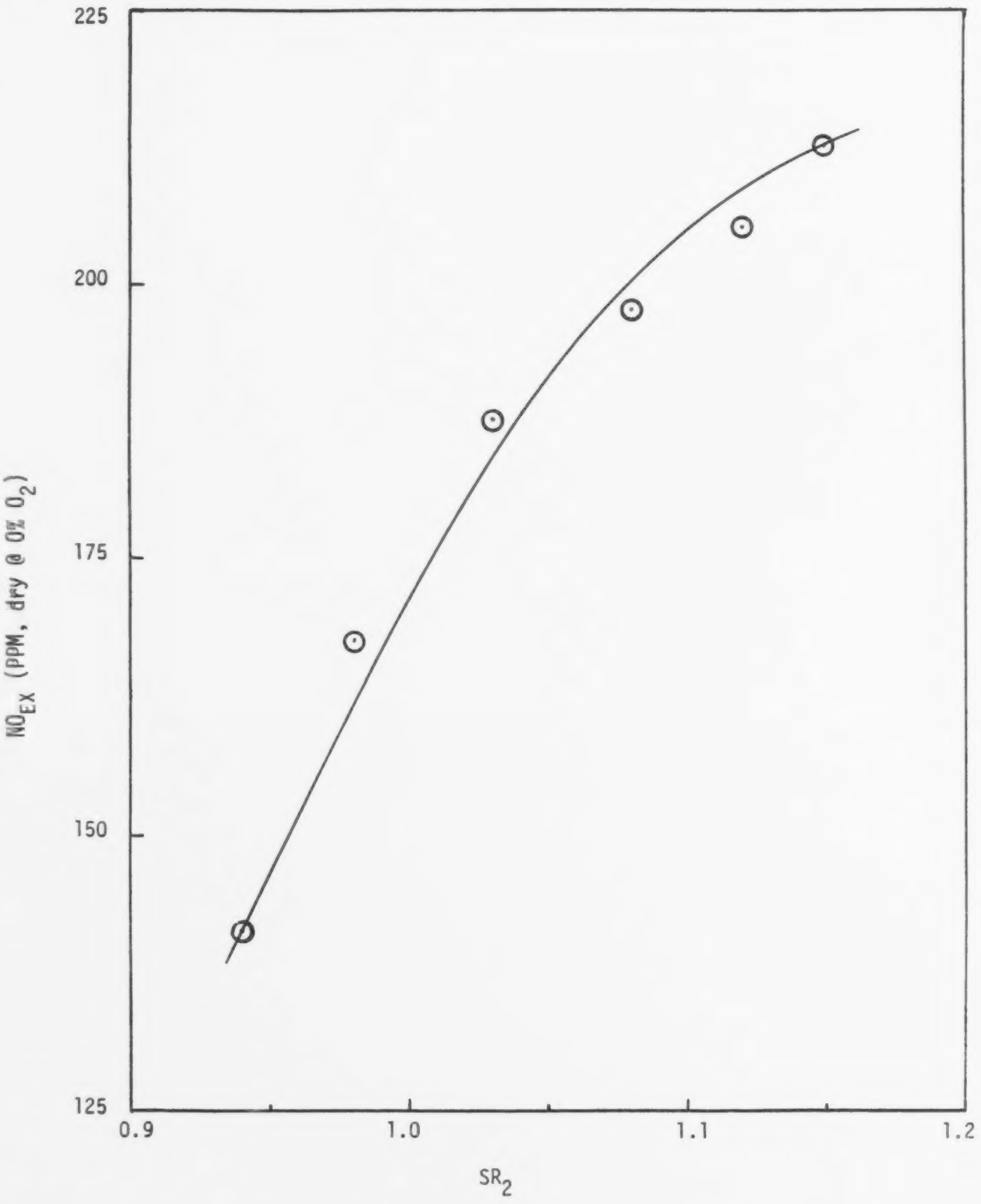

Figure 4-5: Baseline NO_{EX} Versus SR_2

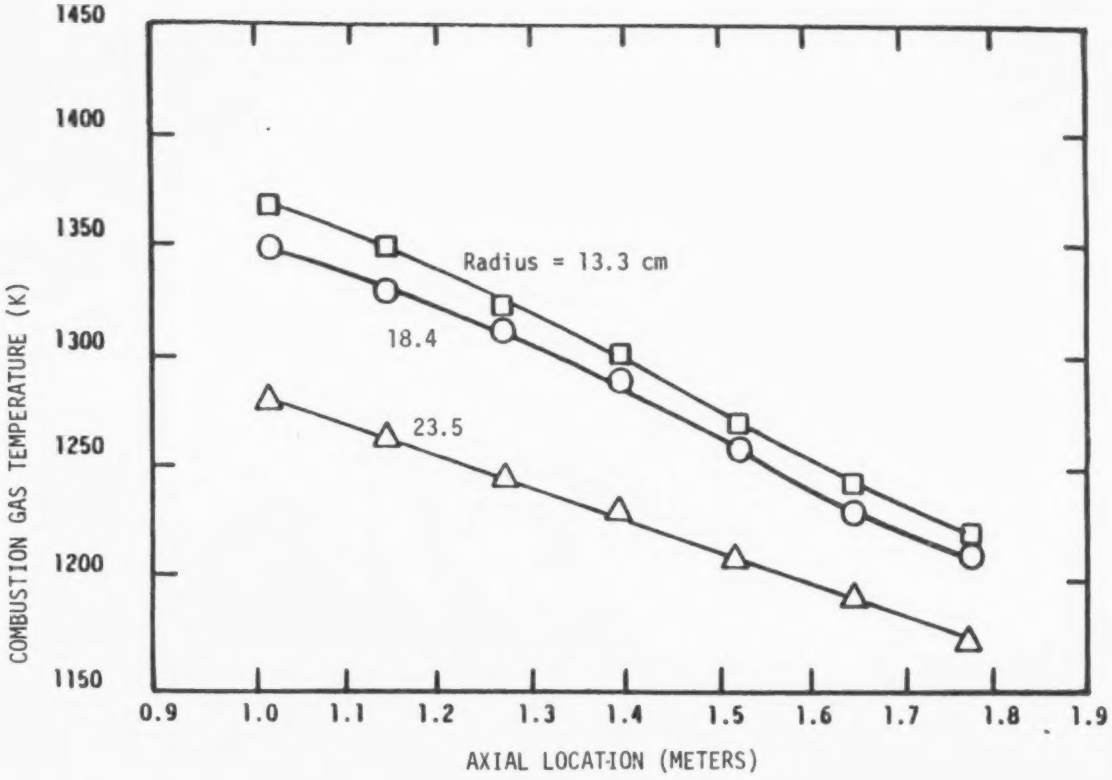

Figure 4-6: Axial Temperature Profiles

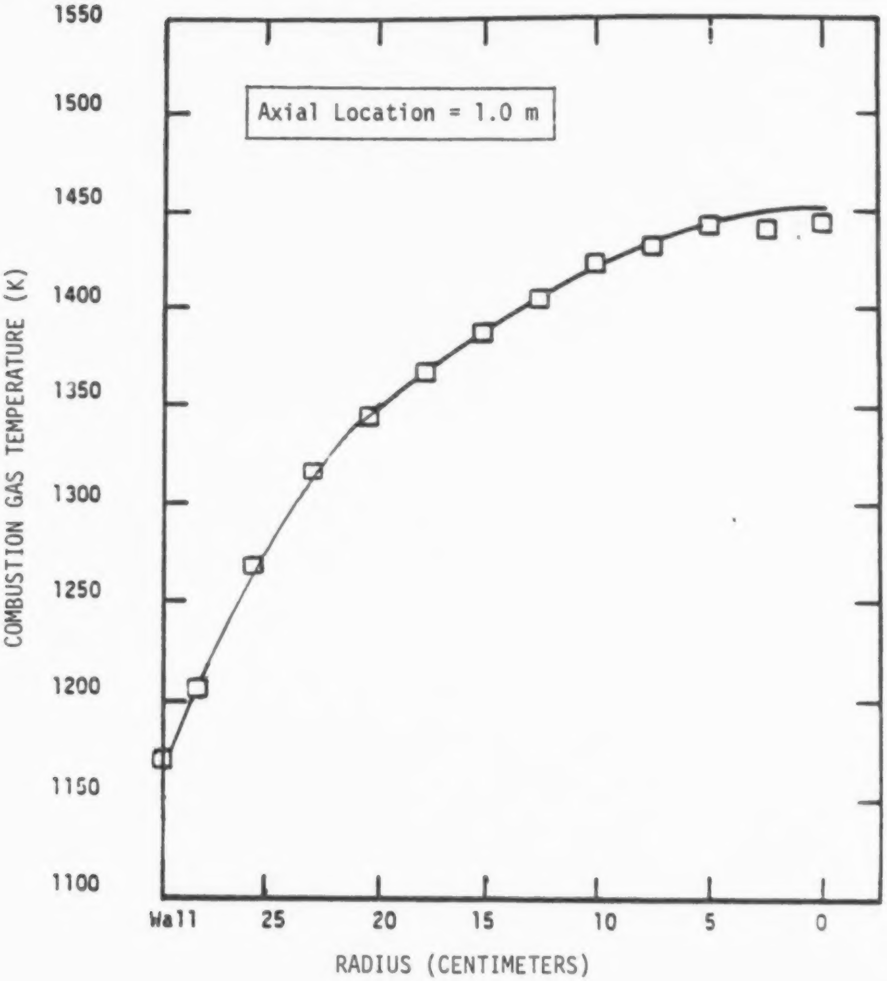

Figure 4-7: Radial Temperature Profile

which secondary natural gas can be injected and burned under fuel-rich conditions without excessive sooting. For secondary fuel oil injection, the primary zone had to be insulated to increase temperature and prevent excessive soot deposits from forming in the fuel-rich zone (see Section 6).

Primary Zone Velocity

A radial profile of the axial component of velocity was measured at the 1.0 m (40 in.) axial location. Figure 4-8 shows that a peak axial velocity of 14.5 m/sec (48 ft/sec) was measured at the boiler centerline. Extrapolating the velocity data to zero at the boiler wall, and drawing the profile such that the area under the curve equals the measured input flow rate, it is observed that the pitot probe measurement is not accurate for velocities less than 3 m/sec (10 ft/sec). This observation is consistent with the fact that for velocities less than 3 m/sec, more than half of the 250 instantaneous differential pressure readings were negative. The Apple microcomputer treats these data as zero readings, biasing the average velocity measurement high. (For low mean velocities, negative fluctuations are possible).

Note that although the bulk average velocity of combustion gas at the 1.0 m boiler plane is 3.4 m/sec (11 ft/sec), the peak velocity is measured at over 4 times this value. The velocity of the gas jet exitting the transition section (0.25 m diameter) is calculated from input flow measurements to be 16.1 m/sec (52.8 ft/sec). Thus, this is further indication that the measured velocity profile represents actual conditions at the 1.0 m boiler plane. The development of the in-flame velocity measurement system in this pilot-scale combustor is considered a valuable by-product of this reburning study.

Primary Zone Species Concentration

Axial and radial profiles of O_2, CO_2, CO, NO, UHC, NH_3, HCN, and N_2O were measured. Significant results are presented here. Figure 4-9 shows an axial

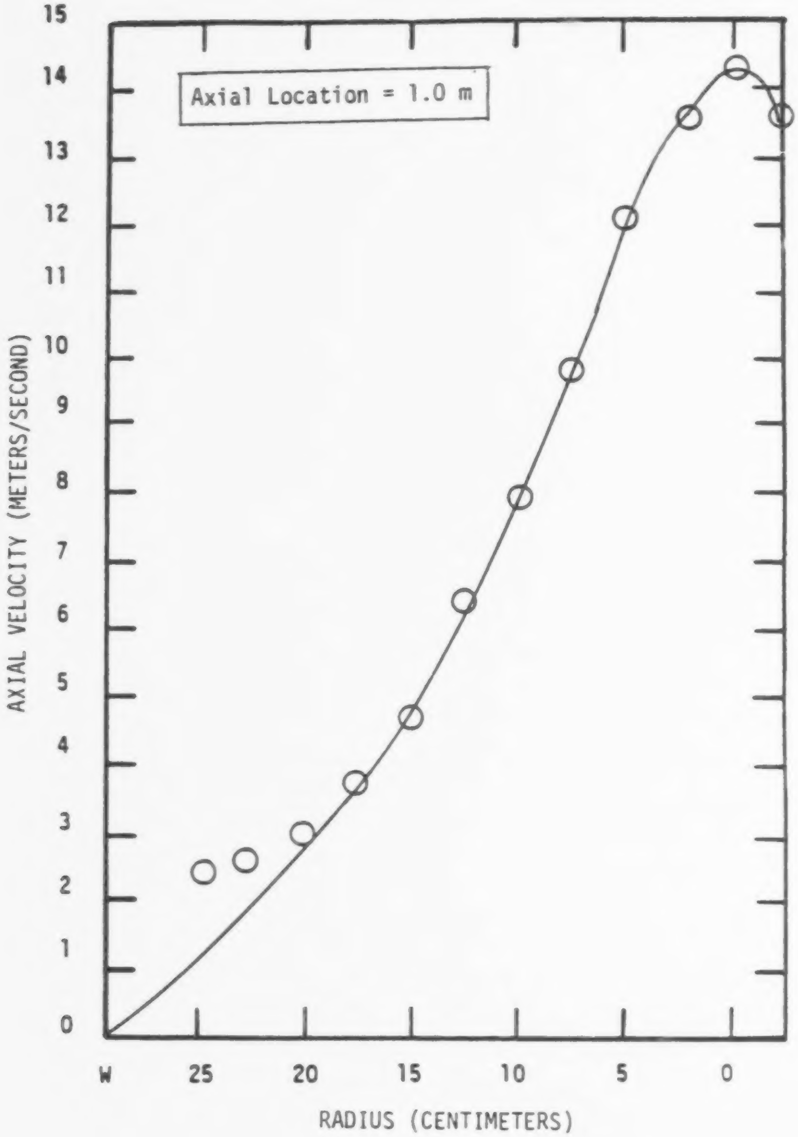

Figure 4-8: Radial Velocity Profile

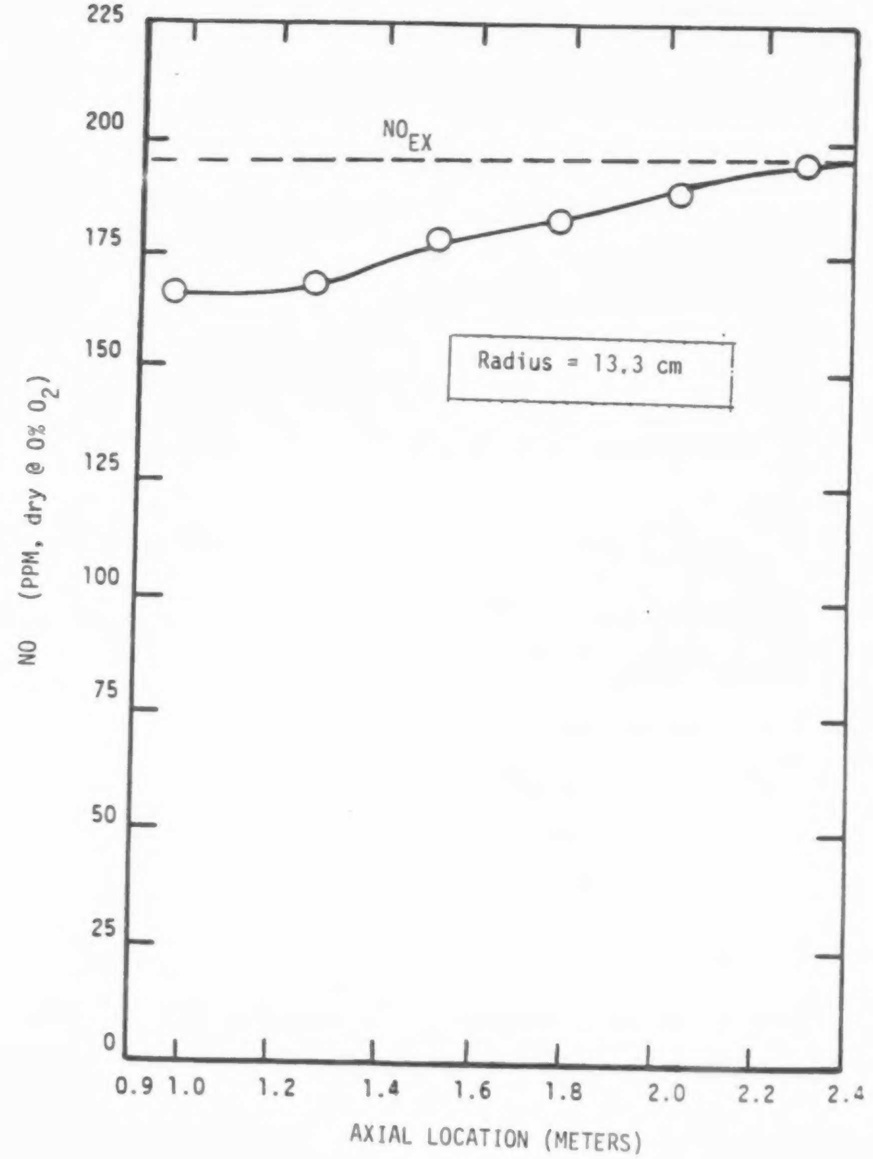

Figure 4-9: Axial NO Profile

profile of NO concentration at the 13.3 cm (5.25 in.) radial location. Two points are made concerning this measurement. First, there is no significant concentration (> 1 ppm) of N_2O, NH_3, and HCN in the post-flame region. Thus, it is inferred that all of the fixed nitrogen exists as NO_x. It is important that no residual HCN or NH_3 concentration from primary fuel combustion exists at the point of secondary fuel injection because the presence of these species, thought to be an integral part of the NO_x destruction mechanism via reburning, could affect the reburning process, making understanding the process more difficult.

A second, more academic point to be made from the NO axial profile is that the rate of NO increase in the post-flame region is approximately 150 ppm/sec. This experimentally determined rate is an order of magnitude slower than the rate predicted by Merryman and Levy [17] for nitrogen dioxide (NO_2) conversion to NO by the reaction:

$$NO_2 + O \longrightarrow NO + O_2,\ k_{4-1} = 1.9 \times 10^{13} \exp(-1060/RT) \qquad (4\text{-}1)$$

Here, the kinetic rate constant (from Engleman [18]) is evaluated at 1322K (1920°F), and equilibrium product concentrations are assured. It has been shown by Lanier [3] that the rate-controlling reaction for NO_2 destruction is the reverse of the following reaction:

$$NO + HO_2 \longrightarrow NO_2 + OH,\ k_{4-2} = 1 \times 10^{13} \exp(-3000/RT) \qquad (4\text{-}2)$$

Here, the predicted rate of NO_2 decomposition is two orders of magnitude faster than the experimentally determined rate (based on equilibrium concentrations of the HO_2 radical at 1322K). However, Lanier has also shown that kinetic processes predict superequilibrium concentrations of the hydroxyl radical (HO_2) well into the post-flame region. The high NO_2 concentrations predicted by kinetics result in O atom depletion, and, thus, slower NO_2 decomposition rates than originally predicted by reaction 4-1.

slower NO_2 decomposition rates than originally predicted by reaction 4-1. This subject is discussed in detail in Chapter 4 of reference [3].

To verify the conversion of NO_2 to NO in the post-flame region of the boiler several attempts were made to quantitatively measure NO_x. Using both wet sampling methods with ion chromatograph analysis for NO_2 and NO_3 detection and dry gas sampling for NO_x measurements using chemiluminescence, it was found that in the boiler and stack at excess air conditions the NO_x concentration consists of 5 to 15 percent NO_2. However, under fuel-rich conditions NO_2 is an excellent oxidizing agent. Thus, as secondary fuel is added and the flame radical pool increases, NO_2 will rapidly decompose to NO.

Figure 4-10 shows radial profiles of O_2 and NO at the 1.0 m (40 in.) axial location. Of significance here is the flatness of the curves, indicating a well-mixed primary flame effluent. While some radial variation is unavoidable in a combustor of this size, (as shown by the CO profile, which is very sensitive to stoichiometry), uniformity of O_2 concentration at the point of secondary fuel injection simplifies fuel injector design. Circumferential uniformity (radial symmetry) is assumed.

4.3 SECONDARY FUEL INJECTION DEFINITION

The data presented in the previous section characterizing conditions in the primary zone are critical to the positioning of the secondary fuel boom and the design of the fuel injection spokes.

Secondary Fuel Injection Location

Several factors were considered in the selection of a secondary fuel injection location. The primary reason for selecting an axial location of 1.02 m (40 in.) for the start of the reburning zone (zone 3) is that ports in the PBS are available for complete temperature, velocity, and species characterization at that location. In addition, this location is downstream of the primary flame (0.9 m flame length), yet sufficiently upstream so that the combustion gas temperature exceeds 1370K (2000°F). Further, combustion gas speciation at this location is nearly uniform (see Figure 4-10). Finally, PBS aerodynamics at the secondary fuel injection point are considered. There is a step change in diameter as the combustion gas exits the transition section and enters the PBS unit. Beer [16] has shown that jet reattachment may be reasonably estimated by assuming a jet spread angle of 9.7 degrees. Using this assumption, flow reattachment is estimated to be 1.0 m into the PBS. This estimation of the step recirculation zone length makes the selection of the 1.0 m axial fuel injection location ideal, in that secondary fuel flow would not be entrained into these recirculation zones. This calculation was checked experimentally by injecting a tracer gas near the boiler wall at the 1.0 m axial location and observing no upstream migration of the gas.

Secondary Fuel Spoke Design

To produce a radially uniform distribution of stoichiometry in zone 3, secondary fuel spokes with carefully selected hole patterns were designed as shown in Figure 2-9. Twelve 1/32 in. diameter holes were drilled in each of eight spokes at radial locations of equal area cross-section. The number of holes per spoke was determined by assuming a maximum secondary flow rate. A second set of spokes with six 1/32 in. diameter holes per spoke was fabricated for low secondary fuel flow rates. Table 4-1 lists the port size and location for each of the two uniform fuel injection spokes.

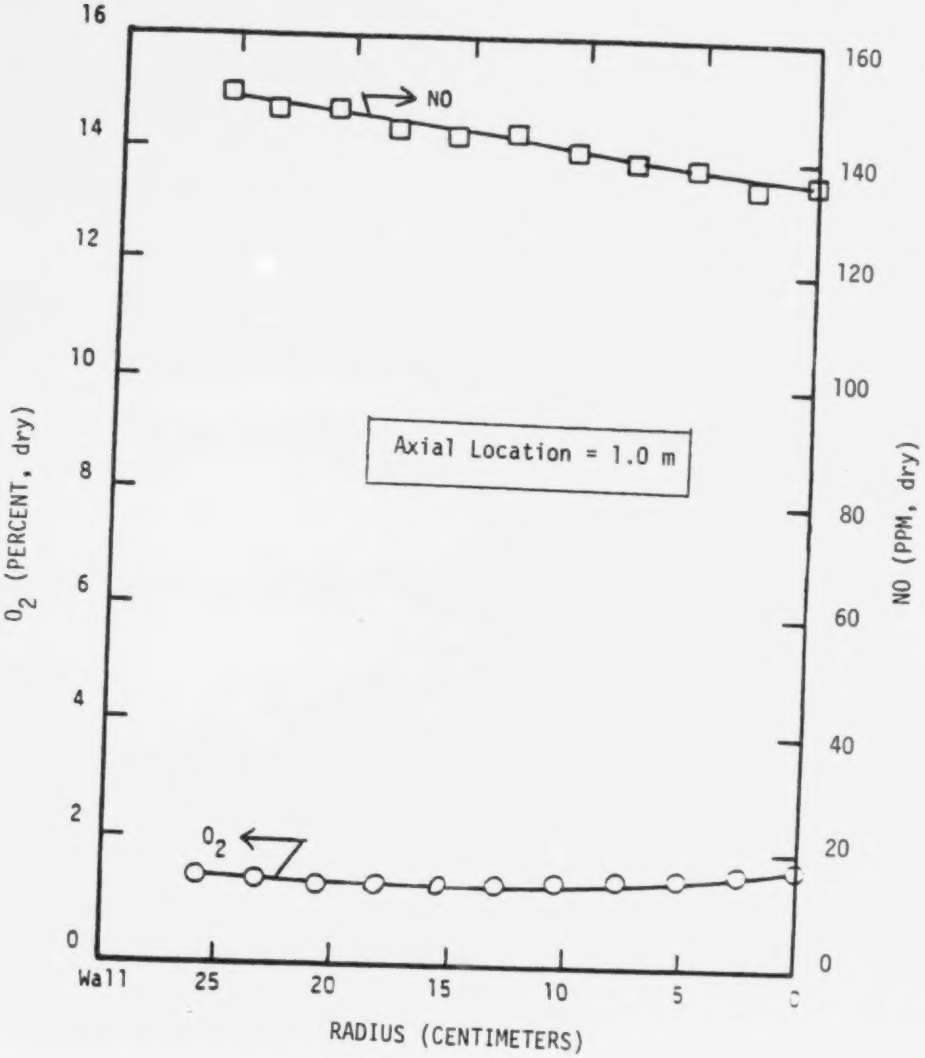

Figure 4-10: Radial O_2 and NO Profiles

TABLE 4-1. SECONDARY NATURAL GAS UNIFORM INJECTION SPOKE SPECIFICATIONS

"12-Hole Spokes"		"6-Hole Spokes"	
Radial Location (cm)	Hole Diameter (mm)	Radial Location (cm)	Hole Diameter (mm)
5.39	0.794	5.39	0.794
6.68	0.794		
7.94	0.794	7.94	0.794
8.89	0.794		
9.52	0.794	9.52	0.794
11.43	0.794		
12.06	0.794	12.06	0.794
13.65	0.794		
15.24	0.794	15.24	0.794
18.41	0.794		
21.59	2 @ 0.397		
24.13	0.794	24.13	0.794
26.67	2 @ 0.397		

Total Flow Area/Spoke = 5.94 mm^2

No. of spokes = 8

Fuel Jet Velocity at Nominal Reburn Load = 79.5 m/sec

Total Flow Area/Spoke = 2.97 mm^2

No. of Spokes = 8

Fuel Jet Velocity at Nominal Reburn Load = 158.9 m/sec

SECTION 5

PBS NATURAL GAS REBURNING TEST RESULTS

The package boiler simulator (PBS) has been used to obtain fundamental insight into the natural gas reburning process. Reburning, as applied to this pilot-scale research facility, is shown schematically in Figure 5-1. As shown in the figure, four zones characterize this application: a precombustion chamber burner zone (zone 1); a primary zone (zone 2); a reburning zone (zone 3); and a burnout zone (zone 4). Characterization of zones 1 and 2 was discussed in Section 4. This section discusses results that show how input parameters influence the reburning process, taking place in zones 3 and 4.

As stated in Section 4, primary load is held constant, at 0.62 MW, and burner stoichiometry is fixed at 0.64 in these reburning tests. Thus, the total load varies with the reburning load. Values for other input parameters are varied individually, over the ranges listed in Table 5-1. The nominal values were chosen to achieve program goals within the practical constraints of hardware design. Section 5-1 documents input/output trials in which input parameters, such as primary NO_x, primary, reburning and burnout zone stoichiometries, residence time, and fuel type, are varied while holding other input parameters constant at nominal settings.

In Section 5-2, zone 3 is looked at in detail to understand the chemical process of reburning. In Section 5.3, the effects of secondary fuel injection method are studied. In Section 5.4, thermal effects on the reburning process are investigated. Additional insight into natural gas reburning was provided by studying final air jet phenomena (Section 5.5) and alternative fuel and air staging strategies (Section 5.6). In the last subsection (Section 5.7) results from trials at high primary NO_x levels are presented.

Most of the material presented in Section 5 has been documented by Lanier in his doctorial dissertation [2]. In addition, Lanier and Mulholland are

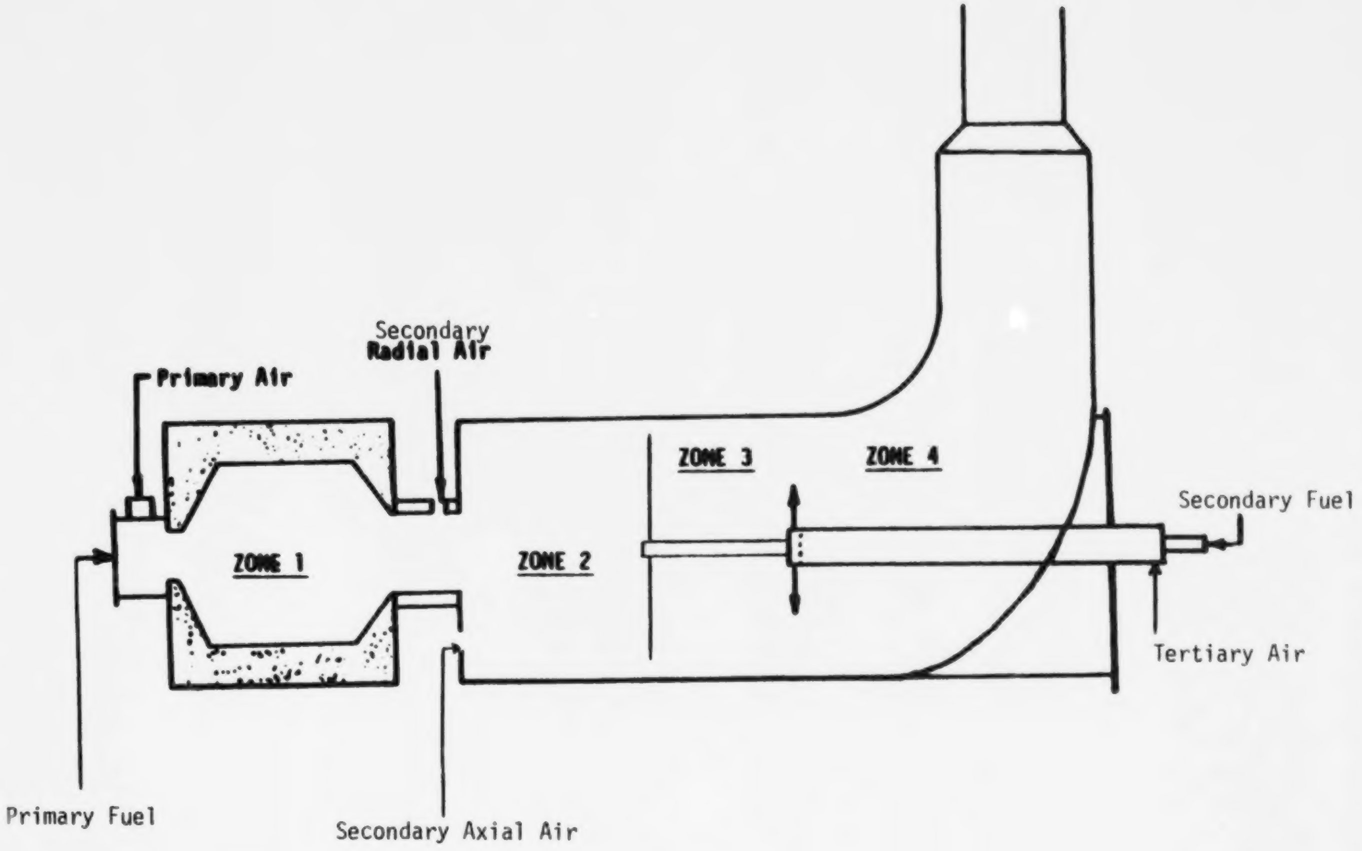
Secondary Radial Air
Primary Air
ZONE 1
ZONE 2
ZONE 3
ZONE 4
Secondary Fuel
Tertiary Air
Primary Fuel
Secondary Axial Air

Figure 5-1: PBS Natural Gas Reburning Schematic

TABLE 5-1. NOMINAL INPUT VARIABLE VALUES

Report Section	Parameter	Symbol	Value	Range
5.1.1	Primary NO_x	NO_{PRI}	200 ppm	50-500 ppm
5.1.1	Reburn Zone Stoichiometry	SR_R or SR_3	0.9	0.7-1.1
	-- Reburn Firing Rate	FR_R	0.12 MW	0-0.23 MW
5.1.2	Secondary Fuel Dopant	$(NH_3)_R$	0, 0.5%	0-1.0%
5.1.3	Reburn Zone Bulk Residence Time	τ_{b3}	200 ms	0-400 ms
	-- Reburn Zone Length	L_3	0.61 m	0-1.22 m
5.1.4	Primary Zone Stoichiometry	SR_{PRI} or SR_2	1.1	0.9-1.2
5.1.5	Burnout Zone Stoichiometry	SR_{EX} or SR_4	1.1	1.0-1.3
5.1.6	Primary Fuel	-	Natural Gas	Fuel Oil
5.3	Reburn Zone Mixing:			
	-- Secondary Air Injection	Ax/Rad	0	$0-\infty$
	-- Secondary Fuel Injection	-	Uniform	Nonuniform
5.4	Reburn Zone Temp	T_3	1370K	1370-1750K
	-- Reburn Zone Insulation	-	None	Boiler Wall and Fuel Boom
	-- Primary Zone Insulation	-	None	Boiler Wall
	-- Secondary Fuel Injection Location	L_2	1.0 m	0.25-1.6 m

preparing 3 technical papers to be published in 1985. These papers, covering detailed reburning chemistry, secondary fuel injection method effects, and thermal effects, appear in modified form in Sections 5.2, 5.3, and 5.4, respectively.

5.1 INPUT/OUTPUT TRIALS

An extensive series of input/output (I/O) tests was performed to evaluate the effect of input parameter variation on the overall reburning process.

5.1.1 Primary NO_x and Reburn Zone Stoichiometry

Initial reburning I/O trials were performed with undoped natural gas and natural gas doped with 0.5 percent ammonia (0.42 percent nitrogen, by weight). Primary NO_x was adjusted from 50 to 200 ppm (measured dry, at zero percent O_2) by varying the amount of ammonia-dopant in the primary natural gas flow. Zone 3 stoichiometry was adjusted by varying the flow rate of secondary natural gas. For these tests, primary and burnout zone stoichiometries were maintained at excess air levels of 3 to 10 percent. The secondary natural gas was injected at 1.02 m (40 in.) and the final air at 1.63 m (64 in.); this resulted in a reburn zone bulk residence time of 200 ms. The boiler was uninsulated, with an average temperature of 1370K (2000°F) at the point of secondary fuel injection. The secondary natural gas was injected through spokes in the fuel boom to produce a uniform SR_3.

Results of these tests are presented in Figures 5-2 and 5-3. The 500 ppm primary NO_x condition was achieved by operating the primary burner at a stoichiometry of 0.95. Reburn parameters, such as temperature and mixing at the secondary fuel injection location, were not significantly changed by this variance from the nominal operating condition. Three significant observations are to be made from these figures: first, NO reduction via reburning is strongly dependent on reburn zone stoichiometry; second, NO reduction via reburning is strongly dependent on primary NO_x concentration; and third, NO

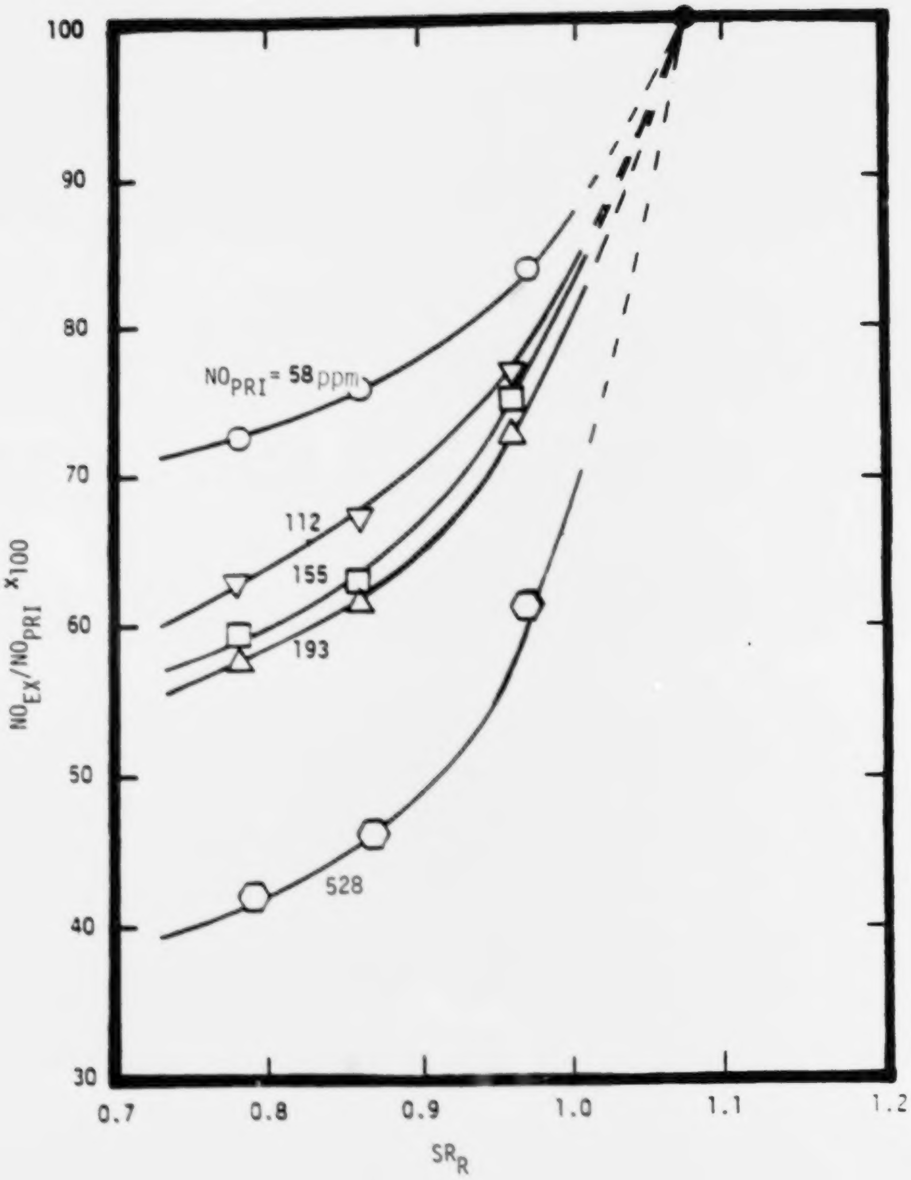

Figure 5-2: Natural Gas Reburning Effectiveness

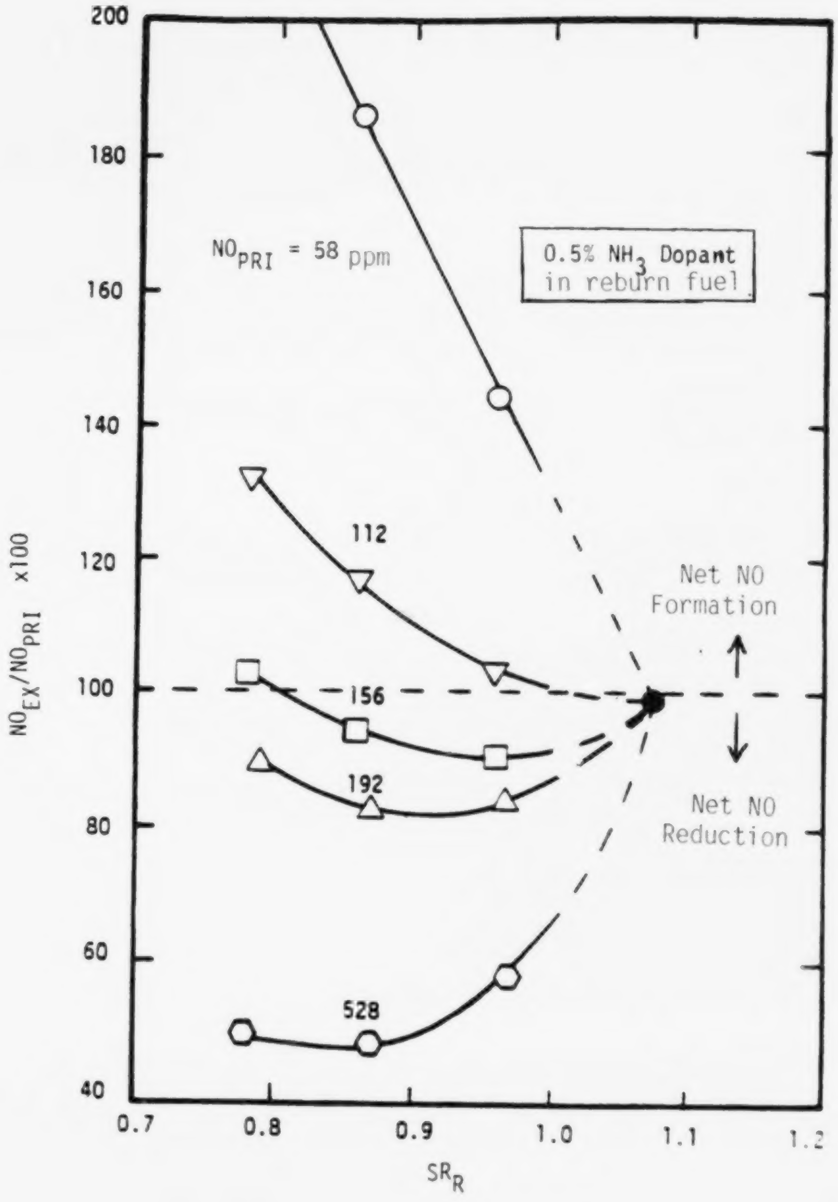

Figure 5-3: Ammonia-Doped Natural Gas Reburning Effectivenss

reduction via reburning is strongly dependent on secondary fuel nitrogen content. Each of these observations is discussed here.

The observation that NO reduction is a function of reburn zone stoichiometry is consistent with the data of Chen _et al_. [12]. However, Chen observed a minimum in the NO reduction versus stoichiometry curve at a reburn zone stoichiometry of 0.9 (see Figure 1-10), whereas no minimum was observed in the tests performed here. Chen _et al_. applied a correction factor to their results to eliminate the dilution effect of secondary fuel and final air addition. In this way, their results represent a net molar destruction of NO. This correction factor increases with increasing reburning load. When this correction factor is removed from Chen's data, the minimum becomes less distinct.

In this study, the "dilution" of secondary fuel and final air injection is not removed from the NO reduction. Though it is important to realize that only a portion of the NO reduction is due to NO destruction, determination of the actual moles of NO destroyed is difficult. Some NO is formed with the addition of secondary fuel (possibly via the prompt NO mechanism); thus, to assume that all of the additional flow from reburning is diluent is misleading. The scale of this experiment is too large for detailed kinetic interpretation; therefore, the utility of applying a correction factor to estimate NO destruction is minimal. NO reductions in this study are represented as a ratio of the stack NO concentration with reburning to the primary NO_x concentration measured at the derated primary load. Figure 5-4 shows the difference between representing the results as a net NO destruction and as overall NO_x reduction.

For fuel-rich reburn zone stoichiometries less than 0.7, the exhaust NO curves seem to approach a minimum. This is consistent with the observation that equilibrium values of total fixed nitrogen species have a minimum at fuel-rich

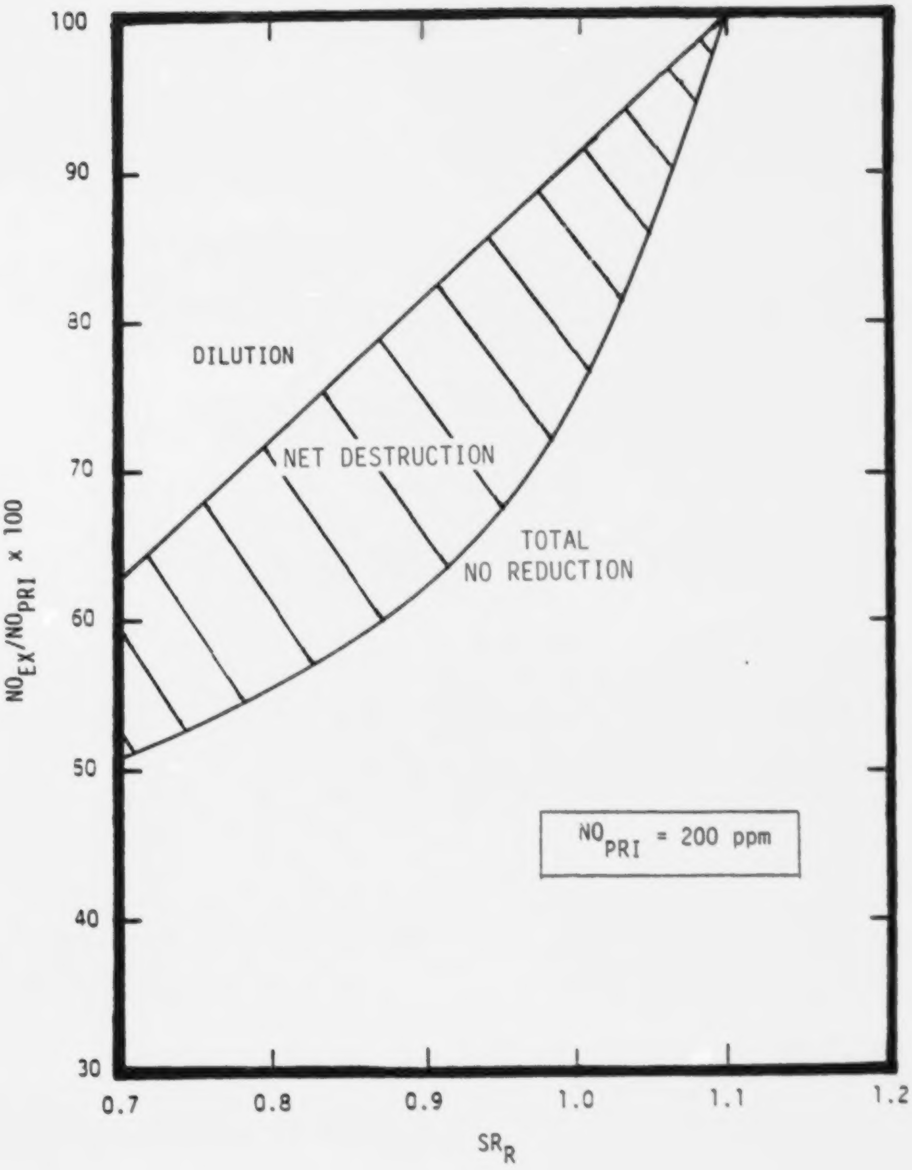

Figure 5-4: Comparison of NO Reduction and Net NO Destruction

stoichiometries, dependent on temperature. Though equilibrium values, typically less than 10 ppm (see Figure 1-5), are never achieved in these reburning tests, the equilibrium driving force towards low NO_x decreases in strength as the reburn zone becomes increasingly fuel-rich. It is hypothesized that for stoichiometries less than 0.7, the NO_{EX} curve will reach a minimum with NO emissions eventually increasing with decreasing SR_3. This is seen for ammonia-doped natural gas reburning.

The nonlinearity of the NO_{EX} curve, with a positive second derivative, suggests that the uniformity of reburn zone stoichiometry should be important in optimizing NO reduction. This is especially true for the case of secondary fuels with high nitrogen content. For example, for the case of 0.5 percent ammonia doped into the secondary natural gas, with 200 ppm primary NO_x, uniform fuel injection results in a 19 percent NO reduction at the optimum SR_3 of 0.9. However, for the hypothetical case of injecting all of the secondary fuel uniformly into half the boiler, with the rich and lean halves of the combustion flow remaining unmixed, an overall NO reduction of about 3 percent would be expected. This is shown in Figure 5-5. The effect of reburn zone stoichiometry uniformity is investigated in Section 5-3.

The second observation derived from Figures 5-2 and 5-3 is that NO reduction via reburning is not first order with primary NO_x. The data plotted in Figure 5-6 clearly show that, as NO_{PRI} increases, NO reductions increase. This contradicts the claim of the MHI researchers [9] that 50 percent NO_x reduction is achieved independent of initial NO_x. The overall rate of change of NO can be expressed by:

$$\frac{d[NO]}{dt} = -k_1 [NO]^a + k_2 \qquad (5\text{-}1)$$

where k_1 is the overall destruction rate constant, a is the overall order of destruction with respect to NO, and k_2 is a formation term which is assumed

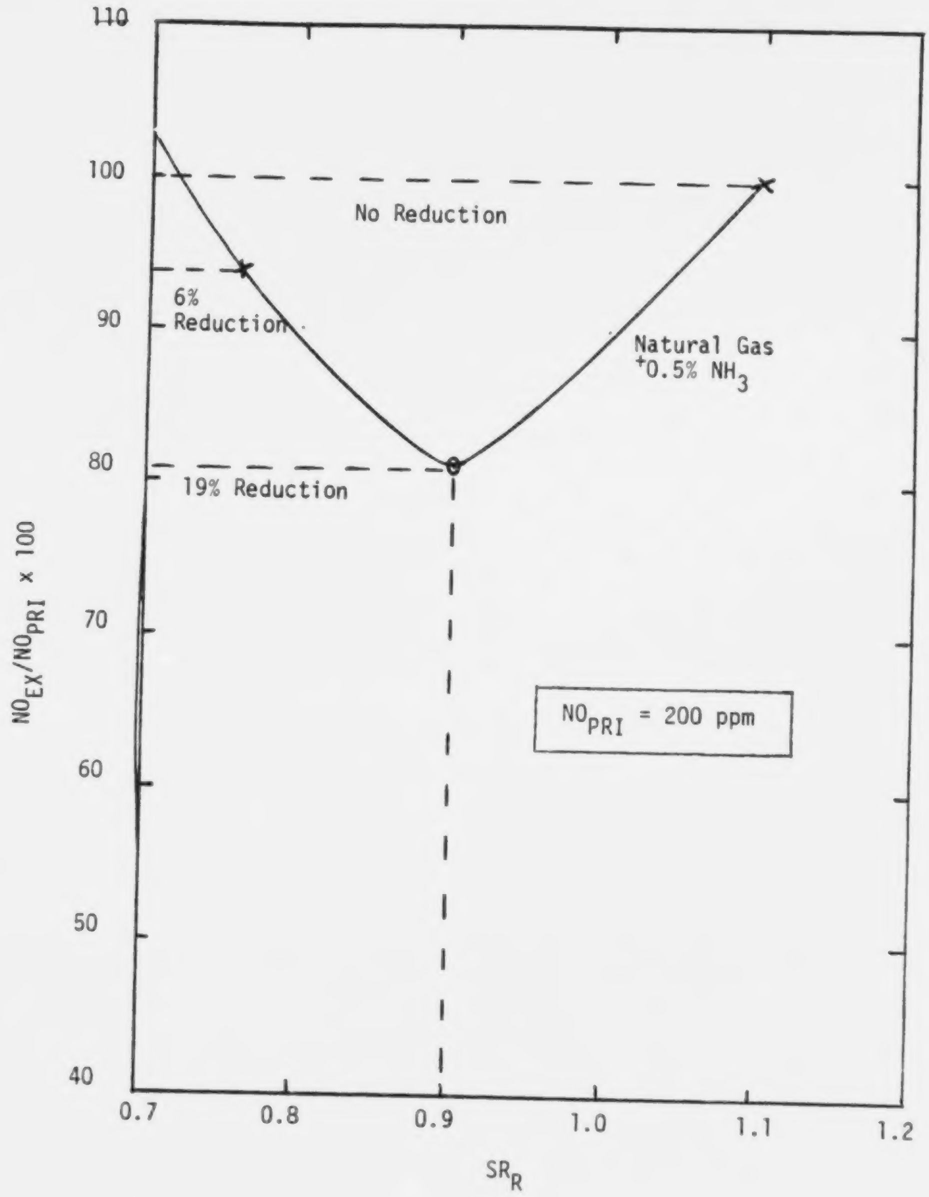

Figure 5-5: Hypothetical Effect of Nonuniform Secondary Fuel Injection

independent of NO concentration. This expression is evaluated for two limit cases. First, if k_2 is small relative to k_1, equation (5-1) may be integrated to yield:

$$\frac{[NO_i]}{[NO]} = \left(1 - (a-1)\ k_1 t\ [NO_i]^{(a-1)}\right)^{\frac{1}{(a-1)}},\ a>1 \qquad (5\text{-}2)$$

Here, as $[NO_i]$ approaches zero $[NO_i]/[NO]$ approaches one. Conversely, if k_2 dominates equation (5-1), integration yields:

$$\frac{[NO_i]}{[NO]} = \frac{1}{1 + \frac{k_2 t}{[NO_i]}} \qquad (5\text{-}3)$$

In this case, as $[NO_i]$ approaches zero, $[NO_i]/[NO]$ approaches zero, and as $[NO_i]$ approaches infinity, $[NO_i/[NO]$ approaches one. The initial NO concentration, $[NO_i]$, is equivalent to the primary NO concentration, NO_{PRI}. It is assumed that for NO_{PRI} greater than 50 ppm, the destruction term (k_1) dominates the formation term (k_2); hence, equation (5-2) is applicable.

To determine the overall reaction order with respect to initial NO_x from the experimental data, results shown in Figure 5-6 are replotted in Figures 5-7 and 5-8. The data are clearly not consistent with either first or second order behavior. For first order behavior (a = 1), $[NO_i]/[NO] = e^{-k_1 t} =$ constant. Thus, a horizontal line would describe the data. For second order behavior (a = 2), $[NO_i]/[NO] = 1 - k_1 t\ [NO_i]$. Thus, a straight line originating from $[NO_i]/[NO] = 1.0$ (at $[NO_i] = 0$) would describe the data. Instead, the data suggest an overall reaction order between 1 and 2. Figure 5-7 shows that the experimental data for SR_3 of 0.78 are best fit with an overall reaction order of 1.5. As seen, agreement is well within data uncertainty bars. For SR_3 of 0.87, the best curve fit is found to be for an overall reaction order of 1.55 (see Figure 5-8). It is not expected that the best fit reaction order be the same for data taken at two different stoichiometries since the term $k_1 t$ represents a gross overall average that may be a function of SR_3.

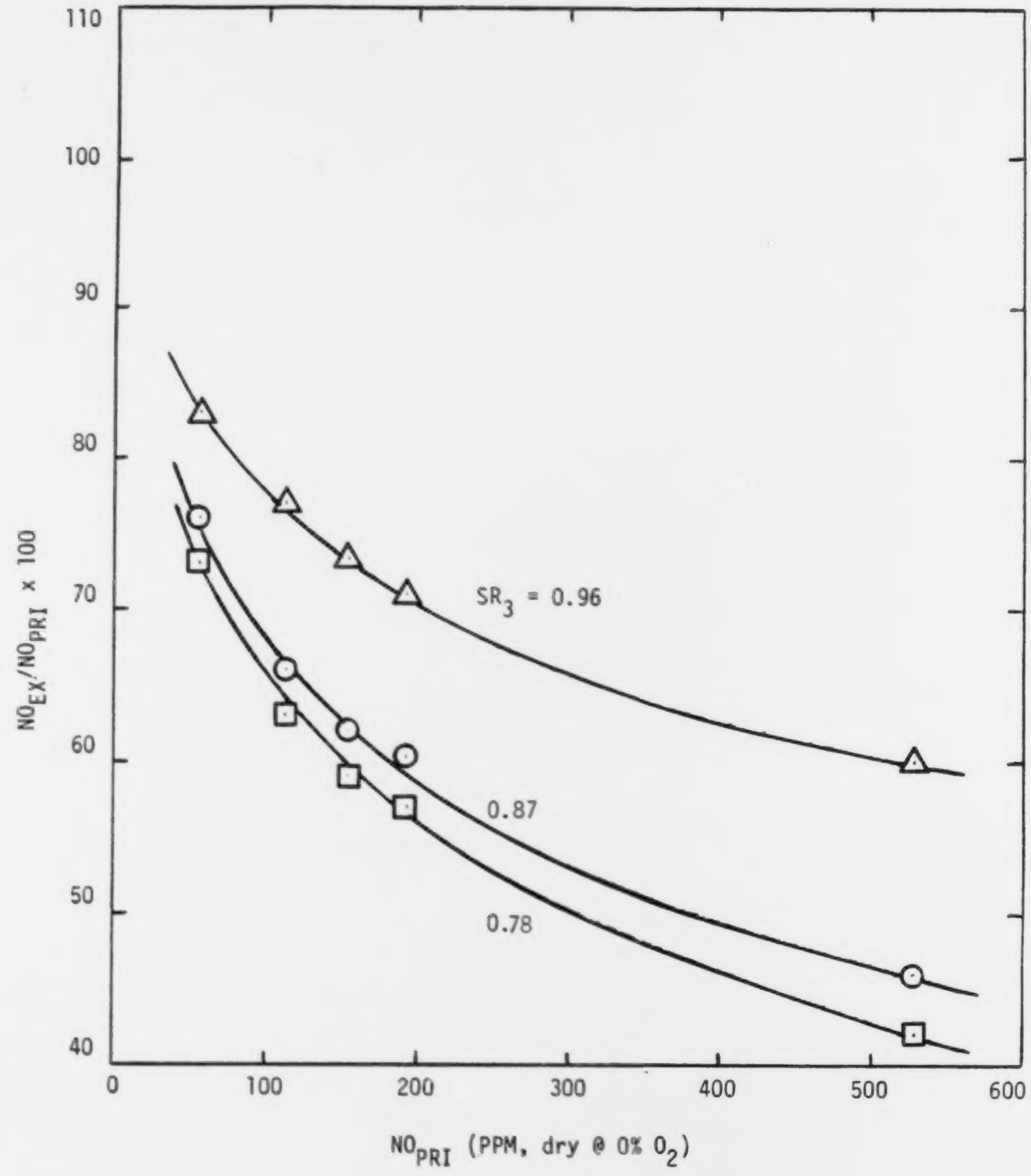

Figure 5-6: Effect of NO_{PRI} for Natural Gas Reburning

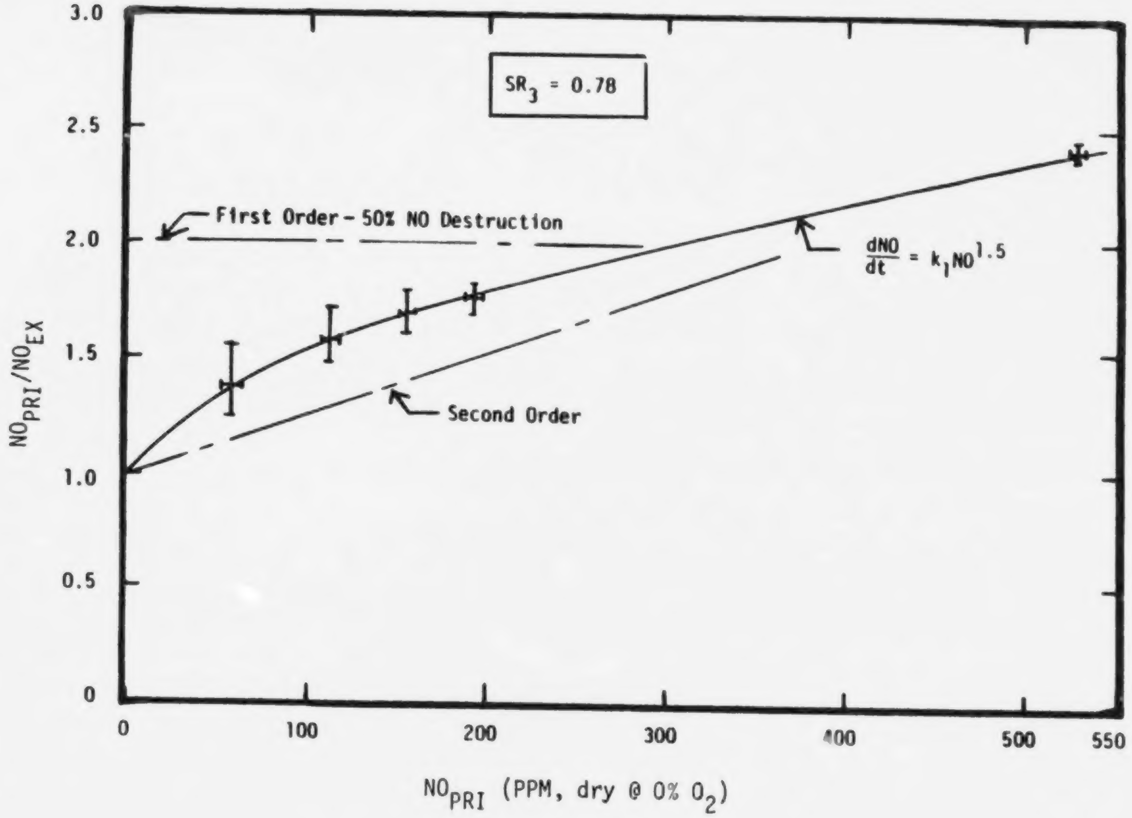

Figure 5-7: Reaction Rate Order Determination for $SR_R = 0.78$

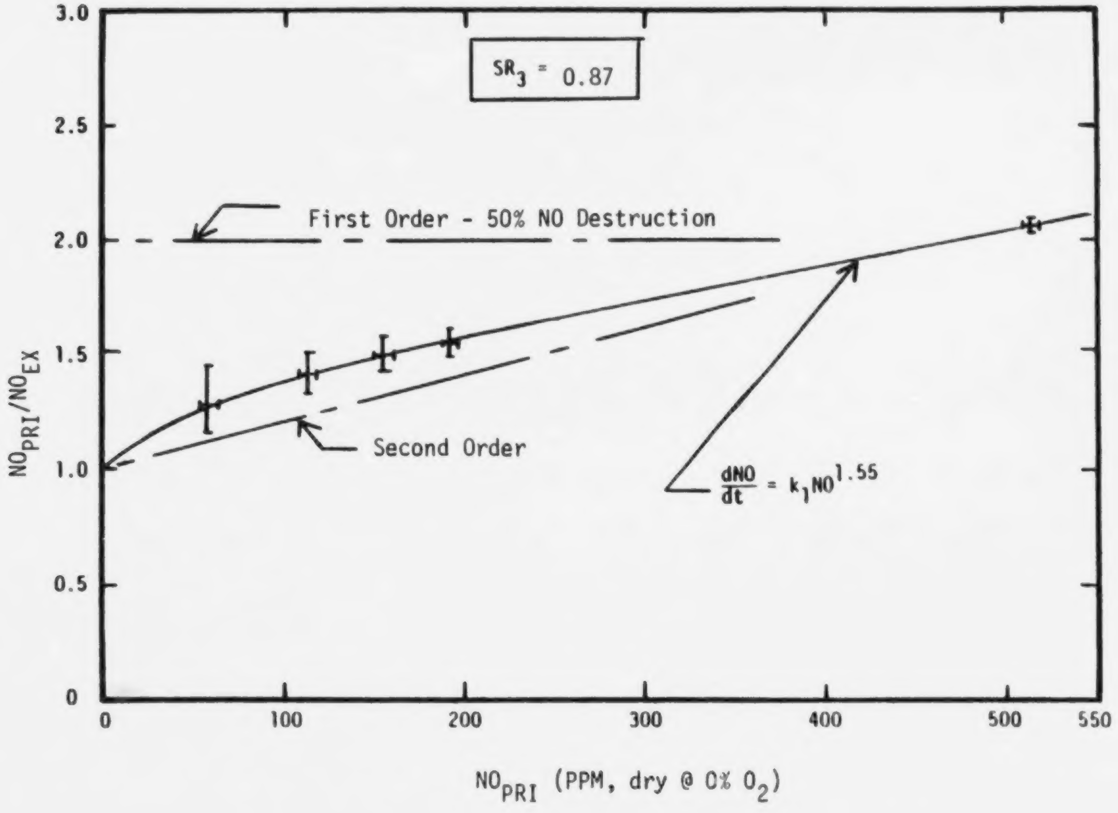

Figure 5-8: Reaction Rate Order Determination for $SR_R = 0.87$

The relatively large uncertainty in the experimental data at low NO_i concentrations precludes extrapolation of data in Figure 5-7 and 5-8 to the zero $[NO_i]$ intercept. Zero intercepts of either zero or unity would be consistent with undoped natural gas data. It may be concluded, however, that NO formation processes such as prompt NO, which would result in a zero intercept, account for less than 50 ppm net NO production. For ammonia-doped secondary fuel, however, NO formation is not negligible. Figure 5-9 shows that exhaust NO becomes very high with respect to $[NO_i]$ for $[NO_i]$ approaching zero. In this case, significant NO is formed by the oxidation of the trace quantities of ammonia added to the secondary fuel.

These simple input/output measurements provide an overall evaluation of hypothesis 1. NO reduction is indeed a strong function of initial NO concentration, and the overall reduction reaction order is approximately 1.5.

The third observation, that NO reduction is strongly dependent on secondary fuel nitrogen content, is clearly seen in Figure 5-10. For NO_{PRI} = 200 ppm, 0.5 percent ammonia (0.42 percent nitrogen, by weight) doped into the secondary fuel results in a maximum NO reduction of 20 percent, as compared to more than 40 percent without ammonia doping. Further, it is seen that for low initial NO_x conditions, reburning with 0.5 percent ammonia-doped natural gas results in increased NO concentration in the stack. The net fractional conversion of NH_3 fuel dopant to NO is found to be between 35 and 40 percent over the ranges of NO_{PRI} (50 to 500 ppm) and SR_R (0.75 to 1.0) tested (see Figure 5-11). The effect of nitrogen in the secondary fuel is discussed next.

5.1.2 Ammonia-Doped Secondary Fuel

As discussed in Section 1, ammonia was selected as a secondary natural gas dopant to simulate fuel-bound nitrogen effects. For the nominal test condition of 200 ppm primary NO_x and 0.86 SR_3, the secondary natural gas was doped with ammonia ranging from zero to 1 percent of the total flow. The

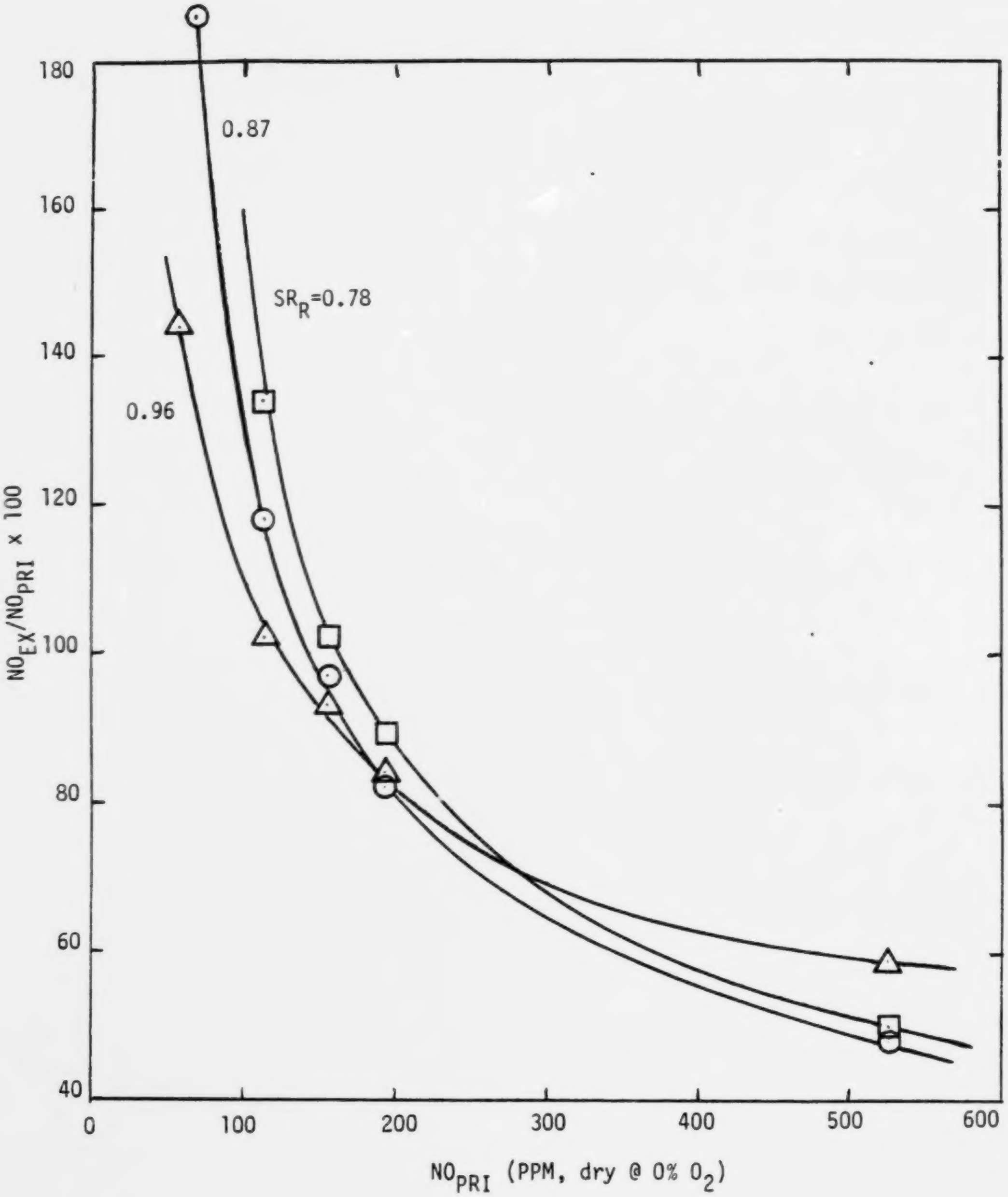

Figure 5-9: Effect of NO_{PRI} for Ammonia-Doped Natural Gas Reburning

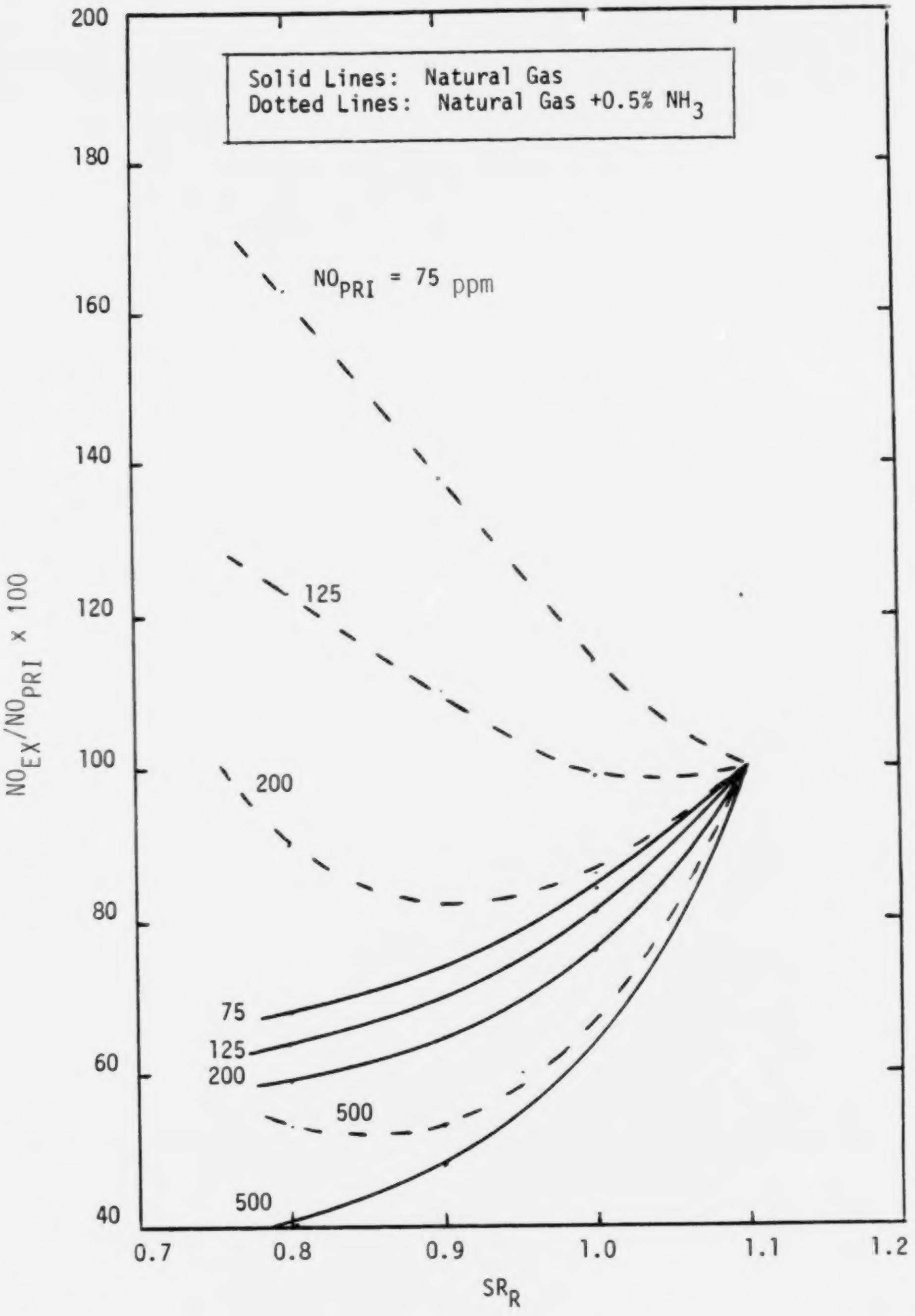

Figure 5-10: Comparison of Undoped and Ammonia-Doped Natural Gas Reburning

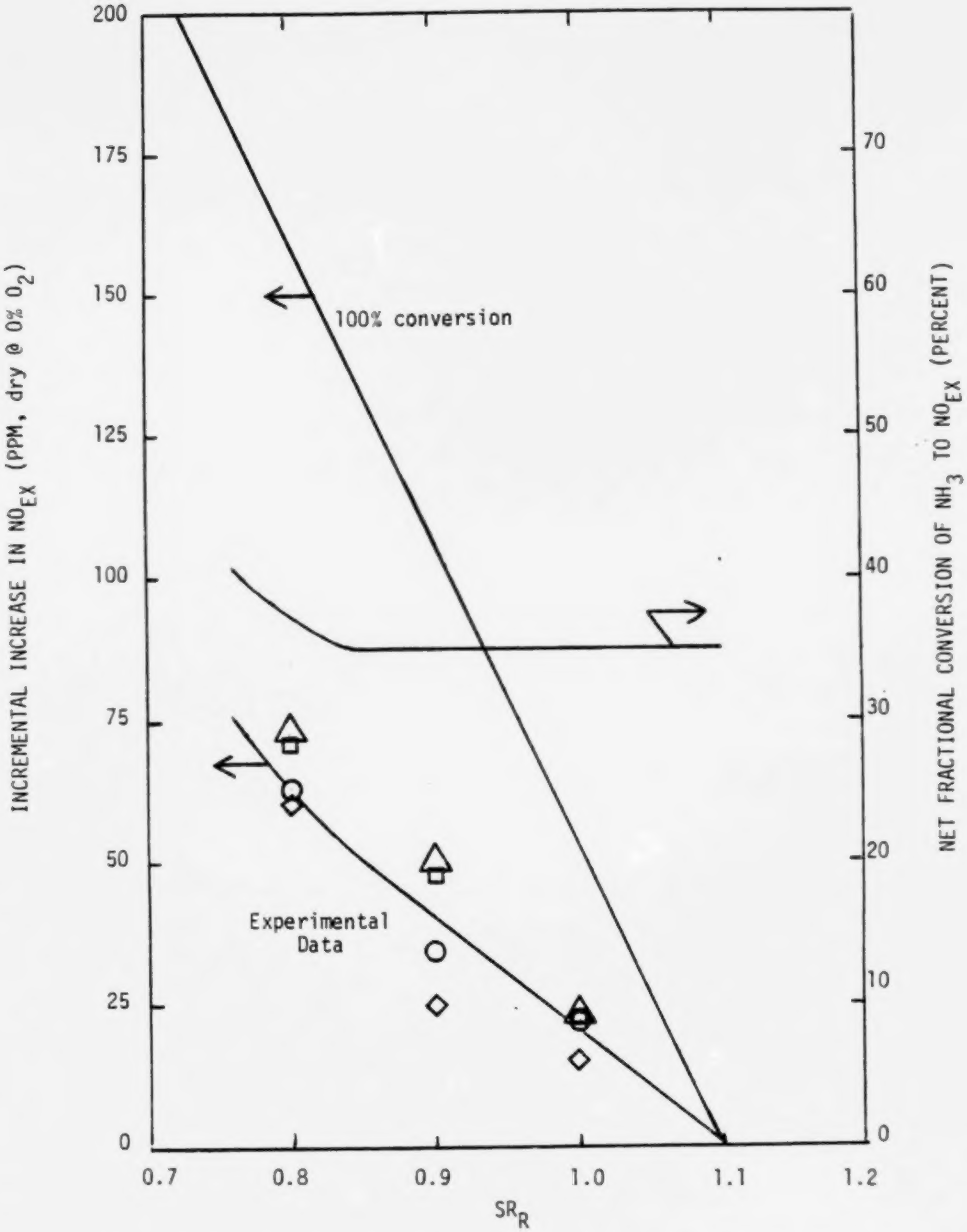

Figure 5-11: Net Fractional Conversion of Ammonia to Exhaust NO

results, shown in Figure 5-12, indicate that increasing ammonia dopant flow rate results in a monotonic increase in exhaust NO.

If it is assumed that the NO destruction process is independent of the NO formation process, the net yield of NO from secondary ammonia oxidation may be calculated as the difference between doped and undoped trials. The fractional conversion is then the ratio of this difference in measured NO to the NO yield for 100 percent conversion of secondary ammonia to NO. Figure 5-13 shows that the net fractional conversion of ammonia dopant to NO is less than 50 percent with the apparent fractional conversion decreasing with increasing dopant flow. This general trend is consistent with numerous fuel NO_x formation studies.

For 0.5 percent ammonia dopant, a wide range of I/O data was obtained. The results shown in Figure 5-11 indicating secondary fuel NO formation to be independent of NO_{PRI} suggest that the NO formation and destruction processes are independent. Detailed tests, discussed in Section 5.2, are required to confirm this behavior.

Based on these results, it is concluded that hypothesis 2 is correct. That is, NO_x reduction by the reburning process is adversely influenced by the presence of bound nitrogen in the secondary fuel, especially for low primary NO_x.

5.1.3 Reburn Zone Residence Time

Reburn zone residence time was varied by holding the location of secondary fuel injection fixed at 1.02 m (40 in.) and varying the location of final air addition. At the nominal final air addition location of 1.63 m (64 in.), the bulk residence time in the reburning zone is approximately 200 ms. By varying the location of final air injection from 1.2 m (48 in.) to 2.30 m (90 in.), the bulk residence time was varied from 67 ms to 420 ms. All other input parameters were held constant at nominal values.

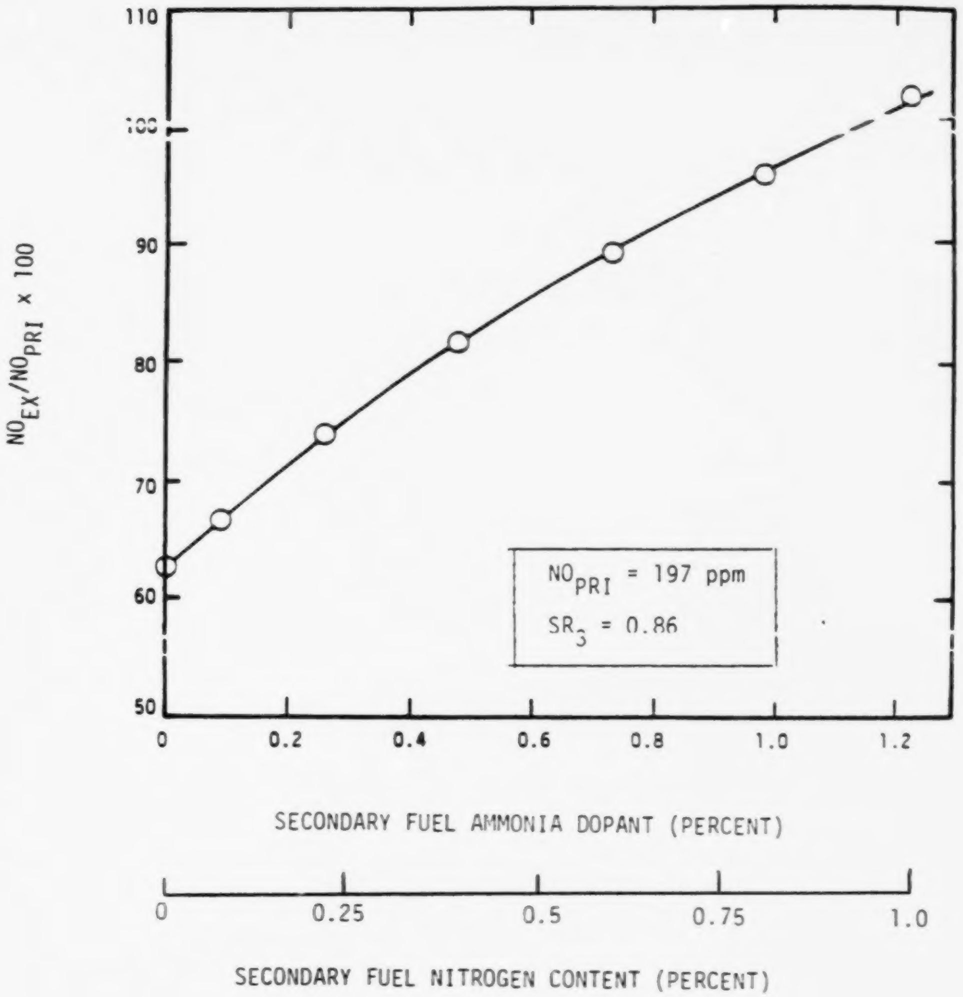

Figure 5-12: Effect of Ammonia Dopant for Natural Gas Reburning

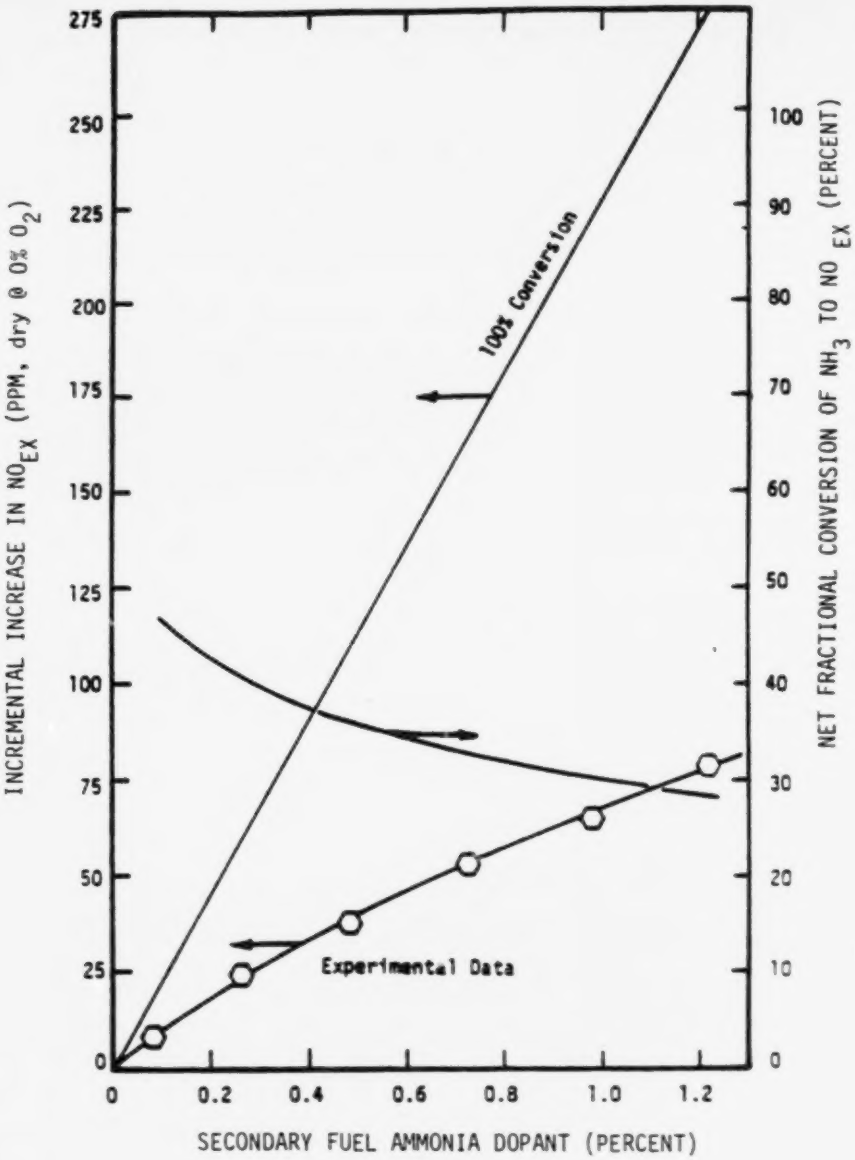

Figure 5-13: Net Fractional Conversion of Ammonia to Exhaust NO

The data shown in Figure 5-14 for both undoped and doped (0.5 percent ammonia) natural gas reburning indicates that NO destruction increases with increasing zone 3 residence time. Further, it is observed that the undoped natural gas secondary fuel curves approach symptotic behavior. This suggests that approximately 66 cm (26 in.) is required to complete the NO destruction reactions for all portions of the flow field. Though the average combustion gas velocity in the boiler is about 3.1 m/sec (12 ft/sec), the peak centerline velocity in zone 2 was shown to be approximately 14 m/sec (47 ft/sec) (see Figure 4-8). Thus, while the bulk reburn zone residence time is about 200 ms, the minimum reburn zone residence time is about 50 ms. This suggests that the characteristic chemical time for the overall reburn zone reactions is about 50 ms. Detailed tests, described in Section 5.2, verify this estimation.

For the ammonia-doped natural gas reburn tests shown in Figure 5-13, net NO reduction is more strongly influenced by reburn zone residence time (relative to undoped tests). This is probably due to the conversion of ammonia to N_2 in the reburn zone. As SR_3 decreases, the amounts of secondary natural gas and secondary ammonia dopant increase, and the dependence of NO reduction on zone 3 residence time becomes more pronounced. The optimum SR_3 and maximum NO reduction for ammonia-doped reburning are obviously functions of residence time.

It should be pointed out that the above arguments are only semi-quantitative, with detailed measurements required to substantiate the results. Residence time tests on the pilot-scale facility are limited due to radial variations in the combustion gas properties, and due to the inability to hold all other parameters perfectly constant. For instance, as reburn zone

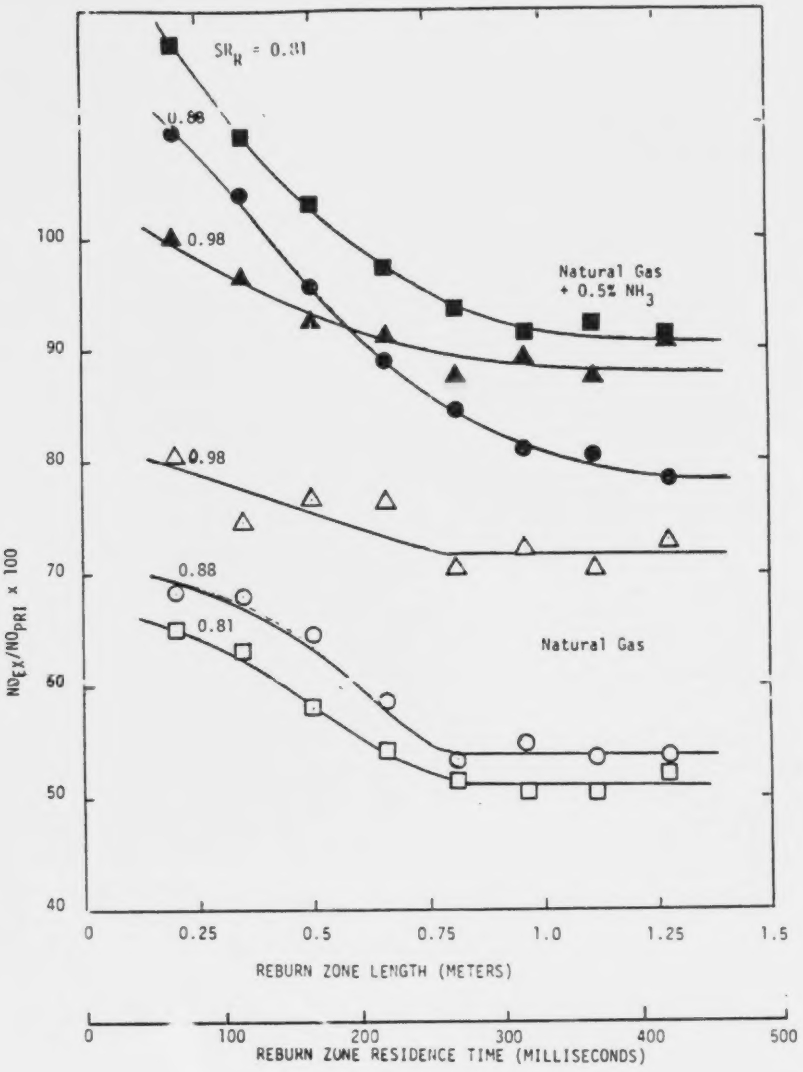

Figure 5-14: Effect of Reburn Zone Length for Natural Gas Reburning

residence time is increased by moving the location of final air addition further downstream in the boiler, the temperature at the point of final air addition changes slightly. Thermal effects on the reburning process are discussed in Section 5.4.

5.1.4 Primary Zone Stoichiometry

The amount of excess air in the primary zone, zone 2, influences both NO production in the primary zone and NO destruction in the reburning zone. For a standard burner, the level of NO_x produced is a function of excess air. For the low NO_x precombustion chamber burner used in this study, primary NO_x was shown to be strongly dependent on excess air (see Figure 4-5). For investigation of the effect of primary zone stoichiometry on the reburning process, primary NO_x was held constant with changing primary excess air by varying the amount of ammonia fed into the primary burner. Thus, the effect of primary zone stoichiometry on the reburning process was isolated.

To quantify the influence of SR_2 on reburning, data was obtained to compare NO reduction at a nominal 200 ppm primary NO_x level for SR_2's ranging from 0.95 to 1.14. The data, shown in Figure 5-15 for undoped natural gas reburning, indicate that the influence of SR_2 is primarily one of determining the amount of secondary fuel necessary to create a fuel-rich reburning stoichiometry. NO reduction is determined predominantly by reburn zone stoichiometry, independent of primary zone stoichiometry. However, for a fuel-rich primary zone, it requires less secondary fuel to reach a fuel-rich reburn zone condition, and secondary flame radicals may be insufficient to drive the NO destruction mechanism to the high levels achieved for a fuel-lean SR_2. Alternatively, with a high excess air level in the primary zone (15 percent or greater), a high flow rate of secondary fuel is required to achieve

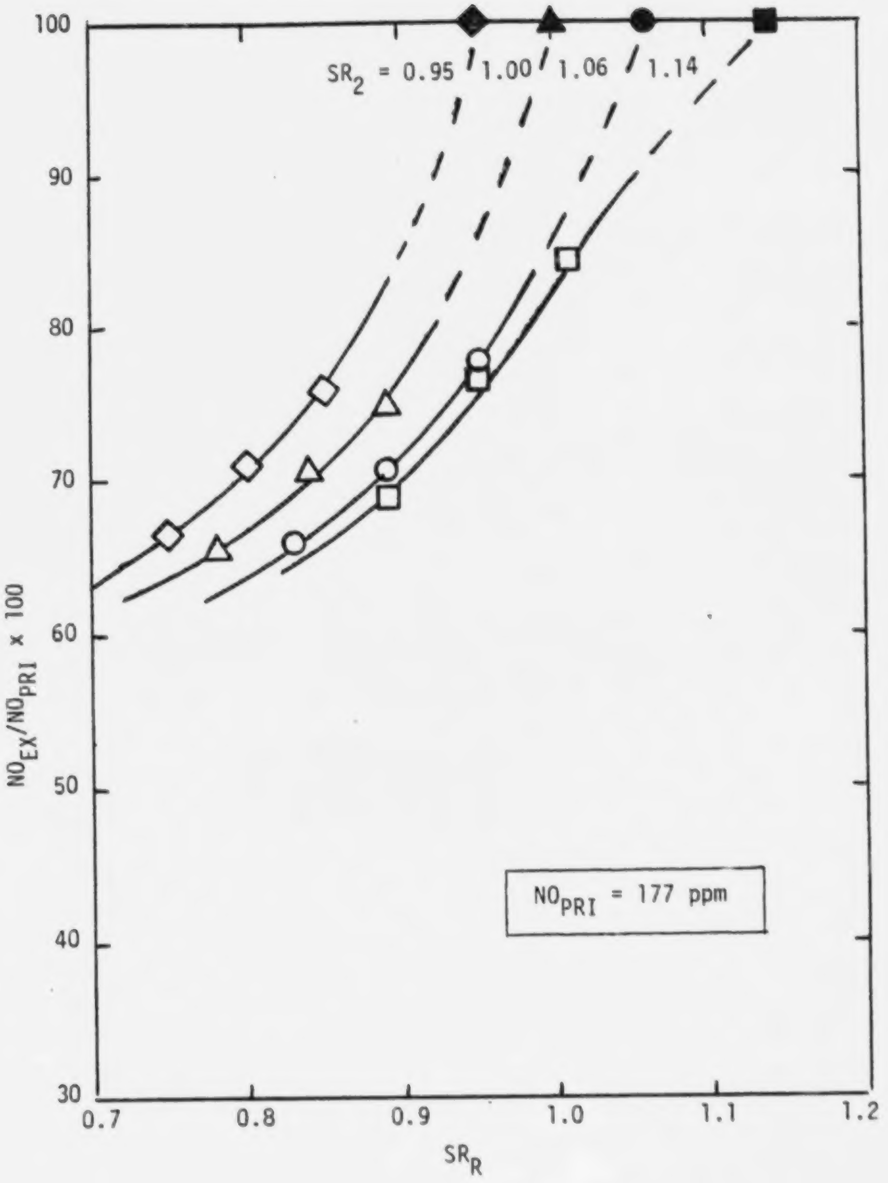

Figure 5-15: Effect of Primary Zone Stochiometry for Natural Gas Reburning

a fuel-rich reburn zone condition. This may result in increased reburn zone NO formation (especially for nitrogen-containing secondary fuels), which reduces the overall NO reduction via reburning. Moreover, in practical applications, higher primary zone excess air level will result in higher primary NO_x concentrations, and, thus, higher overall NO_x concentrations. Assuming that a fuel-lean primary zone is desirable, optimal primary zone stoichiometries for NO_x control by reburning application are found to be between 1.0 and 1.1.

5.1.5 Burnout Zone Stoichiometry

An I/O test series was performed to determine the effect of overall excess air on the reburning process. In this test series, primary and reburn zone stoichiometries were held constant ($SR_2 = 1.07$, $SR_3 = 0.86$), primary NO_x was fixed at 197 ppm, and burnout zone excess air was varied from zero to 20 percent. The data shown in Figure 5-16 show that, with dilution effects removed (NO corrected to zero percent O_2), the influence of final excess air is very small. This is in sharp contrast to the influence of excess air on primary burner NO_x. The long fuel-rich reburn zone residence times and low temperatures at the exit of the reburn zone result in low NO_x formation in the burnout zone. Thus, final excess air level may be chosen to provide sufficient burnout of the secondary fuel without the penalty of increased NO_x emissions.

5.1.6 Primary Fuel

Tests were performed using a distillate fuel oil as the primary fuel, rather than natural gas. The chief difference between the two fuels is the molar carbon-to-hydrogen ratio. For natural gas, the carbon-to-hydrogen ratio is nearly that of methane: 1 to 4. For the distillate fuel oil, the carbon-to-hydrogen ratio is approximately 1 to 2. This results in different carbon dioxide and water concentrations in the fuel-lean primary zone effluent. At zero percent O_2, CO_2 concentration is about 16 percent (dry) for

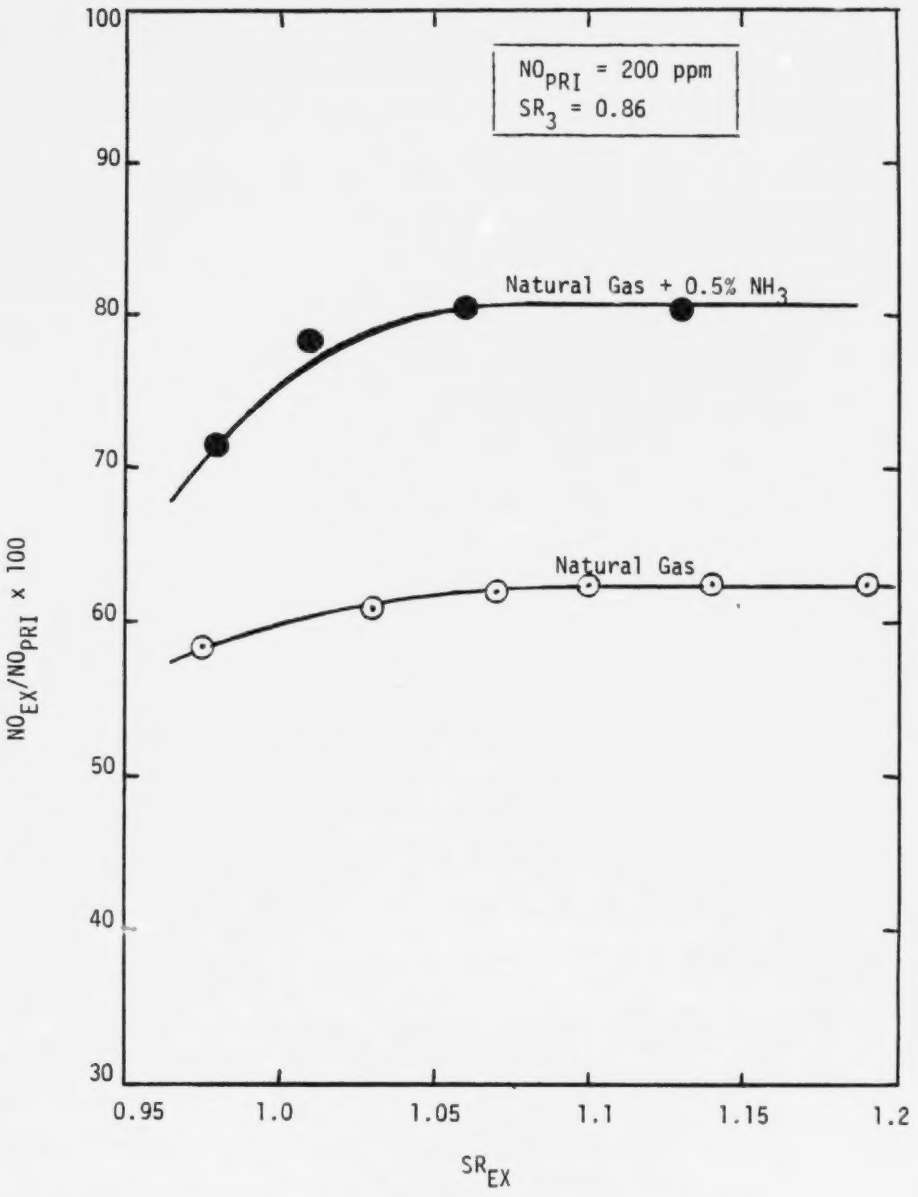

Figure 5-16: Effect of Burnout Zone Stoichiometry for Natural Gas Reburning

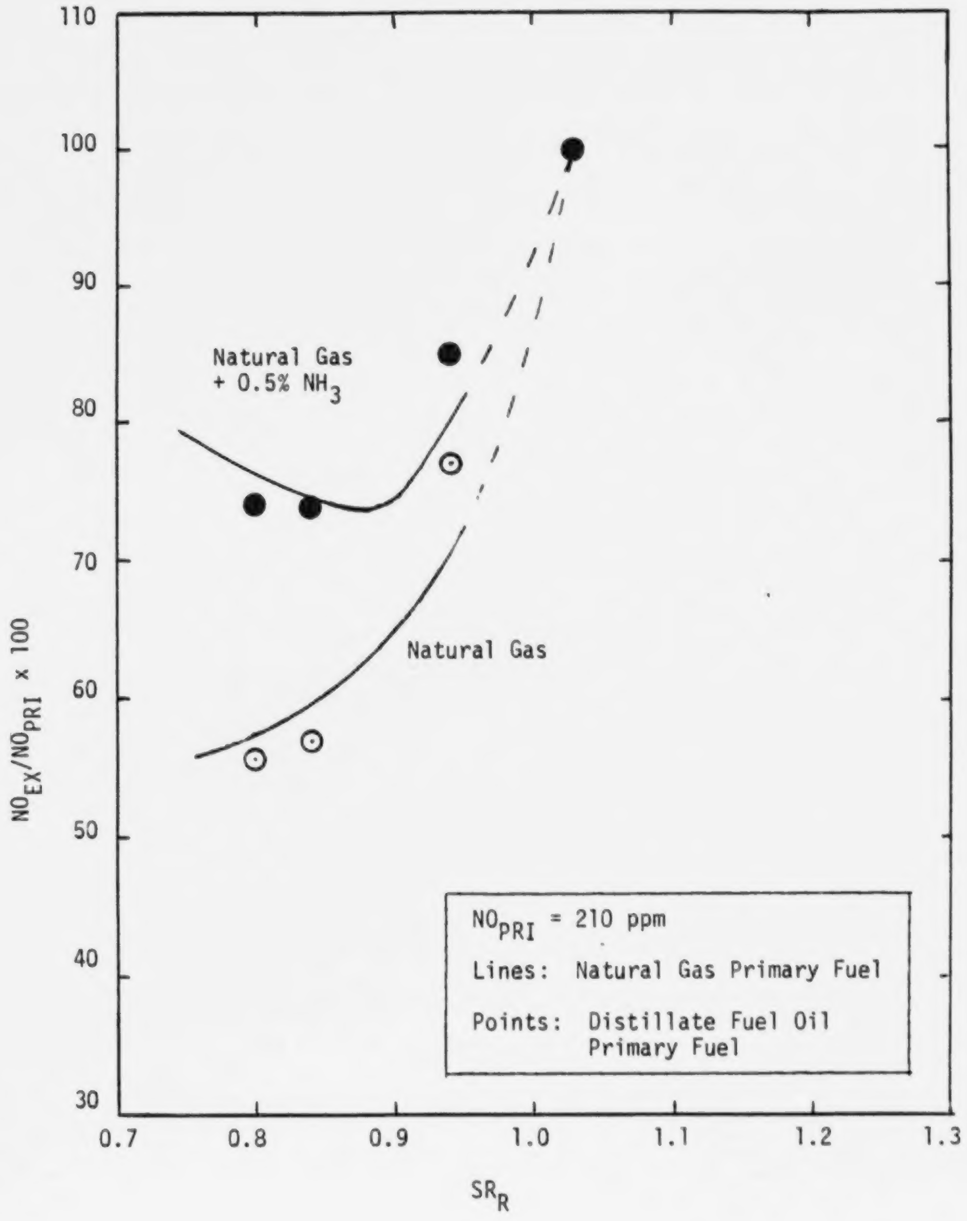

Figure 5-17: Effect of Primary Fuel Type for Natural Gas Reburning

distillate oil, versus 12 percent (dry) for natural gas; H_2O concentration is 12 percent for distillate oil, versus 18 percent for natural gas.

Primary fuel type effects on primary NO were negated by controlling NO_{PRI} by adjusting primary ammonia flow. The data presented in Figure 5-17 show that there is no significant effect of primary burner fuel type when reburning with natural gas at equivalent primary NO_x and reburn zone stoichiometry conditions. This is not surprising since the primary reactions for the proposed NO_x destruction mechanism do not involve CO_2 and H_2O concentrations directly. However, secondary fuel type is important. Fuel oil reburning is discussed in Section 6.

5.2 DETAILED TESTS

A series of tests were performed to measure the thermal, aerodynamic, and chemical conditions in the firetube package boiler during reburning application. Spatial and temporal variation of these measurements provide a better understanding of the physical and chemical processes that characterize the reburning process.

A test matrix of the detailed trials is presented in Table 5-2. An operating condition was established and maintained for the duration of the test. Each test consisted of in-flame axial and radial temperature measurements, radial velocity measurements, and axial and radial chemical species measurements. These tests required a total of about twelve hours to complete, being conducted in a single test day to avoid changes in fixed parameters during overnight load changes. Many of the tests were repeated.

5.2.1 Temperature and Velocity Profiles

Axial temperature profiles as a function of SR_3 are presented in Figure 5-18. These data were taken at a 13.3 cm (5.25 in.) radius. Shown for comparison is the axial temperature profile without reburning. A maximum

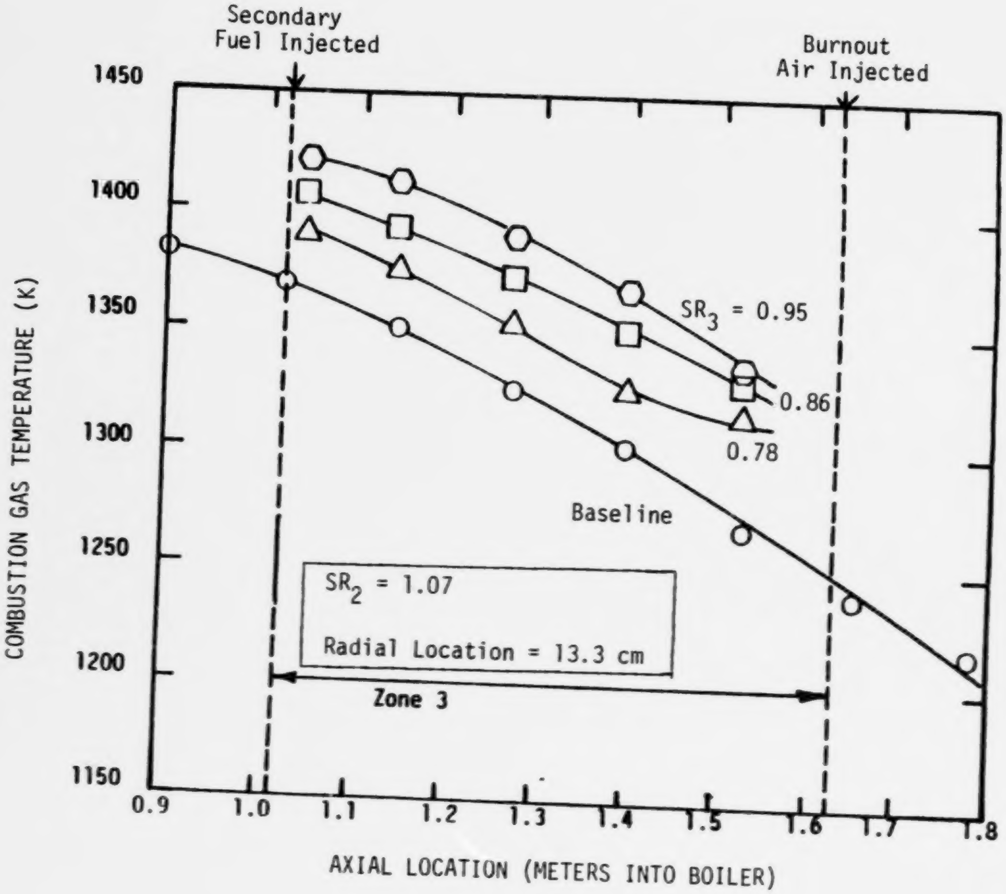

Figure 5-18: Reburn Zone Axial Temperature Profiles

TABLE 5-2. DETAILED TRIAL TEST MATRIX -- NATURAL GAS REBURNING

Figure Number	NO_{PRI} (ppm, dry at 0% O_2)	SR_R	Secondary Fuel Ammonia (percent)	Reburn Zone Length (m)	Insulation
5-25	206	0.97	0	0.61	-
5-26	206	0.86			
5-27	222	0.78			
5-28	122	0.87			
5-29	49	0.86			
5-30	206	0.95	0.5	0.61	-
5-31	198	0.87			
5-32	216	0.78			
5-33	119	0.86			
5-34	69	0.86			
5-54	193	0.86	0	0.69	Zone 2
5-55	185	0.91	0.5		

temperature rise of 66°C (150°F) was achieved, for an SR_3 of 0.95 (which was the closest condition to a stoichiometric fuel/air ratio examined). The temperature at the start of the reburn zone is nominally 1400K (2060°F).

Figure 5-19 shows the radial profiles of temperature as a function of stoichiometry, measured 3.8 cm (1.5 in.) downstream of the secondary fuel injection. Peak temperatures ranged from 1375 to 1425K (2015 to 2105°F). Again, a radial temperature profile without reburning is shown for comparison. The cooling effect of the fuel boom is seen in the shift in boiler peak temperature, from centerline without reburning to approximately 12 cm (4.7 in.) with reburning.

Radial velocity profiles were measured at the entrance of the reburning zone, with secondary natural gas injected 3.8 cm (1.5 in.) upstream. Within the accuracy of the measurements, there were no discernable differences in velocity profiles for the three stoichiometries tested, as shown in Figure 5-20. This is to be expected since the secondary fuel injection mass addition rate is very low, relative to the mass flow rate from zone 2. A peak velocity of 12.8 m/sec (42 ft/sec) was measured at a 6.3 cm (2.5 in.) radius. At the nominal sample radius for axial reburn zone measurements, the velocity is 8.0 m/sec (26 ft/sec). The integrated velocity profile with respect to boiler cross-sectional area results in a mass flow determination within 5 percent of the measured input flows. Data quality was also verified by the high degree of repeatability in these results.

Axial velocity profiles were not measured. It was assumed that the velocity varied axially simply from density (i.e., temperature) variation. Axial temperature varied by only 5 percent over the 16 cm (2 ft.) length of the reburning zone. Thus, for the purpose of reburning zone residence time calculation, a constant velocity is assumed at a given radius. Errors due to

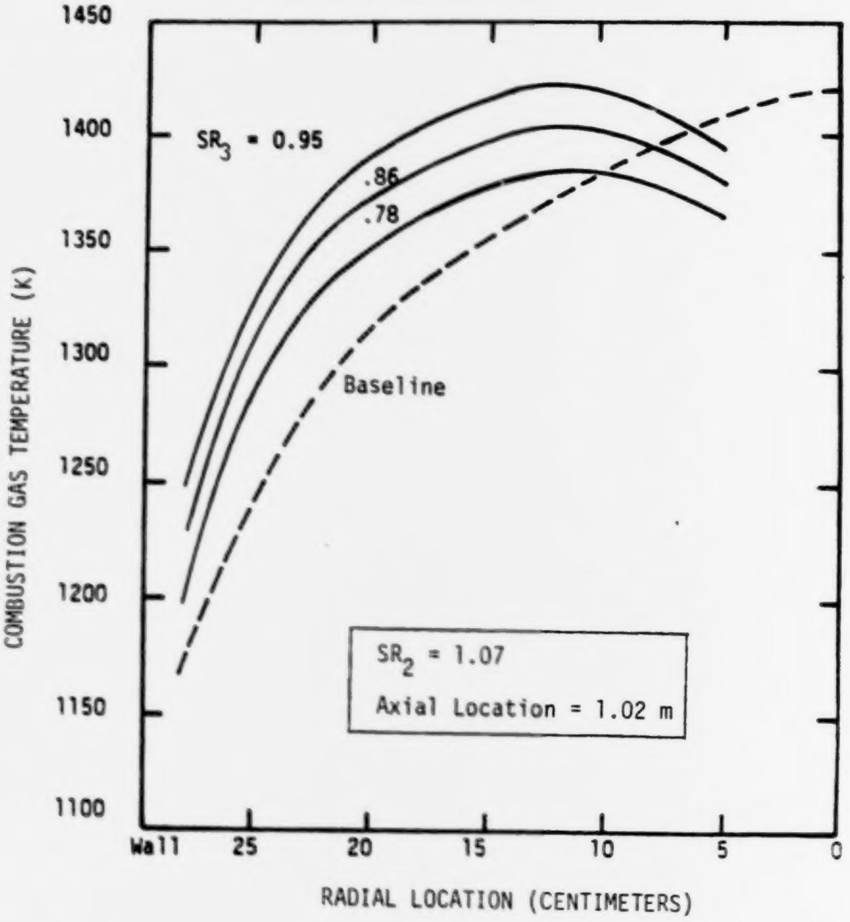

Figure 5-19: Reburn Zone Radial Temperature Profiles

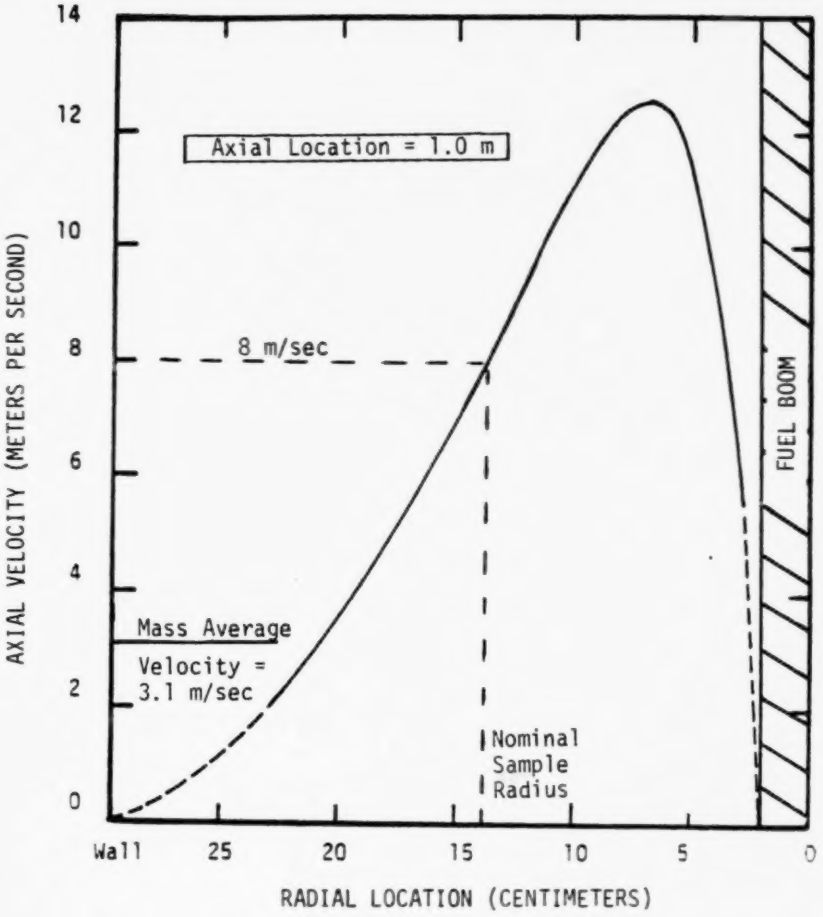

Figure 5-20: Reburn Zone Radial Velocity Profile

axial velocity variation are negligible compared to uncertainty in radial location, determination and velocity measurement.

At the three radial sample port locations of 13.3, 18.4, and 23.5 cm (5.25, 7.25, and 9.25 in.), reburn zone velocities of 8.0, 4.3 and 0.2 m/sec (26, 14, and 0.66 ft/sec) are estimated. The sensitivity of velocity to radius makes the uncertainty of these velocities high.

5.2.2 Uniform Secondary Fuel Injection Validation

Before discussing combustion gas species variation in the reburning zone, it is important to demonstrate that secondary fuel is injected uniformly into the primary zone effluent. If the reburn zone stoichiometry is uniform, then one set of axial measurements, at a nominal radius, will provide a good approximation of the total combustion gas species history in the reburn zone. Further, data from the various test conditions will be comparable given consistently uniform secondary fuel injection.

As discussed in Section 4.3, two sets of fuel injector spokes were constructed for the natural gas reburning tests. For high secondary fuel flow rates, 12-hole spokes were used. Using ammonia doped in the secondary fuel as a tracer, axial profiles of NH_3 were measured for the three nominal reburn load test conditions. Initial NH_3 concentration was calculated from the measured input flow rates. As shown in Figure 5-21, the 12-hole spokes provide good ammonia distribution for the high reburn load conditions (SR_3 of 0.86 and 0.78), but poor distribution for the low reburn load condition (SR_3 of 0.95). Good ammonia distribution is defined by close agreement between the measured NH_3 concentration near the injection point and the calculated NH_3 concentration given uniform distribution. At the lowest secondary fuel addition rate (SR_3=0.95), measured and calculated initial concentrations deviate by more than a factor of 2, which was considered unacceptable.

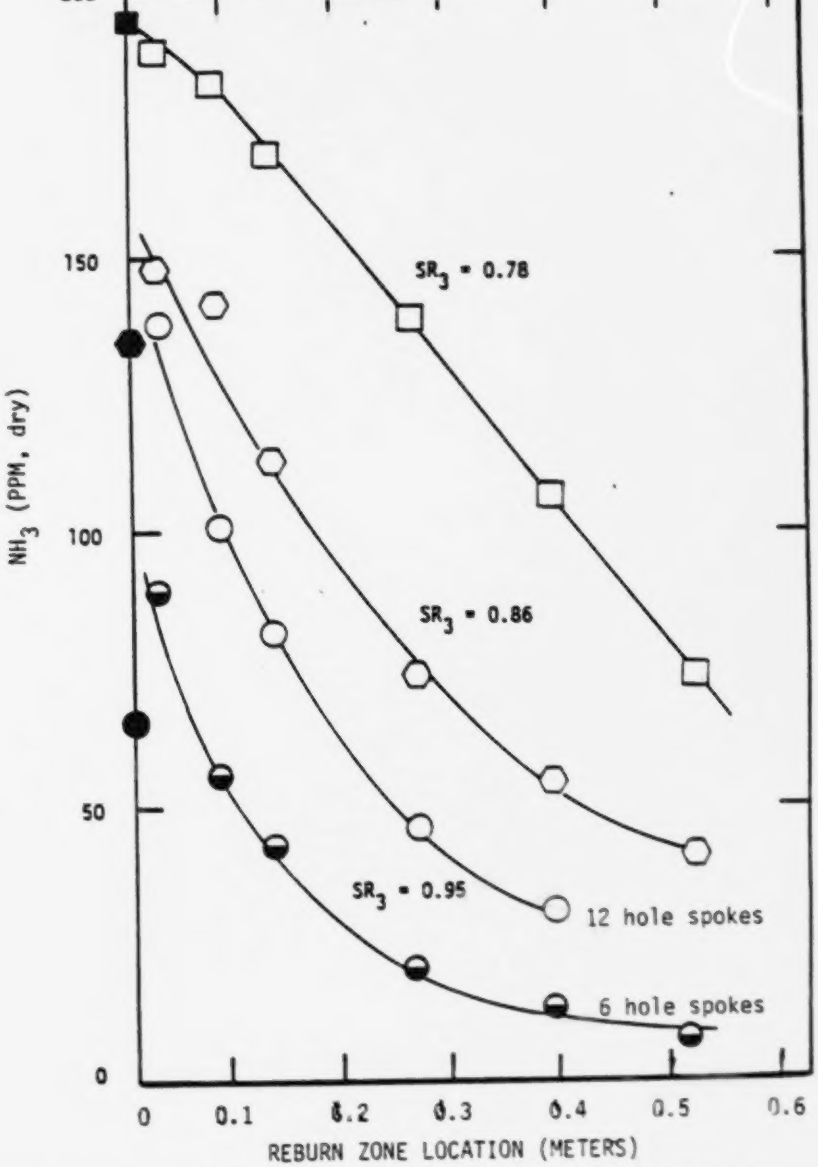

Figure 5-21: Degree of Uniformity of Spoked Secondary Fuel Injection

Analysis of this data indicated that for low secondary fuel flow rates the individual spokes are not acting as plenums. Instead of the secondary fuel and ammonia flow was injected nearer the boiler centerline than the boiler wall. To circumvent this problem, a second set of fuel spokes, each containing only 6 holes, was constructed. These spokes provided NH_3 profiles represented by the half-solid symbols in Figure 5-21. The maximum secondary flow for the second set of spokes was sufficient to achieve an SR_3 of no lower than 0.87 (for the nominal primary operating conditions).

The detailed tests were performed using the 12-hole spokes for the 0.78 and 0.86 SR_3 conditions, and the 6-hole spokes for the 0.95 SR_3 condition.

5.2.3 Chemical Species Characteristics

In-flame species samples were collected at the 13.3 cm (5.25 in.) radial location for each test condition listed in Table 5-2. Of the three sample ports available for axial traverses, this location represents the radius of highest velocity (8.0 m/sec, or 26 ft/sec), and, hence, maximum temporal resolution. Further, mass transport into this jet stream tube should be a minimum, relative to the other two locations.

Carbon and Hydrogen Chemistry

Before presenting nitrogenous species data, it is useful to consider carbon and hydrogen chemistry in the reburning zone. Understanding the destruction of hydrocarbons and the production of flame radicals is necessary for the understanding of nitrogen chemistry in the reburning process.

At the exit of the primary zone ($SR_2 = 1.07$), the temperature and major chemical species of the combustion gas (measured at a 13.3 cm radius) are listed in Table 5-3.

TABLE 5-3. TEMPERATURE AND MAJOR CHEMICAL SPECIATION ENTERING REBURN ZONE

T	(measured by suction pyrometer)	1367K (2000°F)
[H_2O]	(calculated from equilibrium)	17.6%
[CO_2]	(measured, dry)	11.1%
[O_2]	(measured, dry)	1.5%
[N_2]	(calculated by difference, wet)	71.6%

Into the primary zone effluent, natural gas was injected at the three nominal rates necessary to achieve reburn zone stoichiometries of 0.95, 0.86, and 0.78. The NASA equilibrium computer code [1] was used to predict reburn zone temperature, and CO, CO_2 and CH_4 concentrations. This data is compared to experimental values, measured at the 13.3 cm radius, in Table 5-4.

TABLE 5-4. TEMPERATURE AND CO AND CO_2 CONCENTRATIONS IN THE REBURN ZONE

	SR_3	Peak Temperature K(°F)	CO percent, dry	CO_2 percent, dry	CH_4 ppm, dry
Measured	0.95	1422 (2100)	0.90	11.0	-
Calculated		1442 (2136)	1.26	10.87	<1
Measured	0.86	1406 (2070)	1.3	10.9	12,000
Calculated		1358 (1984)	3.34	9.53	<1
Measured	0.78	1389 (2040)	1.7	10.5	-
Calculated		1273 (1831)	4.94	8.62	<1

Comparison of the experimental data and the calculations reveal the unusual situation of the measured temperature exceeding the equilibrium flame temperature (calculated assuming no heat extraction in the reburning zone).

The equilibrium flame temperature for the fuel-rich reburning condition is driven by the overall reaction:

$$CO_2 + CH_4 \longrightarrow 2CO + 2H_2 \qquad (5\text{-}4)$$

This reaction is endothermic by 71.8 kcal/gmole, resulting in the low adiabatic flame temperature calculation. Apparently, reaction 5-4 does not occur to any appreciable extent in the experimental reburning application. This results in the super equilibrium flame temperatures, as well as in high CO_2 concentrations and low CO concentrations. This observation was verified by total unburned hydrocarbon (THC) concentration measurements in the reburn zone for $SR_3 = 0.86$. Unburned hydrocarbons totaling more than 1 percent (dry), as methane, were found to persist in the reburn zone. Reburn zone carbon species profiles are shown in Figure 5-22. The less than complete hydrocarbon consumption is typical of a phenomenon known as cool flames (i.e., flames under 1600K). These flames are generally found to be unstable. As will be discussed in Section 5.4, relatively small increases in reburn zone temperature (achieved by insulating the primary zone boiler walls) resulted in complete hydrocarbon consumption.

Termination of hydrocarbon consumption removes the driving force that produces radical species (O, OH, and H). It is hypothesized that equilibration of the water-gas reaction;

$$CO + H_2O \rightleftharpoons CO_2 + H_2, \qquad (5\text{-}5)$$

describes the partial equilibrium state in the reburn zone. Engleman [17] provides the following empirical equation for the equilibrium constant, K_{5-5}

$$K_{5-5} = 2.39 \times 10^{-5}\ {}^{0.87}\exp\,(9{,}839/RT) \qquad (5\text{-}6)$$

This argument suggests that super equilibrium quantities of CH_4 and H_2 exist in the reburn zone and that flame radicals (such as CH and OH) are depressed, which may significantly impact nitrogen chemistry in the rich zone.

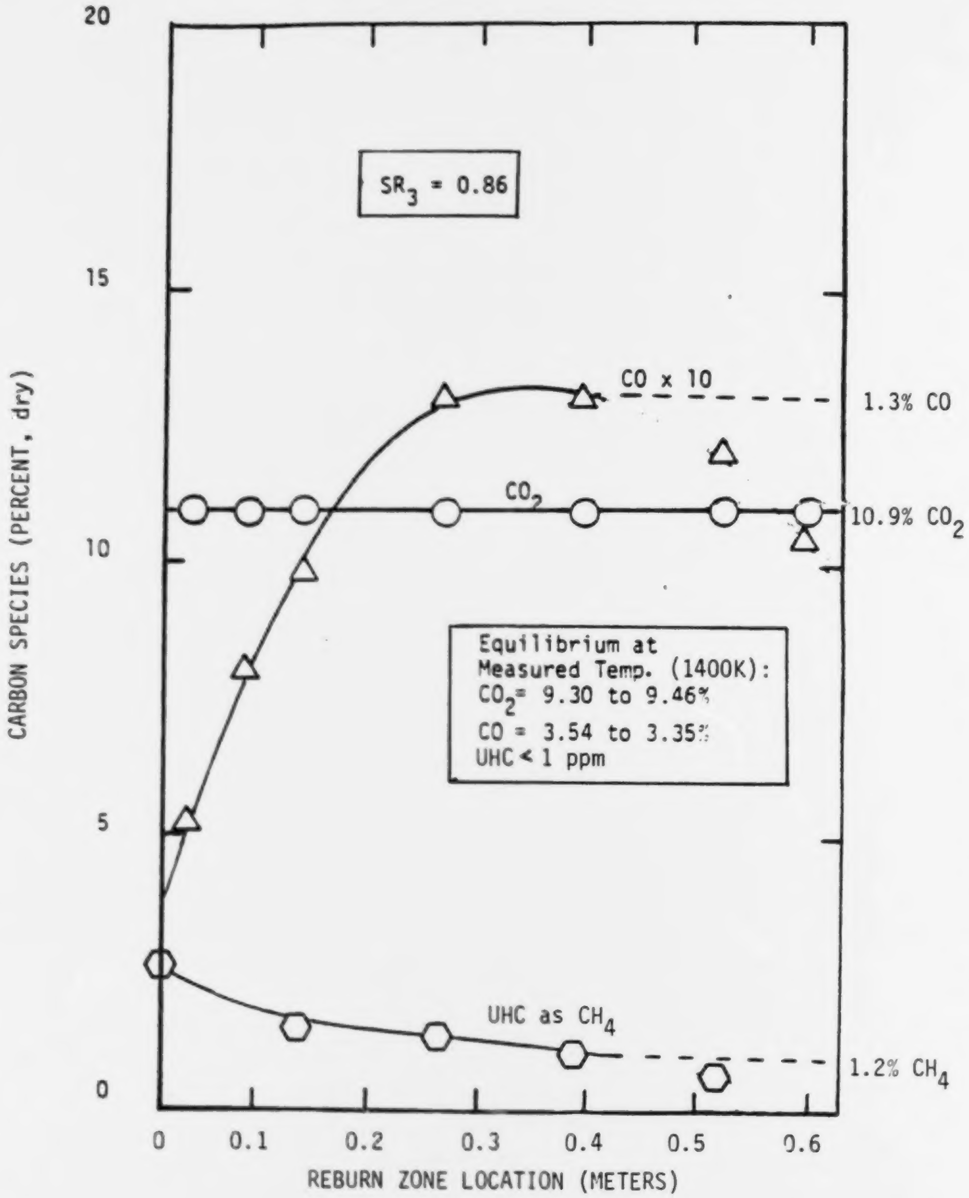

Figure 5-22: Reburn Zone Carbon Species Profiles for Natural Gas Reburning

Without actually measuring H_2 concentrations, two calculations can be made to check this scenerio. First, assuming that the significant product species in the reburning zone are CO_2, CO, CH_4, H_2, H_2O, O_2, and N_2, species concentrations for these seven species can be calculated from the four atom balance equations (O, H, C, N) and the measured concentration profiles of CO_2, CO, and O_2. At $SR_3 = 0.86$, the predicted CH_4 profile is compared to the measured profile in Figure 5-23, with excellent agreement being observed. Also shown in Figure 5-23 is the predicted H_2 profile, which is extremely sensitive to the measured concentrations of O_2, CO_2, and CO.

To further check this calculation, the water-gas equilibrium constant predicted by equation 5-6 is compared to the "measured" equilibrium constant calculated from the following defining equation.

$$K_{5-5} = \frac{[CO_2][H_2]}{[CO]]H_2O]} \qquad (5\text{-}7)$$

This comparison, shown in Figure 5-24, clearly indicates that equilibration of the water-gas reaction is a strong driving force to the kinetic process occurring in the reburn zone, and that partial equilibration is essentially achieved by about 50 ms (at the 0.4 m reburn zone location). It is noted that the approach to partial equilibrium is accomplished by substantial increase in hydrogen concentration.

This data, indicating that approximately half of the secondary fuel is not consumed in the reburning zone, implies that soot formation, via acetylene (C_2H_2) or other higher hydrocarbon formation, can occur. Some sooting was observed during the natural gas reburning tests. For fuel oils, reburning at these low temperatures resulted in excessive sooting. This is discussed in Section 6.

Another implication of the lack of secondary fuel burnout in the reburn zone is that the reduction of free radicals for NO_x destruction

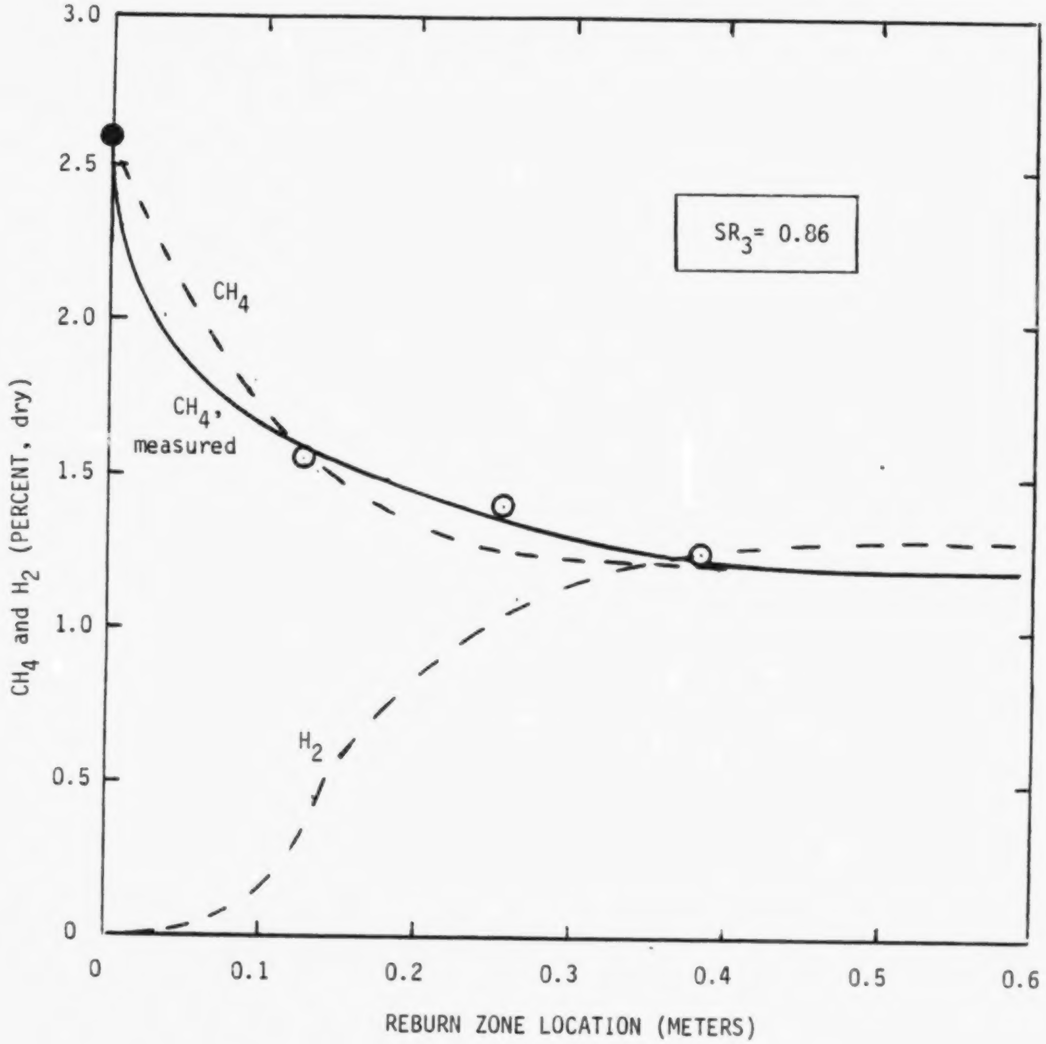

Figure 5-23: Calculated Reburn Zone UHC (as CH_4) and H_2 Profiles for Natural Gas Reburning

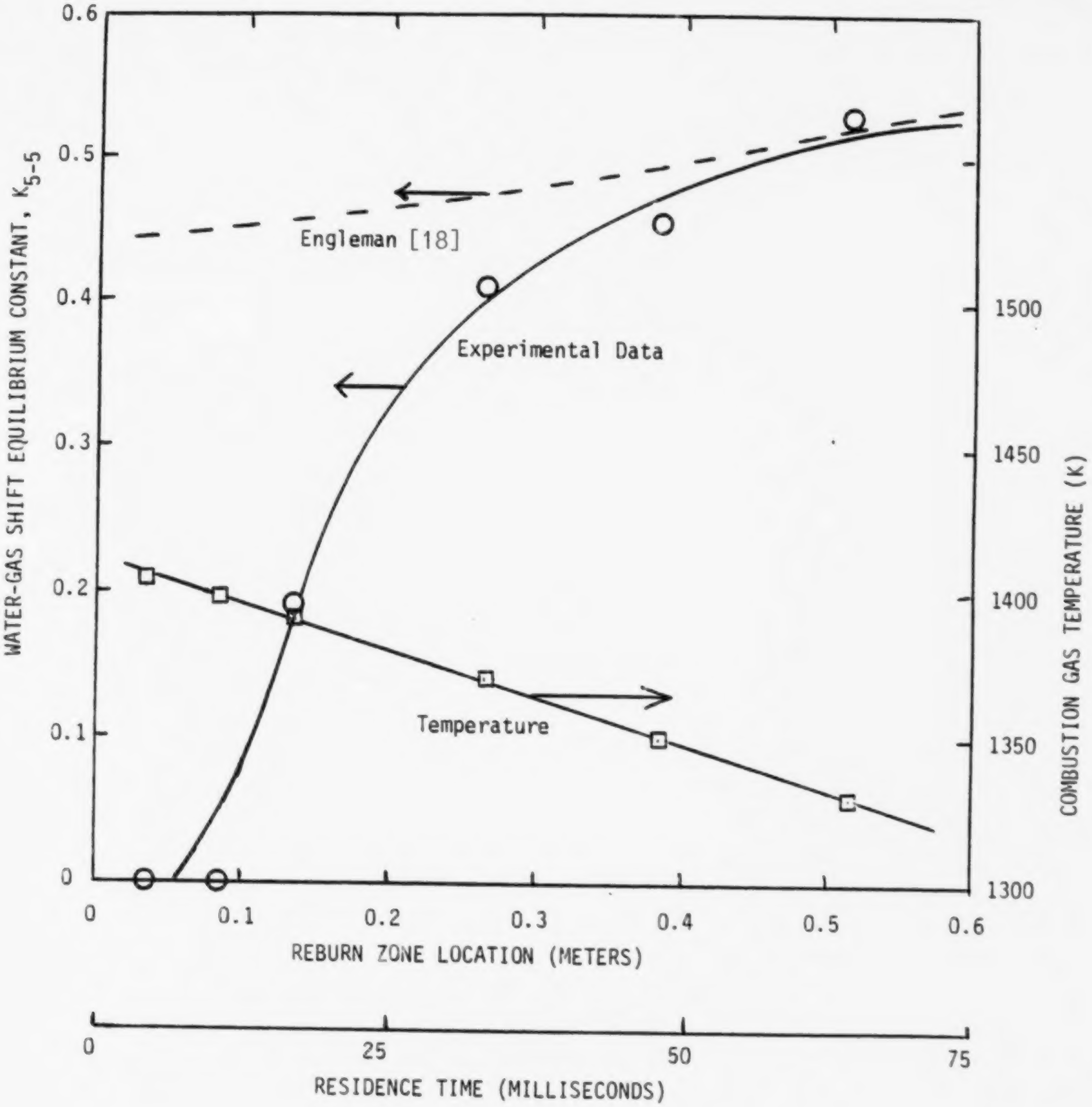

Figure 5-24: Water-Gas Equilibrium Constant

will reduce reburning effectiveness. The nitrogen species chemistry is discussed below.

Nitrogen Chemistry

As defined in Table 5-2, detailed tests were performed on conditions of various reburn zone stoichiometry (0.95, 0.86, 0.78) and primary NO_x concentration (200, 125, and 50 ppm) for both undoped and ammonia doped natural gas secondary fuel. Concentrations of fixed nitrogenous species are plotted against axial location in the reburning zone. Unless otherwise stated, these axial profiles were measured at the 13.3 cm (5.25 in.) radial location. The combustion gas velocity at this radius is about 8 m/sec (26 ft/sec). Thus, residence time can be computed by dividing the length by this velocity.

In comparing nitrogenous species concentrations in zones 2, 3 and 4, measured in dry molar quantities, dilution factors are employed. At the entrance of the reburning zone, secondary fuel is added, increasing the dry molar volume. The resulting dilution factor is defined as:

$$D_{2-3} = \frac{\text{Dry molar flow in zone 2}}{\text{Dry molar flow in zone 2 + molar flow of secondary fuel}} \tag{5-8}$$

Similarly, for converting zone 4 concentrations to equivalent reburn zone concentrations, the following dilution factor is used:

$$D_{4-3} = \frac{\text{Dry molar flow rate in zone 4}}{\text{Dry molar flow rate at zone 3 exit}}$$

For fixed primary load and excess air, these dilution factors are simply a function of SR_3. Table 5-5 lists the dilution factors used for the three nominal reburn zone stoichiometries.

TABLE 5-5. DILUTION FACTORS FOR COMPARING MOLAR QUANTITIES IN PRIMARY, REBURN AND BURNOUT ZONES

SR_3	D_{2-3}	D_{4-3}
0.95	0.988	1.036
0.86	0.976	1.125
0.78	0.963	1.202

Axial concentration profiles of NO, HCN, and NH_3 are presented in Figures 5-25 through 5-34. Several general comments need to be made concerning the preparation of these plots. First, the curve labeled TFN (total fixed nitrogen) represents the summation of NO, HCN, and NH_3. This represents nitrogen that is already in an oxidized state or in a readily oxidizable state. No significant N_2O concentrations were measured during these tests (always less than 1 ppm); hence, N_2O is not shown. Second, data is shown only up to the 1.52 m (60 in.) location. Beyond this point, upstream propagation of the final air (injected at 1.63 m or 64 in.) is observed.

A third comment concerns the HCN profiles. As discussed in Section 3.4, the collection efficiency for HCN was determined to be approximately 70 percent. Therefore, measured HCN concentrations were multiplied by 1.5 (equivalent to a 67 percent collection efficiency) before being plotted. Ammonia collection efficiency was found to be nearly 100 percent, so no correction was required on NH_3 measurements.

A fourth comment concerns the initial concentrations in the reburn zone. Initial NO concentration (represented by a solid circle on the left vertical axis) was determined by measuring primary NO concentration (at the O_2 level of the primary zone exhaust), and correcting that by the dilution of the secondary natural gas (D_{2-3}). Initial NH_3 concentration (represented by a

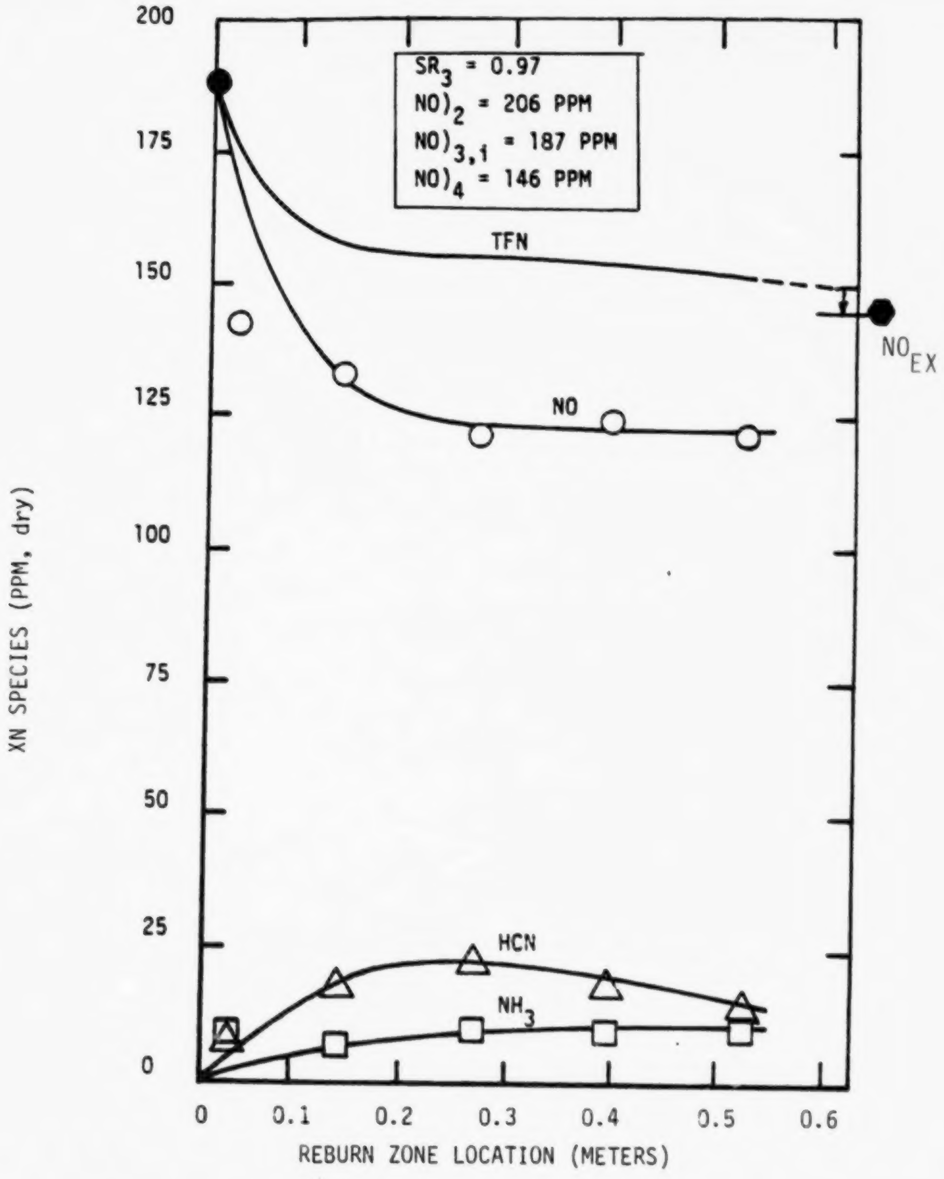

Figure 5-25: Reburn Zone Nitrogen Species Profiles for Natural Gas Reburning, SR_R = 0.97

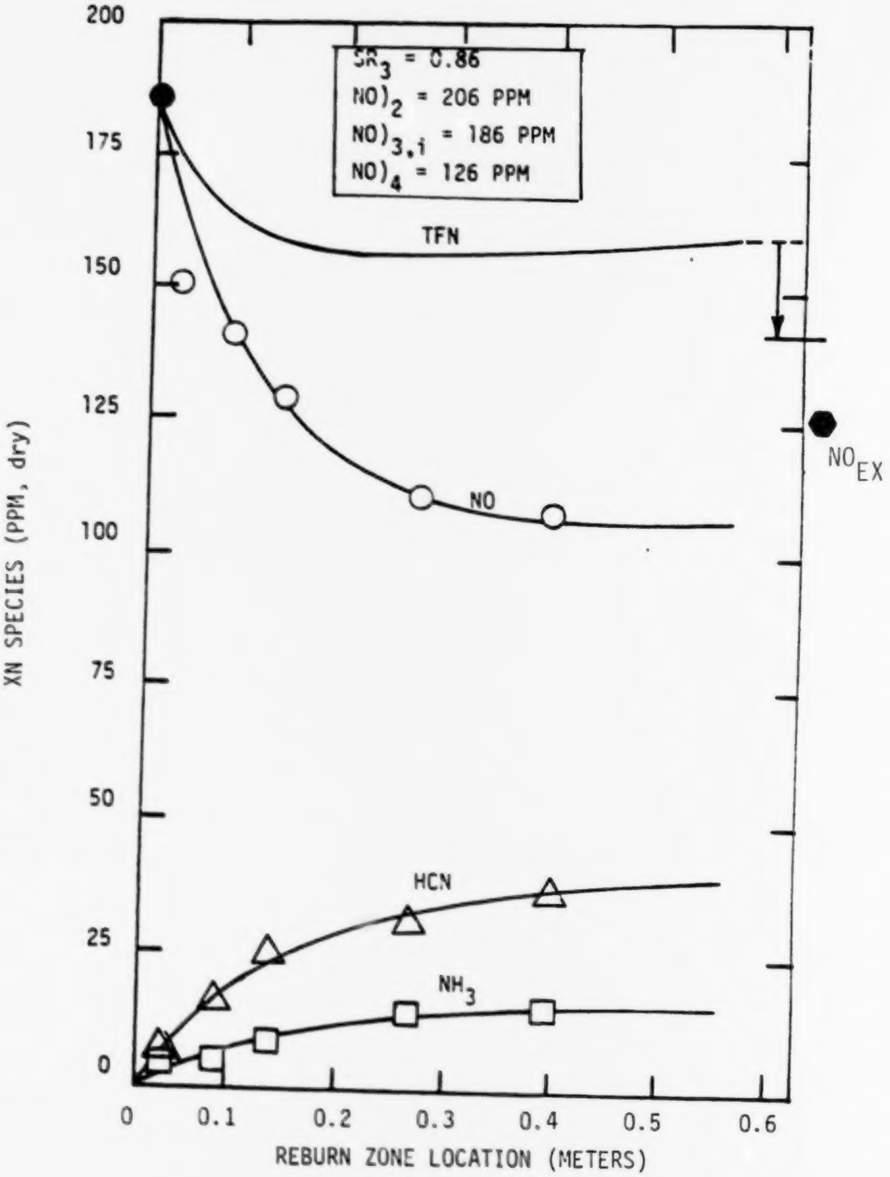

Figure 5-26: Reburn Zone Nitrogen Species Profiles for Natural Gas Reburning, SR_R = 0.86

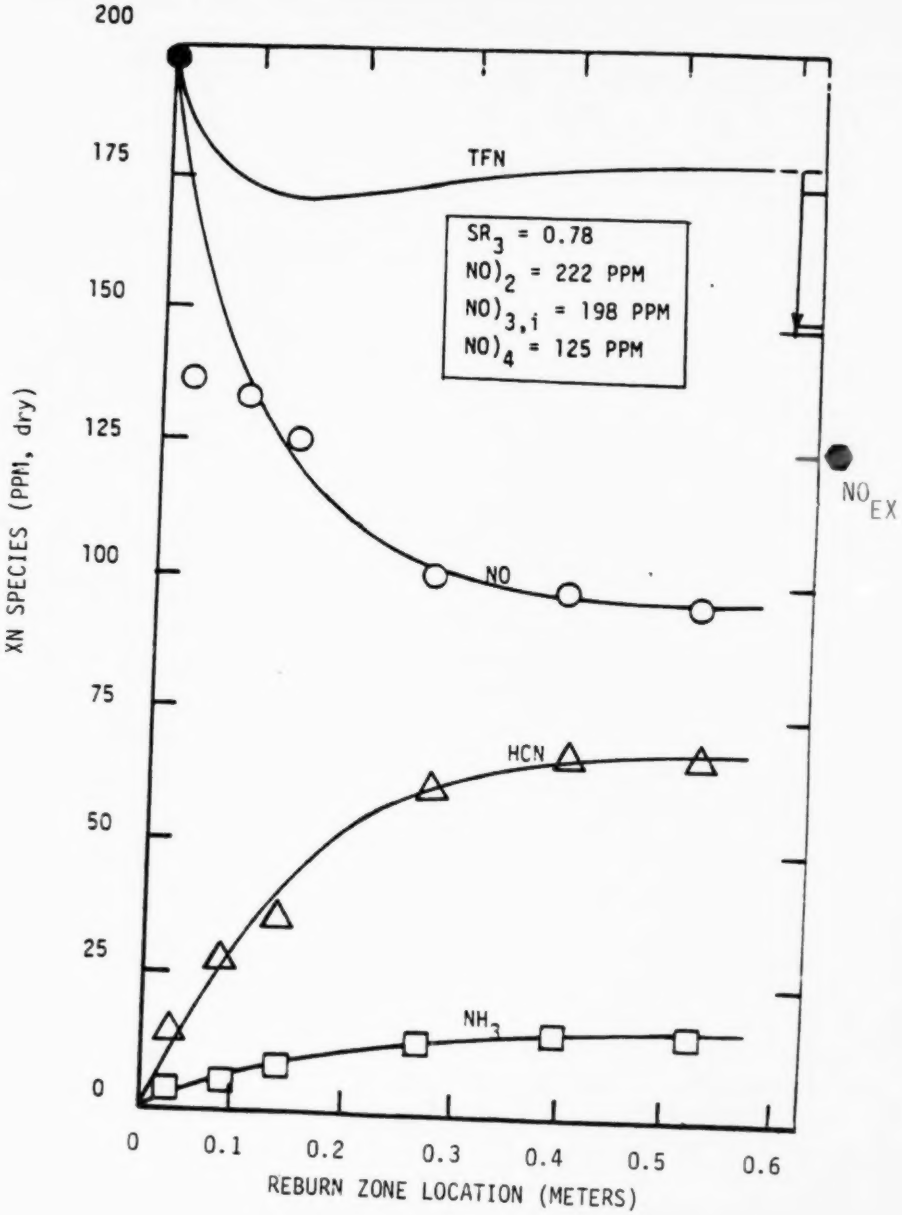

Figure 5-27: Reburn Zone Nitrogen Species Profiles for Natural Gas Reburning, SR_R = 0.78

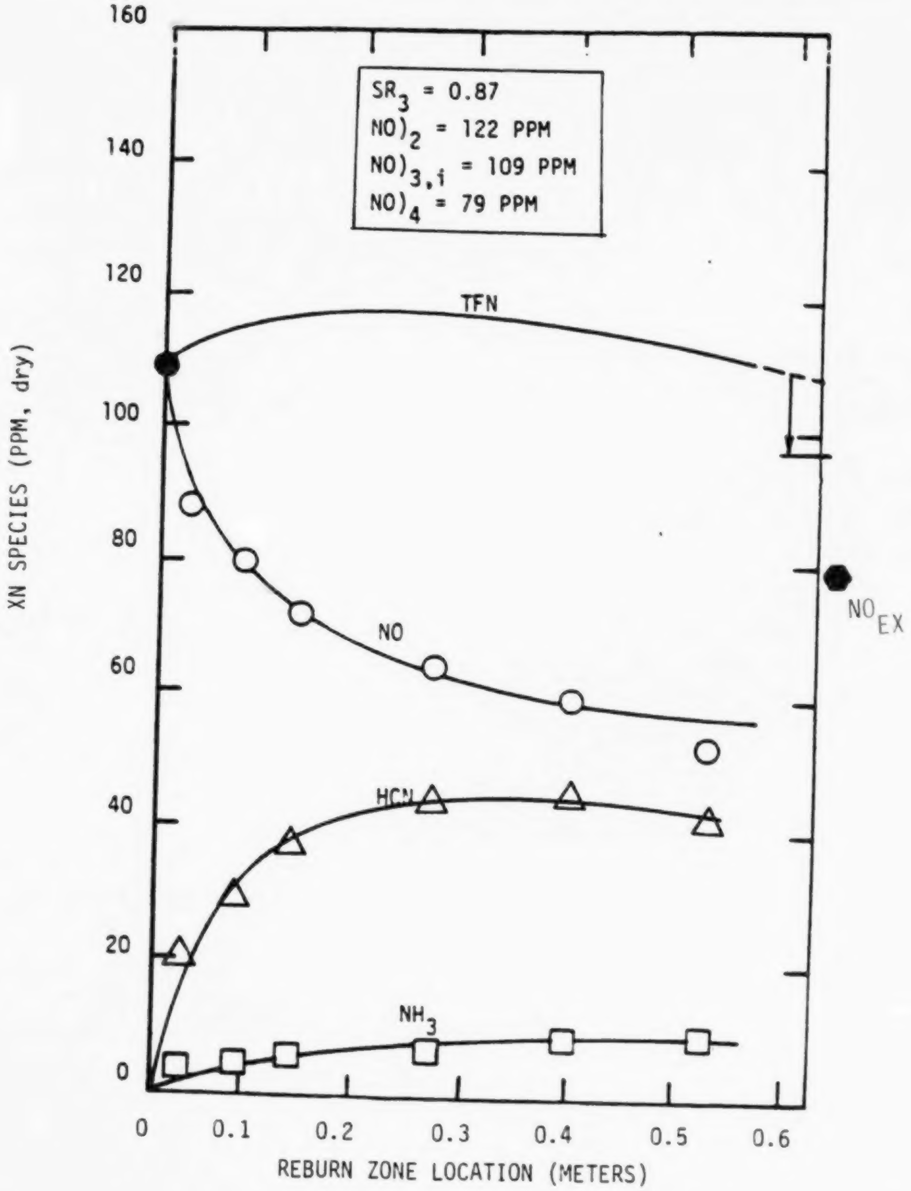

Figure 5-28: Reburn Zone Nitrogen Species Profiles for Natural Gas Reburning, NO_{PRI} = 122 PPM

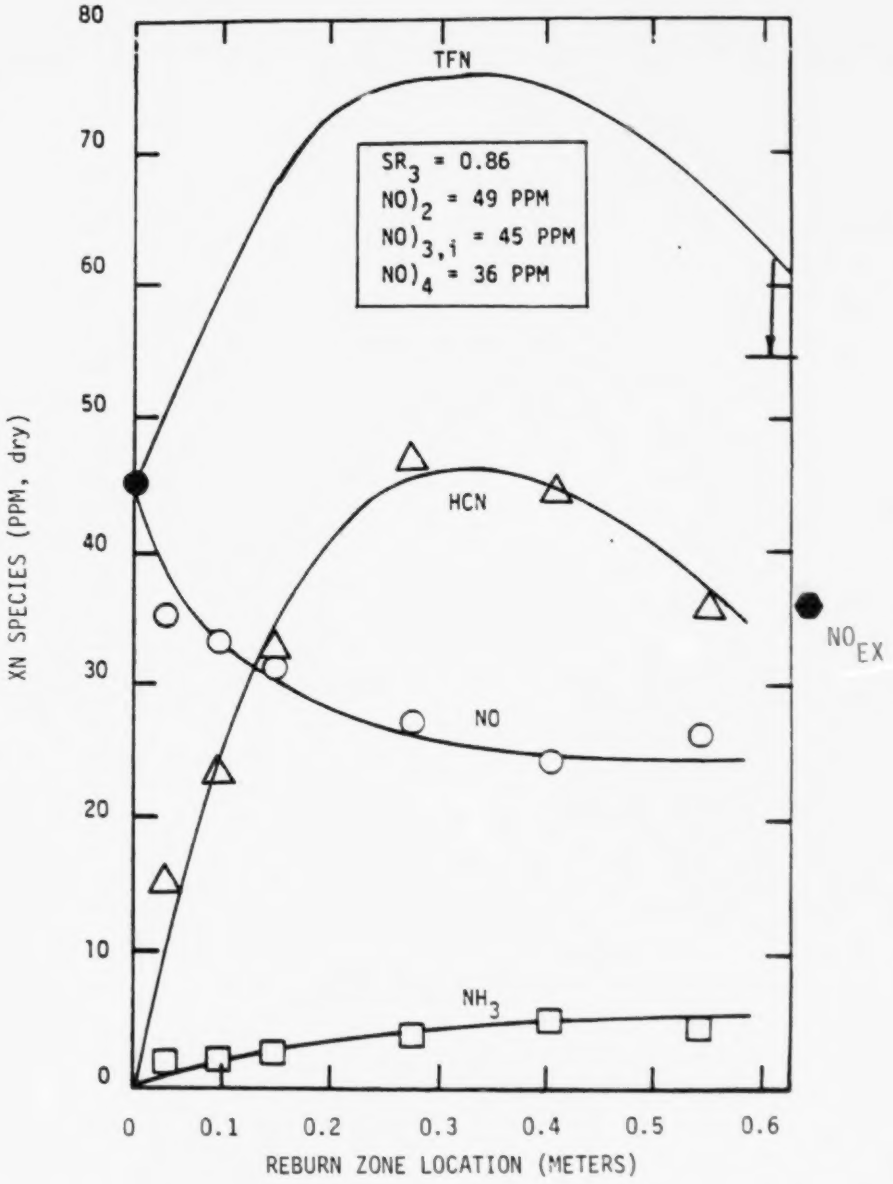

Figure 5-29: Reburn Zone Nitrogen Species Profiles for Natural Gas Reburning, NO_{PRI} = 49 PPM

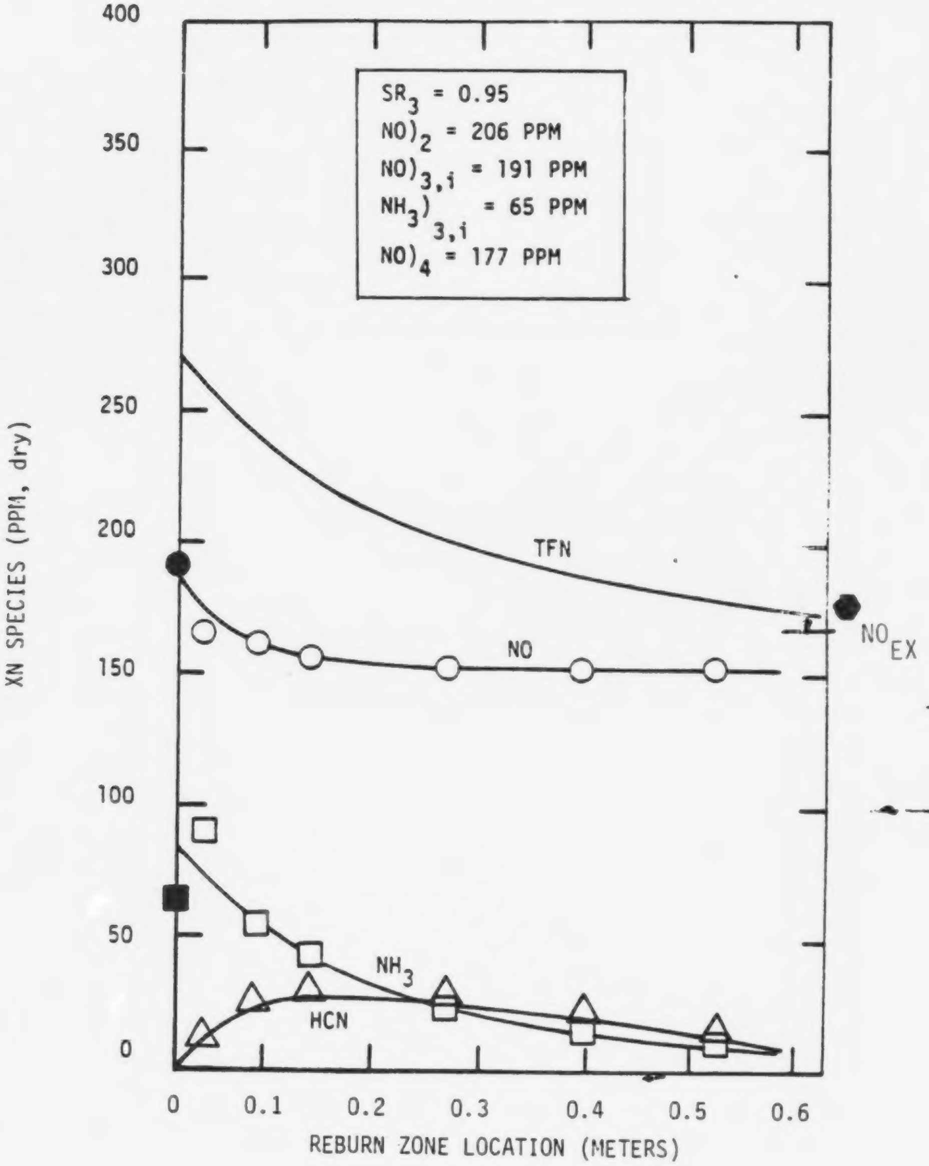

Figure 5-30: Reburn Zone Nitrogen Species Profiles for 0.5% Ammonia-Doped Natural Gas Reburning, SR_R = 0.95

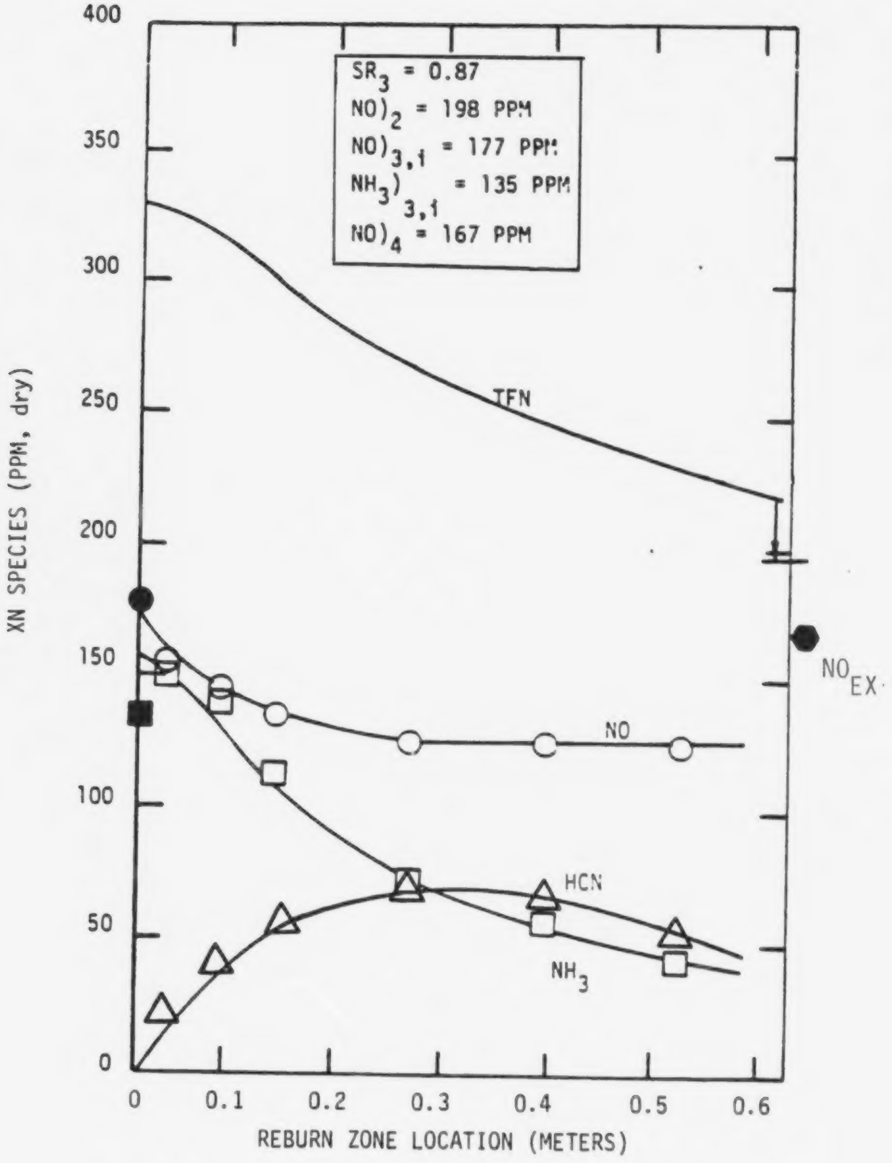

Figure 5-31: Reburn Zone Nitrogen Species Profiles for 0.5% Ammonia-Doped Natural Gas Reburning, SR_R = 0.87

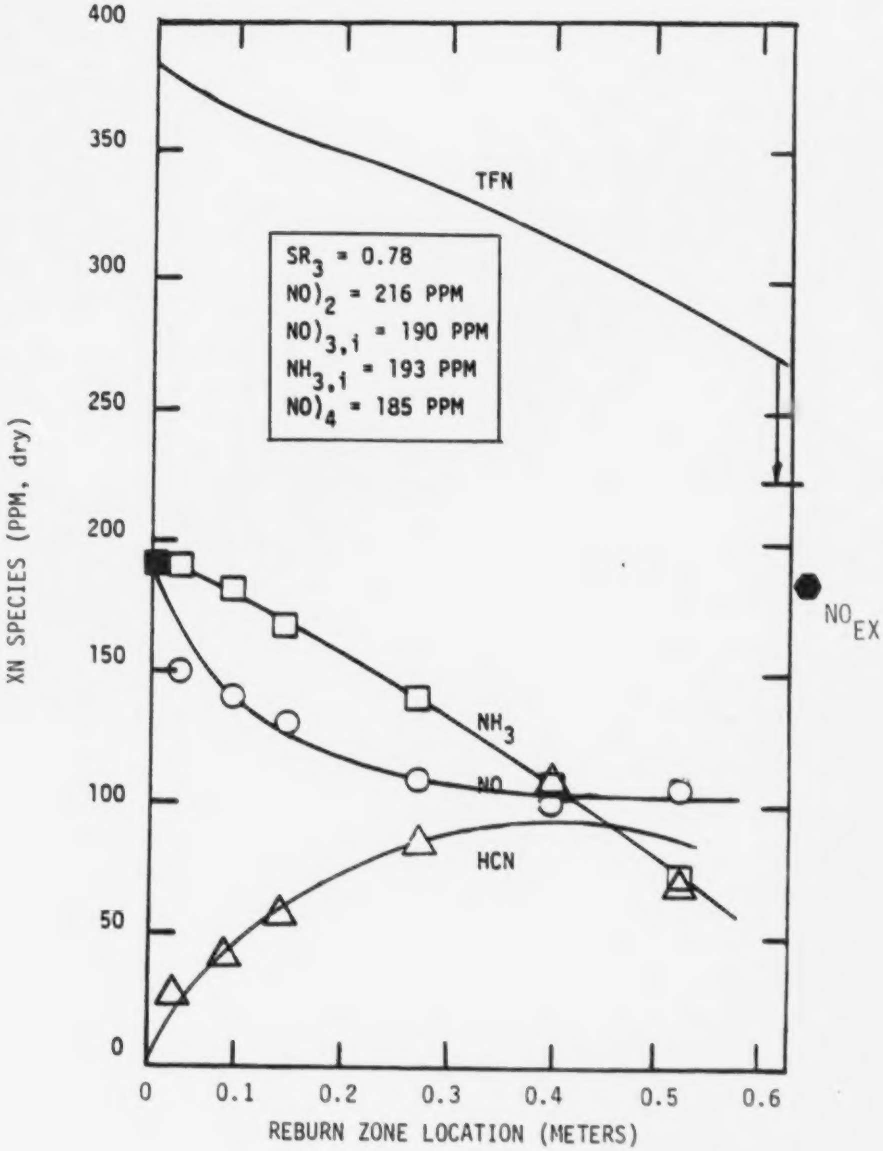

Figure 5-32: Reburn Zone Nitrogen Species Profiles for 0.5% Ammonia-Doped Natural Gas Reburning, SR_R = 0.78

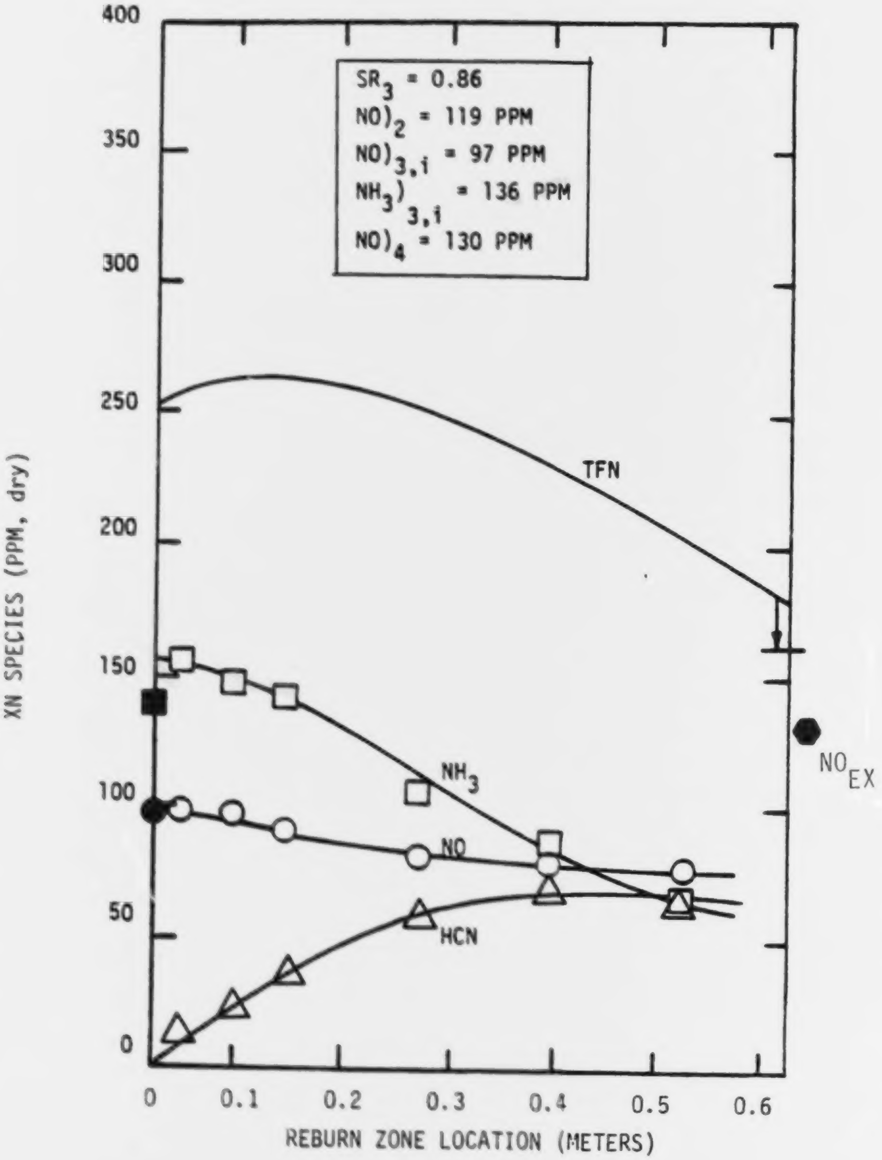

Figure 5-33: Reburn Zone Nitrogen Species Profiles for 0.5% Ammonia-Doped Natural Gas Reburning, NO_{PRI} = 119 PPM

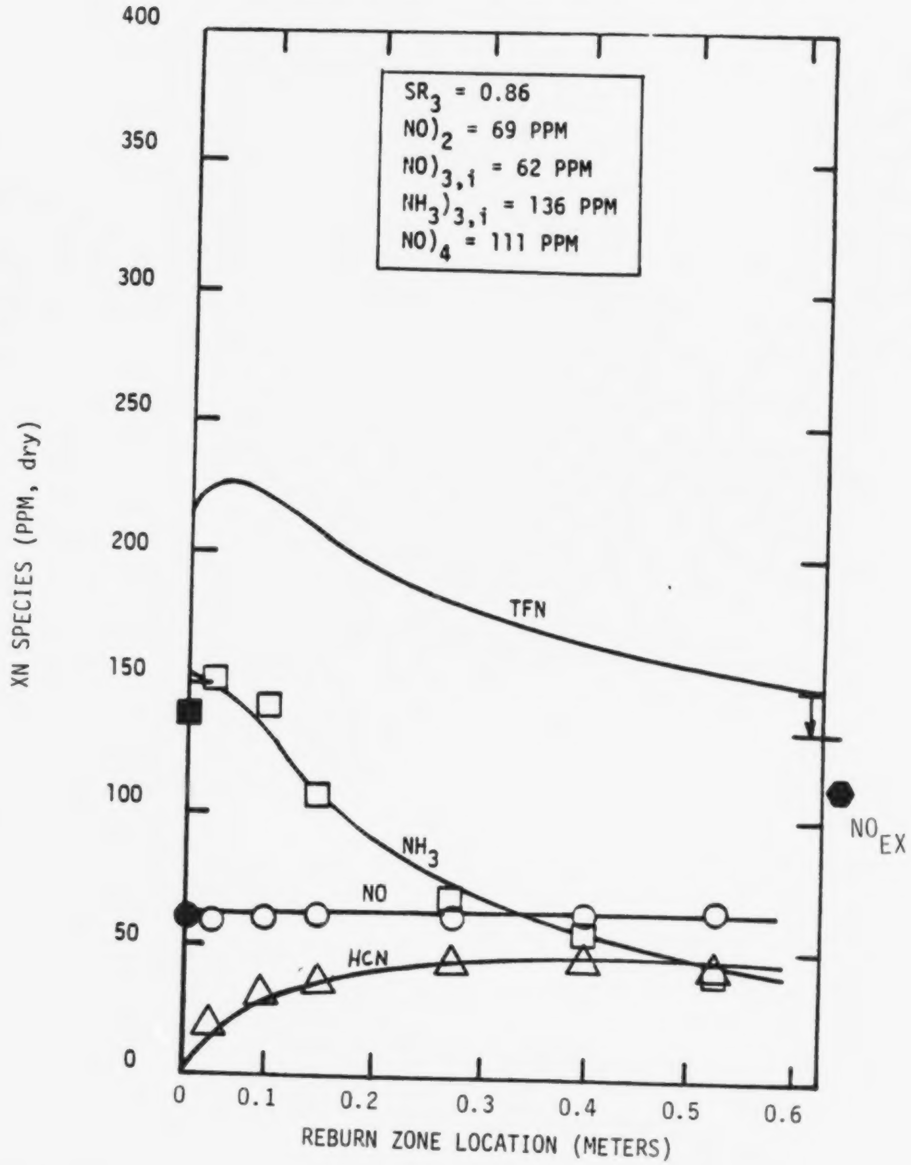

Figure 5-34: Reburn Zone Nitrogen Species Profiles for 0.5% Ammonia-Doped Natural Gas Reburning, NO_{PRI} = 69 PPM

solid square on the left vertical axis) for the ammonia-doped reburn fuel test conditions was determined from the measured molar flow rate of the NH_3 dopant and the calculated molar flow rate at the entrance of the reburning zone. Finally, TFN at the reburn zone exit was converted to a molar concentration representative of the burnout zone, corrected to zero percent O_2. In this way, the molar conversion of TFN to NO_{EX} (represented by a solid hexagon on the right vertical axis) can be seen.

Reduction of NO_x is directly proportional to the formation of N_2. Conversion of N atoms in the reburning zone can be expressed as:

$$[N_{total}] = [HCN] + [NH_3] + [NO] + 2[N_2] = [TFN] + 2[N_2] \qquad (5\text{-}9)$$

Differentiating equation 5-9 results in:

$$d[N_2] = -1/2d[TFN] \qquad (5\text{-}10)$$

Thus, the slope of the TFN profile is directly related to the rate of formation or destruction of molecular nitrogen.

Discussion of data presented in Figures 5-25 through 5-34 is divided into two parts. First, species variation with reburn zone stoichiometry is discussed; and second, species variation with primary NO_x concentration is discussed.

Reburn Zone Stoichiometry Variation:

For undoped natural gas reburning, the following observations are made concerning SR_3 variation from 0.97 to 0.78. NO destruction increases with decreasing SR_3; peak HCN formation increases with decreasing SR_3; and peak NH_3 formation is unaffected by SR_3. These observations shown in Figures 5-25, 5-26, and 5-27, are summarized in Figure 5-35. The HCN concentration profile mirrors the NO concentration profile. The characteristic time for HCN formation and NO destruction is on the order of 50 ms. This is shown in Figure 5-36, where NO profiles have reached a minimum by the 0.4 m reburn zone location (at 50 ms). This agrees with the minimum required local residence time for maximum NO reduction determined from the I/O data (see Section 5.1.1).

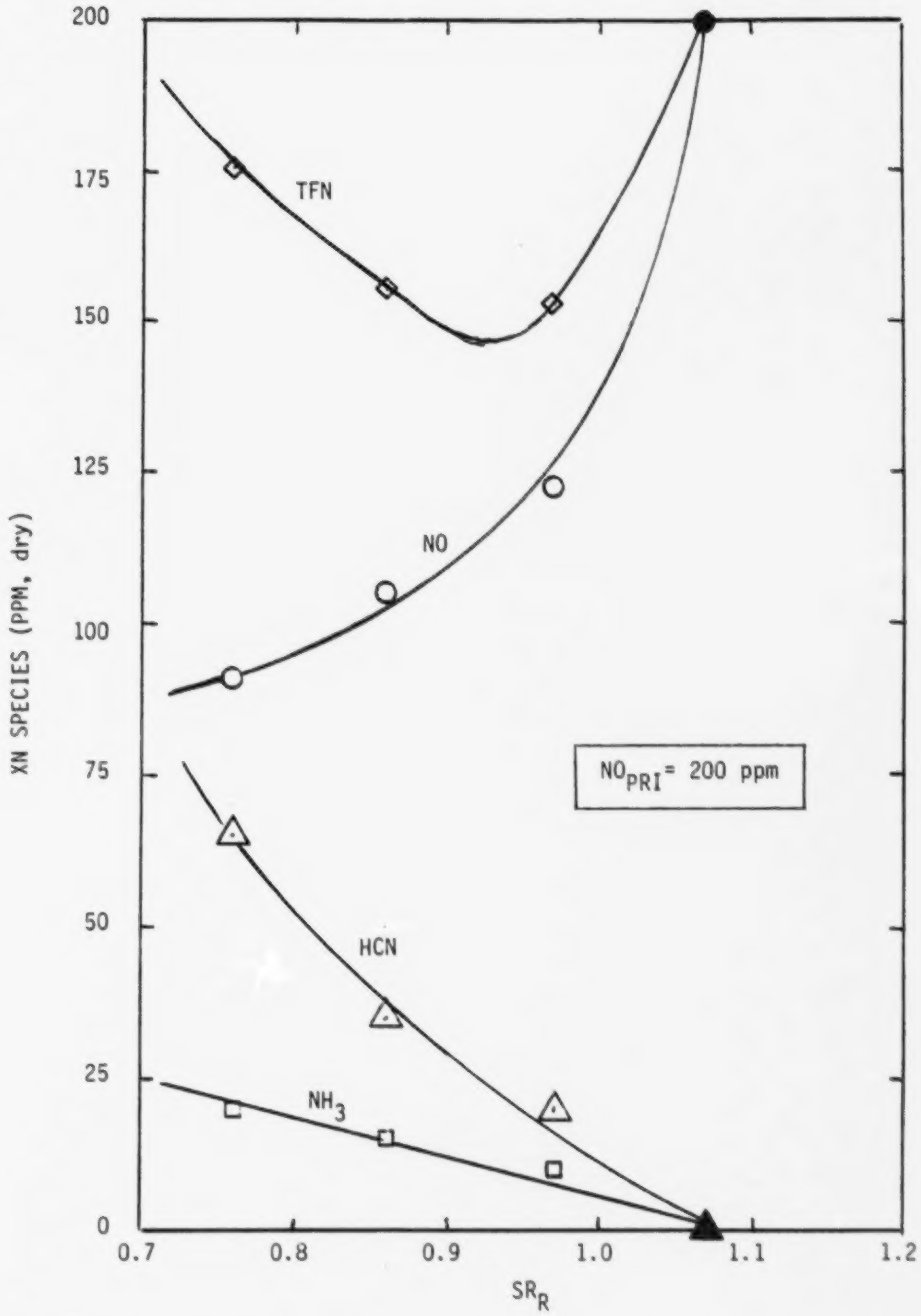

Figure 5-35: Nitrogen Species Concentrations at the Reburn Zone Exit for Natural Gas Reburning

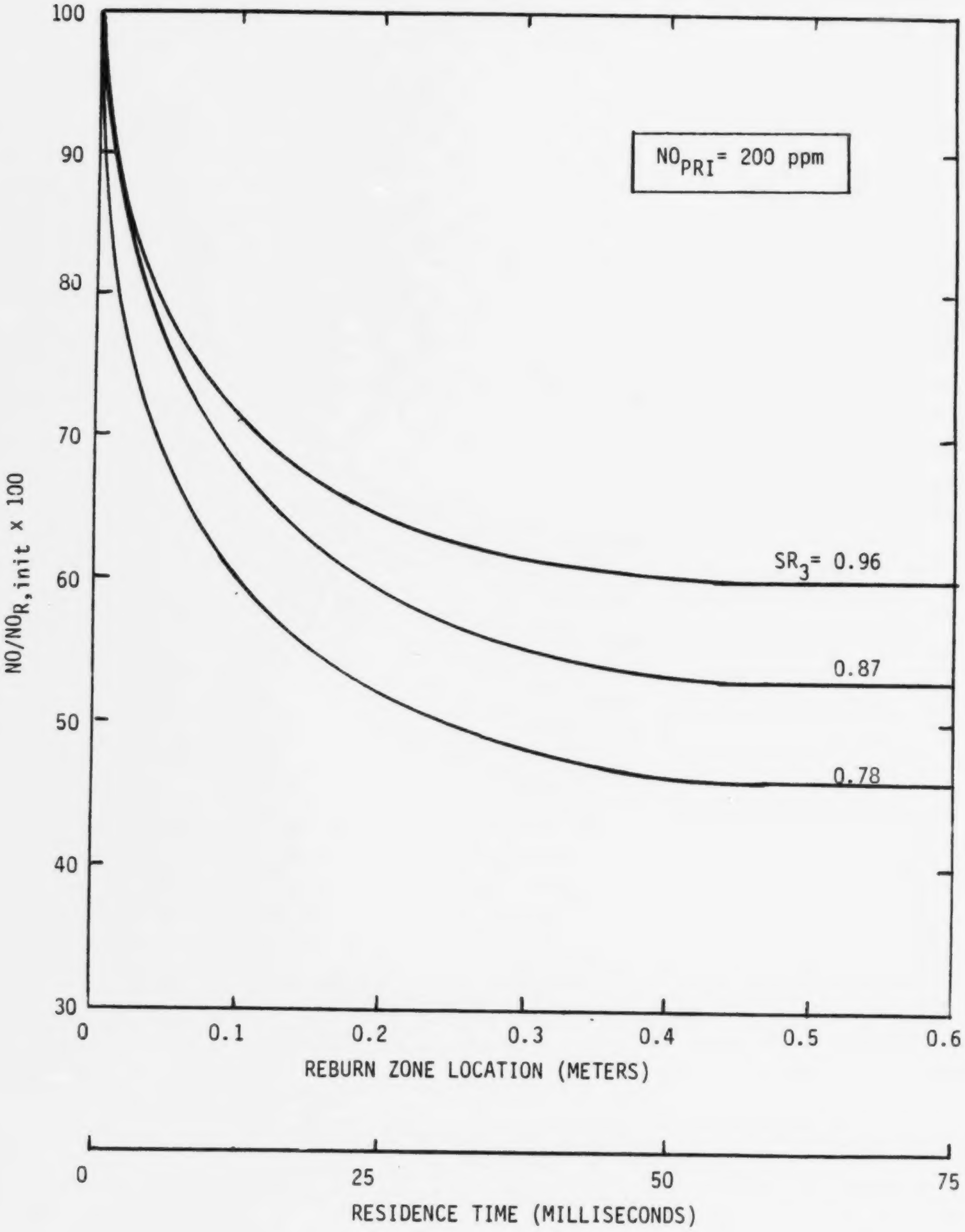

Figure 5-36: Reburn Zone NO Profiles for Natural Gas Reburning

For all three stoichiometries, TFN falls rapidly (within approximately 15 ms) and then levels out. This trend indicates that actual N_2 formation in the reburning zone occurs immediately, essentially independent of stoichiometry. This data conflicts with the I/O data on two counts: first, the I/O data indicate that overall NO_x destruction increases with decreasing SR_3; and second, the I/O data indicate that 50 ms minimum reburn zone residence times are required to maximize NO_x reduction.

To explain these apparent discrepancies, processes in the burnout zone are considered. Pohl et al. [17] have developed an empirical correlation for staged coal combustion which relates the exhaust NO_x level to the concentration of NO, HCN, and NH_3 in the fuel-rich zone. The correlation illustrates two points: first, the fraction of TFN existing as NO is almost completely retained as NO in transitioning from the fuel-rich zone to the fuel-lean exhaust; second, the fractional conversion of HCN and NH_3 to NO is less than 50 percent, with the conversion percentage decreasing as HCN and NH_3 concentrations increase. These points appear to be applicable to the reburn data presented here, as shown in Figure 5-37. For high SR's, where the TFN is largely NO in the reburn zone, nearly 100 percent conversion of TFN to NO is observed. For an SR_3 of 0.78, TFN to NO conversion drops to 84 percent. Assuming 100 percent NO retention in transitioning from zone 3 to zone 4, HCN and NH_3 conversion is estimated to be on the order of 25 percent.

The TFN to NO conversion as a function of TFN composition (which is a function of SR_3) explains both the overall NO reduction increase with decreasing SR_3 and the residence time effects. N_2 is formed in both the reburn and the burnout zones. While the reburn zone N_2 formation occurs rapidly (within 15 ms), independent of SR_3, the N_2 formation in the burnout zone depends on reburn zone stoichiometry and reburn zone residence time, since NO to TFN ratio at the reburn zone exit depends on these parameters.

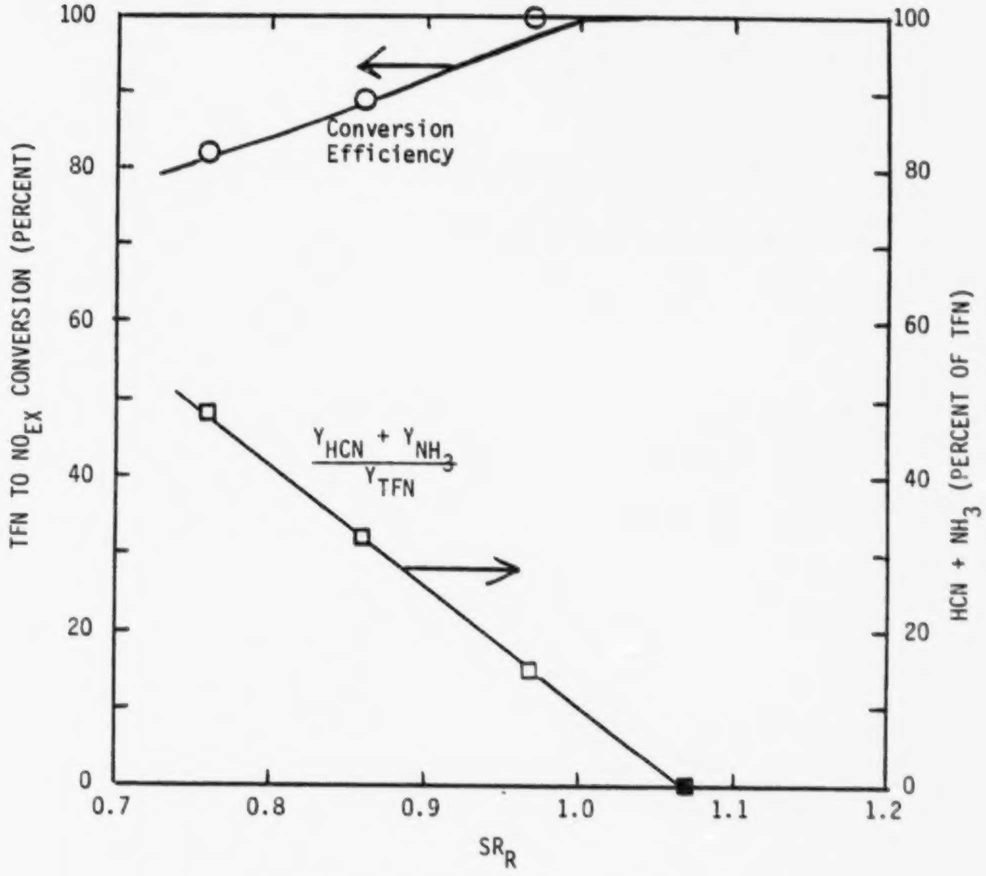

Figure 5-37: TFN to NO Conversion Efficiency in the Burnout Zone for Natural Gas Reburning

Figures 5-30, 5-31, and 5-32 show nitrogen species variation for the three reburn stoichiometry test conditions with 0.5 percent ammonia-doped natural gas secondary fuel. The high ammonia concentration at the start of the reburn zone is reduced considerably in the reburning zone, at a maximum rate of roughly 2000 ppm/sec. The more reburn fuel (and, hence, more ammonia dopant) added, the longer the reburn zone residence time required to reduce the NH_3 concentration. Thus, as SR_3 decreases, greater reburn zone residence times are required for nitrogen-containing secondary fuels.

As in the case of the undoped natural gas reburning fuel, the NO destruction and HCN formation curves as a function of SR_3 mirror each other. However, reburn zone net NO destruction is less than in the undoped trials. This behavior is probably due to the fact that ammonia consumption occurs by two chemical paths: a fixed nitrogen reduction path to form N_2, and an oxidation path to form NO. The NO formation from ammonia injection, or fuel nitrogen, results in increased NO reactions with hydrocarbons to form HCN. Thus, the TFN levels at the exit of the reburn zone are significantly higher for the ammonia-doped natural gas reburning condition than for the undoped condition. As before, TFN conversion to NO in the burnout zone is dependent on the TFN speciation. The fractional conversion of HCN and NH_3 to NO for the doped condition is nearly identical to that of the undoped condition.

Primary NO_x Variation:

To examine the influence of primary NO_x on the reburning process, additional detailed tests were performed, holding SR_3 constant (at a nominal value of 0.86). The NO_x entering the reburning zone was set at three nominal conditions: 200, 125, and 50 ppm. Figures 5-26, 5-28, and 5-29 present nitrogen species profiles under these conditions for undoped natural gas reburning; Figures 5-31, 5-33, and 5-34 present the same data for ammonia-doped natural gas reburning.

The undoped natural gas reburning results indicate that NO_x destruction in the reburning zone is first order with respect to primary NO_x. Percent NO destruction in the reburning zone is plotted versus axial boiler location in Figure 5-38 for the three nominal primary NO_x conditions, as well as for two additional conditions (primary NO_x concentrations of 385 and 528 ppm). For each case, nearly 50 percent destruction was achieved after 50 ms (0.4 m).

No significant variation in HCN formation was seen for the three nominal test conditions. Approximately 45 ppm was formed in each test condition. Thus, as a percentage of the primary NO_x level, the percent HCN concentration increased dramatically as primary NO_x decreased. NH_3 formation varied slightly with primary NO_x, but never exceeded 15 ppm. Thus, the TFN profiles as a function of primary NO_x differ strikingly. For the 206 ppm primary NO_x condition (Figure 5-26), TFN falls sharply in the initial portion of the reburning zone, then levels out. At the intermediate primary NO_x level (122 ppm, Figure 5-28), TFN is essentially constant in the reburning zone. For the low primary NO_x condition (49 ppm, Figure 5-29), TFN actually increases in the reburning zone.

Figure 5-29 clearly demonstrates the existence of an N_2 destruction process in the reburning zone. It is hypothesized that this occurs by the prompt NO mechanism:

$$CH + N_2 \longrightarrow HCN + N \qquad (5\text{-}11)$$

For the data collected, it is hard to quantify the amount of N_2 destruction via this mechanism. However, based on Figure 5-29, it is estimated that between 20 and 50 ppm of fixed nitrogen is formed. This is consistent with the prompt NO measurements of other researchers [4]. It is suggested that

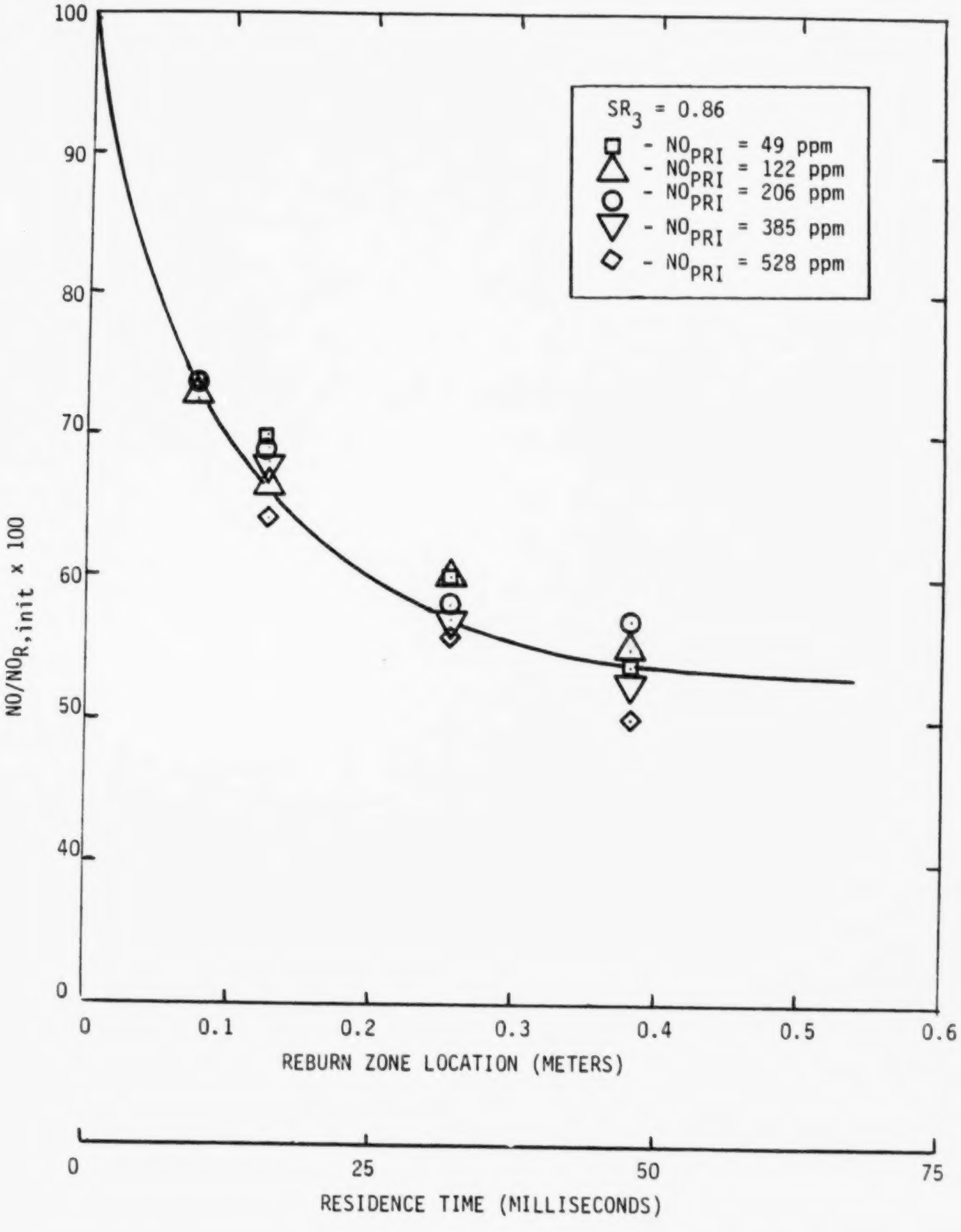

Figure 5-38: Reburn Zone NO Profiles for Natural Gas Reburning

this N_2 destruction is not a strong function of SR_3 over the range tested. The fractional conversion of TFN to N_2 in the burnout zone allows for an overall NO reduction, even at the low primary NO_x condition. It is also pointed out that, due to the fractional conversion of HCN and NH_3 to NO in the burnout zone, an overall NO reduction order of one is not achieved, despite the first order NO destruction observed in the reburning zone.

Reburning with ammonia-doped natural gas resulted in net reburn zone NO reduction that was not first order with respect to primary NO_x. This is shown in Figure 5-39. Assuming that the ammonia oxidation NO formation process is independent of the NO destruction process, the difference between the NO concentration with nitrogen in the secondary fuel and NO concentration with nitrogen-free secondary fuel represents the amount of NO formation by this process. Figure 5-40 shows this difference. The data agreement for the entire range of primary NO_x conditions (50 to 500 ppm) is quite good. Thus, reburn zone fuel-nitrogen NO formation is independent of primary NO_x. Data from the reburn zone stoichiometry variation trials (with primary NO_x held constant at 200 ppm), indicate that the fuel-nitrogen NO formation in the reburn zone is also independent of SR_3. This suggests that the ammonia oxidation reaction is limited by oxygen availability.

Chemical Kinetic Mechanisms:

A qualitative evaluation of the proposed chemical kinetic mechanism for the reburning process is presented here. A more detailed qualitative discussion is presented by Lanier [2]. The utility of the pilot-scale results in evaluating the kinetic mechanisms is somewhat limited, due to spatial variations in measured parameters. However, qualitative conclusions can be drawn.

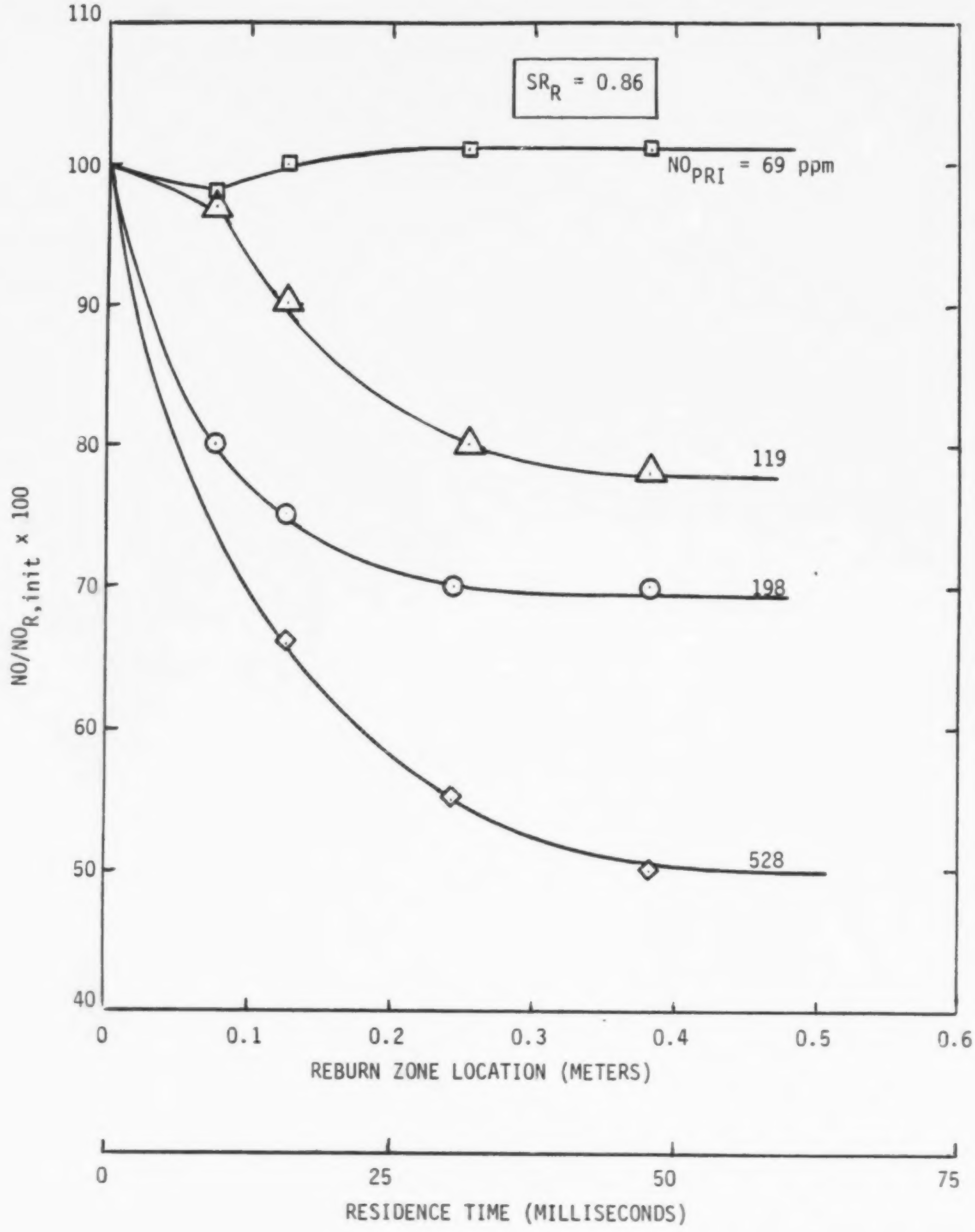

Figure 5-39: Reburn Zone NO Profiles for 0.5% Ammonia-Doped Natural Gas Reburning

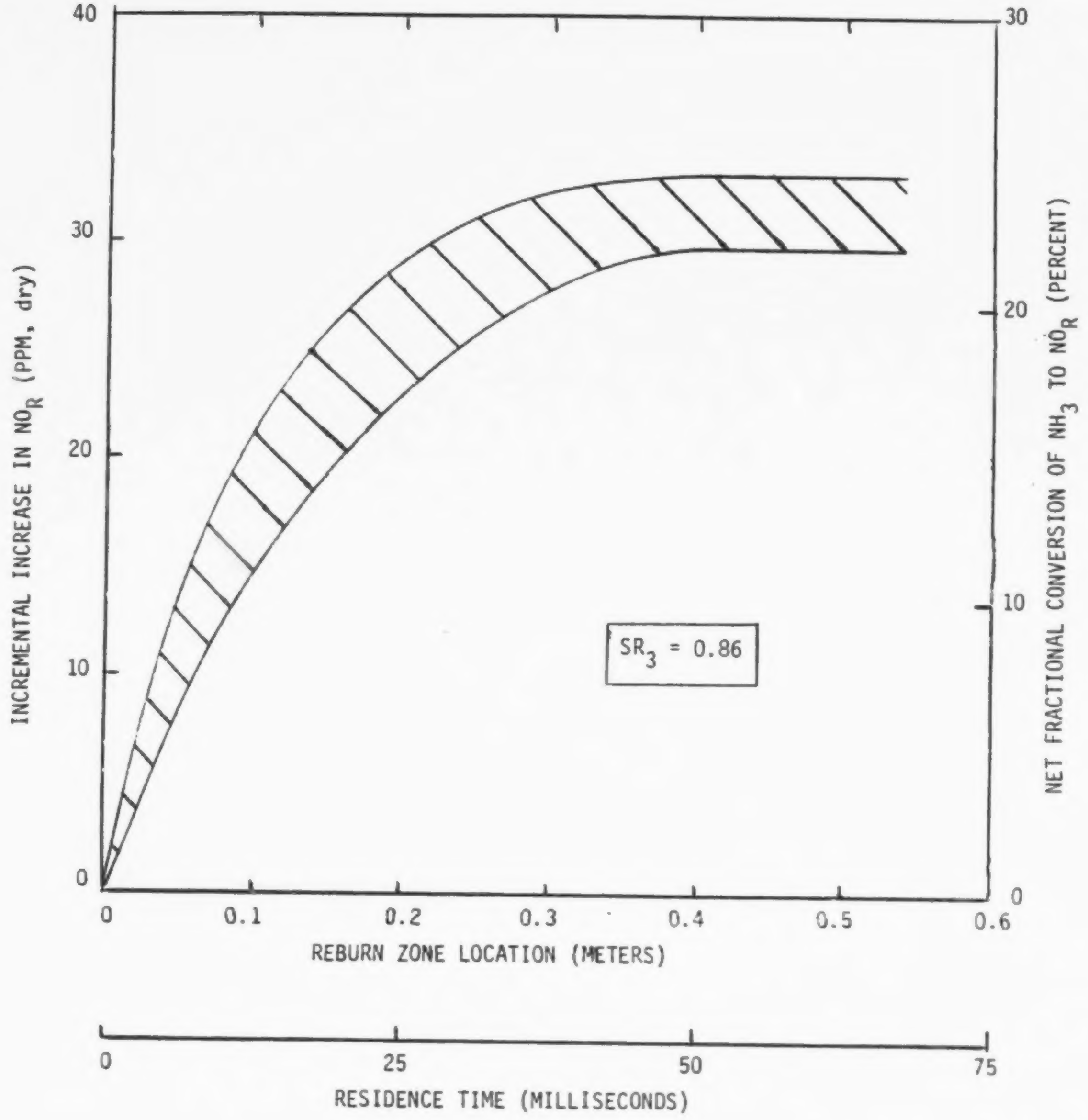

Figure 5-40: Net Conversion of Ammonia to NO in the Reburn Zone

NO destruction by reaction with the methylidyne radical producing HCN appears to be significant in the reburning zone.

$$NO + CH \longrightarrow HCN + O \qquad (5\text{-}12)$$

Reaction 5-12 results in about a 50 percent destruction in NO at a reburn stoichiometry of 0.86. However, it was proposed in Figure 1-5 that reactions involving O and OH radicals convert HCN into a partially equilibrated pool of NH_i species.

$$HCN + O(OH) \longrightarrow NH_i + \ldots \qquad (5\text{-}13)$$

Reaction between NH_i species and NO would then produce other intermediates (N and N_2O), and finally N_2. These latter steps in the NO_x destruction model do not appear to occur to any appreciable extent in the reburning zone. This suggests that the OH radical or O atom concentrations are quickly depleted in the reburning zone. N_2 formation in the reburning zone occurs only within the first 15 ms.

N_2 formation also occurs in the burnout zone, where HCN and NH_3 are converted to either N_2 or NO. It is suggested that in the burnout zone more flame radicals are produced, resulting in reaction 5-13. N_2 can then be formed by one of two proposed routes.

$$\text{Route 1:}\quad \begin{array}{l} NH + OH \longrightarrow N + H_2O \\ N + NO \longrightarrow N_2 + O \end{array} \qquad (5\text{-}14)$$

$$\text{Route 2:}\quad \begin{array}{l} NH\ (NH_2) + NO \longrightarrow N_2O + H(H_2) \\ N_2O + H \longrightarrow N_2 + O_2 \end{array} \qquad (5\text{-}15)$$

NO formation can occur by two routes, as well.

$$\text{Route 1:}\quad \begin{array}{l} NH + OH \longrightarrow N + H_2O \\ N + OH \longrightarrow NO + H \end{array} \qquad (5\text{-}16)$$

$$\text{Route 2:}\quad NH + OH \longrightarrow NO + H \longrightarrow NO + H_2 \qquad (5\text{-}17)$$

It was observed that a net 25 percent of the HCN and NH_3 get converted to NO in the burnout zone.

NO formation from N_2 destruction can also occur via the prompt NO_x mechanism:

$$CH + N_2 \longrightarrow HCN + N \qquad (5\text{-}18)$$

It was estimated in the reburn experiments that 20 to 50 ppm of HCN was formed in the reburning zone via this reaction. Fuel-bound nitrogen, simulated by NH_3 fuel-dopant, can result in NO formation in the reburn zone as well as in the burnout zone. In the reburn zone, with primary zone excess air set at approximately 10 percent, between 20 and 30 ppm of NO is formed, independent of primary NO_x or reburn stoichiometry. Further, fuel nitrogen increases reburn zone HCN concentration, which partially converts to NO in the burnout zone. Thus, prompt NO and fuel NO production in the reburning process can reduce reburning effectiveness in reducing NO_x. For low primary NO_x values (less than 100 ppm), these NO formation processes become very significant.

Having addressed the first three hypotheses concerning natural gas reburning in the PBS, the final two hypotheses, concerning secondary fuel injection effects and thermal effects, are investigated in Sections 5.3 and 5.4, respectively.

5.3 SECONDARY FUEL INJECTION METHOD STUDIES

As discussed in Section 1, Chen et al. [12] have found that there is an optimum stoichiometry in the fuel-rich region for NO_x destruction. Figure 1-10, taken from the work of Chen et al., shows that NO_x destruction is maximized when the secondary fuel (propane) injection rate is sufficient to achieve a rich-zone stoichiometry of 90 percent theoretical air. This optimum is accentuated when the secondary fuel contains a significant quantity of fuel-bound nitrogen (0.86 percent nitrogen by weight, achieved here with ammonia-doping). Therefore, local variations of stoichiometry within the fuel-rich zone, governed by fuel injection techniques and mixing parameters, would appear to be important in optimizing reburning effectiveness.

5.3.1 Spoked Secondary Fuel Injection

A series of experiments were performed to quantify the influence of secondary fuel injection parameters on the overall effectiveness of reburning. The experimental approach was to: first, establish a baseline reburning condition wherein the secondary fuel is injected in such a manner that the stoichiometry in the fuel-rich region is spatially uniform; and, second, distort the secondary fuel injection scheme from the uniform baseline condition.

To establish a spatially uniform stoichiometry in the fuel-rich reburning zone, it was necessary to match the radial distribution of secondary fuel addition to the radial distribution of free oxygen flux, as discussed in Section 4. Special operational procedures and reburn fuel boom designs were utilized to achieve that baseline requirement. Operationally, the staged combustion air was introduced in the all-radial mode, producing a premixed primary flame in the boiler radiant section. The resultant radial profile of O_2 concentration at the secondary fuel addition plane was essentially flat.

Further, the location of secondary fuel injection was selected to be 1.016 m downstream of the radiant section front wall, just downstream of the point at which the flow from the prechamber constriction (including staged combustion air) should have reattached to the boiler wall. Thus, at the plane of secondary fuel injection, the flow should contain minimum swirl, no reverse flow, and nearly constant radial oxygen concentration profile.

To match the secondary fuel flow to the free oxygen flux, the secondary fuel boom was equipped with eight interchangeable spokes attached to eight parallel water-cooled spokes. Twelve holes were drilled into each fuel spoke allowing the radial distribution of secondary fuel addition to match incoming O_2 flux distribution. Thus, secondary fuel was introduced through 96 individual jets aimed circumferentially, as shown in Figure 5-41a. Achievement of spatially uniform stoichiometry in the fuel-rich region was verified by doping the reburning fuel with 0.5 percent ammonia and measuring the NH_3 concentration just downstream of the injection plane at several radial locations. For a reburn zone stoichiometry of 0.86 or richer, deviation between measured NH_3 concentration and that calculated from the known flow rates was less than 5 percent, indicating uniform injection. To achieve similar agreement at lower reburn loads, six-hole injector spokes were required.

All tests were performed by maintaining the primary fuel, primary air, and staged combustion air flow rates constant. As reburning was applied, the total boiler heat release rate was increased but the thermal and fluid mechanic conditions at the secondary fuel injection plane remained essentially constant.

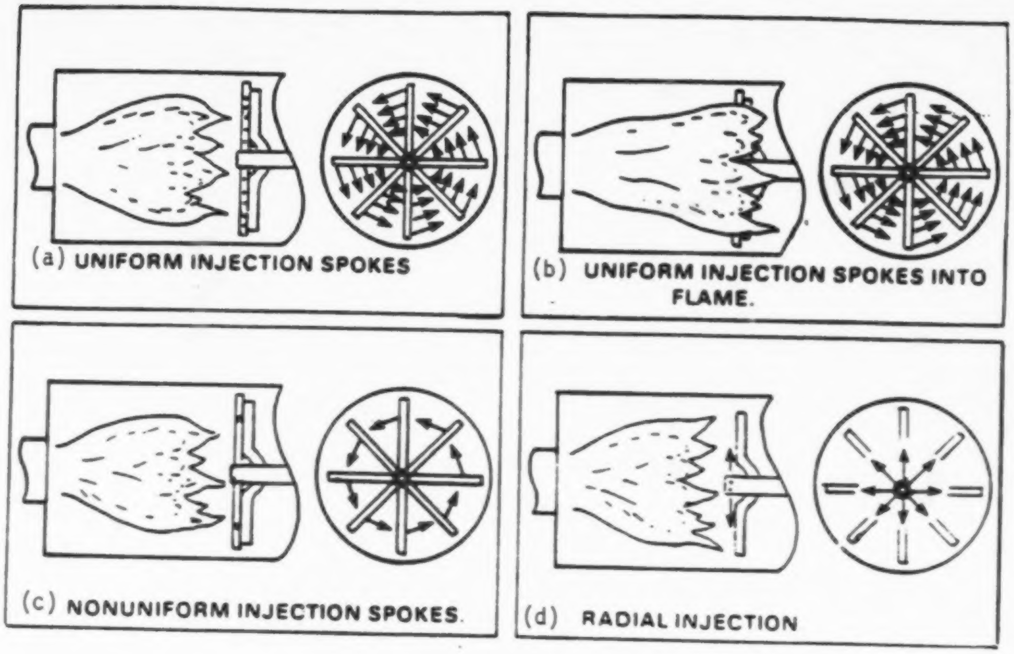
(a) UNIFORM INJECTION SPOKES

(b) UNIFORM INJECTION SPOKES INTO FLAME.

(c) NONUNIFORM INJECTION SPOKES.

(d) RADIAL INJECTION

Figure 5-41: Secondary Fuel Injection Schematics

In this section, data are presented comparing results from the spatially uniform trials to results from three series of tests with severe perturbations to the method of secondary fuel injection. The first perturbation mode, shown schematically in Figure 5-41b, was to utilize the spoked fuel injectors employed in the baseline trials, but to change the mode of staged combustion air addition from all-radial (premixed flame) to all-axial (axial diffusion flame). In the second perturbation mode, the baseline spokes were replaced with spokes having two injection ports very close together at a nominal radius of 18.4 cm (Figure 5-41c). The third perturbation mode involved replacing the eight fuel spokes with caps, each having a single 2.78 mm port, that inject fuel radially outward from the centerline boom (Figure 5-41d).

Results from the four test series are presented in Figure 5-42 as a plot of the exhaust to primary NO_x ratio versus the stoichiometry ratio in the fuel-rich reburning region. The solid lines in this figure represent results from the baseline (spatially uniform stoichiometry) trials, obtained using natural gas and natural gas doped with 0.5 percent ammonia as the reburning fuel. In all four test series, the NO_x concentration and excess air level at the plane of secondary fuel injection was fixed at 200 ppm (measured dry, corrected to zero percent O_2) and 7 percent, respectively, and the exhaust excess air level was maintained constant at 10 percent. As shown in this figure, there was no discernible influence of secondary fuel injection method on the extent of NO_x reduction.

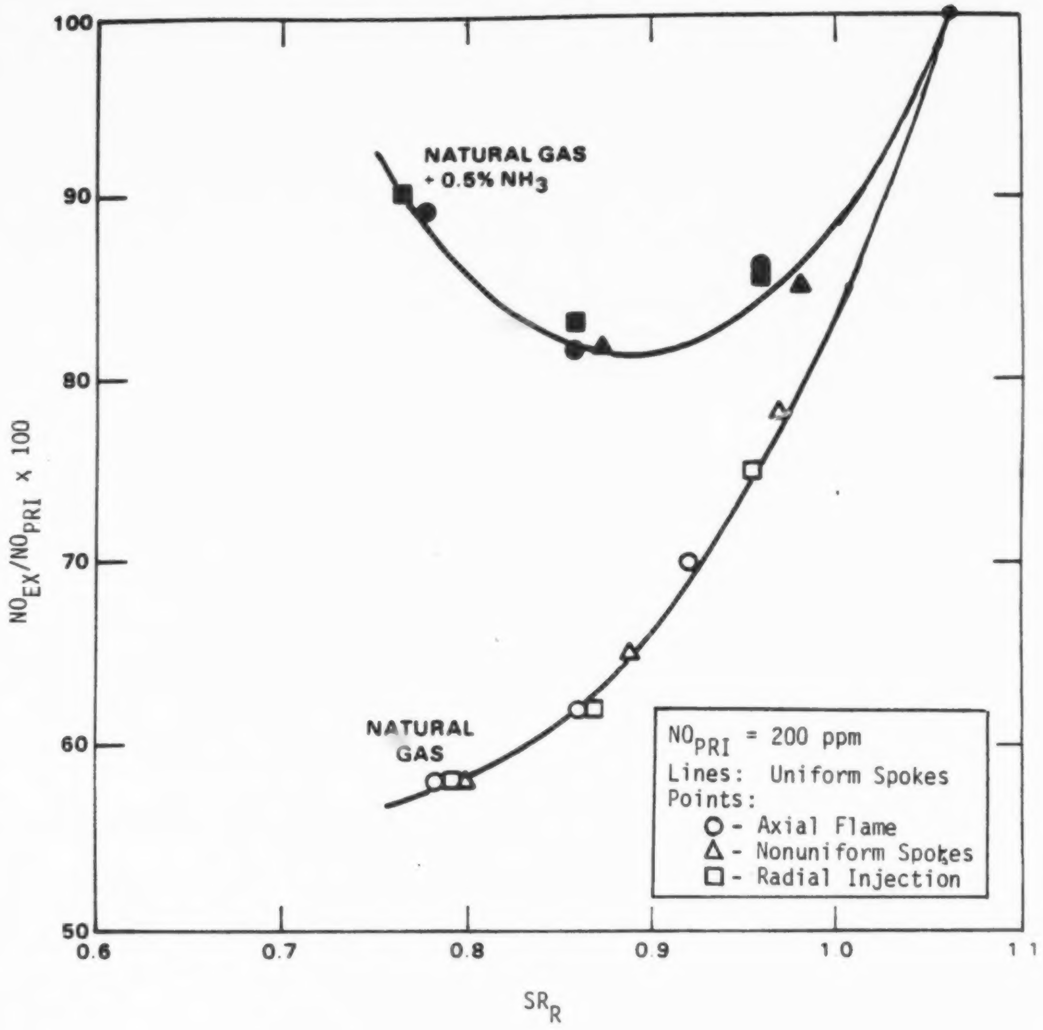

Figure 5-42: Effect of Secondary Fuel Injection Method

Note that, for a relatively small spread in maximum to minimum local stoichiometry, the basic reburning system characteristic is piece-wise linear, and a nonuniform injection pattern would produce overall results equivalent to uniform injection. However, the perturbation tests were designed to produce a large variation in radial distribution of stoichiometry in the fuel-rich region. With the two-hole spoke injector, for example, all of the secondary fuel was injected into the wall region of the boiler facility. In this case, the center portion of the flow should have remained at the stoichiometry of the primary flame (7 percent excess air). Considering the wide variation in secondary fuel injection method examined and the general shape of the NO_x versus rich-zone stoichiometry curves, the data in Figure 5-42 suggest that strong radial mass transport was occurring, resulting in far greater uniformity of rich zone stoichiometry than expected. Turbulent processes are obviously capable of generating radial mass transport, but the apparent extent of that transport was surprising.

A series of in-flame tests were performed using the nonuniform spoke injector configuration which introduces the secondary fuel through two holes (in each of the eight spokes). This configuration was shown schematically in Figure 5-41c. These holes are nominally located at the 17.8 and 19.05 cm (7 and 7.5 in.) radial locations and are oriented such that each jet is directed toward the adjacent spoke. Each jet is, therefore, entering the system with a velocity vector tangent to its firing circle and should be initially moving radially outward. Further, the swirl imparted by these jets should force more of the flow toward the wall.

The locations of the two holes in this nonuniform spoke injector were based on the available radial locations for inserting the in-flame sampling probe. Axial probing ports are located 13.3, 18.4, and 23.5 cm from the boiler centerline. Thus, the secondary fuel is being injected 0.635 cm (0.25 in.) on either side of the 18.4 cm sampling location and should be forced radially outward toward the 23.5 cm sampling location. Without strong radial mass transport, samples extracted from the 13.3 cm radial location should be characterized by primary flame conditions.

Under nominal reburning conditions, axial profiles of CO concentration at each sampling port location were measured; the profiles are presented in Figure 5-43. Of particular interest relative to mixing phenomena is the observation that the CO concentration, 2.54 cm into the fuel-rich zone and at the 13.3 cm radial location, is equal to or greater than the CO measured at larger radii. Considering the pumping action of the fuel jets, the initial fuel jet orientation and the radially outward force of the induced swirl, high CO concentration at this location was unexpected. Note that the term "high concentration" is quantified as approximately 14,000 ppm; it compares to 500 ppm at the same location without reburning.

The data in Figure 5-43 clearly indicate that a substantial amount of secondary fuel was radially transported from its injection point (17.8 cm) to the 13.3 cm sampling radius over an axial distance of 2.54 cm. This would indicate that the minimum apparent turbulent mixing length is 4.5 cm. An upper limit Prandtl mixing length can be calculated from the measured velocity profile by assuming 100 percent turbulent intensity (i.e., mean axial velocity equals fluctuating velocity). The radial profile of mean axial velocity was measured 3.5 cm downstream of the secondary fuel injection plane. At the 18.4 cm radial location, the upper limit mixing length, based on classical

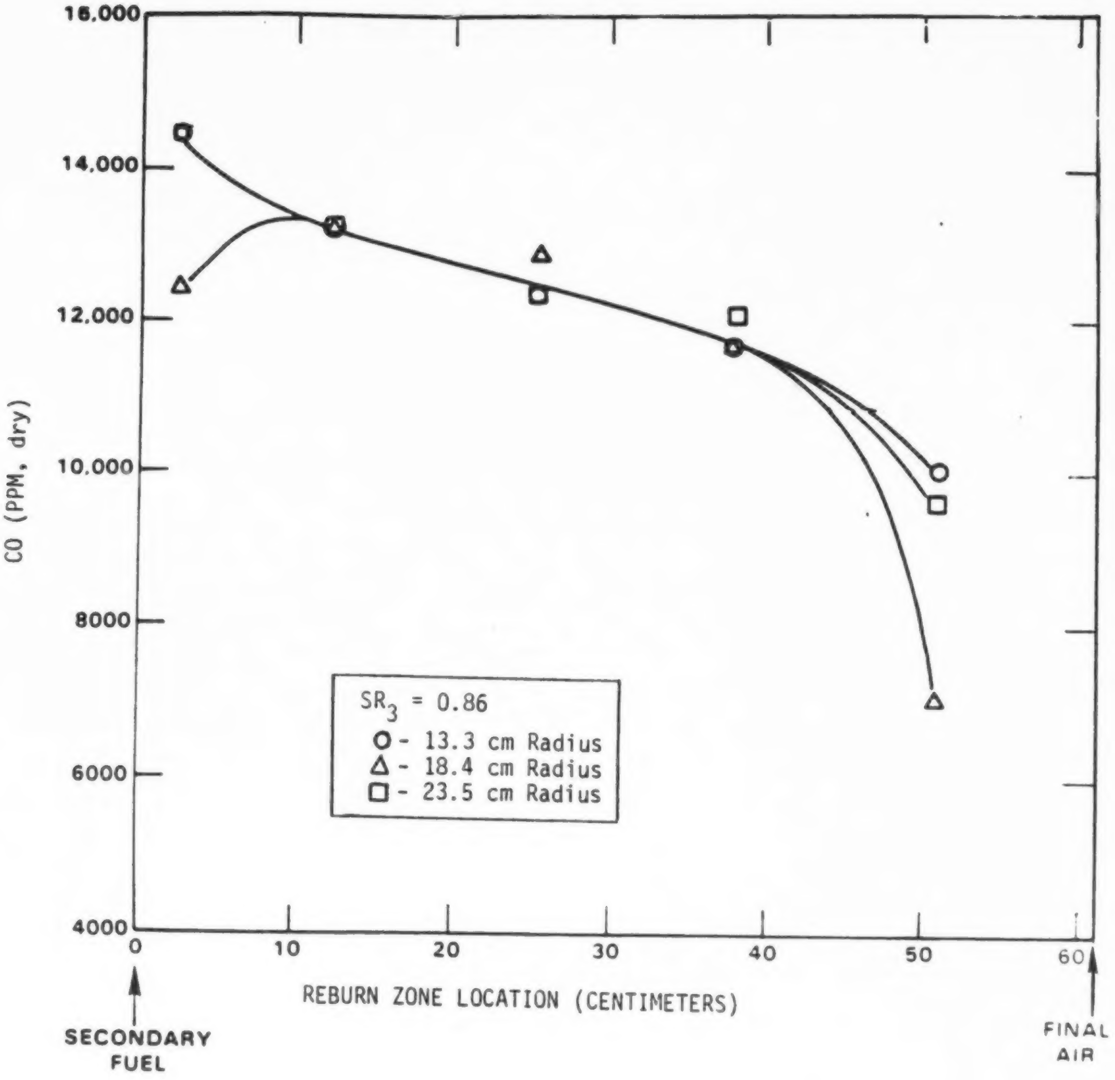

Figure 5-43: Reburn Zone CO Profiles with Nonuniform Spoke Injection

turbulence theory, is calculated to be 4.6 cm. Thus, the maximum turbulent mixing length calculated from classical turbulence theory is only 1 mm greater than the lower limit mixing length indicated by the CO data. Considering the magnitude of CO concentration observed at the first sampling location, the initial ballistic trajectory of the fuel jets, the induced swirl, and the gross nature of assuming 100 percent turbulent intensity, it is concluded that radial mass transport is occurring by means other than what is describable by classical turbulence theory.

Two possible sources of enhanced radial mass transport were considered. First, for the injection schemes examined, it is possible that wakes formed behind the fuel spokes and water cooling lines dominated the mixing process, eliminating any significant influence associated with initial fuel jet trajectory. Considering the physical size of the spokes (0.6 cm diameter), it is unlikely that such wakes could influence the mixing process sufficiently to cause the results described in Figures 5-42 and 5-43. A more likely possibility is that the main flow contained large scale eddy structures which dominated secondary fuel transport.

5.3.2 Unspoked Secondary Fuel Injection

To examine these two possible explanations of enhanced radial mass transport, a new secondary fuel addition boom was constructed without the external spokes and cooling lines. Instead, secondary fuel was injected from interchangeable nozzle tips containing eight radial ports. Six nozzles were constructed which allowed the secondary fuel injection velocity to be varied between 15 and 150 m/sec. One of the nozzles (2.78 mm port diameter) replicates the injection pattern of the capped injector of Figure 5-41d (less the protruding water cooling lines). Results from tests using this nozzle on the new boom are compared with results from the capped injector in Figure 5-44. As shown, NO_x destruction efficiency was 5 to 10 percent less with the new boom.

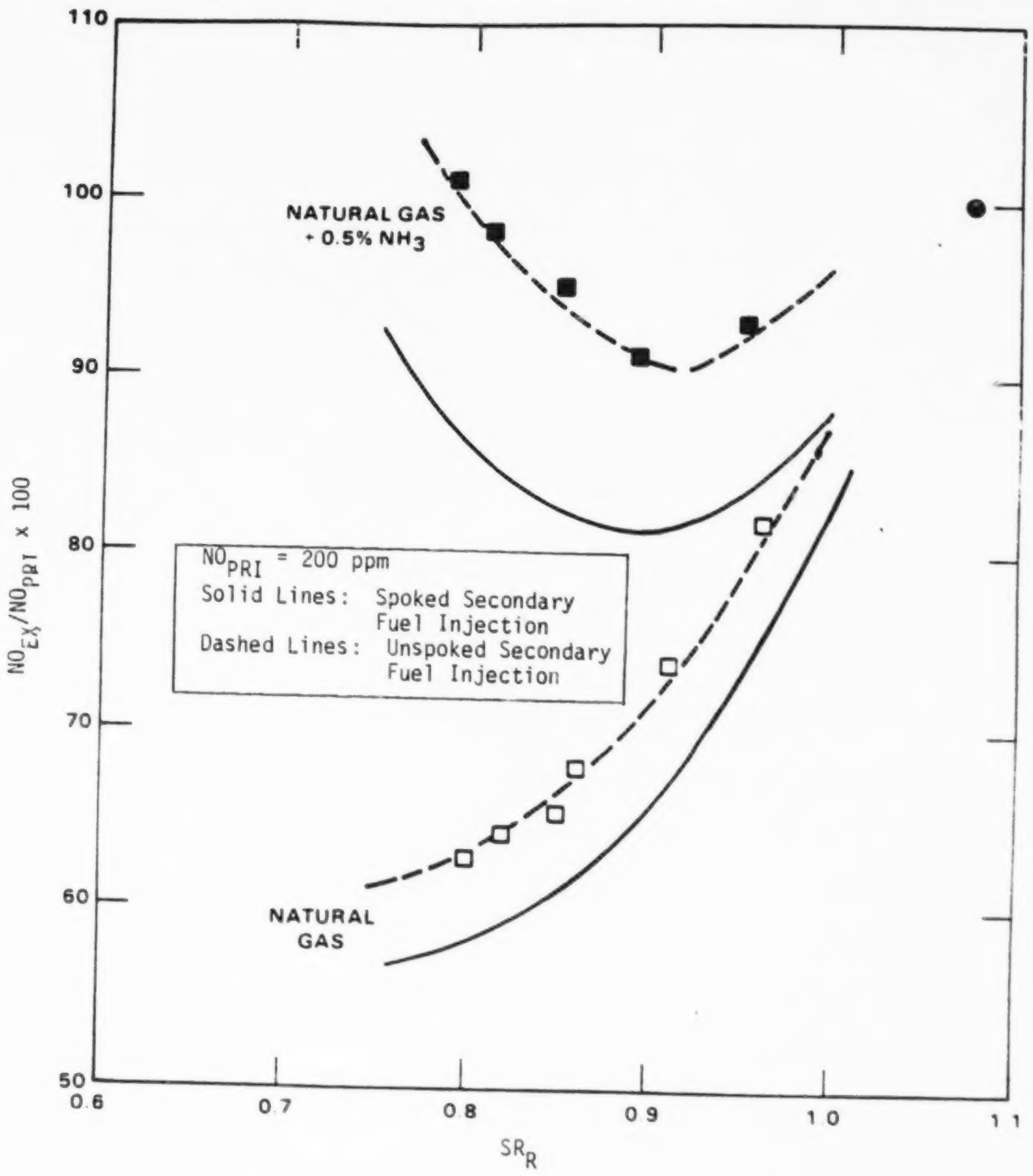

Figure 5-44: Comparison of Spoked and Unspoked Secondary Fuel Injection

The results described in Figure 5-44 clearly indicate that the presence of radial spokes significantly enhanced NO_x destruction. This finding is consistent with the hypothesis that wakes formed by the spokes enhanced secondary fuel mixing sufficiently to dominate fuel jet effects. The results are not conclusive, however. Removal of the fuel spokes and water lines from the fuel addition boom represented a significant system modification. In addition to removing the flow disturbance bodies and their associated wakes, use of the new fuel addition boom reduced the amount of heat extraction at the point of secondary fuel injection and removed a series of hot metal surfaces that could have a catalytic effect. Thus, the enhancement of NO_x destruction caused by the spokes might be due to system influences as well as mixing effects. Further studies could investigate the thermal and catalytic effects of water-cooled stainless steel spokes on the reburning process. The purpose of this study is to investigate combustion aerodynamic effects on reburning.

To investigate further the hypothesis that wakes caused by the spokes dominated the mixing process and, hence, eliminated secondary fuel jet effects, a test series was performed to examine the influence of initial jet velocity in the absence of radial solid bodies in the flow. If the hypothesis were true, large variation of the fuel jet velocity into a flow field without the flow disturbances caused by the spokes would result in significant variations in the degree of radial uniformity of rich-zone stoichiometry. This, in turn, would result in significant variation in the amount of NO_x destruction. Jet penetration calculations indicate that, with the large port diameter (low velocity) nozzle tip, the secondary fuel would be rapidly turned by the main flow and would remain within about 10 cm of the centerline boom. For the small diameter (high velocity) nozzle, the eight fuel jets should penetrate to the boiler wall.

Results from tests using all six nozzles, tabulated in Table 5-6, show that an order of magnitude variation in initial jet velocity produced no discernible variation in fractional NO_x reduction for either high (196 ppm) or low (64 ppm) primary NO_x conditions. Thus, even without the flow disturbances caused by the fuel injection spokes, sufficient mixing did occur to result in NO_x reductions independent of fuel jet velocity. Based on the results tabulated in Table 5-6, the differences described in Figure 5-44 appear to be due to system influences rather than mixing effects. It is now postulated that the primary flame contains large turbulent eddies (or coherent structures) which dominate radial mass transport of the secondary fuel.

TABLE 5-6. TEST RESULTS FOR VARIOUS RADIAL SECONDARY FUEL INJECTOR NOZZLES

Fuel Port Diameter (mm)	Secondary Fuel Jet Injection Velocity (m/sec)	NO_{EX}/NO_{PRI}[a] (at NO_{PRI}=196 ppm, dry at 0% O_2)	NO_{EX}/NO_{PRI}[a] (at NO_{PRI}=64 ppm, dry at 0% O_2)
6.35	14.6	65	75
5.56	19	63	75
4.76	26	64	75
3.97	37	64	74
2.78	76	65	75
1.98	150	64	75
Uniform spokes	-	61	72

[a] Nominal stoichiometries: $SR_{PRI} = 1.05$, $SR_R = 0.85$.

5.3.3 Turbulent Eddy Size

A review of recent work in the coherent structure area revealed a series of experiments being performed at the California Institute of Technology by

Professor Frank Marble and Mr. Duane Smith. They are examining the formation of large eddies in premixed methane/air flames undergoing sudden expansions. For conditions substantially the same as those at the entrance to the radiant section in the current reburning study, they have observed coherent structures with a characteristic dimension on the order of the step height. For the current experiments, the step height is the difference between the boiler radius and the throat radius (approximately 17 cm). The unpublished photographic evidence from Cal Tech leaves a distinct impression that the eddies are capable of upstream (as well as normal) mass transport. Upstream transport in a region of relatively large mean axial velocity is, of course, not possible within the context of classical turbulence theory.

A simple experiment was devised to determine if upstream transport of secondary fuel was occurring. Detection of upstream transport would provide direct evidence that coherent structures exist in flow and would rationalize the lack of influence of secondary fuel injection method. Further, it would indicate that the effective rotational speed of the eddies exceeded their translational speed.

The test which was devised involved radial secondary fuel injection. Staged combusion air was injected in the all-axial mode to increase the main flow axial momentum in the wall region. With the boom installed but without secondary fuel injection, an axial traverse of stable species was performed in the primary flame just upstream of the fuel boom. Immediately following this test, secondary fuel flow (doped with 0.5 percent ammonia) was initiated at a rate commensurate with an overall reburn zone stoichiometry of 0.85. An axial traverse in the region upstream of secondary fuel injection was then repeated.

Results from these two tests are presented in Figure 5-45. The plots of CO and NH_3 concentration profiles clearly indicate that secondary fuel has been transported upstream. As shown, the NH_3 profiles converge approximately 8 cm upstream of the fuel boom while the CO profiles converge approximately 11 cm upstream of the boom. This minor difference in convergence locations is probably related to the relative reactivity of NH_3 and CO. To a first approximation, the location at which the two CO profiles converge, relative to the fuel boom, may be equated to the effective radius of the eddy structures. On this basis, the characteristic dimension of the structures is estimated to be approximately 22 cm.

The findings described here raise question as to the generality of the boiler simulator test results. Are the results specific to the unique geometry and operation of the modified research facility? To address this question, extensive input/output tests were performed in a commercial North American boiler fitted with a conventional burner (see Section 7). Results from these tests were nearly identical to results from the research boiler simulator. This is strong evidence indicating a generality of the results for smaller firetube package boilers, but it does not imply an absence of secondary fuel nozzle effects for larger scale devices, such as wall-fired watertube boilers.

5.3.4 Conclusions

In conclusion, the foregoing experimental investigation has demonstrated that the effectiveness of the reburning process as a NO_x control technique is not significantly influenced by secondary fuel jet parameters in the firetube package boiler. It has been observed that large scale structures exist in the reacting flow, causing this lack of influence of secondary fuel jet parameters. These eddy structures are found to transport fluid across distances significantly in excess of what can be predicted by classical

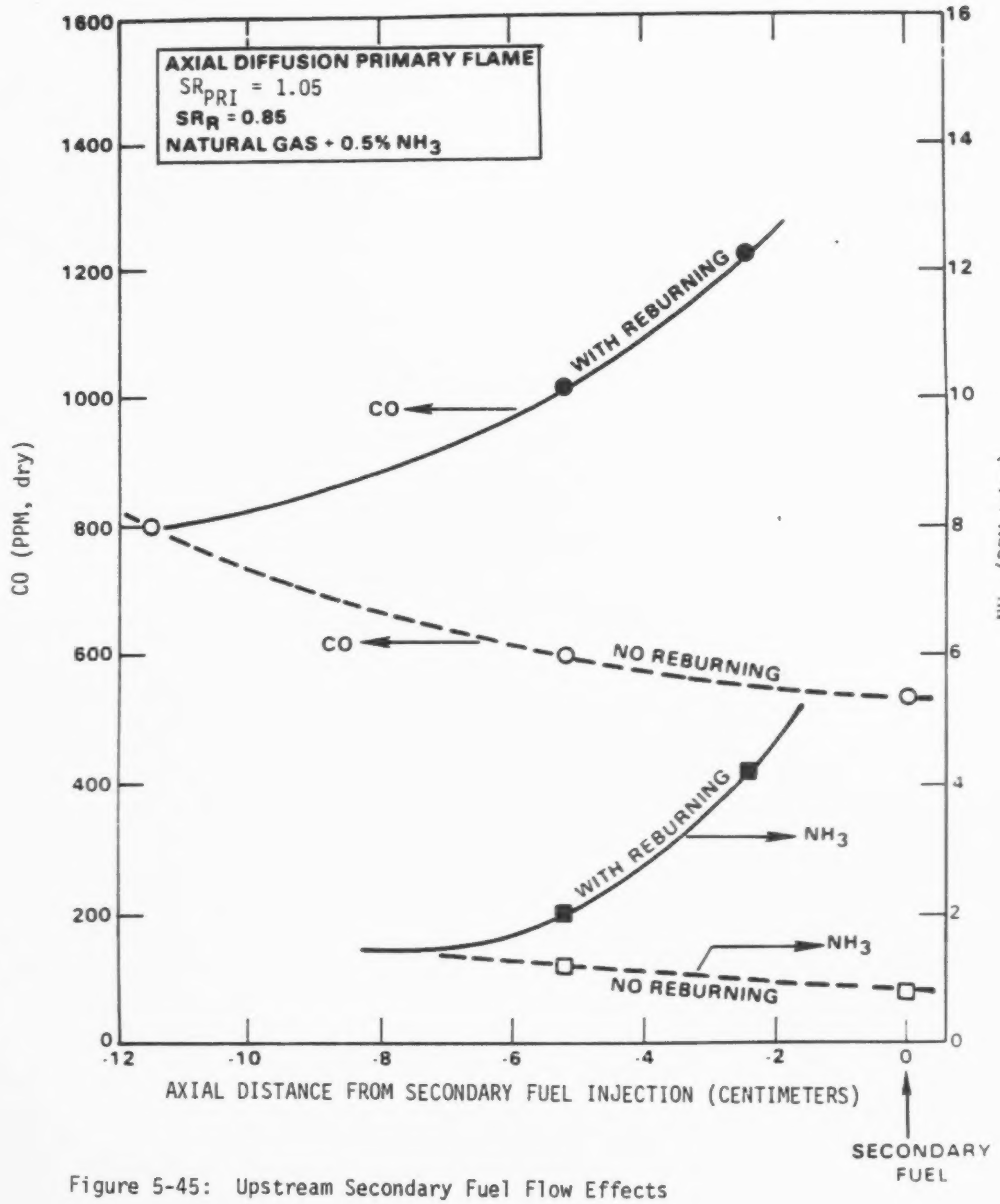

Figure 5-45: Upstream Secondary Fuel Flow Effects

turbulence theory. In addition, it was seen that the large eddies were capable of upstream mass transport, even in regions of relatively high positive mean axial velocity. This implies that the effective rotational speed of the eddies exceeds their translational speed. Additional fundamental study would help to better understand the nature of these large structures.

From a practical perspective, the experimental findings indicate that optimum application of reburning to firetube package boilers may be simpler than originally expected. Most firetube boilers have access plates on the rear furnace wall, which is an ideal location for inserting secondary fuel and final air addition hardware. The presence of large scale turbulent structures in the primary combustion flow should simplify fuel injector design.

5.4 REBURNING ZONE THERMAL ENVIRONMENT STUDIES

Four methods of varying reburn zone temperatures to determine thermal effects on the reburning process were tried. First, primary burner load was varied to vary the primary zone heat release. Second, the reburning zone was insulated to reduce reburn zone heat extraction. Third, the primary zone was insulated to increase temperatures at the reburn zone entrance. Finally, the secondary fuel injection axial location was varied to vary the amount of heat extraction prior to the reburning zone. Results from each of these trials are presented in this section.

5.4.1 Primary Load Variation

The simplest approach to increasing reburn zone temperatures was to increase primary load, since this required no physical modification to the PBS. Primary load was increased from the nominal value 0.60 MW (2.0 x 10^6 Btu/Hr) to 0.78 MW (2.7 x 10^6 Btu/Hr). Baseline (without reburning) temperatures were increased between 94 and 150°C (200 and 300°F), as shown in Figure 5-46. The primary flame length also increased, extending into the boiler to the 1.17 m (46 in.) axial location. At the nominal primary load condition, the flame

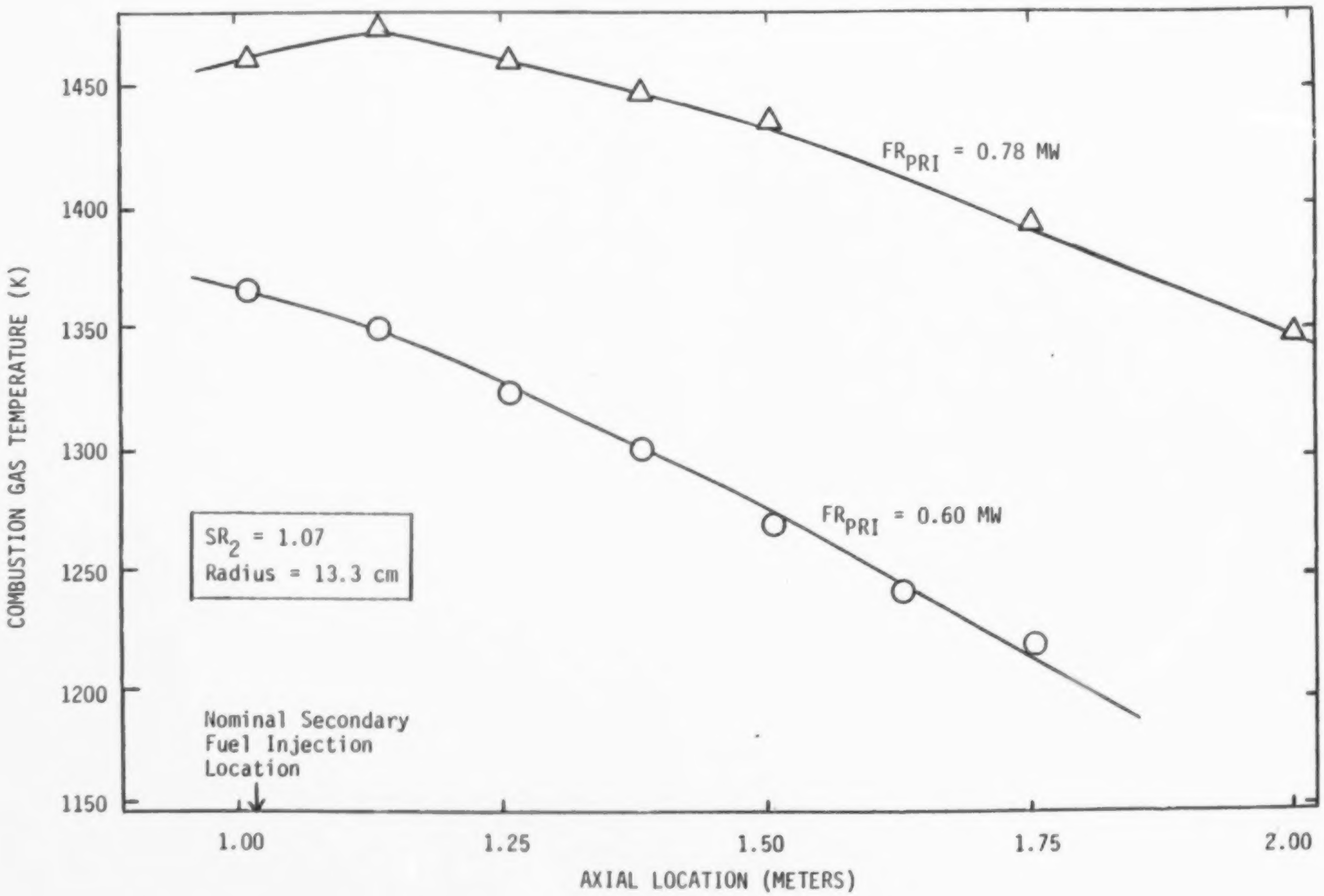

Figure 5-46: Baseline Temperature Profile with Increased Primary Load

extended to the 0.89 m (35 in.) axial location. Thus, to inject secondary fuel at the end of the visible primary flame, the nominal injection point would have to be moved downstream approximately 0.25 m (10 in.). Rather than change the nominal secondary fuel injection location, alternate methods of increasing reburn zone temperature were investigated.

Primary load was halved to evaluate reburning effectiveness at reduced boiler temperatures (see Figure 5-46 for baseline temperature profile). It was found that when the burnout air was injected at temperatures less than 1100 K (1500°F), NO emissions were drastically reduced. Over 90 percent NO reduction (to less than 10 ppm) was achieved under this condition. However, under this condition, burnout becomes a problem as CO and UHC emissions increase rapidly as temperature decreases. The data shown in Figure 5-47 illustrate this phenomenon. It is apparent that this overall NO reduction in the stack is due to a mechanism other than the reburning mechanism. This phenomenon was also observed locally, in the burnout air jet, under full load conditions. This is discussed in Section 5.5. Possible mechanisms that have been hypothesized to explain these data are thermal de-NO_x, reverse-Zeldovich and heterogeneous soot reactions.

5.4.2 Insulated Reburning Zone

The boiler walls in the reburning zone, and the reburning fuel boom, were insulated with a layer of 5.1 cm (2 in.) thick insulating blanket. As shown in Figure 5-48, this effectively eliminated heat loss in the reburning region, resulting in a flat temperature profile. The peak temperature in the reburning zone was increased by less than 38°C (100°F), however. A limited series of I/O tests were performed under these conditions, with a slight reduction in the amount of overall NO reduction observed. Data from these tests are compared to uninsulated tests in Figure 5-49. Increased reburning

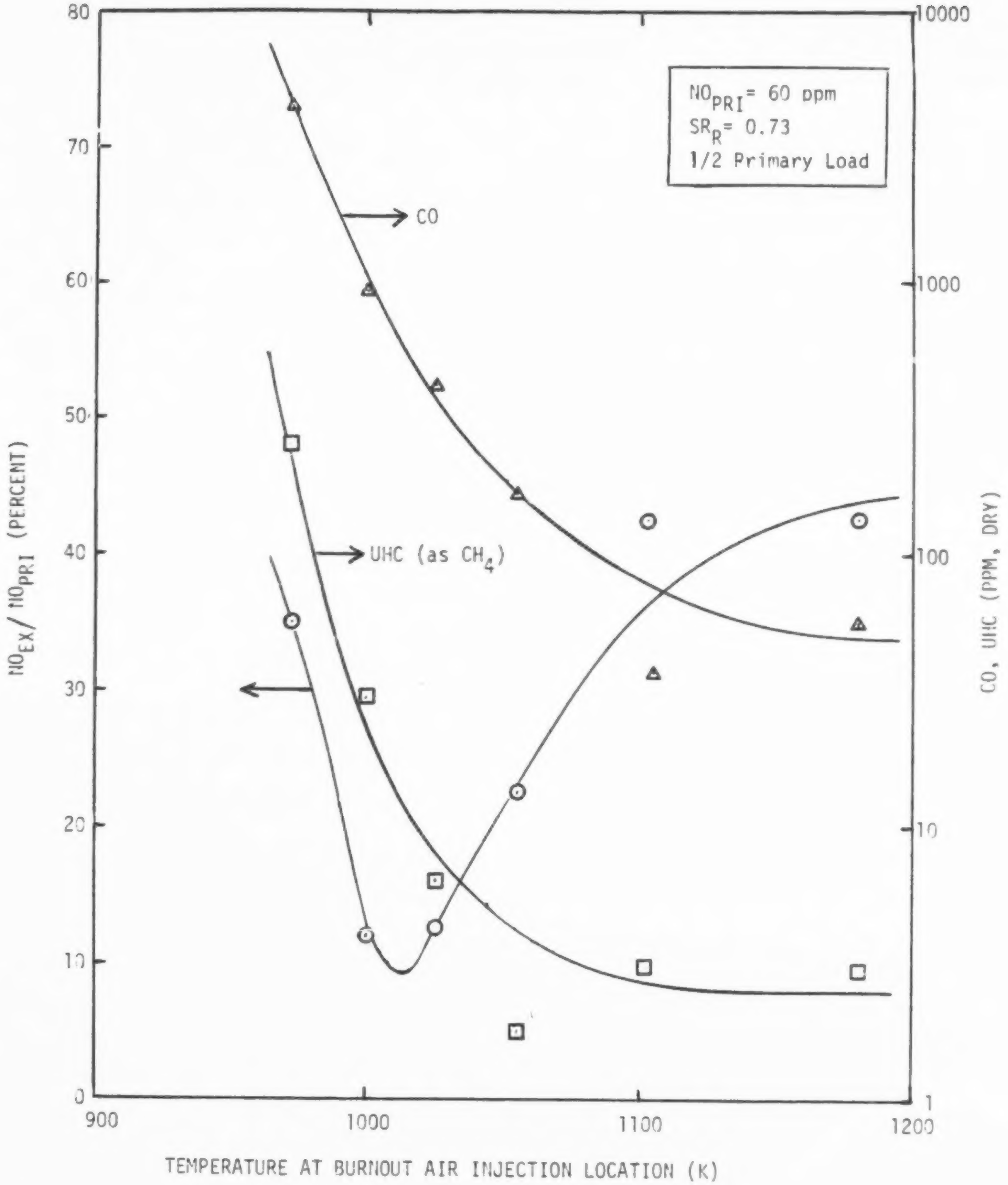

Figure 5-47: Reburning Effectiveness at Low Temperatures

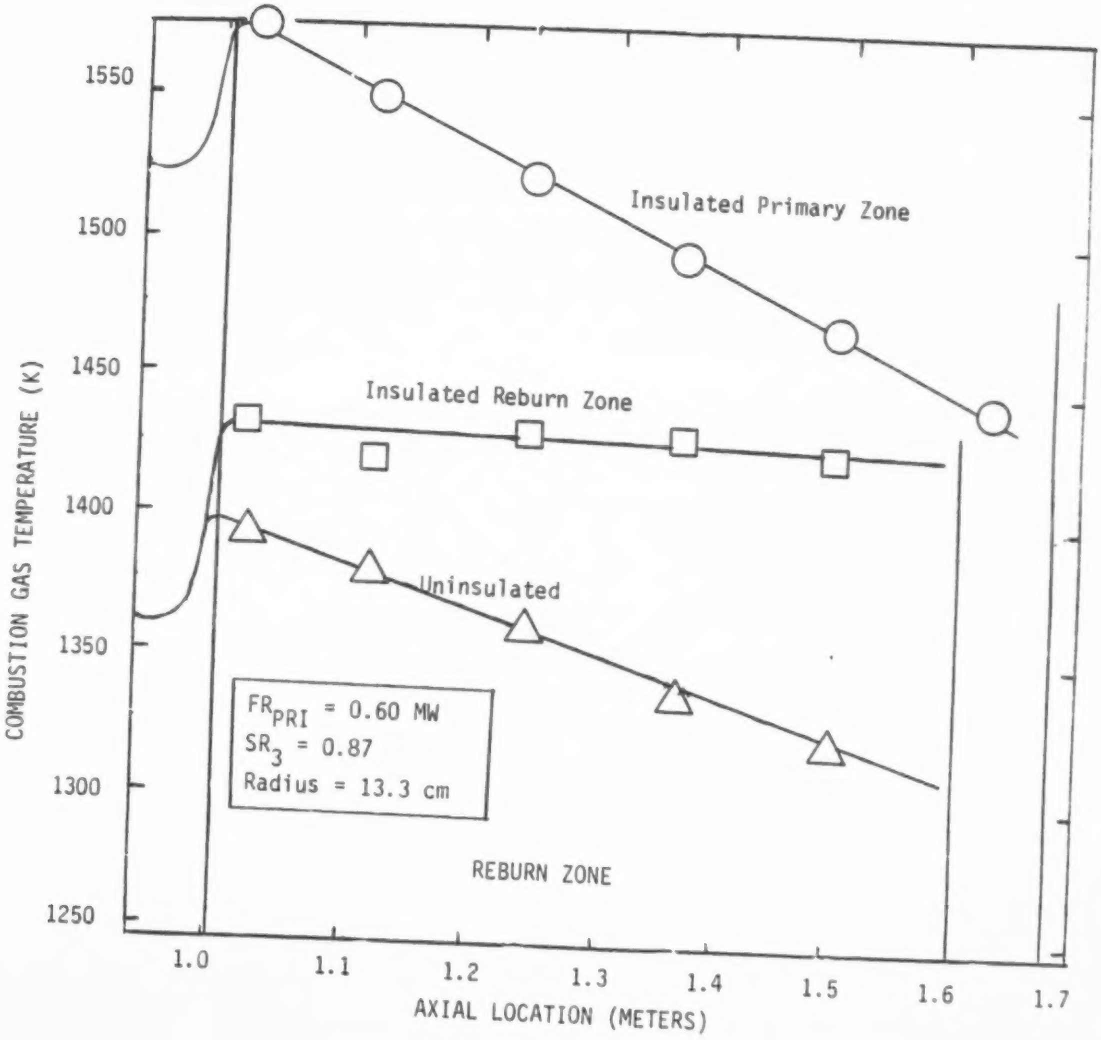

Figure 5-48: Reburn Zone Temperature Profile with Insulated Primary Zone and Insulated Reburn Zone

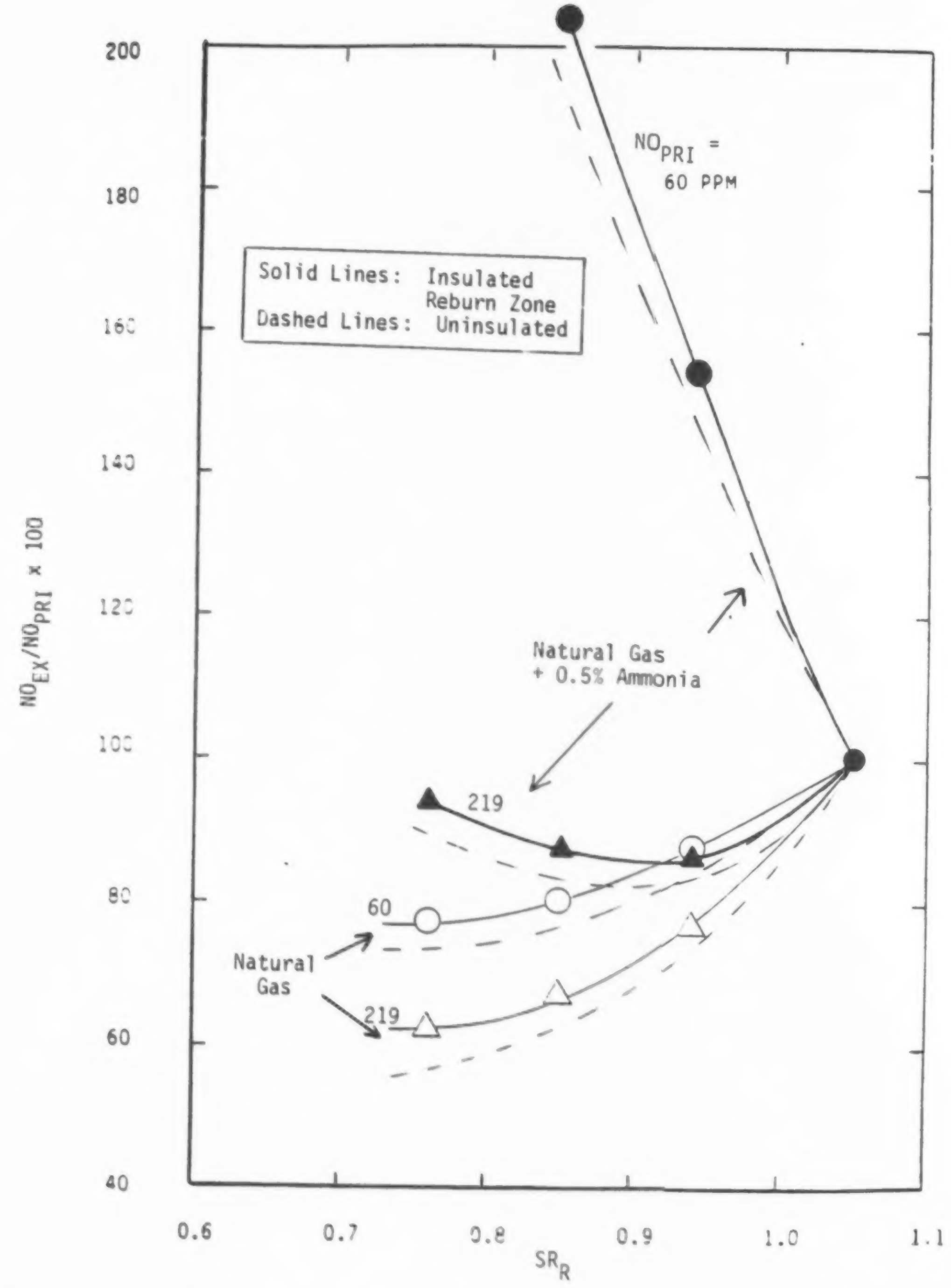

Figure 5-49: Natural Gas Reburning Effectiveness with Insulated Reburn Zone

zone temperatures slightly decreased reburning effectiveness in reducing NO_x. This seems to contradict the argument that increasing fuel-rich zone temperature should increase the equilibrium driving force for NO_x destruction. One possible explanation for the unexpected result is that reburning zone insulation decreased reburn zone residence times significantly (due to the combustion gas density and cross-sectional area decreases). Another possible explanation is that insulating the reburning zone did not increase peak reburning temperatures significantly, but did increase the temperature of combustion gas entering the burnout zone. This may have the effect of increasing fractional conversion of HCN and NH_3 to NO in the burnout zone.

Rather than investigate these results further, a third approach for increasing reburn zone temperature was taken: insulation of the primary zone. This approach would have minimal effect on reburn zone residence time (combustion gas density changes could be countered by increasing the reburn zone length to maintain constant reburn zone residence time) and would increase peak reburn zone temperature significantly.

5.4.3 Insulated Primary Zone

A 2.54 cm (1 in.) thick Fiberfrax® ceramic blanket layer of insulation was cemented to the boiler wall of the primary flame zone in the PBS. Baseline tests (without reburning) were repeated to characterize the primary zone with insulation. An axial temperature profile measured at the 13.3 cm (5.25 in.) radial location is presented in Figure 5-50. Baseline temperature was increased by about 150°C (300°F) in the post-flame region.

Axial temperature and velocity profiles for the insulated primary zone test condition are compared to those for the uninsulated tests under nominal reburn conditions. These plots are shown in Figures 5-50 and 5-51. Measured peak reburn temperature increased from 1460K (2070°F) to 1590K (2400°F). Peak velocity increased from 13 to 16 m/sec (43 to 52 ft/sec.).

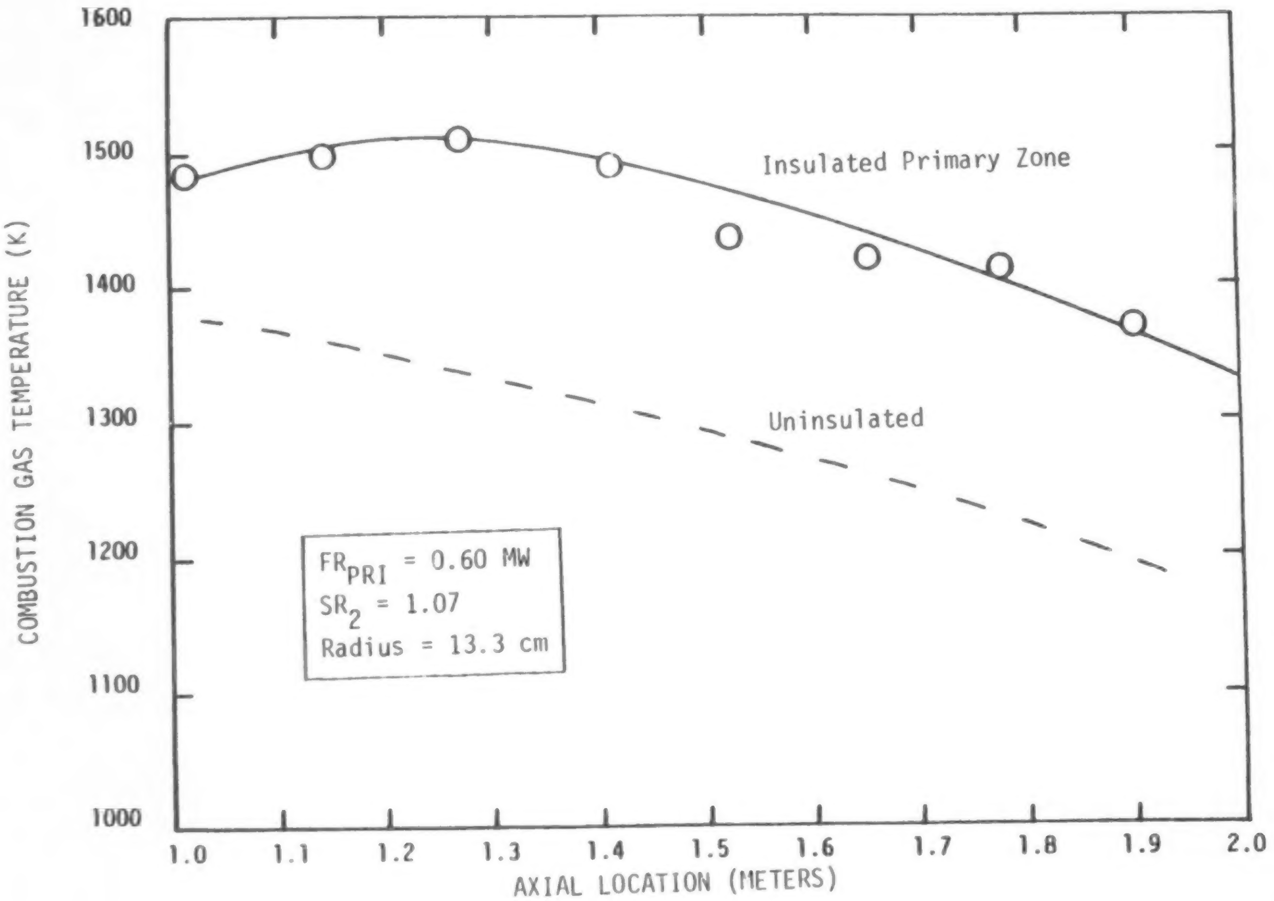

Figure 5-50: Baseline Temperature Profile with Insulated Primary Zone

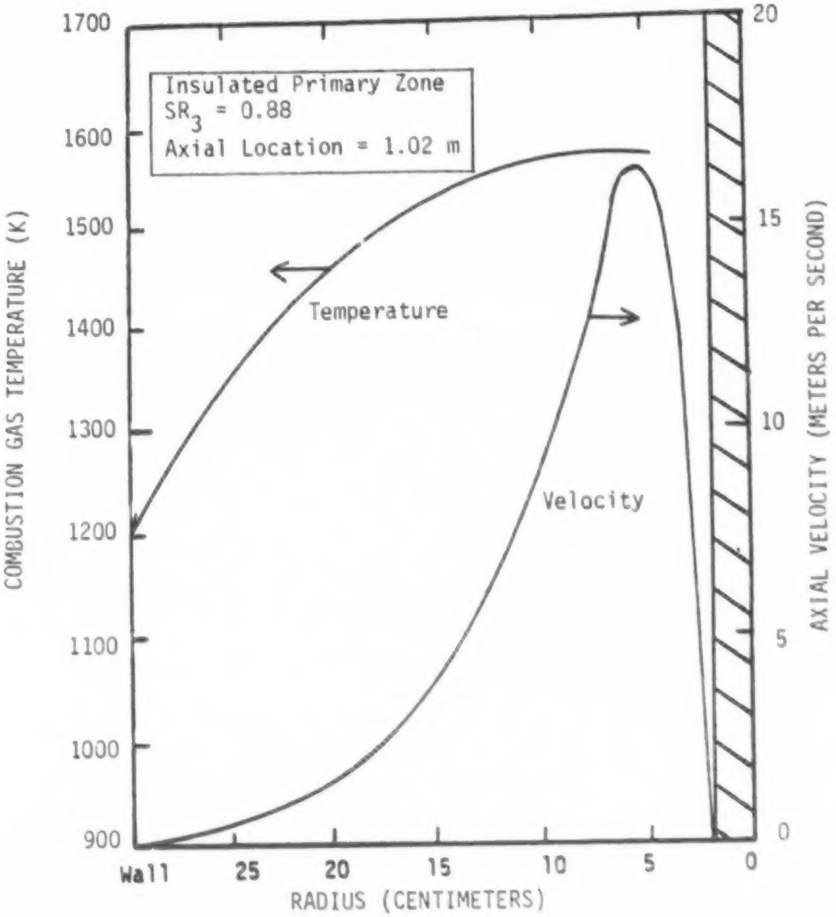

Figure 5-51: Reburn Zone Radial Velocity Profile with Insulated Primary Zone

Input/output reburn tests were performed with the primary zone insulated, using the spoked secondary fuel injector to achieve a uniform spatial distribution of SR_3. The axial length of the reburn zone was increased to 69 cm (27 in.) to keep the mass averaged residence time at approximately 200 ms. Parametric tests were conducted with SR_3 variation from 0.78 to 0.96, primary NO_x variation from 75 to 200 ppm, and undoped and ammonia-doped natural gas secondary fuels. Results indicated that there was no net influence of increasing temperature on the extent of overall NO reduction. Figure 5-52 presents a comparison of the high and low temperature trials for the 86 and 189 ppm primary NO_x conditions. To understand the reason for this apparent lack of influence of reburn zone thermal environment, detailed tests are required.

Axial concentration profiles of CO_2, CO, and THC (represented as CH_4), measured at the 13.3 cm radial location, are plotted in Figure 5-53 for SR_3 equal to 0.89. These data are compared to equivalent data taken for the uninsulated reburn test condition. As expected, the higher reburn zone resulted in much greater destruction of the hydrocarbon fuel, and much higher concentration of CO. At the reburn zone exit the CO and CO_2 concentrations approach their equilibrium values at the measured temperature (CO: 1.8%; CO_2: 10.6%).

Measured nitrogenous species concentration profiles for SR_3 equal to 0.9 and primary NO_x equal to 190 ppm are presented in Figures 5-54 and 5-55, for undoped and doped natural gas reburning. Though data to make a direct comparison of these results with low temperature results at exactly the same operating conditions are not available, there are some obvious observations that can be made. First, HCN concentrations peak almost immediately for the high temperature condition. Further, this peak is significantly higher (50 percent higher) than the peak at the low temperature test condition. Reburn

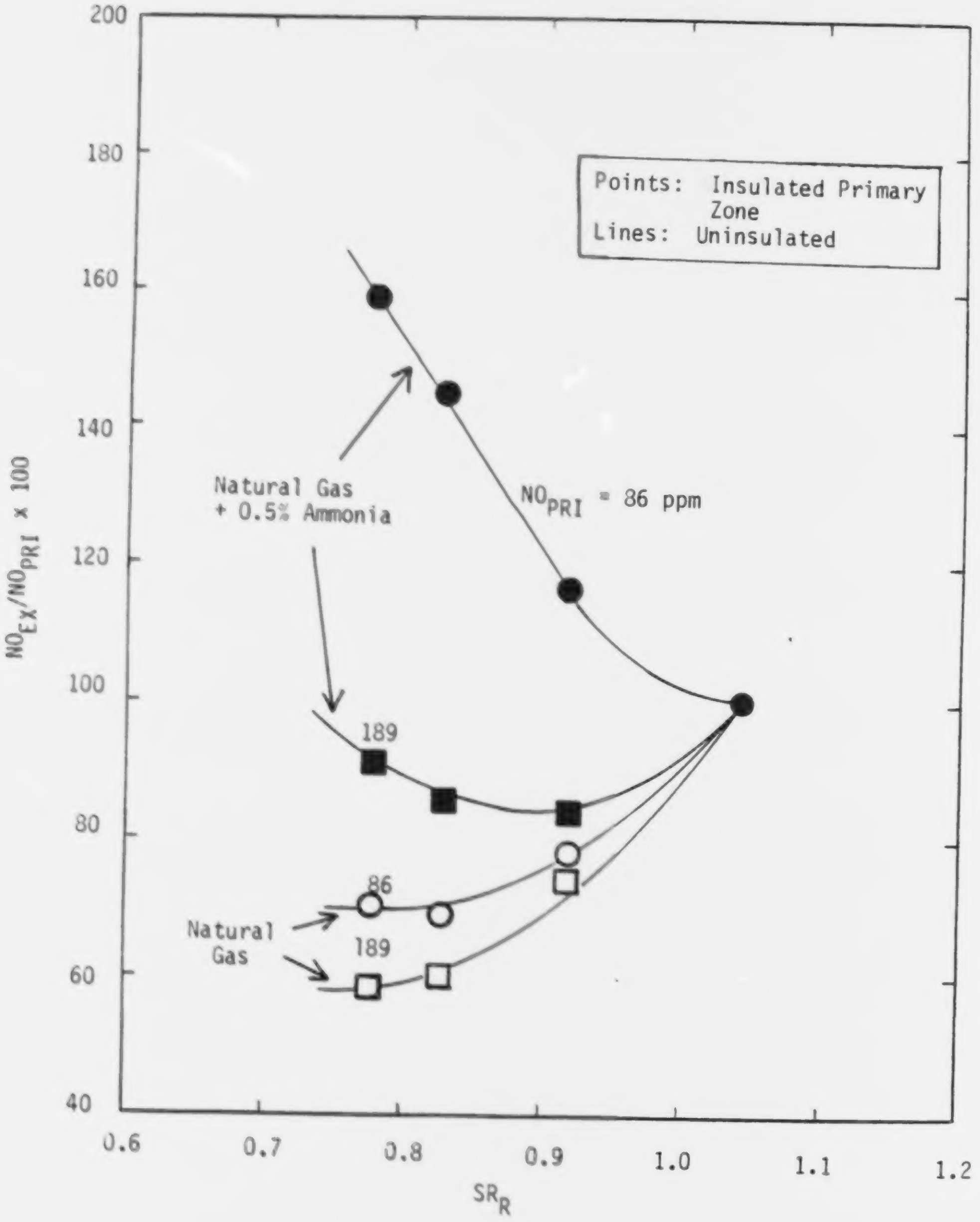

Figure 5-52: Natural Gas Reburning Effectiveness with Insulated Primary Zone

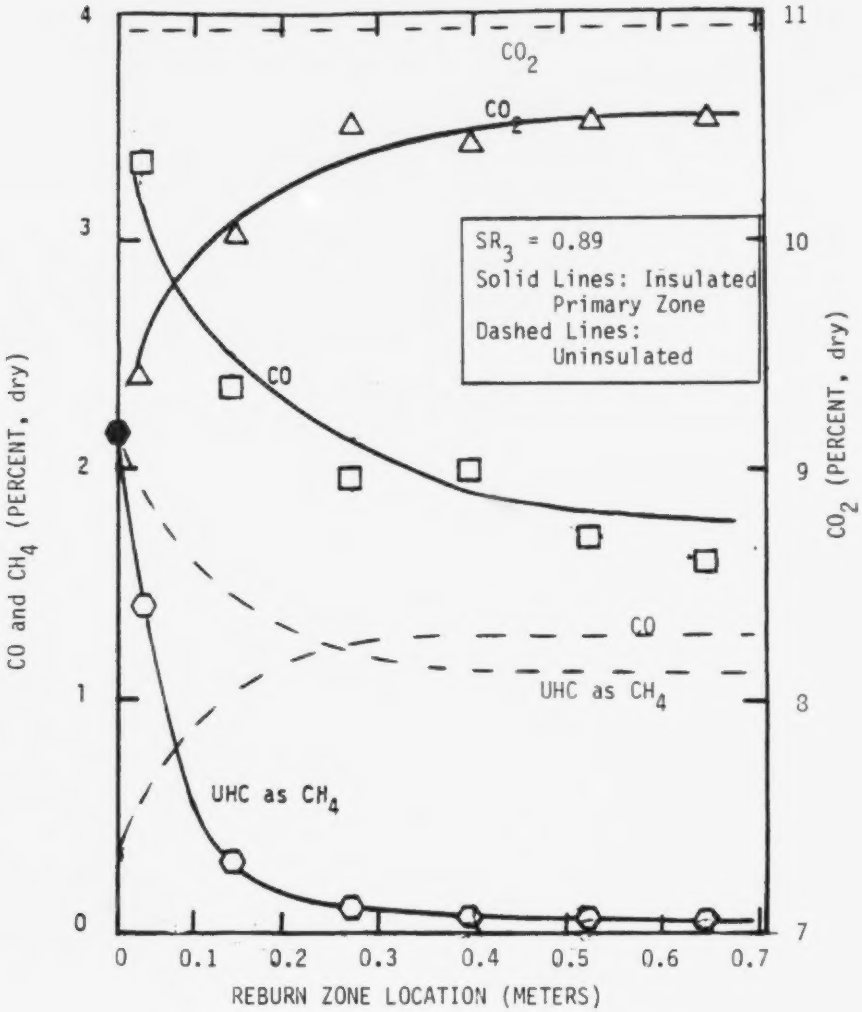

Figure 5-53: Reburn Zone Carbon Species Profiles for Natural Gas Reburning with Insulated Primary Zone

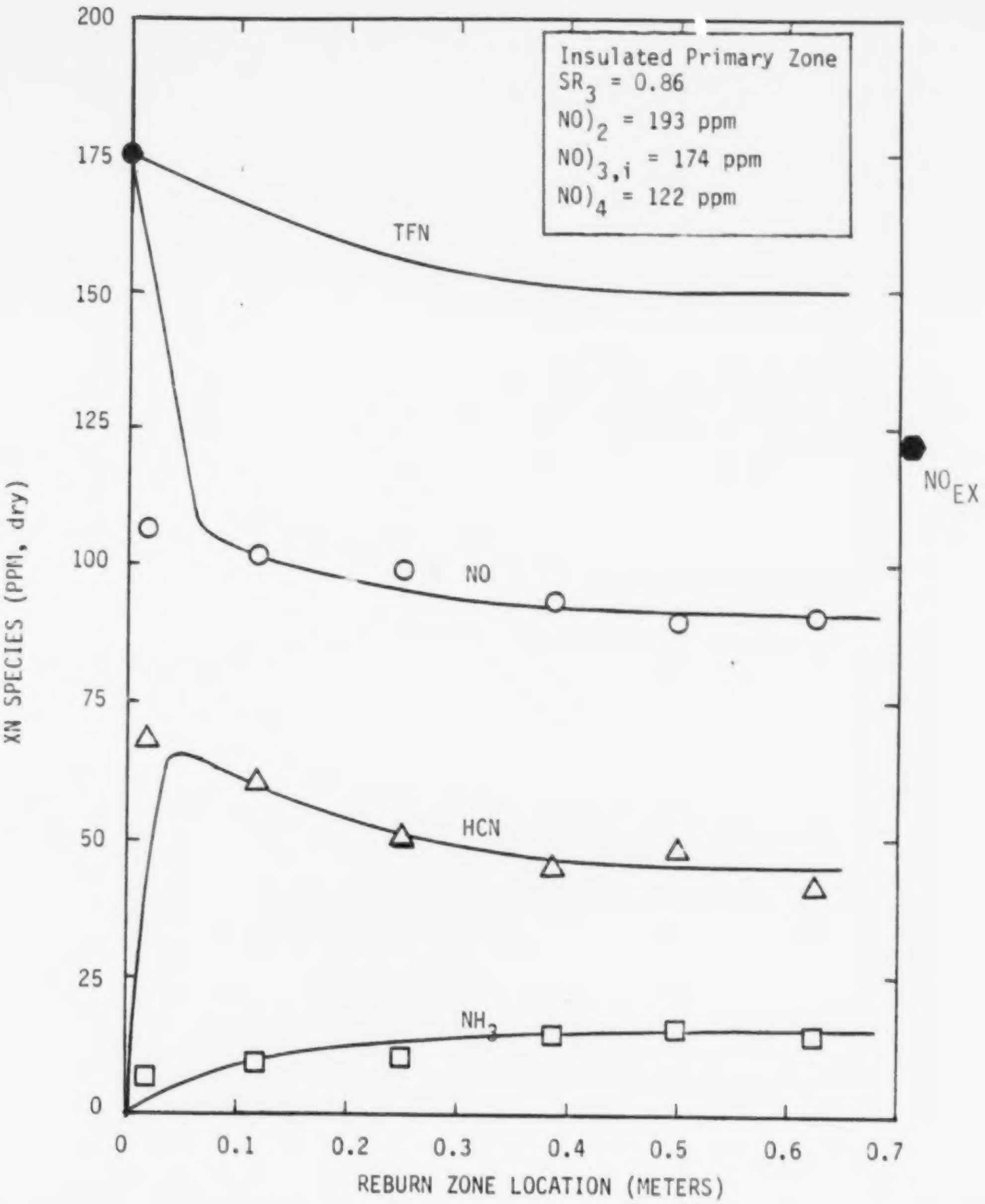

Figure 5-54: Reburn Zone Nitrogen Species Profiles for Natural Gas Reburning with Insulated Primary Zone

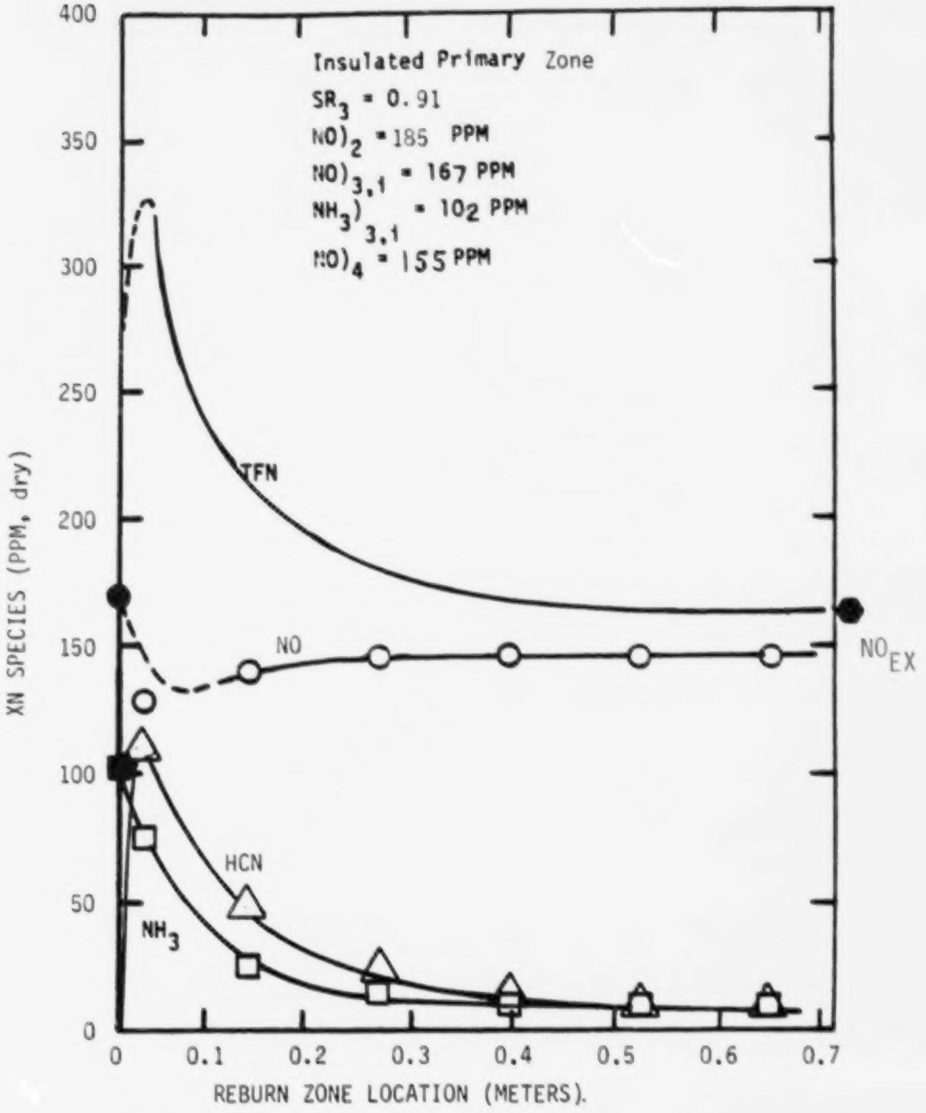

Figure 5-55: Reburn Zone Nitrogen Species Profiles for 0.5% Ammonia-Doped Natural Gas Reburning with Insulated Primary Zone

zone NO destruction is only slightly greater for the high temperature condition. Thus, the increase in hydrocarbon radicals caused by the increase in reburn zone temperature increased HCN formation by increasing the destruction of both NO and N_2. The net result is that overall NO destruction remains nearly constant.

In this test series, results were compared from test conditions in which not only reburn zone temperature was varied, but primary zone flame shape (the primary flame was 25 cm (10 in.) longer for the insulated primary zone test condition), reburn zone residence time (reburn zone length was limited to 69 cm (27 in.) due to boom design), and burnout zone temperature as well. Although it is impossible to vary only temperature in a practical system, a final test series was designed to better approximate this parametric variation of reburn zone temperature.

5.4.4 Secondary Fuel Injection Location

New primary burner operating conditions and a new secondary fuel injector were used to vary reburn zone temperature via secondary fuel injection location variation (and, hence, primary zone heat extraction variation). To provide a shorter primary flame length, SR_1 equal to 0.91 was established. With a primary fuel of undoped natural gas, a primary NO_x of 230 ppm was obtained at 6 percent excess air. The visible primary flame extended only 25 cm (10 in.) into the boiler. At 25 cm (10 in.) into the boiler, the centerline baseline temperature was 1730K (2650°F); at 102 cm (40 in.), the peak temperature was 1575K (2375°F).

A third-generation fuel boom was constructed to allow for secondary fuel injection through a side port in the PBS. This configuration, shown in Figure 5-56, is identical to the fuel oil reburning configuration, shown in Figure 6-1. Secondary natural gas was injected at 25 cm (10 in.) and 102 cm (40 in.), with 4 fuel jets originating from the boiler centerline directed

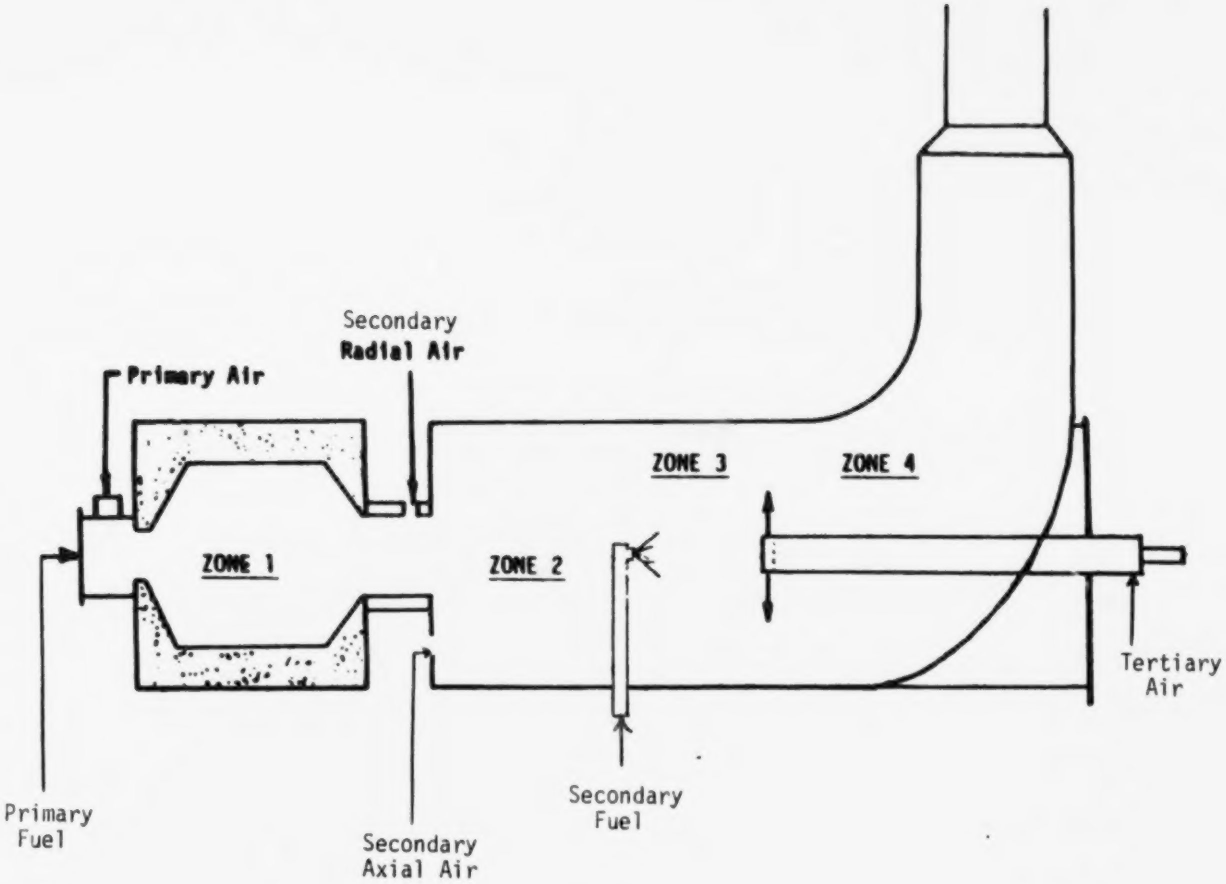
Secondary
Radial Air
Primary Air
ZONE 1
ZONE 2
ZONE 3
ZONE 4
Primary
Fuel
Secondary
Axial Air
Secondary
Fuel
Tertiary
Air

Figure 5-56: PBS Natural Gas Reburning Schematic with Secondary Fuel Boom # 3

downstream. Downstream orientation of the high velocity fuel jets resulted in the need to increase reburn zone length for maximum NO reduction. Reburn zone length was varied for each test condition by changing the location of final air addition. In this way, maximum NO reductions (minimums on the NO_{EX}/ NO_{PRI} curves) could be compared for the different fuel-injection locations.

Baseline radial temperature profiles at secondary fuel injection locations are shown in Figure 5-57. Input/output test results of NO measurements for undoped and ammonia-doped natural gas reburning are plotted as a function of reburn zone bulk residence time in Figures 5-58 and 5-59, respectively. For the low reburn load condition (SR_3 of 0.95), maximum NO reduction is decreased by 5 to 10 percent at the higher reburn zone temperatures. However, for the higher reburn load conditions (SR_3's of 0.85 and 0.79), maximum NO reduction is increased by 5 to 10 percent at the higher reburn zone temperatures. These trends are consistent for both doped and undoped natural gas reburning.

Figures 5-60, 5-61 and 5-62 show the same three sets of plots for a different primary burner operating condition. Here, SR_1 was set at 1.10 and zone 2 was eliminated. Due to the higher temperatures in the precombustion chamber burner, a primary NO_x level of 1050 ppm was established. The peak temperature at the 25 cm (10 in.) boiler location was 1879K (2900°F); at 102 cm (40 in.) the peak temperature was 1590K (2400°F). The results shown in Figures 5-61 and 5-62 show the same trends as those in 5-58 and 5-59. That is, for the low reburn load condition (SR_3 of 0.99), NO emissions increased by 10-20 percent with increased temperature; for the higher reburn load conditions (SR_3's of 0.89 and 0.80), NO emissions decreased by about 5 percent.

These results can be understood by simply considering equilibrium. Under fuel-lean conditions, increased temperature results in increasing equilibrium

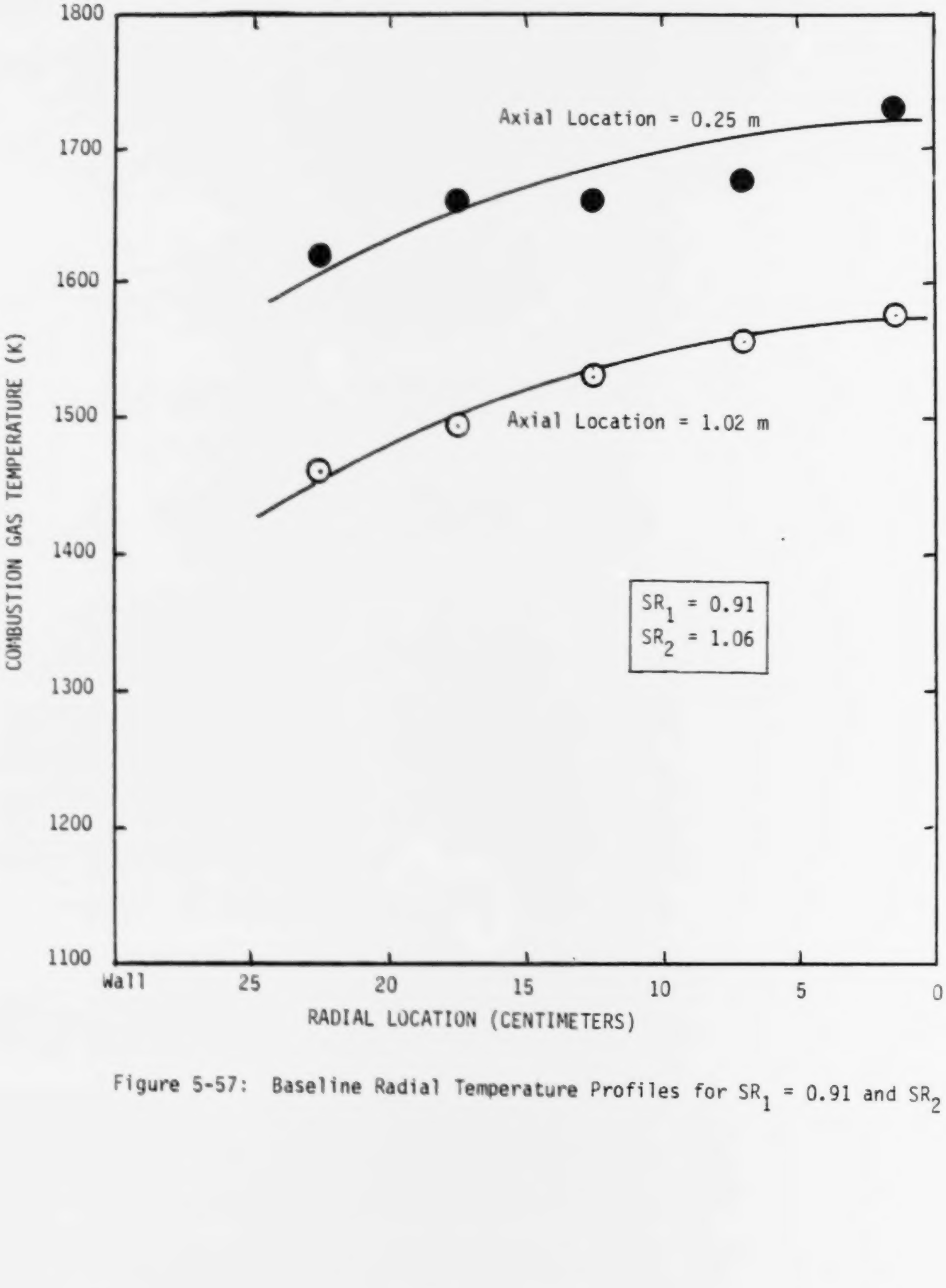

Figure 5-57: Baseline Radial Temperature Profiles for $SR_1 = 0.91$ and $SR_2 = 1.06$

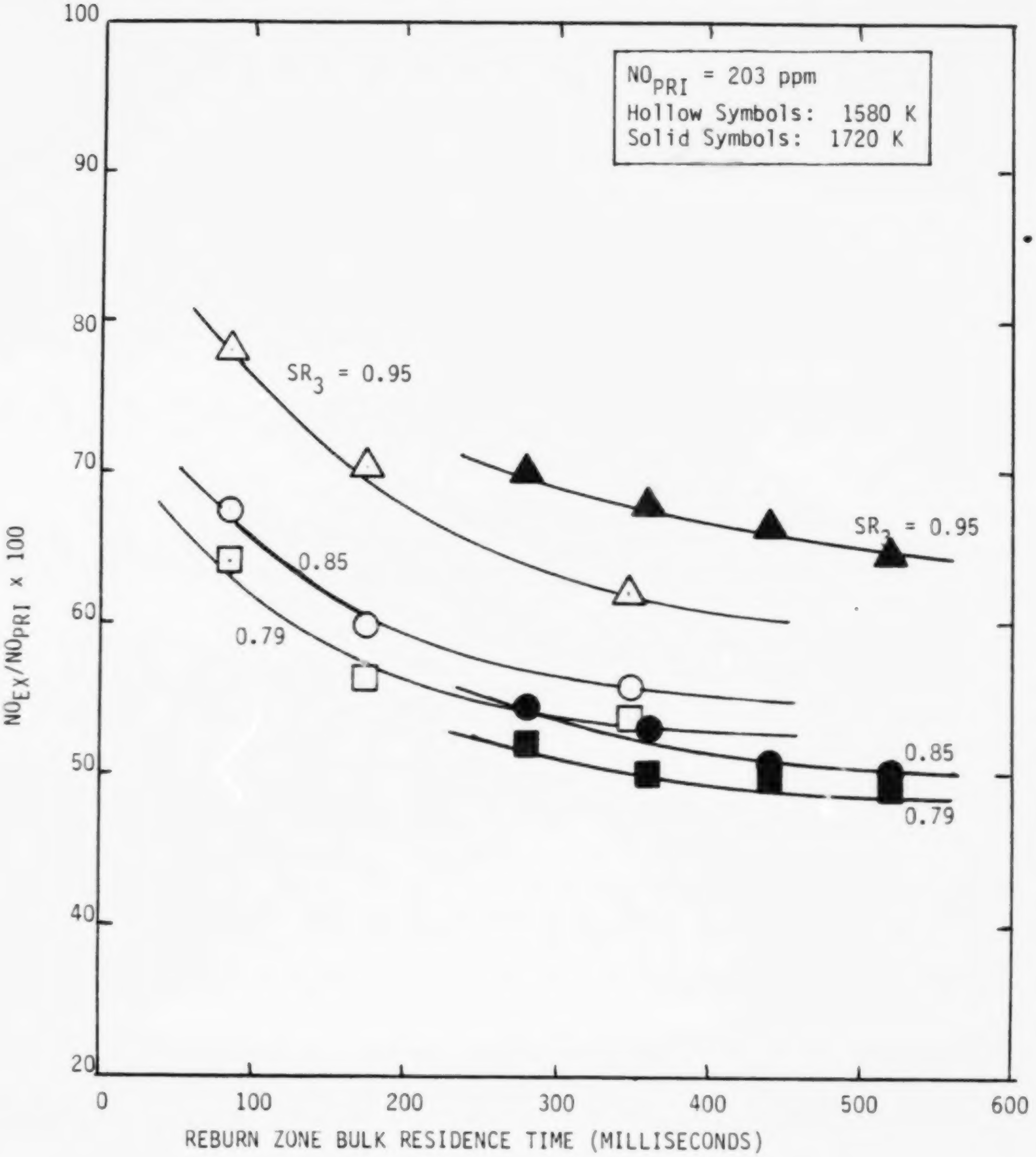

Figure 5-58: Thermal Effects for Natural Gas Reburning

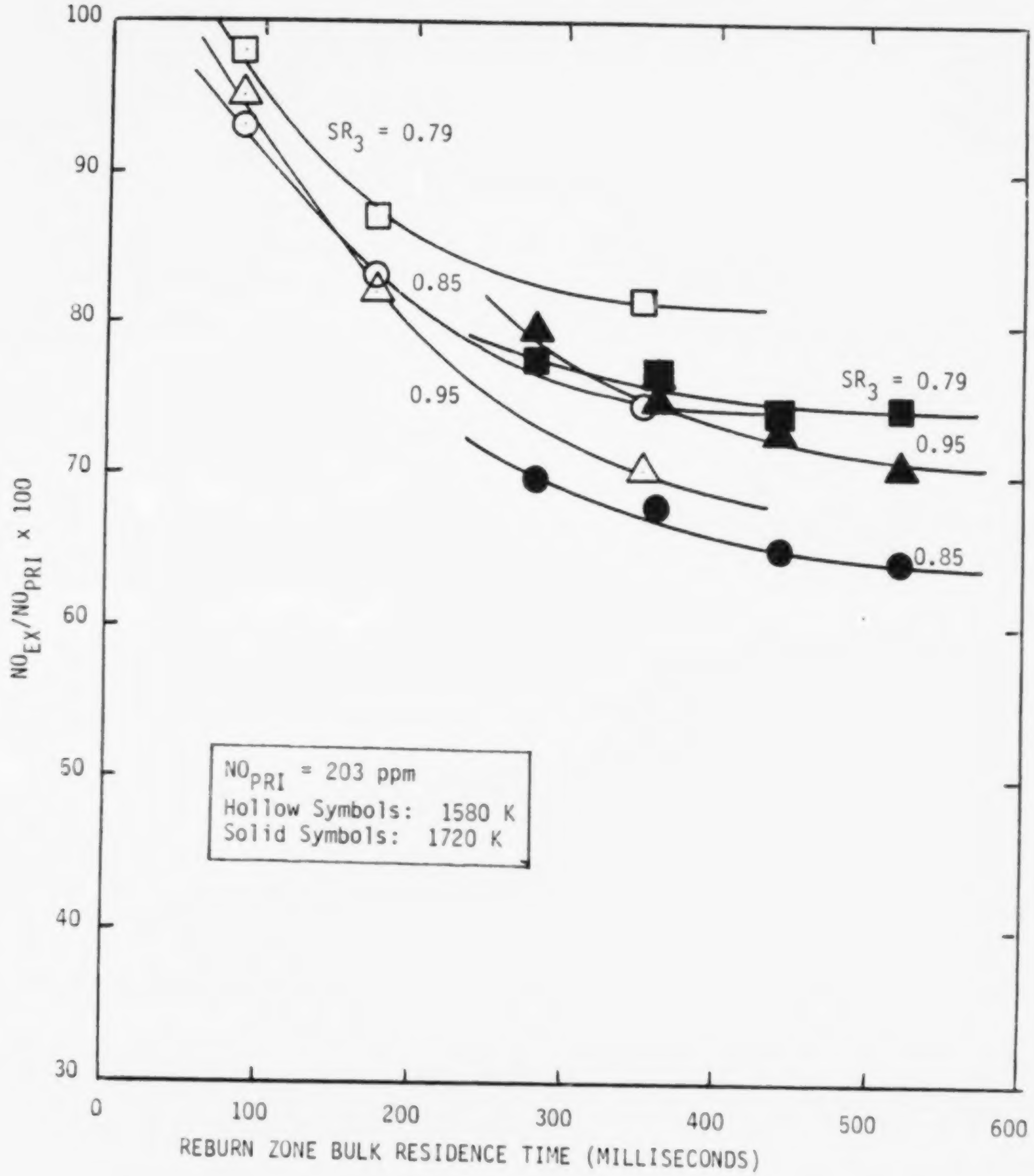

Figure 5-59: Thermal Effects for 0.5% Ammonia-Doped Natural Gas Reburning

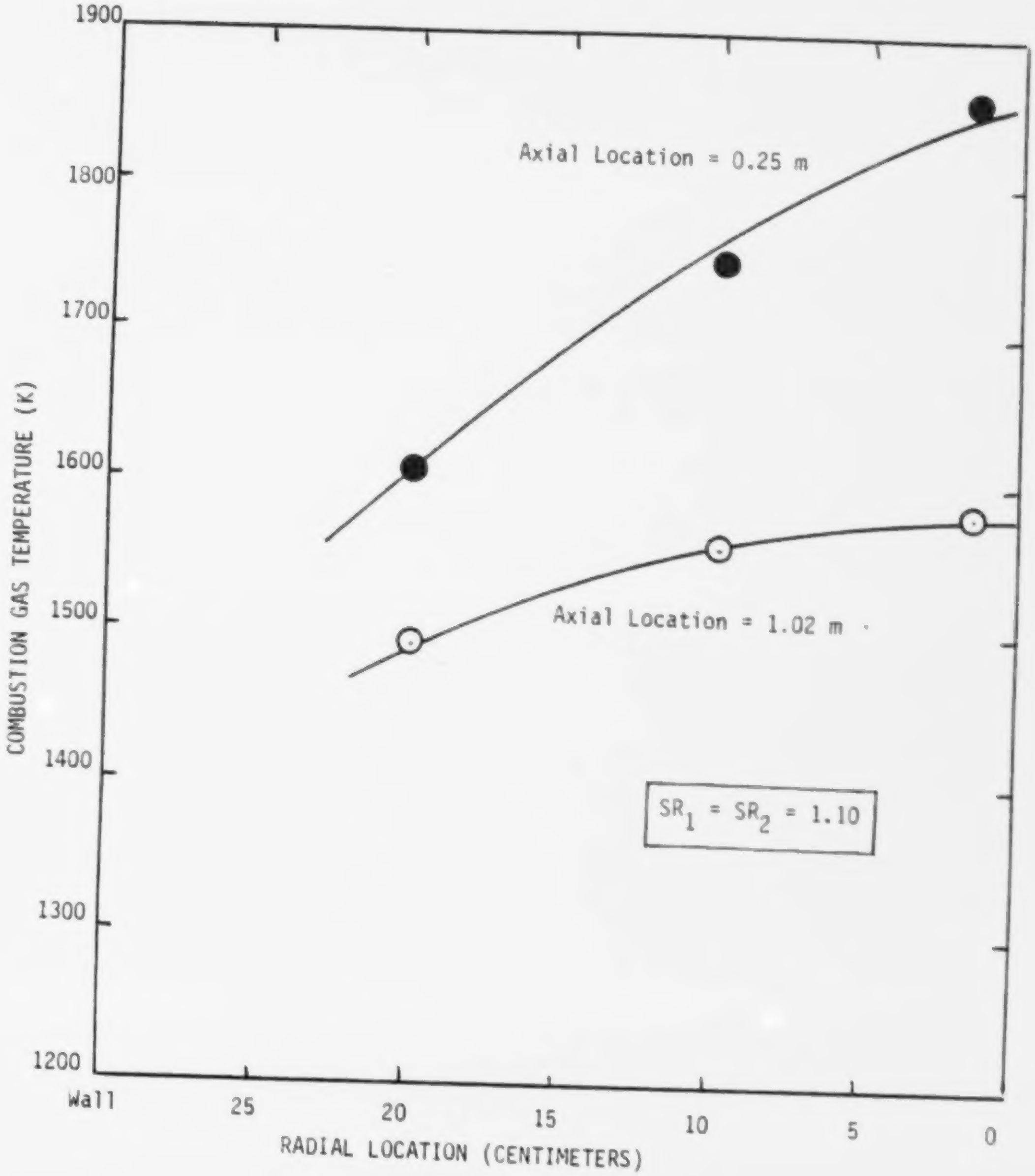

Figure 5-60: Baseline Radial Temperature Profiles for $SR_1 = SR_2 = 1.10$

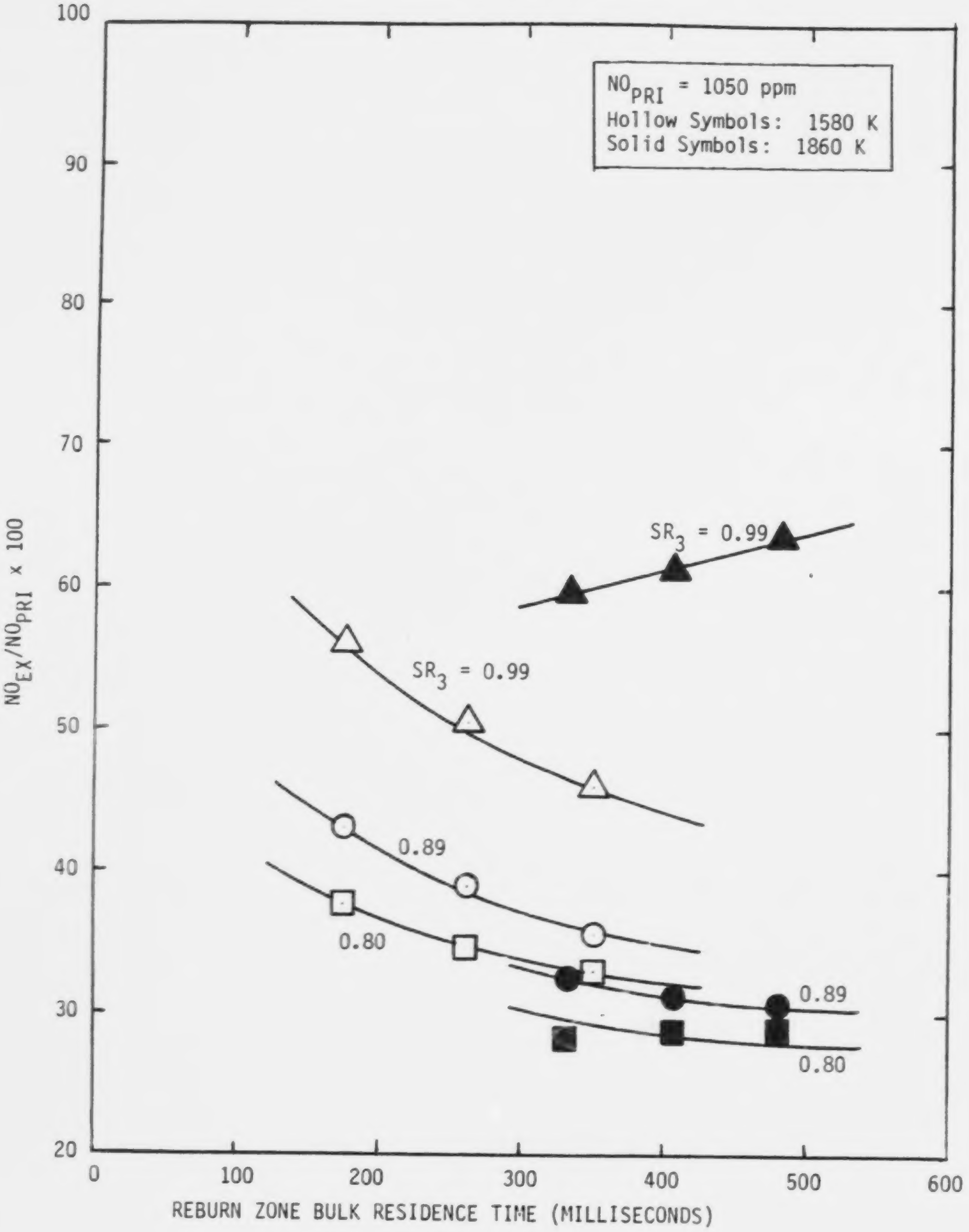

Figure 5-61: Thermal Effects for Natural Gas Reburning, NO_{PRI} = 1050 PPM

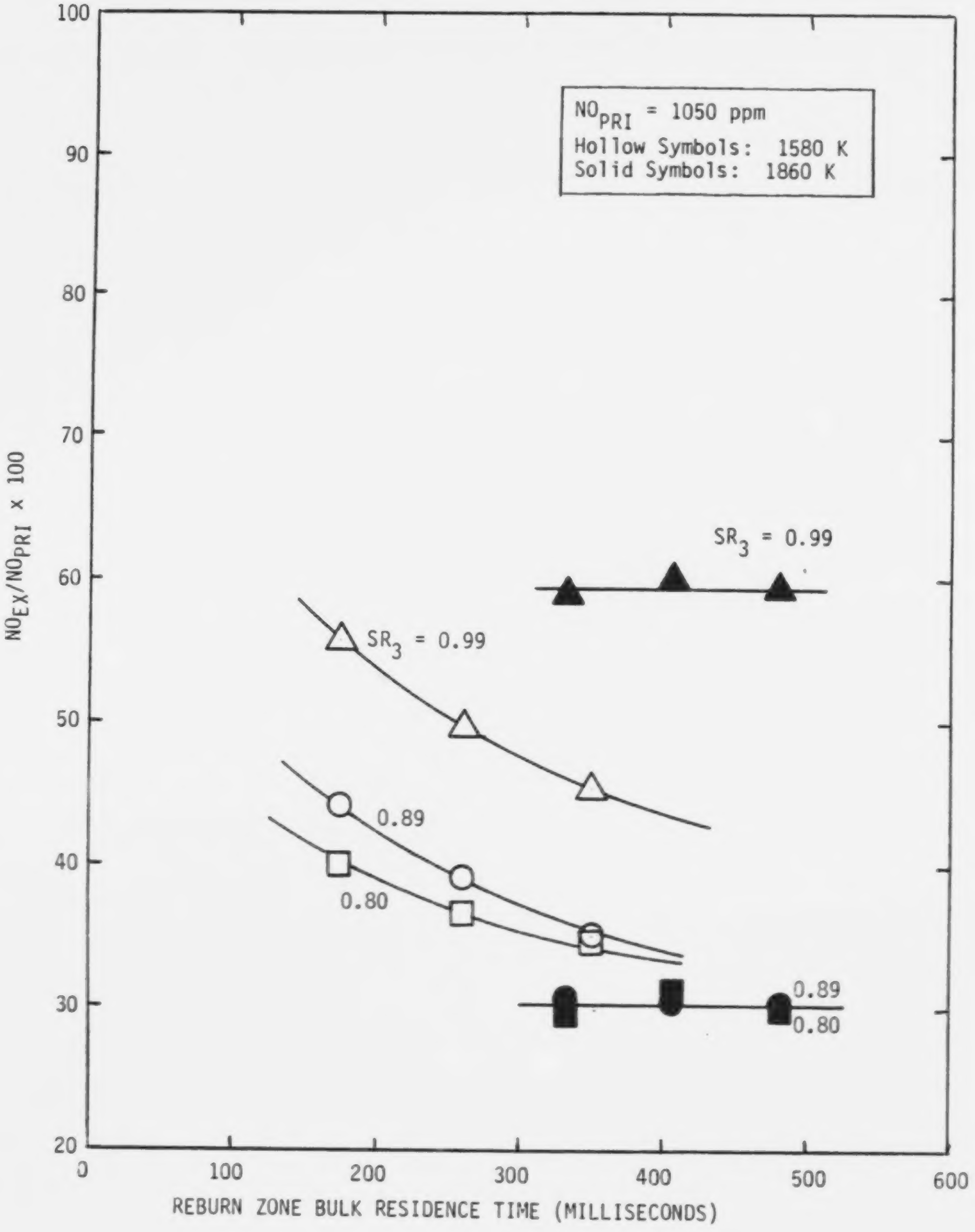

Figure 5-62: Thermal Effects for 0.5% Ammonia-Doped Natural Gas Reburning, NO_{PRI} = 1050 PPM

NO_x; however, for stoichiometric ratios less than 0.9, increasing temperature lowers equilibrium NO_x. Thus, the equilibrium driving force changes as reburning conditions are made increasingly fuel-rich. Considering that local stoichiometries may vary widely in the reburn zone (with the nearly point-source secondary fuel injection provided by the side-port injection fuel boom), the degree to which the data trends follow equilibrium predictions is remarkable. It should be noted that only the data trends are predicted by equilibrium; the magnitude of NO emissions still greatly exceed equilibrium NO concentrations.

5.4.5 Conclusions

Thus, it is concluded that increasing reburn zone temperature does improve NO_x reduction under fuel-rich conditions for stoichiometries less than 0.90. It is believed that this was not observed for the first three test series designed to increase reburn zone temperatures due to lack of control over other critical reburn parameters.

The first 5 hypotheses, stated in Section 1.4, have now been evaluated. These results will be summarized in Section 8. The following two sections describe PBS natural gas reburning tests that provide further insight into the natural gas reburning process.

5.5 STAGED AIR JET STUDIES

Reburning fuel and air staging effects have been studied both from an overall perspective (via input/output tests) and from a detailed analysis (via in-flame sampling). While performing detailed tests, a phenomenon was observed in the burnout air jet stream: NO was reduced to values less than 10 ppm (dry, corrected to zero percent O_2). This large NO destruction was found to be very localized, existing only in the air jet stream; the destruction did not appear to result in a significant overall NO_{EX} reduction. The phenomenon of NO_x destruction in staged air jets has been observed by other investigators [18,19], but the cause of this destruction is not understood. In this section, the observed phenomenon of NO destruction in the burnout air jet is documented, key parameters governing this destruction are identified, possible explanations of this phenomenon are suggested and evaluated, and conclusions are drawn as to the potential for optimizing this NO destruction mechanism in reburning application.

5.5.1 Observed Phenomenon

A test was conducted to document the phenomenon of burnout air jet NO destruction. At the low NO_{PRI} (67 ppm) and nominal reburn load (SR_R = 0.87) conditions, an axial traverse of various gas species at the 13.3 cm (5.25 in.) radial location was taken in the reburn and burnout zones. Secondary fuel was injected downstream (using fuel boom #3) at the 1.02 m (40 in.) axial location; final, or burnout, air was injected radially at the 1.63 m (64 in.) axial location. The burnout air boom is constructed with eight 1.27 cm (0.5 in.) diameter holes (spaced 45 degrees apart) through which burnout air is injected radially into the boiler at initial velocities ranging from 15 to 75 m/sec (50 to 250 ft/sec), depending on reburn load (SR_R's ranging from 0.96 to 0.78). At the nominal reburn load used in this test, eight radial air jets of 38 m/sec (125 ft/sec) velocity were established. Into these jets diffuses fuel-rich reburn zone effluent, with a bulk average velocity of 3.1 m/sec (10 ft/sec), and a peak velocity (at the boiler centerline) approaching 15 m/sec (50 ft/sec). Thus, the burnout zone consists of eight inverse diffusion flames, with the fuel made up of CO and H_2, primarily.

In Figure 5-63 it is shown that, in the reburn zone, NO was reduced rapidly to a steady state value of 39 ppm. In the burnout zone, NO increased, due to a partial conversion of reburn zone HCN and NH_3 to NO, to an exhaust

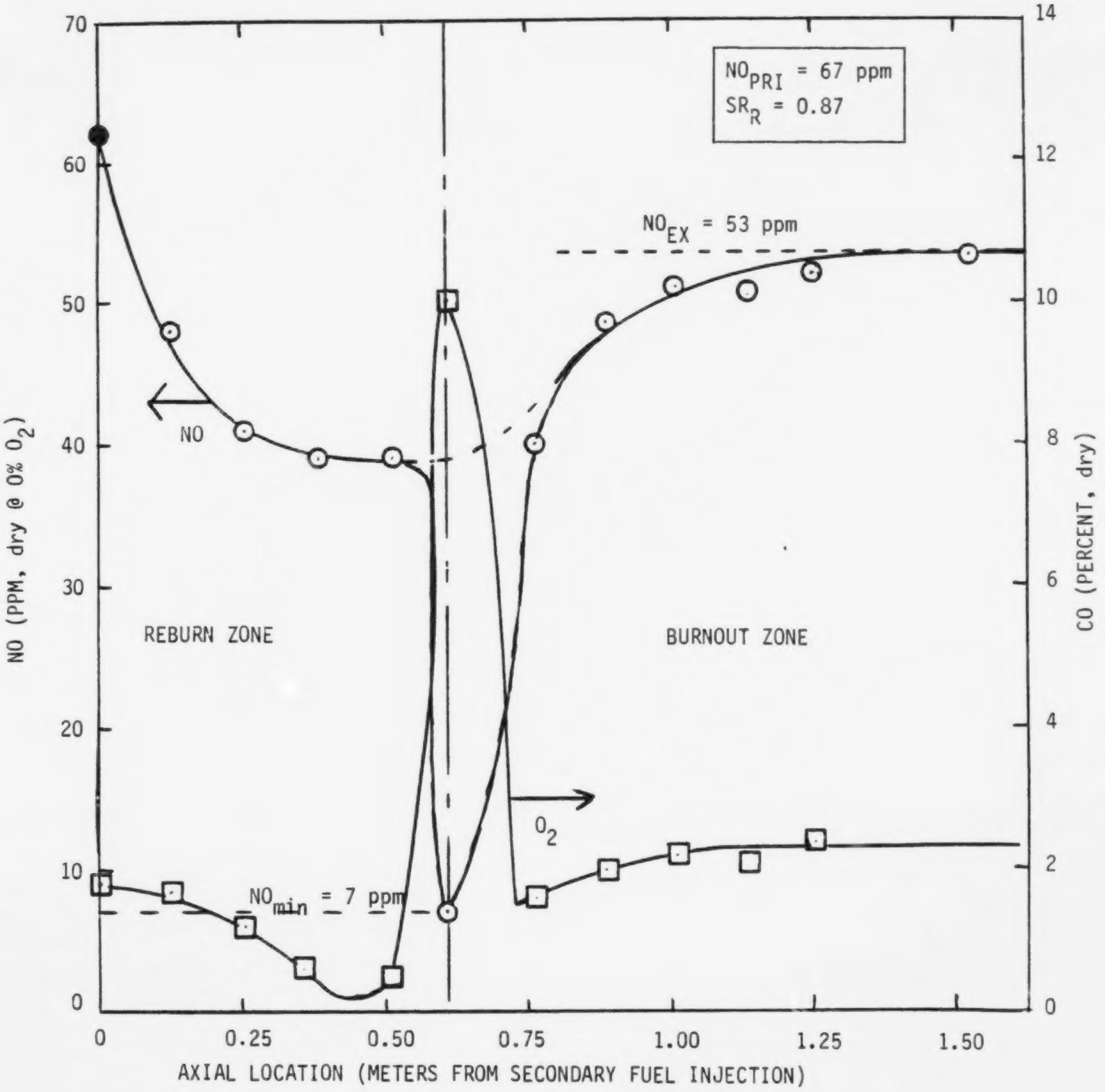

Figure 5-63: Axial NO and O$_2$ Profiles through the Burnout Air Jet

value of 53 ppm. In the burnout air jet, a net molar destruction of NO of over 80 percent was observed. At the minimum NO level (about 7 ppm, dry at zero percent O_2), measured at the center of the air jet, a carbon balance calculation indicates that the combustion gas composition at this location is roughly an equal mixture of reburn zone effluent (or fuel) and air.

From the axial profile shown in Figure 5-63 it would appear that the NO destruction is very localized, confined to the air jet environment. Two tests were performed to assess the extent of this destruction in the radial and in the circumferential directions. Gas species measurements were taken at three radii (13.3, 18.4 and 23.5 cm), and the results are tabulated in Table 5-7.

TABLE 5-7. RADIAL NO AND O_2 VARIATION IN THE BURNOUT AIR JET

Radius (cm)	NO without jet (ppm, dry @ 0% O_2)	NO with jet (ppm, dry @ 0% O_2)	O_2 with jet (percent, dry)
13.3	30	3	11
18.4	30	5	6
23.5	30	15	4

NO_{PRI} = 59 ppm
SR_R = 0.87
SR_{EX} = 1.08

Clearly, burnout air jet NO destruction decreases as distance from the jet source increases; however, even at large radii significant NO reduction is observed. Thus, the data suggest that NO destruction occurs in the air jet across the entire boiler radius.

Circumferential variations in NO were observed by investigating a single air jet. At the 13.3 cm radius sample location, NO concentrations of less than 5 ppm were recorded within 10 degrees of either side of the air jet (see Figure 5-64). With eight spokes located symmetrically, each 45 degrees apart, the data suggest that nearly half the flow area (but less than half the flow, as will be discussed in the next paragraph) is in the air jet NO destruction region. The relatively low peak O_2 concentration measured in the air jet in this test (3.4 percent, as opposed to 11 percent measured in other tests) suggests that the axial location of the sample probe was slightly off the air jet centerline. Repeatability of measurements highly sensitive to sample location is difficult in the large scale facility.

Results from these radial and circumferential sampling tests provide a means to make an order of magnitude estimation of the total moles of NO destroyed in the burnout air jets. To calculate this mass average NO destruction, two simplifying assumptions are made. First, based on the O_2 and CO_2 measurements in the peak NO destruction areas of the air jet, it is assumed that the quantity of primary zone effluent that sees this zone is equal to the total flow of burnout air. This assumption means that roughly 20 percent of the reburn zone effluent passes through the air jet for the nominal reburn load test condition. Intuitively, it would be expected that a majority of the reburn zone exhaust would bypass the high velocity (high total pressure) air jets and mix downstream. A second assumption is that of the 20 percent of the reburn zone flow that enters the jet, all but 3 ppm of the NO is destroyed. None of the NO in the remaining 80 percent flow is destroyed. Based on these assumptions, for the 60 ppm NO_{PRI} condition where the reburn zone NO concentration is 30 ppm, the burnout zone NO concentration after air jet NO destruction is 24.6 ppm. Thus, only a 5.4 ppm overall reduction in NO is realized by the air jet NO destruction phenomenon.

It is emphasized that this is an order of magnitude computation. The assumptions that 20 percent of the flow experiences nearly complete NO destruction and 80 percent of the flow experiences no NO destruction are

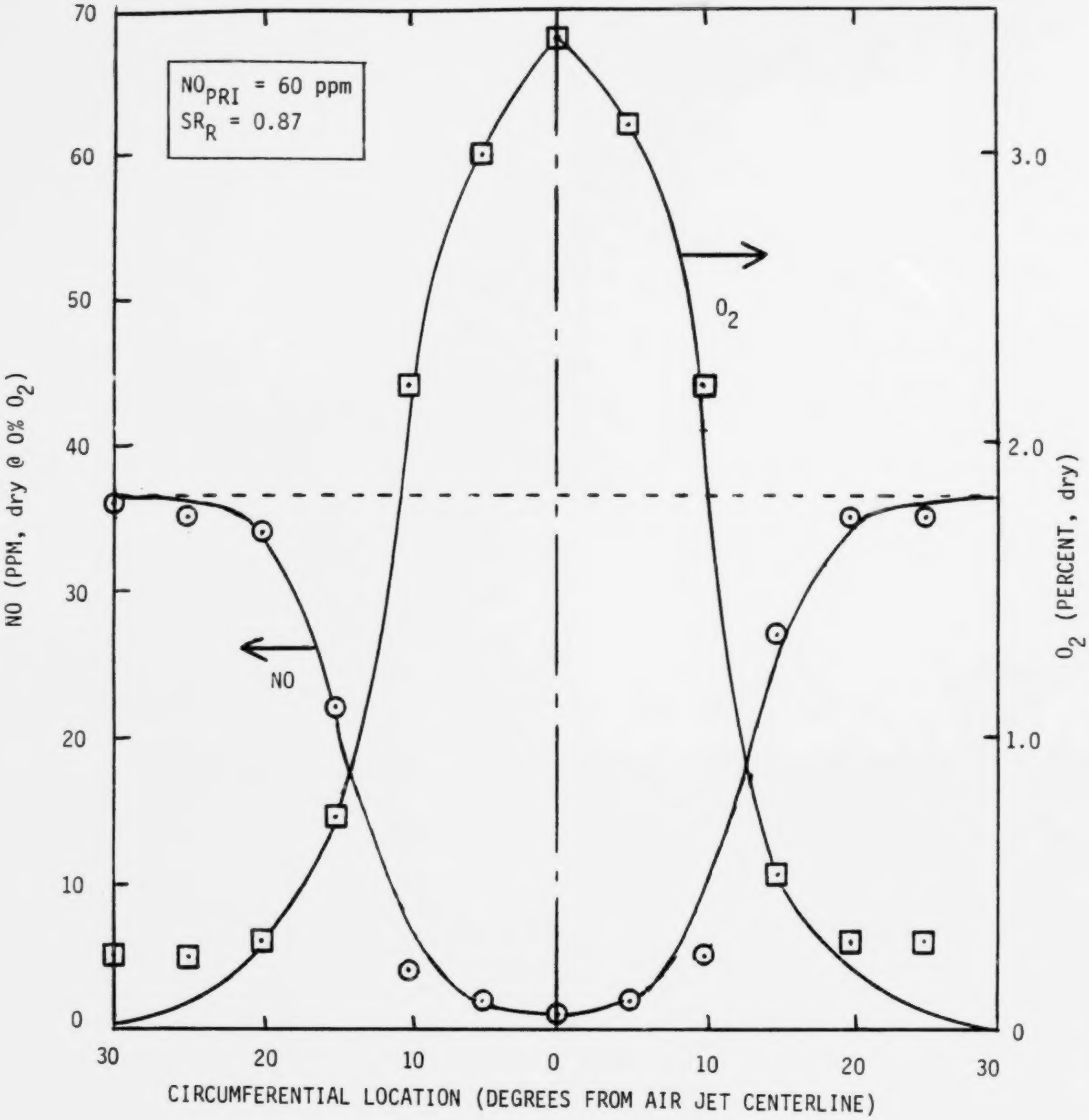

Figure 5-64: Circumferential NO and O_2 Profiles in the Burnout Air Jet

obviously oversimplifications. In addition, with NO formation processes occurring in the burnout zone as well, it is impossible to measure the destruction term alone in the large scale facility. Nonetheless, the computation does confirm the observation that the air jet NO destruction phenomenon does not significantly effect overall NO emissions.

Before trying to understand and optimize this NO destruction phenomenon, it is necessary to demonstrate that the destruction is real, not simply a conversion of one fixed nitrogen species to another. Samples were taken in and out of the air jet to determine concentrations of NO, NO_2, NO_3, HCN and NH_3. These tests were repeated several times. Table 5-9 lists the results of these measurements. A reduction in TFN of 86% (to less than 10 ppm) was measured. Although every fixed nitrogen species could not be measured in these tests, it is not expected that any other nitrogenous species, other than N_2, is formed in a natural gas reburning and air flame. Therefore, it is concluded that the observed N_2 formation in the air jet is real.

So far, the NO destruction in the air jet has been termed a "phenomenon", as the mechanism of this destruction is unknown. In the following sections, the cause of this destruction is investigated.

TABLE 5-8. FIXED NITROGEN SPECIES IN THE BURNOUT AIR JET

Species	Concentration Without Jet (ppm, dry @ 0% O_2)	Concentration With Jet (ppm, dry @ 0% O_2)	Percent Reduction
O_2	0.35	11.25	-
NO	30	3	90%
NO_2 + NO_3	(<5)	(<5)	-
HCN	11	2	82%
NH_3	4.0	1.4	65%
TFN	45	6.4	86%

5.5.2 Key Parameters

The dependence of the air jet NO destruction phenomenon on reburn load (and SR_R), NO_{PRI}, jet composition, air jet flow and temperature has been studied.

For the low NO_{PRI} condition (66 ppm), air jet NO concentrations at three reburn loads (corresponding to $SR_R = 0.98$, 0.88 and 0.79) were measured. As shown in Figure 5-65, NO destruction in the air jet increased as reburn load increased (i.e., SR_R decreased). NO destructions of as high as 95 percent were measured. With no reburning, no NO destruction was found. It is concluded that flame radical species are necessary to destroy NO. With reburning, some air jet NO destruction is observed even for overall fuel-lean SR_R's. Without reburning, air must be staged into a fuel-rich environment to achieve NO destruction. This discrepancy is explained by the observation that in reburning, even at fuel-lean reburn zone conditions, flame species (such as CO) exist entering the burnout zone due to insufficient reburn zone residence time and mixing. Thus, it is concluded that for staging air into long, well-mixed fuel-rich zones, NO destruction approaches 0 as the fuel-rich stoichiometry approaches 1.0.

Two NO_{PRI} conditions were considered at nominal reburn loads. As already stated, for the low NO_{PRI} test condition with reburn zone exit NO concentrations less than 50 ppm (dry), minimum NO values of less than 5 ppm were observed in the air jet. For the high NO_{PRI} condition (approximately 200 ppm), with a reburn zone exit NO concentration of about 130 ppm, minimum NO values in the air jet at the 13.3 cm radial location were found to be in the range of 10 to 25 ppm. Although uncertainty in the NO analyzer accuracy below 10 ppm and uncertainty in the exact sample location for these highly localized

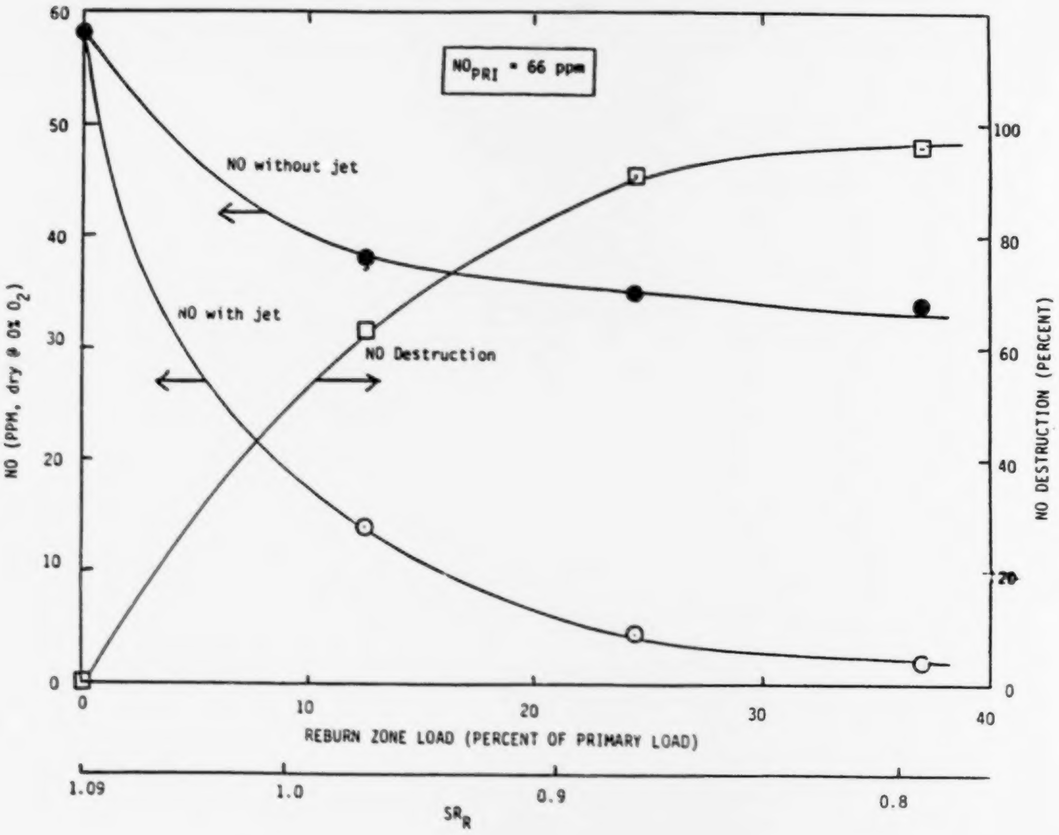

Figure 5-65: Effect of Reburn Zone Load on Burnout Air Jet NO Destruction

destructions make conclusive results difficult to obtain, the data suggest that a 90 percent destruction of NO is achieved in the burnout air jet independent of NO_{PRI} in the range of zero to 200 ppm. Computing the total molar destruction of NO for the 200 ppm NO_{PRI} condition as done previously for the 60 ppm NO_{PRI} condition, a total destruction of 23.4 ppm is realized by the air jets (from 130 ppm NO in the reburn zone effluent). As before, NO formation processes in the burnout zone dominate and stack NO values actually increase over reburn zone NO values.

Jet composition was also considered as a parameter controlling the local NO destruction. A small amount of air compressor lubricating oil was observed to have contaminated the compressor air that was used for burnout air. To eliminate this oil contamination as a potential contributor to the air jet NO destruction (via hydrocarbon reactions, as in reburning), dry bottled air was used. As shown in Table 5-9, no significant change in the air jet NO level was measured in changing from compressor air to bottled air. A second test was conducted using bottled molecular nitrogen in place of the burnout air. There was no destruction of NO using the pure N_2 (chemically inert at the injection conditions), as expected. Thus, NO destruction in the burnout air jet is apparently dependent on oxygen reactions, either directly or indirectly.

TABLE 5-9. EFFECT OF JET COMPOSITION ON NO DESTRUCTION

Jet Composition	NO without jet (ppm, dry)	NO with jet (ppm, dry at 0% O_2)	Percent Reduction
Compressor air	40	9.4	77
Bottled Air	40	6.4	84
Bottled N_2	40	39.5 (corrected)	0

Dependence of air jet NO destruction on air jet flow is shown in Figure 5-66. Minimum NO concentrations (of less than 5 ppm) are achieved when the air jet flow is sufficient to drive local O_2 levels to 6 percent and higher. This data appears to be consistent with radial sampling at a fixed air flow rate (Table 5-7), where at the outer sampling radius (23.5 cm) NO levels were higher and O_2 levels lower than at the inner sampling radii (13.3 and 18.4 cm).

Air jet NO reduction dependence on temperature (measured at the final air injection location, but without air flow) is shown in Figure 5-67. Temperature variation was achieved by operating the PBS with a fuel-rich primary zone (and no reburning). By varying the location of staged air injection, and by changing the fuel-rich zone stoichiometry, temperatures ranging from 1250K (1800°F) to 1800K (2800°F) were achieved. The results shown in Figure 5-67 indicate that at temperatures greater than 1600K (2420°F), NO destruction in the air jet decreases.

Also plotted in Figure 5-67 are equilibrium NO values for atmospheric methane/air combustion at 10 percent excess air. It is interesting to note that the equilibrium NO trend proximates the air jet NO curve shifted to lower temperatures. Variations in local temperatures and stoichiometries in the air jet are probably high, dependent on the physical and thermal mixing rates of the hot "fuel" (comprised primarily of CO and H_2) and the unpreheated air. Considering these variations, it is remarkable how closely the experimental curve measured at local conditions and the equilibrium curve calculated at overall conditions agree.

From this investigation of key parameters influencing the air jet NO destruction, a theory as to the cause of the destruction emerges. The fuel-rich reburn zone effluent, consisting of combustion products and products of incomplete combustion (i.e., CO and H_2), is mixed with the burnout air and

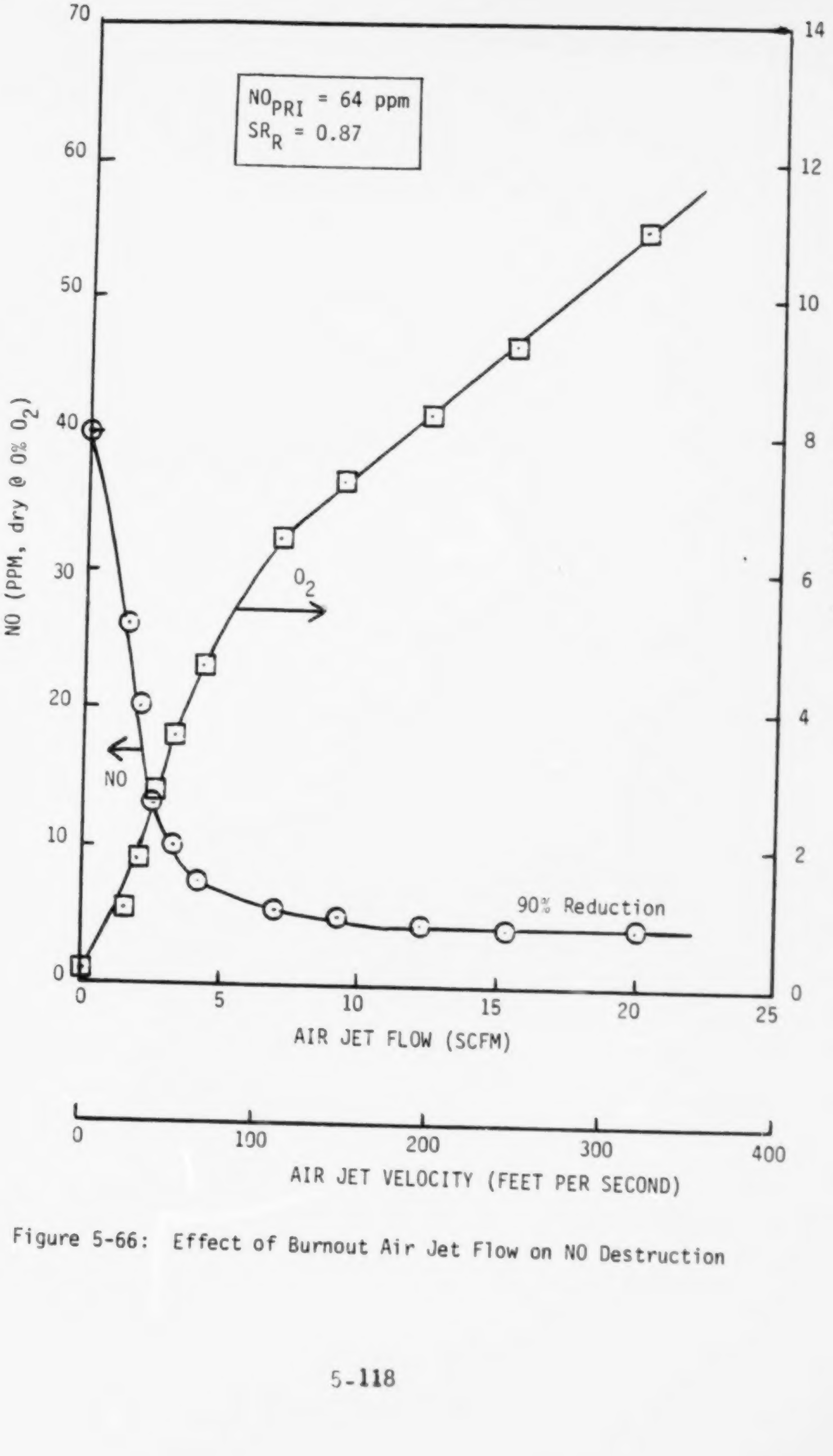

Figure 5-66: Effect of Burnout Air Jet Flow on NO Destruction

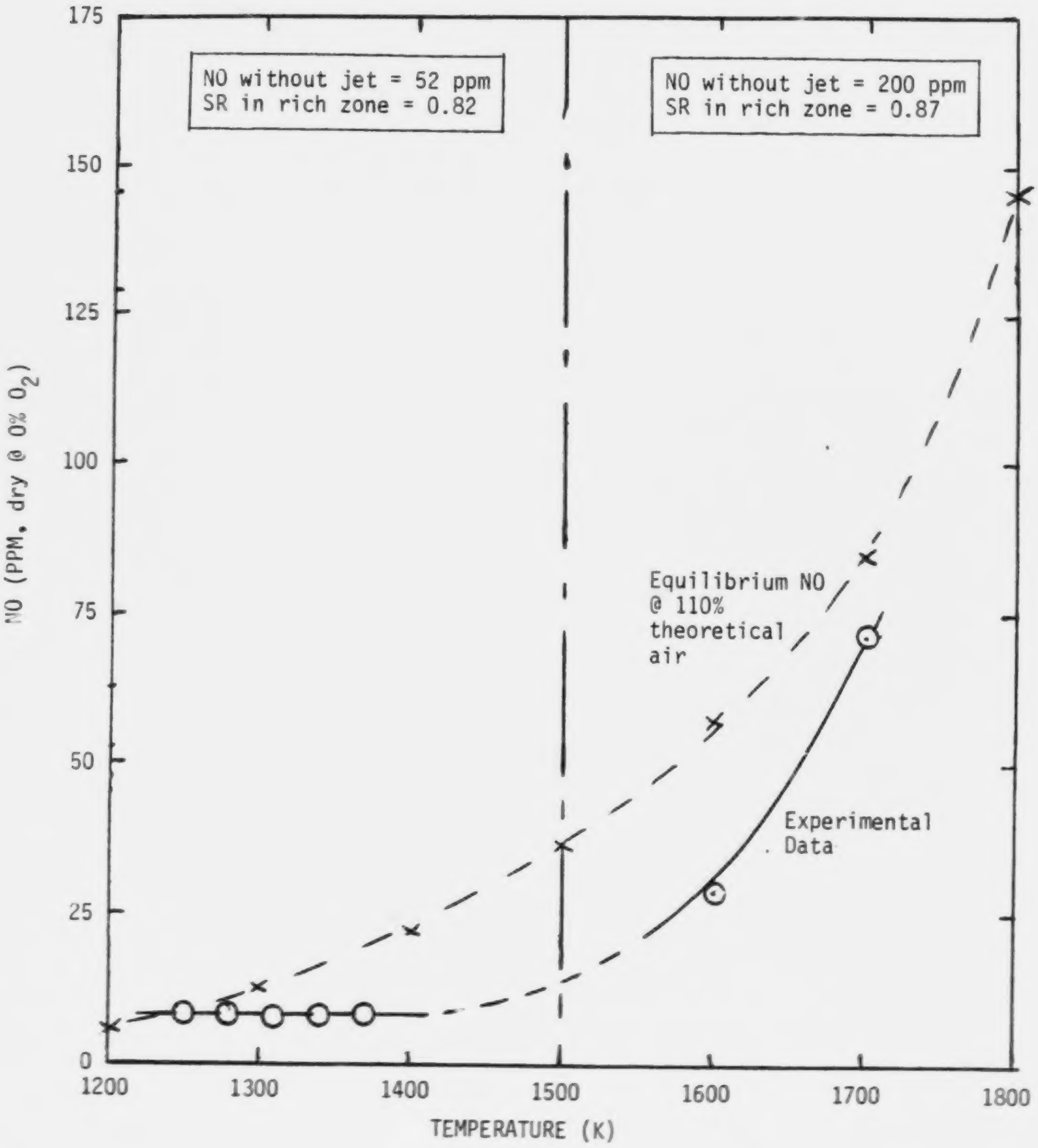

Figure 5-67: Effect of Temperature on Burnout Air Jet NO Destruction

various flame radicals (i.e., O, H and OH radicals) are produced. It is postulated that these radicals, formed as the fuel enters the jet stream, provide a "boost" towards equilibrium by increasing kinetic reaction rates by several orders of magnitude. As the fuel continues to diffuse into the air jet the mixture becomes increasingly fuel-lean and is rapidly quenched. Thus, the large NO destruction occurring at the fringes of the jet stream results in minimum NO levels approaching equilibrium values (at near stoichiometric conditions, the environment where burning initially occurs) that are frozen at the jet center. This theory suggests that as the jet expands at larger boiler radii, the reduction at the jet fringes occurs farther from the jet centerline and the thermal quenching rate decreases as more of the hot reburn zone effluent is mixed with the air jet. Thus, the minimum NO location and level should change as the sample radius changes. This was observed, with the minimum NO at the 23.5 cm radial location being higher and occurring farther upstream.

Possible reaction mechanisms by which the NO approaches equilibrium in the air jet are considered next.

5.5.3 Possible Mechanisms

Three hypotheses as to the mechanism of NO destruction in the burnout air jet are proposed and evaluated here. First, the thermal de-NO_x reaction pathway (involving ammonia reactions) is considered. Second, the reverse Zeldovich mechanism is evaluated as a possible NO destruction path, given superequilibrium concentrations of flame radicals. Third, a nonuniform mixing theory is presented as a qualitative explanation of air jet NO destruction. In this theory, kinetic analysis cannot be used to predict NO destruction without quantifying the fluid mechanics of the system.

Thermal De-NO_x

Exxon's "Thermal De-NO_x" process [20] involves ammonia injection into combustion product gases in a very narrow temperature window, between 1200K (1700°F) and 1300K (1880°F). At temperatures above 1300K, NH_3 is oxidized to H_2O and NO, while below 1200K, NH_3 goes unreacted. Within the temperature window, however, the dominant NH_3 reaction path is through NO to form N_2. Hydrogen injection with the ammonia can shift this temperature window to lower temperatures. Ammonia injection in the presence of a catalyst can lower the temperature regime for NO destruction even further.

It has been hypothesized that ammonia produced in the fuel-rich reburning zone may result in thermal de-NO_x in the burnout air jet. Two tests were performed to evaluate this hypothesis. First, ammonia was injected into the boiler, operated without reburning, to determine whether or not thermal de-NO_x would occur in the PBS. Second, ammonia was injected with the burnout air to enhance any thermal de-NO_x occurring in the air jet in reburning application.

Under nominal primary load conditions (load = 0.59 MW; excess air = 10 percent), at an exhaust NO condition of 190 ppm, a small amount of ammonia (about 0.25 percent by volume of the total fuel flow) was injected at various locations in the boiler. Figure 5-68 shows that a 45 percent reduction in NO was achieved for ammonia injection at 1244K (1780°F). The temperature window for NO destruction by ammonia injection for these tests was approximately 1170 to 1280K (1650 to 1850°F). At the low temperature conditions (less than 1250K) significant quantities of ammonia (over 40 ppm) were measured in the stack gas. These results are in close agreement with published thermal de-NO_x data. Thus, it is concluded that NO destruction via thermal de-NO_x can occur in the PBS. Next, reburning (SR_R = 0.89) was applied to the PBS. The same amount of ammonia injected in the previous test was injected with the burnout air in this test.

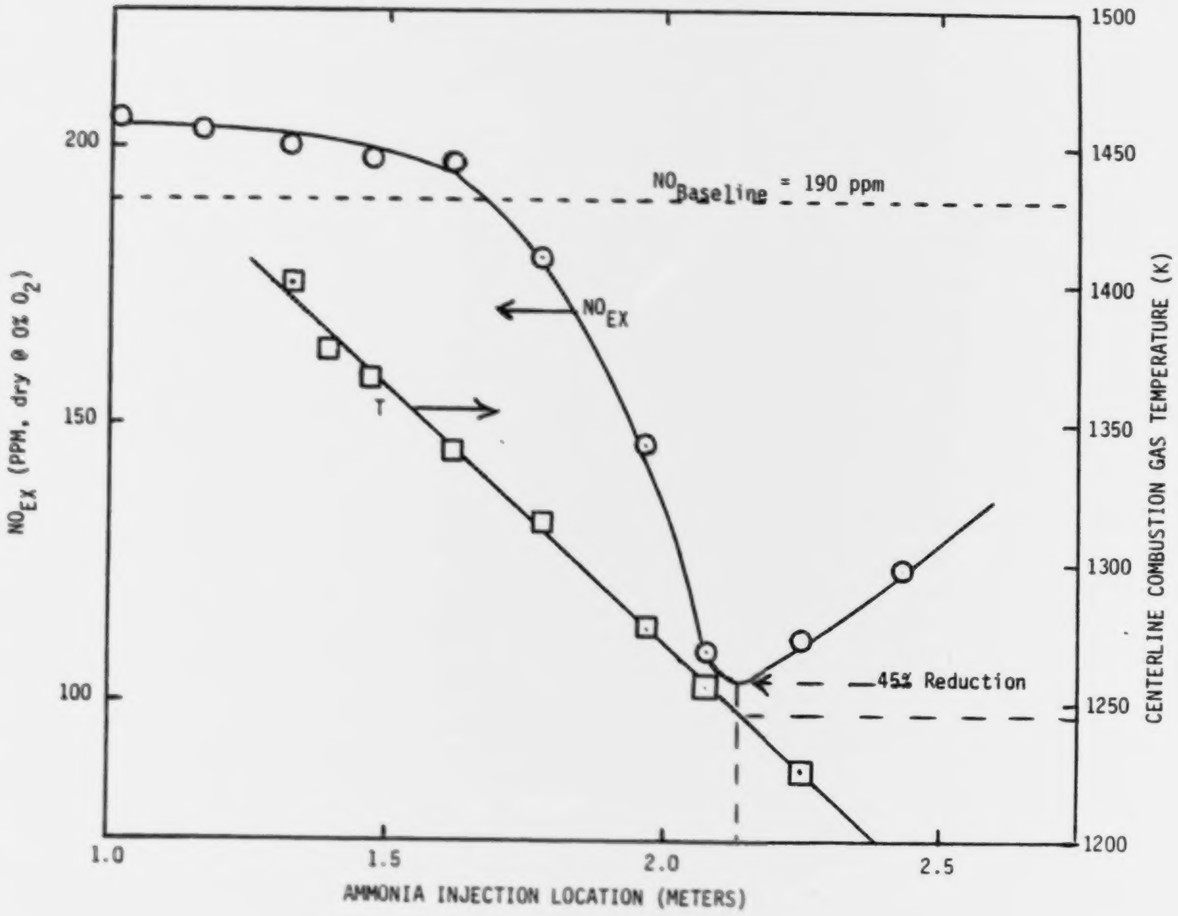

Figure 5-68: Thermal De-NO$_x$ in the PBS

NO_x emissions more than doubled, from 112 ppm (40 percent net NO reduction) with reburning alone to 242 ppm (30 percent net NO formation) with reburning plus ammonia injection (see Table 5-10). No ammonia was measured in the stack. Locally, in the air jet, the NO increased from 35 ppm (without ammonia) to 183 ppm (with ammonia). Thus, ammonia injection did not enhance NO destruction with reburning; instead, ammonia injection resulted in NO formation.

TABLE 5-10. REBURNING WITH AMMONIA INJECTION IN THE BURNOUT AIR JET

Burnout Air Injection	NO_{EX} (ppm, dry @ 0% O_2)	NO_{EX}/NO_{PRI} (percent)	NO_{airjet} (ppm, dry @ 0% O_2)
Without NH_3	112	35	60
With NH_3	242	183	130

This result is not surpising in that the mean temperature at the burnout air injection location with reburning in the PBS was typically about 1350K (1970°F), well above the temperature necessary for thermal de-NO_x. At 1350K, the NH_3 oxidizes to form NO (and H_2O). It is also noted that even had the reburning thermal environment been correct for thermal de-NO_x, ammonia reactions with NO would account for only a very small part of the NO destruction observed in the air jet, since ammonia concentrations at the reburn zone exit are typically very small. Without reburning, an NO destruction of 45 percent was achieved for an ammonia injection level that would result in 300 ppm of NH_3 unreacted. Measured NH_3 concentrations at the exit of the reburn zone were typically less than 10 ppm. For these reasons, thermal de-NO_x is eliminated as a possible mechanism of air jet NO destruction.

Reverse Zeldovich

A second mechanism to be investigated is the so-called "reverse", or "back", Zeldovich mechanism. This mechanism involves flame radical reactions with NO to form N_2, the reverse direction of the thermal NO formation mechanism first proposed by Zeldovich (see Section 1). To evaluate the hypothesis that reverse Zeldovich reactions are responsible for the NO destruction in the air jet, hand-calculations involving the forward and back reactions of the following reaction set are made:

$$O_2 + M \rightleftharpoons 2O + M \qquad (5\text{-}19)$$

$$N_2 + O \rightleftharpoons NO + N \qquad (5\text{-}20)$$

$$N + O_2 \rightleftharpoons NO + O \qquad (5\text{-}21)$$

where $K_{5-19} = 177T^{-0.24}\exp(-119,\ 118/RT)$ g-mole/cm^3

$k_{f5-20} = 8 \times 10^{13}\exp(-75{,}500/RT)$ cm^3/g-mole·K

$k_{r5-20} = 6.6 \times 10^{9}T^{1.0}\exp(-6{,}260/RT)$ cm^3/g-mole·K

$k_{f5-21} = 1.62 \times 10^{13}$ cm^3/g-mole·K

$k_{r5-21} = 1.5 \times 10^{9}T^{1.0}\exp(-38{,}700/RT)$ cm^3/g-mole·K

For this set of reactions, the rate equation of N_2 formation is:

$$\frac{d[N_2]}{dt} = k_{r5-20}\,[NO][N] - k_{f5-20}\,[N_2][O] \qquad (5\text{-}22)$$

The oxygen molecule/atom equilibrium constant is given by

$$K_{5-19} = \frac{[O]^2}{[O_2]} \qquad (5\text{-}23)$$

or,

$$[O] = K_{5-19}^{1/2}\,[O_2]^{1/2}.$$

If the N atom reactions are considered to be infinitely fast, then

$$\frac{d[N]}{dt} = k_{f5-20}[N_2][O] - k_{f5-21}[N][O_2] - k_{r5-20}[NO][N]$$

$$+ k_{r5-21}[NO][O] = 0 \qquad (5\text{-}24)$$

Plugging equations (5-24) and (5-23) into (5-22), and converting species concentrations into mole fractions, yields:

$$dY_{N_2}/dt = (K_{5-19}\ Y_{O_2})^{1/2}(RT/P)^{-1/2}(K_{r5-20}Y_{NO}(K_{f5-20}Y_{N_2}+K_{r5-21}Y_{NO})/$$

$$(K_{f5-21}Y_{O_2}+K_{r5-20}Y_{NO}) - K_{f5-20}Y_{N_2})\ \text{sec}^{-1} \qquad (5\text{-}25)$$

Equation (5-25) can be evaluated at various temperatures for specified O_2, N_2, H_2O and NO mole fractions. Equilibrium values of Y_{O_2}, Y_{N_2} and Y_{H_2O} for methane/air combustion at 10 percent excess air are 0.0174, 0.7213 and 0.1725, respectively. Assuming dry NO values of 200 and 50 ppm (Y_{NO} values of 165.5×10^{-6} and 41×10^{-6}), equation (5-25) is evaluated at temperatures ranging from 1000 to 2000K (1340 to 3140°F), with results tabulated in column (a) of Table 5-11. Note that

$$\frac{dY_{NO}}{dt} = -2\,\frac{dY_{N_2}}{dt} \qquad (5\text{-}26)$$

These calculations show that the reverse Zeldovich mechanism is not significant for this reaction set given realistic residence times (less than 1 second). The only radical generating step in this mechanism is the oxygen equilibrium reaction. At 1300K, this results in $Y_O = 3.7 \times 10^{-9}$. However, air jet superequilibrium concentrations of CO have been measured; it is expected that superequilibrium values of various flame radicals, such as H, O and OH, exist in the air jet as well. To show how the Zeldovich kinetics might change given superequilibrium flame species concentrations, a second calculation is made with the oxygen equilibrium constraint relaxed, and assuming an O atom mole fraction of 0.001. This calculation should be performed for a full set of C, H, N and O system reactions, as there are several O atom consumers other than the Zeldovich reactions. However, the hand calculation performed here is useful in demonstrating the potential effect caused by superequilibrium concentrations of flame radicals.

Plugging equation (5-24) into (5-22) and converting species concentrations into mole fractions yields

$$dY_{N_2}/dt = Y_O(RT/P)^{-1}(K_{r5-20}Y_{NO}(K_{f5-20}Y_{N_2} + K_{r5-21}Y_{NO})/(K_{f5-21}Y_{O_2} + K_{r5-20}Y_{NO}) - K_{f5-20}Y_{N_2})\ \text{sec}^{-1} \qquad (5\text{-}27)$$

TABLE 5-11. ZELDOVICH REACTION RATE CALCULATIONS

Temp (K)	(a)O_2-O Equilibrium dY_{NO}/dt (ppm/sec)		Rate Acceleration Factor	(b)Y_O=0.001 dY_{NO}/dt (ppm/sec)	
	$Y_{NO}=165.5\times10^{-6}$	$Y_{NO}=41\times10^{-6}$		$Y_{NO}=165.5\times10^{-6}$	$Y_{NO}=71\times10^{-6}$
2000	+330	+345	11	+3600	+3800
1900	+54	+59	25	+1400	+1500
1800	+7.6	+8.4	62	+470	+520
1700	+0.83	+0.94	170	+140	+160
1600	+0.069	+0.080	520	+36	+42
1500	$+3.6 \times 10^{-3}$	$+4.8 \times 10^{-3}$	1900	+6.8	+9.1
1400	$+8.4 \times 10^{-5}$	$+1.9 \times 10^{-4}$	8000	+0.67	+1.5
1300	-3.2×10^{-6}	$+5.2 \times 10^{-6}$	4.2×10^{4}	-0.13	+0.22
1200	-3.3×10^{-7}	$+3.7 \times 10^{-8}$	3.0×10^{5}	-0.010	+0.011
1100	-1.1×10^{-8}	-4.7×10^{-10}	3.0×10^{6}	-0.033	-1.4×10^{-3}
1000	-1.6×10^{-10}	-1.2×10^{-11}	4.2×10^{7}	-6.7×10^{-3}	-5.0×10^{-4}

Thus, the "rate acceleration factor" due to superequilibrium O atom concentration is:

$$\frac{dY_{N_2}/dt)_{5-27}}{dY_{N_2}/dt)_{5-25}} = Y_O \, (K_{5-19} Y_{O_2})^{-1/2} (RT/P)^{-1/2} \qquad (5\text{-}28)$$

The results tabulated in Table 5-11 indicate that, given a superequilibrium concetration of O atoms, the Zeldovich reaction rates are significantly increased. Although the hand calculations of a single reacation set do not indicate that the back Zeldovich mechanism is at work in the air jet, they do suggest that high reaction rates are possible. In reality, when the entire set of C, H, N and O system reactions interact, equilibrium NO at temperatures less than 1300K for 10 percent excess air is less than 10 ppm. Therefore, the reaction rate dY_{NO}/dt is negative, and NO is destroyed, in the burnout air jet. The reaction path to equilibrium may be through H or OH radical species. Regardless of the actual reaction pathway, it seems evident that superequilibrium flame species must be present near the air jet to drive the NO concentration rapidly towards equilibrium.

Nonuniform Mixing Rate Theory

The theory that superequilibrium concentrations of flame species at the air jet drive NO equilibrium suggests that if the thermal quenching rate and stoichiometry of the reacting flow as it enters the air jet are known, the air jet speciation can be predicted. A third theory suggests that nonuniform mixing rates, governed by turbulent flow parameters, result in microscopic fuel-rich and fuel-lean pockets within the air jet. To make quantitative predictions, chemical kinetic theory must be integrated with turbulent fluid mechanic theory. Here, a qualitative argument is made that in a diffusion flame (be it oxidizer diffusing into fuel or fuel into oxidizer), mixing does not occur on a molecular level but in discrete gaseous pockets whose size and dissipation rate depend on physical gas mixing parameters. Species concentrations in these pockets may vary widely, depending on composition and heat transfer rates. These pockets mix in the air jet and sample probe, resulting in average species concentration readings that cannot be predicted on the basis of kinetics alone. In the burnout air jet, fuel-rich pockets are heated from combustion on the edges, and NO is driven towards equilibrium.

5.5.4 Conclusions

In reburning application, significant NO destruction has been observed in the burnout air jet. This destruction of NO is apparently an actual N_2 formation process, with minimum NO values approaching equilibrium values (at the reduced combustion temperatures and exhaust stoichiometry near the boiler radiant section exit) of less than 5 ppm. Parameters that influence this reduction are the fuel-rich zone stoichiometry, the air jet flow rate, and the temperature. It has been shown that the NO destruction path is not by ammonia reactions, but via reactions involving flame radicals (such as O, H and OH). These radicals are suggested to exist in elevated quantities in the air jet.

It was shown that the reverse Zeldovich mechanism is a possible reaction path for this NO destruction. It is hypothesized that mixing rates between the fuel and oxidizer might substantially effect the overall air jet NO destruction. Tests with variable injection patterns in the burnout air boom were inconclusive. It is recommended that the air jet NO destruction phenomenon be studied further in a small-scale reactor where fuel-rich effluent can be passed through an air sheet. Study is also recommended on inverse diffusion flames (i.e., fuel diffusing into an air jet). In a small scale combustor, the NO destruction mechanism can be studied more carefully by seeding the fuel and air flows with various flame species.

Finally, it is noted that the phenomenon of air jet NO destruction is not unique to reburning; it was first observed in conventional air staging applications. While kinetic theory is useful in predicing reaction rates of highly mixed flames, an integrated kinetic and mixing theory is needed to understand combustion in air (and fuel) jets.

5.6 ALTERNATIVE STAGING STRATEGIES

A final series of tests was performed in the PBS to compare various fuel and air staging strategies. Five firing arrangements were considered: baseline (unstaged) firing, air staging, conventional reburning, biased reburning, and advanced biased reburning. The fuel staging tests were performed for both fuel-lean and fuel-rich primary zone stoichiometries. In all tests, burner precombustion chamber parameters were held constant (0.59 MW load, SR_1 = 0.65, primary fuel dopant = 0.75% NH_3). The firing arrangements are shown schematically in Figure 5-69.

Each firing arrangement represents a stepwise variation of another firing arrangement. Going from unstaged combustion to air staging requires that a portion of the combustion air be diverted to a downstream location. Reburning involves staging fuel as well. Biased reburning consists of combining the staged fuel and air streams. Advanced biased reburning is the term used to describe the firing conditions between conventional reburning and biased reburning where some, but not all, of the staged air is mixed with the staged fuel. Researchers at KVB [21] have reported as high as 90 percent NO reduction via advanced biased reburning. As will be shown, such reductions can be achieved only by staging large amounts of fuel and air and by operating a large portion of the combustor fuel-rich.

5.6.1 Air Staging

A baseline test condition of 188 ppm NO was established at nominal load and excess air conditions. Air was then removed from the radial air injectors

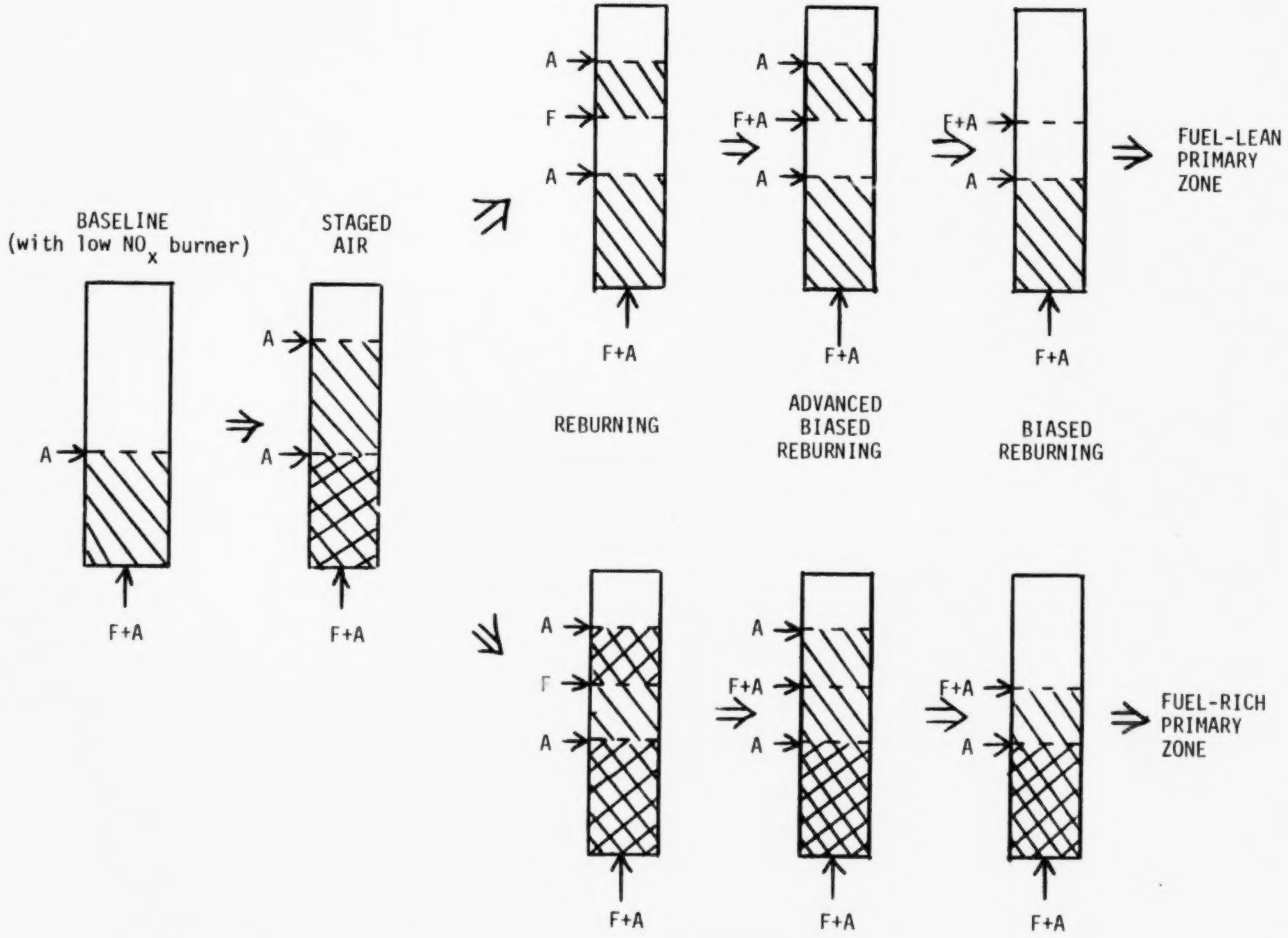
BASELINE
(with low NO_x burner)
STAGED
AIR
A
F
F+A
REBURNING
ADVANCED
BIASED
REBURNING
BIASED
REBURNING
FUEL-LEAN
PRIMARY
ZONE
FUEL-RICH
PRIMARY
ZONE

Figure 5-69: Alternative PBS Firing Strategies

and injected through the staged air boom. This resulted in a fuel-rich primary zone with an air-to-fuel stoichiometry of 0.88. The staged air was injected at the 1.02 m (40 in.) and 1.93 m (76 in.) axial locations. The results, plotted in Figure 5-70, are compared with natural gas reburning results with a fuel-rich zone stoichiometry of 0.88. Air staging resulted in NO reductions of more than 40 percent. This percent reduction is dependent on the primary burner hardware and operation. In the PBS tests, the low NO_x prechamber burner, which is itself operated in a staged air baseline condition, can produce very low NO_x emissions. Further air staging would not be expected to yield as high a percent NO reduction as that achievable with a conventional burner producing a high NO concentration in the baseline condition. Nonetheless, even with the prechamber primary burner, air staging was found to be just as effective in reducing NO emissions as conventional reburning.

The mechanisms of NO reduction are very different in air staging and reburning. Air staging NO reductions are achieved by reducing NO formation in the primary flame; with reburning, NO produced by the primary flame is actually destroyed. There are two advantages of reburning over air staging. First, with reburning, only a small portion of the boiler radiant section is operated fuel-rich. With air staging, there is no fuel lean primary zone. Second, reburning can be coupled with air staging or other NO_x control technologies to achieve greater reductions.

One final note on this comparison should be made. In reburning, additional load is added to the boiler in the secondary fuel. To maintain a constant total load, the primary load would be reduced. Typically, at derated primary burner operation, primary flame mixing intensities are reduced and less NO is produced in the primary flame. Thus, there is an additional

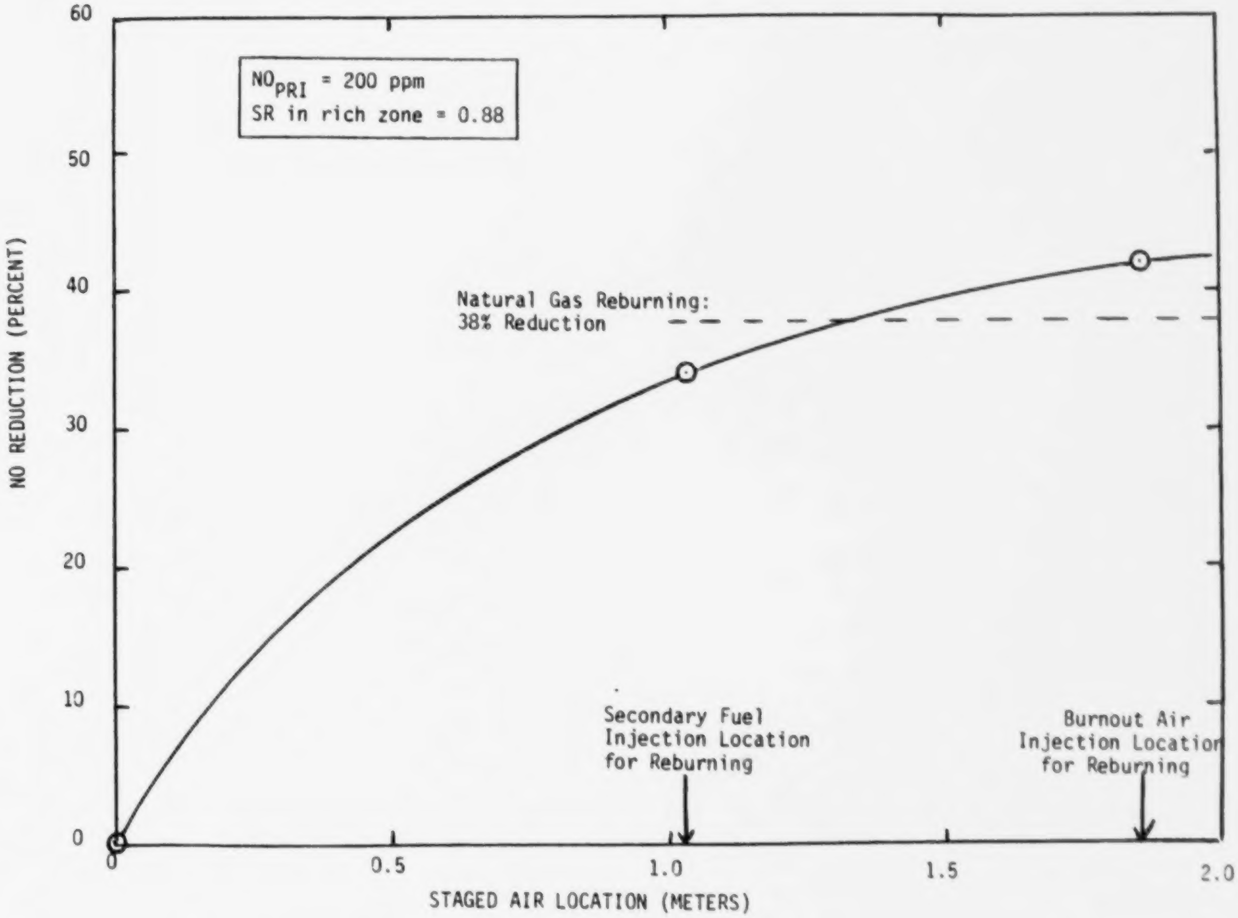

Figure 5-70: Staged Air NO Reduction in PBS

reduction associated with reburning application due to the primary load reduction. This reduction, which is very dependent on burner hardware, is coupled to the reburning reduction described in this section. Thus, the overall NO reduction via reburning in a practical application would be higher than the 38 percent shown in Figure 5-70. As described in Section 7, the reburning application tests on a conventional firetube package boiler were conducted at constant total load.

5.6.2 Biased Reburning

Biased reburning involves mixing the staged fuel and air streams. To observe the effect of premixing staged fuel and air as an extension of conventional reburning, reburn zone length was reduced from 0.9 m to zero, the biased reburning condition. As shown in Figure 5-71, NO reductions decreased as reburn zone lengths shortened. At the biased reburning condition, only a 12 percent NO reduction was achieved, less than the 20 percent reduction that would have been achieved for zero net NO destruction. (With zero destruction of primary zone NO and zero formation of NO in the reburning and burnout zones due to the added load, the NO concentration measured in the stack exhaust for the reburn load applied in this test would be 20 percent less than the NO concentration in the exhaust without reburning).

Another way to compare conventional and biased reburning in a continuous manner is to remove air from the staged air flow and add it to the staged fuel flow (so-called advanced biased reburning), until all of the staged air is injected with the staged fuel (biased reburning). Data obtained in this manner are plotted in Figure 5-72 for both fuel-lean and fuel-rich primary zone stoichiometries. For SR_{PRI} of 1.09, conventional reburning, with a reburn zone stoichiometry of 0.88, yielded a reduction in NO of about 40 percent. As air was added to the secondary fuel, SR_R increased and NO

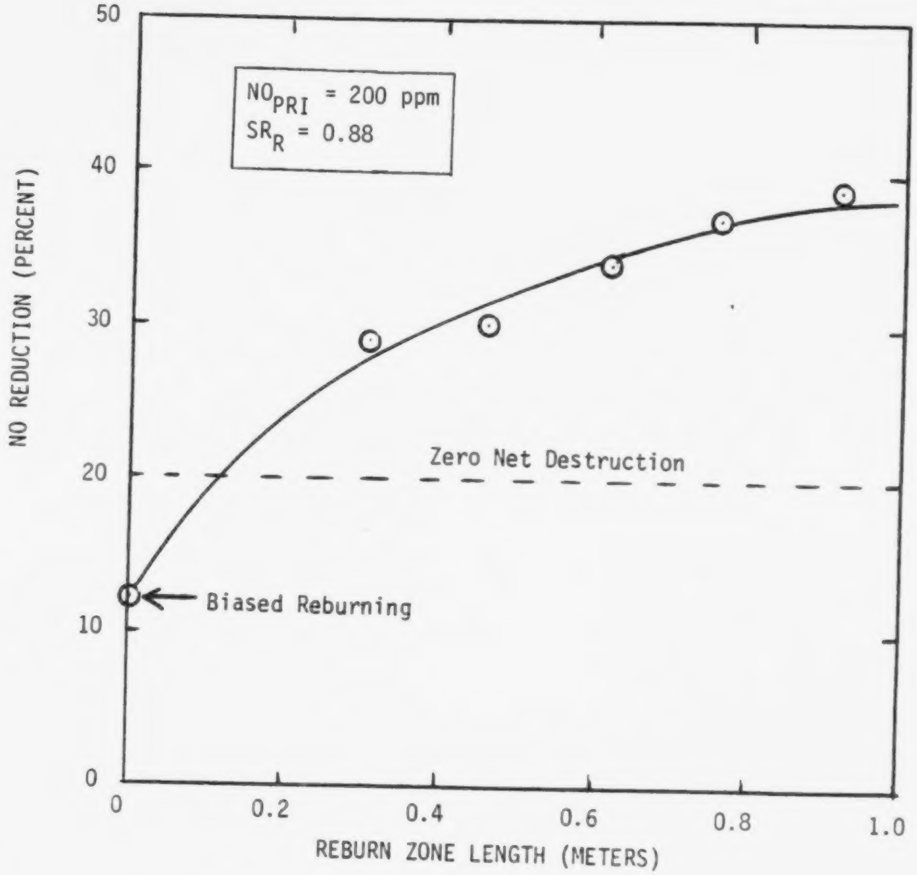

Figure 5-71: Natural Gas Reburning Versus Biased Reburning

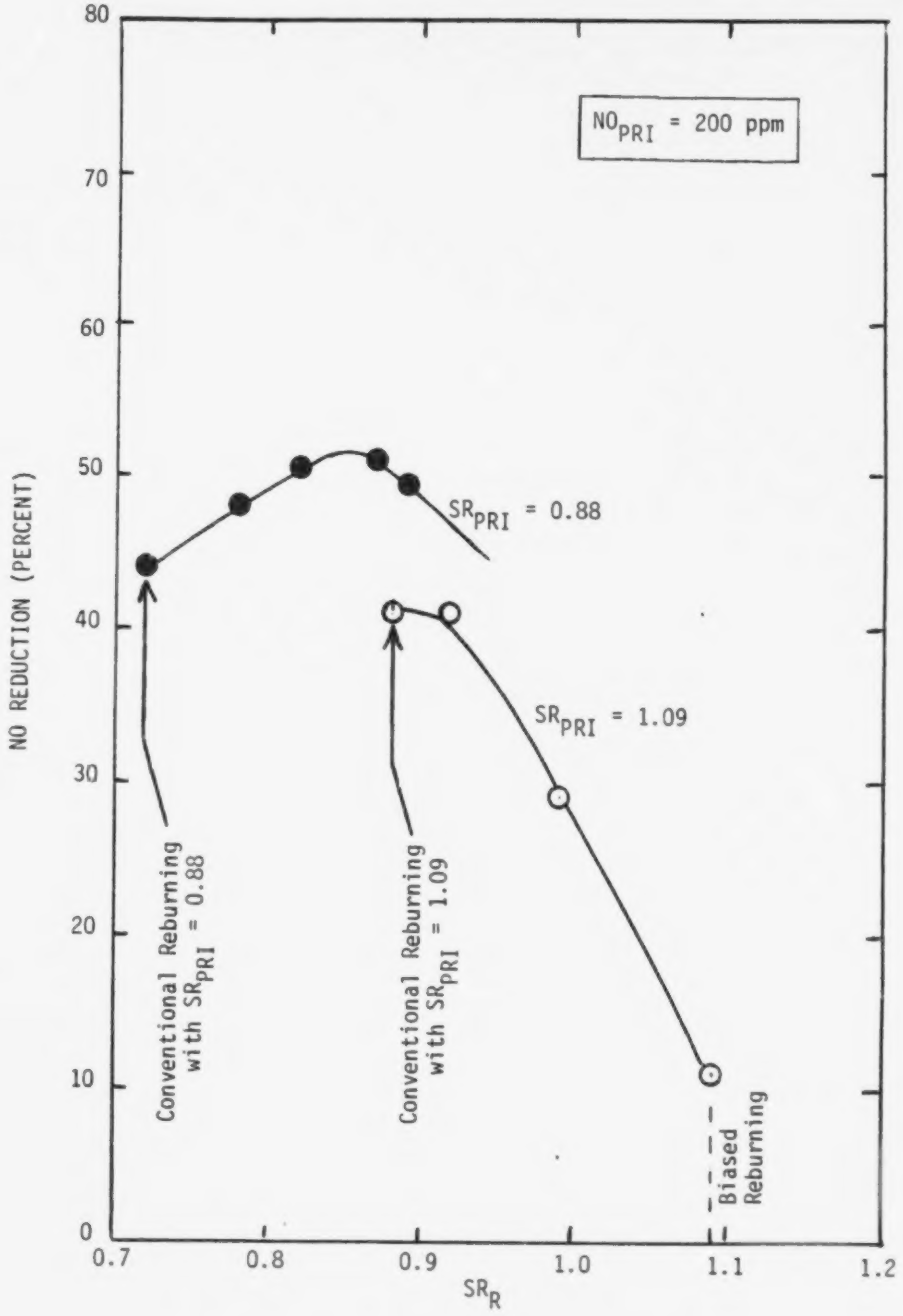

Figure 5-72: Natural Gas Reburning Versus Advanced Biased Reburning

reductions decreased. Thus, for the fuel-lean SR_{PRI} test condition, maximum NO reductions were achieved for conventional reburn firing.

However, for a fuel-rich primary zone (SR_{PRI} = 0.88) reburn application, where conventional reburning produces a reburn zone stoichiometry of 0.71, advanced biased reburning does result in a maximum NO reduction for a reburn zone stoichiometry of 0.85. The 52 percent NO reduction at this condition represents a reduction from the baseline condition with a fuel-lean primary zone. The reason for this optimum (shown by the solid symbols in Figure 5-72) will be discussed in Section 5.6.3.

Advanced biased reburning with a fuel-rich primary zone can result in high NO reductions due to significant reductions in NO formation as well as due to NO destruction. In a practical application of advanced biased reburning, reductions in absolute primary zone NO formation (in terms of moles of NO) are achieved in three ways: (1) fuel and air from the primary burner are diverted to the staged injectors; (2) the primary burner load is derated so that the fuel remaining is combusted with lower mixing intensities, hence, lower NO (in terms of concentration, or lbs per Btu); and (3) the primary zone is operated fuel-rich. Coupled to this reduction is a net molar destruction of primary NO achieved by reburning. In the tests conducted in the PBS, reduction in NO was limited by: (1) a baseline condition of low NO due to the use of the precombustion chamber burner; (2) a constant primary load operation (and, thus, zero NO reduction due to primary burner derating); and (3) a limitation in the amount of reburn load due to a limitation in staged air flow. Thus, the 90 percent NO reduction achieved by KVB researchers [21] could not be achieved in these tests.

5.6.3 Optimum Reburn Zone Stoichiometry

These tests raise the following question as to reburning application: What is the optimum reburn zone stoichiometry? The answer is dependent on both boiler hardware and boiler operation. A hypothetical example is presented here, based on the conventional and biased reburning test results. Results from tests on a commercial boiler, discussed in Section 7, support this scenario.

Two sets of curves are presented in Figure 5-73. Four components that characterize the total NO reduction via reburning can be identified and quantified in the pilot-scale reburn tests. For conventional reburning, four curves representing these components of NO reduction are drawn (dashed lines in Figure 5-73a) as a function of reburn zone stoichiometry, which is proportional to reburn load. Curve 1 represents the reduction in moles of NO_{PRI} due to fuel and air diversion to staged locations. This reduction is proportional to the reburn load (it can be thought of as a reburn load dilution); hence, it is represented by a straight line on this graph. Curve 2 represents the reduction in NO_{PRI} concentration due to the primary burner derating. As primary load decreases, the primary fuel and air mixing intensity decreases resulting in a decrease in the concentration of NO formed in the primary zone. This curve is specific to a given burner hardware. In the PBS tests the primary load was held constant to eliminate this source of NO reduction. In the hypothetical example shown in Figure 5-73a, a typical NO reduction curve with load variation is shown. In a specific reburning application, this trend could be measured. Curve 3 represents the primary NO reduction due to primary air staging. Again, this reduction is characteristic of a particular burner application. For a specific system this reduction in NO could be measured as a function of the primary zone stoichiometry. In this example, it is assumed that a 20 percent reduction in the primary NO level is achieved by staging primary combustion air. Curve 4 represents the net NO destruction due to reburning application. This curve is calculated from the

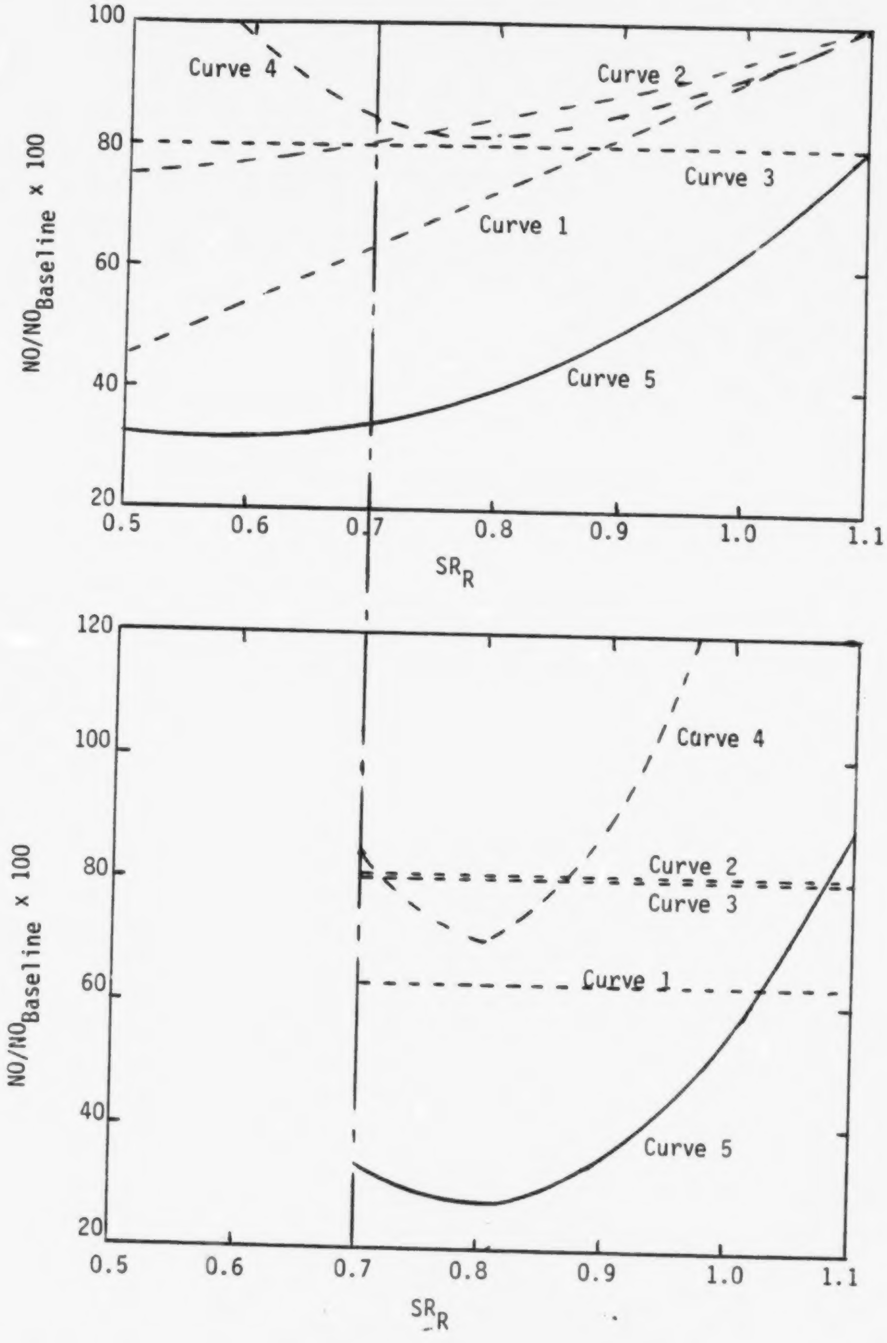

Figure 5-73: Optimum Reburning Stoichiometry
Curve 1: Reburn load dilution; Curve 2: Primary load reduction; Curve 3: Primary stoichiometry reduction; Curve 4: Net NO destruction; Curve 5: Total NO reduction.

measured total NO reduction and the measured NO reductions in the primary zone. That is,

$$(NO_{EX}/NO_{Baseline})_{curve\ 5} = (NO_{PRI}/NO_{Baseline})_{primary} \times (NO_{EX}/NO_{PRI})_{curve\ 4} \quad (5\text{-}29)$$

where

$$(NO_{PRI}/NO_{Baseline})_{primary} = (FR_{PRI}/FR_{TOT})_{curve\ 1} \times (NO\ @\ FR_{PRI}/NO\ @\ FR_{TOT})_{curve\ 2} \times (NO\ @\ SR_{PRI}/NO\ @\ SR_{EX})_{curve\ 3}. \quad (5\text{-}30)$$

This approach to studying overall NO reductions via reburning is useful in understanding the optimum reburn zone stoichiometry. Though a minimum in the exhaust NO curve does not occur until sufficient load is diverted to drive the reburn zone stoichiometry to less than 0.7, there is a minimum in the net NO destruction curve at an SR_R of approximately 0.8. This is more fuel-rich than the optimum NO destruction stoichiometry of 0.9 found by Chen et al. [12], Differences in net NO destruction optimums are to be expected as these curves are dependent on many combustion parameters, such as temperature and mixing rate that are hardware-specific. Chen's results were obtained on a bench-scale (30 kW) furnace using propane as the reburning fuel.

In Figure 5-73b, biased reburning is considered. At a reburning load sufficient to drive the reburn zone stoichiometry to 0.7 without biased reburning, staged air is transferred to the secondary fuel flow (advanced biased reburning) until all of the staged air is injected with the staged fuel (biased reburning). Under these conditions of fixed primary and reburning loads, the primary NO reductions (curves 1, 2 and 3) remain constant. Therefore, the NO reduction curve mirrors the NO net destruction curve over the range of SR_R's achieved by advanced biased reburning variation. Thus, the exhaust NO level can decrease for advanced biased reburning, as the minimum shifts to a higher SR_R. The shape of the net NO destruction curve changes with advanced biased reburning as well.

A fundamental question in reburning application is raised: Why is the shape of the net NO destruction curve (#4) as it is? The first observation to be made is that this curve represents both NO formation and NO destruction processes in the reburning and burnout zones. These processes depend on such quantities as fuel type and fuel nitrogen content, temperature, stoichiometry, load, and thermal and physical mixing rates, parameters that were studied individually, as has been discussed. These parameters determine kinetic reaction rates that accelerate the system towards equilibrium. Therefore, the shape of the net NO destruction curve should be similar to that of equilibrium at typical reburn conditions. This is observed to be qualitatively true in that minimums in the total fixed nitrogen equilibrium curves occur at stoichiometries between 0.6 and 1.0 for methane/air combustion at 1 atmosphere and various temperatures (see Figure 5-74). For temperatures typical of PBS reburning application (1400 to 1600K), the minimum in equilibrium TFN is near a stoichiometry of 0.9, with the curve rising steeply as stoichiometry increases from the optimum and with much less of a slope as stoichiometry decreases. The magnitude of the measured exhaust NO is much greater than the equilibrium values predicted in the reburning zone, however. Equilibrium is only the driving force of the kinetic rates, allowing for prediction of the direction of the reburning NO curves, but not of the magnitude. Reburning is a kinetically-controlled process, governed by mixing and quenching rates.

5.6.4 Conclusions

There are many different staged fuel and air firing arrangements that can provide significant NO_x reduction. In a practical application, fuel burnout, surface area heat release, surface corrosion, and hardware modification must be considered in addition to NO reduction. Air staging can often provide as much NO reduction as reburning in applications to unstaged boilers. However, with

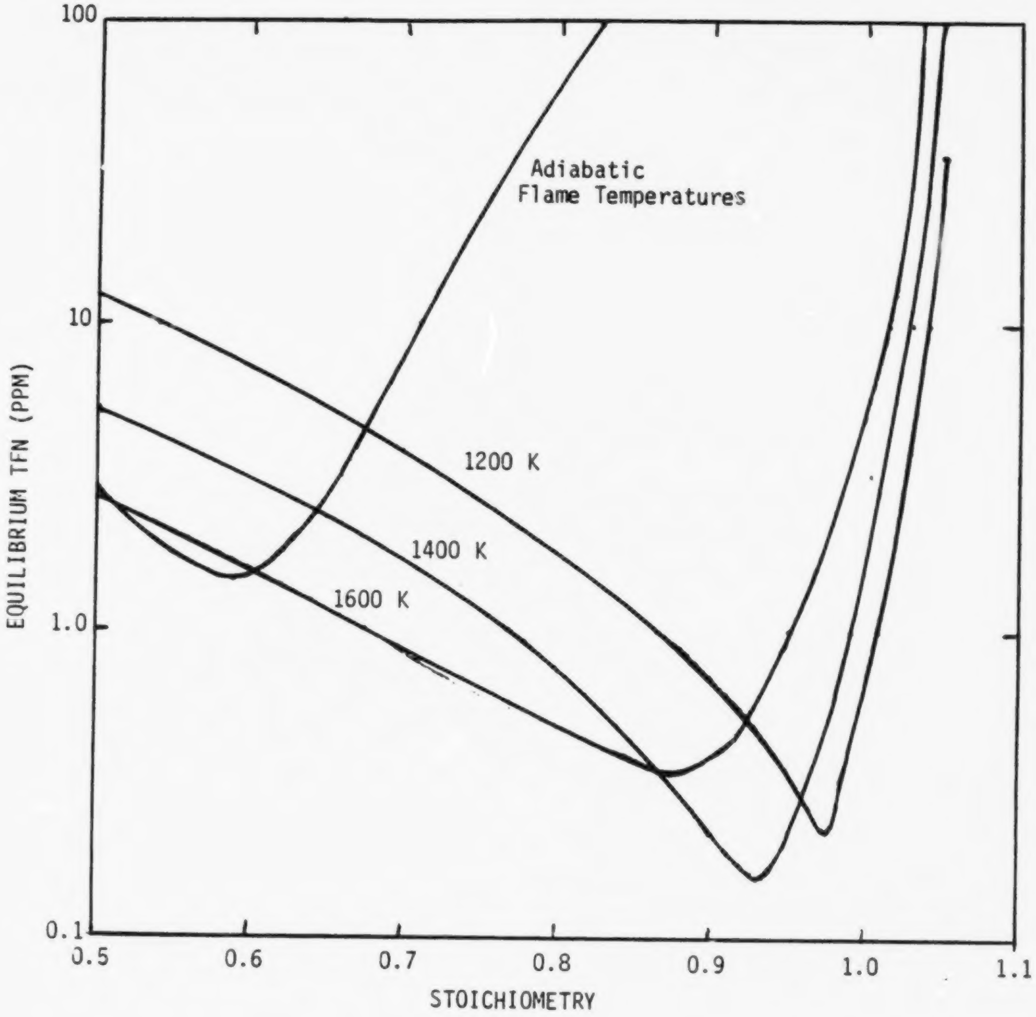

Figure 5-74: Equilibrium TFN for Methane/Air Combustion at 1 Atmosphere

reburning, the fuel-rich zone, a corrosive environment, is much smaller than that for air staging to achieve an equivalent NO reduction. In addition, reburning can be coupled with other NO_x control technologies to decrease NO_x emissions further.

There exists a stoichiometry that maximizes NO destruction via fuel staging. This maximum NO destruction is predicted by equilibrium, though kinetic rates are insufficient for equilibrium NO levels to be obtained. This NO destruction is coupled with NO reductions in the primary zone due to primary load and stoichiometry variation. Thus, the overall NO reduction via reburning is maximized for reburn zone stoichiometries much less than the optimum net NO destruction stoichiometry. For the PBS natural gas reburning tests, maximum NO reduction occurred at a reburn stoichiometry less than 0.7, whereas the maximum net NO destruction stoichiometry was between 0.8 and 0.85.

Advanced biased reburning, which consists of mixing a portion of the staged air with the staged fuel, can enhance reburn NO reductions at high reburn loads, or low reburn zone stoichiometries. This enhancement by advanced biased reburning is due to minimizing primary NO_x formation while maximizing reburn zone NO destruction. At high reburn zone stoichiometries (greater than 0.8), adding air to the staged fuel increases NO_x emissions.

Use of advanced biased reburning may be necessary in some applications. For coal reburning, transport air is injected with the staged coal. For natural gas reburning in combustion exhausts at low temperatures (less than 1350K), advanced biased reburning is necessary to permit good burnout of the staged fuel. This minimum reburning temperature is greater for fuel oils, as will be discussed in the following section. Tests on the PBS have shown that biased air/staging allows for natural gas reburning at greatly reduced temperatures.

5.7 HIGH PRIMARY NO REBURNING

A short series of tests were performed to investigate reburning effectiveness for primary NO levels of about 1000 ppm. It has been shown that for primary NO levels in the range of 50 to 500 ppm, reburning effectiveness increases with increasing NO_{PRI}. In Figure 5-2 it was shown that for a reburn zone stoichiometry of 0.8, the reduction of primary NO increased from 28 percent for NO_{PRI} of 58 ppm to 58 percent for NO_{PRI} of 528 ppm. For NO_{PRI} of 1016 ppm, greater than 60 percent of the primary NO was reduced. Thus, for increasing primary NO, reburning effectiveness approaches a maximum of 60 to 65 percent NO reduction for natural gas reburning. If reductions in primary NO levels are taken into account (reductions due to reductions in load and excess air), the overall effectiveness of natural gas reburning at these high initial NO conditions may exceed 80 percent. In the reburning tests described here, primary zone conditions were held constant during reburning application.

In addition to extending the range of NO_{PRI} considered in these natural gas reburning studies, it was desired to evaluate the effect of reburning fuel nitrogen under the high NO_{PRI} condition. It was hypothesized that under high NO_{PRI} conditions, reburning fuel nitrogen may enhance reburning effectiveness since the path for the nitrogen conversion to molecular nitrogen is through NO. In Figure 5-75 results are shown comparing natural gas reburning effectiveness with ammonia-doped natural gas reburning effectiveness for NO_{PRI} = 1016 ppm. As hypothesized, the presence of fuel nitrogen (in the form of NH_3) enhanced reburning NO reduction. A maximum reduction of 75 percent was achieved with the ammonia-doped natural gas, as compared to 60 percent for the undoped natural gas. Recall that for NO_{PRI} of less than 500 ppm fuel nitrogen inhibited NO reduction. More study is needed in this area. Simulating fuel nitrogen with NH_3 may be misleading because the NH_3 represents an advanced stage in the nitrogen chemical mechanism. Also, it is possible that some thermal de-NO_x reactions contributed to the NO reduction in the ammonia-doped reburning tests.

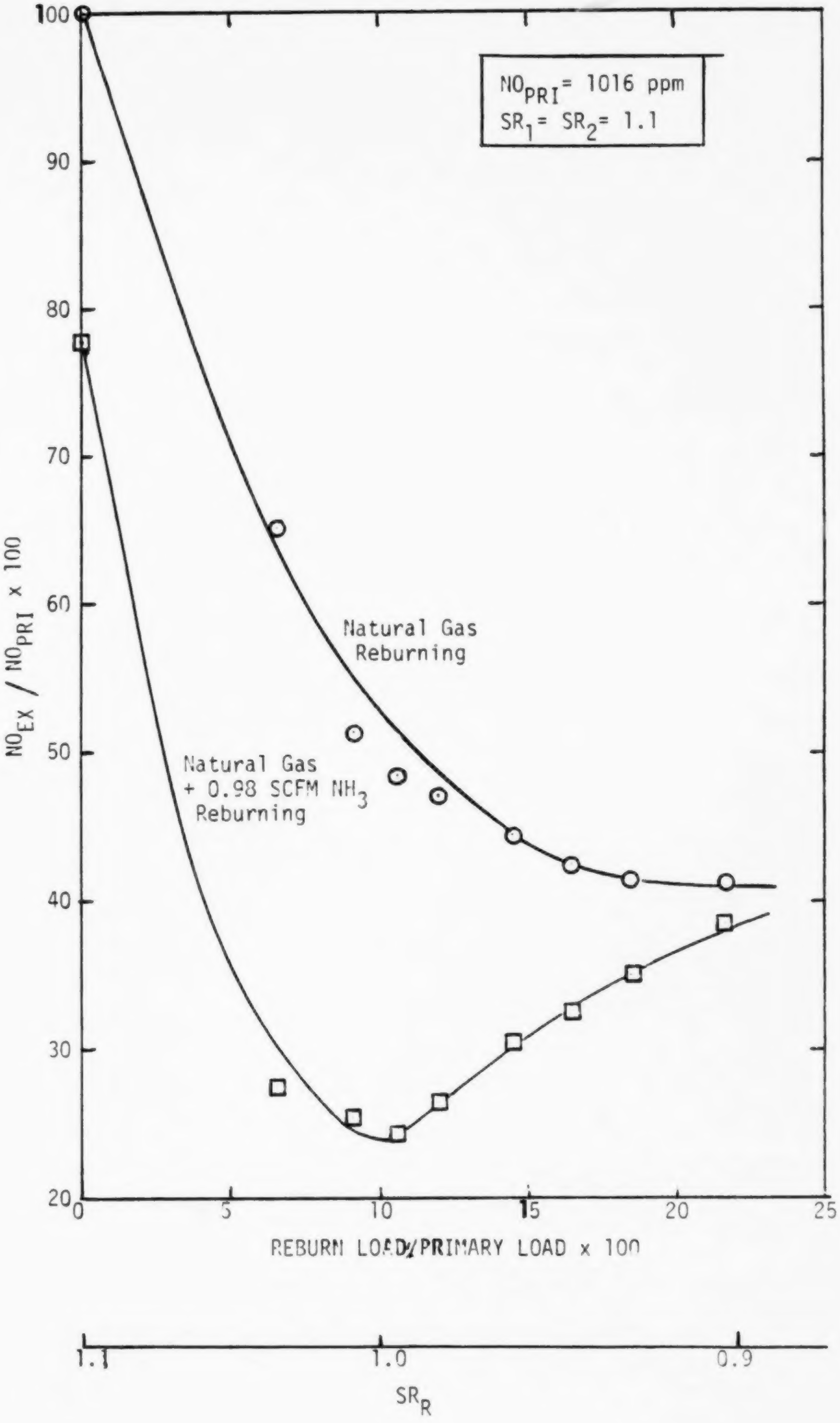

Figure 5-75: Reburning Effectiveness for NO_{PRI} = 1016 ppm

SECTION 6

PRS FUEL OIL REBURNING TEST RESULTS

Reburning with a distillate fuel oil and a distillate/residual fuel oil mixture (termed here, heavy fuel oil) was applied to the pilot-scale package boiler simulator. Whereas gaseous fuel combustion is predominantly a chemical phenomenon, fuel oil combustion is strongly dependent on physical phenomena, such as droplet atomization, mixing, and vaporization. Kinetic considerations must be coupled with considerations of the physical processes that control fuel oil burning. In this section, results are presented to characterize fuel oil reburning in a firetube package boiler, with emphasis given to those characteristics that distinguish fuel oil reburning from natural gas reburning.

As was stated in Section 4, primary load was held constant, at 0.62 MW, and burner prechamber zone stoichiometry was fixed at 0.6. Test parameters were varied individually over the ranges described in Table 6-1. In Section 6-1, input/output trials are documented in which stack emission measurements are used to characterize the effects on reburning efficiency of primary NO_x, reburn zone stoichiometry, secondary fuel nitrogen content, reburn zone residence time, primary and burnout zone stoichiometries, primary fuel, secondary fuel nozzle, and reburn zone temperature. In Section 6-2, a detailed look at the reburning zone under selected conditions is made to better understand the physical and chemical processes of fuel oil reburning.

Parts of the material contained in Section 6 were presented at the 1985 Joint Symposium on Stationary Combustion NO_x Control in Boston [22] and the 1985 Joint Power Generation Conference in Milwaukee [23].

6.1 INPUT/OUTPUT TRIALS

An extensive series of input/output (I/O) tests were performed for parametric study of fuel oil reburning. Distillate fuel oil was injected

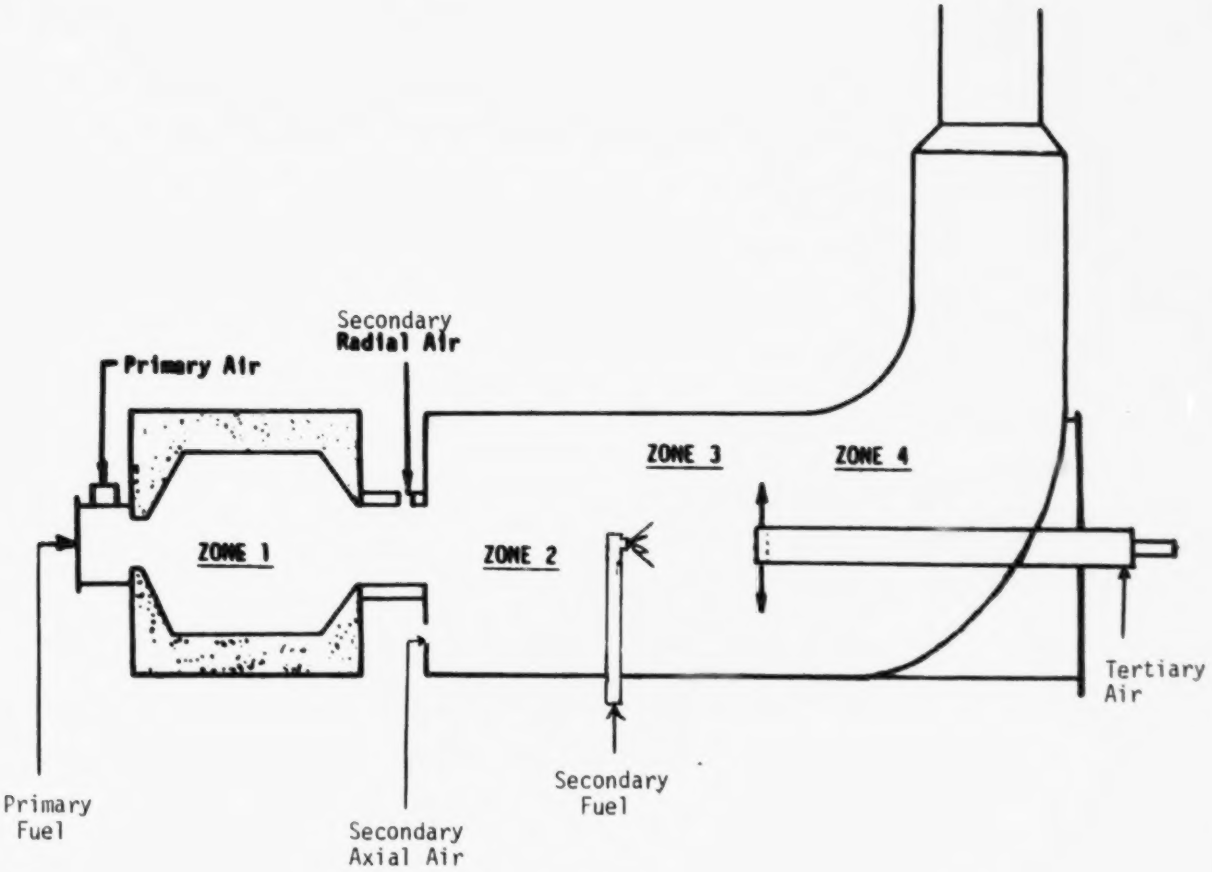
Secondary
Radial Air
Primary Air
ZONE 3
ZONE 4
ZONE 1
ZONE 2
Tertiary
Air
Secondary
Fuel
Primary
Fuel
Secondary
Axial Air

Figure 6-1: PBS Fuel Oil Reburning Schematic

TABLE 6-1. INPUT PARAMETERS -- FUEL OIL REBURNING

Section	Parameter	Symbol	Nominal Value	Range
6.1.1	Primary NO_x	NO_{PRI}	200 ppm	50-500 ppm
6.1.1	Reburn Zone Stoichiometry	SR_R or SR_3	0.9	0.8-1.1
	-- Reburn Firing Rate	FR_R	0.12 MW	0-0.18 MW
6.1.2	Secondary Fuel Dopant	$(C_5H_5N)_R$	0	0, 0.5% N_2
6.1.3	Reburn Zone Bulk Residence Time	b,3	200 ms	0-400 ms
	-- Reburn Zone Length	L_3	0.61 m	0-1.22 m
6.1.4	Primary Zone Stoichiometry	SR_{PRI} or SR_2	1.1	0.9-1.2
6.1.5	Burnout Zone Stoichiometry	SR_{EX} or SR_4	1.1	1.0-1.3
6.1.6	Primary Fuel	-	Natural Gas	Fuel Oils
6.1.7	Secondary Fuel Nozzle	-	Delavan	Delavan, Sonicore
6.1.8	Reburn Zone Temperature	T_3	1590K	1370-1750K
	-- Primary Zone Installation	-	Boiler Walls	None
	-- Secondary Fuel Injection Location	L_2	1.0 m	0-1.6 m

unheated through a secondary fuel injector inserted through a side port in the boiler, as shown in Figure 6-1. The fuel oil spray was directed in the downstream (rather than upstream) direction to provide a well-defined reburn zone. The residual/distillate fuel oil mixture was heated to approximately 93°C (200°F) before injection to ensure good atomization.

6.1.1 Primary NO_x and Reburn Zone Stoichiometry

Initial fuel oil reburning I/O trials were performed for three primary NO_x levels (nominally, 80, 140, and 200 ppm). Zone 3 stoichiometry was adjusted by varying the flow rate of secondary fuel. For these tests, primary and burnout zone stoichiometries were maintained between 5 and 10 percent excess air. Secondary fuel was injected at 1.0 m (40 in.), and final air was injected at 1.6 m (64 in.); this resulted in a reburn zone bulk residence time of about 200 ms. These nominal conditions are the same as those used in natural gas reburning tests. The boiler primary zone was insulated to reduce boiler heat extraction, allowing sufficiently high reburn zone inlet temperatures to avoid excessive sooting.

Results of these tests are shown in Figures 6-2 and 6-3. The data trends of exhaust NO are consistent with those of natural gas reburning. The data are replotted in Figure 6-4 as a function of NO_{PRI}. Clearly, NO_x reduction is not first order with respect to NO_{PRI}; as NO_{PRI} is decreased, reburn effectiveness decreases. Further, as reburn load is increased and reburn zone stoichiometry becomes more fuel-rich (over the range tested), NO_x reduction is enhanced, except when the reburn fuel contains significant quantities of nitrogen. The heavy fuel oil (distillate/residual oil mixture) has a 0.14 percent nitrogen content (see Table 2-1), which results in a secondary flame

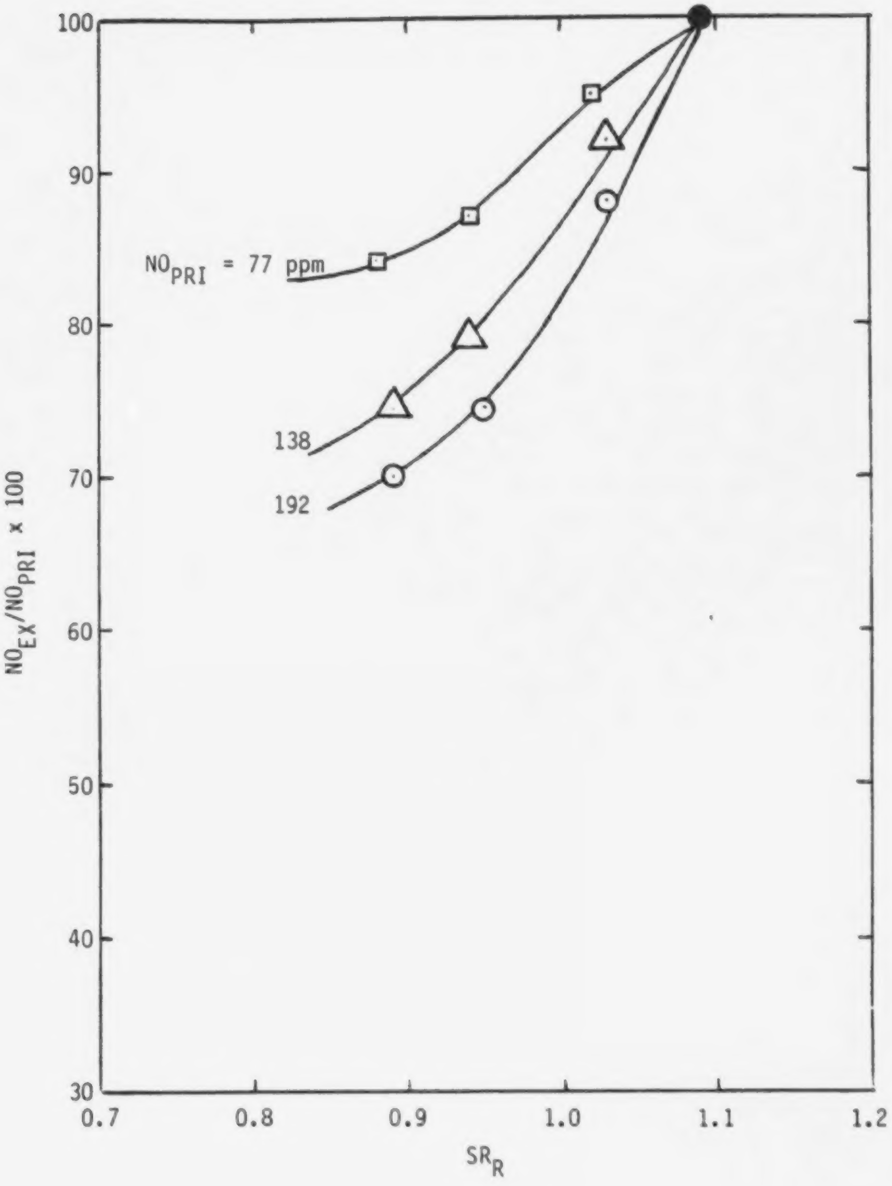

Figure 6-2: Distillate Fuel Oil Reburning Effectiveness

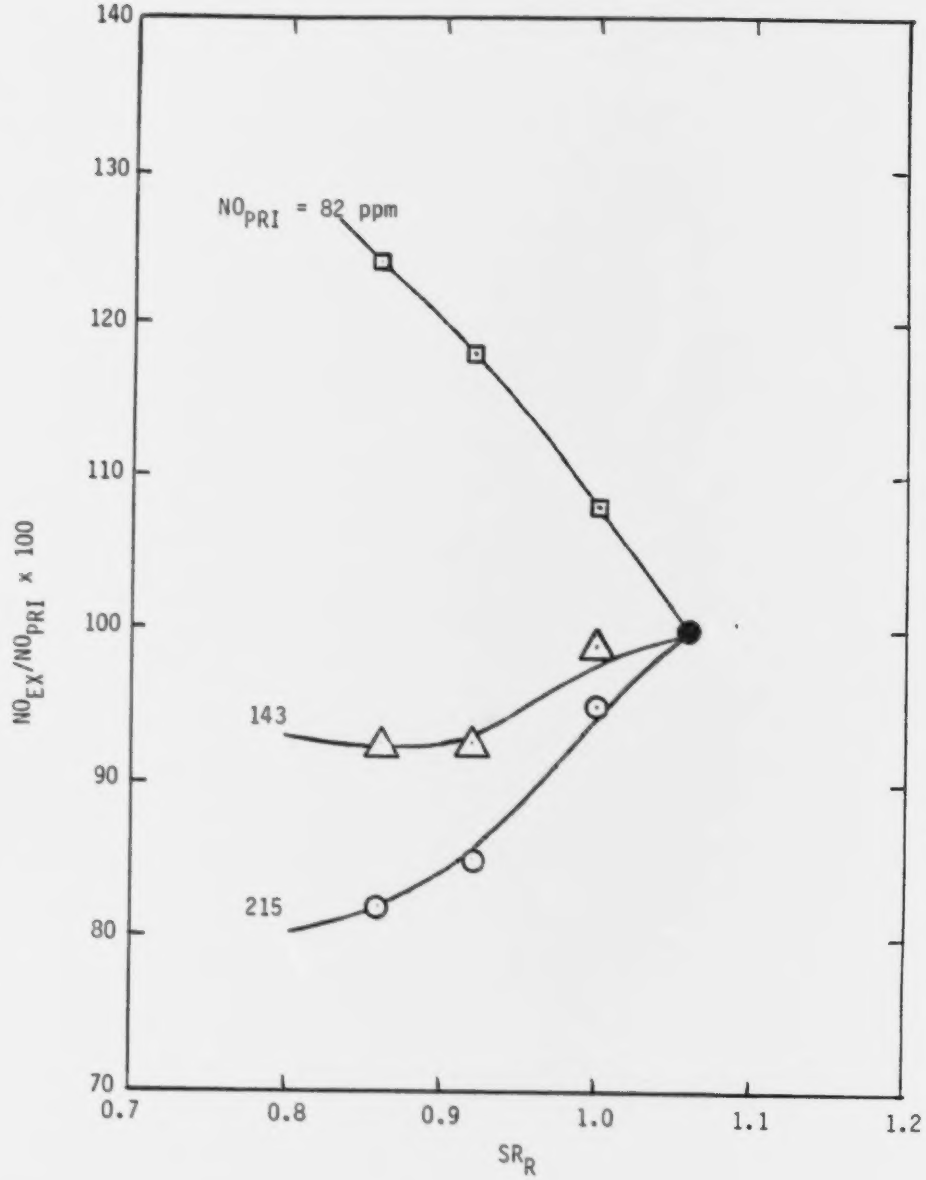

Figure 6-3: Heavy Fuel Oil Reburning Effectiveness

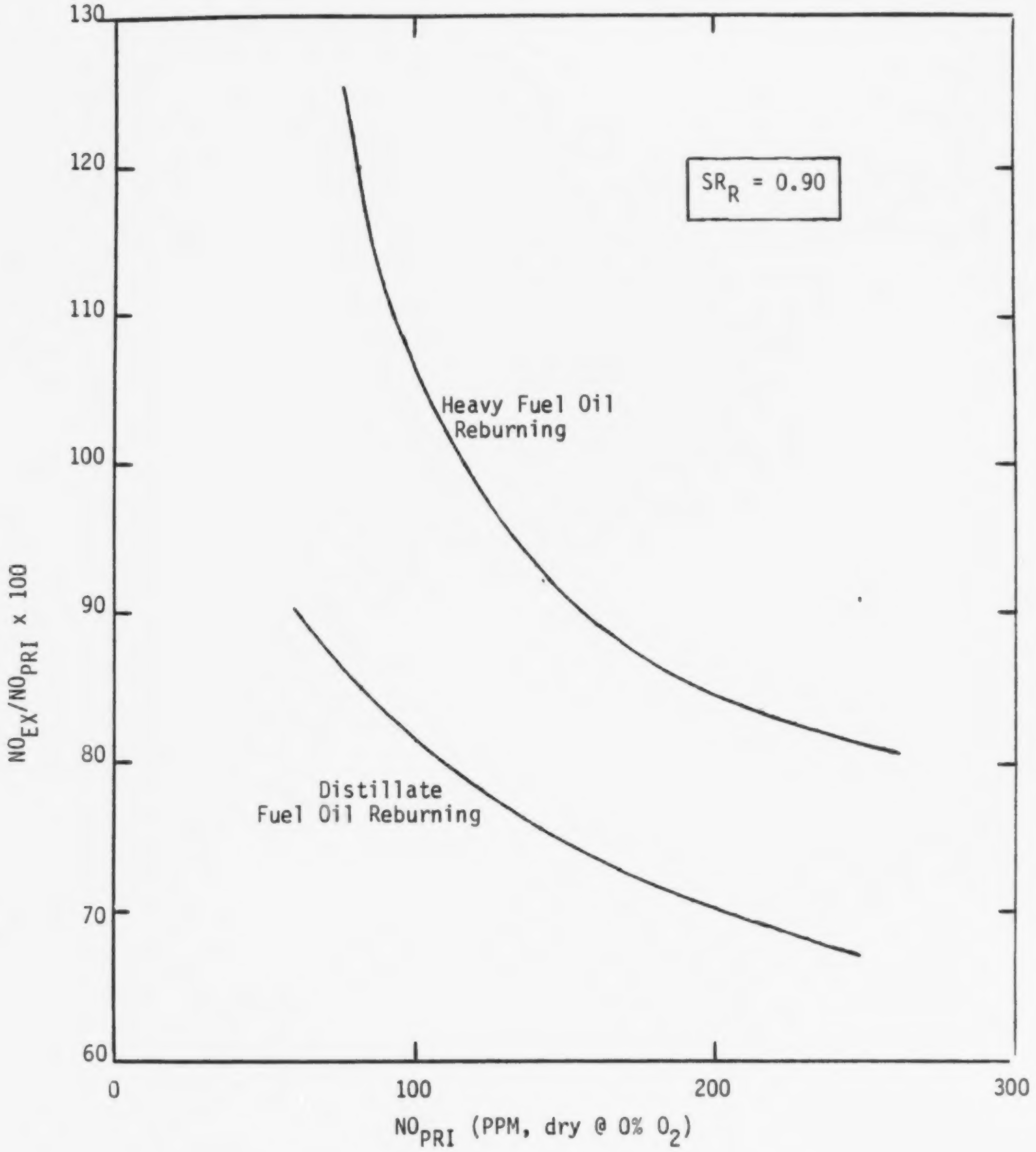

Figure 6-4: Effect of NO_{PRI} for Fuel Oil Reburning

NO_x formation that can be significant at low NO_{PRI} concentrations. In addition, the requirement that the fuel droplets vaporize prior to burning reduces the effective reburn zone residence time for gas phase kinetics. Fuel-bound nitrogen contained in the secondary fuel oil is converted to NO_x.

Assuming that reburning with a heavy fuel oil without nitrogen would yield NO_x reductions similar to that of distillate fuel oil (possibly a poor assumption given differences in fuel oil volatility), a net conversion of secondary fuel nitrogen to NO_{EX} of about 50 percent is observed. This result appears to be independent of primary NO and reburn zone stoichiometry. This result will be investigated further in the next section discussing the pyridine-doped distillate fuel oil reburning results.

It is shown in Figure 6-5 that fuel oil reburning is significantly less effective in reducing primary NO_x than natural gas reburning under identical operating conditions. The NO_x reduction curves shown in Figure 6-5 are obtained by cross-plotting the data against various parameters, then normalizing the results to a set of nominal conditions. The apparent result is surprising in that it was hypothesized in Section 1 that the higher carbon-to-hydrogen ratio in fuel oils (compared to natural gas) would produce higher concentrations of the methyldine radical (CH) in the reburning zone, causing increased NO_x destruction (hypothesis 6). While the heavy oil mixture contains significant fuel-bound nitrogen that reduces reburning effectiveness in reducing NO_x, the distillate oil is nearly nitrogen free. The carbon-to-hydrogen ratio of fuel oils being nearly twice that of natural gas (roughly 1:2 for oils compared to 1:4 for methane), it was expected that greater NO_x reductions would be achieved with the distillate oil.

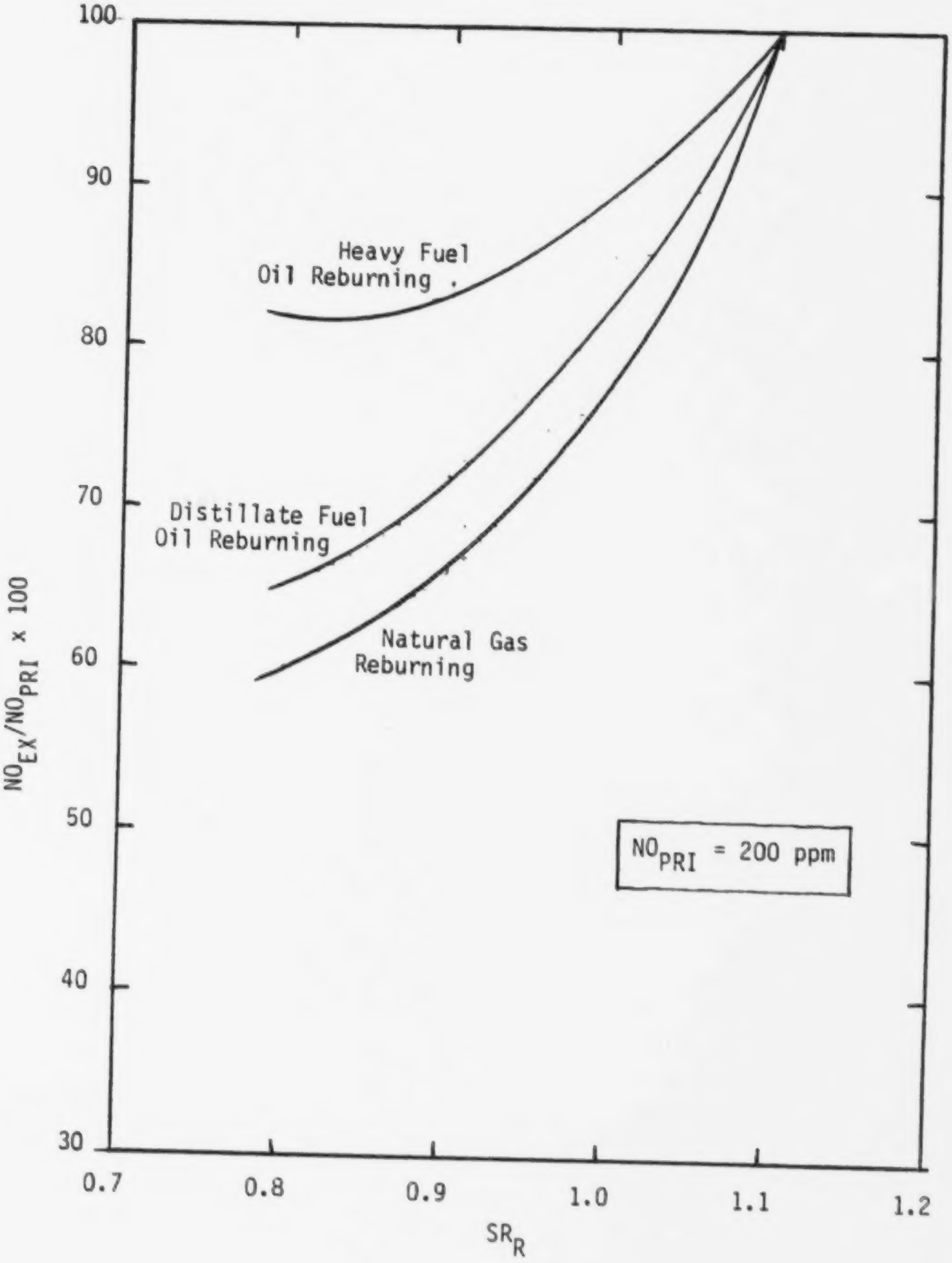

Figure 6-5: Comparison of Natural Gas and Fuel Oil Reburning

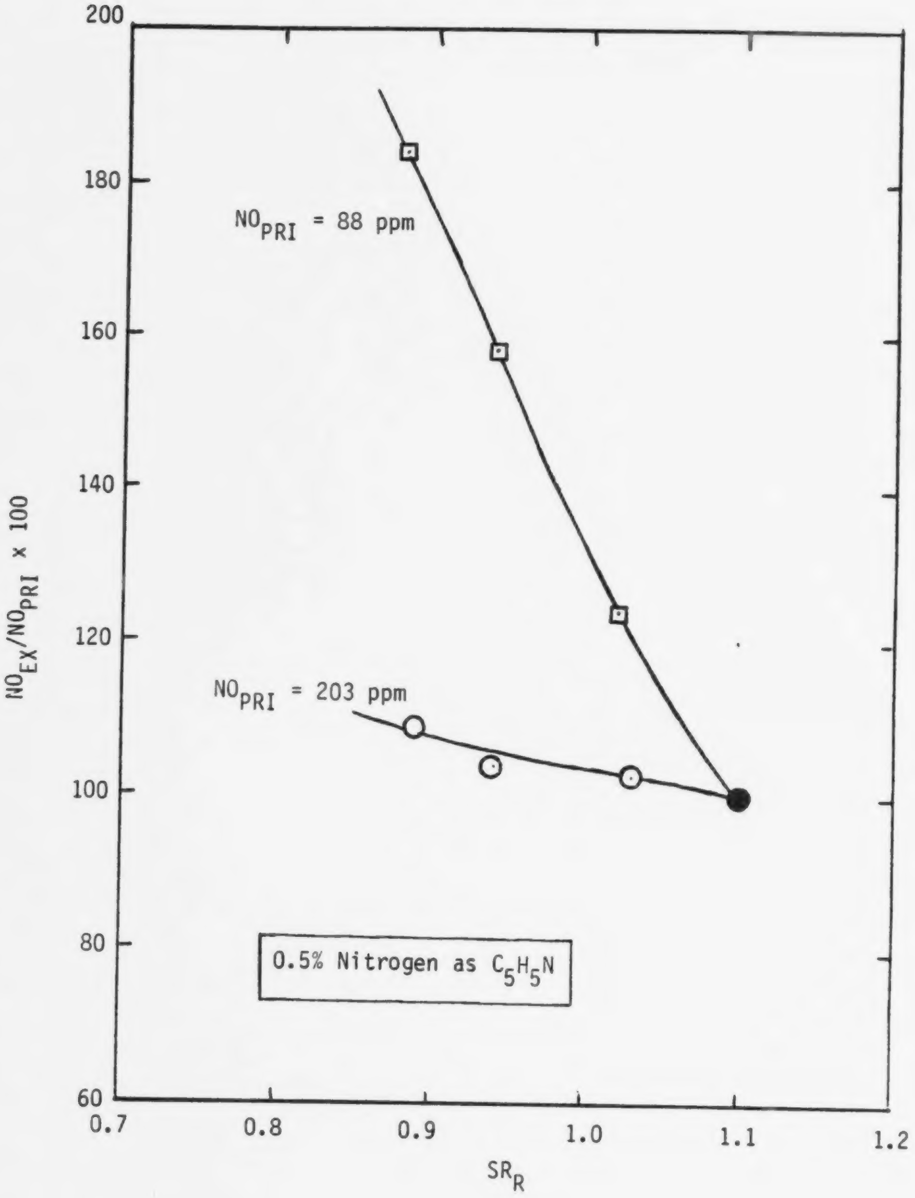

Figure 6-6: Pyridine-Doped Distillate Fuel Oil Reburning Effectiveness

An explanation of this anamolous behavior is presented in Section 6.1.3. The danger of parametric testing is that it may lead to conclusions that are true only for the test conditions established. As will be shown, residence time tests and detailed sampling experiments demonstrate that physical phenomena associated with fuel oil reburning make direct comparison to natural gas reburning results misleading. Before discussing further the comparison of natural gas and fuel oil reburning, bound nitrogen effects on fuel oil reburning are discussed.

6.1.2 Pyridine-Doped Secondary Fuel

Pyridine (C_5H_5N) was selected as a nitrogenous fuel dopant for fuel oil reburning tests. Because pyridine is a light, volatile liquid, it was mixed only with the distillate fuel oil. A 50 gallon batch mixture of pyridine and distillate fuel oil was prepared to achieve a 0.5 percent fuel nitrogen content.

Results shown in Figure 6-6 demonstrate the significant effect of secondary fuel-bound nitrogen on reburning effectiveness. As was the case with ammonia-doped natural gas reburning, pyridine-doped distillate fuel oil reburning resulted in conditions in which the formation of NO_x from the fuel-bound nitrogen was greater than the reduction of NO_x via reburning. This effect is magnified at low initial NO_x levels for two reasons: first, NO_x reduction at low NO_{PRI} concentration is less than the NO_x reduction at high NO_{PRI} concentration; and, second, the NO_x formation from secondary fuel-bound nitrogen is mostly independent of NO_{PRI}, and, hence, represents a larger fraction of the total NO_x emission at lower NO_{PRI} levels.

The net fractional conversion of secondary fuel pyridine to NO_{EX} was found to be approximately 40 percent for all conditions tested. This is slightly higher than the conversion percentage of ammonia to NO_{EX} in natural gas reburning. It was shown that about 35 percent of the ammonia dopant was converted to NO_{EX} (see Figure 5-11). This result, shown in Figure 6-7, indicates that net fuel-bound nitrogen formation in reburning application is independent of NO_{PRI} and SR_R. As already noted, the heavy fuel oil, containing 0.14 percent nitrogen, was characterized by a net 50 percent conversion of secondary fuel nitrogen to NO_{EX}. Thus, fractional conversion of fuel nitrogen to exhaust NO depends on the amount and form of fuel nitrogen contained in the secondary fuel.

These results further support hypothesis 2. That is, NO_x reduction by reburning is adversely affected by secondary fuel-bound nitrogen.

6.1.3 Reburn Zone Residence Time

Reburn zone bulk residence time was varied from 100 to 400 ms by varying the location of final air addition. In Figures 6-8 and 6-9, data are plotted for distillate and heavy fuel oil reburning, respectively, at 185 ppm NO_{PRI}. As the reburn zone length increases, NO_x emissions decrease, indicating that fuel oil reburning is very much kinetically controlled over this range in reburn zone lengths.

Figure 6-10 shows a comparison of residence time effects on NO_x reduction for natural gas and light and heavy fuel oils. For natural gas reburning, a reburn zone length of about 0.63 m (25 in.) is required to achieve maximum NO_x reduction. (The shallow slope of the NO_x reduction curve beyond 0.63 m is probably due to the effect of reduced temperatures at the point of final air

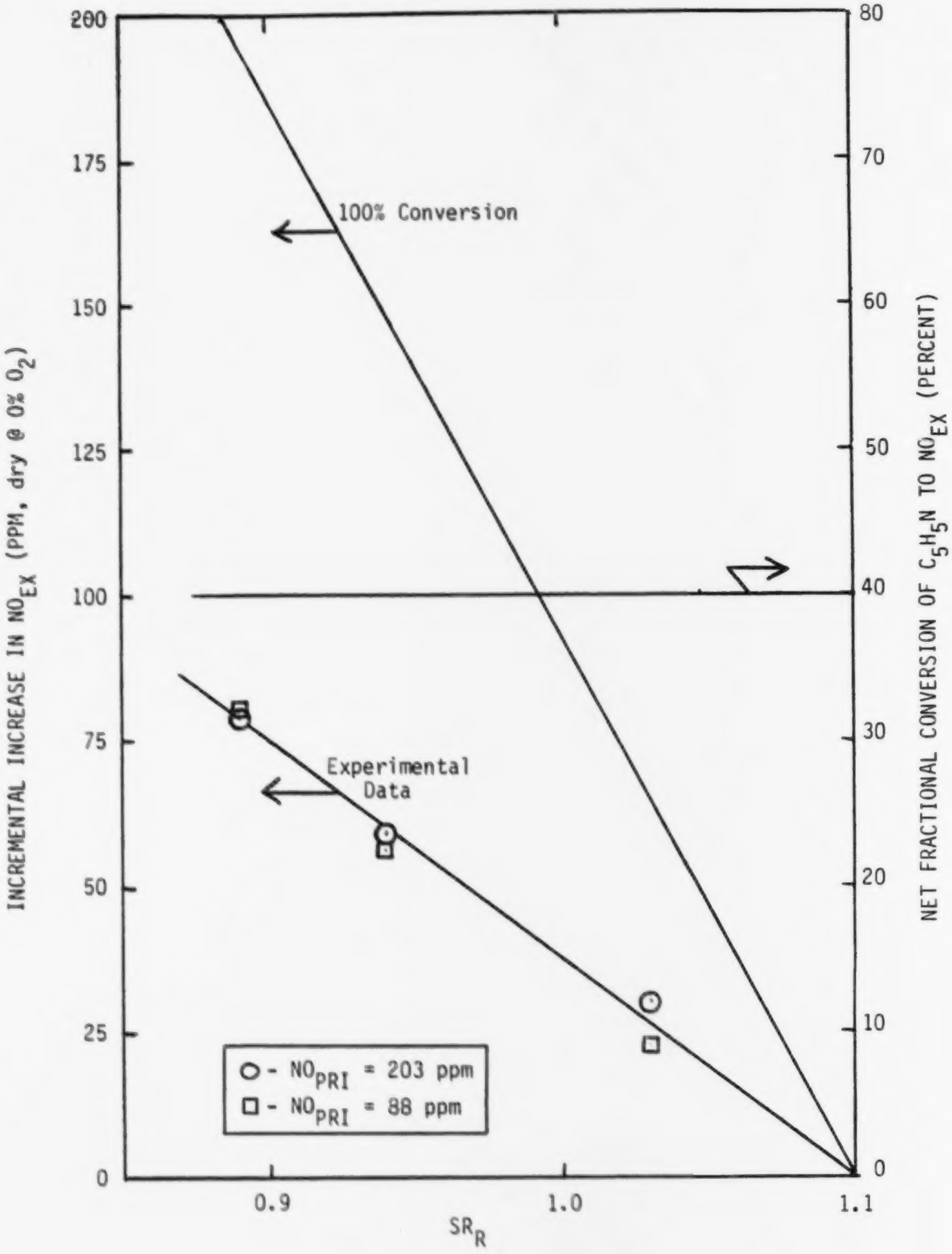

Figure 6-7: Net Fractional Conversion of Pyridine to NO$_{EX}$

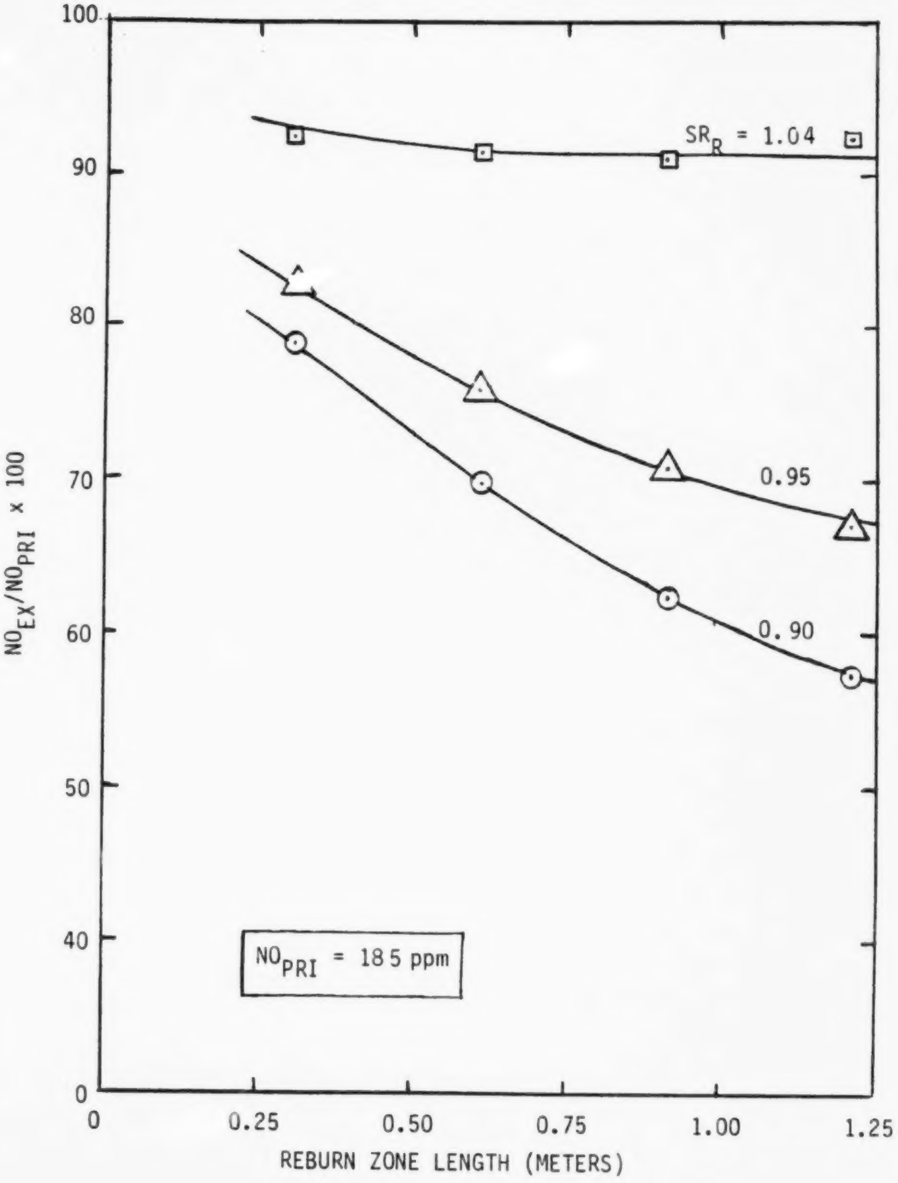

Figure 6-8: Effect of Reburn Zone Residence Time for Distillate Fuel Oil Reburning

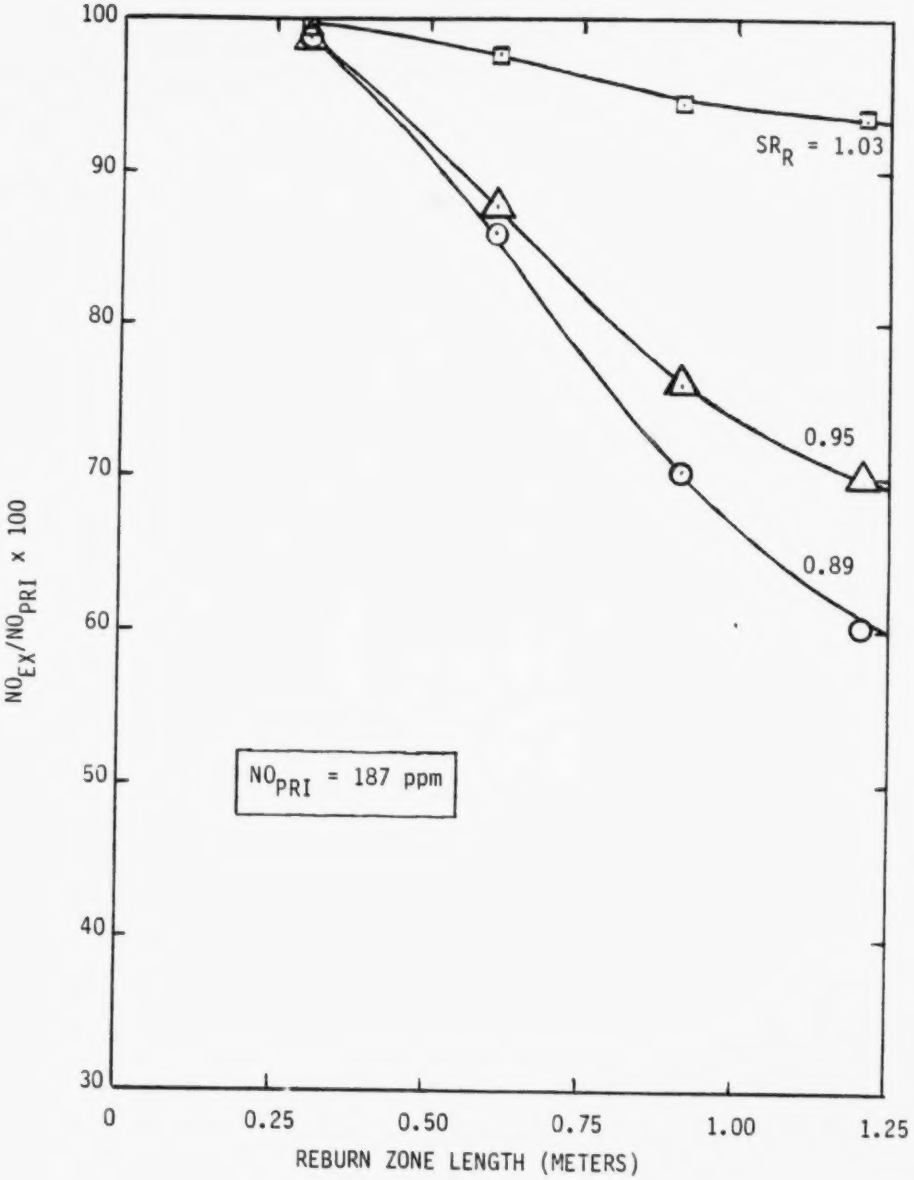

Figure 6-9: Effect of Reburn Zone Residence Time for Heavy Fuel Oil Reburning

addition). For distillate oil reburning, approximately 1.0 m (39 in.) reburn zone length is required. For heavy fuel oil reburning, about 1.3 m (51 in.) reburn zone length is required. With a peak velocity in the reburn zone of about 12 m/sec (40 ft/sec), these distances suggest characteristic reburning times of 50 ms for natural gas, 85 ms for light oil, and 105 ms for heavy oil. If the gas phase chemical times for reburn zone reactions is assumed to be equal for each fuel (50 ms), this data suggests that the distance required for droplet vaporization for the distillate oil is 35 cm (14 in.), and for heavy fuel oil, 65 cm (26 in.). Photographs of the secondary fuel oil spray indicate that the droplets persist several inches into the reburn zone. Given the high initial velocity of the droplets and the existence of some large droplets in the spray, the increased residence time requirement for fuel oil reburning is not surprising.

The requirement for longer reburn zone residence times for fuel oils will be investigated further in Section 6.2, where detailed measurements are presented. It is clear from the input/output data that reburning effectives for natural gas and fuel oils should not be compared at constant reburn zone lengths, since the overall characteristic NO_x reduction times differ. Figure 6-10 shows that the maximum reduction achieved by fuel oil reburning exceeds the maximum reduction achieved by natural gas reburning by about 5 percent. Thus, the conclusion that could be drawn from the data presented in Section 6.1.1, that natural gas reburning is more effective at reducing NO_x than fuel oil reburning, is not true when sufficient reburn zone residence times for maximum NO_x reduction are provided. For optimum reburn application, greater NO_x reduction may be achieved with fuel oil reburning than with natural gas reburning. Although there is only a weak indication of this conclusion (a 5 percent difference in NO_x is hardly statistically significant, given the

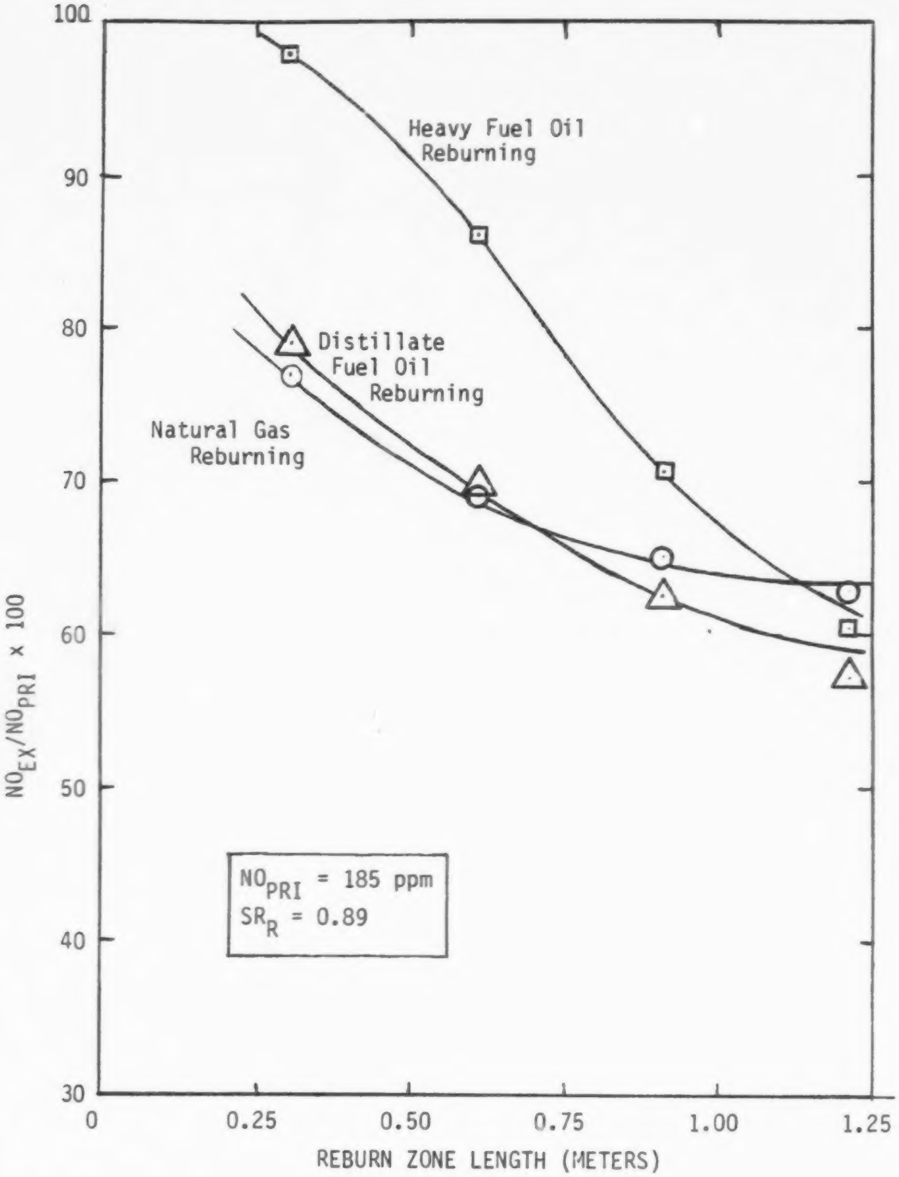

Figure 6-10: Comparison of Natural Gas and Fuel Oil Reburning with Residence Time

myriad of parameters that must be held constant), this result can be attributed to the higher carbon-to-hydrogen ratio of the fuel oils (resulting in more hydrocarbon flame radicals).

Figure 6-11 further demonstrates the significance of reburn zone residence time. For low primary NO_x, no NO_x reduction was realized for heavy fuel oil reburning with the nominal 0.61 m (24 in.) reburn zone length. However, as reburn zone length increased, NO_x reductions were achieved, and the optimum reburn zone stoichiometry changed. For short reburn zone lengths, optimum reburn loads are small to minimize NO_x formation from fuel-bound NO_x. For longer reburn zone lengths, optimum reburn load increases to take advantage of increased NO_x destruction by flame radicals.

The influence of reburn zone residence time on pyridine-doped distillate fuel oil reburning is shown in Figure 6-12. As reburn zone residence time increases, NO_x reduction increases and the net fraction of fuel nitrogen producing NO_x decreases. Thus, optimum reburn zone lengths are greater for nitrogen-containing fuels.

6.1.4 Primary Zone Stoichiometry

Primary zone stoichiometry was varied from 0.95 to 1.16 with other parameters held constant. Figure 6-13 shows the effect of this variation on NO_x reduction for distillate fuel oil reburning. Figure 6-14 shows this effect for heavy fuel oil reburning. Both sets of curves show that variation in primary zone stoichiometry does not significantly influence NO_x reduction for primary zone excess airs less than 10 percent. However, as primary zone stoichiometry increases, more secondary fuel is required to achieve a desired

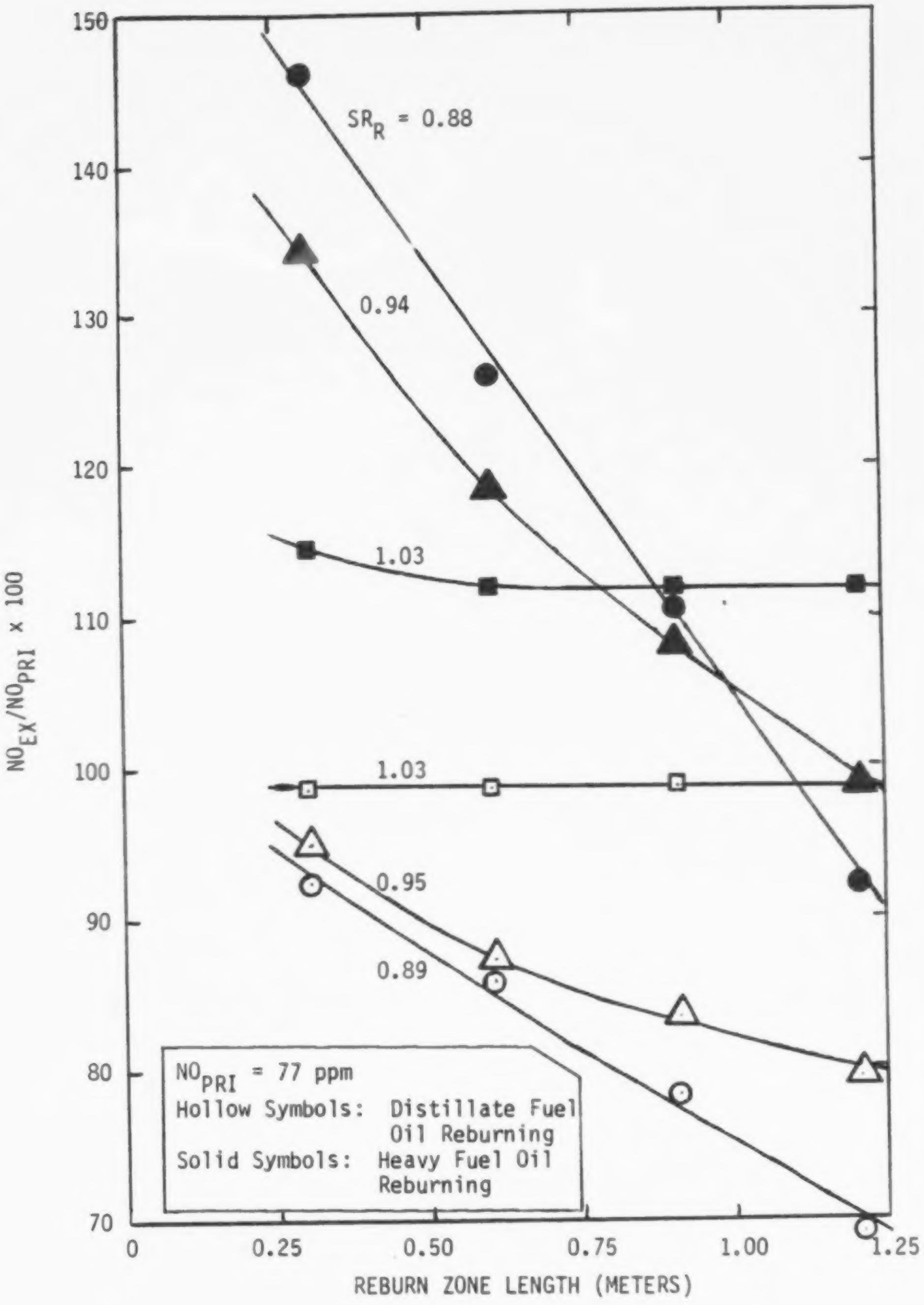

Figure 6-11: Effect of Reburn Zone Residence Time for Low NO_{PRI}

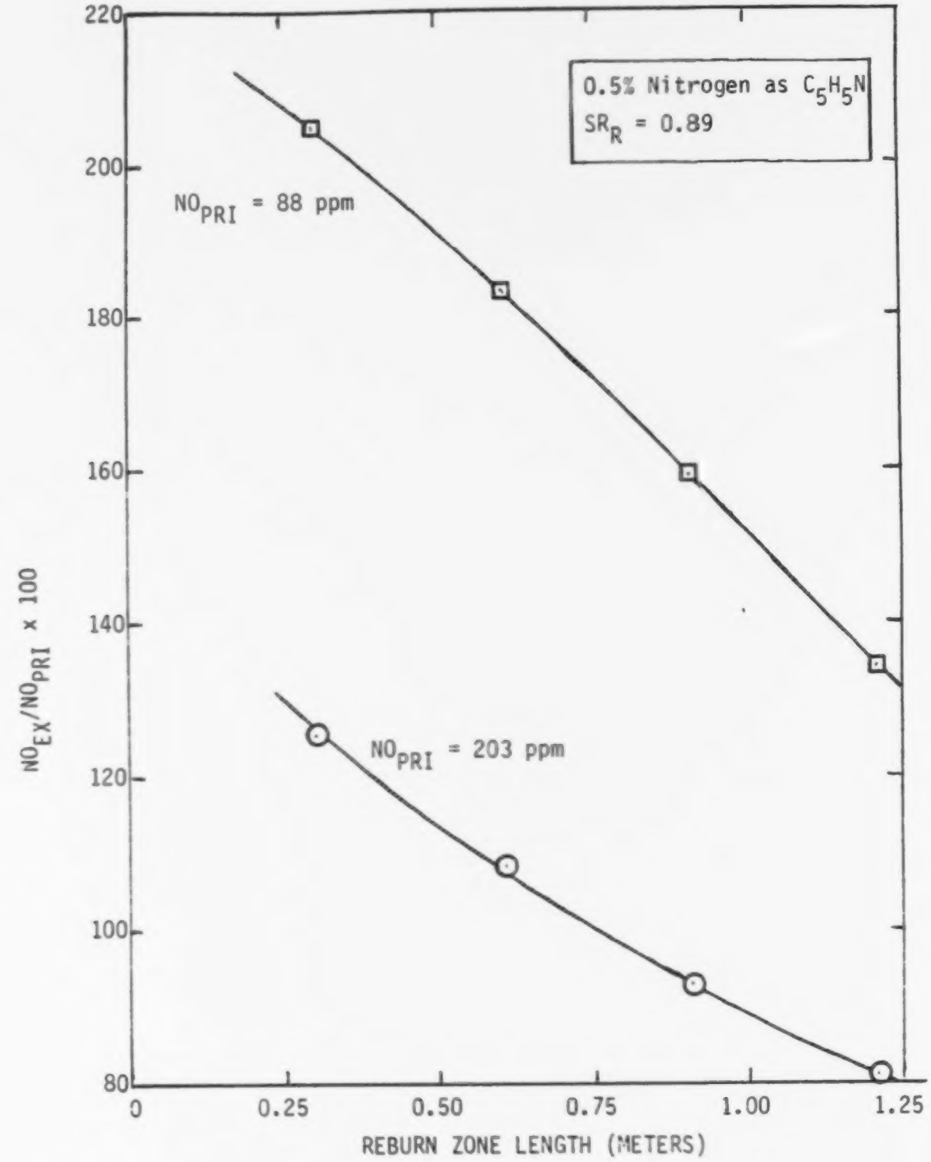

Figure 6-12: Effect of Reburn Zone Residence Time for Pyridine-Doped Distillate Fuel Oil Reburning

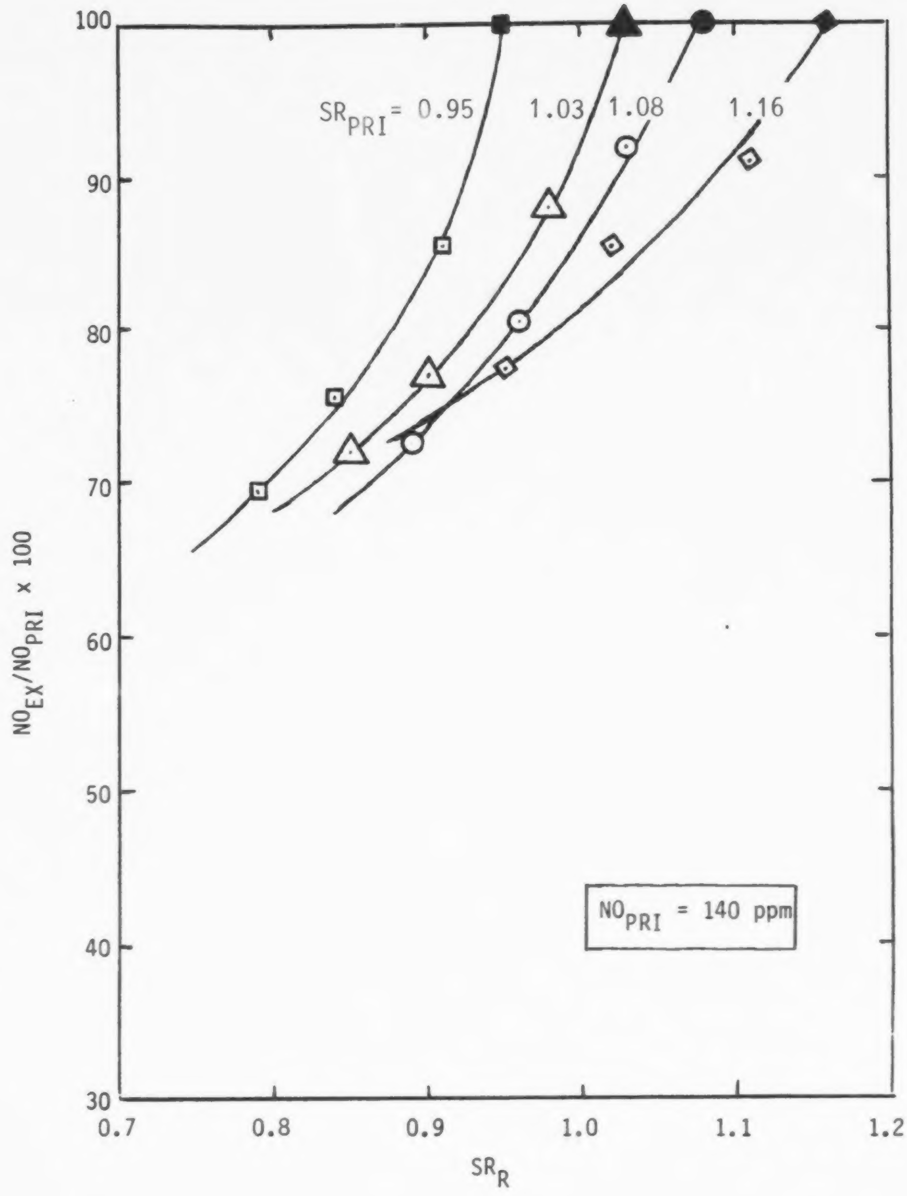

Figure 6-13: Effect of Primary Zone Stoichiometry for Distillate Fuel Oil Reburning

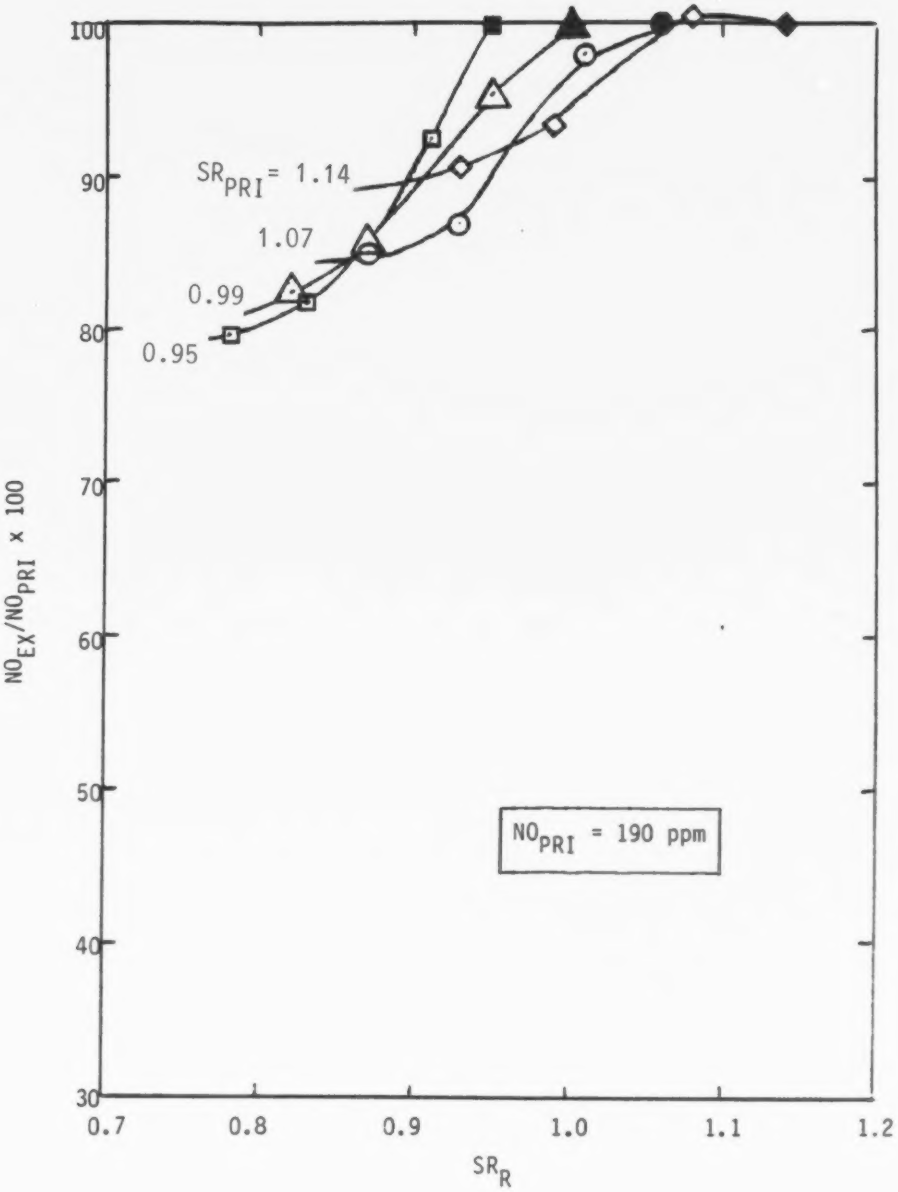

Figure 6-14: Effect of Primary Zone Stoichiometry for Heavy Fuel Oil Reburning

reburn zone stoichiometry. Also, in a practical application, primary zone excess air would effect NO_{PRI}. In these tests, however, this effect was eliminated by adjusting primary ammonia flow to maintain a constant NO_{PRI}. In reburn application tests to an actual boiler, described in Section 7, the total affect of primary zone stoichiometry variation is investigated.

6.1.5 Burnout Zone Stoichiometry

Figure 6-15 shows NO_x reduction curves as a function of burnout zone stoichiometry for both distillate and heavy fuel oil reburning. As in the natural gas reburnin tests, it is seen that NO_x is relatively independent of final excess air amount, due to the low combustion gas temperatures at the point of final air addition. The heavy fuel oil reburning test condition was the most sensitive to burnout zone stoichiometry, possibly indicating that some of the fuel is not completely decomposed in the reburn zone in those tests.

6.1.6 Primary Fuel

For distillate fuel oil reburning, both natural gas and distillate oil were used as the primary fuel. As with natural gas reburning, no effect of primary fuel composition on the reburning process was observed. Thus, it is concluded that the relative amounts of primary zone CO_2 and H_2O concentrations are not important in reburning application; only the concentration of NO_{PRI} impacts reburning. This is consistent with the proposed NO_x destruction mechanism involving NO_x reactions secondary fuel radicals, independent of primary fuel composition. Of course, primary fuel type does effect primary NO_x formation. This dependence was eliminated from these tests by varying the amount of ammonia dopant in the primary flow.

Figure 6-16 shows the lack of influence of primary fuel type on distillate oil reburning.

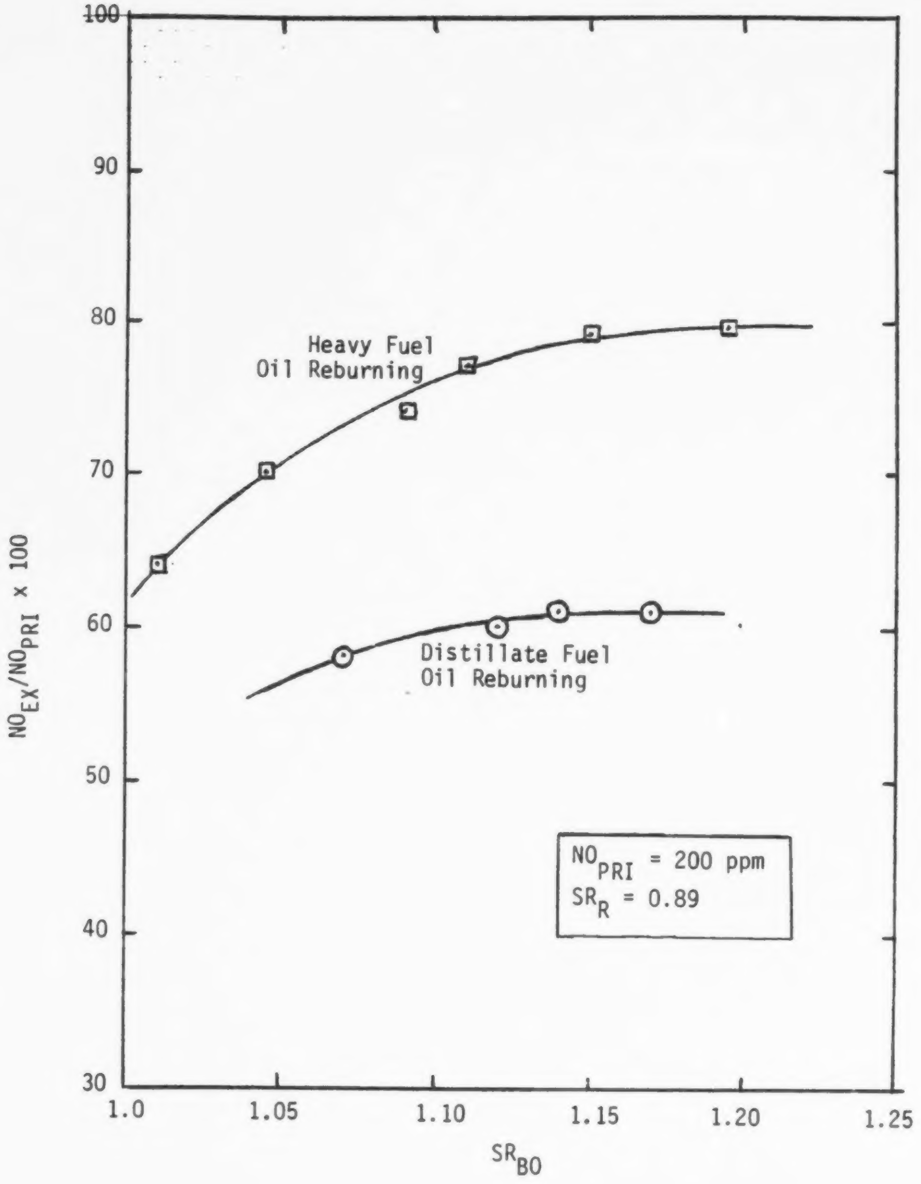

Figure 6-15: Effect of Burnout Zone Stoichiometry for Fuel Oil Reburning

6.1.7 Secondary Fuel Atomization

Secondary fuel oil was fired with various nozzle and injector types. Varied were atomizer type (air-atomized versus pressure-atomized), nozzle capacity (affecting droplet size) spray angle, and spray direction. All tests were performed with natural gas primary fuel, distillate oil reburning fuel, and 200 ppm NO_{PRI}. Results are summarized in Table 6-2.

No influence on reburning effectiveness (NO_x reduction) was observed for variation in atomizer type, nozzle capacity, or spray angle. The air-atomized sonicare nozzle used approximately 1 scfm of air to atomize the fuel oil. According to the manufacturer, droplets ranging from 0.1 to 10 micrometers are produced by this nozzle operated at design conditions. For the hollow cone spray, pressure-atomized Hago and Delavan nozzles, a Sauter Mean Diameter (SMD) on the order of 200 micrometers is produced. The dependence of SMD on supply pressure has been shown to be:

$$\text{SMD} \propto \frac{1}{p^{0.3}}$$

Thus, as pressure decreases, SMD increases. Using an oversized nozzle at reduced pressures can produce the same flow, with larger droplets, as using a properly sized nozzle. In this way, droplet sizes were varied from 200 to 500 micrometers, with no detectable effect on reburning NO_x reductions. Considering the wide range in droplet sizes (including the fine mist produced by the air-atomizing nozzle), it is surprising that no effect on reburning effectiveness was observed. Droplet burning time has been shown to be proportional to the square of the droplet diameter (d^2 burning law). It was expected that larger droplets would delay the reburning gas-phase kinetics and result in less NO_x reduction. This was not observed.

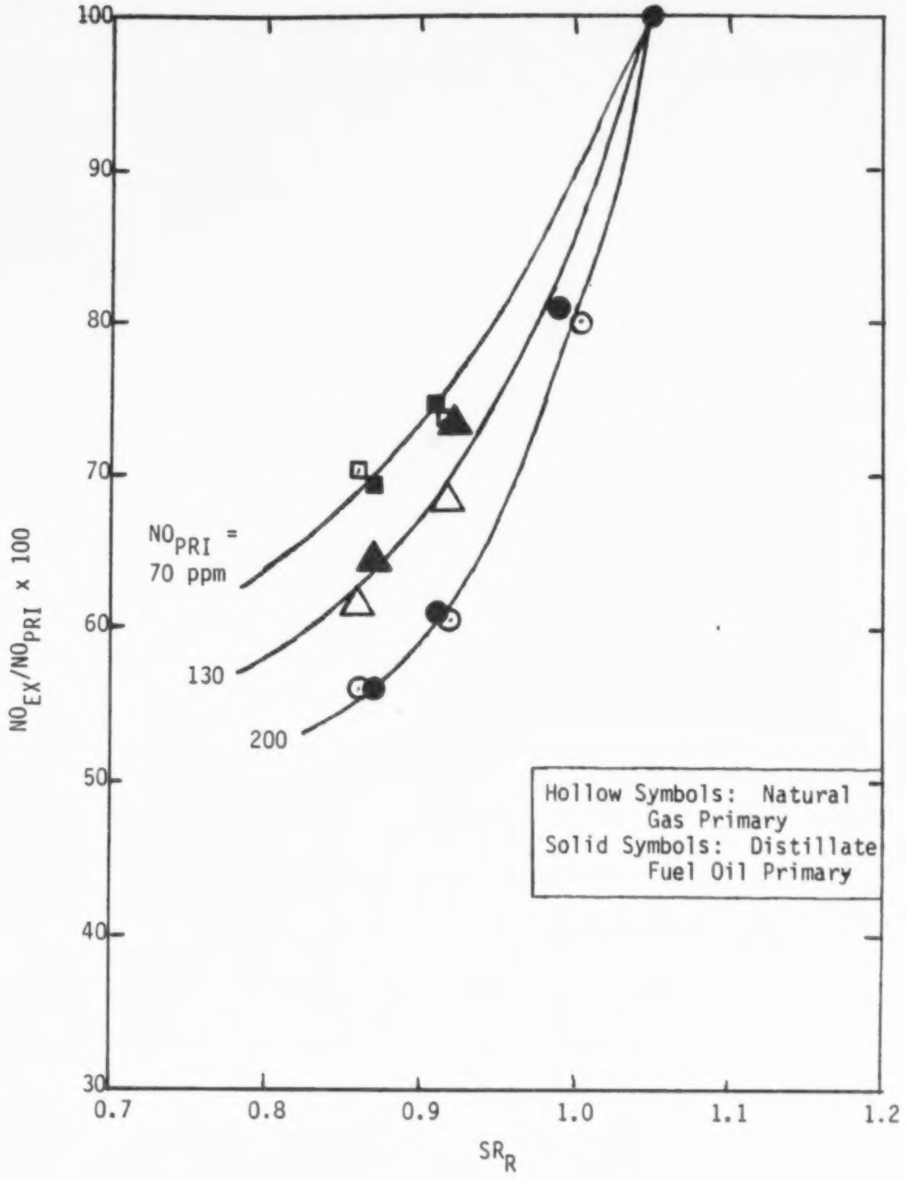

Figure 6-16: Effect of Primary Fuel Type for Distillate Fuel Oil Reburning

TABLE 6-2. EFFECT OF SECONDARY FUEL OIL NOZZLE

Test Variable	Nozzle Manufacturer	Atomizer Type	Nozzle Capacity (gph)	Spray Angle	Spray Direction	NO_x Reduction (percent) $SR_3=0.96$	$SR_3=0.86$	$SR_3=0.78$
Atomizer Type	Sonicore 052	Air	3.5	30°	Upstream	-	-	35
Spray Direction	Hago	Pressure	3.5	30°	Upstream	-	26	34
	Hago	Pressure	3.5	30°	Downstream	-	23	29
Spray Angle	Delavan WDA	Pressure	4.0	45°	Downstream	9	25	29
	Delavan WDA	Pressure	4.0	30°	Downstream	13	25	29
	Delavan WDA	Pressure	4.0	90°	Downstream	10	25	31
Droplet Size	Delavan WDA	Pressure	5.0	45°	Downstream	10	24	30
	Delavan WDA	Pressure	3.0	45°	Downstream	10	25	29
	Delavan WDA	Pressure	2.0	45°	Downstream	9	22	-

Variation in secondary fuel spray angle, from 30° to 90°, also resulted in no measurable difference in NO_x reduction. This result is consistent with the natural gas mixing tests in which secondary natural gas fuel injection mode had no effect on reburning effectiveness. Apparently, secondary fuel oil injection parameters, such as droplet size and spray angle, have no effect on the reburning process in the firetube package boiler. It has been shown that large scale mixing phenomena in the firetube radiant section (see Section 5-3) dominate reburn zone mixing and, together with reburn chemistry, control the reburning process. This result may be applicable only to the firetube package boiler class.

Secondary fuel oil was injected both countercurrent and cocurrent to the combustion gas flow stream. In each case, the fuel oil was injected 1.0 m (40 in.) into the boiler. This resulted in a difference in the amount of NO_x reduction of 3 to 5 percent, with greater reduction achieved in the countercurrent (upstream) injection scheme. This difference may be due to a difference in secondary fuel residence time prior to final air addition. For countercurrent injection, the reburn zone is effectively lengthened due to the upstream momentum of the fuel spray. Thus, the effect on NO_x reduction is not thought to be an atomizer effect.

6.1.8 Reburn Zone Thermal Environment

As stated at the start of Section 6, fuel oil reburning in the uninsulated PBS resulted in excessive sooting in the fuel-rich reburning zone. Therefore, nominal fuel oil reburning tests were performed with primary zone boiler walls insulated. This resulted in a combustion gas temperature of 1590K (2400°F) at the point of secondary fuel injection, an increase of 150°C (300°F) over the uninsulated combustion gas temperature (as described in Section 5.4).

A comparison of the NO_x reduction achieved for distillate fuel oil reburning under the insulated and uninsulated primary zone conditions is presented in Figure 6-17. The uninsulated test yielded 5 percent greater reductions than the insulated test for the conditions tested. This result seems to contradict the natural gas reburning data where increased temperature enhanced NO_x reduction under fuel-rich conditions. Several possible explanations can be hypothesized. In the uninsulated test condition, not only was the temperature at the point of secondary fuel addition lower (thus, decreasing reburn zone NO_x destruction), the temperature at the point of final air addition was lower. This may result in an increased percent conversion of fixed nitrogen to molecular nitrogen in the burnout zone. Further, lower reburn zone temperatures result in longer residence times, which enhances NO_x reduction. Finally, the presence of excessive sooting in the uninsulated test may have caused NO_x destruction reactions with the soot. Sooting was too great to reburn with heavy fuel oil without primary zone insulation.

A second test was performed to evaluate thermal effects on reburning. The burner prechamber was operated fuel-lean (at 20 percent excess air). Secondary fuel was injected at various locations in the boiler with temperatures greater than 1530K (2300°F). Primary NO_x was very high (1175 ppm) at this condition due to the nearly adiabatic primary flame zone in the prechamber producing large amounts of thermal NO_x. A baseline axial temperature profile is presented in Figure 6-18. Secondary fuel was injected at the boiler entrance, at a temperature of 1850K (2870°F), and 1.0 m (40 in.)

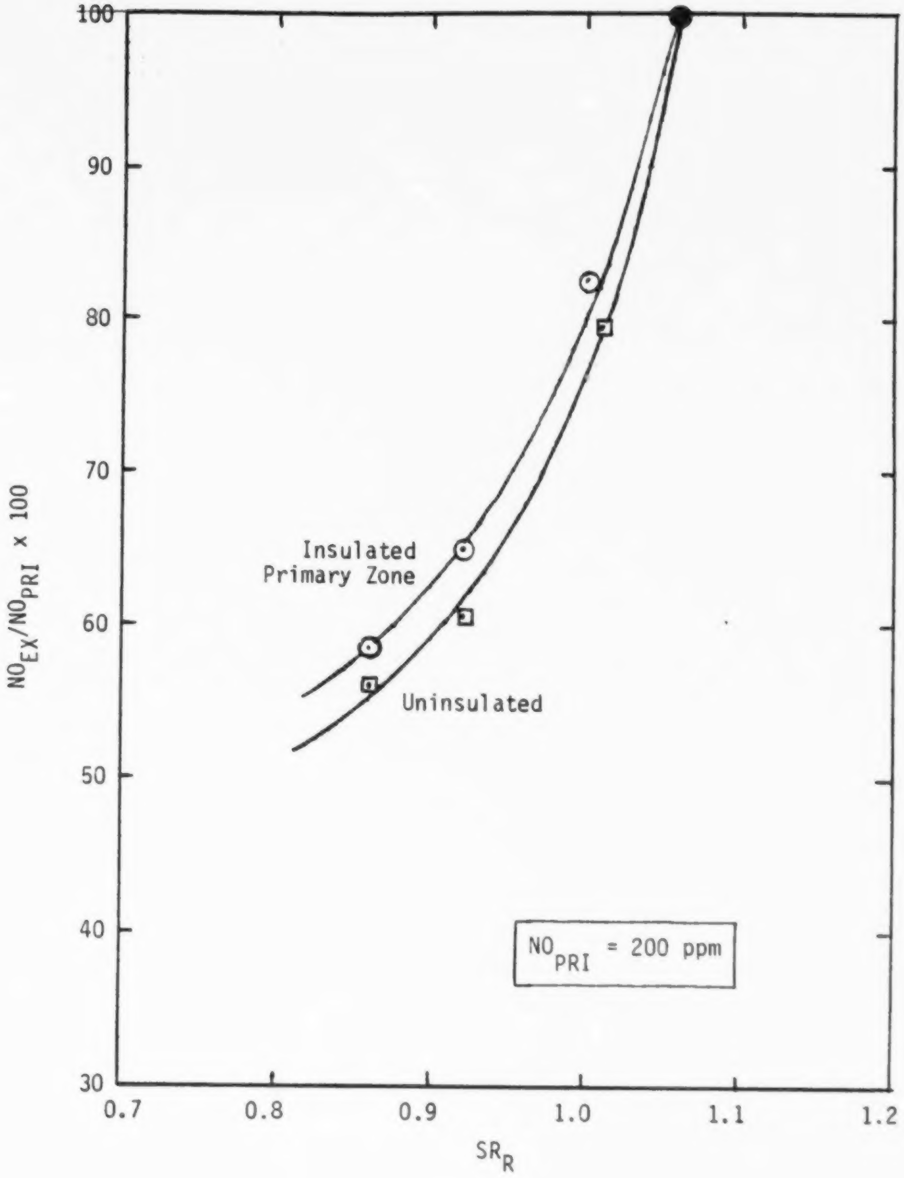

Figure 6-17: Effect of Primary Zone Insulation for Distillate Fuel Oil Reburning

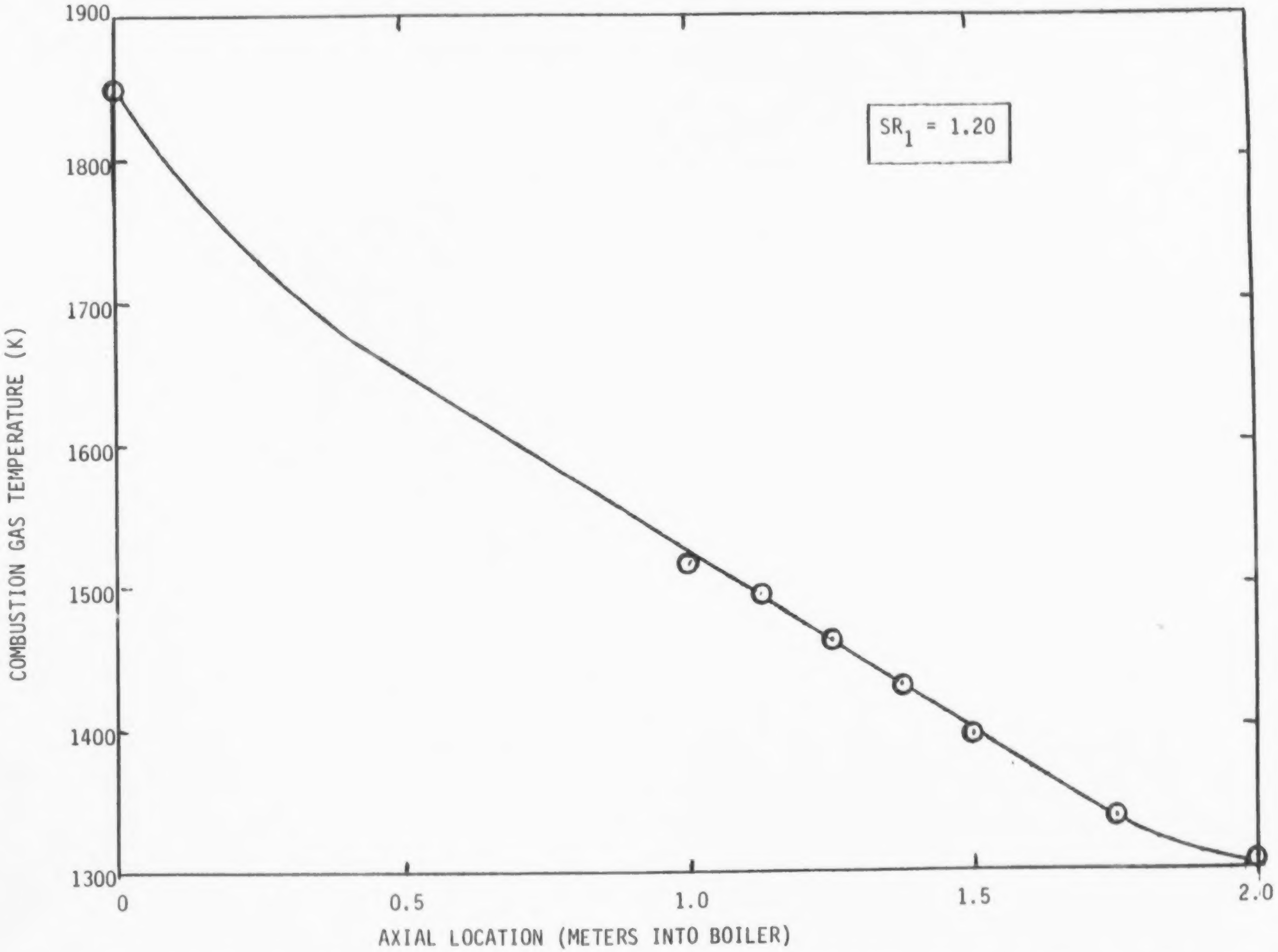

Figure 6-18: Baseline Centerline Temperature Profile for Fuel-Lean Prechamber Burner Operation

into the boiler, at 1530K (2300°F). Results are plotted in Figure 6-19. The low temperature reburn condition yielded significantly greater NO_x reductions than the high temperature reburn condition. However, fuel-rich reburning conditions were not attained during these tests. This result is consistent with natural gas reburning results where, under fuel-lean reburn zone conditions, increased temperature reduced NO_x reduction. Unfortunately, limitations in the oil feed rate capacity prevented testing under fuel-rich conditions for this mode of primary burner operation.

Further tests were conducted for oil reburning to evaluate thermal effects under fuel-rich conditions. Primary excess air levels were reduced to achieve these test conditions. Results from these tests demonstrate that under fuel-rich conditions, increased temperature enhances fuel oil reburning effectiveness.

6.2 DETAILED TESTS

Detailed tests, involving the measurement of reburn zone combustion gas species profiles, were performed for a variety of fuel oil reburning test conditions, as summarized in Table 6-3. Plots of measured fixed nitrogen species (NO, HCN, and NH_3) in the reburn zone are shown in Figures 6-20 through 6-30. These plots show the destruction of NO and the formation of HCN and NH_3 as functions of reburn zone location (or residence time). The trends for fuel oil reburning are essentially the same as those for natural gas reburning (discussed in Section 5.2). NO destruction increases (and HCN formation increases) as reburn zone stoichiometry decreases from 1.03 to 0.87. Percent NO_x destruction in the reburn zone is nearly independent of NO_{PRI} for distillate fuel oil rburning. This first order behavior in the reburn zone is consistent with the results from undoped natural gas reburning. Net NO_x destruction decreases with decreasing NO_{PRI} for heavy oil reburning.

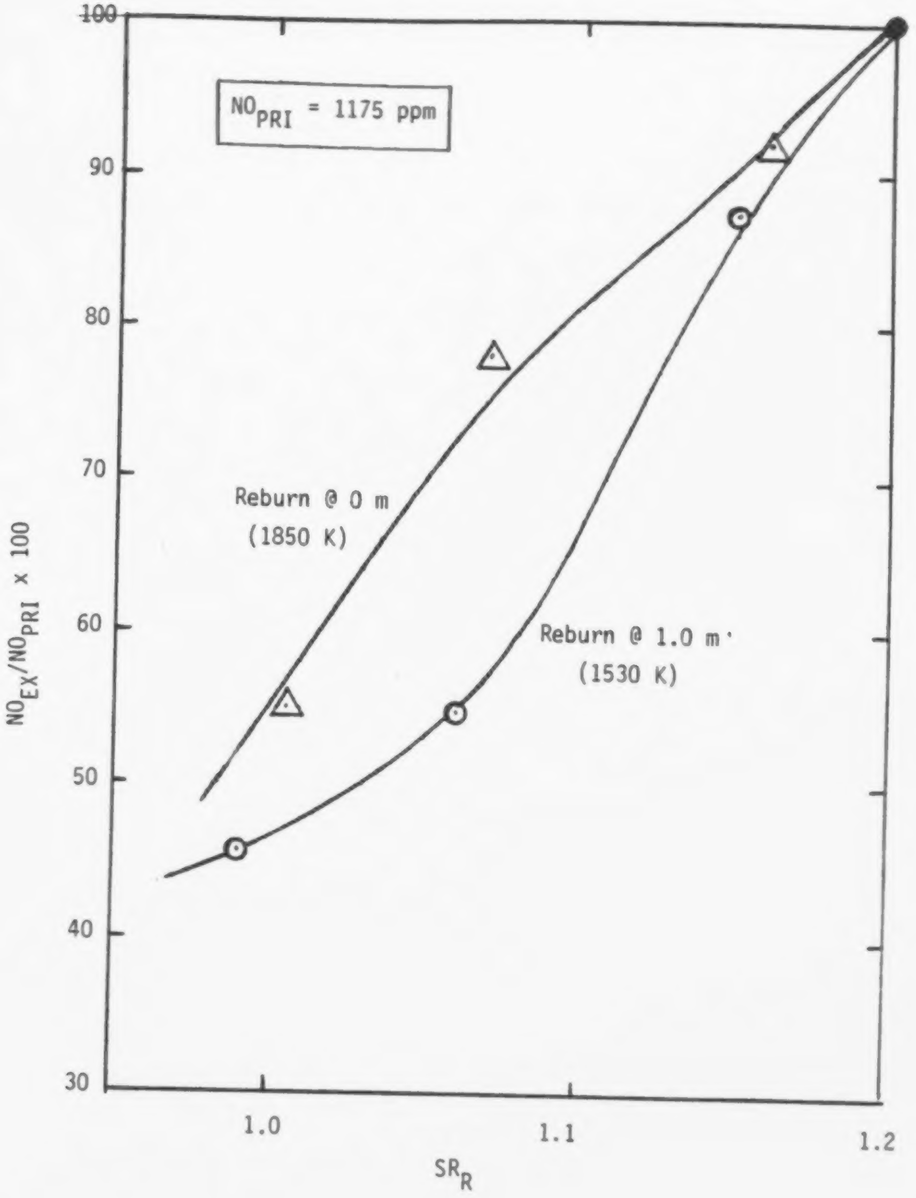

Figure 6-19: Thermal Effects for Fuel-Lean Distillate Fuel Oil Reburning

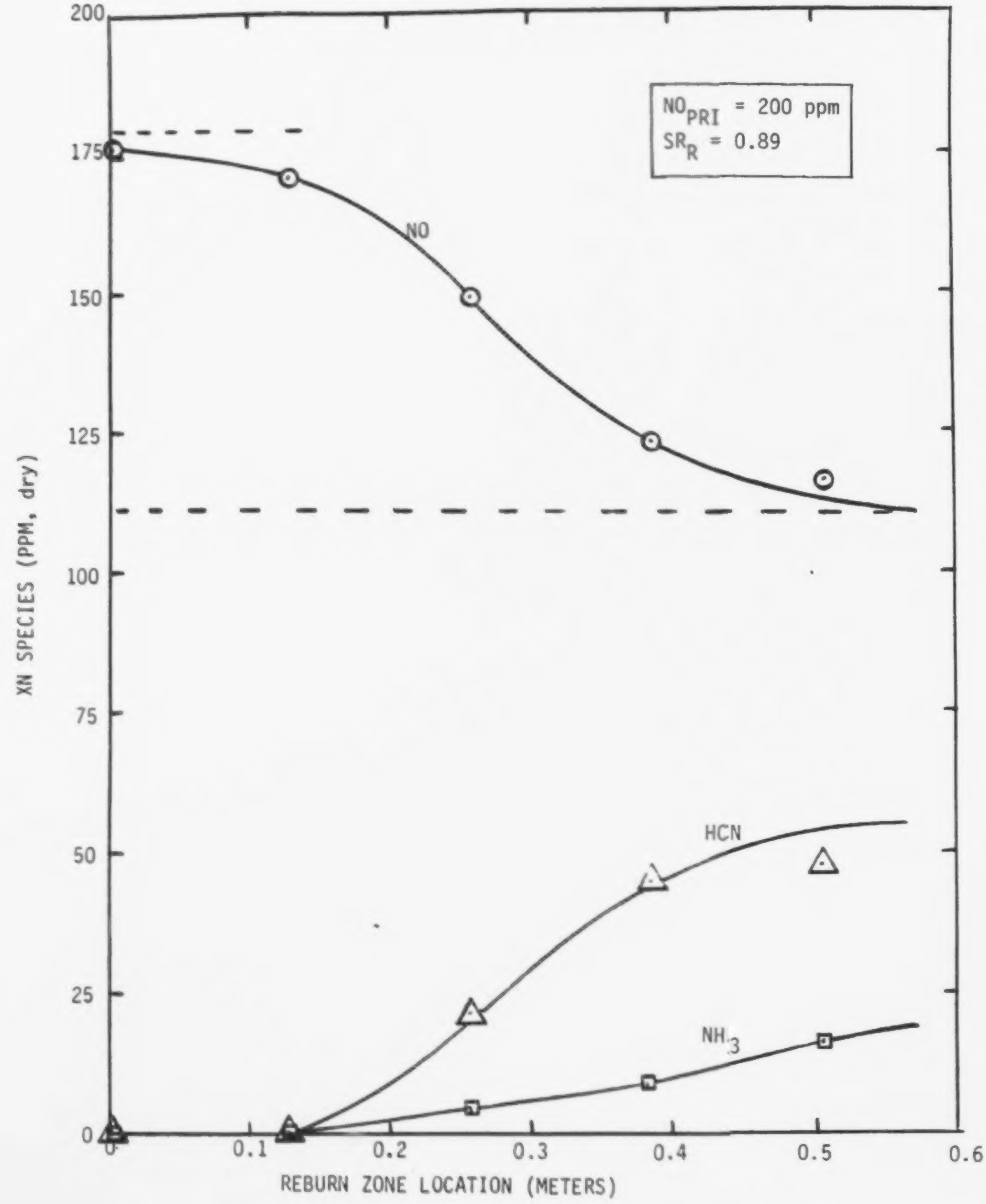

Figure 6-20: Reburn Zone Nitrogen Species Profiles for Distillate Fuel Oil Reburning, SR$_R$ = 0.89

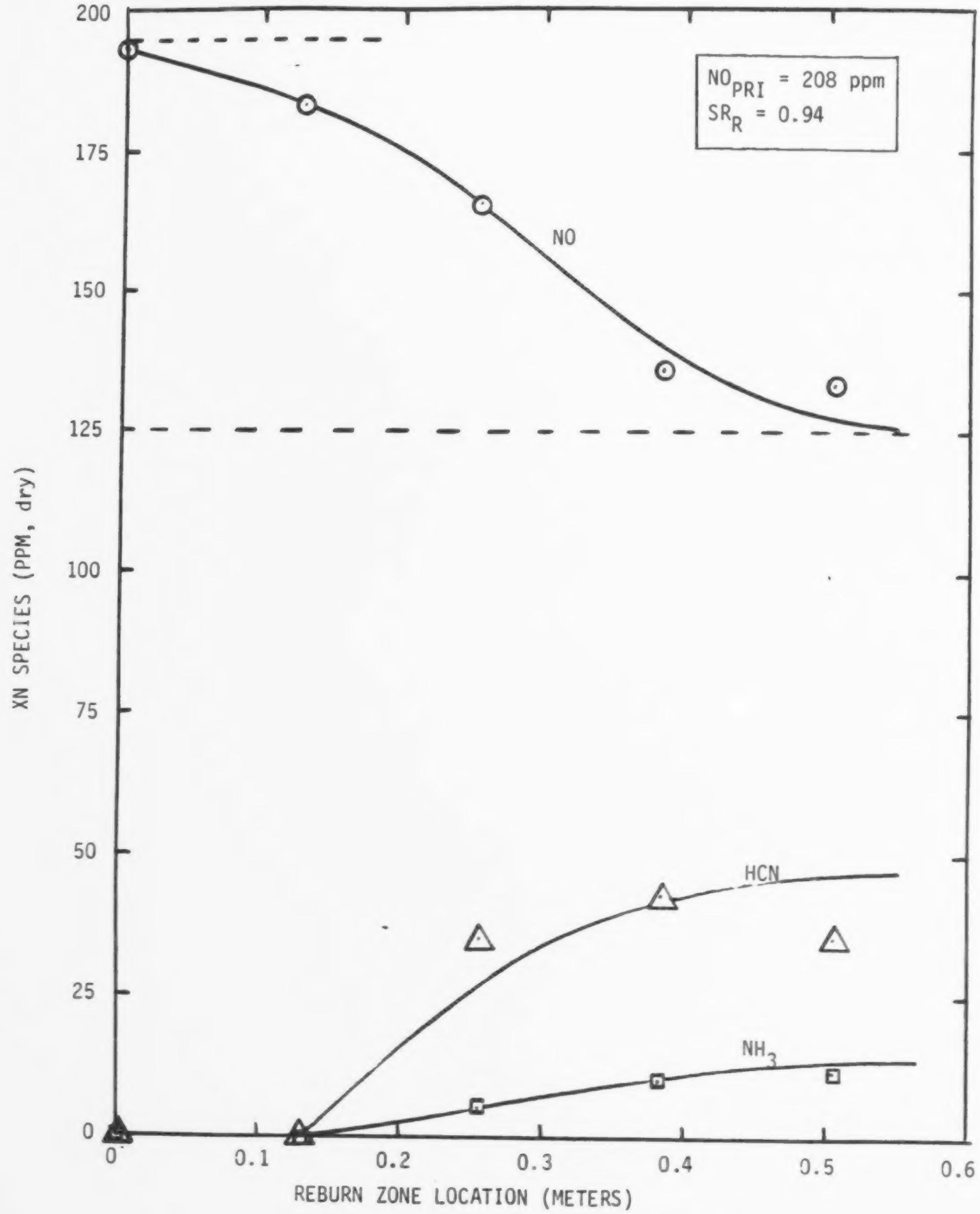

Figure 6-21: Reburn Zone Nitrogen Species Profiles for Distillate Fuel Oil Reburning, SR_R = 0.94

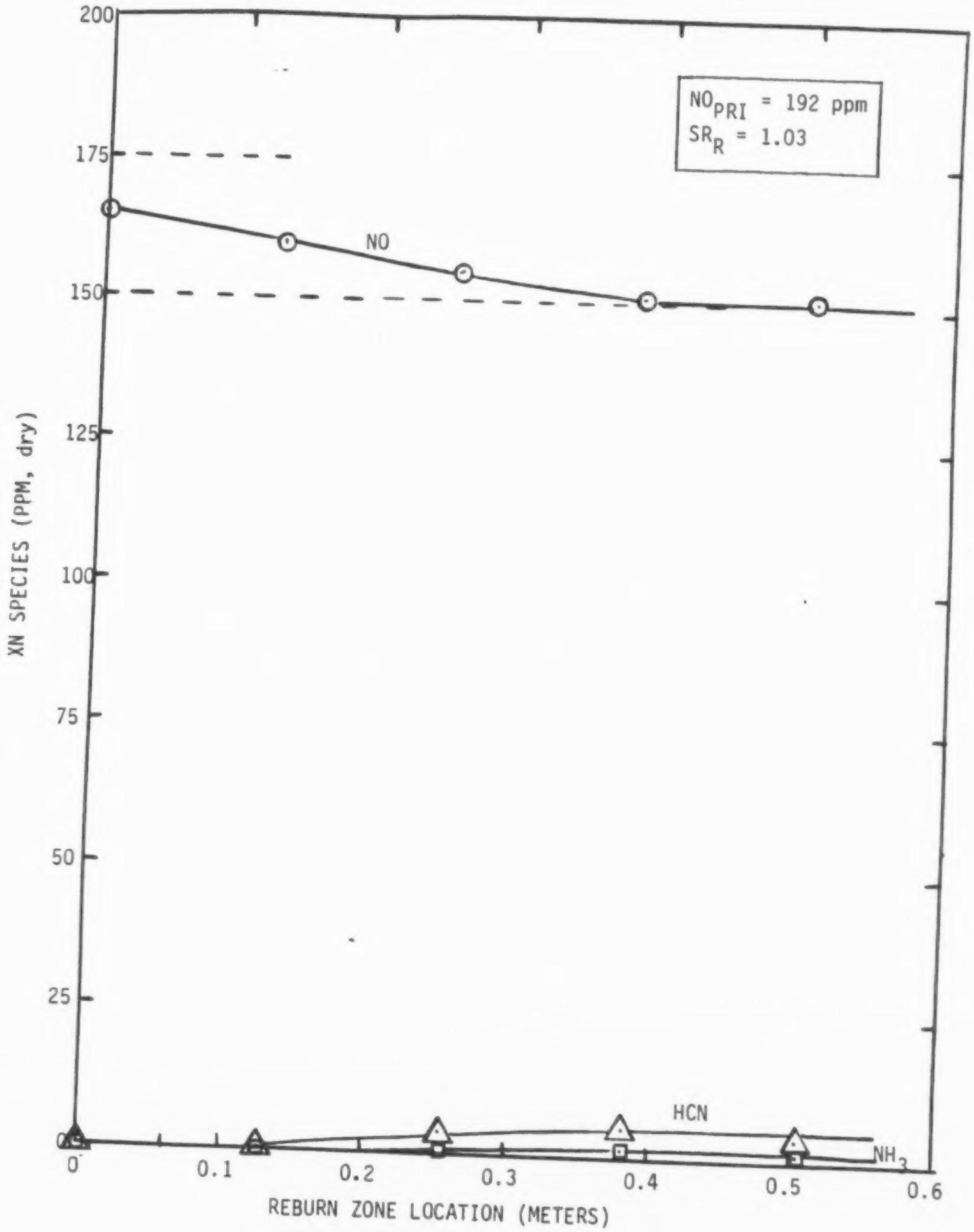

Figure 6-22: Reburn Zone Nitrogen Species Profiles for Distillate Fuel Oil Reburning, SR_R = 1.03

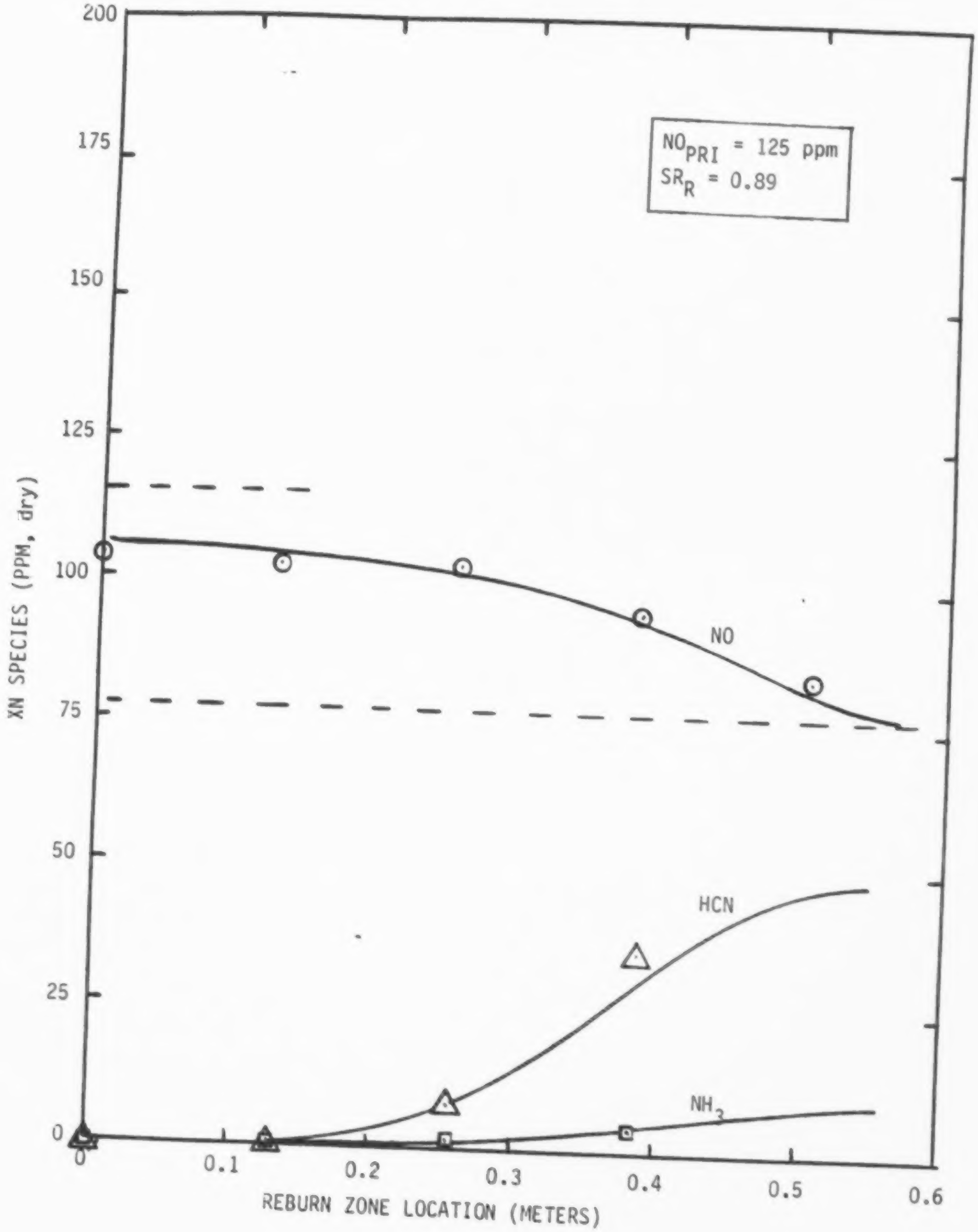

Figure 6-23: Reburn Zone Nitrogen Species Profiles for Distillate Fuel Oil Reburning, NO_{PRI} = 125 PPM

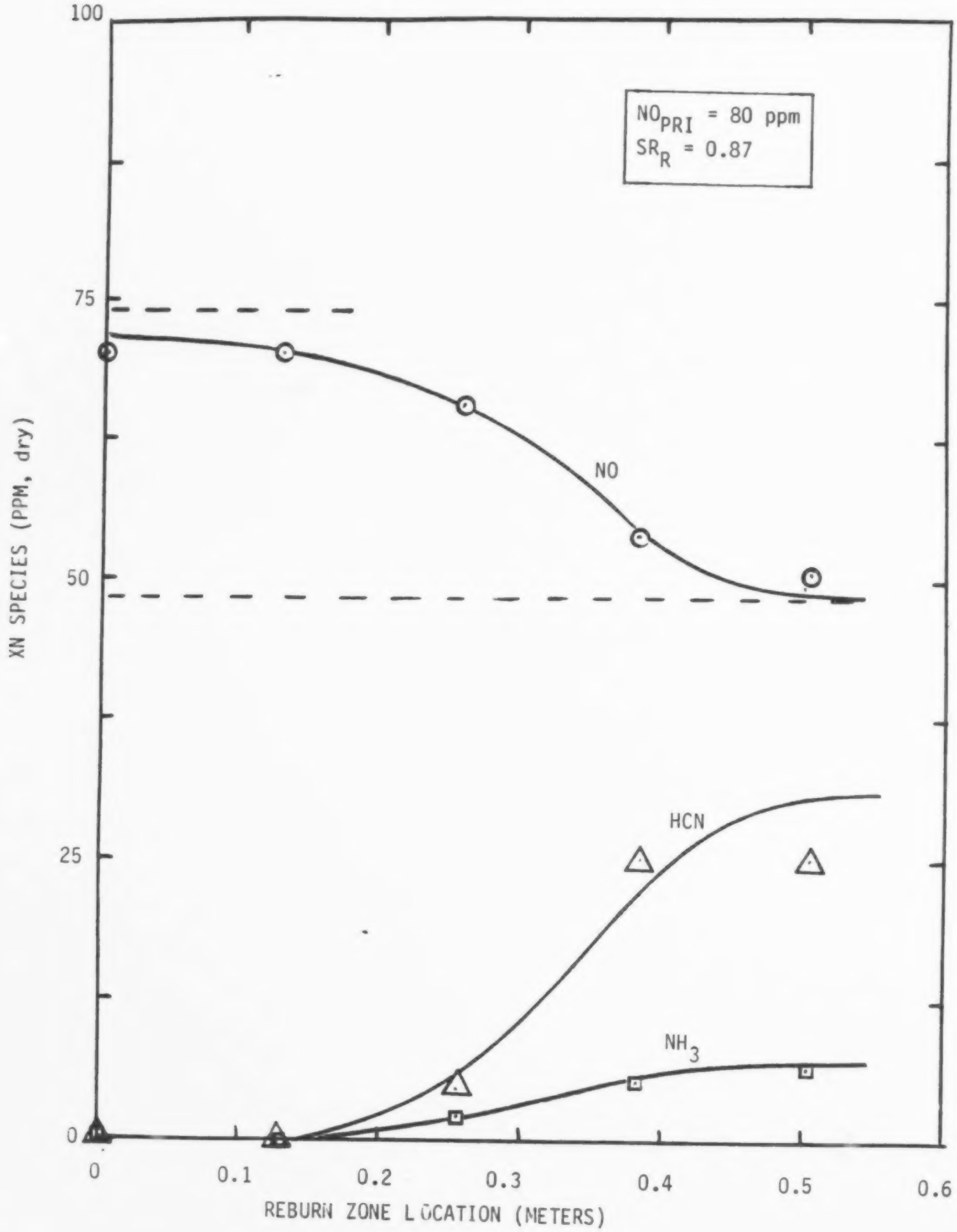

Figure 6-24: Reburn Zone Nitrogen Species Profiles for Distillate Fuel Oil Reburning, NO_{PRI} = 80 PPM

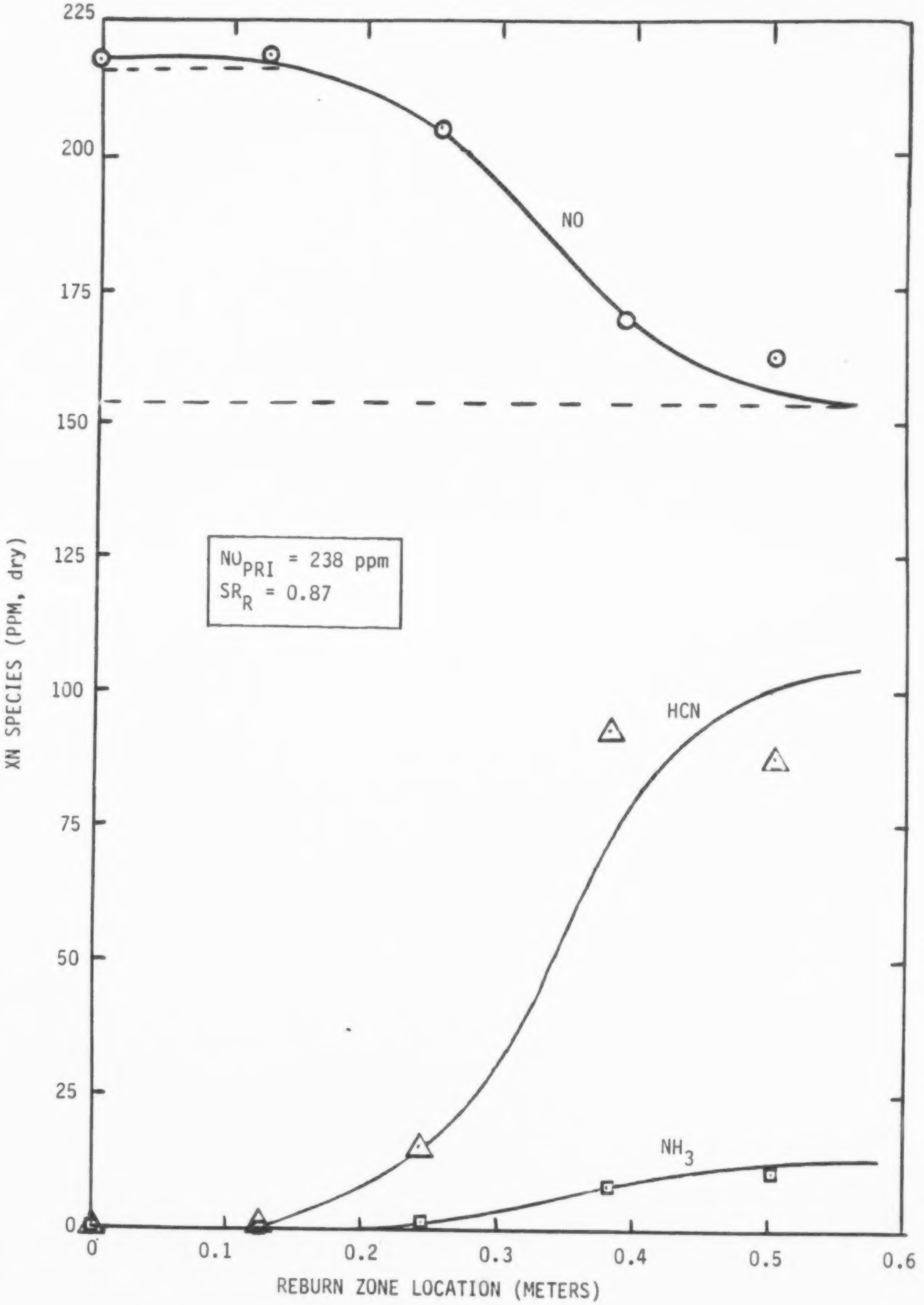

Figure 6-25: Reburn Zone Nitrogen Species Profiles for Heavy Fuel Oil Reburning, SR_R = 0.87

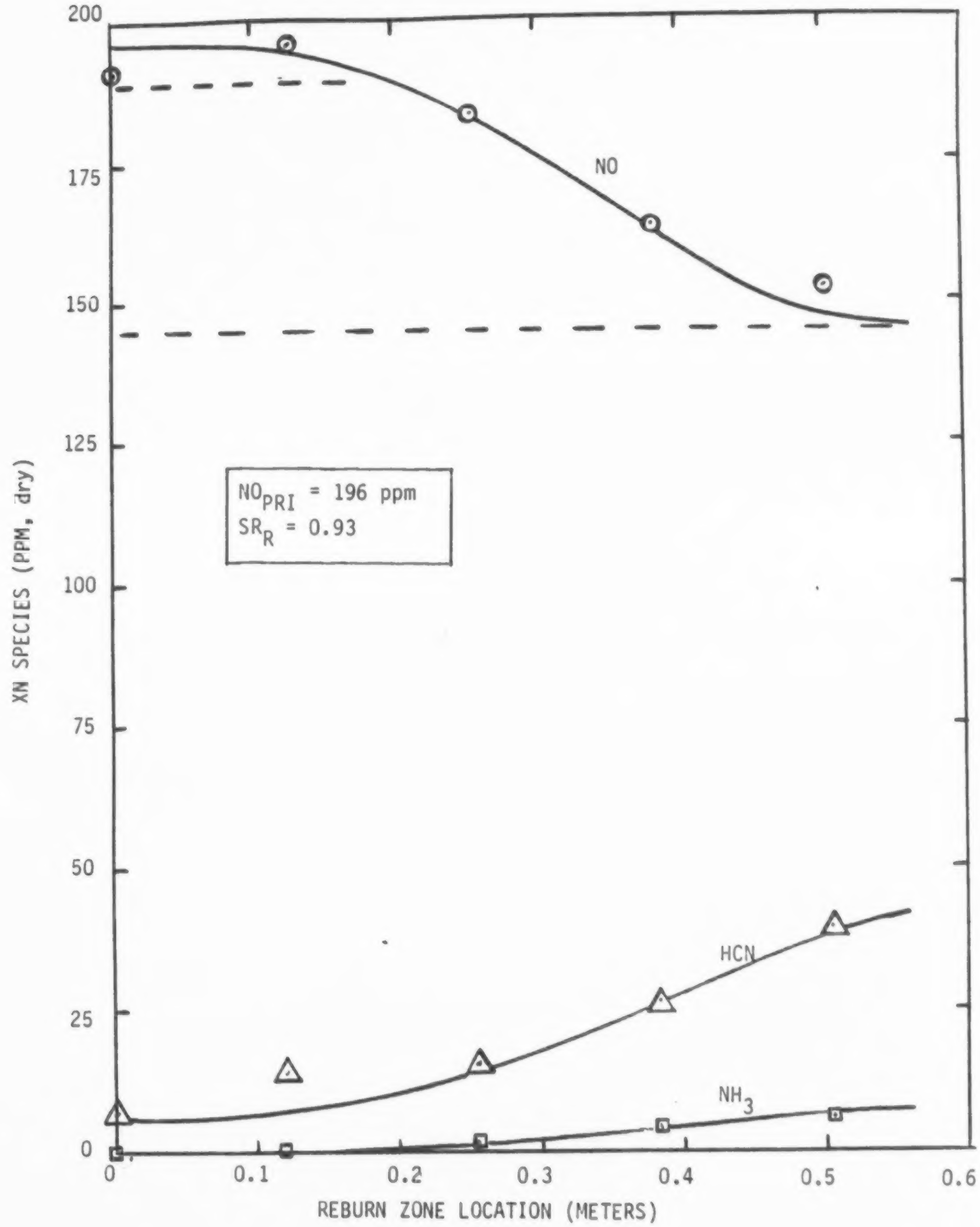

Figure 6-26: Reburn Zone Nitrogen Species Profiles for Heavy Fuel Oil Reburning, SR_R = 0.93

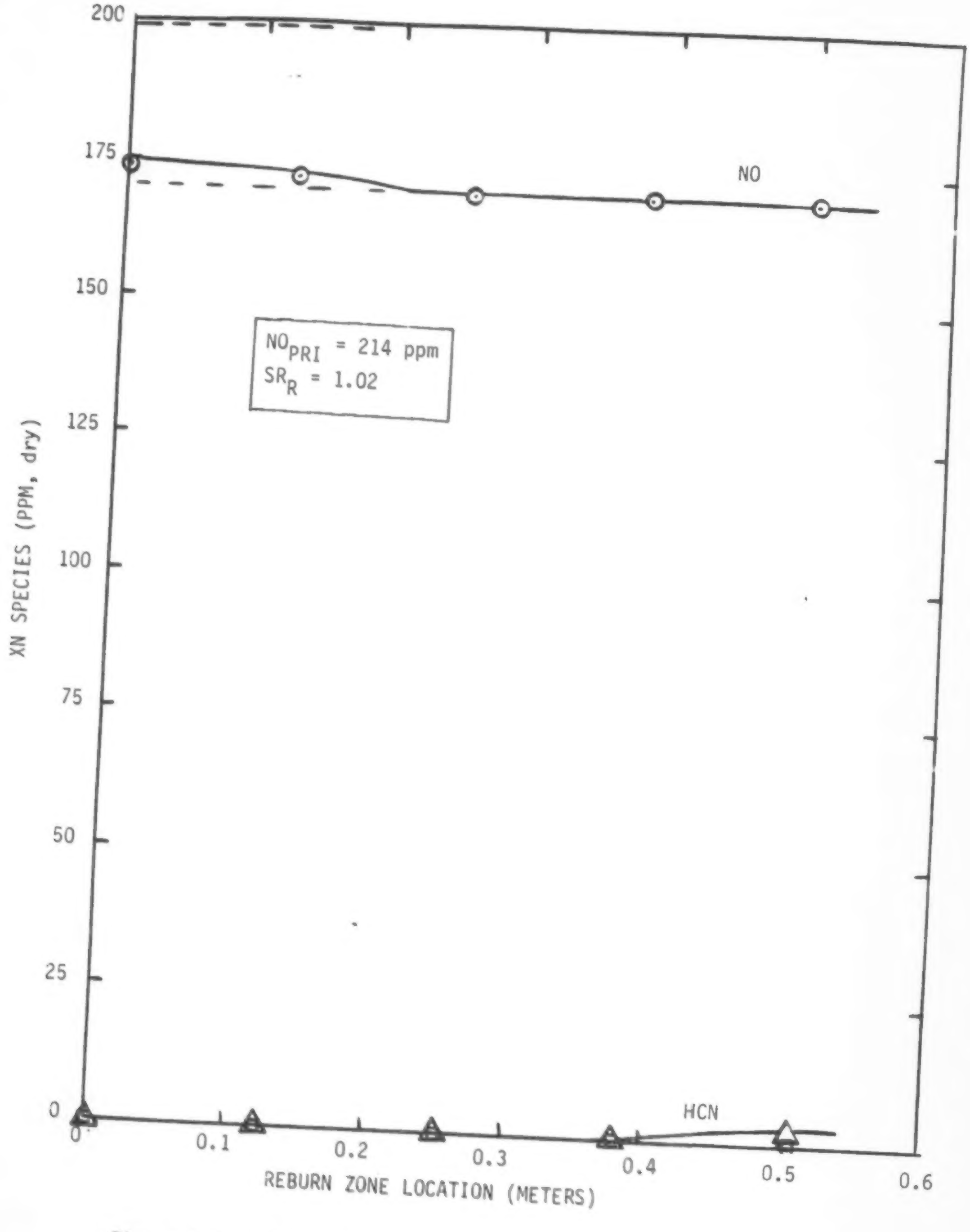

Figure 6-27: Reburn Zone Nitrogen Species Profiles for Heavy Fuel Oil Reburning, SR_R = 1.02

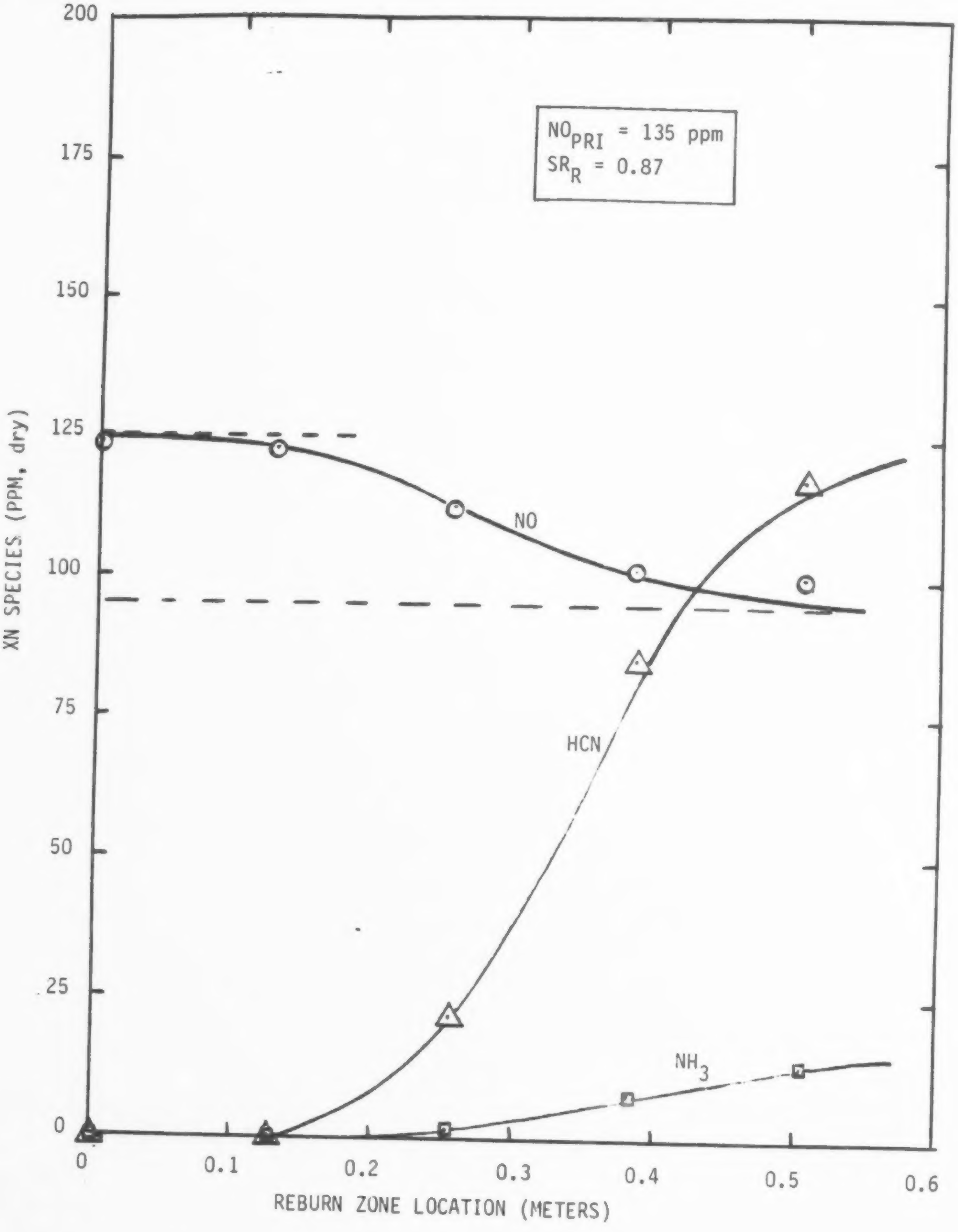

Figure 6-28: Reburn Zone Nitrogen Species Profiles for Heavy Fuel Oil Reburning, NO_{PRI} = 135 PPM

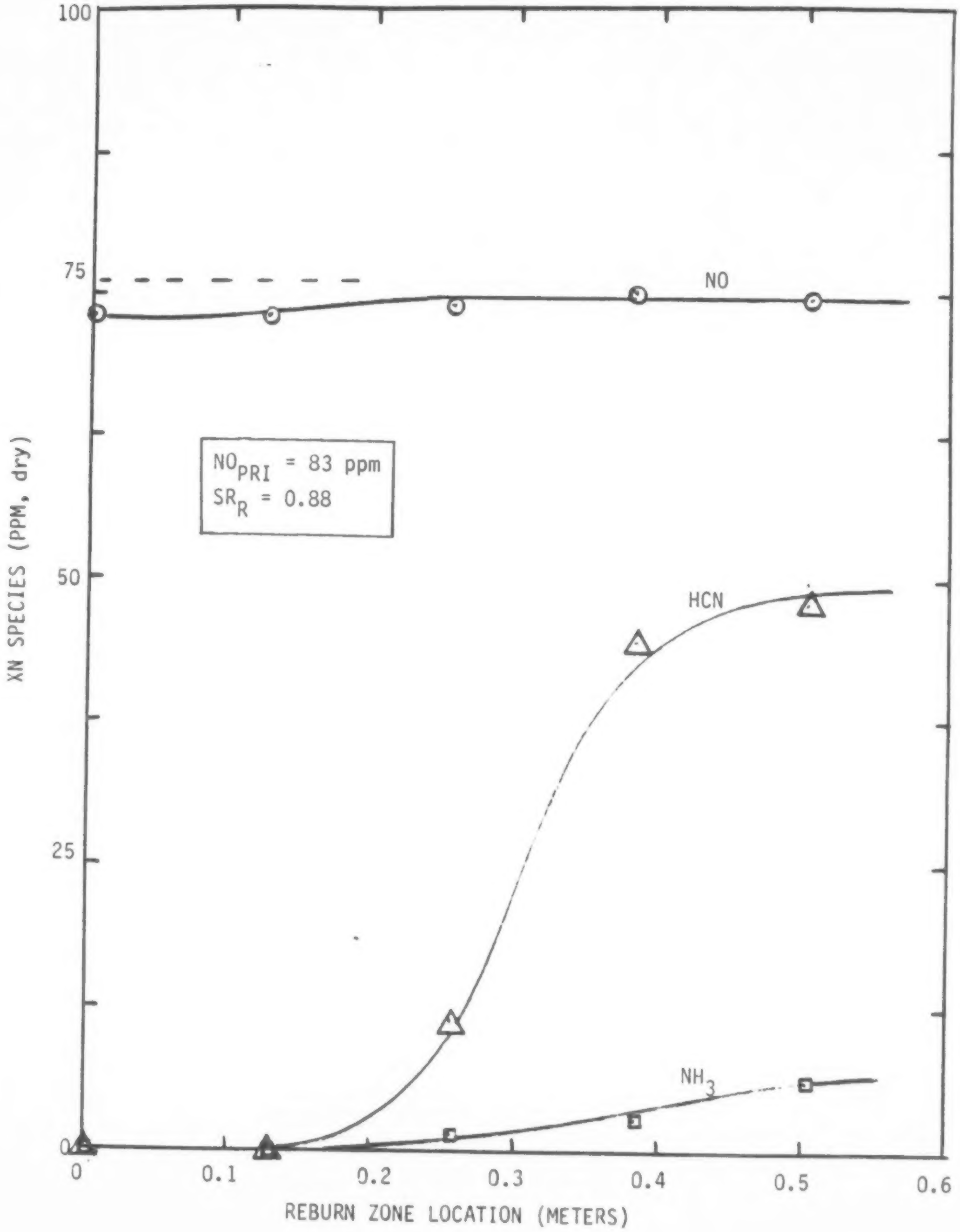

Figure 6-29: Reburn Zone Nitrogen Species Profiles for Heavy Fuel Oil Reburning, NO$_{PRI}$ = 83 PPM

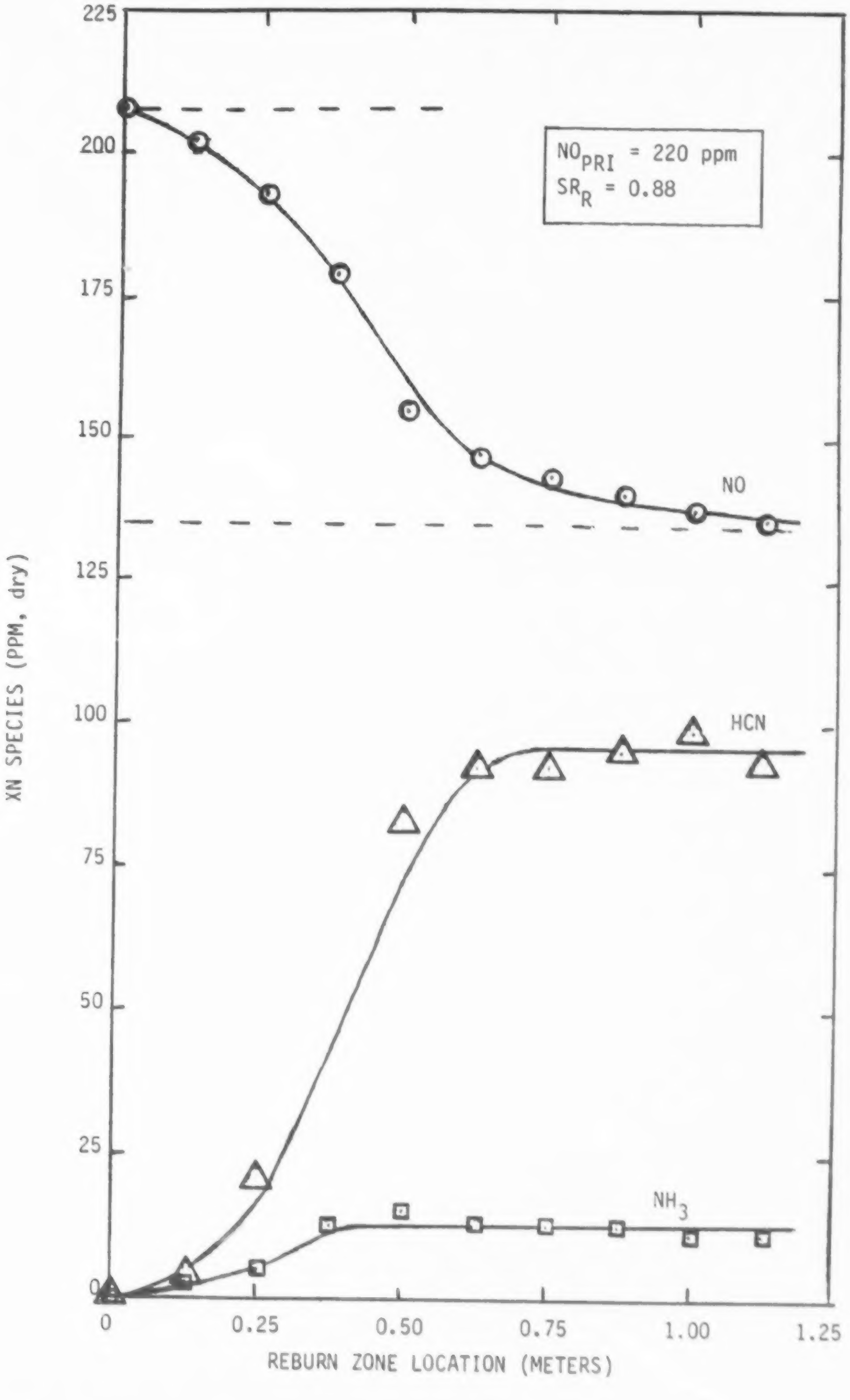

Figure 6-30: Reburn Zone Nitrogen Species Profiles for Heavy Fuel Oil Reburning, Long Reburn Zone Residence Time

TABLE 6-3. DETAILED TRIAL TEST MATRIX -- FUEL OIL REBURNING

Figure Number	NO_{PRI} (ppm, dry at 0% O_2)	SR_R	Secondary Fuel Oil	Reburn Zone Length (m)
6-20	200	0.89	Distillate	0.61
6-21	208	0.94		
6-22	192	1.03		
6-23	125	0.89		
6-24	80	0.87		
6-25	238	0.88	Heavy	0.61
6-26	196	0.93		
6-27	214	1.02		
6-28	135	0.87		
6-29	83	0.88		
6-30	220	0.88	Heavy	1.22

Similarly, ammonia-doped natural gas reburning and pyridine-doped distillate oil reburning exhibited this trend. Fuel nitrogen either inhibits the destruction of primary NO_x (by consuming CH radicals and forming HCN), or forms NO in the reburn zone, resulting in a net increase NO concentration in the reburn zone.

HCN collection efficiency for these fuel oil reburning tests is assumed to be approximately 70 percent, based on the tests described in Section 3.4. NH_3 collection efficiency is nearly 100 percent. Cyanide electrode interference of unburned oil in the in-flame sample solutions was circumvented by repeated filtering. The impact of this procedure on HCN collection efficiency was not determined. This method was followed for each sample analysis, regardless of the amount of unburned fuel in the samples. The HCN measurements provided repeatable trends of HCN concentration. The detailed measurement results (from fuel oil reburning tests) are consistent with natural gas reburning results in that:

1. HCN is the major intermediate fixed nitrogen species in the reburn zone.
2. In addition to being formed by NO destruction, HCN is formed by the destruction of N_2 in the reburn zone.
3. HCN decomposition rates in the reburn zone are slow, if the HCN decomposes at all.
4. NH_3 concentrations never exceed 25 ppm in the reburn zone.
5. HCN and NH_3 are fractionally converted to NO in the burnout zone; NO retention as NO in the burnout zone is nearly 100 percent.
6. Molecular nitrogen is formed in both the reburn zone and the burnout zone.

The chief difference between fuel oil and natural gas reburning is the NO_x destruction rate in the reburn zone. In Figure 6-31, detailed NO concentration data from five separate tests have been interpolated and plotted against reburn zone residence time for identical operating conditions. Five secondary fuel types are considered: natural gas, natural gas doped with 0.4 percent nitrogen in the form of ammonia, distillate fuel oil, distillate fuel oil doped with 0.5 percent nitrogen in the form of pyridine, and heavy fuel oil (containing 0.14 percent nitrogen). Three observations are made from this plot:

1. NO reaction times are 2 to 3 times longer for oil reburning than for gas reburning.
2. Fuel nitrogen reduces net NO destruction.
3. Nitrogen-free fuel oil reburning yields slightly less NO reductions than natural gas reburning.

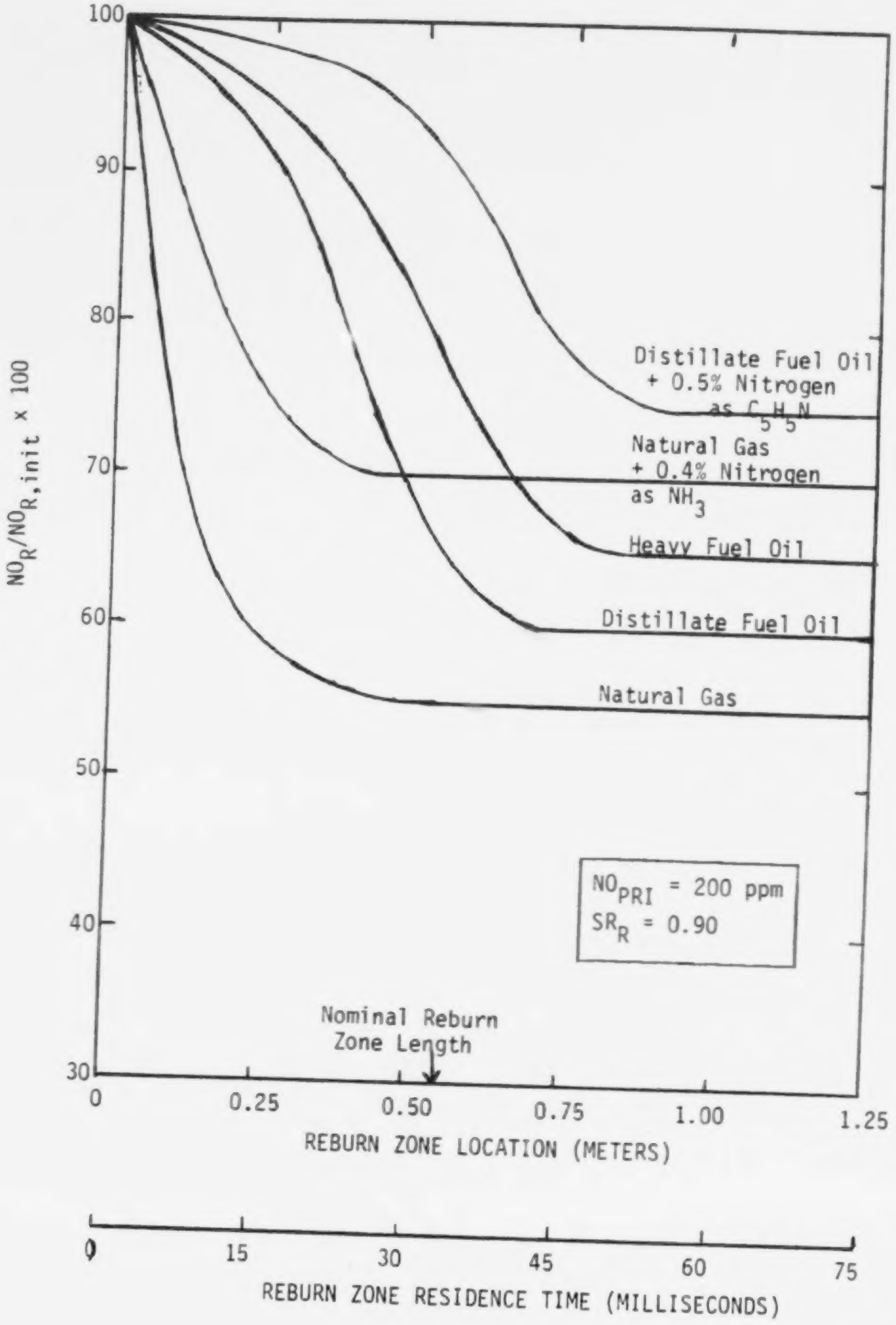

Figure 6-31: Comparison of Reburn Zone NO Profiles for Natural Gas and Fuel Oil Reburning

The first difference between natural gas and fuel oil reburning, that NO reaction times are 2 to 3 times longer for oil reburning than for gas reburning, is probably exagerated. The oil droplets were injected downstream into the combustion gas flow at velocities several times greater than the gas flow. The reburn zone residence time resolutions are based on the combustion gas velocity at the sample radius. Before the droplets have vaporized, they travel at speeds exceeding the gas flow; hence, the actual residence times of the droplets entering the reburn zone are less than those indicated in Figure 6-31. The natural gas jet velocity also exceeds the combustion gas velocity by as much as a factor of 10. However, those jets are oriented radially, perpendicular to the net combustion gas flow. In addition, the natural gas would be expected to mix more quickly with the combustion gases from the primary zone.

The second difference, that fuel nitrogen reduces net NO destruction, is due to the fact that the reburn zone net NO destruction consists of a combination of formation and destruction processes. Some of the secondary fuel nitrogen is oxidized in the reburn zone and results in increased NO concentrations.

The third difference that was observed is more surprising. Although the nitrogen-free distillate fuel oil reburning tests produced slightly greater overall NO reductions than did natural gas reburning tests, in the reburn zone NO reductions were less for distillate fuel oil reburning. Reasons for this are unclear, but the temperature at the burnout air injection location appears to be important. It has been observed that the lower the burnout zone temperature, the less the NO emission (see Section 5.4). This is the opposite temperature dependence that is observed in the reburn zone. Moreover, it has been observed that when the burnout air temperature decreases to the point of failure to burnout CO, NO emissions decrease at an accelerated rate. It was also observed for fuel oil reburning, conditions at which incomplete burnout of CO occurred were more frequent than for natural gas reburning. Therefore, it is postulated that the thermal environment that enhances NO reduction in the burnout zone leads to incomplete combustion of fuel species.

Further study is needed in the area of thermal quenching of the reburning flame. It has been observed that locally in the burnout air jet characterized by high O_2 levels, high CO and low NO concentrations (approaching equilibrium values) coexist (see Section 5.5). As the CO burns out in Zone 4, NO levels increase. This relationship is being studied in on-going experiments in the PBS.

SECTION 7

NORTH AMERICAN BOILER REBURNING APPLICATION TEST RESULTS

Tests performed on the pilot-scale package boiler simulator (PBS) equipped with a low-NO_x research burner have entailed extensive modification of boiler hardware and boiler operating conditions to provide fundamental insight into the chemistry and physics of natural gas and fuel oil reburning (Sections 4, 5 and 6). A series of experiments were performed on a commercial firetube package boiler to determine the representativeness of results obtained from the PBS tests, and to assess the practicality of an actual retrofit application. These tests are described here in three subsections: baseline tests, natural gas reburning tests, and fuel oil reburning tests.

7.1 Baseline Tests

A North American scotch-type package boiler, described in Section 2.3, was used for these reburning application tests. Both light (No. 2) and heavy (net No. 5) fuel oils were fired in the primary burner. Total boiler load was held constant during the reburning tests, requiring that, as secondary load increases, main burner load increases.

Baseline testing consisted of measuring the exhaust emissions, centerline temperature profile, and visible flame length as a function of main burner firing rate for both distillate and heavy fuel oils. Exhaust NO concentration, measured on a dry basis and corrected to zero percent O_2, is presented in Figure 7-1 as a function of the percent of full load. The full load NO emission level for the distillate oil (containing 0.01 percent nitrogen) is approximately 83 ppm; for the heavy fuel oil (containing 0.14 percent nitrogen), the full load emission is 200 ppm. From Figure 7-1 it is observed that exhaust NO emissions decrease between 5 and 15 percent as primary load is dropped. This is characteristic of most boilers where

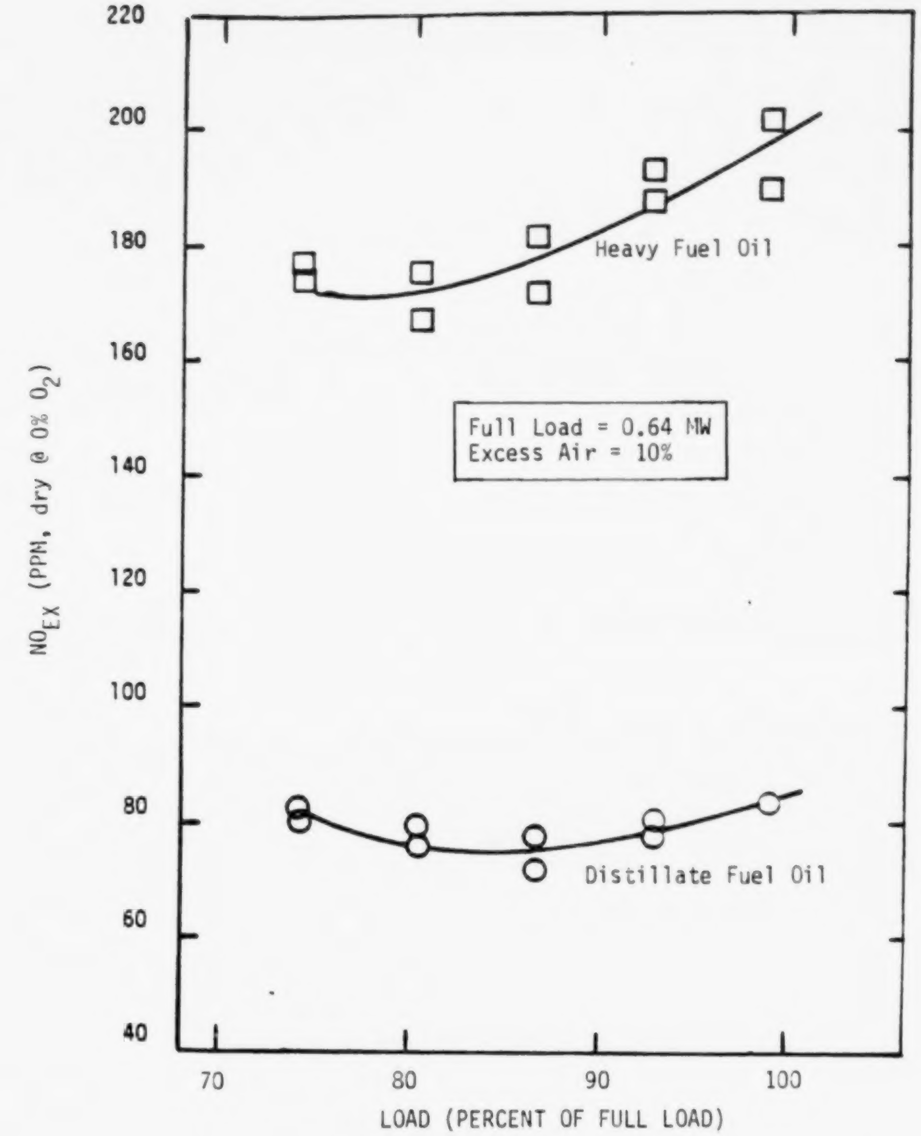

Figure 7-1: Effect of Load on Baseline NO_{EX}

burner derating results in reduced flame zone mixing intensities, and hence, reduced NO_x.

With a practical burner, there is no well-defined flame shape. Primary flame length fluctuations of up to 0.5 m (1.6 ft) were observed. The average flame length decreased noticeably with decrasing load, from about 2.5 m (8.2 ft) at full load to about 1.5 m (4.9 ft) at 75 percent of full load (see Figure 7-2). The reduced primary flame length allows for secondary fuel injection near the end of the visible flame with sufficient boiler length remaining for reburning. Figure 7-3 presents axial temperature profiles as measured on the boiler centerline for the heavy fuel oil. Temperatures were measured with a suction pyrometer at 25 cm (10 in.) intervals, with profiles recorded at five different firing rates. At the nominal secondary fuel injection point the centerline baseline temperature is about 1530 K (2300F). Tests on the research boiler simulator indicated that at this temperature, oil reburning leads to soot deposition on the water-cooled booms and on the boiler walls. Reburning in thermal environments less than 1600 K (2420°F) should be restricted to gaseous fuels.

Based on the baseline tests, nominal operating conditions were defined. The heavy fuel oil was chosen as the nominal primary fuel because it provided an initial NO_x level comparable to the nominal primary NO_x concentration used in PBS testing. A nominal secondary fuel injection location of 1.52 m (60 in.) was defined, based on flame length and temperature measurements. The final air injection location was selected to be 2.13 m (84 in.), providing a rich-zone bulk residence time of approximately 220 ms.

Reburning, as applied to the North American boiler, is shown schematically in Figure 7-4. A comparison of operating parameters for the North American boiler and the PBS is presented in Table 7-1.

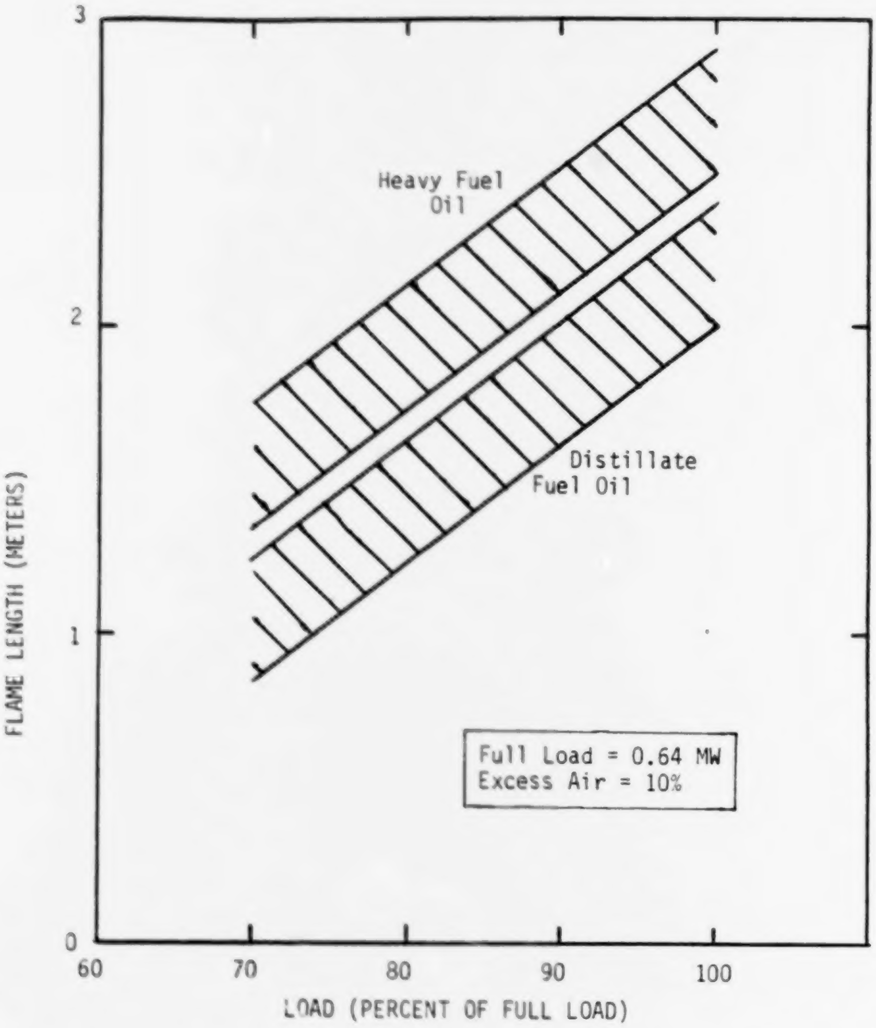

Figure 7-2: Effect of Load on Primary Flame Length

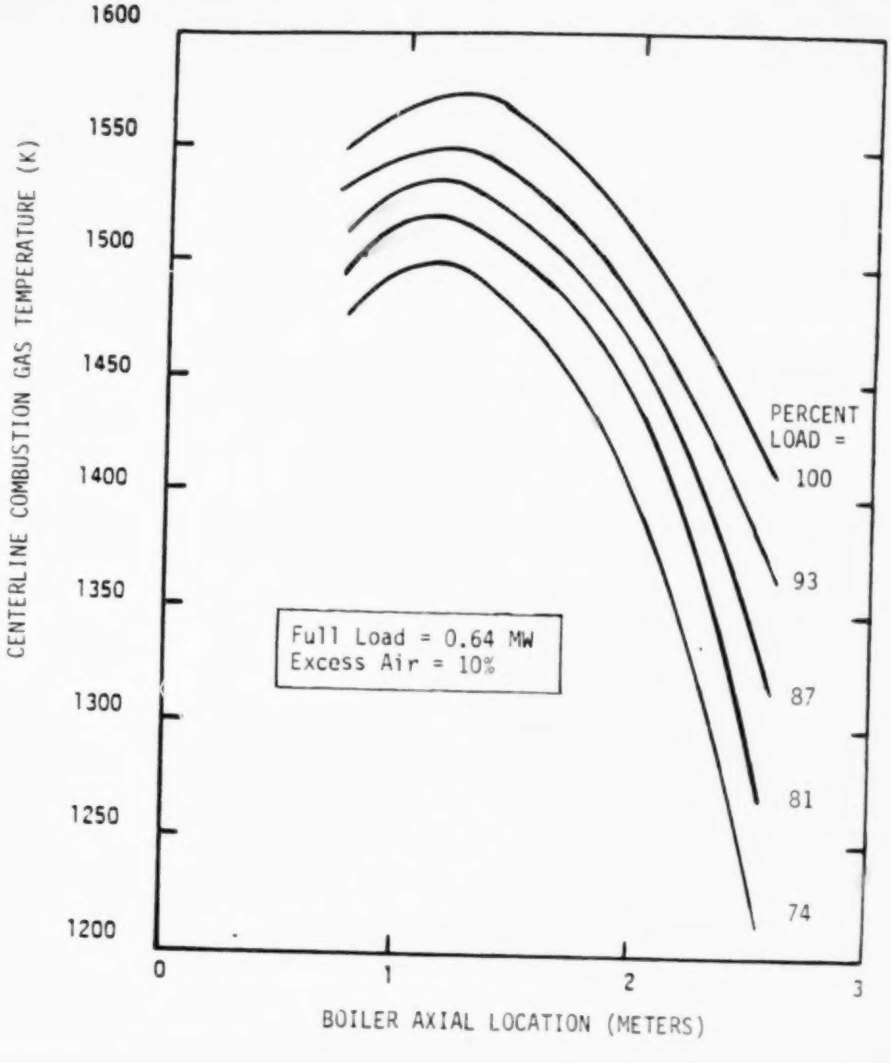

Figure 7-3: Baseline Axial Temperature Profiles

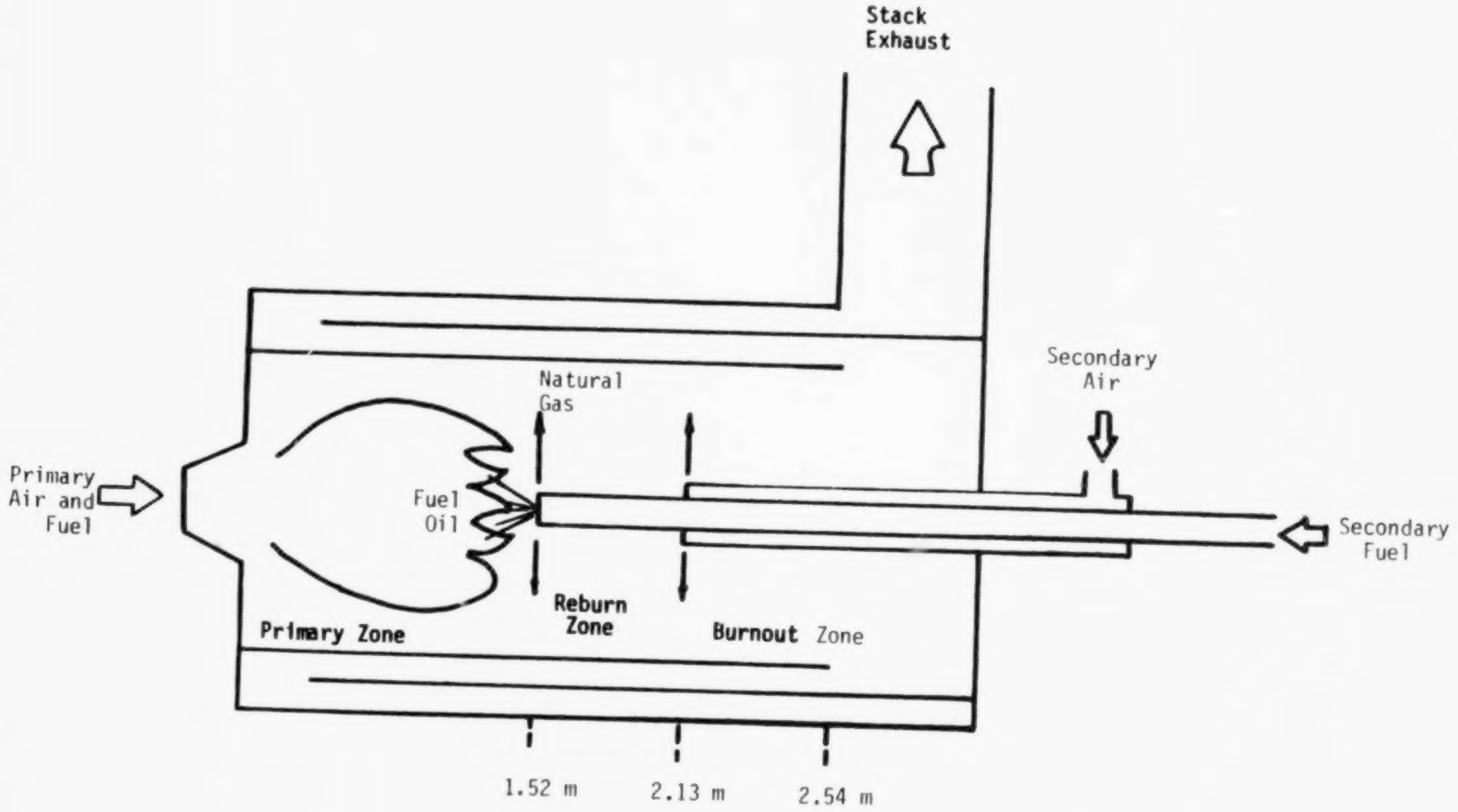
Stack
Exhaust
Secondary
Air
Natural
Gas
Primary
Air and
Fuel
Fuel
Oil
Secondary
Fuel
Reburn
Zone
Primary Zone
Burnout Zone
1.52 m
2.13 m
2.54 m

Figure 7-4: North American Boiler Reburning Application Schematic

TABLE 7-1. COMPARISON OF PBS AND NORTH AMERICAN BOILER OPERATING PARAMETERS

Research Facility (PBS) Fundamental Reburning Study	North American Boiler Reburning Application Study
o Constant primary load	o Constant total load
o Low NO_x prechamber burner	o Commercial swirl air burner
o Reburn zone temperature: 2000-2400°F	o Reburn zone temperature: 2300°F
o Reburn zone bulk residence time: 200 ms	o Reburn zone bulk residence time: 220 ms
o Input/output and detailed data	o Input/output data only

7.2 NATURAL GAS REBURNING TESTS

Single parameter variation tests were conducted on the major reburning process variables, including stoichiometry, initial NO_x, reburn fuel nitrogen, and residence time, using natural gas secondary fuel. Baseline tests (without reburning) were conducted prior to and at the conclusion of each test series to define primary zone effluent compositions. Results presented here have also been presented in ASME publication [24].

Initial NO and Rich-Zone Stoichiometry

Figure 7-5 presents plots of natural gas reburning NO_x reduction versus the fraction of total boiler load contributed by the secondary fuel. Reburn zone stoichiometry is shown as an alternate abscissa. Primary and burnout zone stoichiometries were held at 1.1.

As reburn load increases, several factors contribute to improved NO reduction. First, reduction in primary load results in a reduction in the primary NO_x due to reduced mixing intensities for derated primary burner operation. Second, the availability of more hydrocarbon radicals results in

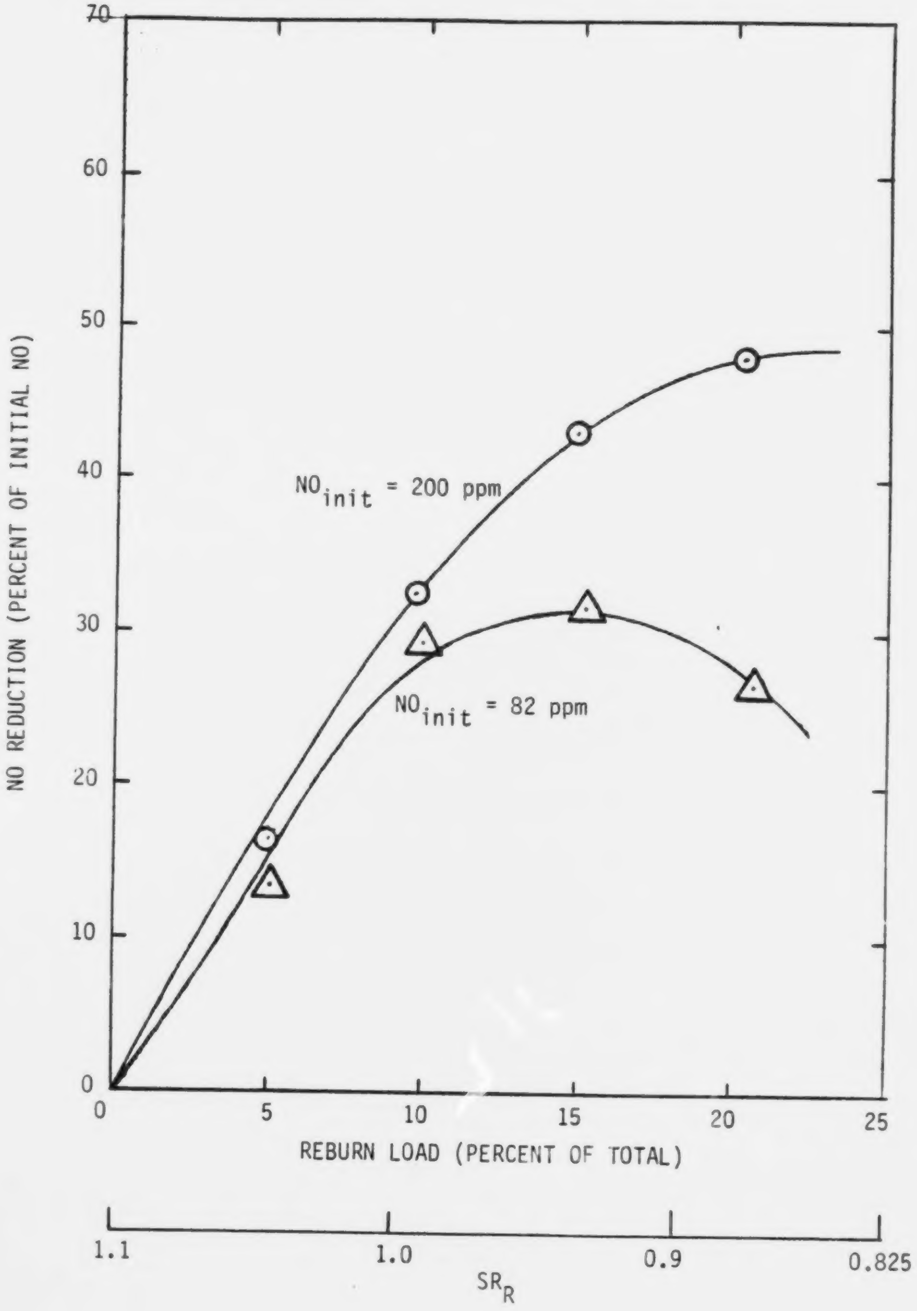

Figure 7-5: Natural Gas Reburning Effectiveness

increased destruction of primary NO_x. Third, an increasing portion of the total fuel is consumed in a low-temperature, fuel-rich environment, not conducive to NO_x formation. Thus, the low-NO_x secondary burner heat release "dilutes" the relatively high NO_x primary burner effluent. This dilution component is strongly coupled to the destruction component of NO_x reduction and cannot be straightforwardly isolated.

In Figure 7-6, data points are plotted in the same manner as PBS data plots. The solid lines on these plots represent PBS data. As is shown, agreement between the two facilities is well within the indicated data uncertainty bands. Figure 7-6 indicates that at least two of the results obtained in the PBS tests may be generalized to the firetube package boiler class. Clearly, primary NO_x concentration influences the degree of NO_x reduction under a given set of reburning conditions. North American boiler tests yielded significantly smaller reductions for the low primary NO_x condition than for the high initial NO_x condition. For the distillate primary fuel condition (primary NO_x of 75 ppm), with 20 percent of the total load used for reburning, primary NO_x is reduced by 28 percent; for the heavy fuel oil condition (primary NO_x of 180 ppm), a 38 percent reduction is realized under the same conditions. From results of PBS testing where primary NO_x concentrations were varied from 50 to 500 ppm, reaction orders with respect to NO_{PRI} between 1.5 and 1.6 were observed for rich-zone stoichiometries between 1.0 and 0.8.

The second PBS result confirmed is the lack of dependence on secondary fuel injection method. Reburning in the North American boiler utilized the second generation fuel boom. With this injector, secondary natural gas is injected radially from the boiler centerline. This boom made modification of the North American boiler much simpler than if the spoked injector had been used. With

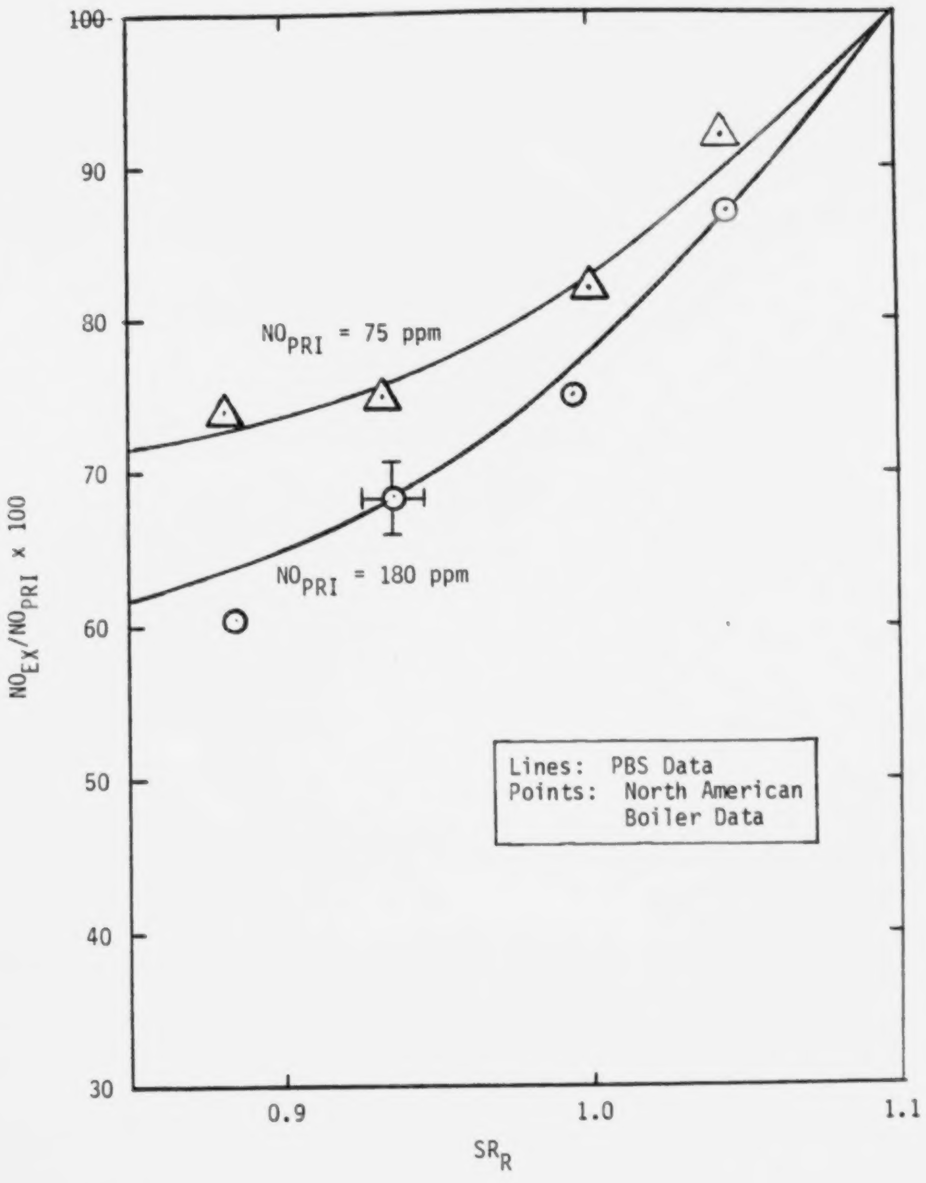

Figure 7-6: Comparison of PBS and North American Boiler Natural Gas Reburning Results

the simple radial injector design, NO_x reductions were achieved nearly identical to reductions achieved in the PBS using a wide range of secondary fuel injection techniques. Thus, large scale mixing processes in the firetube package boiler eliminate the need to inject secondary fuel uniformly, significantly simplifying the design of reburning retrofit hardware for the firetube package boiler class.

Reburn Fuel Nitrogen

When ammonia was doped into the secondary natural gas stream, NO_x reductions decreased. Figure 7-7 shows this data trend for ammonia dopoing of up to 1.5 percent. This trend is nearly identical to the PBS data trend. Though not directly comparable to fuels containing nitrogen (doping with a cyano compound like hydrogen cyanide would more closely model fuel-bound nitrogen evolution, but would also present increased safety hazards), these tests confirm that fuel nitrogen is an important factor in the reburning mechanism.

Reburn Zone Residence Time

Reburn zone length was varied from 30 to 160 cm (12 to 64 in.) by shifting the location of secondary fuel injection. Final air injection location was fixed at 2.13 m (84 in.). Injecting final air beyond 2.13 m resulted in burnout residence times too short to achieve sufficient fuel burnout prior to thermal quenching, causing high CO stack emissions. Figure 7-8 shows NO_x reduction as a function of secondary fuel injection location for natural gas reburning of 15 percent. As the secondary fuel boom was inserted farther into the boiler, increased quenching of the primary flame occurred, causing excessive sooting and high stack CO measurements. The data indicate that 95 percent of the maximum NO_x reduction for the North American boiler application is achieved within a reburn zone bulk residence time of approximately 200 ms. This result agrees with the results from the PBS tests,

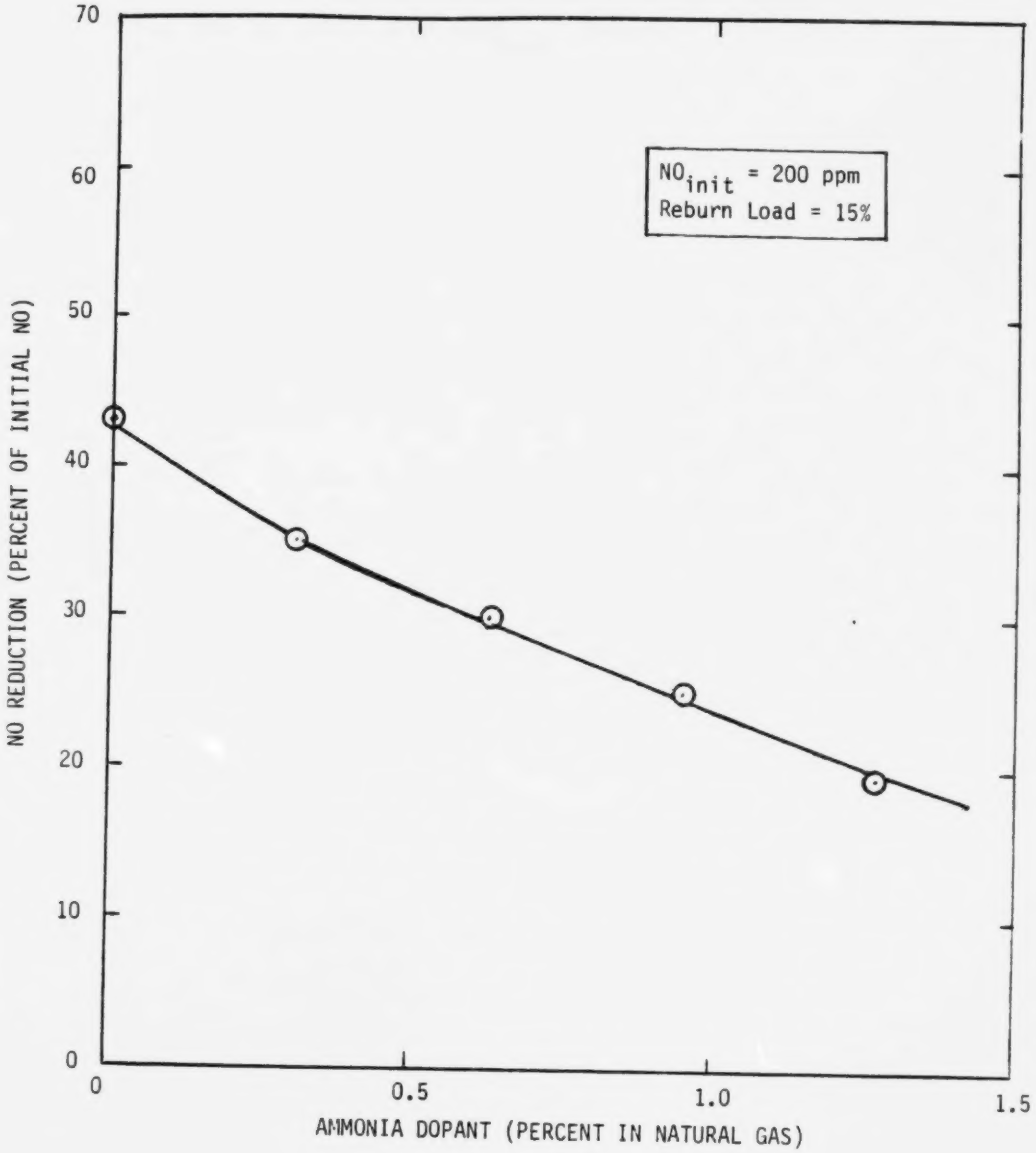

Figure 7-7: Effect of Ammonia-Doping of Secondary Natural Gas

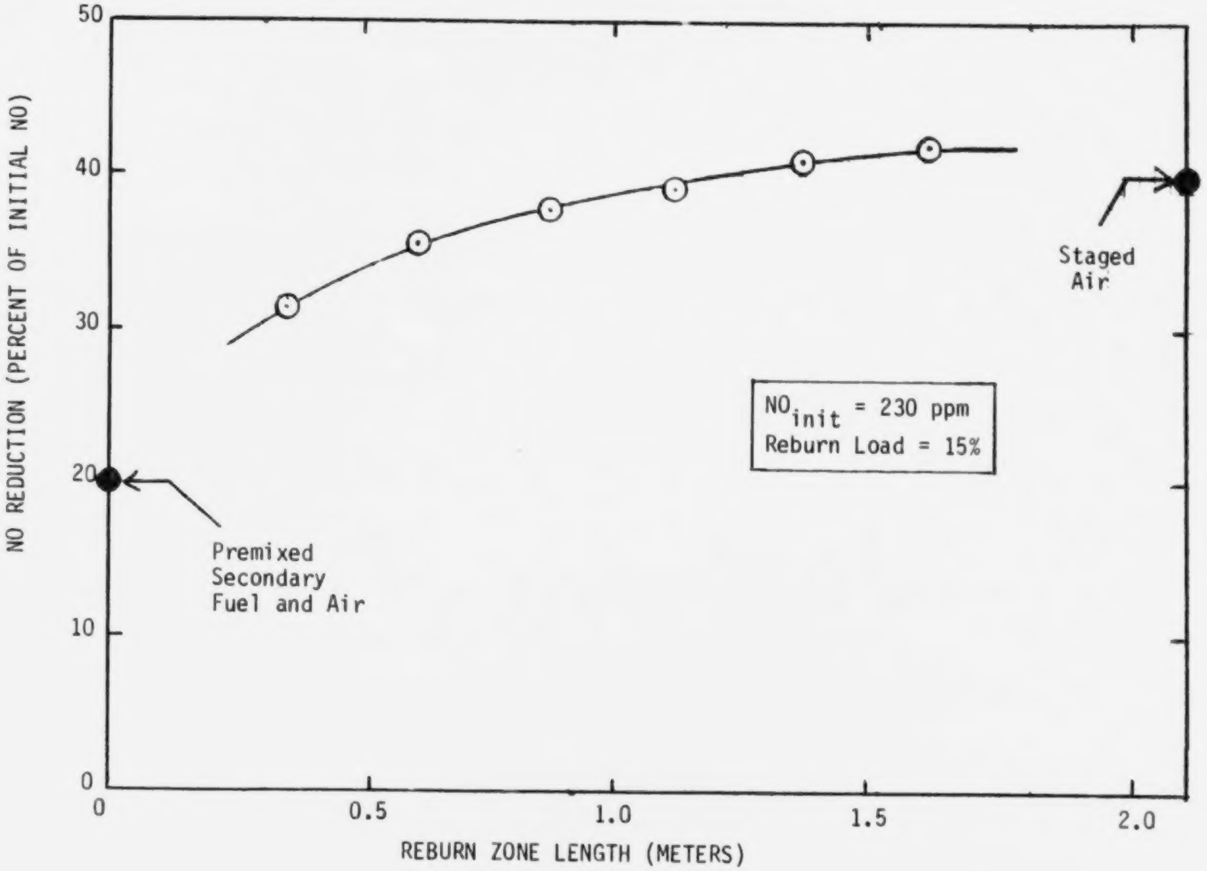

Figure 7-8: Effect of Secondary Natural Gas Injection Location

where detailed measurements indicated that a minimum local residence time of 50 ms (characteristic of the 200 ms bulk residence time condition) was necessary to complete nitrogen species reactions.

Optimization Example

To utilize the aforementioned results in a practical application, an example is presented in which realistic reburning operating conditions are applied to achieve an optimum reduction in NO_x. This example is broken into 4 steps, as shown in Figure 7-9. The initial condition selected is full-load operation firing heavy fuel oil at 15 percent excess air. The NO_{EX} emission level at that condition is 230 ppm. The first step is to reduce the primary flame excess air from 15 to 10 percent. This reduces the exhaust NO_x emission level to 198 ppm. Next, the boiler load is reduced by 20 percent, holding excess air constant at 10 percent. This reduces the NO_x emission level to 164 ppm. Third, secondary flow of natural gas and final air is initiated to return the boiler to full load with a stack excess air of 10 percent. Accomplishing the third step sets the fuel-rich zone stoichiometry at 0.88. This causes the exhaust NO_x emission level to drop to 99 ppm. To return the overall excess air to 15 percent, the final air flow rate is increased causing the exhaust NO_x emission level to increase to 101 ppm.

In this example, overall NO_x reduction via reburning is achieved by means of primary load reduction, primary excess air reduction, and the destruction and dilution effects of staged fuel combustion, as shown in Figure 7-10. The example illustrates a net 56 percent reduction in NO_x achievable by reburning; approximately the reduction claimed by Mitsubishi [10]. It is noted that the 56 percent NO_x reduction is achieved by diverting only 20 percent of the main burner load and that larger emission reductions are possible. Process

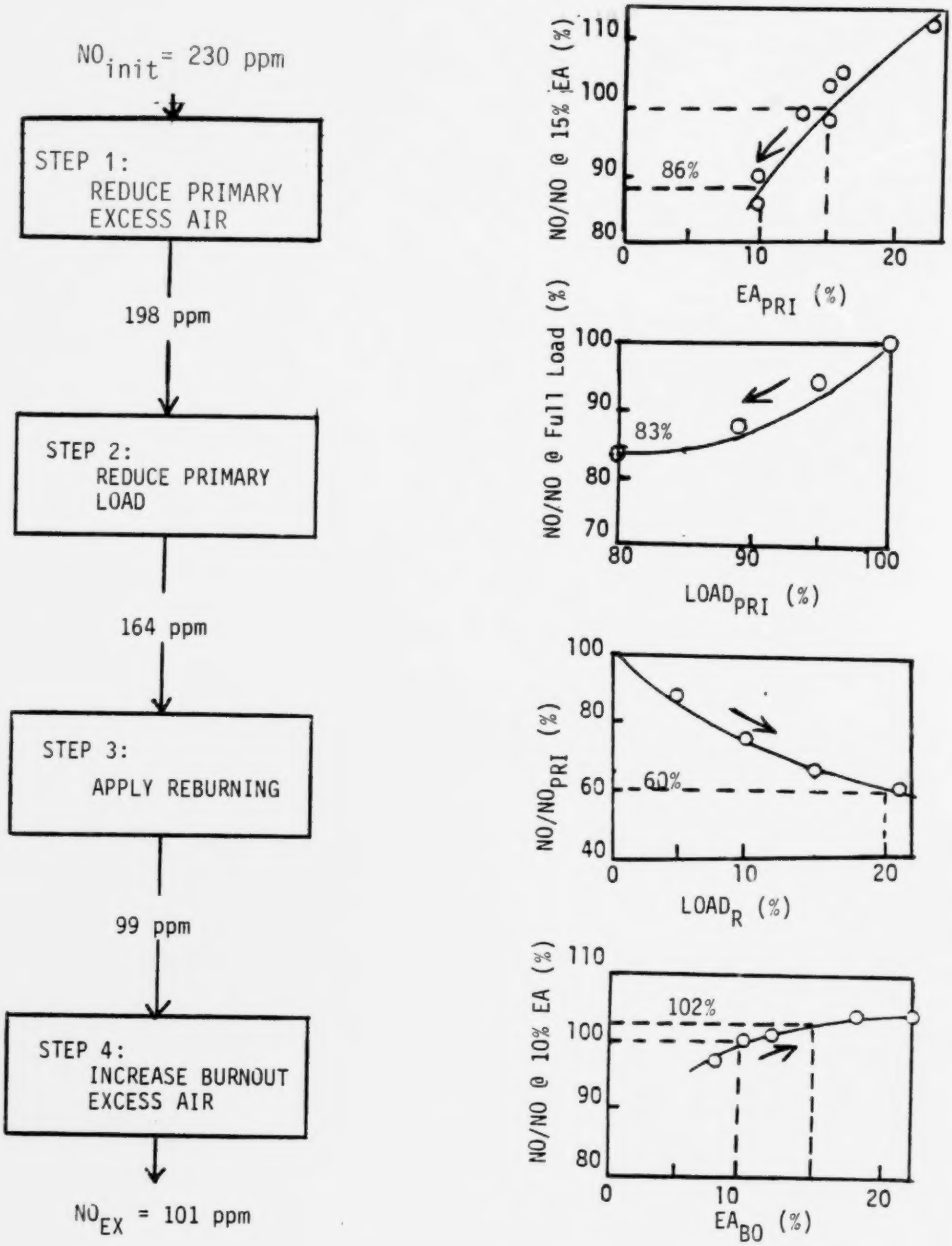

Figure 7-9: Natural Gas Reburning Application Example

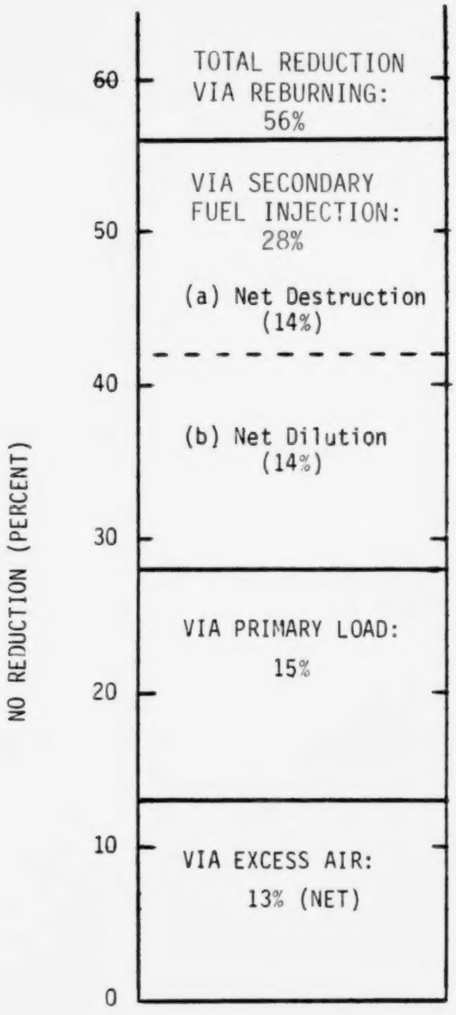

Figure 7-10: Natural Gas Reburning Application Example Results Summary

optimization, however, is best left to industries (such as the boiler manufacturers) who intend commercial application of this technology.

The results from the natural gas reburning application tests are summarized in the following two conclusions:

- NO_x reductions of 50% and greater are achievable with the application of reburning to firetube package boilers.
- Retrofit modifications for natural gas reburning require minimal cost and effort.

The input/output demonstration tests provide little insight into the chemistry and physics of reburning, but do verify results obtained from the fundamental PBS tests. Thus, hypotheses 9 and 10 are verified for natural gas reburning.

7.3 FUEL OIL REBURNING TESTS

Single parameter variation tests using light and heavy fuel oils as secondary fuels were conducted on the major reburning process variables. These tests were conducted in the same manner as the natural gas reburning tests, described in the previous section. As in the case of the natural gas reburning tests, these tests address hypotheses 9 and 10.

Nominal secondary fuel and air injection locations had to be changed from those for natural gas reburning due to high CO stack measurements. A longer burnout zone is required for fuel oil reburning than natural gas reburning. Final air was injected at 1.63 m (64 in.); secondary fuel at 1.02 m (40 in.).

Initial NO_x, Reburn Zone Stoichiometry, and Fuel Nitrogen

Figure 7-11 presents plots of fuel oil reburning NO_x reduction versus the fraction of total boiler load contributed by the secondary fuel. As was the case in the PBS tests, the data clearly show the strong dependence of NO_x reduction on primary NO_x, reburn zone stoichiometry, and fuel nitrogen.

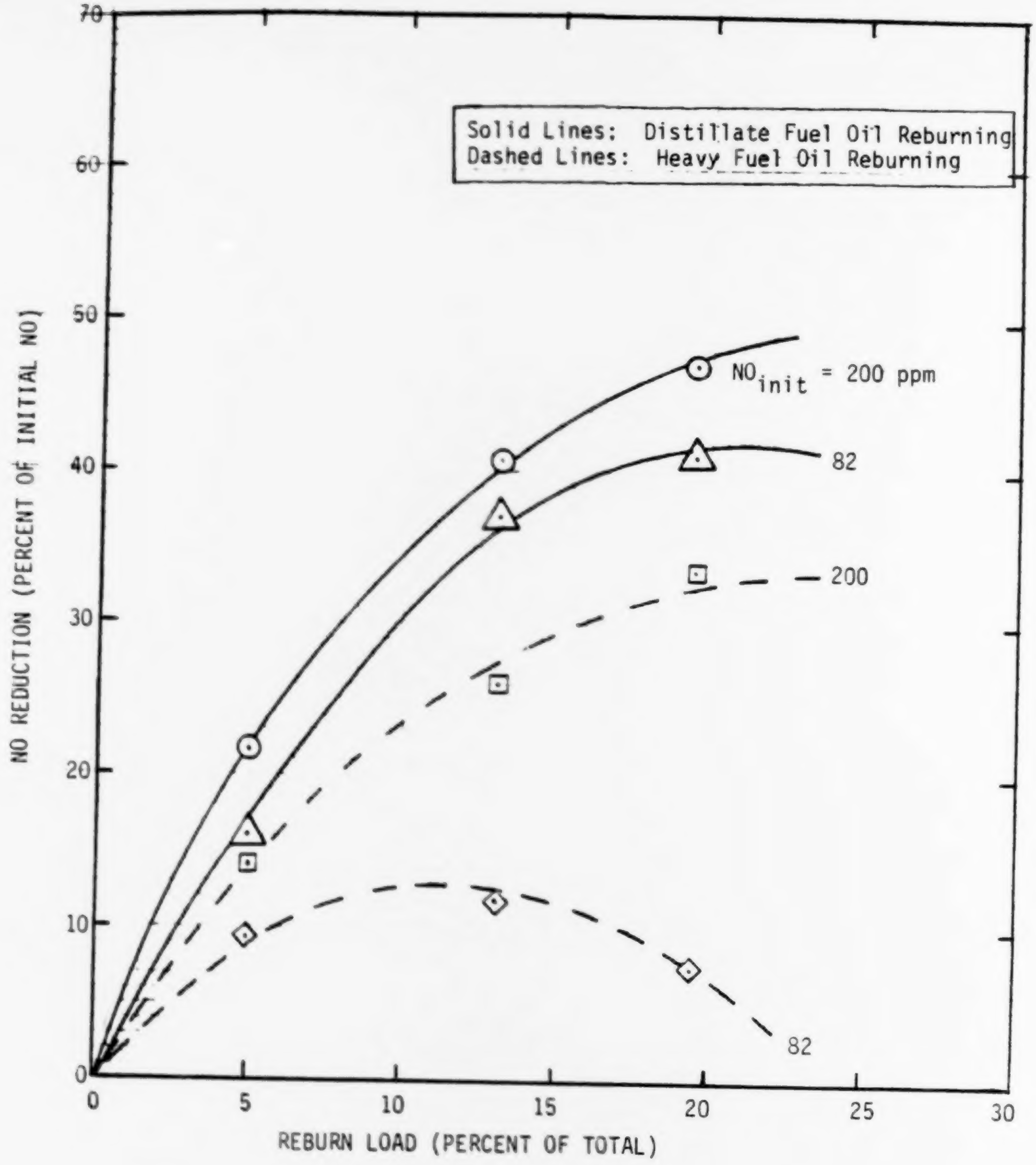

Figure 7-11: Fuel Oil Reburning Effectiveness

Compared directly to PBS data, as shown in Figure 7-12, the North American boiler data are in agreement to a remarkable degree. Agreement with PBS results for distillate and heavy fuel oil reburning tests at low primary NO_x conditions (75 ppm) was also excellent.

Reburn Zone Residence Time

Figure 7-13 shows the effect of varying the location of secondary fuel injection while leaving the final air injection location constant for distillate fuel oil reburning. In one limit, all of the fuel is injected with the final air at 2.13 m (84 in.), in the other limit, all of the fuel is injected in the primary burner, and only air is staged. It is interesting to note that the maximum NO_x reduction occurs for the staged air condition. Thus, the advantage of reburning over air staging in this application is not an enhanced NO_x reduction, but a shorter fuel-rich zone. At the low radiant zone temperatures characteristic of the firetube package boiler, considerable soot deposits formed in the fuel-rich region. Minimizing the fuel-rich zone length is desirable in most practical applications.

Optimization Examples

Reburning application examples for light and heavy fuel oil secondary fuels are presented to demonstrate optimum reduction of NO_x from an initial level of 230 ppm. Figures 7-14 and 7-15 outline the 4-step examples, as was shown in the natural gas reburning example (Figure 7-9).

The initial condition selected is full-load operation firing heavy fuel oil at 15 percent excess air. The NO_x emission level at that condition is 230 ppm. The first step is to reduce the primary flame excess air from 15 to 10 percent. This reduces the exhaust NO_x emission level to 198 ppm. Next, the boiler load is reduced by 20 percent, holding excess air constant at 10 percent. This reduces the NO_x emission level to 164 ppm. Third, secondary

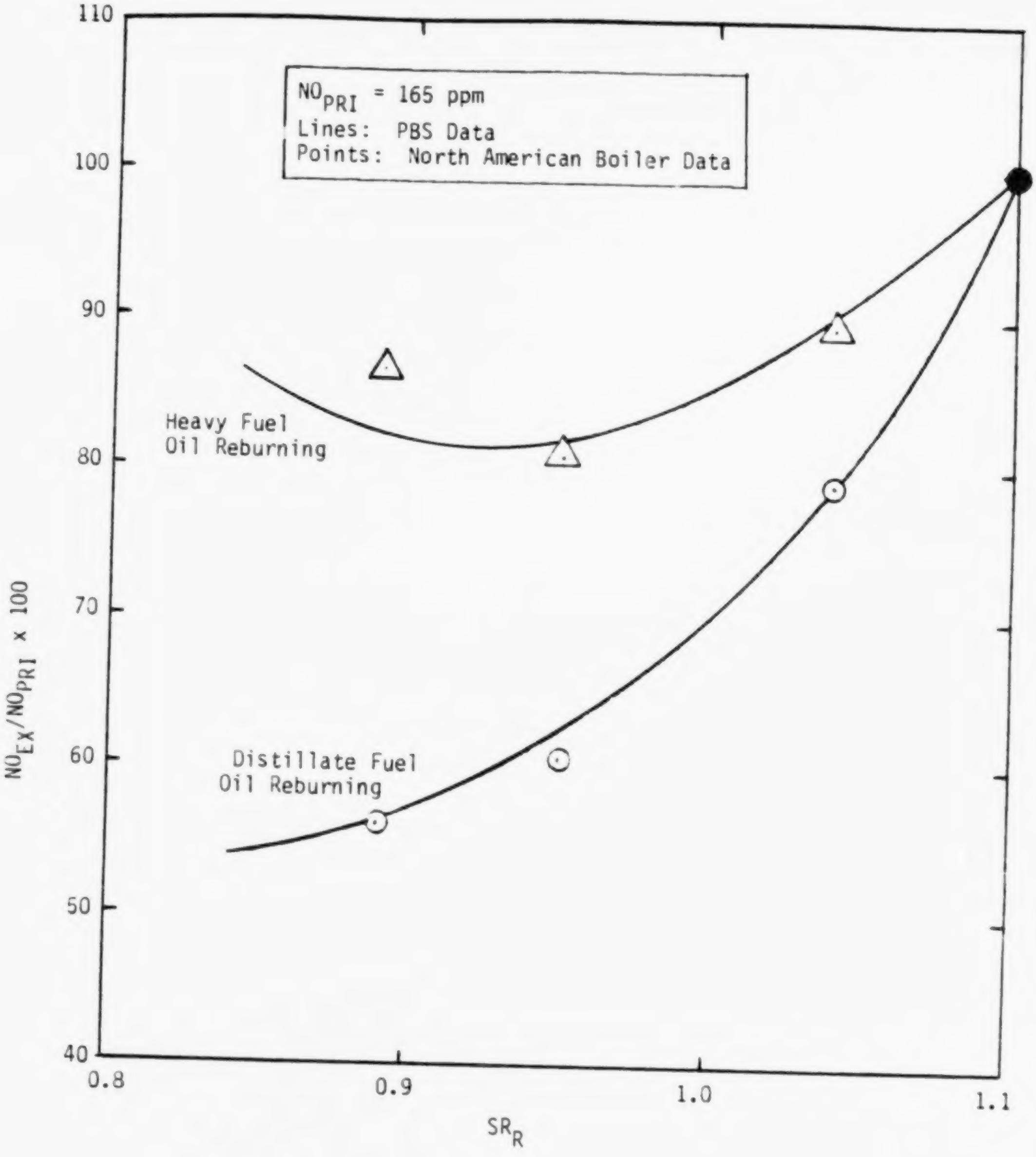

Figure 7-12: Comparison of PBS and North American Boiler Fuel Oil Reburning Results

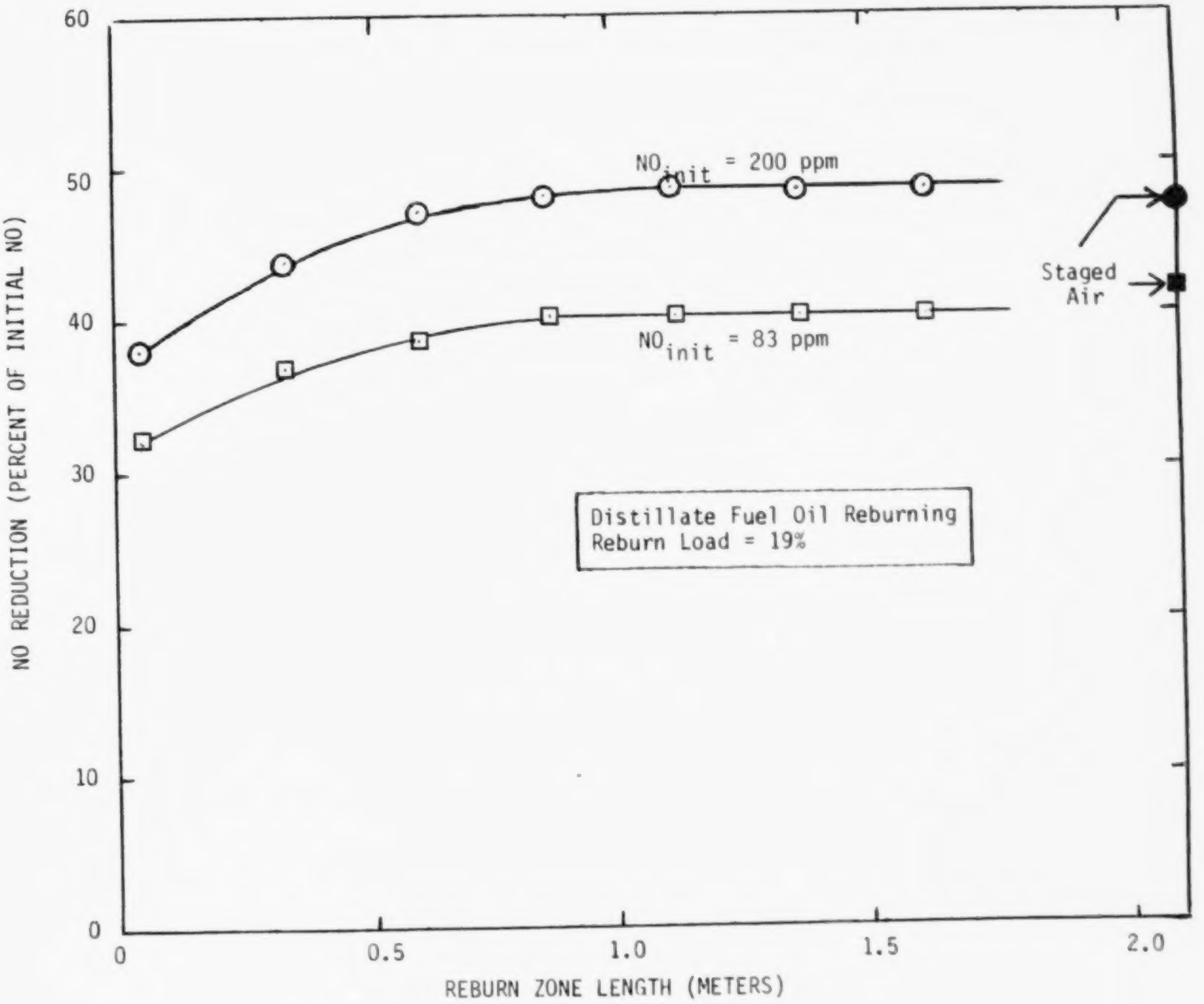

Figure 7-13: Effect of Secondary Fuel Oil Injection Location

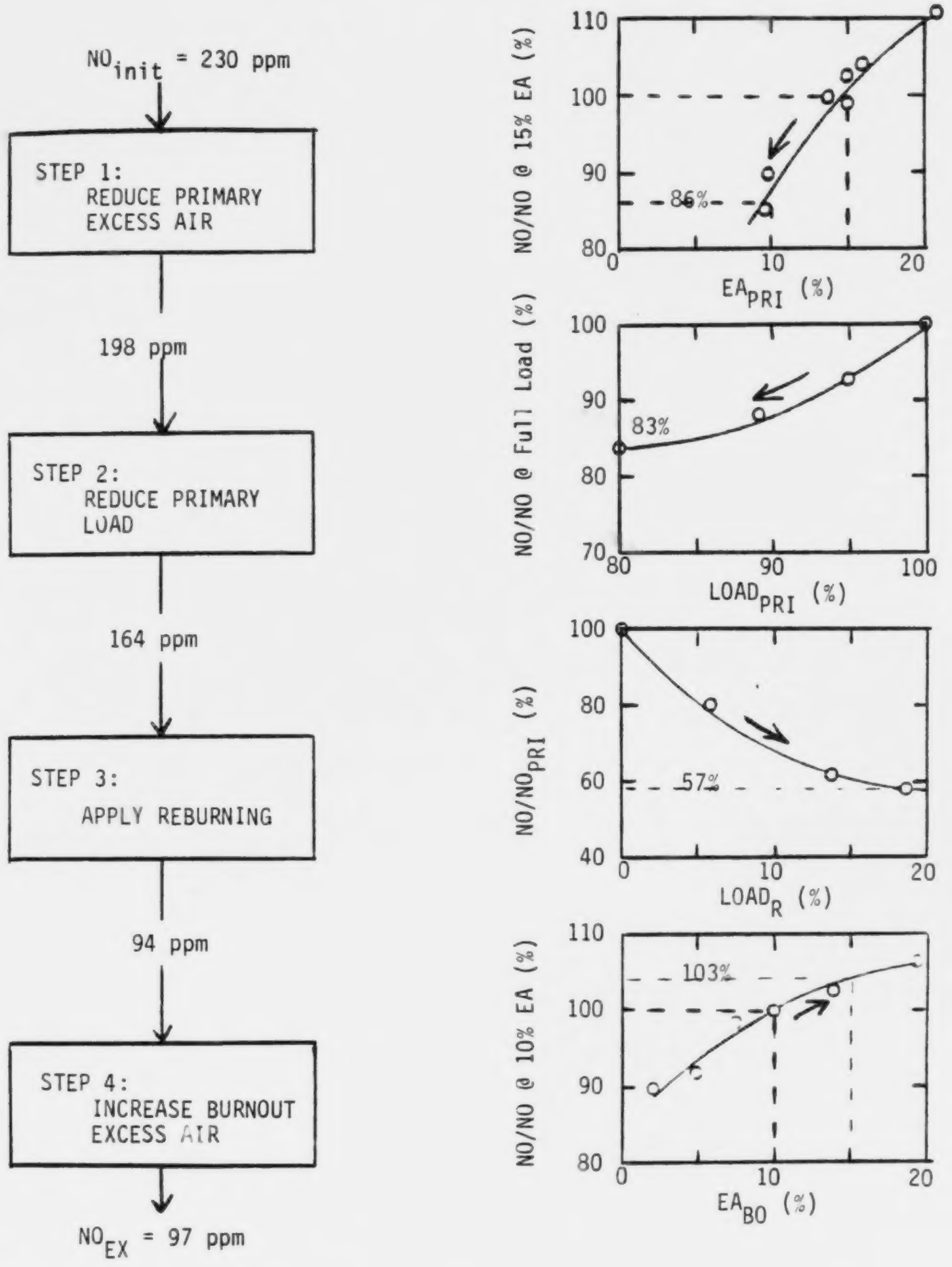

Figure 7-14: Distillate Fuel Oil Reburning Application Example

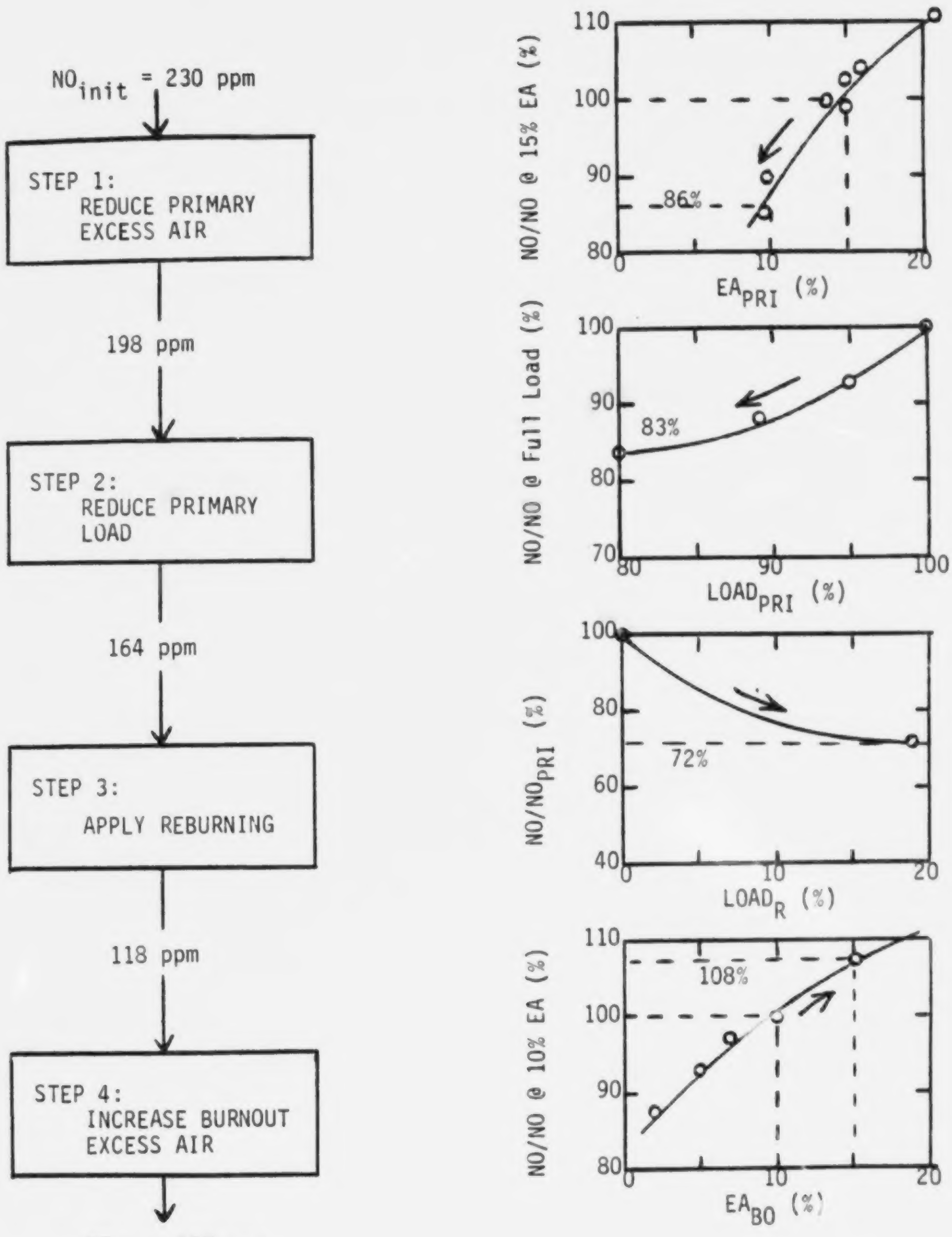
NO_init = 230 ppm
STEP 1: REDUCE PRIMARY EXCESS AIR
198 ppm
STEP 2: REDUCE PRIMARY LOAD
164 ppm
STEP 3: APPLY REBURNING
118 ppm
STEP 4: INCREASE BURNOUT EXCESS AIR
NO_EX = 127 ppm
NO/NO @ 15% EA (%)
110
100
90
80
86%
0
10
20
EA_PRI (%)
NO/NO @ Full Load (%)
100
90
80
70
83%
80
90
100
LOAD_PRI (%)
NO/NO_PRI (%)
100
80
60
40
72%
0
10
20
LOAD_R (%)
NO/NO @ 10% EA (%)
110
100
90
80
108%
0
10
20
EA_BO (%)

Figure 7-15: Heavy Fuel Oil Reburning Application Example

flows of fuel oil and final air are initiated to return the boiler to full load with a stack excess air of 10 percent. This results in a fuel-rich zone stoichiometry of 0.88. For distillate fuel oil reburning, with a 0.61 m (24 in.) reburn zone length, a 43 percent NO reduction is realized. For heavy fuel oil reburning, with a 0.92 m (36 in.) reburn zone length, a 28 percent NO reduction is obtained. Returning the overall excess air to 15 percent causes the exhaust NO_x emission to increase, by 3 percent in the case of distillate fuel oil reburning, and by 8 percent in the case of heavy fuel oil reburning.

In these examples, overall NO_x reductions of 58 and 45 percent via distillate and heavy fuel oil reburning, respectively, are achieved by means of primary load reduction, primary excess air reduction, and the destruction and dilution effects of staged fuel combustion. These examples illustrate that net 50 percent reductions in NO_x (and greater) are achievable by reburning with light or heavy fuel oils.

It is significant that the distillate fuel oil, containing almost no nitrogen, requires approximately only 200 ms (or 2 ft) of reburn zone to achieve a net 50 percent NO_x reduction; this is about the same reburn zone length required to achieve a 50 percent NO_x reduction by natural gas reburning. However, for the less volatile heavy fuel oil, containing 0.14 percent nitrogen, longer reburn zone residence times (and/or higher reburn loads) are needed to achieve similar reductions. For residual fuel oils with high nitrogen contents, 50 percent NO_x reductions via reburning may not be possible without modifying the boiler (e.g., making the boiler longer to allow for increased reburn zone residence times necessary to reduce fuel-bound nitrogen NO formation).

SECTION 8

CONCLUSIONS

This study of the application of reburning to firetube package boilers has demonstrated reburning to be an effective NO_x control technology, and has provided a better understanding of the physical and chemical processes associated with gaseous and liquid fuel reburning. Tables 8-1 and 8-2 contain test results from the package boiler simulator and the North American boiler, respectively. The ten hypotheses listed in Section 1-4 have been addressed. Each is discussed here.

The first hypothesis stated that overall NO_x destruction chemistry should be second order with respect to the level of NO_x produced in the primary flame. This hypothesis was based on the simple notion that 2 NO molecules would be required to form N_2. Experimental results from natural gas reburning tests (described in Section 5) indicate that the overall reaction order with respect to NO_{PRI} is approximately 1.5. That is,

$$\frac{d[NO_x]}{dt} = -k\,[NO_x]^{1.5} \qquad (8\text{-}1)$$

Though the pilot-scale test boiler is too large to obtain fundamental chemistry data, the boiler volume was sufficiently characterized (by axial and radial temperature, velocity, and species concentration profiles) to determine gross chemical properties, such as the overall NO_x destruction rate order. The finding that the rate dependence is greater than first order with NO_{PRI}, which implies that the NO_x reduction benefit of reburning diminishes as primary NO_x concentration is reduced, is true of both the gaseous and liquid fuels.

In Section 1.4 it was hypothesized that fuel-bound nitrogen would decrease NO_x reduction by reburning with ammonia-doped natural gas (hypothesis

TABLE 8-1. SUMMARY OF PBS TEST RESULTS AT NOMINAL OPERATING CONDITIONS*

Secondary Fuel	Percent NO_x Reduction: $(1 - NO_{EX}/NO_{PRI}) \times 100\%$	
	b,R = 200 ms	b,R = 400 ms
Natural gas	35	40
Natural gas + 0.4% nitrogen as NH_3	12	20
Distillate oil	30	44
Distillate oil + 0.5% nitrogen as C_5H_5N	-8	20
Heavy oil	15	40

*Nominal Operating Conditions: NO_{PRI} = 200 ppm, dry at 0% O_2
$SR_{PRI} = 1.1$
$SR_R = 0.9$
$SR_{EX} = 1.1$
$T_{init,R}$ = 1590K (2400°F)

TABLE 8-2. SUMMARY OF NORTH AMERICAN BOILER TEST RESULTS AT NOMINAL OPERATING CONDITIONS*

Secondary Fuel	Percent NO_x Reduction: $(1 - NO_{EX}/NO_{init}) \times 100\%$
Natural gas	56 (a)
Distillate oil	58 (a)
Heavy oil	45 (b)

(a) b,R = 220 ms
(b) b,R = 310 ms

*Nominal Operating Conditions: NO_{init} = 230 ppm, dry at 0% O_2
FR_R/FR_{TOT} = 20%
EA = 15%
$T_{init,R}$ = 1530K (2300°F)

2) and fuel oil (hypothesis 7). This was found to be true, as significant increases in NO_x emissions were observed when reburning with nitrogen-containing fuels. Ammonia-doped natural gas, pyridine-doped distillate fuel oil, and heavy fuel oil (containing 0.14 percent nitrogen by weight) were tested extensively. The detrimental effect of fuel-bound nitrogen on NO_x emissions can be minimized by maximizing the residence time of the fuel-rich reburning zone, allowing more of the secondary fuel nitrogen to go to molecular nitrogen before oxidation in the burnout zone. Further, NO_x formation from secondary fuel nitrogen appears to be independent of primary NO_x; thus, at high primary NO_x conditions, secondary fuel nitrogen may not significantly effect net NO_x reduction via reburning.

In hypothesis 3, it was suggested that the characteristic times for NO_x, HCN and NH_3 reactions are significant to the overall reburning process, and that each of the time constants is influenced by parameters such as stoichiometry, temperature, and bound nitrogen content in the secondary fuel. Although the chemical processes responsible for NO_x destruction are closely coupled (and not easily isolated in the pilot-scale package boiler simulator), the data suggest fuel-rich reburn zone reaction pathways for HCN and the amine species, as shown in Figures 8-1 and 8-2, respectively. As indicated, in addition to fuel-bound nitrogen evolution, HCN is formed by two basic mechanisms involving the methylidyne radical:

$$CH + NO \longrightarrow HCN + O \qquad (8\text{-}2)$$

$$CH + N_2 \longrightarrow HCN + N \qquad (8\text{-}3)$$

HCN formed in the fuel-rich reburn zone either exits unreacted or is reduced to an amine species, principally the radical imidogen (NH). The dominant species in the equilibrium reactions between amine species is ammonia (NH_3). In the reburn zone, the amines may react with an oxidizing species to form NO, react

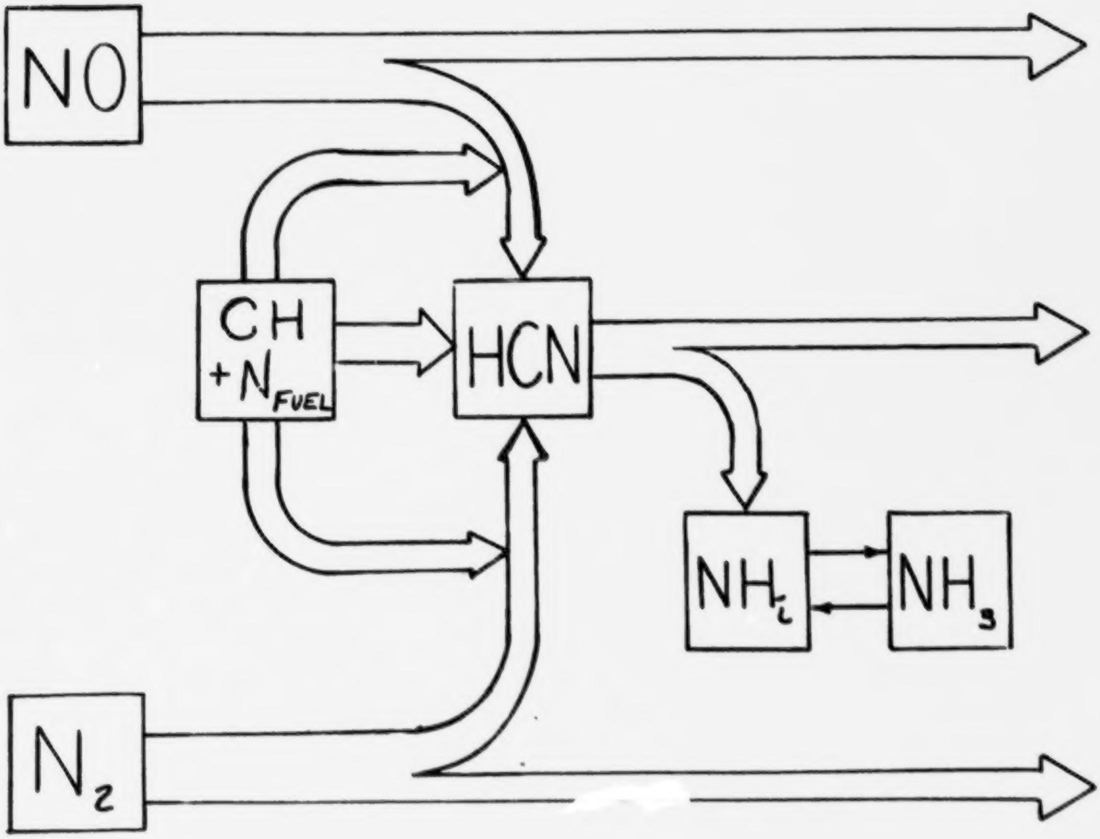
NO
CH + N_{FUEL}
HCN
NH_i
NH_3
N_2

Figure 8-1: HCN Reaction Pathways in the Reburn Zone

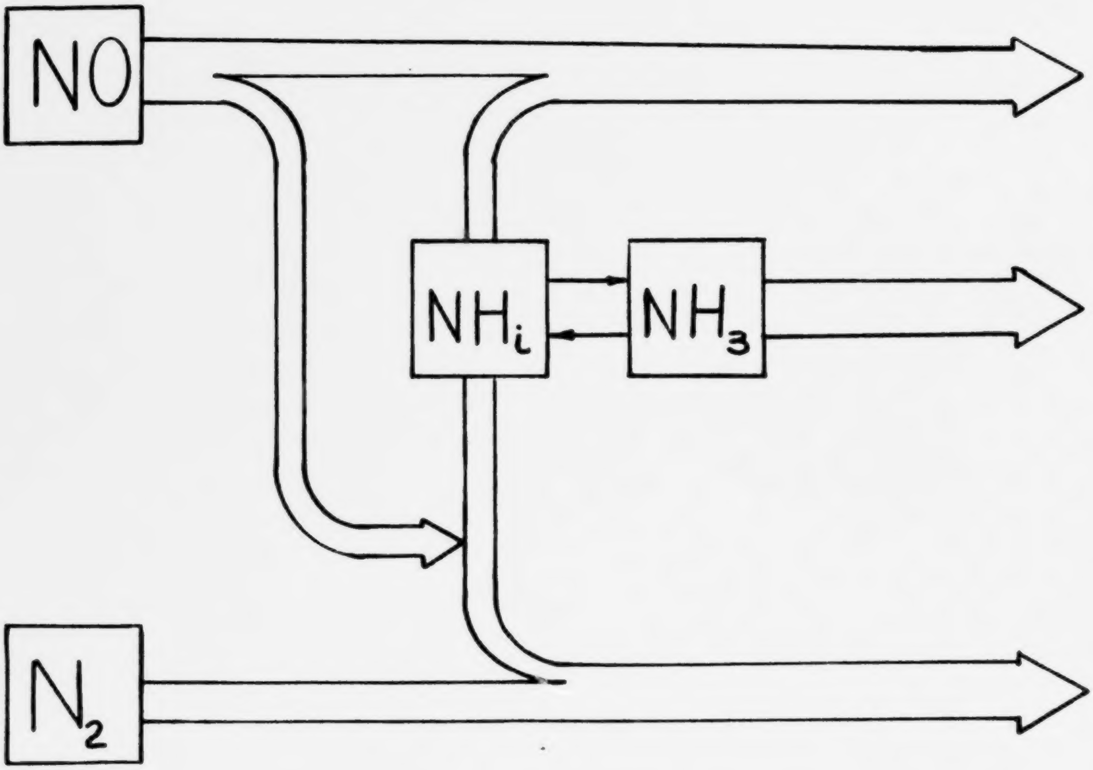
NO
NH$_i$
NH$_3$
N$_2$

Figure 8-2: NH$_3$ Reaction Pathways in the Reburn Zone

with NO molecules to form N_2, or exit unreacted. In the burnout zone, HCN and amines are converted to either NO or N_2. Almost 100 percent of the NO in the reburn zone is retained as NO in the exhaust.

Reburn zone NO and HCN profiles are influenced dramatically by stoichiometry and fuel nitrogen. NO destruction increases with decreasing stoichiometry in the reburn zone. Net NO reduction in the reburn zone decreases with increasing secondary fuel-bound nitrogen. In these experiments, reburn zone temperature had a large effect on the amount of soot formation and the rates of nitrogenous species reactions in the reburn zone.

Reburn zone N_2 formation was observed to continue as long as hydrocarbon radicals were present. For natural gas reburning, maximum N_2 formation occurs at approximately 15 ms into the reburn zone. However, maximum overall NO_x reduction with natural gas reburning requires a minimum of 50 ms. This difference in characteristic residence times is due to the continued rearrangement of fixed nitrogen species (TFN) that maximize N_2 formation in the burnout zone. The low fractional conversion (40 percent or less) of NH_3 and HCN to NO in the burnout zone (compared to the 100 percent retention of NO as NO in transition to the burnout zone) makes formation of these species in the fuel-rich reburn zone favorable for overall N_2 formation. Thus, the reburn zone serves two functions in the NO_x reduction process: first, N_2 is formed in the first 15 ms of the fuel-rich zone; second, HCN and amines are formed within about 50 ms, and are partially converted to N_2 in the burnout zone.

The above evaluation of hypothesis 3 deals with gas phase reactions characteristic of reburning. In hypothesis 8 it was stated that fuel oil reburning would result in an increase of characteristic reaction times. This was observed for the distillate and heavy fuel oils tested. The light distillate oil, requiring no preheat for atomization (2.47 cs viscosity at

40°C), required approximately 85 ms in the reburn zone to achieve maximum NO_x reduction. The heavy fuel oil (a mixture of distillate and residual oils), requiring about 93°C (200°F) preheat for atomization (4.63 cs viscosity at 100°C), requires approximately 105 ms to achieve maximum NO_x reduction. Thus, the increase in overall reaction time for fuel oil reburning over the gas phase reaction time appears to correlate with the grade (and volatility) of the fuel oil. Insufficient data was collected to quantify this relation.

Hypothesis 4 stated that increasing temperature enhances NO_x destruction in the reburning process. Temperature was found to be a difficult parameter to study in the pilot-scale facility. Increasing temperature in the reburn zone under fuel-rich conditions increases N_2 formation; however, increasing temperature in the burnout zone under fuel-lean conditions effects the conversion of HCN and amines to NO and N_2. Competing effects result in NO_x reduction dependence on temperature to be weaker than originally thought. However, it was shown that increasing reburn zone temperature results in increased NO_x reductions for reburn zone stoichiometries less than 0.9.

In hypothesis 5 it was stated that "secondary fuel injector design will effect NO_x reduction". This hypothesis was found to be invalid for natural gas and fuel oil reburning in the firetube package boiler. The reason for this lack of effect of secondary fuel injection mode is that large scale turbulent structures in the boiler dominate the mixing rate of the primary zone effluent and the secondary fuel. This conclusion appears to be true for reburning application to boilers in the firetube package boiler class, but may not be true of other sizes and types of boilers.

It was hypothesized in hypothesis 6 that the higher carbon-to-hydrogen ratio in fuel oils than in natural gas would result in increased NO_x destruction via the methyldine radical. For distillate fuel oil reburning, with reburn zone residence times increased to allow for droplet vaporization time requirements, the doubling of the carbon-to-hydrogen ratio resulted in only about 5 percent greater NO_x reductions. Further, fuel-rich zone NO_x destruction was actually greater for natural gas reburning than for fuel oil reburning. For heavy fuel oil reburning, the existence of significant fuel-bound nitrogen (a negative influence on NO_x reduction) overshadows the effect of the higher carbon-to-hydrogen ratio, resulting in higher NO_x emissions than for natural gas reburning. Thus, it is concluded that NO_x reduction is only weakly dependent on secondary fuel carbon-to-hydrogen ratio.

In hypothesis 9 it was stated that "results obtained on the research simulator are applicable to a commercial system". This hypothesis was confirmed in tests performed on a North American boiler. The input/output test results agree to a remarkable degree with results obtained from the firetube package boiler simulator tests. This conclusion demonstrates the generality of the results obtained in this test program to the firetube package boiler class.

Finally, hypothesis 10 claimed that 50 percent NO_x reductions could be obtained in a practical reburn application. This was shown to be true for natural gas and distillate fuel oil reburning, with initial NO_x concentration of 230 ppm (measured dry, at zero percent O_2). A 45 percent NO_x reduction was achieved for heavy fuel oil reburning. Reductions of greater than 50 percent are obtainable by increasing reburning load.

Thus, all of the original hypotheses have been addressed. Hypotheses 2, 3, 7, 8, 9 and 10 are correct as originally stated. Hypotheses 4 and 6 were shown to be only weakly valid. Further testing of fuel oil reburning at higher temperatures is recommended. Hypothesis 1 was shown to be incorrect as stated, with quantitative measurements of NO_x destruction rate order being presented.

Hypothesis 5 was also shown to be incorrect for the class of firetube package boilers.

Modification of pilot-scale boiler facilities for reburning proved to be relatively simple. Access ports on the back end of the boiler provide a convenient location for inserting staged air and fuel injectors. Secondary air and fuel supply systems and secondary burner safeguard systems are incorporated into the boiler operating management system.

Reburning is one of many NO_x control technologies presently available. Other NO_x control strategies include low NO_x burners, low excess air systems, staged air, flue gas recirculation, selective catalytic reduction, and ammonia non-catalytic reduction. To meet current New Source Performance Standards (NSPS) on NO_x there exist several alternatives for NO_x control, many of which require less hardware modification and/or less cost than reburning application. However, natural gas reburning can be coupled with other NO_x control techniques to achieve very low NO_x emissions. Therefore, the application of reburning is likely to be most attractive when very low NO_x emissions are desired. With reburning, the technology exists to control NO_x emissions to a level of 0.1 lb as NO_2/million Btu for natural gas and 0.15 lb as NO_2/million Btu for fuel oil.

REFERENCES

[1] Gorden, S., and McBride, B. J., "Computer Program for Calculation of Complex Chemical Equilibrium Compositions, Rocket Performance, Incident and Reflected Shocks, and Chapman-Jonguet Detonations," NASA SP-273, Interim Revision, March 1976.

[2] Zeldovich, Ya. B., "The Oxidation of Nitrogen in Combustion and Explosions," Acta Physicochimica, USSR, Vol. 21 (4), p. 577, 1946.

[3] Lanier, W. S., An Investigation of Chemical and Mixing Phenomena Associated with Reburning Applied to Firetube Package Boilers, Ph.D. Dissertation, University of Virginia, 1984.

[4] Glassman, I., Combustion, Academic Press, New York, 1977.

[5] Fenimore, C. P., Thirteenth Symposium (International) on Combustion, The Combustion Institute, p. 373, 1971.

[6] Patry, M., and Engel, G., Compte Renda Hebd. des Seances de l'Academie des Sciences, Vol. 31, p. 1302, 1950.

[7] Meyerson, A. L., Taylor, F. R., and Faunce, B. G., Sixth Symposium (International) on Combustion, The Combustion Institute, p. 897, 1973.

[8] Reed, R. D., "Process for the Disposal of Nitrogen Oxide," John Zink Company, U. S. Patent 1274637, 1969.

[9] Wendt, J.O.L., Sternling, C. V., and Matovich, M. A., Fourteenth Symposium (International) on Combustion, The Combustion Institute, p. 897, 1973.

[10] Takahashi, Y., Sakai, M., Murakami, N., Sengcka, T., Kawamura, T., Kunimoto, T., Haneda, H., Hirayama, A., Muraishi, K., and Kaneko, S., "Development of Mitsubishi 'MACT' In-Furnace NO_x Removal Process," Mitsubishi Heavy Industries, Ltd., Technical Review, Vol. 18, No. 2, 1981. Presented at the U.S.-Japan NO_x Information Exchange, Tokyo, Japan, May 25-30, 1981.

[11] Kelly, J. T., Pam, R. L., and Suttmann, S. T., "Fuel Staging for Pulverized Coal Furnace NO_x Control," In: Proceedings of the 1982 Joint Symposium on Stationary Combusion NO_x Control, Vol. I, EPA-600/9-85-022a (NTIS PB85-235604), July 1985.

[12] Chen, S. L., Clark, W. C., Heap, M. P., Pershing, D. W., and Seeker, W. R., "NO_x Reduction by Reburning with Gas and Coal -- Bench Scale Studies," In: Proceedings of the 1982 Joint Symposium on Stationary Combustion NO_x Control, Vol. I, EPA-600/9-85-022a (NTIS PB85-235604), July 1985.

[13] England, G., Heap, M. O., Payne, R., and Pershing, D. W., "The Development of Design Criteria for Low NO_x Oil Burners Suitable for Application to TEOR Steamers," Air Pollution Control Association, 1982.

[14] Merryman, E. L., and Levy, A., Fifteenth Symposium (International) on Combustion, The Combustion Institute, p. 647, 1979.

[15] Engleman, V. S., "Survey and Evalution of Kinetic Data on Reactions in Methane/Air Combustion," EPA-600/2-76-003 (NTIS PB248139), January 1976.

[16] Beer, J. M., and Chigier, N. A., Combustion Aerodynamics, John Wiley and Sons, New York, 1972.

[17] Pohl, J. H., Chen, S. L., Heap, M. P., and Pershing, D. W., "Correlation of NO_x Emissions with Basic Physical and Chemical Characteristics of Coal," In: Proceedings of the 1982 Joint Symposium on Stationary Combustion NO_x Control, Vol. II, EPA-600/9-85-022b (NTIS PB85-235612), July 1985.

[18] Wendt, J. O. L., Pershing, D. W., Lee, J. W., and Glass, J. W., "Pulverized Coal Combustion: NO_x Formation Mechanisms Under Fuel-Rich and Staged Combustion Conditions," Seventeenth Symposium (International On Combustion, 1978, pp. 77-87.

[19] Johnson, S. A., and Cioffi, P. L., "Development of an Advanced Combustion System to Minimize NO_x Emissions from Coal-Fired Boilers," presented at the 1978 Joint Power Generation Conference, Dallas, Texas, September 1978.

[20] Lyon, R. K., Varga, G. M., Jr., Ruterbories, B. H., Tomsho, M., Hardy, J., Freund, H., Muzio, L. J., and Robinson, J. M., "The Exxon Thermal De-NO_x Process," Institution of Chemical Engineers Symposium Series, Vol. 57, 1979.

[21] Yang, R. J., Garcia, F. J., and Hunter, S. C., "Screening and Optimization of In-Furnace NO_x Reduction Processes for Refinery Process Heater Applications," In: Proceedings: 1985 Joint Symposium on Stationary Combustion NO_x Control, Vol. 1, EPA-600/9-86-021a (NTIS PB86-225042), July 1986.

[22] Mulholland, J. A., and Hall, R. E., "The Effect of Fuel Nitrogen in Reburning Application to a Firetube Package Boiler," In: Proceedings: 1985 Joint Symposium on Stationary Combustion NO_x Control, Vol. I, EPA-600/9-86-021a (NTIS PB86-225042), July 1986.

[23] Mulholland, J. A., and Hall, R. E., "Fuel Oil Reburning Application for NO_x Control to Firetube Package Boilers," ASME Paper 85-JPGC-APC-6, 1985.

[24] Mulholland, J. A., and Lanier, W. S., "Application of Reburning for NO_x Control to a Firetube Package Boiler," ASME Paper 84-JPGC-APC-3, 1984.

APPENDIX A

QUALITY ASSURANCE/QUALITY CONTROL REPORT

CONTENTS OF APPENDIX A

Page

QA/QC OBJECTIVES A-4

DATA QUALITY PARAMETER DEFINITION A-4

DATA QUALITY ASSESSMENT A-6

CONCLUSIONS A-7

LIST OF FIGURES

Figure	Title	Page
A-1	In-Flame Temperature Measurement Accuracy	A-10
A-2	Velocity Measurement Accuracy	A-11

LIST OF TABLES

Table	Title	Page
A-1	Data Accuracy	A-8
A-2	Data Precision	A-9
A-3	Velocity Accuracy Calculation Worksheet	A-12

QUALITY ASSURANCE/QUALITY CONTROL REPORT

QA/QC OBJECTIVES

As specified in Section 2.0 of the Low NO_x/Reburn Combustion Test Facility Quality Assurance Project Plan, the Quality Assurance (QA) objectives are to assess and document the accuracy and precision of the following measurements:

- Stack and in-flame combustion gas species measurements
- In-flame temperature and velocity measurements
- Process control measurements

An overall data completeness goal of 90 percent was established in the QA/QC plan. Data representativeness was ensured by establishing sampling techniques that provided thorough mapping of the boiler sample volume.

DATA QUALITY PARAMETER DEFINITION

The primary QA parameters, accuracy and precision, are measured as follows. For combustion gas species measured by continuous emission monitors (CEM's), specific ion electrodes, and gas chromatography, repeated calibrations on known standards provide a comparison of the measured value to the actual value. These readings are recorded in a QA/QC logbook located at the facility. Thus, for NO, CO_2, CO, O_2, THC, HCN, NH_3, and N_2O measurements, accuracy is calculated in terms of percent difference between the measured value and the known standard concentration. CEM instrument readings (NO, CO_2, CO, O_2 and THC) are recorded continuously on strip chart recorders during testing. These recordings provide an estimate of precision, measured in terms of the percent difference between the maximum data fluctuations and the mean value. For HCN, NH_3, and N_2O measurements, duplicate samples are taken at each point and relative percent differences (TPD) are calculated as a precision estimate.

For in-flame temperature measurement via suction pyrometry, accuracy is estimated from the flow-rate versus temperature calibration curve. The assymptote line temperature for high suction flow rates, assumed to be the actual temperature, is compared to the temperature measurement at the operating flow rate, accuracy is represented as the percent difference. Precision is estimated from the fluctuation of the thermocouple reading (monitored on a digital readout) over the measurement time period (approximately 1 min.); it is represented as percent of mean. Accuracy of the velocity measurement is determined by integrating the radial velocity profile across the boiler cross-section, and comparing that calculated flow to the measured input flow (by means of a percent difference). Multiple (2 or 3) velocity readings are taken at each test point, with precision measured in terms of percent difference from the mean.

Process control instrumentation have accuracies determined by calibration with standard devices of known, high quality, calibration. For flow element calibrations, clean, factory-calibrated laminar flow elements are the calibration standards used for comparison. These standards are not used for testing. Accuracy is determined annually. Precision is measured each test day by comparison of multiple readings (approximately every half hour for steady state operation).

Data completeness is quantified by calculating the percent of all data recorded that meets accuracy and precision goals (as defined in the QA/QC plan). Data representativeness is not quantified. Based on the sampling methods established, documented in detail in the QA/QC plan, sufficient data representativeness was achieved.

DATA QUALITY ASSESSMENT

Accuracy and precision measurements are summarized in Tables A-1 and A-2. As shown in Table A-1, QA data accuracy goals were achieved for each measurement except the secondary atomizing air flow. However, because this is such a small flow rate, an accuracy of ±10 percent is sufficient to assure that the accuracy of the reduced data is well within the accuracy goal specified.

Accuracies of temperature and velocity measurements were determined from Figures A-1 and A-2, respectively. Velocity accuracy was found to be ±7.5 percent (see Table A-3). Suction pyrometer temperature accuracy was found to be ±0.42 percent (±10°F). The operating parameters that characterize the reburning application, such as stoichiometric ratios and firing rates, have accuracies that are calculated using Kline and McClintock's root-sum-square addition method.[1] For a result, R, determined from n variables, V, the statistical propagation of uncertainty is given by

$$\delta R = \left(\frac{\delta R}{\delta V_1} \delta V_1{}^2 + \frac{\delta R}{\delta V_2} \delta V_2{}^2 + \ldots + \frac{\delta R}{\delta V_n} \delta V_n{}^2 \right)^{1/2}.$$

Here, the variable V_i is described by

$$V_i = V_i \pm \delta V_i,$$

and the result is described by

$$R = R \pm \delta R.$$

The accuracy, or percent difference, of the result is then,

$$\text{Percent Accuracy} = \frac{\delta R}{R} \times 100.$$

Accuracy of NH_3 and HCN, once collected in solution, met QA/QC goals. Recalibration of electrodes were always within 10 percent of the initial calibration. However, the sample train collection efficiencies are not represented in this number. For NH_3, sample train collection efficiency, measured by pulling a known standard gas through the sample train, under conditions identical to those in tests, was found to be 98 percent. However, for HCN measurement, sample train collection efficiency was only 70%. These values were repeatable.

---

[1] Kline, S. J., and McClintock, F.A., "Describing Uncertainties in Single-Sample Experiments," Mechanical Engineering, January 1953.

Precision measurements are summarized in Table A-2. All QA precision goals were achieved.

Data completeness was found to be better than 95 percent. Approximately 2000 test conditions were established (see Appendix B), with many (five to thirty) output and input measurements taken at each condition.

CONCLUSIONS

The quality of data taken during the reburning study is consistent with the overall goals of the project. The data are of sufficient quality to provide fundamental insight into reburning application to firetube package boilers, both in terms of data trends and absolute data values. The data are being published in scientific journals to make the results available to the technical community.

TABLE A-1. DATA ACCURACY

Parameter Measured	Typical Value	Range	Measured Accuracy (± percent)	QA/QC Accuracy Goal (± percent)
FLOW:				
Primary Air (SCFM)	200	50-500	3%	5%
Secondary Air (SCFM)	100	20-200	3%	5%
Tertiary Air (SCFM)	75	20-200	3%	5%
Fire Eye Cooling Air (SCFM)	3	1-10	2.5%	5%
Sec. Fuel Nozzle Cooling Air	3	1-10	5%	5%
Primary Atomizing Air (SCFM)	20	4-40	1%	5%
Secondary Atomizing Air (SCFM)	1	0.4-1.2	10%	5%
Primary Natural Gas (SCFM)	33	5-50	3%	5%
Secondary Natural Gas (SCFM)	8	2-20	3%	5%
Primary Oil (GPH)	13	2-20	1%	5%
Secondary Oil (GPH)	3	0.5-5	3%	5%
Primary Ammonia (SCFM)	0.25	0.03-3	5%	5%
Secondary Ammonia (SCFM)	0.05	0.01-1	5%	5%
Firing Rate[a] (MBTU/HR)	2.5	2-4	2.5%	4.1%
Stoichiometric Ratio[a]	1.1	0.5-1.5	3.9%	6.1%
Doped N_2[a] (% of fuel)	0.5	0.1-1	5.8%	7.1%
Temperature (°F)	2000	1000-3000	0.42%	2%
Velocity (FPS)	50	10-100	7.5%	10%
Combustion Gas Species:				
NO (ppm, dry)	200	1-1000	1%	2.5%
O_2 (%, dry)	2	0.2-21	1%	2.5%
CO_2 (%, dry)	12	5-20	1%	5%
CO (ppm, dry)	20	5-50,000	2%	5%
THC (ppm, dry)	10	5-50,000	2%	5%
NH_3 (ppm, solution)	0.5	0.1-10	5%	10%
HCN (ppm, solution)	1	0.1-10	10%	10%
N_2O (ppm, dry)	<5	1-10	10%	10%

[a] Accuracy calculated using Kline and McClintock's root-sum-square addition method for computing propagation of uncertainties.

TABLE A-2. DATA PRECISION

Parameter Measured	Typical Value	Range	Measured Precision (± Percent)	QA/QC Precision Goal (± Percent)
FLOW:				
Primary Air (SCFM)	200	50-500	3%	-
Secondary Air (SCFM)	100	20-200	3%	-
Tertiary Air (SCFM)	75	20-200	5%	-
Fire Eye Cooling Air (SCFM)	3	1-10	10%	-
Sec. Fuel Nozzle Cooling Air	3	1-10	10%	-
Primary Atomizing Air (SCFM)	20	4-40	10%	-
Secondary Atomizing Air (SCFM)	1	0.4-1.2	10%	-
Primary Natural Gas (SCFM)	33	5-50	1%	-
Secondary Natural Gas (SCFM)	8	2-20	2.5%	-
Primary Oil (GPH)	13	2-20	1%	-
Secondary Oil (GPH)	3	0.5-5	1%	-
Primary Ammonia (SCFM)	0.25	0.03-3	2%	-
Secondary Ammonia (SCFM)	0.05	0.01-1	2%	-
Firing Rate[a] (MBTU/HR)	2.5	2-4	1.0%	2.5%
Stoichiometric Ratio[a]	1.1	0.5-1.5	2.2%	2.5%
Doped N_2[a] (% of fuel)	0.5	0.1-1	3.2%	5%
Temperature (°F)	2000	1000-3000	0.5%	5%
Velocity (FPS)	50	10-100	2%	5%
Combustion Gas Species:				
NO (ppm, dry)	200	1-1000	2.5%	5%
O_2 (%, dry)	2	0.2-21	5%	5%
CO_2 (%, dry)	12	5-20	2%	5%
CO (ppm, dry)	20	5-50,000	10%	10%
THC (ppm, dry)	10	5-50,000	10%	10%
NH_3 (ppm, solution)	0.5	0.1-10	10%	20%
HCN (ppm, solution)	1	0.1-10	10%	20%
N_2O (ppm, dry)	<5	1-10	20%	20%

[a] Accuracy calculated using Kline and McClintock's root-sum-square addition method for computing propagation of uncertainties.

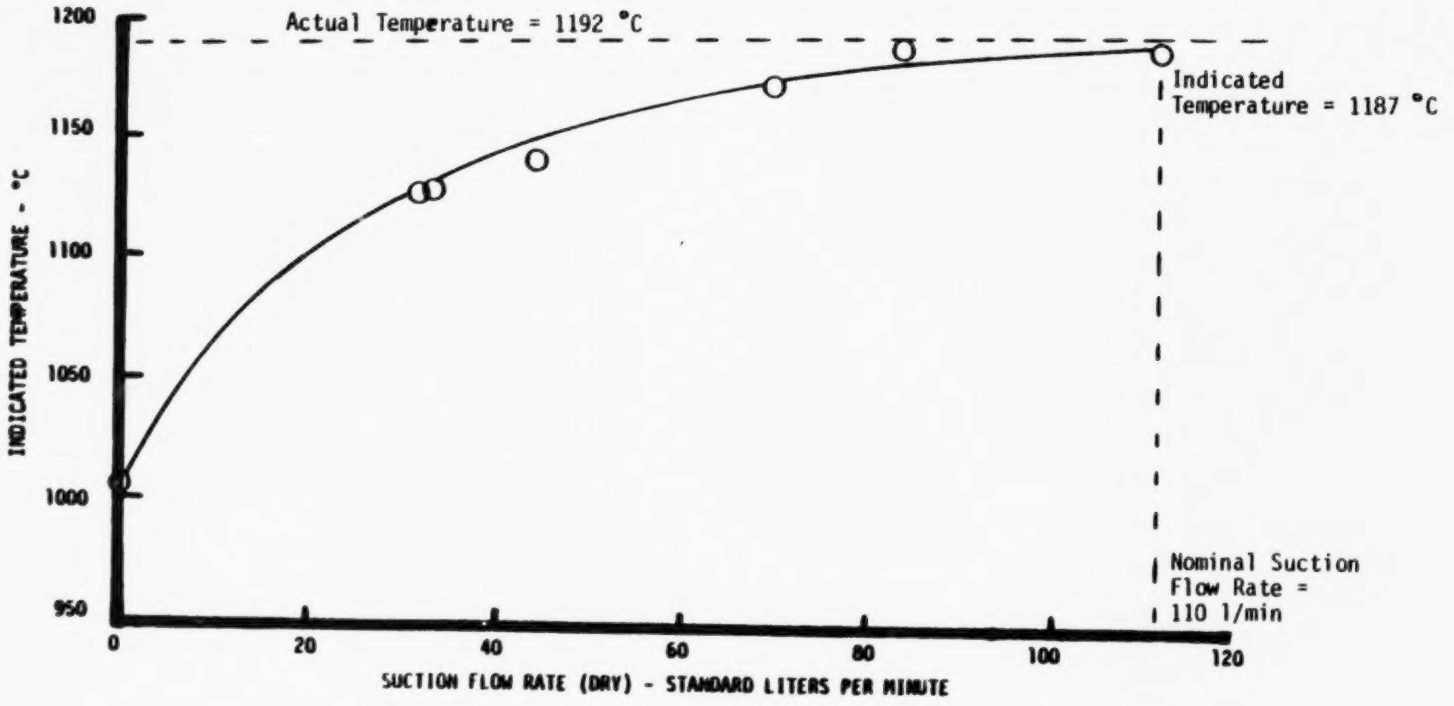

Figure A-1: In-Flame Temperature Measurement Accuracy

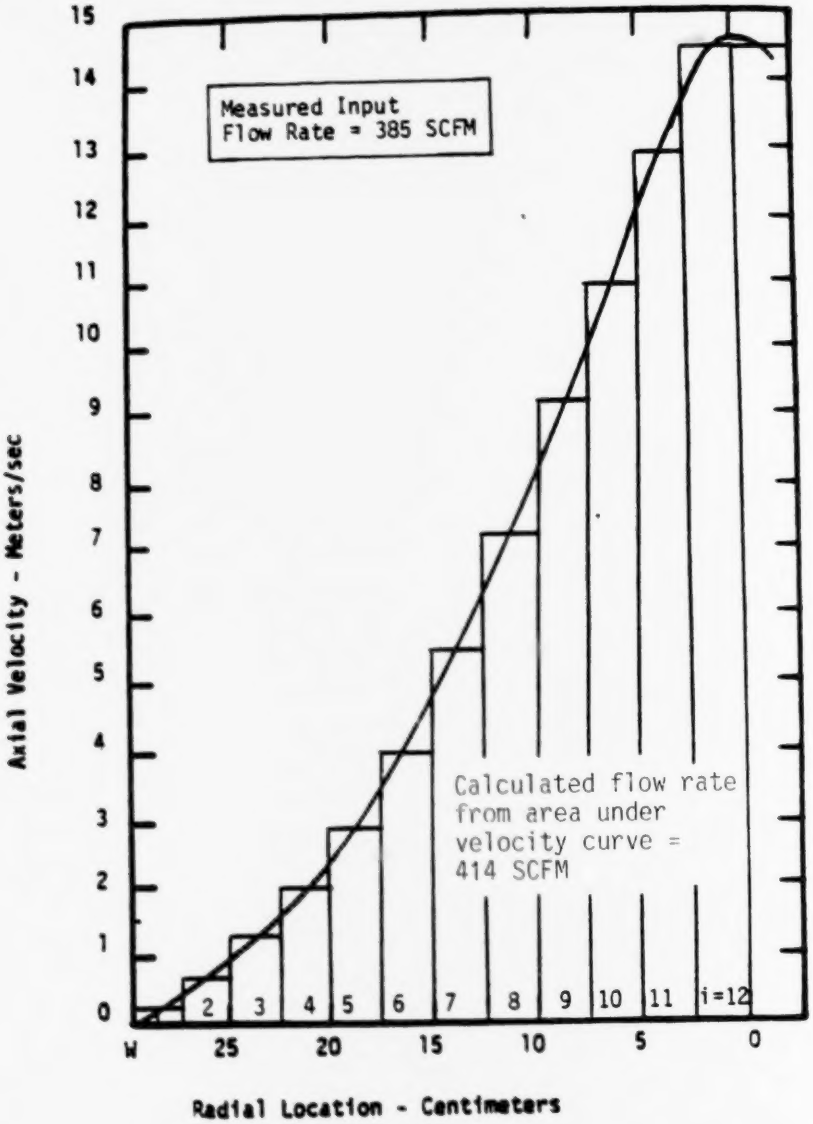

Figure A-2: Velocity Measurement Accuracy

TABLE A-3. VELOCITY CALIBRATION WORKSHEET

i	V_i (m/sec)	T_i (K)	A_i (cm^2)	V_iA_i/T_i (m·cm^2/sec·K)
1	0.2	1200	452	0.075
2	0.7	1250	412	0.231
3	1.2	1290	373	0.347
4	2.0	1320	334	0.506
5	2.9	1340	295	0.638
6	4.0	1360	255	0.750
7	5.3	1380	216	0.830
8	7.1	1400	177	0.898
9	9.1	1420	137	0.878
10	11.0	1430	98	0.754
11	12.8	1440	59	0.524
12	14.5	1450	20	0.200

$$\text{Calculated SCFM} = 62.4 \sum_{i=1}^{12} V_iA_i/T_i = 414 \text{ SCFM}$$

$$\text{Measured input SCFM} = \dot{m}_{fuel} + \dot{m}_{air} = 385 \text{ SCFM}$$

$$\text{Percent difference} = \frac{414-385}{385} \times 100 = 7.5\%$$

APPENDIX B

DATA SUMMARY

CONTENTS OF APPENDIX B

Page

DATA SUMMARY SHEETS B-4

Package Boiler Simulator (PBS):

- Natural Gas Baseline B-5
- No. 2 (Distillate) Fuel Oil Baseline B-11
- Natural Gas Reburning B-15
- No. 2 (Distillate) Fuel Oil Reburning B-48
- No. 5 (Heavy) Fuel Oil Reburning B-58
- Fuel Comparison, Reburning B-63

North American Boiler:

- No. 2 (Distillate) Fuel Oil Baseline B-67
- No. 5 (Heavy) Fuel Oil Baseline B-70
- Natural Gas Reburning B-73
- No. 2 (Distillate) Fuel Oil Reburning B-78
- No. 5 (Heavy) Fuel Oil Reburning B-81

PBS Tests Performed After October 1, 1984 . . . . B-84

Raw Data Sheets B-90

- Package Boiler Simulator (PBS) B-91
- North American Boiler B-98

LIST OF TABLES

Table	Title	Page
B-1	Secondary Fuel Nozzles	B-3

TABLE B-1. SECONDARY FUEL NOZZLES

Boom	Nozzle	Fuel	Hole Pattern
B1 (centerline)	R1	Gas	8 spokes: - 6 1/32" diameter holes/spoke - uniform injection
	R2	Gas	8 spokes: - 12 1/32" diameter holes/spoke - uniform injection
	R3	Gas	8 spokes: - 6 1/32" diameter holes/spoke - uniform injection
	N1	Gas	8 spokes: - 2 5/64" diameter holes/spoke - nonuniform injection
	N2	Gas	8 caps: - 1 7/64" diameter hole/cap - radial injection
	N3	Gas	4 caps - 1 7/64" diameter hole/cup - radial injection
B2 (centerline)	N1	Gas	8 7/64" diameter holes; radial injection
	N2	Gas	8 5/32" diameter holes; radial injection
	N3	Gas	8 3/16" diameter holes; radial injection
	N4	Gas	8 7/32" diameter holes; radial injection
	N5	Gas	8 1/4" diameter holes; radial injection
	N6	Gas	8 5/64" diameter holes; radial injection
	N7	Gas	4 5/32" diameter holes (one side); radial injection
	N8	Gas	1 1/4" diameter hole; radial injection
B3 (side wall)	N9	Gas	5 5/32" diameter holes; downstream injection
	S052	Oil	Sonicore air-atomizing nozzle, model 052
	H ---	Oil	Hago pressure-atomizing nozzle, 3.5 gph, 45 degree spray angle
	D ---	Oil	Delavan type WDA pressure-atomizing nozzle, hollow cone spray, 2-5 gph, 30-90 degree spray nozzle

DATA SUMMARY SHEETS

PBS FACILITY:

NATURAL GAS BASELINE

Data Summary Sheet

TEST: Natural Gas Baseline FACILITY: PBS PAGE: 1

		1	2	3	4	5	6	7	8	9	10	11	12	13	14	15	16	17	18	19	20
DATE & DATA BOOK #	Data Pt. #	FR_{TOT}	FR_{SEC}/FR_{PRI}	PRI FUEL	SEC FUEL	SR_1	SR_2	SR_3	SR_4	PRI FUEL DOPANT	SEC FUEL DOPANT	SEC FUEL INJ	FINAL AIR INJ	PRI ZONE MIXING	SEC FUEL NOZZLE	INJ. ZONE	SAMPLE LOCATION AXIAL	RADIAL	SAMPLE TYPE(S)		TEST VARIABLE
A-1		MW	%							% N_2 by wt	% N_2 by wt	in. into boiler	in. into boiler	sec air ax/rad			in. into boiler	in. radius			
4/20/83	1	0.59	0	NG	–	0.80	1.06	–	–	0	–	–	–	1	–	–	St	–	CEMS		I/O –
	2					0.72															SR_1
	3					0.63															
	4					0.55															
	5					0.99	1.24														
	6					0.81	1.06							0							
	7						1.00														
	8					0.72	1.06														
	9					0.64															
	10					0.55															
4/21	1	0.59	0	NG	–	0.80	1.05	–	–	0	–	–	–	∞	–	–	St	–	CEMS		I/O –
	2					0.71															SR_1
	3					0.62															
	4					0.53															
5/3	1	0.59	0	NG	–	0.78	1.02	–	–	0	–	–	–	1	–	–	St	–	CEMS		I/O –
	2									0.14											$(NH_3)_{PRI}$
	3									0.26											
	4									0.39											
	5									0.63											
	6									0.65											
	7					0.68															SR_1
	8					0.59															
	9					0.52															
5/4	2	0.59	0	NG	–	0.80	1.02	–	–	0.65	–	–	–	0	–	–	St	–	CEMS		I/O –
	3					0.70															SR_1
	4					0.60															
	5					0.51															
	6					1.01															
5/5	2	0.59	0	NG	–	0.80	1.02	–	–	0.65	–	–	–	∞	–	–	St	–	CEMS		I/O –
	3					0.69															SR_1

C.F. 620

Data Summary Sheet

TEST : Natural Gas Baseline FACILITY : PBS PAGE : 2

		1	2	3	4	5	6	7	8	9	10	11	12	13	14	15	16	17	18	19	20
DATE & DATA BOOK #	Data Pt. #	FR_{TOT}	$\frac{FR_{SEC}}{FR_{PRI}}$	PRI FUEL	SEC FUEL	SR_1	SR_2	SR_3	SR_4	PRI FUEL DOPANT	SEC FUEL DOPANT	SEC FUEL INJ	FINAL AIR INJ	PRI ZONE MIXING	SEC FUEL NOZZLE	INS. ZONE	SAMPLE LOCATION		SAMPLE TYPE(S)		TEST VARIABLE
																	AXIAL	RADIAL			
A-1		MW	%							% N_2 by wt	% N_2 by wt	in. into boiler	in. into boiler	sec air $\frac{ax}{rad}$			in. into boiler	in. radius			
5/5	4	0.59	0	NG	–	0.60	1.02	–	–	0.65	–	–	–	∞	–	–	st	–	CEMS		SR_1
	5					0.49															
	6					0.71								1							
	7					0.67															
	8					0.73															
	9					0.75															
	10					0.70															
	11									0.50											(NH_3)
	12									0.35											
	13									0.21											
	14									0.11											
	15									0											
5/25	1-11	0.59	0	NG	–	0.64	1.05	–	–	0.65	–	–	–	1	–	–	40	0-11½	T		D
5/26	1-15	0.59	0	NG	–	0.65	1.06	–	–	0.65	–	–	–	0	–	–	40	0-11½	T		D
6/2	1-22	0.58	0	NG	–	0.67	1.07	–	–	0.65	–	–	–	1	–	–	40	0-10	CEMS	, V	D
6/3	1-35	0.58	0	NG	–	0.67	1.07	–	–	0.65	–	–	–	0	–	–	40	0-10	CEMS	, V, T	D
	36-70	0.58	0	NG	–	0.67	1.07	–	–	0.65	–	–	–	∞	–	–	40	0-10	CEMS	, V, T	D
6/15	1-11	0.59	0	NG	–	0.66	1.03	–	–	0.65	–	–	–	0	–	–	40	0-10	CEMS		D
6/16	1-11	0.59	0	NG	–	0.56	1.04	–	–	0.65	–	–	–	0	–	–	40	0-10	CEMS		D
A-2																					
6/21	17-44	0.59	0	NG	–	0.62	1.00	–	–	0	–	–	–	0	–	–	40	0-10	CEMS	, T	D
7/8	1-6	0.59	0	NG	–	0.63	1.03	–	–	0	–	–	–	0	–	–	40	0-10	CEMS		D
	7-8																30-40	5¼	CEMS	, HCN, NH_3	
7/11	1-11	0.59	0	NG	–	0.63	1.08	–	–	0.65	–	–	–	0	–	–	40	0-10	CEMS		D
	12-22																30-60	5¼	CEMS,	HCN, NH_3,	T
7/13	1-13	0.59	0	NG	–	0.63	1.09	–	–	0.65	–	–	–	0	–	–	40-116	5¼	CEMS		D
7/15	31-41	0.60	0	NG	–	0.61	1.07	–	–	0.65	–	–	–	0	–	–	40	0-10	CEMS		D
7/21	25-31	0.59	0	NG	–	0.61	1.06	–	–	0.65	–	–	–	0	–	–	40	0-10	CEMS		D
7/22	21-28	0.59	0	NG	–	0.63	1.08	–	–	0.65	–	–	–	0	–	–	40	0-10	CEMS		D
A-3																					

C.F. 620

Data Summary Sheet

TEST: Natural Gas Baseline FACILITY: PBS PAGE: 3

		1	2	3	4	5	6	7	8	9	10	11	12	13	14	15	16	17	18	19	20
DATE & DATA BOOK #	Data Pt. #	FR_{TOT}	FR_{SEC}/FR_{PRI}	PRI FUEL	SEC FUEL	SR_1	SR_2	SR_3	SR_4	PRI FUEL DOPANT	SEC FUEL DOPANT	SEC FUEL INJ	FINAL AIR INJ	PRI ZONE MIXING	SEC FUEL NOZZLE	INS. ZONE	SAMPLE LOCATION AXIAL	RADIAL	SAMPLE TYPE(S)		TEST VARIABLE
A-3		MW	%							$\%N_2$ by wt	$\%N_2$ by wt	in. into boiler	in. into boiler	sec air ax/rad			in. into boiler	in. radius			
7/27	35-41	0.60	0	NG	–	0.61	1.07	–	–	0.65	–	–	–	0	–	–	40	0-10	CEMS		D
7/28	37-43	0.60	0	NG	–	0.60	1.05	–	–	0.16	–	–	–	0	–	–	40	0-10	CEMS		D
7/29	41-47	0.59	0	NG	–	0.62	1.08	–	–	0.16	–	–	–	0	–	–	40	0-10	CEMS		D
8/1	42-48	0.60	0	NG	–	0.61	1.06	–	–	0	–	–	–	0	–	–	40	0-10	CEMS		D
8/3	25-31	0.59	0	NG	–	0.61	1.07	–	–	0	–	–	–	0	–	–	40-65	9 1/4	T		D
	32-38																40-70	5 1/4	T		
	39-45																40-70	7 1/4	T		
8/11	9-14	0.60	0	NG	–	0.62	1.07	–	–	0.65	–	–	–	0	–	–	40-90	5 1/4	CEMS		D
8/29	38-44	0.59	0	NG	–	0.62	1.07	–	–	0.65	–	–	–	0	–	–	40	0-10	CEMS		D
A-6																					
12/12	3-9	0.57	0	NG	–	0.64	1.07	–	–	0	–	–	–	0	–	–	10	0-10	CEMS		D
	10	0.57	0	NG	–	0.64	1.07	–	–	0	–	–	–	0	–	–	St	–	CEMS		I/o- AIR STAGING
	11						0.98	–	1.06				64								
	12						0.89														
	13						0.79														
	14						0.71														
	15	0.57	0	NG	–	0.64	0.71	–	1.06	0	–	–	52	0	–	–	St	–	CEMS		I/o- AIR STAGING
	16												76								
	17												88								
12/13	2-6	0.59	0	NG	–	0.62	1.04	–	–	0	–	–	–	0	–	–	10	1-9	T		D
	8	0.59	0	NG	–	0.71	1.06	–	–	0	–	–	–	0	–	–	St	–	CEMS		I/o- AIR STAGING
	9						0.97	–	1.08				64								
	10						0.89														
	11						0.82														
	12						0.77														
	13					0.85	0.90														
	14						1.08	–	–				–								
A-7																					
1/12/[illegible]	1,16	0.59	0	NG	–	0.63	1.05	–	–	0.65	–	–	–	0	–	–	St	–	CEMS		I/o- AIR STAGING
	2						0.96	–	1.05				64								

C.F. 620

Data Summary Sheet

TEST: Natural Gas Baseline

FACILITY: PBS

PAGE: 4

		1	2	3	4	5	6	7	8	9	10	11	12	13	14	15	16	17	18	19	20
DATE & DATA BOOK #	Data Pt. #	FR_{TOT}	FR_{SEC}/FR_{PRI}	PRI FUEL	SEC FUEL	SR_1	SR_2	SR_3	SR_4	PRI FUEL DOPANT	SEC FUEL DOPANT	SEC FUEL INJ	FINAL AIR INJ	PRI ZONE MIXING	SEC FUEL NOZZLE	INS. ZONE	SAMPLE LOCATION AXIAL	RADIAL	SAMPLE TYPE(S)		TEST VARIABLE
		MW	%							% N_2 by wt	% N_2 by wt	in. into boiler	in. into boiler	sec air ax/rad			in. into boiler	in. radius			
A-7																					
1/12	3	0.59	0	NG	–	0.63	0.96	–	1.05	0.65	–	–	40	0	–	–	St	–	CEMS		I/o- AIR STAGING
	4						0.87	–				–	64								
	5							–				–	56								
	6							–				–	48								
	7							0.96				40	64								
	8						0.78	–				–	64								
	9							0.86				40	64								
	10							–				–	56								
	11							–				–	48								
	12						0.68	–				–	64								
	13							0.77				40	64								
	14							–				–	56								
	15							–				–	48								
A-8																					
2/14	2-7	0.59	0	NG	–	0.65	1.13	–	–	0.65	–	–	–	1	–	–	40	0-9	T		I/O- LOAD
	14-18	0.66															40	0-8	T		
	21-25	0.75															40	0-8	T		
2/15	2-6	0.78	0	NG	–	0.65	1.14	–	–	0.65	–	–	–	1	–	–	40	0-8	T		
	8-15																40-90	6¼	T		
2/22	2-7	0.59	0	NG	–	0.65	1.06	–	–	0.65	–	–	–	0	–	PRI	40	1-11	T		D- INSULATED
	12-26																40-90	5¼	CEMS	,T	
	28-42																4	0-8	CEMS	,V	
A-9																					
4/6	2-8	0.59	0	NG	–	0.65	1.07	–	–	0.65	–	–	–	0	–	PRI	40-80	5¼	CEMS		D
	9-15																40-80	7¼	CEMS		
	16-22																40-80	9¼	CEMS		
B-4																					
6/8	12-26	0.59	0	NG	–	0.66	1.08	–	–	0	–	–	–	0	–	PRI	90	0-8	T,V		D
6/14	20-26	0.59	0	NG	–	1.21	–	–	–	0.65	–	–	–	0	–	PRI	40-80	0	T		D
	27-34																40-75	5¼	T		

C.F. 620

Data Summary Sheet

TEST : Natural Gas Baseline FACILITY : PBS PAGE : 5

DATE & DATA BOOK #	Data Pt. #	1 FR$_{TOT}$	2 $\frac{FR_{SEC}}{FR_{PRI}}$	3 PRI FUEL	4 SEC FUEL	5 SR$_1$	6 SR$_2$	7 SR$_3$	8 SR$_4$	9 PRI FUEL DOPANT	10 SEC FUEL DOPANT	11 SEC FUEL INJ	12 FINAL AIR INJ	13 PRI ZONE MIXING	14 SEC FUEL NOZZLE	15 INS. ZONE	16 SAMPLE LOCATION AXIAL	17 SAMPLE LOCATION RADIAL	18 SAMPLE TYPE(S)	19	20 TEST VARIABLE
B-4		MW	%							% N_2 by wt	% N_2 by wt	in. into boiler	in. into boiler	sec.air ~~ax~~ rad			in. into boiler	in. radius			
6/14	35-40	0.59	0	NG	-	1.21	-	-	-	0.65	-	-	-	0	-	PRI	40	0-11	T		D
	41																0	2	T		
A-10																					
7/9	55-59	0.59	0	NG	-	0.91	1.06	-	-	0	-	-	-	0	-	PRI	40	0-8	T		D
	60-61																10	0-8	T		
8/9	2-6	0.59	0	NG	-	1.10	-	-	-	0	-	-	-	0	-	PRI	10	0-8	CEMS		D
	7-12																40	0-8	CEMS		
	53-55																40	0-7	T		
	56-58																10	0-7	T		

C.F. 620

PBS FACILITY:

NO. 2 (DISTILLATE) FUEL OIL BASELINE

Data Summary Sheet

TEST: No. 2 Fuel Oil Baseline FACILITY: PBS PAGE: 6

		1	2	3	4	5	6	7	8	9	10	11	12	13	14	15	16	17	18	19	20
DATE & DATA BOOK #	Data Pt. #	FR_{TOT}	FR_{SEC}/FR_{PRI}	PRI FUEL	SEC FUEL	SR_1	SR_2	SR_3	SR_4	PRI FUEL DOPANT	SEC FUEL DOPANT	SEC FUEL INJ	FINAL AIR INJ	PRI ZONE MIXING	SEC FUEL NOZZLE	INS. ZONE	SAMPLE LOCATION AXIAL	RADIAL	SAMPLE TYPE(S)		TEST VARIABLE
B-1		MW	%							$\% N_2$ by wt	$\% N_2$ by wt	in. into boiler	in. into boiler	sec.air ax/rad			in. into boiler	in. radius			
10/3/83	4	0.51	0	#2	–	0.74	1.24	–	–	0	–	–	–	0	–	–	St	–	CEMS		I/O-LOAD
10/11	4	0.57				0.76	1.23														
	7	0.82				0.73	1.08														
	8	0.63	0	#2	–	0.70	1.08	–	–	0	–	–	–	0	–	–	St	–	CEMS		I/O-SR_1
	9					0.63															
	10					0.58															
	11					0.75															
	12					0.72															
	13					0.82															
	14					0.89															
	15					0.99															
	16	0.63	0	#2	–	0.69	1.07	–	–	0	–	–	–	0	–	–	St	–	CEMS		I/O-SR_2
	17						0.97														
	18						1.03														
	19						1.12														
	20						1.16														
	21-24	0.63	0	#2	–	0.68	1.05	–	–	0	–	–	–	0	–	–	St	–	CEMS		I/O-Atom. AIR
12/15	4	0.64	0	#2	–	0.73	1.05	–	–	0.50	–	–	–	0	–	–	St	–	CEMS		I/O-SR_1
	5					0.70															
	6					0.80															
	7					0.86															
	8					0.97															
	10					0.56															
	11					0.64															
	13					0.68															
	14					0.61															
12/16	1	0.60	0	#2	–	0.68	1.03	–	–	0	–	–	–	0	–	–	St	–	CEMS		I/O-$(NH_3)_{FD}$
	2									0.09											
	3									0.22											
	4									0.36											

C.F. 620

Data Summary Sheet

TEST : No. 2 Fuel Oil Baseline FACILITY : PBS PAGE : 7

DATE & DATA BOOK #	Data Pt. #	1	2	3	4	5	6	7	8	9	10	11	12	13	14	15	16	17	18	19	20
		FR_{TOT}	$\frac{FR_{SEC}}{FR_{PRI}}$	PRI FUEL	SEC FUEL	SR_1	SR_2	SR_3	SR_4	PRI FUEL DOPANT	SEC FUEL DOPANT	SEC FUEL INJ	FINAL AIR INJ	PRI ZONE MIXING	SEC FUEL NOZZLE	INS. ZONE	SAMPLE LOCATION		SAMPLE TYPE(S)		TEST VARIABLE
																	AXIAL	RADIAL			
B-1		MW	%							% N_2 by wt	% N_2 by wt	in. into boiler	in. into boiler	secair ax/rad			in. into boiler	in. radius			
12/16	5	0.60	0	#2	-	0.68	1.03	-	-	0.52	-	-	-	0	-	-	St	-	CEMS		I/o - $(NH_3)_{PRI}$
	6					0.56				0.52											
	7									0.36											
	8									0.22											
	9									0.09											
	10									0											
	11	0.60	0	#2	-	0.55	1.05	-	-	0	-	-	-	0	-	-	St	-	CEMS		I/o - SR_2
	12									0.52											
	13						1.02			0											
	14									0.52											
	15						0.99			0											
	16									0.52											
	17						0.97			0											
	18									0.52											
	19						0.96			0											
	20									0.52											
	21	0.60	0	#2	-	0.55	1.03	-	-	0	-	-	-	0	-	-	St	-	CEMS		I/o - AIR MIXING
	22									0.52											
	23									0				1							
	24									0.52											
	25									0				7							
	26									0.52											
12/19	1	0.60	0	#2	-	0.58	1.01	-	-	0	-	-	-	0	-	-	St	-	CEMS		I/o - SR_1
	2					0.66															
	3					0.69															
	4					0.73															
	5					0.78															
	6					0.83															
	7					0.87															
	9-14	0.60	0	#2	-	0.58	1.05	-	-	0.52	-	-	-	0	-	-	90-90	7¼	CEMS		D

C.F. 620

Data Summary Sheet

TEST : No. 2 Fuel Oil Baseline FACILITY : PBS PAGE : 8

DATE & DATA BOOK #	Data Pt. #	1 FR$_{TOT}$	2 $\frac{FR_{SEC}}{FR_{PRI}}$	3 PRI FUEL	4 SEC FUEL	5 SR$_1$	6 SR$_2$	7 SR$_3$	8 SR$_4$	9 PRI FUEL DOPANT	10 SEC FUEL DOPANT	11 SEC FUEL INJ	12 FINAL AIR INJ	13 PRI ZONE MIXING	14 SEC FUEL NOZZLE	15 INJ. ZONE	16 SAMPLE LOCATION AXIAL	17 SAMPLE LOCATION RADIAL	18 SAMPLE TYPE(S)	19	20 TEST VARIABLE
B-1		MW	%							$\%N_2$ by wt	$\%N_2$ by wt	in. into boiler	in. into boiler	sec air $\frac{ax}{rad}$			in. into boiler	in. radius			
12/19	17-25	0.60	0	#2	-	0.58	1.05	-	-	0.52	-	-	-	0	-	-	10	0-10	CEMS		D
12/20	2-19	0.60	0	#2	-	0.58	1.01	-	-	0.52	-	-	-	0	-	-	40	0-10	CEMS	, T	D
	20-29																10	0-11	T		
1/18/84	1-13	0.60	0	#2	-	0.60	1.10	-	-	0	-	-	-	0	-	-	10	0-11	T		D
	14-20																40	0-11	T		
	21-29																50-130	0	T		
	30-40																40	0-8	V		
1/19	2-7	0.60	0	#2	-	0.58	1.09	-	-	0.52	-	-	-	0	-	-	40	0-10	CEMS		D
	9-18																35-125	9 1/4	CEMS		
	20-29																35-125	5 1/4	CEMS		
	31-40																35-125	0	CEMS		
	41	0.60	0	#2	-	0.58	1.09	-	-	0.52	-	-	-	0	-	-	St	-	CEMS		I/o-$(NH_3)_{PRI}$
	42									0.36											
	43									0.22											
	44									0.09											
	45									0											
B-2																					
2/2	11-15	0.61	0	#2	-	0.58	1.06	-	-	0.52	-	-	-	0	-	-	90-80	5 1/4	T		D

C.F. 620

PBS FACILITY:

NATURAL GAS REBURNING

Data Summary Sheet

TEST: Natural Gas Reburning FACILITY: PBS PAGE: 9

DATE & DATA BOOK #	Data Pt. #	1	2	3	4	5	6	7	8	9	10	11	12	13	14	15	16	17	18	19	20
		FR_{TOT}	FR_{SEC}/FR_{PRI}	PRI FUEL	SEC FUEL	SR_1	SR_2	SR_3	SR_4	PRI FUEL DOPANT	SEC FUEL DOPANT	SEC FUEL INJ	FINAL AIR INJ	PRI ZONE MIXING	SEC FUEL NOZZLE	INJ. ZONE	SAMPLE LOCATION AXIAL	RADIAL	SAMPLE TYPE(S)		TEST VARIABLE
A-2		MW	%							% N_2 by wt	% N_2 by wt	in. into boiler	in. into boiler	sec air ax/rad			in. into boiler	in. radius			
6/15	12	0.69	17	NG	NG	0.66	1.03	0.875	1.02	0.65	0	40	64	0	B1R1	-	St	-	CEMS		I/O
	13	0.74	25					0.82													
	14	0.66	12					0.92													
6/16	12	0.67	13	NG	NG	0.56	1.04	0.92	1.09	0.65	0	40	64	0	B1R1	-	St	-	CEMS		I/O
	13	0.71	20					0.865													
	14	0.74	26					0.83													
	15											35½									
	16											52									I₃
6/20	2	0.66	12	NG	NG	0.62	1.01	0.90	1.02	0.65	0	40	64	0	B1R2	-	St	-	CEMS		I/O
	3	0.74	25					0.81													
	4	0.82	39					0.73													
	5	0.84	42					0.71													
	8	0.66	12					0.90		0.35											
	9	0.74	25					0.80													
	10	0.82	39					0.73													
	12	0.66	12					0.90		0											
	13	0.74	25					0.81													
	14	0.82	39					0.73													
	16	0.82	39					0.73		0.13											
	17	0.74	25					0.80													
	18	0.66	12					0.90													
6/21	2	0.66	12	NG	NG	0.62	1.01	0.90	1.02	0.65	3.43	40	64	0	B1R2	-	St	-	CEMS		I/O
	3	0.74	25					0.80													
	4	0.82	39					0.73													
	6	0.66	12					0.90		0.35											
	7	0.74	25					0.81													
	8	0.82	39					0.73													
	10	0.66	12					0.90		0.13											
	11	0.74	25					0.80													
	12	0.82	39					0.73													

C.F. 620

Data Summary Sheet

TEST : Natural gas Reburning　　FACILITY : FFS　　PAGE : 10

		1	2	3	4	5	6	7	8	9	10	11	12	13	14	15	16	17	18	19	20
DATE & DATA BOOK #	Data Pt. #	FR_{TOT}	FR_{SEC}/FR_{PRI}	PRI FUEL	SEC FUEL	SR_1	SR_2	SR_3	SR_4	PRI FUEL DOPANT	SEC FUEL DOPANT	SEC FUEL INJ	FINAL AIR INJ	PRI ZONE MIXING	SEC FUEL NOZZLE	INS. ZONE	SAMPLE LOCATION AXIAL	RADIAL	SAMPLE TYPE(S)		TEST VARIABLE
A-2		MW	%							% N_2 by wt	% N_2 by wt	in. into boiler	in. into boiler	secair ax/rad			in. into boiler	in. radius			
6/21	13	0.82	39	NG	NG	0.62	1.01	0.73	1.02	0	0.43	40	64	0	BIRZ	–	St	–	CEMS		I/0
	14	0.74	25					0.80													
	15	0.66	12					0.90													
	45-51	0.66	12	NG	NG	0.62	1.00	0.89	1.01	0.35	0.43	40	64	0	BIRZ	–	40-65	7 1/4	T		D
	52											40							CEMS		I/0-
	53											46									f_3
	54											52									
	55											58									
	56											61 3/4									
7/12	1-5	0.66	12	NG	NG	0.63	1.08	0.97	1.09	0.65	0	40	64	0	BIRZ	–	40-60	5 1/4	CEMS	HCN, NH_3	D
	6																60	7 1/4	CEMS	HCN, NH_3	
7/13	14-18	0.66	12	NG	NG	0.61	1.06	0.95	1.07	0.65	0	40	64	0	BIRZ	–	40-60	5 1/4	T		D
7/14	2-6	0.74	24	NG	NG	0.62	1.07	0.86	1.07	0.65	0	40	64	0	BIRZ	–	40-55	5 1/4	CEMS,	HCN, NH_3,	N_2O
	7-13																40-70	5 1/4	T		D
	14-18																40-60	7 1/4	T		
	19-27																40	1-9	T,	V	
7/15	2-7	0.82	38	NG	NG	0.61	1.07	0.78	1.07	0.65	0	40	64	0	BIRZ	–	40-60	5 1/4	CEMS	HCN, NH_3,	N_2O
	8-14																40-70	5 1/4	T		D
	15-29																40	1-10	T, V		
7/21	2-6	0.66	12	NG	NG	0.61	1.06	0.95	1.07	0.65	0.43	40	64	0	BIRZ	–	40-55	5 1/4	CEMS	HCN, NH_3,	N_2O
	7-11																40-55	7 1/4	CEMS		D
	13-23																40-65	5 1/4	T		
	32-36																40	3-11	T		
7/22	2-7	0.74	24	NG	NG	0.63	1.08	0.87	1.08	0.65	0.43	40	64	0	BIRZ	–	40-60	5 1/4	CEMS,	HCN, NH_3,	N_2O
	8-20																40	2-10	T,	V	D
A-3																					
7/27	2-7	0.82	38	NG	NG	0.62	1.08	0.78	1.07	0.65	0.41	40	64	0	BIRZ	–	40-60	5 1/4	CEMS	HCN, NH_3,	N_2O
	8-13																40-60	7 1/4	CEMS		D
	14-2																40-10	5 1/4	T		
	21-33																40	1-9	T,	V	

C.F. 620

Data Summary Sheet

TEST: Natural Gas Reburning FACILITY: PBS PAGE: 11

DATE & DATA BOOK #	Data Pt. #	1 FR_{TOT}	2 FR_{SEC}/FR_{PRI}	3 PRI FUEL	4 SEC FUEL	5 SR_1	6 SR_2	7 SR_3	8 SR_4	9 PRI FUEL DOPANT	10 SEC FUEL DOPANT	11 SEC FUEL INJ	12 FINAL AIR INJ	13 PRI ZONE MIXING	14 SEC FUEL NOZZLE	15 INJ. ZONE	16 SAMPLE LOCATION AXIAL	17 SAMPLE LOCATION RADIAL	18 SAMPLE TYPE(S)	19	20 TEST VARIABLE
A-3		MW	%							% N_2 by wt	% N_2 by wt	in. into boiler	in. into boiler	sec air ax/rad			in. into boiler	in. radius			
7/28	3-8	0.74	24	NG	NG	0.62	1.08	0.87	1.07	0.16	0	40	64	0	BIR2	–	40-60	5 1/4	CEMS,	HCN, NH_3, N_2O	
	9-14																40-60	7 1/4	CEMS		D
	15-21																40-70	5 1/4	T		
	22-34																40	1-9	T, V		
7/29	2	0.74	25	NG	NG	0.62	1.08	0.86	1.07	0.16	0.43	40	64	0	BIR2	–	St	–	CEMS		I/O
	3	0.70	19					0.91													
	4	0.66	12					0.96													
	6-11	0.74	25					0.86									40-60	5 1/4	CEMS,	HCN, NH_3, N_2O	
	12-18																40-65	7 1/4	CEMS		D
	19-25																40-70	5 1/4	T		
	26-38																40	1-9	T, V		
8/1	6-11	0.74	24	NG	NG	0.61	1.07	0.86	1.06	0	0	40	64	0	BIR2	–	40-60	5 1/4	CEMS,	HCN, NH_3	
	12-19																40-65	7 1/4	CEMS		D
	20-26																40-70	5 1/4	T		
	27-39																40	1-9	T, V		
8/2	3-8	0.74	24	NG	NG	0.62	1.08	0.87	1.07	0	0.43	40	64	0	BIR2	–	40-60	5 1/4	CEMS,	HCN, NH_3	
	9-15																40-70	7 1/4	CEMS		D
	16-22																40-70	5 1/4	T		
	24-29										0						40-65	7 1/4	CEMS,	HCN, NH_3	
	30-35																40-65	9 1/4	CEMS,	HCN, NH_3	
	37-43																40-70	7 1/4	T		
8/3	3-15	0.66	12	NG	NG	0.62	1.08	0.96	1.08	0.65	0	40	64	0	BIR2	–	40	1-9	T, V		D
	17-23	0.74	24	NG	NG	0.61	1.07	0.86	1.07	0	0	40	64	0	BIR2	–	40-70	9 1/4	T		D
8/18	3-8	0.74	24	NG	NG	0.62	1.08	0.86	1.07	0	0.43	40	64	0	BIR2	–	40-60	5 1/4	CEMS,	HCN, NH_3	D
	11-17																40-70	T			
8/23	3-8	0.66	12	NG	NG	0.61	1.06	0.95	1.07	0.65	0.43	40	64	0	BIR3	–	40-60	5 1/4	CEMS,	HCN, NH_3	D
	9-11																40-50	7 1/4	CEMS,	HCN, NH_3	
	12																40	9 1/4	CEMS,	HCN, NH_3	
8/24	3-8	0.66	12	NG	NG	0.61	1.07	0.96	1.08	0.65	0	40	64	0	BIR3	–	40-60	5 1/4	CEMS,	HCN, NH_3	D
	9-17																40-70	5 1/4	T		

C.F. 620

Data Summary Sheet

TEST: Natural Gas Reburning FACILITY: PBS PAGE: 12

DATE & DATA BOOK #	Data Pt. #	1	2	3	4	5	6	7	8	9	10	11	12	13	14	15	16	17	18	19	20
		FR_{TOT}	$\frac{FR_{SEC}}{FR_{PRI}}$	PRI FUEL	SEC FUEL	SR_1	SR_2	SR_3	SR_4	PRI FUEL DOPANT	SEC FUEL DOPANT	SEC FUEL INJ	FINAL AIR INJ	PRI ZONE MIXING	SEC FUEL NOZZLE	INS. ZONE	SAMPLE LOCATION AXIAL	RADIAL	SAMPLE TYPE(S)		TEST VARIABLE
A-3		MW	%							$\% N_2$ by wt	$\% N_2$ by wt	in. into boiler	in. into boiler	sec air ax/rad			in. into boiler	in. radius			
8/24	18-29	0.66	12	NG	NG	0.61	1.07	0.96	1.08	0.65	0	40	64	0	B1R3	—	40	1-9	T,	V	D
	30-35																40	1-10	CEMS		
8/25	4-10	0.74	24	NG	NG	0.62	1.08	0.87	1.08	0.65	0.42	40	64	0	B1R3	—	40-70	5 1/4	CEMS,	HCN, NH_3	D
	11-13																40-50	7 1/4	CEMS,	HCN, NH_3	
	15-20	0.74	24	NG	NG	0.61	1.08	0.87	1.08	0.65	0	40	64	0	B1R3	—	40-70	5 1/4	CEMS		D
	22-24	0.74	24	NG	NG	0.61	1.08	0.87	1.08	0	0	40	64	0	B1R3	—	63-64	5 1/4	CEMS		D
8/26	3-16	0.74	24	NG	NG	0.62	1.08	0.87	1.08	0	0	40	64	0	B1R3	—	40-65	5 1/4	CEMS		D
	17-23																65	7 1/4	CEMS		
	24-31																65	9 1/4	CEMS		
	32-35																62-64	5 1/4	CEMS,	HCN, NH_3	
A-4																					
8/29	2	0.66	12	NG	NG	0.62	1.07	0.96	1.07	0.65	0	40	64	0	B1N1	—	St	–	CEMS		I/O-Mixing
	3	0.74	24					0.86													
	4	0.82	38					0.78													
	6	0.66	12					0.96		0.35											
	7	0.74	24					0.86													
	8	0.82	38					0.78													
	10	0.66	12					0.96		0.13											
	11	0.74	24					0.86													
	12	0.82	38					0.78													
	14	0.66	12					0.96		0											
	15	0.74	24					0.86													
	16	0.82	38					0.78													
	18	0.66	12					0.96		0	0.42										
	19	0.74	24					0.86													
	20	0.82	38					0.78													
	22	0.66	12					0.96		0.13											
	23	0.74	24					0.86													
	24	0.82	38					0.78													
	26	0.66	12					0.96		0.35											

C.F. 620

Data Summary Sheet

TEST : Natural Gas Reburning FACILITY : PBS PAGE : 13

		1	2	3	4	5	6	7	8	9	10	11	12	13	14	15	16	17	18	19	20
DATE & DATA BOOK #	Data Pt. #	FR_{TOT}	$\frac{FR_{SEC}}{FR_{PRI}}$	PRI FUEL	SEC FUEL	SR_1	SR_2	SR_3	SR_4	PRI FUEL DOPANT	SEC FUEL DOPANT	SEC FUEL INJ	FINAL AIR INJ	PRI ZONE MIXING	SEC FUEL NOZZLE	INS. ZONE	SAMPLE LOCATION AXIAL	RADIAL	SAMPLE TYPE(S)		TEST VARIABLE
A-4		MW	%							$\% N_2$ by wt	$\% N_2$ by wt	in. into boiler	in. into boiler	sec air $\frac{ax}{rad}$			in. into boiler	in. radius			
8/29	27	0.74	24	NG	NG	0.62	1.07	0.86	1.07	0.35	0.42	40	64	0	BIN1	–	St	–	CEMS		I/O –
	28	0.82	38					0.78													Mixing
	30	0.66	12					0.96		0.65											
	31	0.74	24					0.86													
	32	0.82	38					0.78													
8/30	3-7	0.74	24	NG	NG	0.61	1.06	0.85	1.06	0.65	0	40	64	0	BIN1	–	40-60	5 1/4	CEMS	HCN, NH_3	
	8-12																40-60	7 1/4	CEMS	HCN, NH_3	
	13-17																40-60	9 1/4	CEMS	HCN, NH_3	
8/31	3-8	0.74	24	NG	NG	0.60	1.05	0.85	1.05	0.65	0.42	40	64	0	BIN1	–	40-60	5 1/4	CEMS	HCN, NH_3	
	9-14																40-60	7 1/4	CEMS	HCN, NH_3	
	15-20																40-60	9 1/4	CEMS	HCN, NH_3	
9/1	2	0.66	12	NG	NG	0.60	1.05	0.94	1.05	0.65	0	40	64	0	BIN2	–	St	–	CEMS		I/O–
	3	0.74	24					0.84													Mixing
	4	0.82	38					0.76													
	6	0.66	12					0.94		0.35											
	7	0.74	24					0.84													
	8	0.82	38					0.76													
	10	0.66	12					0.94		0.13											
	11	0.74	24					0.84													
	12	0.82	38					0.76													
	14	0.66	12					0.94		0											
	15	0.74	24					0.84													
	16	0.82	38					0.76													
	17	0.82	38					0.76		0	0.42										
	18	0.74	24					0.84													
	19	0.66	12					0.94													
	22	0.66	12					0.94		0.13											
	23	0.74	24					0.84													
	24	0.82	38					0.76													
	26	0.66	12					0.94		0.35											

C.F. 620

Data Summary Sheet

TEST: Natural Gas Reburning FACILITY: PBS PAGE: 14

DATE & DATA BOOK #	Data Pt. #	1 FR_{TOT}	2 $\frac{FR_{SEC}}{FR_{PRI}}$	3 PRI FUEL	4 SEC FUEL	5 SR_1	6 SR_2	7 SR_3	8 SR_4	9 PRI FUEL DOPANT	10 SEC FUEL DOPANT	11 SEC FUEL INJ	12 FINAL AIR INJ	13 PRI ZONE MIXING	14 SEC FUEL NOZZLE	15 INS. ZONE	16 SAMPLE LOCATION AXIAL	17 RADIAL	18 SAMPLE TYPE(S)	19	20 TEST VARIABLE
A-4		MW	%							% N_2 by wt	% N_2 by wt	in. into boiler	in. into boiler	sec air $\frac{ax}{rad}$			in. into boiler	in. radius			
9/1	27	0.74	29	NG	NG	0.60	1.05	0.84	1.05	0.35	0.42	40	64	0	BINZ	—	St	—	CEMS		I/O-Mixing
	28	0.82	38					0.76													
	30	0.66	12					0.94		0.65											
	31	0.74	29					0.84													
	32	0.82	38					0.76													
	34	0.66	12					0.94		0	0			∞							
	35	0.74	29					0.84													
	36	0.82	38					0.76													
	38	0.66	12					0.94		0.13											
	39	0.74	29					0.84													
	40	0.82	38					0.76													
	42	0.66	12					0.94		0.35											
	43	0.74	29					0.84													
	44	0.82	38					0.76													
	46	0.66	12					0.94		0.65											
	47	0.74	29					0.84													
	48	0.82	38					0.76													
	49	0.82	38					0.76		0.65	0.42										
	50	0.74	29					0.84													
	51	0.66	12					0.94													
	54	0.66	12					0.94		0.35											
	55	0.74	29					0.84													
	56	0.82	38					0.76													
	58	0.66	12					0.94		0.13											
	59	0.74	29					0.84													
	60	0.82	38					0.76													
	62	0.66	12					0.94		0											
	63	0.74	29					0.84													
	69	0.82	38					0.76													
9/2	4-7	0.74	29	NG	NG	0.60	1.05	0.85	1.05	0.65	0.42	40	64	∞	BINZ	—	35-40	5 1/4	CEMS	NH_3	D

C.F. 620

Data Summary Sheet

TEST: Natural Gas Reburning FACILITY: PBS PAGE: 15

		1	2	3	4	5	6	7	8	9	10	11	12	13	14	15	16	17	18	19	20
DATE & DATA BOOK #	Data Pt. #	FR_{TOT}	$\frac{FR_{SEC}}{FR_{PRI}}$	PRI FUEL	SEC FUEL	SR_1	SR_2	SR_3	SR_4	PRI FUEL DOPANT	SEC FUEL DOPANT	SEC FUEL INJ	FINAL AIR INJ	PRI ZONE MIXING	SEC FUEL NOZZLE	INJ. ZONE	SAMPLE LOCATION AXIAL	SAMPLE LOCATION RADIAL	SAMPLE TYPE(S)	SAMPLE TYPE(S)	TEST VARIABLE
A-4		MW	%							% N_2 by wt	% N_2 by wt	in. into boiler	in. into boiler	sec.air ax/rad			in. into boiler	in. radius			
9/13	2	0.66	12	NG	NG	0.60	1.05	0.94	1.05	0.65	0	40	64	0	BIRZ	3	St	–	CEMS		I/O-T_A
	3	0.74	24					0.85													
	4	0.82	38					0.76													
	6	0.66	12					0.94													
	7	0.74	24					0.85													
	8	0.82	38					0.76													
	10	0.66	12					0.94													
	11	0.74	24					0.85													
	12	0.82	38					0.76													
	14	0.66	12					0.94			0.42										
	15	0.74	24					0.85													
	16	0.82	38					0.76													
	18	0.66	12					0.94													
	19	0.74	24					0.85													
	20	0.82	38					0.76													
	22	0.66	12					0.94													
	23	0.79	24					0.85													
	24	0.82	38					0.76													
	27-37	0.74	24	NG	NG	0.60	1.05	0.85	1.05	0.65	0	40	64	0	BIRZ	3	40-85	5 1/4	CEMS		D
9/14	3-8	0.74	24	NG	NG	0.61	1.06	0.86	1.06	0.65	0	40	64	0	BIRZ	3	40-65	5 1/4	CEMS	HCN, NH_3	
	9-16																40-75	5 1/4	I		
	17-24																40-75	7 1/4	I		
	25-28																40-70	9 1/4	I		
	30-37	0.74	24	NG	NG	0.61	1.06	0.86	1.06	0.65	0.42	40	64	0	BIRZ	3	40-75	5 1/4	CEMS	HCN, NH_3	
A-5																					
9/19	2	0.66	12	NG	NG	0.63	1.08	0.97	1.07	0.65	0	40	64	0	BIRZ	–	St	–	CEMS		I/O-T_A
	3										0.42										
	4	0.74	24					0.87			0										
	5										0.42										
	6	0.82	38					0.78			0										

C.F. 620

Data Summary Sheet

TEST: Natural Gas Reburning FACILITY: PBS PAGE: 16

DATE & DATA BOOK #	Data Pt. #	1	2	3	4	5	6	7	~~8~~	9	10	11	12	13	14	15	16	17	18	19	20
		FR_{TOT}	$\frac{FR_{SEC}}{FR_{PRI}}$	PRI FUEL	SEC FUEL	SR_1	SR_2	SR_3	SR_4	PRI FUEL DOPANT	SEC FUEL DOPANT	SEC FUEL INJ	FINAL AIR INJ	PRI ZONE MIXING	SEC FUEL NOZZLE	INS. ZONE	SAMPLE LOCATION AXIAL	RADIAL	SAMPLE TYPE(S)		TEST VARIABLE
A-5		MW	%							$\%N_2$ by wt	$\%N_2$ by wt	in. into boiler	in. into boiler	sec air ax/rad			in. into boiler	in. radius			
9/19	7	0.82	38	NG	NG	0.63	1.08	0.78	1.07	0.65	0.42	40	64	0	BIRZ	–	St	–	CEMS		I/O-
	8	0.66	12					0.97			0		68								I_R
	9										0.42										
	10	0.74	24					0.87			0										
	11										0.42										
	12	0.82	38					0.78			0										
	13										0.42										
	14	0.66	12					0.97			0		50								
	15										0.42										
	16	0.74	24					0.87			0										
	17										0.42										
	18	0.82	38					0.78			0										
	19										0.42										
	22	0.66	12					0.97			0		57								
	23										0.42										
	24	0.74	24					0.87			0										
	25										0.42										
	26	0.82	38					0.78			0										
	27										0.92										
	28-33	0.74	24	NG	NG	0.63	1.08	0.87	1.08	0.65	0.42	40	50	0	BIRZ	–	45-70	5 1/4	CEMS		D
	34-44	0.74	24	NG	NG	0.63	1.08	0.87	1.08	0.65	0.42	40	68	0	BIRZ	–	40-90	5 1/4	CEMS		D
9/20	2-10	0.74	24	NG	NG	0.62	1.07	0.86	1.06	0.65	0.42	40	68	0	BIRZ	–	40-70	5 1/4	CEMS	HCN, NH_3	D
	12-17																45-70	7 1/4	CEMS	HCN, NH_3	
	18-23																45-70	9 1/4	CEMS	HCN, NH_3	
	24	0.74	24	NG	NG	0.61	1.06	0.85	1.06	0.65	0.42	40	68	0	BIRZ	–	St	–	CEMS		I/O-
	25								1.01												SR_{80}
	26								0.98												
	27								1.13												
9/21	2	0.74	24	NG	NG	0.61	1.06	0.85	1.06	0.65	0.42	40	50	0	BIRZ	–	St	–	CEMS		I/O-
	3								1.01												I_R

C.F. 620

Data Summary Sheet

TEST: Natural Gas Reburning
FACILITY: PBS
PAGE: 17

DATE & DATA BOOK #	Data Pt. #	1	2	3	4	5	6	7	8	9	10	11	12	13	14	15	16	17	18	19	20
		FR_{TOT}	FR_{SEC}/FR_{PRI}	PRI FUEL	SEC FUEL	SR_1	SR_2	SR_3	SR_4	PRI FUEL DOPANT	SEC FUEL DOPANT	SEC FUEL INJ	FINAL AIR INJ	PRI ZONE MIXING	SEC FUEL NOZZLE	INS. ZONE	SAMPLE LOCATION AXIAL	SAMPLE LOCATION RADIAL	SAMPLE TYPE(S)		TEST VARIABLE
A-5		MW	%							% N_2 by wt	% N_2 by wt	in. into boiler	in. into boiler	sec.air ax/rad			in. into boiler	in. radius			
9/21	4	0.74	24	NG	NG	0.61	1.06	0.85	0.98	0.65	0.42	40	50	0	BIRZ	-	St	-	CEMS		I/O - ϵ_R
	5								1.13												
	6								1.06			40	64								
	7								1.01												
	8								0.98												
	9								1.13												
	10								1.13			35	64								
	11								0.98												
	12								1.01												
	13								1.06												
	15	0.66	12	NG	NG	0.94	1.09	0.97	1.08	0.65	0	40	64	0	BIRZ	-	St	-	CEMS		I/O - T_R
	16										0.42										
	17	0.74	24					0.87			0										
	18										0.42										
	19	0.82	38					0.79			0										
	20										0.42										
	21-25	0.74	24	NG	NG	0.94	1.09	0.87	1.08	0.65	0.42	40	64	0	BIRZ	-	40-60	5¼	CEMS		D
	26-30	0.74	24	NG	NG	0.94	1.09	0.87	1.08	0.65	0	40	64	0	BIRZ	-	40-60	5¼	CEMS		D
	32-36	0.74	24	NG	NG	0.94	1.09	0.87	1.08	0	0	40	64	0	BIRZ	-	40-60	5¼	CEMS		D
9/22	1	0.82	38	NG	NG	0.62	1.08	0.78	1.07	0	0	40	64	0	BIRZ	-	40	3-11	T		D
	3	0.65	9	NG	NG	0.62	0.94	0.87	1.05	0.65	0	40	64	0	BIRZ	-	St	-	CEMS		I/O - SR_{ART}
	4										0.42										
	6	0.67	13				0.98				0										
	7										0.42										
	9	0.71	18				1.03				0										
	10										0.42										
	12	0.74	23				1.08				0										
	13										0.42										
	15	0.76	27				1.12				0										
	16										0.42										

Data Summary Sheet

TEST: Natural Gas Reburning FACILITY: PBS PAGE: 18

		1	2	3	4	5	6	7	8	9	10	11	12	13	14	15	16	17	18	19	20
DATE & DATA BOOK #	Data Pt. #	FR_{TOT}	$\frac{FR_{SEC}}{FR_{PRI}}$	PRI FUEL	SEC FUEL	SR_1	SR_2	SR_3	SR_4	PRI FUEL DOPANT	SEC FUEL DOPANT	SEC FUEL INJ	FINAL AIR INJ	PRI ZONE MIXING	SEC FUEL NOZZLE	INS. ZONE	SAMPLE LOCATION AXIAL	SAMPLE LOCATION RADIAL	SAMPLE TYPE(S)		TEST VARIABLE
A-5		MW	%							% N_2 by wt	% N_2 by wt	in. into boiler	in. into boiler	sec air $\frac{ax}{rad}$			in. into boiler	in. radius			
9/22	18	0.77	31	NG	NG	0.62	1.15	0.88	1.05	0.65	0	40	64	0	BIR2	–	St	–	CEMS		I/o – SR_{PRI}
	19										0.42										
	21					0.62	1.13				0										
	22										0.42										
	24					0.61	1.03				0										
	25										0.42										
	27					0.58	0.94				0										
	28										0.42										
	30					0.60	0.97				0										
	31										0.42										
9/23	3-7	0.74	24	NG	NG	0.62	1.09	0.87	1.08	0.65	0	40	64	0	BIR2	–	40-60	5¼	CEMS	HCN, NH3	▷
	9	0.65	9	NG	NG	0.61	1.07	0.98	1.08	0.65	0	40	64	0	BIN3	–	St	–	CEMS		I/o – Mixing
	10										0.54										
	11	0.74	24					0.86			0										
	12										0.42										
	13	0.79	33					0.81			0										
	14										0.42										
	16	0.65	9					0.98		0.16	0										
	17										0.54										
	18	0.74	24					0.86			0										
	19										0.42										
	20	0.79	33					0.81			0										
	21										0.42										
	23	0.65	12					0.96		0	0										
	24										0.42										
	25	0.74	24					0.86			0										
	26										0.42										
	27	0.79	33					0.81			0										
	28										0.42										
	29	0.66	12					0.96		0.16	0										

C.F. 620

Data Summary Sheet

TEST: Natural Gas Reburning FACILITY: PBS PAGE: 19

DATE & DATA BOOK #	Data Pt. #	1	2	3	4	5	6	7	8	9	10	11	12	13	14	15	16	17	18	19	20
		FR_{TOT}	FR_{SEC}/FR_{PRI}	PRI FUEL	SEC FUEL	SR_1	SR_2	SR_3	SR_4	PRI FUEL DOPANT	SEC FUEL DOPANT	SEC FUEL INJ	FINAL AIR INJ	PRI ZONE MIXING	SEC FUEL NOZZLE	INS. ZONE	SAMPLE LOCATION AXIAL	RADIAL	SAMPLE TYPE(S)		TEST VARIABLE
A-5		MW	%							$\%N_2$ by wt	$\%N_2$ by wt	in. into boiler	in. into boiler	sec.air ax/rad			in. into boiler	in. radius			
9/23	30	0.66	12	NG	NG	0.61	1.07	0.96	1.08	0.16	0.42	90	69	0	BIN3	–	St	–	CEMS		I/c - Mixing
	31									0.65	0										
	32										0.42										
9/26	3-7	0.74	29	NG	NG	0.62	1.08	0.87	1.07	0.65	0	40	64	0	B1R3	–	40 Lc	5 ¼	CEMS	HCN, NH3	D
	9	0.65	9	NG	NG	0.57	0.94	0.86	1.03	0.65	0	40	64	0	B1R3	–	St	–			I/c - SR_{PRI}
	10										0.42										
	11	0.67	13								0										
	12										0.42										
	13	0.70	18								0										
	14										0.42										
	15	0.74	29								0										
	16										0.42										
9/27	2	0.65	9	NG	NG	0.62	0.99	0.91	1.08	0.65	0	40	69	0	BIR3	–	St	–	CEMS		I/c - SR_{PRI}
	3										0.42										
	4	0.67	13					0.88			0										
	5										0.42										
	6	0.70	18					0.84			0										
	7										0.42										
	8	0.74	24					0.80			0										
	9										0.42										
	11	0.65	9				1.02	0.91	1.03		0										
	12										0.42										
	13	0.67	13					0.90			0										
	14										0.42										
	15	0.70	18					0.86			0										
	16										0.42										
	17	0.74	29					0.82			0										
	18										0.42										
	20	0.67	13				1.09	0.97	1.08		0										
	21										0.42										

C.F. 620

Data Summary Sheet

TEST: Natural Gas Reburning FACILITY: PPS PAGE: 20

		1	2	3	4	5	6	7	8	9	10	11	12	13	14	15	16	17	18	19	20
DATE & DATA BOOK #	Data Pt. #	FR_{TOT}	FR_{SEC}/FR_{PRI}	PRI FUEL	SEC FUEL	SR_1	SR_2	SR_3	SR_4	PRI FUEL DOPANT	SEC FUEL DOPANT	SEC FUEL INJ	FINAL AIR INJ	PRI ZONE MIXING	SEC FUEL NOZZLE	INS. ZONE	SAMPLE LOCATION AXIAL	RADIAL	SAMPLE TYPE(S)		TEST VARIABLE
A-5		MW	%							$\%N_2$ by wt	$\%N_2$ by wt	in. into boiler	in. into boiler	sec.air ~~ax~~/rad			in. into boiler	in. radius			
9/27	22	0.80	18	NG	NG	0.62	1.09	0.93	1.03	0.65	0	40	64	0	BIR3	–	St	–	CEMS		I/O – SR_{AA4}
	23										0.42										
	24	0.74	24					0.88			0										
	25										0.42										
	27	0.65	9			0.57	0.92	0.84	1.02	0.65	0										
	28										0.42										
	29	0.67	13					0.81			0										
	30										0.42										
	31	0.70	18					0.78			0										
	32										0.42										
	33	0.74	24					0.74			0										
	34										0.42										
9/28	2	0.74	24	NG	NG	0.62	1.07	0.86	1.07	0.65	0	40	64	0	BIR3	–	St	–	CEMS		I/O – $(N_2)_R$
	3										0.07										
	4										0.21										
	5										0.40										
	6										0.60										
	7										0.81										
	8										1.01										
	9	0.74	24	NG	NG	0.62	1.07	0.86	1.07	0.65	0	40	64	0	BIR3	–	St	–	CEMS		I/O – SR_{80}
	10								0.97												
	11								1.03												
	12								1.10												
	13								1.14												
	14								1.19												
	12-28	0.74	24	NG	NG	0.61	1.05	0.85	1.05	0	0.42	40	64	0	BIN3	–	40-60	5 1/4	CEMS,	HCN, NH_3	D
	29										0.42						St	–	CEMS		I/O
	30										0										
A-6 11/29	2	0.74	24	NG	NG	0.62	1.03	0.83	1.03	0.65	0	40	64	0	B2N1	–	St	–	CEMS		I/O

C.F. 620

Data Summary Sheet

TEST: Natural Gas Reburning FACILITY: PBS PAGE: 21

DATE & DATA BOOK #	Data Pt. #	1	2	3	4	5	6	7	8	9	10	11	12	13	14	15	16	17	18	19	20
		FR_{TOT}	$\frac{FR_{SEC}}{FR_{PRI}}$	PRI FUEL	SEC FUEL	SR_1	SR_2	SR_3	SR_4	PRI FUEL DOPANT	SEC FUEL DOPANT	SEC FUEL INJ	FINAL AIR INJ	PRI ZONE MIXING	SEC FUEL NOZZLE	INS. ZONE	SAMPLE LOCATION AXIAL	SAMPLE LOCATION RADIAL	SAMPLE TYPE(S)	SAMPLE TYPE(S)	TEST VARIABLE
A6		MW	%							$\%N_2$ by wt	$\%N_2$ by wt	in. into boiler	in. into boiler	secair $\frac{ax}{rad}$			in. into boiler	in. radius			
11/29	3	0.74	24	NG	NG	0.62	1.03	0.83	1.03	0.65	0.42	40	64	0	B2N1	-	St	-	CEMS		I/α L_{ARI}
	4										0	50	74								
	5										0.42										
	6										0	60	84								
	7										0.42										
	8										0	70	94								
	9										0.42										
	10										0	80	104								
11/30	2	0.74	24	NG	NG	0.63	1.04	0.83	1.04	0.65	0	72	84	0	B2N1	-	St	-	CEMS		I/o - L_{ARI}
	3										0.42										
	4										0	60									
	5										0.42										
	6										0	48									
	7										0.42										
	8										0	36									
	9										0.42										
	10										0	24									
	11										0.42										
	12										0	12									
	13										0.42										
	16	0.82	38					0.75			0	12									
	17										0.42										
	18										0.42	24									
	19										0										
	20										0	36									
	21										0.42										
	22										0.42	48									
	23										0										
	24										0	60									
	25										0.42										

C.F. 620

Data Summary Sheet

TEST: Natural Gas Reburning FACILITY: PBS PAGE: 22

DATE & DATA BOOK #	Data Pt. #	1 FR$_{TOT}$	2 $\frac{FR_{SEC}}{FR_{PRI}}$	3 PRI FUEL	4 SEC FUEL	5 SR$_1$	6 SR$_2$	7 SR$_3$	8 SR$_4$	9 PRI FUEL DOPANT	10 SEC FUEL DOPANT	11 SEC FUEL INJ	12 FINAL AIR INJ	13 PRI ZONE MIXING	14 SEC FUEL NOZZLE	15 INS. ZONE	16 SAMPLE LOCATION AXIAL	17 SAMPLE LOCATION RADIAL	18 SAMPLE TYPE(S)	19 SAMPLE TYPE(S)	20 TEST VARIABLE
A-6		MW	%							% N_2 by wt	% N_2 by wt	in. into boiler	in. into boiler	sec air ax/rad			in. into boiler	in. radius			
12/1	2	0.66	12	NG	NG	0.63	1.05	0.94	1.06	0.65	0	72	84	0	B2N1	-	St	-	CEMS		I/O - L_{PRI}
	3										0.42										
	4										0	60									
	5										0.42										
	6										0	48									
	7										0.42										
	8										0	36									
	9										0.42										
	10										0	24									
	11										0.42										
	12										0	12									
	13										0.42										
	16	0.74	24					0.85			0	12	84								τ_R
	17										0.42										
	18										0		72								
	19										0.42										
	20										0		60								
	21										0.42										
	22										0		48								
	23										0.42										
12/6	2	0.74	24	NG	NG	0.64	1.05	0.85	1.05	0.65	0	72	84	∞	B2N1	-	St	-	CEMS		I/O - L_{PRI}
	3											60									
	4											48									
	5											36									
	6											24									
	7											12									
12/7	2	0.74	24	NG	NG	0.63	1.04	0.83	1.09	0	0	40	52	0	B2N1	-	St	-	[illegible]		I/O - τ_R
	3										0.42										
	4										0		64								
	5										0.42										

C.F. 620

Data Summary Sheet

TEST: Natural Gas Reburning FACILITY: PBS PAGE: 23

		1	2	3	4	5	6	7	8	9	10	11	12	13	14	15	16	17	18	19	20
DATE & DATA BOOK #	Data Pt. #	FR_{TOT}	$\frac{FR_{SEC}}{FR_{PRI}}$	PRI FUEL	SEC FUEL	SR_1	SR_2	SR_3	SR_4	PRI FUEL DOPANT	SEC FUEL DOPANT	SEC FUEL INJ	FINAL AIR INJ	PRI ZONE MIXING	SEC FUEL NOZZLE	INS. ZONE	SAMPLE LOCATION AXIAL	RADIAL	SAMPLE TYPE(S)		TEST VARIABLE
A-6		MW	%							$\% N_2$ by wt	$\% N_2$ by wt	in. into boiler	in. into boiler	sec air $\frac{ax}{rad}$			in. into boiler	in. radius			
12/7	6	0.74	24	NG	NG	0.63	1.04	0.83	1.04	0	0	40	76	0	B2N1	-	St	-	CEMS		I/o - τ_R
	7										0.42										
	8										0		88								
	9										0.42										
	11										0		94								
	12										0.42										
	13										0		100								
	14										0.42										
	17-25	0.74	24	NG	NG	0.63	1.04	0.83	1.04	0	0	40	88	0	B2N1	-	40-88	7 1/4	CEMS	HCN, NH_3	D
12/8	3-11	0.74	24	NG	NG	0.63	1.04	0.83	1.04	0	0.42	40	88	0	B2N1	-	90-88	7 1/4	CEMS	HCN, NH_3	D
	15-18	0.74	24	NG	NG	0.63	1.04	0.83	1.04	0	0	40	88	0	B2N1	-	60-80	5 1/4	CEMS	HCN, NH_3	D
12/9	3-5	0.74	24	NG	NG	0.64	1.05	0.84	1.06	0	0	40	64	0	B2N1	-	50-60	5 1/4	CEMS	HCN, NH_3	D
	6-8	0.74	24	NG	NG	0.64	1.05	0.84	1.06	0	0.42	40	64	0	B2N1	-	50-60	5 1/4	CEMS	HCN, NH_3	D
	9-11	0.74	24	NG	NG	0.64	1.05	0.84	1.06	0	0.42	40	64	0	B2N1	-	50-60	9 1/4	CEMS	HCN, NH_3	D
12/15	2	0.66	12	NG	NG	0.98	1.12	1.00	1.10	0.65	0	40	64	0	B2N1	-	St	-	CEMS		I/o -
	3										0.42										High
	4	0.74	24					0.89			0										NO_{PRI}
	5										0.42										
	6	0.82	38					0.80			0										
	7										0.42										
A-7																					
1/4	2	0.74	24	NG	NG	0.62	1.04	0.84	1.05	0	0	40	64	0	B2N1	-	St	-	CEMS		I/o -
	3									0.65											Mixing
	6									0					B2N6						
	7									0.65											
	8									0					B2N2						
	9									0.65											
	10									0					B2N3						
	11									0.65											
	12									0					B2N4						

C.F. 620

Data Summary Sheet

TEST: Natural Gas Reburning FACILITY: PBS PAGE: 24

		1	2	3	4	5	6	7	8	9	10	11	12	13	14	15	16	17	18	19	20
DATE & DATA BOOK #	Data Pt. #	FR_{TOT}	FR_{SEC}/FR_{PRI}	PRI FUEL	SEC FUEL	SR_1	SR_2	SR_3	SR_4	PRI FUEL DOPANT	SEC FUEL DOPANT	SEC FUEL INJ	FINAL AIR INJ	PRI ZONE MIXING	SEC FUEL NOZZLE	INS. ZONE	SAMPLE LOCATION AXIAL	RADIAL	SAMPLE TYPE(S)		TEST VARIABLE
A-7		MW	%							% N_2 by wt	% N_2 by wt	in. into boiler	in. into boiler	secair ax/rad			in. into boiler	in. radius			
1/4	13	0.74	24	NG	NG	0.63	1.04	0.84	1.05	0.65	0	40	64	0	BZN4	–	St	–	CEMS		I/o-
	14									0					BZN5						Mixing
	15									0.65											
1/12	17	0.74	24	NG	NG	0.63	1.05	0.84	1.04	0.65	0	40	64	0	BZN5	–	St	–	CEMS		I/o-
	18										0.42										SR_{PRI}
	19						0.92	0.74			0										
	20										0.42										
	21	0.68	15					0.80			0										
	23	0.62	5				0.87	0.83			0										
	26	0.74	24	NG	NG	0.64	–	0.97	1.05	0.65	0	0	64	0	BZN5	–	St	–	CEMS		I/o-
	27										0.42										ADV.
	28							0.86			0										BIAS
	29										0.92										
	30							0.73			0.92										
	31										0										
1/13	3	0.74	24	NG	NG	0.85	–	1.08	–	0.65	0	0	–	0	BZN5	–	St	–	CEMS		I/o-
	4										0.42										ADV.
	5							0.97	1.08		0		64								BIAS
	6										0.42										
	7							0.89			0										
	8										0.42										
	9							0.85			0										
	10										0.42										
	11							0.76			0										
	12										0.42										
2/9	3-7	0.74	24	NG	NG	0.64	1.06	0.85	1.06	0.65	0	40	64	0	BIR2	–	40-60	7¼	CEMS	,UHC	D
	9-14																40-60	5¼			
A-8																					
2/23	2	0.66	12	NG	NG	0.66	1.04	0.92	1.04	0.65	0	51	78	0	BIR2	2	St	–	CEMS		I/o-
	3										0.42										τ_2

C.F. 620

Data Summary Sheet

TEST: Natural Gas Reburning FACILITY: PBS PAGE: 25

		1	2	3	4	5	6	7	8	9	10	11	12	13	14	15	16	17	18	19	20
DATE & DATA BOOK #	Data Pt. #	FR_{TOT}	FR_{SEC}/FR_{PRI}	PRI FUEL	SEC FUEL	SR_1	SR_2	SR_3	SR_4	PRI FUEL DOPANT	SEC FUEL DOPANT	SEC FUEL INJ	FINAL AIR INJ	PRI ZONE MIXING	SEC FUEL NOZZLE	INS. ZONE	SAMPLE LOCATION AXIAL	SAMPLE LOCATION RADIAL	SAMPLE TYPE(S)		TEST VARIABLE
A-8		MW	%							% N_2 by wt	% N_2 by wt	in. into boiler	in. into boiler	sec.air ax/rad			in. into boiler	in. radius			
2/23	4	0.74	24	NG	NG	0.66	1.04	0.83	1.04	0.65	0	51	78	0	BIR2	2	St	-	CEMS		I/o-L_2
	5										0.42										
	6	0.78	32					0.78			0										
	7										0.42										
	8	0.66	12	NG	NG	0.66	1.04	0.92	1.04	0.65	0	40	67	0	BIR2	2	St	-	CEMS		I/o
	10										0.42										
	11	0.74	24					0.83			0										
	12										0.42										
	13	0.78	32					0.78			0										
	14										0.42										
	17	0.66	12					0.92		0.16	0										
	18										0.42										
	19	0.74	24					0.83			0										
	20										0.42										
	21	0.78	32					0.78			0										
	22										0.42										
	25	0.66	12					0.92		0	0										
	26										0.42										
	27	0.74	24					0.83			0										
	28										0.42										
	29	0.78	32					0.78			0										
	30										0.42										
	33	0.66	12			0.96	1.13	1.01	1.13	0.65	0										
	34										0.42										
	35	0.74	24					0.91			0										
	36										0.42										
	37	0.78	32					0.88			0										
	38										0.42										
	41	0.66	12					1.01		0	0										
	42										0.42										

C.F. 620

Data Summary Sheet

TEST: Natural Gas Reburning

FACILITY: PBS

PAGE: 26

		1	2	3	4	5	6	7	8	9	10	11	12	13	14	15	16	17	18	19	20
DATE & DATA BOOK #	Data Pt. #	FR_{TOT}	$\frac{FR_{SEC}}{FR_{PRI}}$	PRI FUEL	SEC FUEL	SR_1	SR_2	SR_3	SR_4	PRI FUEL DOPANT	SEC FUEL DOPANT	SEC FUEL INJ	FINAL AIR INJ	PRI ZONE MIXING	SEC FUEL NOZZLE	INJ. ZONE	SAMPLE LOCATION AXIAL	RADIAL	SAMPLE TYPE(S)		TEST VARIABLE
A-8		MW	%							% N_2 by wt	% N_2 by wt	in. into boiler	in. into boiler	secair ax/rad			in. into boiler	in. radius			
2/23	43	0.74	24	NG	NG	0.96	1.13	0.91	1.13	0	0	40	67	0	B1R2	2	St	-	CEMS		I/O
	44										0.42										
	45	0.78	32					0.88			0										
	46										0.42										
	50-56	0.74	24	NG	NG	0.66	1.07	0.86	1.07	0.65	0	40	67	0	B1R2	2	41-70	5¼	CEMS		D
2/24	3-8	0.74	24	NG	NG	0.66	1.07	0.86	1.06	0.65	0	40	67	0	B1R2	2	41-65	5¼	CEMS,	HCN, NH$_3$	D
	11-20																40	1-10	T, V		
2/27	3-11	0.74	24	NG	NG	0.67	1.08	0.86	1.07	0.65	0.42	40	67	0	B1R2	2	41-80	5¼	CEMS		D
	13-17																40	1-10	CEMS		
2/28	6-12	0.71	21	NG	NG	0.66	1.07	0.89	1.09	0.65	0.49	40	67	0	B1R3	2	41-80	5¼	CEMS		D
	14-20																40	1-7	V		
2/29	3-8	0.70	19	NG	NG	0.66	1.08	0.91	1.11	0.65	0.42	40	67	0	B1R3	2	41-65	9¼	CEMS		D
	10-15																41-65	5¼	CEMS,	HCN, NH$_3$	
3/1	3-11	0.70	18	NG	NG	0.66	1.09	0.92	1.12	0.65	0.42	40	67	0	B1R3	2	41-80	5¼	T		D
3/2	2	0.74	24	NG	NG	0.67	1.09	0.87	1.08	0.65	0	40	64	0	B3N1	2	St	-	CEMS		I/O-
	3										0.42										τ_3
	4										0.42	40	52								
	5										0										
	6										0	40	76								
	7										0.42										
	8										0.42	40	88								
	9										0										
	14									0	0	40	88								
	15										0.42										
	16										0.42	40	76								
	17										0										
	18										0	40	64								
	19										0.42										
	20										0.42	40	52								
	21										0										

C.F. 620

Data Summary Sheet

TEST : Natural Gas Reburning FACILITY : PBS PAGE : 27

		1	2	3	4	5	6	7	8	9	10	11	12	13	14	15	16	17	18	19	20
DATE & DATA BOOK #	Data Pt. #	FR_{TOT}	$\frac{FR_{SEC}}{FR_{PRI}}$	PRI FUEL	SEC FUEL	SR_1	SR_2	SR_3	SR_4	PRI FUEL DOPANT	SEC FUEL DOPANT	SEC FUEL INJ	FINAL AIR INJ	PRI ZONE MIXING	SEC FUEL NOZZLE	INS. ZONE	SAMPLE LOCATION		SAMPLE TYPE(S)		TEST VARIABLE
																	AXIAL	RADIAL			
A-8		MW	%							% N_2 by wt	% N_2 by wt	in. into boiler	in. into boiler	sec air $\frac{ax}{rad}$			in. into boiler	in. radius			
	22	0.74	24	NG	NG	0.67	1.09	0.87	1.08	0	0	40	46	0	B2N1	2	St	-	CEMS		I/O -
	23										0.42										τ_3
	27	0.66	12	NG	NG	0.66	1.07	0.97	1.08	0	0	40	64	0	B2N1	2	St	-	CEMS		I/O
	28										0.42										
	29									0.65	0.42										
	30										0										
	31	0.74	24					0.87		0.65	0										
	32										0.42										
	33									0	0.42										
	34										0										
	35	0.82	39					0.78		0	0										
	36										0.42										
	37									0.65	0.42										
	38										0										
A-9																					
4/4	2	0.62	6	NG	NG	0.94	1.07	1.01	1.08	0.65	0.63	40	64	0	B2N1	2	St	-	CEMS		I/O - Mixing
	3	0.66	12					0.96													
	4	0.70	18					0.90													
	5	0.74	24					0.86													
	6	0.77	30					0.82													
	7	0.79	34					0.80													
	10	0.62	6					1.01							B2N7						
	11	0.66	12					0.96													
	12	0.70	18					0.90													
	13	0.74	24					0.86													
	14	0.77	30					0.82													
	15	0.79	34					0.80													
4/5	2	0.62	6	NG	NG	0.93	1.11	1.05	1.11	0.65	0.63	40	64	0	B2N7	2	St	-	CEMS		I/O - Mixing
	3	0.66	12					0.99													
	4	0.70	18					0.94													

C.F. 620

Data Summary Sheet

TEST : Natural Gas Reburning FACILITY : PBS PAGE : 28

		1	2	3	4	5	6	7	8	9	10	11	12	13	14	15	16	17	18	19	20
DATE & DATA BOOK #	Data Pt. #	FR_{TOT}	$\frac{FR_{SEC}}{FR_{PRI}}$	PRI FUEL	SEC FUEL	SR_1	SR_2	SR_3	SR_4	PRI FUEL DOPANT	SEC FUEL DOPANT	SEC FUEL INJ	FINAL AIR INJ	PRI ZONE MIXING	SEC FUEL NOZZLE	INS. ZONE	SAMPLE LOCATION AXIAL	RADIAL	SAMPLE TYPE(S)		TEST VARIABLE
		MW	%							% N_2 by wt	% N_2 by wt	in. into boiler	in. into boiler	sec air ax/rad			in. into boiler	in. radius			
	5	0.74	24	NG	NG	0.93	1.11	0.89	1.11	0.65	0.63	40	64	0	B2N7	2	St	-	CEMS		I/o- Mixing
	6	0.77	30					0.85													
	7	0.79	34					0.83													
	9	0.62	6					1.05							B2N1						
	10	0.66	12					0.99													
	11	0.70	18					0.94													
	12	0.74	24					0.89													
	13	0.77	30					0.85													
	14	0.79	34					0.83													
	17	0.62	6			0.65	1.06	1.00	1.06		0.63				B2N7						
	28										0.42										
	18	0.66	12					0.95			0.63										
	27										0.42										
	19	0.70	18					0.89			0.63										
	26										0.42										
	20	0.74	24					0.85			0.63										
	25										0.42										
	21	0.77	30					0.81			0.63										
	22										0.42										
	23	0.79	34					0.79			0.63										
	24										0.42										
	30	0.62	6					1.00			0.63				B2N1						
	31										0.42										
	32	0.66	12					0.95			0.63										
	33										0.42										
	34	0.70	18					0.89			0.63										
	35										0.42										
	36	0.74	24					0.85			0.63										
	37										0.42										
	38	0.77	30					0.81			0.63										

C.F. 620

Data Summary Sheet

TEST: Natural Gas Reburning FACILITY: PBS PAGE: 29

		1	2	3	4	5	6	7	8	9	10	11	12	13	14	15	16	17	18	19	20
DATE & DATA BOOK #	Data Pt. #	FR_{TOT}	FR_{SEC}/FR_{PRI}	PRI FUEL	SEC FUEL	SR_1	SR_2	SR_3	SR_4	PRI FUEL DOPANT	SEC FUEL DOPANT	SEC FUEL INJ	FINAL AIR INJ	PRI ZONE MIXING	SEC FUEL NOZZLE	INJ. ZONE	SAMPLE LOCATION AXIAL	RADIAL	SAMPLE TYPE(S)		TEST VARIABLE
A-9		MW	%							$\% N_2$ by wt	$\% N_2$ by wt	in. into boiler	in. into boiler	sec air ~~ax~~ rad			in. into boiler	in. radius			
9/5	39	0.77	30	NG	NG	0.65	1.06	0.81	1.06	0.65	0.42	40	64	0	B2N1	2	St	–	CEMS		I/o –
	40	0.79	34					0.79			0.63										Mixing
	41										0.42										
4/6	25-41	0.79	34	NG	NG	0.65	1.07	0.79	1.05	0.65	0.42	40	64	0	B2N7	2	40-80	9 1/4	CEMS		D
	52-72																40-80	5 1/4	CEMS		
4/9	2,13	0.63	6	NG	NG	0.67	1.09	1.02	1.07	0.65	0	40	64	0	B2N7	2	St	–	CEMS		I/o –
	3,14	0.66	12					0.96													Mixing
	4,15	0.70	18					0.91													
	5	0.74	24					0.86													
	6	0.78	30					0.82													
	7	0.80	34					0.80													
	17	0.63	6					1.02							B2N1						
	18	0.66	12					0.96													
	19	0.70	18					0.91													
	20	0.74	24					0.86													
	21	0.78	30					0.82													
	22	0.80	34					0.80													
	26	0.63	6					1.02							B2N8						
	27	0.66	12					0.96													
	28	0.70	18					0.91													
	29	0.74	24					0.86													
	30	0.78	30					0.82													
	31	0.80	34					0.80													
	8	0.80	34	NG	NG	0.67	1.09	0.80	1.07	0.65	0.45	40	64	0	B2N7	2	St	–	CEMS		I/o –
	9	0.74	24				0.94	0.76													SReas
	10						1.09	0.87													
	23						1.09	0.87							B2N1						
	24						0.94	0.76													
5/4	2	0.66	12	NG	NG	0.65	1.06	0.95	1.07	0.65	0	40	69	0	B2N7	2	St	–	CEMS		I/o –
	3										0.42										Mixing

C.F. 620

Data Summary Sheet

TEST: Natural Gas Reburning FACILITY: PBS PAGE: 30

DATE & DATA BOOK #	Data Pt. #	1 FR	2	3	4	5	6	7	8	9	10	11	12	13	14	15	16	17	18	19	20
		FR_{TOT}	FR_{SEC}/FR_{PRI}	PRI FUEL	SEC FUEL	SR_1	SR_2	SR_3	SR_4	PRI FUEL DOPANT	SEC FUEL DOPANT	SEC FUEL INJ	FINAL AIR INJ	PRI ZONE MIXING	SEC FUEL NOZZLE	INS. ZONE	SAMPLE LOCATION AXIAL	RADIAL	SAMPLE TYPE(S)		TEST VARIABLE
A-9		MW	%							$\%N_2$ by wt	$\%N_2$ by wt	in. into boiler	in. into boiler	sec.air ax/rad			in. into boiler	in. radius			
5/4	4	0.74	24	NG	NG	0.65	1.06	0.86	1.07	0.65	0	40	64	0	B2N7	2	St	-	CEMS		I/o - Mixing Air Plugged
	5										0.42										
	8	0.66	12					0.96		0.20	0										
	9										0.42										
	10	0.74	24					0.86			0										
	11										0.42										
	14	0.66	12					0.95		0	0										
	15										0.42										
	16	0.74	24					0.86			0										
	17										0.42										
	20	0.66	12					0.95		0.65	0				B2N1						
	21										0.42										
	22	0.74	24					0.86			0										
	23										0.42										
	26	0.66	12	NG	NG	0.65	1.06	0.95	1.07	0.65	0	40	64	0	B2N1	2	St	-	CEMS		I/o - Mixing
	27										0.42										
	28	0.74	24					0.86			0										
	29										0.42										
	30	0.82	38					0.77			0										
	31										0.42										
	34	0.66	12					0.95		0.20	0										
	35										0.42										
	36	0.74	24					0.85			0										
	37										0.42										
	38	0.82	38					0.77			0										
	39										0.42										
	42	0.66	12					0.95		0	0										
	43										0.42										
	44	0.74	24					0.85			0										
	45										0.42										

C.F. 620

Data Summary Sheet

TEST : Natural Gas Reburning FACILITY : PBS PAGE : 31

		1	2	3	4	5	6	7	8	9	10	11	12	13	14	15	16	17	18	19	20
DATE & DATA BOOK #	Data Pt. #	FR_{TOT}	$\frac{FR_{SEC}}{FR_{PRI}}$	PRI FUEL	SEC FUEL	SR_1	SR_2	SR_3	SR_4	PRI FUEL DOPANT	SEC FUEL DOPANT	SEC FUEL INJ	FINAL AIR INJ	PRI ZONE MIXING	SEC FUEL NOZZLE	INJ. ZONE	SAMPLE LOCATION AXIAL	RADIAL	SAMPLE TYPE(S)		TEST VARIABLE
A-9		MW	%							% N_2 by wt	% N_2 by wt	in. into boiler	in. into boiler	sec air $\frac{ax}{rad}$			in. into boiler	in. radius			
5/4	46	0.82	38	NG	NG	0.65	1.06	0.77	1.07	0	0	40	64	0	B2N1	2	St	-	CEMS		I/o -
	47										0.42										Mixing
4/10	2	0.66	12	NG	NG	0.67	1.10	0.98	1.10	0.65	0	40	48	0	B2N1	2	St	-	CEMS		I/o -
	3										0.42										τ_R
	4	0.74	24					0.88			0										
	5										0.42										
	6	0.80	34					0.81			0										
	7										0.42										
	8	0.66	12					0.98			0		54								
	9										0.42										
	10	0.74	24					0.88			0										
	11										0.42										
	12	0.80	34					0.81			0										
	13										0.42										
	14	0.66	12					0.98			0		60								
	15										0.42										
	16	0.74	24					0.88			0										
	17										0.42										
	18	0.80	34					0.81			0										
	19										0.42										
	23	0.66	12					0.98			0		66								
	24										0.42										
	25	0.74	24					0.88			0										
	26										0.42										
	27	0.80	34					0.81			0										
	28										0.42										
	29	0.66	12					0.98			0		72								
	30										0.42										
	31	0.74	24					0.88			0										
	32										0.42										

C.F. 620

Data Summary Sheet

TEST: Natural Gas Reburning FACILITY: PBS PAGE: 32

		1	2	3	4	5	6	7	8	9	10	11	12	13	14	15	16	17	18	19	20
DATE & DATA BOOK #	Data Pt. #	FR_{TOT}	$\frac{FR_{SEC}}{FR_{PRI}}$	PRI FUEL	SEC FUEL	SR_1	SR_2	SR_3	SR_4	PRI FUEL DOPANT	SEC FUEL DOPANT	SEC FUEL INJ	FINAL AIR INJ	PRI ZONE MIXING	SEC FUEL NOZZLE	INS. ZONE	SAMPLE LOCATION AXIAL	RADIAL	SAMPLE TYPE(S)		TEST VARIABLE
A-9		MW	%							$\% N_2$ by wt	$\% N_2$ by wt	in. into boiler	in. into boiler	sec air $\frac{ax}{rad}$			in. into boiler	in. radius			
4/10	33	0.80	34	NG	NG	0.67	1.10	0.81	1.10	0.65	0	40	72	0	BZNI	2	St	-	CEMS		$I/o-\tau_R$
	34										0.42										
	35	0.66	12					0.98			0		78								
	36										0.42										
	37	0.74	24					0.88			0										
	38										0.42										
	39	0.80	34					0.81			0										
	40										0.42										
	41	0.66	12					0.98			0		84								
	42										0.42										
	43	0.74	24					0.88			0										
	44										0.42										
	45	0.80	34					0.81			0										
	46										0.42										
	47	0.66	12					0.98			0		90								
	48										0.42										
	49	0.74	24					0.88			0										
	50										0.42										
	51	0.80	34					0.81			0										
	52										0.42										
4/11	2	0.66	12	NG	NG	0.70	1.09	0.97	1.08	0	0	48	49	0	BZNI	2	St	-	CEMS		$I/o-\tau_R$
	3										0.42										
	4	0.74	24					0.87			0										
	5										0.42										
	6	0.80	34					0.81			0										
	7										0.42										
	8	0.66	12					0.97			0		55								
	9										0.42										
	10	0.74	24					0.87			0										
	11										0.42										

C.F. 620

Data Summary Sheet

TEST : Natural Gas Reburning FACILITY : PBS PAGE : 33

		1	2	3	4	5	6	7	8	9	10	11	12	13	14	15	16	17	18	19	20
DATE & DATA BOOK #	Data Pt. #	FR_{TOT}	$\frac{FR_{SEC}}{FR_{PRI}}$	PRI FUEL	SEC FUEL	SR_1	SR_2	SR_3	SR_4	PRI FUEL DOPANT	SEC FUEL DOPANT	SEC FUEL INJ	FINAL AIR INJ	PRI ZONE MIXING	SEC FUEL NOZZLE	INS. ZONE	SAMPLE LOCATION AXIAL	RADIAL	SAMPLE TYPE(S)		TEST VARIABLE
A-9		MW	%							% N_2 by wt	% N_2 by wt	in. into boiler	in. into boiler	sec air $\frac{ax}{rad}$			in. into boiler	in. radius			
4/11	12	0.80	34	NG	NG	0.70	1.09	0.81	1.08	0	0	48	55	0	B2N1	2	St	-	CEMS		I/o - τ_R
	13										0.42										
	14	0.66	12					0.97			0		61								
	15										0.42										
	16	0.74	24					0.87			0										
	17										0.42										
	18	0.80	34					0.81			0										
	19										0.42										
	22	0.66	12					0.97			0		67								
	23										0.42										
	24	0.74	24					0.87			0										
	25										0.42										
	26	0.80	34					0.81			0										
	27										0.42										
	28	0.66	12					0.97			0		73								
	29										0.42										
	30	0.74	24					0.87			0										
	31										0.42										
	32	0.80	34					0.81			0										
	33										0.42										
	36	0.65	12	NG	NG	0.65	1.08	0.86	1.07	0.65	0	47	49	0	B2N1	2	St	-	CEMS		I/o - τ_R
	37										0.42										
	38	0.73	25					0.86			0										
	39										0.42										
	40	0.78	35					0.80			0										
	41										0.42										
A-10																					
5/17	2	0.80	35	NG	NG	0.65	1.07	0.79	1.08	0.65	0	40	64	0	B3N9	2	St	-	CEMS		I/o
	3										0.62										
	4	0.79	24					0.86			0.62										

C.F. 620

Data Summary Sheet

TEST: Natural Gas Reburning FACILITY: PBS PAGE: 34

DATE & DATA BOOK #	Data Pt. #	1 FR$_{TOT}$	2 $\frac{FR_{SEC}}{FR_{PRI}}$	3 PRI FUEL	4 SEC FUEL	5 SR_1	6 SR_2	7 SR_3	8 SR_4	9 PRI FUEL DOPANT	10 SEC FUEL DOPANT	11 SEC FUEL INJ	12 FINAL AIR INJ	13 PRI ZONE MIXING	14 SEC FUEL NOZZLE	15 INS. ZONE	16 SAMPLE LOCATION AXIAL	17 RADIAL	18 SAMPLE TYPE(S)	19	20 TEST VARIABLE
A-10		MW	%							%N_2 by wt	%N_2 by wt	in. into boiler	in. into boiler	sec air $\frac{ax}{rad}$			in. into boiler	in. radius			
5/17	5	0.74	24	NG	NG	0.65	1.07	0.86	1.08	0.65	0	40	64	0	B3N9	2	St	-	CEMS		I/o
	6	0.66	12					0.96			0										
	7										0.62										
7/10	2	0.76	28	NG	NG	0.64	0.95	0.75	1.08	0.65	0	40	64	0	B3N9	2	St	-	CEMS		I/o - SR_2
	3										0.42										
	4	0.71	20					0.80			0.42										
	5										0										
	6	0.66	12					0.85			0										
	7										0.42										
	10	0.76	28				1.06	0.83		0.28	0										
	11										0.42										
	12	0.71	20					0.89			0.42										
	13										0										
	14	0.66	12					0.95			0										
	15										0.42										
	18	0.76	28				0.95	0.74		0.28	0										
	19										0.42										
	20	0.71	20					0.79			0.42										
	21										0										
	22	0.66	12					0.85			0										
	23										0.42										
	27	0.76	28				1.00	0.78		0.38	0										
	28										0.42										
	29	0.71	20					0.84			0.42										
	30										0										
	31	0.66	12					0.89			0										
	32										0.42										
	36	0.76	28				1.14	0.95		0.23	0										
	37										0.42										
	38	0.71	20					1.01			0.42										

C.F. 620

Data Summary Sheet

TEST: Natural Gas Reburning FACILITY: PBS PAGE: 35

		1	2	3	4	5	6	7	8	9	10	11	12	13	14	15	16	17	18	19	20
DATE & DATA BOOK #	Data Pt. #	FR_{TOT}	FR_{SEC}/FR_{PRI}	PRI FUEL	SEC FUEL	SR_1	SR_2	SR_3	SR_4	PRI FUEL DOPANT	SEC FUEL DOPANT	SEC FUEL INJ	FINAL AIR INJ	PRI ZONE MIXING	SEC FUEL NOZZLE	INS. ZONE	SAMPLE LOCATION AXIAL	RADIAL	SAMPLE TYPE(S)		TEST VARIABLE
A-10		MW	%							$\%N_2$ by wt	$\%N_2$ by wt	in. into boiler	in. into boiler	sec air ~~ax~~ rad			in. into boiler	in. radius			
7/10	39	0.71	20	NG	NG	0.64	1.14	0.95	1.08	0.23	0	40	64	0	B3N9	2	St	-	CEMS		I/O - SR_2
	40	0.66	12					1.01			0										
	41										0.42										
	44	0.76	28	NG	NG	0.64	1.06	0.83	1.13	0.28	0	40	64	0	B3N9	2	St	-	CEMS		I/O - SR_4
	45								1.10												
	46								1.05												
	47								1.00												
	48								0.94												
7/13	2	0.66	12	NG	NG	0.91	1.06	0.95	1.07	0	0	40	52	0	B3N9	2	St	-	CEMS		I/O - Temp
	3										0.42										
	4	0.73	24					0.85			0.42										
	5										0										
	6	0.76	29					0.82			0										
	7	0.79	35					0.79			0										
	8										0.42										
	9	0.79	35					0.79			0.42	40	64								
	10										0										
	11	0.73	24					0.85			0										
	12										0.42										
	13	0.66	12					0.95			0.42										
	14										0										
	16	0.66	12					0.95			0	40	76								
	17										0.42										
	18	0.73	24					0.85			0.42										
	19										0										
	20	0.79	35					0.79			0										
	21										0.42										
	28	0.66	12					0.95			0	40	88								
	29										0.42										
	30	0.73	24					0.85			0.42										

C.F. 620

Data Summary Sheet

TEST: Natural Gas Reburning FACILITY: PBS PAGE: 36

		1	2	3	4	5	6	7	8	9	10	11	12	13	14	15	16	17	18	19	20
DATE & DATA BOOK #	Data Pt. #	FR_{TOT}	$\frac{FR_{SEC}}{FR_{PRI}}$	PRI FUEL	SEC FUEL	SR_1	SR_2	SR_3	SR_4	PRI FUEL DOPANT	SEC FUEL DOPANT	SEC FUEL INJ	FINAL AIR INJ	PRI ZONE MIXING	SEC FUEL NOZZLE	INS. ZONE	SAMPLE LOCATION AXIAL	RADIAL	SAMPLE TYPE(S)		TEST VARIABLE
		MW	%							% N_2 by wt	% N_2 by wt	in. into boiler	in. into boiler	sec air $\frac{ax}{rad}$			in. into boiler	in. radius			
A-10 7/13	31	0.73	24	NG	NG	0.91	1.06	0.85	1.07	0	0	40	88	0	B3N9	2	St	-	CEMS		I/o-Temp.
	32	0.79	35					0.79			0										
	33										0.42										
	35	0.79	35					0.79			0	10	88								
	36										0.42										
	37	0.73	24					0.85			0.42										
	38										0										
	39	0.66	12					0.95			0										
	40										0.42										
	41	0.66	12					0.95			0.42	10	76								
	42										0										
	43	0.73	24					0.85			0										
	44										0.42										
	45	0.79	35					0.79			0.42										
	46										0										
	47	0.79	35					0.79			0	10	64								
	48										0.42										
	49	0.73	24					0.85			0.42										
	50										0										
	51	0.66	12					0.95			0										
	52										0.42										
	53	0.66	12					0.95			0.42	10	52								
	54										0										
	55	0.73	24					0.85			0										
	56										0.42										
	57	0.79	35					0.79			0.42										
	58										0										
8/9	15	0.82	39	NG	NG	1.10	-	0.80	1.10	0	0	10	88	0	B3N9	2	St	-	CEMS		I/o-Temp.
	16										0.42										
	17	0.82	39								0.42	10	76								

C.F. 620

Data Summary Sheet

TEST: Natural Gas Reburning

FACILITY: PBS

PAGE: 37

		1	2	3	4	5	6	7	8	9	10	11	12	13	14	15	16	17	18	19	20
DATE & DATA BOOK #	Data Pt. #	FR_{TOT}	$\frac{FR_{SEC}}{FR_{PRI}}$	PRI FUEL	SEC FUEL	SR_1	SR_2	SR_3	SR_4	PRI FUEL DOPANT	SEC FUEL DOPANT	SEC FUEL INJ	FINAL AIR INJ	PRI ZONE MIXING	SEC FUEL NOZZLE	INS. ZONE	SAMPLE LOCATION AXIAL	RADIAL	SAMPLE TYPE(S)		TEST VARIABLE
A-10		MW	%							$\% N_2$ by wt	$\% N_2$ by wt	in. into boiler	in. into boiler	sec air $\frac{ax}{rad}$			in. into boiler	in. radius			
8/9	18	0.82	39	NG	NG	1.10	–	0.80	1.10	0	0	10	76	0	B3N9	2	St	–	CEMS		I/o- Temp.
	19	0.74	24					0.89			0.42										
	20										0.42										
	21	0.66	12					0.99			0.42										
	22										0										
	23	0.66	12					0.99			0	10	88								
	24										0.42										
	25	0.74	24					0.89			0.42										
	26										0										
	27	0.74	24					0.89			0	10	64								
	28										0.42										
	29	0.66	12					0.99			0.42										
	30										0										
	31	0.82	39					0.80			0										
	32										0.42										
	34	0.82	39					0.80			0	40	64								
	35										0.42										
	36	0.74	24					0.89			0.42										
	37										0										
	38	0.66	12					0.99			0										
	39										0.42										
	40	0.66	12					0.99			0.42	40	76								
	41										0										
	42	0.74	24					0.89			0										
	43										0.42										
	44	0.82	39					0.80			0.42										
	45										0										
	46	0.82	39					0.80			0	40	88								
	47										0.42										
	48	0.74	24					0.89			0.42										

C.F. 620

Data Summary Sheet

TEST: Natural Gas Reburning FACILITY: PBS PAGE: 38

		1	2	3	4	5	6	7	8	9	10	11	12	13	14	15	16	17	18	19	20
DATE & DATA BOOK #	Data Pt. #	FR_{TOT}	$\frac{FR_{SEC}}{FR_{PRI}}$	PRI FUEL	SEC FUEL	SR_1	SR_2	SR_3	SR_4	PRI FUEL DOPANT	SEC FUEL DOPANT	SEC FUEL INJ	FINAL AIR INJ	PRI ZONE MIXING	SEC FUEL NOZZLE	INS. ZONE	SAMPLE LOCATION AXIAL	RADIAL	SAMPLE TYPE(S)		TEST VARIABLE
A-10		MW	%							$\% N_2$ by wt	$\% N_2$ by wt	in. into boiler	in. into boiler	sec air $\frac{ax}{rad}$			in. into boiler	in. radius			
8/9	49	0.74	24	NG	NG	1.10	–	0.89	1.10	0	0	40	88	0	B3N9	2	St	–	CEMS		I/o -
	50	0.66	12					0.99			0										Temp.
	51										0.42										

C.F. 620

Data Summary Sheet

TEST: Natural Gas Reburning FACILITY: PBS PAGE: 39

		1	2	3	4	5	6	7	8	9	10	11	12	13	14	15	16	17	18	19	20
DATE & DATA BOOK #	Data Pt. #	FR_{TOT}	FR_{SEC}/FR_{PRI}	PRI FUEL	SEC FUEL	SR_1	SR_2	SR_3	SR_4	PRI FUEL DOPANT	SEC FUEL DOPANT	SEC FUEL INJ	FINAL AIR INJ	PRI ZONE MIXING	SEC FUEL NOZZLE	INS. ZONE	SAMPLE LOCATION AXIAL	SAMPLE LOCATION RADIAL	SAMPLE TYPE(S)		TEST VARIABLE
B-2		MW	%							$\%N_2$ by wt	$\%N_2$ by wt	in. into boiler	in. into boiler	secair ax/rad			in. into boiler	in. radius			
1/16/86	2	0.68	10	#2oil	NG	0.57	1.06	0.96	1.06	0.51	0	40	64	0	BZN5	-	St	-	CEMS		I/O
	3										0.42										
	4	0.76	19					0.87			0										
	5										0.42										
	6	0.80	23					0.83			0										
	7										0.42										
	10	0.68	10					0.96		0.16	0										
	11										0.42										
	12	0.76	19					0.87			0.42										
	13										0										
	14	0.80	23					0.83			0										
	15										0.42										
	18	0.68	10					0.96		0	0										
	19										0.42										
	20	0.76	19					0.87			0										
	21										0.42										
	22	0.80	23					0.83			0										
	23										0.42										
1/17	2	0.68	10	#2	NG	0.57	1.06	0.97	1.06	0.51	0	40	64	0	BZN1	-	St	-	CEMS		I/O
	3										0.42										
	4	0.76	19					0.88			0										
	5										0.42										
	6	0.80	23					0.84			0										
	7										0.42										
2/7	2	0.66	9	#2	NG	0.57	1.03	0.99	1.03	0.51	0	40	64	0	BZN2	-	St	-	CEMS		I/O
	3										0.51										
	4	0.75	20					0.84			0										
	5										0.42										
	6	0.78	23					0.80			0										
	7										0.42										

C.F. 620

Data Summary Sheet

TEST: Natural Gas Reburning → FACILITY: PBS PAGE: 40

		1	2	3	4	5	6	7	8	9	10	11	12	13	14	15	16	17	18	19	20
DATE & DATA BOOK #	Data Pt. #	FR_{TOT}	FR_{SEC}/FR_{PRI}	PRI FUEL	SEC FUEL	SR_1	SR_2	SR_3	SR_4	PRI FUEL DOPANT	SEC FUEL DOPANT	SEC FUEL INJ	FINAL AIR INJ	PRI ZONE MIXING	SEC FUEL NOZZLE	INS. ZONE	SAMPLE LOCATION AXIAL	RADIAL	SAMPLE TYPE(S)		TEST VARIABLE
B-2		MW	%							$\% N_2$ by wt	$\% N_2$ by wt	in. into boiler	in. into boiler	sec air ax/rad			in. into boiler	in. radius			
2/7	10	0.67	10	#2	NG	0.57	1.03	0.92	1.03	0.16	0	40	64	0	BZNZ	–	St	–	CEMS		I/O
	11										0.42										
	12	0.75	20					0.84			0										
	13										0.42										
	14	0.78	23					0.80			0										
	15										0.42										
	18	0.67	10					0.92		0	0										
	19										0.42										
	20	0.75	20					0.84			0										
	21										0.42										
	22	0.78	23					0.80			0										
	23										0.42										

C.F. 620

PBS FACILITY:

NO. 2 (DISTILLATE) FUEL OIL REBURNING

Data Summary Sheet

TEST: No. 2 Fuel Oil Reburning FACILITY: PBS PAGE: 41

DATE & DATA BOOK #	Data Pt. #	1	2	3	4	5	6	7	8	9	10	11	12	13	14	15	16	17	18	19	20
		FR_{TOT}	FR_{SEC}/FR_{PRI}	PRI FUEL	SEC FUEL	SR_1	SR_2	SR_3	SR_4	PRI FUEL DOPANT	SEC FUEL DOPANT	SEC FUEL INJ	FINAL AIR INJ	PRI ZONE MIXING	SEC FUEL NOZZLE	INS. ZONE	SAMPLE LOCATION AXIAL	SAMPLE LOCATION RADIAL	SAMPLE TYPE(S)		TEST VARIABLE
B-2		MW	%							% N_2 by wt	% N_2 by wt	in. into boiler	in. into boiler	sec air ax/rad			in. into boiler	in. radius			
1/25/84	2	0.68	14	NG	#2oil	0.64	1.06	0.91	1.06	0.65	–	40	64	0	B2505[illegible]	–	St	–	CEMS		I/O
	8	0.72	18					0.86													
1/26	2	0.68	14	NG	#2	0.64	1.05	0.90	1.05	0.65	–	40	64	0	B2505[illegible]	–	St	–	CEMS		I/O- SR_4
	3								1.09												
	4								1.12												
	5								1.16												
	7	0.74	20					0.89	1.05												
	8								1.10												
	9								1.12												
	10								1.14												
1/30	2	0.73	19	NG	#2	0.64	1.05	0.84	1.06	0.65	–	40	64	0	B2505[illegible]	–	St	–	CEMS		I/O
	4	0.68	14					0.90													
	5	0.63	6					0.99													
	8	0.73	19					0.84		0											
	9	0.68	14					0.90													
	10	0.63	6					0.99													
	13	0.73	19					0.84		0.18											
	14	0.68	19					0.90													
	15	0.63	6					0.99													
	18	0.73	19			0.97	1.07	0.85		0.21											
	19	0.68	14					0.91													
	20	0.63	6					1.00													
	23	0.73	19					0.85		0											
	24	0.68	14					0.91													
	25	0.63	6					1.00													
2/10	2,8	0.73	19	NG	#2	0.63	1.06	0.85	1.06	0.65	–	40	64	0	B2505[illegible]	–	St	–	CEMS		I/O-
	3-7																40-60	5 1/4	CEMS		D
	9											40	88				St	–	CEMS		I/O
	10											40	76								
	19											40	72								

C.F. 620

Data Summary Sheet

TEST: No. 2 Fuel Oil Reburning → FACILITY: PBS PAGE: 42

		1	2	3	4	5	6	7	8	9	10	11	12	13	14	15	16	17	18	19	20
DATE & DATA BOOK #	Data Pt. #	FR_{TOT}	$\frac{FR_{SEC}}{FR_{PRI}}$	PRI FUEL	SEC FUEL	SR_1	SR_2	SR_3	SR_4	PRI FUEL DOPANT	SEC FUEL DOPANT	SEC FUEL INJ	FINAL AIR INJ	PRI ZONE MIXING	SEC FUEL NOZZLE	INJ. ZONE	SAMPLE LOCATION AXIAL	RADIAL	SAMPLE TYPE(S)		TEST VARIABLE
B-2		MW	%							% N_2 by wt	% N_2 by wt	in. into boiler	in. into boiler	sec air ax/rad			in. into boiler	in. radius			
2/10	11-18	0.73	19	NG	#2	0.63	1.06	0.85	1.06	0.65	–	40	72	0	B2S052	–	40-70	5¼	CEMS		D
B-3																					
3/6	2	0.63	6	NG	#2	0.66	1.03	0.95	1.03	0	–	40	64	0	B2S052	2	St	–	CEMS		I/o
	3	0.69	13					0.88													
	4	0.73	19					0.82													
	7	0.63	6					0.96		0.16											
	8	0.69	13					0.88													
	9	0.73	19					0.83													
	12	0.63	6					0.96		0.65											
	13	0.69	13					0.88													
	14	0.73	19					0.83													
	17	0.63	6			0.95	1.18	1.10	1.17	0.65											
	18	0.69	13					1.01													
	19	0.73	19					0.95													
	22	0.63	6					1.10		0.16											
	23	0.69	13					1.01													
	24	0.73	19					0.95													
	27	0.63	6					1.10		0											
	28	0.69	13					1.01													
	29	0.73	19					0.95													
3/7	3-10	0.73	19	NG	#2	0.65	1.09	0.88	1.08	0.65	–	40	64	0	B2S052	2	40-80	7¼	CEMS		D
3/8	3-10	0.73	19	NG	#2	0.65	1.07	0.86	1.08	0.65	–	40	64	0	B2S052	2	40-80	7¼	CEMS		D
	15-22																40-80	5¼	CEMS		
3/12	9-11	0.73	19	NG	#2	0.65	1.09	0.88	1.09	0.65	–	40	64	0	B2S052	2	40-80	5¼	CEMS,	HCN, NH_3	D
3/13	3-6	0.73	19	NG	#2	0.65	1.08	0.87	1.08	0.65	–	40	64	0	B2S052	2	40-60	5¼	HCN,	NH_3	D
	10-14																29-37	5¼	CEMS		
3/14	3-11	0.73	19	NG	#2	0.65	1.07	0.87	1.07	0.65	–	40	64	0	B2S052	2	35-81	5¼	T		D
	16-26																40	2-10	CEMS	, T	
3/15	2,6	0.73	19	NG	#2	0.65	1.07	0.86	1.07	0.65	–	40	64	0	B2S052	2	St	–	CEMS		I/o -
	3											40	76								τ_R

C.F. 620

Data Summary Sheet

TEST: No. 2 Fuel Oil Reburning FACILITY: PBS PAGE: 43

		1	2	3	4	5	6	7	8	9	10	11	12	13	14	15	16	17	18	19	20
DATE & DATA BOOK #	Data Pt. #	FR_{TOT}	$\frac{FR_{SEC}}{FR_{PRI}}$	PRI FUEL	SEC FUEL	SR_1	SR_2	SR_3	SR_4	PRI FUEL DOPANT	SEC FUEL DOPANT	SEC FUEL INJ	FINAL AIR INJ	PRI ZONE MIXING	SEC FUEL NOZZLE	INS. ZONE	SAMPLE LOCATION AXIAL	RADIAL	SAMPLE TYPE(S)		TEST VARIABLE
B-3		MW	%							$\% N_2$ by wt	$\% N_2$ by wt	in. into boiler	in. into boiler	sec.air ~~ax~~ rad			in. into boiler	in. radius			
3/15	4	0.73	19	NG	#2	0.65	1.07	0.86	1.07	0.65	-	40	52	0	B2SOS2	2	St	-	CEMS		I/O -
	5											40	46								Ta
	10-12	0.73	19	NG	#2	0.65	1.07	0.86	1.07	0.65	-	40	64	0	B2SOS2	2	30-40	5 1/4	CEMS		D
3/28	3-10	0.73	19	NG	#2	0.66	1.07	0.87	1.08	0.65	-	40	64	0	B2SOS2	2	30-70	5 1/4	CEMS,	HCN, NH_3	D
4/12	2	0.64	6	NG	#2	0.63	1.05	0.98	1.09	0.65	-	40	64	0	B2H3.5	2	St	-	CEMS		I/O
	3	0.68	14					0.91													
	4	0.72	21					0.86													
	5	0.72	21					0.86		0.44											
	6	0.68	14					0.91													
	7	0.64	6					0.98													
	10	0.64	6					0.98		0.26											
	11	0.68	14					0.91													
	12	0.72	21					0.86													
	13	0.72	21					0.86		0.12											
	14	0.68	14					0.91													
	15	0.64	6					0.98													
	18	0.64	6					0.98		0											
	19	0.68	14					0.91													
	20	0.72	21					0.86													
4/13	3-10	0.72	21	NG	#2	0.66	1.07	0.88	1.08	0.65	-	40	64	0	B2H3.5	2	35-80	5 1/4	CEMS,	UHC	D
	11-18																35-80	7 1/4	CEMS		
	23-30																25-80	9 1/4	CEMS		
4/19	5-13	0.72	21	NG	#2	0.65	1.07	0.87	1.10	0.65	-	40	64	0	B2H2.5	2	30-80	5 1/4	CEMS	UHC	D
4/20	3-11	0.72	21	NG	#2	0.65	1.08	0.88	1.10	0.65	-	40	64	0	B2H2.5	2	30-80	5 1/4	CEMS,	HCN, NH_3	D
4/23	3-8	0.72	21	NG	#2	0.65	1.07	0.88	1.09	0.65	-	40	64	0	B2H3.5	2	40	1-11	T		D
	11-13																40-50	5 1/4	T		
4/25	4-11	0.72	21	NG	#2	0.66	1.07	0.88	1.09	0.65	-	40	64	0	B2H3.5	2	30-70	7 1/4	CEMS	, HCN	D
4/26	3-11	0.72	21	NG	#2	0.66	1.07	0.88	1.09	0.65	-	40	64	0	B2H3.5	2	30-90	5 1/4	T		D
	13-21																35-90	7 1/4	T		
	22-20																35-90	9 1/4	T		

C.F. 620

Data Summary Sheet

TEST: No. 2 Fuel Oil Reburning FACILITY: PBS PAGE: 44

DATE & DATA BOOK #	Data Pt. #	1	2	3	4	5	6	7	8	9	10	11	12	13	14	15	16	17	18	19	20
		FR_{TOT}	FR_{SEC}/FR_{PRI}	PRI FUEL	SEC FUEL	SR_1	SR_2	SR_3	SR_4	PRI FUEL DOPANT	SEC FUEL DOPANT	SEC FUEL INJ	FINAL AIR INJ	PRI ZONE MIXING	SEC FUEL NOZZLE	INJ. ZONE	SAMPLE LOCATION AXIAL	RADIAL	SAMPLE TYPE(S)		TEST VARIABLE
B-3		MW	%							% N_2 by wt	% N_2 by wt	in. into boiler	in. into boiler	sec. air ax/rad			in. into boiler	in. radius			
4/27	3,4	0.72	21	NG	#2	0.66	1.07	0.88	1.10	0.65	–	40	64	0	B2H3.5	2	40,50	5 1/4	HCN		D
4/30	3-18	0.72	21	NG	#2	0.65	1.07	0.87	1.09	0.65	–	40	64	0	B2H3.5	2	40	1-10	T, V		D
B-4																					
5/21	2	0.64	8	NG	#2	0.65	1.06	0.99	1.08	0.65	–	40	64	0	B3H3.5	2	St	–	CEMS		I/O
	3	0.68	14					0.94													
	4	0.72	21					0.88													
5/22	3-8	0.72	21	NG	#2	0.66	1.08	0.90	1.10	0.65	–	40	64	0	B3D4.0	45°, 2	40-70	5 1/4	CEMS,	HCN, NH_3	D
5/23	3-8	0.72	21	NG	#2	0.69	1.08	0.90	1.08	0.65	–	40	64	0	B3D4.0	45°, 2	35-60	9 1/4	CEMS		D
	9-14																35-60	7 1/4	CEMS		
	15-22																35-70	5 1/4	CEMS		
5/24	3-8	0.67	14	NG	#2	0.65	1.07	0.94	1.11	0.65	–	40	64	0	B3D4.0	45°, 2	40-70	5 1/4	CEMS,	HCN, NH_3	D
5/30	3-8	0.62	5	NG	#2	0.66	1.08	1.03	1.10	0.65	–	40	64	0	B3D4.0	45°, 2	40-70	5 1/4	CEMS,	HCN, NH_3	D
	10	0.62	5	NG	#2	0.66	1.08	1.03	1.09	0.65	–	40	64	0	B3D4.0	45°, 2	St	–	CEMS		I/O
	11	0.68	14					0.95													
	12	0.72	21					0.89													
	15	0.72	21					0.89		0.20											
	16	0.68	14					0.94													
	17	0.62	5					1.03													
	20	0.62	5					1.02		0											
	21	0.68	14					0.94													
	22	0.72	21					0.88													
5/31	3-9	0.72	21	NG	#2	0.66	1.08	0.89	1.08	0.20	–	40	64	0	B3D4.0	45°, 2	40-70	5 1/4	CEMS,	HCN, NH_3	D
	13-20																35-80	5 1/4	T		
6/4	3-8	0.72	21	NG	#2	0.65	1.06	0.87	1.09	0	–	40	64	0	B3D4.0	45°, 2	40-70	5 1/4	CEMS,	HCN, NH_3	D
6/5	3-8	0.72	21	NG	#2	0.66	1.09	0.89	1.10	0.65	–	40	64	0	B3D4.0	45°, 2	40-70	5 1/4	CEMS,	HCN, NH_3	D
	10-19	0.68	14	NG	#2	0.66	1.09	0.95	1.10	0.65	–	40	64	0	B3D4.0	45°, 2	40-90	5 1/4	T		D
	20-27	0.62	5	NG	#2	0.66	1.09	1.03	1.14	0.65	–	40	64	0	B3D4.0	45°, 2	40-10	5 1/4	T		D
6/6	2,6	0.72	21	NG	#2	0.66	1.09	0.90	1.10	0.65	–	40	64	0	B2D4.0	45°, 2	St	–	CEMS		I/O
	3												49								T_R
	4												54								

C.F. 620

Data Summary Sheet

TEST: No. 2 Fuel Oil Reburning FACILITY: PBS PAGE: 45

		1	2	3	4	5	6	7	8	9	10	11	12	13	14	15	16	17	18	19	20
DATE & DATA BOOK #	Data Pt. #	FR_{TOT}	FR_{SEC}/FR_{PRI}	PRI FUEL	SEC FUEL	SR_1	SR_2	SR_3	SR_4	PRI FUEL DOPANT	SEC FUEL DOPANT	SEC FUEL INJ	FINAL AIR INJ	PRI ZONE MIXING	SEC FUEL NOZZLE	INS. ZONE	SAMPLE LOCATION AXIAL	RADIAL	SAMPLE TYPE(S)		TEST VARIABLE
B-4		MW	%							% N_2 by wt	% N_2 by wt	in. into boiler	in. into boiler	sec.air ax/rad			in. into boiler	in. radius			
6/6	5	0.72	21	NG	#2	0.66	1.09	0.90	1.10	0.65	-	40	59	0	B3D4.0,	45°, 2	St	-	CEMS		I/O-
	7												69								τ_R
	8												74								
	9												79								
	10												84								
	11												89								
	12												94								
	16-21	0.62	5	NG	#2	0.66	1.09	1.04	1.10	0.65	-	40	64	0	B3D4.0,	45°, 2	50-90	≤ 1/4	T		D
6/8	2-9	0.68	14	NG	#2	0.66	1.08	0.95	1.08	0	-	40	64	0	B3D4.0,	45°, 2	40	0-9	V		D
6/12	2	0.72	21	NG	#2	0.66	1.05	0.90	1.11	0.65	-	40	64	0	B3D4.0,	45°, 2	St	-	CEMS		I/O-
	3	0.68	14					0.95													Nozzles
	4	0.62	5					1.04													
	6	0.72	21					0.90							4.0, 30°						
	7	0.68	14					0.95													
	8	0.62	5					1.04													
	10	0.72	21					0.90							4.0, 90°						
	11	0.68	14					0.95													
	12	0.62	5					1.04													
	14	0.72	21					0.90							5.0, 45°						
	15	0.68	14					0.95													
	16	0.62	5					1.04													
	18	0.72	21					0.90							3.0, 45°						
	19	0.68	14					0.95													
	20	0.62	5					1.04													
	22	0.68	14					0.95							2.0, 45°						
	23	0.62	5					1.04													
	26	0.72	21	NG	#2	0.66	1.09	0.90	1.11	0.65	-	40	64	0	B3D4.0,	45°, 2	St	-	CEMS		I/O-
	27	0.68	14					0.95													SR_2
	28	0.62	5					1.04													
	31	0.72	21			0.65	1.08	0.89	1.11	0.20											

C.F. 620

Data Summary Sheet

TEST: No. 2 Fuel Oil Reburning FACILITY: PBS PAGE: 46

		1	2	3	4	5	6	7	8	9	10	11	12	13	14	15	16	17	18	19	20
DATE & DATA BOOK #	Data Pt. #	FR_{TOT}	FR_{SEC}/FR_{PRI}	PRI FUEL	SEC FUEL	SR_1	SR_2	SR_3	SR_4	PRI FUEL DOPANT	SEC FUEL DOPANT	SEC FUEL INJ	FINAL AIR INJ	PRI ZONE MIXING	SEC FUEL NOZZLE	INJ. ZONE	SAMPLE LOCATION AXIAL	RADIAL	SAMPLE TYPE(S)		TEST VARIABLE
B-4		MW	%							$\%N_2$ by wt	$\%N_2$ by wt	in. into boiler	in. into boiler	sec air ax/rad			in. into boiler	in. radius			
6/12	32	0.68	14	NG	#2	0.65	1.08	0.95	1.11	0.20	—	40	64	0	B3D4.0	45°, 2	St	–	CEMS		I/o- SR_2
	33	0.62	5					1.03													
	35	0.72	21			0.65	0.95	0.79	1.11	0.20											
	36	0.68	14					0.84													
	37	0.62	5					0.91													
	42	0.72	21					0.79		0.44											
	43	0.68	14					0.84													
	44	0.62	5					0.91													
6/13	2	0.72	21	NG	#2	0.66	1.16	0.96	1.11	0.20	—	40	64	0	B3D4.0	45°, 2	St	–	CEMS		I/o- SR_2
	3	0.68	14					1.02													
	4	0.62	5					1.11													
	7	0.72	21				1.09	0.90													
	8	0.68	14					0.95													
	9	0.62	5					1.04													
	12	0.72	21				1.03	0.85													
	13	0.68	14					0.90													
	14	0.62	5					0.98													
	17	0.72	21					0.85		0.26											
	18	0.68	14					0.90													
	19	0.62	5					0.98													
6/14	2	0.72	21	NG	#2	1.21	—	0.99	1.13	0.65	—	40	64	—	B3D4.0	45°, 2	St	–	CEMS		I/o- Temp.
	3	0.68	14					1.06	1.16												
	4	0.62	5					1.15	1.21												
	7	0.72	21					1.00	1.14	0											
	8	0.68	14					1.06	1.17												
	9	0.62	5					1.15	1.22												
	11	0.72	21					1.00	1.14			40	52								
	12											40	76								
	13											40	88								
	16	0.72	21					1.01	1.16	0.65		0	64								

C.F. 620

Data Summary Sheet

TEST: No.2 Fuel Oil Reburning FACILITY: PBS PAGE: 47

		1	2	3	4	5	6	7	8	9	10	11	12	13	14	15	16	17	18	19	20
DATE & DATA BOOK #	Data Pt. #	FR_{TOT}	FR_{SEC}/FR_{PRI}	PRI FUEL	SEC FUEL	SR_1	SR_2	SR_3	SR_4	PRI FUEL DOPANT	SEC FUEL DOPANT	SEC FUEL INJ	FINAL AIR INJ	PRI ZONE MIXING	SEC FUEL NOZZLE	INS. ZONE	SAMPLE LOCATION AXIAL	RADIAL	SAMPLE TYPE(S)		TEST VARIABLE
B-4		MW	%							$\%N_2$ by wt	$\%N_2$ by wt	in. into boiler	in. into boiler	sec.air ax/rad			in. into boiler	in. radius			
6/14	17	0.68	14	NG	#2	1.21	-	1.08	1.19	0.65	-	0	64	-	B3D4.0	45°, 2	St	-	CEMS		I/O-
	18	0.62	5					1.17	1.24												Temp.

C.F. 620

Data Summary Sheet

TEST: No. 2 Fuel Oil Reburning

FACILITY: PBS

PAGE: 48

		1	2	3	4	5	6	7	8	9	10	11	12	13	14	15	16	17	18	19	20
DATE & DATA BOOK #	Data Pt. #	FR_{TOT}	FR_{SEC}/FR_{PRI}	PRI FUEL	SEC FUEL	SR_1	SR_2	SR_3	SR_4	PRI FUEL DOPANT	SEC FUEL DOPANT	SEC FUEL INJ	FINAL AIR INJ	PRI ZONE MIXING	SEC FUEL NOZZLE	INS. ZONE	SAMPLE LOCATION AXIAL	RADIAL	SAMPLE TYPE(S)		TEST VARIABLE
B-5		MW	%							% N_2 by wt	% N_2 by wt	in. into boiler	in. into boiler	sec air ax/rad			in. into boiler	in. radius			
8/6/80	2	0.72	21	NG	#2	0.65	1.08	0.89	1.10	0.65	0.5	40	64	0	B3MS.5	30°, 2	St	-	CEMS		I/o - $(C_5H_5N)_R$
	3	0.68	14					0.94													
	4	0.62	5					1.03													
	7	0.72	21					0.88		0											
	8	0.68	14					0.94													
	9	0.62	5					1.02													
	11	0.72	21	NG	#2	0.65	1.08	0.88	1.10	0	0.5	40	52	0	B3MS.5	30°, 2	St	-	CEMS		I/o - τ_R
	12												64								
	13												76								
	14												88								
	15-19	0.72	21	NG	#2	0.65	1.08	0.88	1.10	0	0.5	40	88	0	B3MS.5	30° 2	40-80	5 1/4	CEMS		D
	22-26									0.65							40-80	5 1/4	CEMS		
	27	0.72	21	NG	#2	0.65	1.08	0.88	1.10	0.65	0.5	40	88	12	B3MS.5	30° 2	St	-	CEMS		I/o - τ_R
	28												76								
	29												64								
	30												52								

C.F. 620

Data Summary Sheet

TEST: No. 2 Fuel Oil Reburning FACILITY: PBS PAGE: 49

DATE & DATA BOOK #	Data Pt. #	1	2	3	4	5	6	7	8	9	10	11	12	13	14	15	16	17	18	19	20
		FR_{TOT}	$\frac{FR_{SEC}}{FR_{PRI}}$	PRI FUEL	SEC FUEL	SR_1	SR_2	SR_3	SR_4	PRI FUEL DOPANT	SEC FUEL DOPANT	SEC FUEL INJ	FINAL AIR INJ	PRI ZONE MIXING	SEC FUEL NOZZLE	INJ. ZONE	SAMPLE LOCATION AXIAL	RADIAL	SAMPLE TYPE(S)		TEST VARIABLE
B-2		MW	%							$\% N_2$ by wt	$\% N_2$ by wt	in. into boiler	in. into boiler	sec air ax/rad			in. into boiler	in. radius			
1/31/89	2	0.74	19	#2	#2	0.56	1.02	0.83	1.03	0.52	–	40	64	0	B2S0SZ	–	St	–	CEMS		I/O
	3	0.69	13					0.89													
	4	0.63	6					0.96													
	7	0.74	19					0.83		0											
	8	0.69	13					0.89													
	9	0.63	6					0.96													
2/1	3	0.73	19	#2	#2	0.59	1.05	0.86	1.06	0.14	–	40	64	0	B2S0SZ	–	St	–	CEMS		I/O
	4	0.73	19					0.86		0.52											
	5	0.68	13					0.91		0.14											
	6	0.62	6					0.99		0.14											
2/2	4	0.74	19	#2	#2	0.91	1.07	0.87	1.07	0	–	40	64	0	B2S0SZ	–	St	–	CEMS		I/O
	5									0.52											
	6	0.69	13					0.93		0.52											
	7									0											
	8	0.64	6					1.00		0											
	9									0.52											
	16-22	0.75	18	#2	#2	0.58	1.06			0.52	–	40	64	0	B2S0SZ	–	40-70	5¼	T		D
	23-29	0.71	13														40-70	5¼	T		
	30-36	0.65	6														40-70	5¼	T		

C.F. 620

PBS FACILITY:

NO. 5 (HEAVY) FUEL OIL REBURNING

Data Summary Sheet

TEST : No. 5 Fuel Oil Reburning FACILITY : PBS PAGE : 50

		1	2	3	4	5	6	7	8	9	10	11	12	13	14	15	16	17	18	19	20
DATE & DATA BOOK #	Data Pt. #	FR_{TOT}	$\frac{FR_{SEC}}{FR_{PRI}}$	PRI FUEL	SEC FUEL	SR_1	SR_2	SR_3	SR_4	PRI FUEL DOPANT	SEC FUEL DOPANT	SEC FUEL INJ	FINAL AIR INJ	PRI ZONE MIXING	SEC FUEL NOZZLE	INS. ZONE	SAMPLE LOCATION AXIAL	SAMPLE LOCATION RADIAL	SAMPLE TYPE(S)		TEST VARIABLE
D-1		MW	%							$\%N_2$ by wt	$\%N_2$ by wt	in. into boiler	in. into boiler	sec air ax/rad			in. into boiler	in. radius			
6/19/84	2	0.72	22	NG	#5 Oil	0.65	1.06	0.86	1.11	0.65	–	40	64	0	B3D4.0	45°, 2	St	–	CEMS		I/o
	3	0.68	15					0.92													
	4	0.62	6					1.00													
	7	0.72	22					0.86		0											
	8	0.68	15					0.92													
	9	0.62	6					1.00													
	12	0.72	22					0.86		0.20											
	13	0.68	15					0.92													
	14	0.62	6					1.00													
	18	0.72	22	NG	#5	0.65	1.06	0.86	1.08	0.65	–	40	64	0	B3D4.0	45°, 2	St	–	CEMS		I/o -
	19												52								T_R
	20												76								
	21												82								
6/21	3-8	0.72	22	NG	#5	0.65	1.06	0.87	1.09	0.65	–	40	64	0	B3D4.0	60°, 2	40-70	9 1/4	CEMS		D
	10-15																45-70	7 1/4	CEMS		
	17-31																40-95	5 1/4	CEMS		
	32	0.68	15	NG	#5	0.65	1.06	0.92	1.12	0.65	–	40	52	0	B3D4.0	60° 2	St	–	CEMS		I/o -
	33												64								T_R
	34												76								
	35												82								
	36												88								
	37	0.62	6					1.01				40	88								
	38												82								
	39												76								
	40												64								
	41												52								
6/22	3	0.72	22	NG	#5	0.65	1.06	0.87	1.10	0	–	40	52	0	B3D4.0	60° 2	St	–	CEMS		I/o -
	4												64								T_R
	5												76								
	6												88								

C.F. 620

Data Summary Sheet

TEST: No. 5 Fuel Oil Reburning FACILITY: PBS PAGE: 51

		1	2	3	4	5	6	7	8	9	10	11	12	13	14	15	16	17	18	19	20
DATE & DATA BOOK #	Data Pt. #	FR_{TOT}	FR_{SEC}/FR_{PRI}	PRI FUEL	SEC FUEL	SR_1	SR_2	SR_3	SR_4	PRI FUEL DOPANT	SEC FUEL DOPANT	SEC FUEL INJ	FINAL AIR INJ	PRI ZONE MIXING	SEC FUEL NOZZLE	INJ. ZONE	SAMPLE LOCATION AXIAL	SAMPLE LOCATION RADIAL	SAMPLE TYPE(S)		TEST VARIABLE
D-1		MW	%							$\%N_2$ by wt	$\%N_2$ by wt	in. into boiler	in. into boiler	sec.air ax/rad			in. into boiler	in. radius			
6/22	8	0.68	15	NG	#5	0.65	1.06	0.92	1.10	0	-	40	52	0	B3D4.0, 30°	2	St	-	CEMS		I/o- τ_a
	9												64								
	10												76								
	11												88								
	12	0.62	6					1.01				40	88								
	13												76								
	14												64								
	15												52								
	16	0.72	22	NG	#5	0.65	1.06	0.88	1.11	0	-	10	64	0	B3D6.0, 45°	2	St	-	CEMS		I/o- Temp
	17	0.68	15					0.93													
	18	0.62	6					1.02													
	19	0.62	6					1.02		0.65											
	20	0.68	15					0.93													
	21	0.72	22					0.88													
	22	0.72	22	NG	#5	0.65	1.06	0.88	1.11	0.65	-	10	52	0	B3D6.0, 45°	2	St	-	CEMS		I/o- Temp.
	23												70								
	24												76								
	25												58								
6/29	8	0.72	22	NG	#5	0.64	1.14	0.93	1.15	0.30	-	40	64	0	B3D4.9, 45°	2	St	-	CEMS		I/o- SR_2
	9	0.68	15					0.99													
	10	0.62	6					1.08													
	11	0.62	6				1.06	1.01	1.07	0.34											
	12	0.68	15					0.93													
	13	0.72	22					0.87													
	14	0.72	22				1.06	0.87	1.07	0.65											
	15	0.68	15					0.93													
	16	0.62	6					1.01													
	17	0.62	6				1.00	0.96	1.02	0.43											
	18	0.68	15					0.88													
	19	0.72	22					0.82													

C.F. 620

Data Summary Sheet

TEST: No. 5 Fuel Oil Reburning FACILITY: PBS PAGE: 52

		1	2	3	4	5	6	7	8	9	10	11	12	13	14	15	16	17	18	19	20
DATE & DATA BOOK #	Data Pt. #	FR_{TOT}	FR_{SEC}/FR_{PRI}	PRI FUEL	SEC FUEL	SR_1	SR_2	SR_3	SR_4	PRI FUEL DOPANT	SEC FUEL DOPANT	SEC FUEL INJ	FINAL AIR INJ	PRI ZONE MIXING	SEC FUEL NOZZLE	INS. ZONE	SAMPLE LOCATION AXIAL	SAMPLE LOCATION RADIAL	SAMPLE TYPE(S)		TEST VARIABLE
D-1		MW	%							% N_2 by wt	% N_2 by wt	in. into boiler	in. into boiler	sec air ax/rad			in. into boiler	in. radius			
6/29	20	0.72	22	NG	#5	0.64	0.95	0.78	0.98	0.65	–	40	64	0	B3D4.0	45° 2	St	–	CEMS		I/O- SR_2
	21	0.68	15					0.83													
	22	0.62	6					0.91													
7/4	3-9	0.72	22	NG	#5	0.64	1.06	0.87	1.09	0.65	–	40	64	0	B3D4.0	45° 2	40-80	5¼	CEMS,	HCN, NH_3	D
	15	0.72	22	NG	#5	0.64	1.00	0.82	1.06	0.43	–	40	64	0	B3D4.0	45° 2	St	–	CEMS		I/O- SR_2
	16	0.68	15					0.87													
	17	0.62	6					0.95													
	18	0.62	6				0.95	0.91	1.04	0.65											
	19	0.68	15					0.83													
	20	0.72	22					0.78													
7/11	3-9	0.72	22	NG	#5	0.65	1.06	0.87	1.08	0.65	–	40	64	0	B3D4.0	45° 2	40-80	5¼	CEMS	HCN, NH_3	D
7/16	3-12	0.68	15	NG	#5	0.66	1.07	0.93	1.11	0.65	–	40	64	0	B3D4.0	45° 2	40-90	5¼	CEMS	HCN, NH_3	D
	13-15																70-90	7¼	CEMS		
	16-17																80, 90	9¼	CEMS		
7/19	3-9	0.62	6	NG	#5	0.65	1.07	1.02	1.14	0.65	–	40	64	0	B3D4.0,	45° 2	40-80	5¼	CEMS,	HCN, NH_3	D
7/20	3-10	0.72	22	NG	#5	0.65	1.08	0.88	1.10	0.65	–	40	64	0	B3D4.0	45° 2	40-80	5¼	CEMS,	HCN, NH_3	D
7/23	3-9	0.72	22	NG	#5	0.65	1.07	0.88	1.09	0.13	–	40	64	0	B3D4.0	45° 2	40-80	5¼	CEMS,	HCN, NH_3	D
7/24	16-26	0.72	22	NG	#5	0.65	1.08	0.88	1.10	0	–	40	88	0	B3D4.0	45° 2	40-100	5¼	CEMS,	HCN, NH_3	D
7/25	3-5	0.72	22	NG	#5	0.65	1.07	0.88	1.09	0.65	–	40	64	0	B3D4.0	45° 2	50-60	5¼	CEMS,	HCN, NH_3	D
	6-8																50-60	7¼	CEMS,	HCN, NH_3	
	9-11																50-60	9¼	CEMS,	HCN, NH_3	
	16	0.72	22	NG	#5	0.65	1.07	0.88	1.09	0.65	–	40	64	0	B3D4.0,	45° 2	St	–	CEMS		I/O- SR_4
	17								1.01												
	18								1.05												
	19								1.11												
	20								1.15												
	21								1.18												
7/26	3-9	0.72	22	NG	#5	0.65	1.06	0.87	1.09	0.13	–	40	64	0	B3D4.0	45° 2	40-80	5¼	CEMS,	HCN, NH_3	D
	15	0.72	22	NG	#5	0.65	1.08	0.88	1.10	0.65	–	10	64	0	B3D4.0	45° 2	St	–	CEMS		I/O- Temp.
	16												76								

C.F. 620

Data Summary Sheet

TEST: No. 5 Fuel Oil Reburning FACILITY: BBS PAGE: 53

DATE & DATA BOOK #	Data Pt. #	1 FR_{TOT}	2 $\frac{FR_{SEC}}{FR_{PRI}}$	3 PRI FUEL	4 SEC FUEL	5 SR_1	6 SR_2	7 SR_3	8 SR_4	9 PRI FUEL DOPANT	10 SEC FUEL DOPANT	11 SEC FUEL INJ	12 FINAL AIR INJ	13 PRI ZONE MIXING	14 SEC FUEL NOZZLE	15 INJ. ZONE	16 SAMPLE LOCATION AXIAL	17 SAMPLE LOCATION RADIAL	18 SAMPLE TYPE(S)	19	20 TEST VARIABLE
D-1		MW	%							$\%N_2$ by wt	$\%N_2$ by wt	in. into boiler	in. into boiler	sec. air $\frac{ax}{rad}$			in. into boiler	in. radius			
7/26	17	0.72	22	NG	#5	0.65	1.08	0.88	1.10	0.65	-	10	88	0	B3D4.0	45° 2	St	-	CEMS		I/o-Temp.
	18-23	0.72	22	NG	#5	0.65	1.08	0.88	1.10	0.65	-	10	88	0	B3D4.0	45° 2	40-65	5 1/4	CEMS		
	24	0.68	15	NG	#5	0.65	1.08	0.94	1.11	0.65	-	10	88	0	B3D4.0	45° 2	St	-	CEMS		Δ I/o-Temp
	25												64								
	26	0.62	6					1.02	1.14			10	64								
	27												88								
	28	0.62	6					1.02	1.13	0		10	88								
	29												64								
	30	0.68	52					0.94	1.10			10	64								
	31												88								
	32	0.72	22					0.87	1.09			10	88								
	33												76								
	34												64								
8/3	6	0.72	22	NG	#5	0.64	1.16	0.94	1.08	0.26	-	40	64	0	B3D4.0	45° 2	St	-	CEMS		I/o-SR_2
	7	0.68	15					1.01													
	8	0.62	6					1.10	1.16												
	9	0.62	6				1.06	1.01	1.08	0.27											
	10	0.68	15					0.93													
	11	0.72	22					0.87													
	12	0.72	22				1.00	0.82		0.31											
	13	0.68	15					0.87													
	14	0.62	6					0.95													
	15	0.62	6				0.95	0.91		0.45											
	16	0.68	15					0.83													
	17	0.72	22					0.78													
	18	0.72	22				0.95	0.78		0.27											
	19	0.68	15					0.83													
	20	0.62	6					0.91													

C.F. 620

PBS FACILITY:

FUEL COMPARISON, REBURNING

Data Summary Sheet

TEST: Fuel Comparison Reburning FACILITY: PBS PAGE: 54

DATE & DATA BOOK #	Data Pt. #	1 FR$_{TOT}$	2 $\frac{FR_{SEC}}{FR_{PRI}}$	3 PRI FUEL	4 SEC FUEL	5 SR$_1$	6 SR$_2$	7 SR$_3$	8 SR$_4$	9 PRI FUEL DOPANT	10 SEC FUEL DOPANT	11 SEC FUEL INJ	12 FINAL AIR INJ	13 PRI ZONE MIXING	14 SEC FUEL NOZZLE	15 INS. ZONE	16 SAMPLE LOCATION AXIAL	17 SAMPLE LOCATION RADIAL	18 SAMPLE TYPE(S)	19	20 TEST VARIABLE
D-1		MW	%							%N_2 by wt	%N_2 by wt	in. into boiler	in. into boiler	sec air ax/rad			in. into boiler	in. radius			
7/3/89	3	0.72	22	NG	#5	0.66	1.08	0.88	1.11	0	-	40	64	0	B3D4.0	45° 2	St	-	CEMS		I/O- #5
	4	0.68	15					0.94													
	5	0.62	6					1.03													
	6	0.62	6					1.03													
	7	0.68	15					0.94					52								
	8	0.72	22					0.88													
	9	0.72	22					0.88													
	10	0.68	15					0.94					76								
	11	0.62	6					1.03													
	12	0.62	6					1.03													
	13	0.68	15					0.94					88								
	14	0.72	22					0.94													
	20	0.72	22					0.88													
	21	0.68	15					0.88		0.65			52								
	22	0.62	6					0.95													
	23	0.62	6					1.03													
	24	0.68	15					1.03					64								
	25	0.72	22					0.95													
	26	0.72	22					0.89													
	27	0.68	15					0.89					76								
	28	0.62	6					0.95													
	29	0.62	6					1.03													
	30	0.68	15					1.03					88								
	31	0.72	22					0.95													
	34	0.72	22	NG	#2	0.66	1.08	0.89	1.11	0	-	40	52	0	B3D4.0	45° 2	St	-	CEMS		I/O- #2
	35	0.68	15					0.89													
	36	0.62	6					0.95													
	37	0.62	6					1.03													
	38	0.68	15					1.03					64								
	39	0.72	22					0.95													
								0.89													

C.F. 620

Data Summary Sheet

TEST: Fuel Comparison Reburning FACILITY: PBS PAGE: 55

		1	2	3	4	5	6	7	8	9	10	11	12	13	14	15	16	17	18	19	20
DATE & DATA BOOK #	Data Pt. #	FR_{TOT}	$\frac{FR_{SEC}}{FR_{PRI}}$	PRI FUEL	SEC FUEL	SR_1	SR_2	SR_3	SR_4	PRI FUEL DOPANT	SEC FUEL DOPANT	SEC FUEL INJ	FINAL AIR INJ	PRI ZONE MIXING	SEC FUEL NOZZLE	INJ. ZONE	SAMPLE LOCATION AXIAL	RADIAL	SAMPLE TYPE(S)		TEST VARIABLE
D-1		MW	%							$\%N_2$ by wt	$\%N_2$ by wt	in. into boiler	in. into boiler	sec air $\frac{ax}{rad}$			in. into boiler	in. radius			
7/3	40	0.72	22	NG	#2	0.66	1.08	0.89	1.11	0	–	40	76	0	B3D9.045°	2	St	–	CEMS		I/O-#2
	41	0.68	15					0.95													
	42	0.62	6					1.03													
	43	0.62	6					1.03					88								
	44	0.68	15					0.95													
	45	0.72	22					0.89													
	46	0.72	22					0.90		0.65			88								
	47	0.68	15					0.95													
	48	0.62	6					1.04													
	49	0.62	6					1.04					76								
	50	0.68	15					0.95													
	51	0.72	22					0.90													
	52	0.72	22					0.90					64								
	53	0.68	15					0.95													
	54	0.62	6					1.04													
	55	0.62	6					1.04					52								
	56	0.68	15					0.95													
	57	0.72	22					0.90													
	60	0.63	6	NG	NG	0.66	1.08	1.02	1.11	0	–	40	52	0	B3N9	2	St	–	CEMS		I/O-NG
	61	0.69	16					0.93													
	62	0.73	23					0.88													
	63	0.73	23					0.88					64								
	64	0.69	16					0.93													
	65	0.63	6					1.02													
	66	0.63	6					1.02					76								
	67	0.69	16					0.93													
	68	0.73	23					0.88													
	69	0.73	23					0.88					88								
	70	0.69	16					0.93													
	71	0.63	6					1.02													

C.F. 620

Data Summary Sheet

TEST: Fuel Comparison Reburning FACILITY: PBS PAGE: 56

DATE & DATA BOOK #	Data Pt. #	1	2	3	4	5	6	7	8	9	10	11	12	13	14	15	16	17	18	19	20
		FR_{TOT}	FR_{SEC}/FR_{PRI}	PRI FUEL	SEC FUEL	SR_1	SR_2	SR_3	SR_4	PRI FUEL DOPANT	SEC FUEL DOPANT	SEC FUEL INJ	FINAL AIR INJ	PRI ZONE MIXING	SEC FUEL NOZZLE	INS. ZONE	SAMPLE LOCATION AXIAL	SAMPLE LOCATION RADIAL	SAMPLE TYPE (S)		TEST VARIABLE
D-1		MW	%							$\% N_2$ by wt	$\% N_2$ by wt	in. into boiler	in. into boiler	sec air ax/rad			in. into boiler	in. radius			
7/3	72	0.63	6	NG	NG	0.66	1.08	1.02	1.11	0.65	-	40	88	0	B3N9	2	St	-	CEMS		I/o-NG
	73	0.69	16					0.94													
	74	0.73	23					0.88													
	75	0.73	23					0.88													
	76	0.69	16					0.94					76								
	77	0.63	6					1.02													
	78	0.63	6					1.02													
	79	0.69	16					0.94					64								
	80	0.73	23					0.88													
	81	0.73	23					0.88													
	82	0.69	16					0.94					52								
	83	0.63	6					1.02													

C.F. 620

NORTH AMERICAN BOILER FACILITY:
NO. 2 (DISTILLATE) FUEL OIL BASELINE

Data Summary Sheet

TEST: No. 2 Fuel Oil Baseline FACILITY: N. A. PAGE: 57

		1	2	3	4	5	6	7	8	9	10	11	12	13	14	15	16	17	18	19	20
DATE & DATA BOOK #	Data Pt. #	FR_{TOT}	FR_{SEC}/FR_{TOT}	PRI FUEL	SEC FUEL	SR_1	SR_2	SR_3	SR_4	PRI FUEL DOPANT	SEC FUEL DOPANT	SEC FUEL INJ	FINAL AIR INJ	PRI ZONE MIXING	SEC FUEL NOZZLE	INS. ZONE	SAMPLE LOCATION AXIAL	SAMPLE LOCATION RADIAL	SAMPLE TYPE(S)		TEST VARIABLE
C-1		MW	%							$\% N_2$ by wt	$\% N_2$ by wt	in. into boiler	in. into boiler	sec air ~~ax~~ rad			in. into boiler	in. radius			
11/9/83	1	0.65	O	No.2	–	–	1.10	–	–	–	–	–	–	–	–	–	St	–	CEMS	UHC	D
	2	0.60															25-105 St	O –	T CEMS	 UHC	
	3	0.56															25-10.5 St	O –	T CEMS	 UHC	
	4	0.52															25-105 St	O –	T CEMS	 UHC	
	5	0.48															25-105 St	O –	T CEMS	 UHC	
11/9	A	0.60	0	No.2	–	–	1.10	–	–	–	–	–	–	–	–	–	25-105 St	O –	T CEMS		I/O-LOAD
	B	0.56																			
	C	0.52																			
	D	0.48																			
11/16	99	0.53	0	No.2	–	–	1.10	–	–	–	–	–	–	–	–	–	St	–	CEMS		D
	110																				
11/17	143	0.52	0	No.2	–	–	1.10	–	–	–	–	–	–	–	–	–	20-100 St	O –	T CEMS		D
8/14/84	1	0.65	0	No.2	–	–	1.10	–	–	–	–	–	–	–	–	–	40-100 St	O –	T CEMS		I/O-LOAD
	2	0.60																			
	4	0.56																			
	6,7	0.53																			
	28	0.53	0	No.2	–	–	1.13	–	–	–	–	–	–	–	–	–	St	–	CEMS		I/O-EA
	29						1.17														
	30						1.08														
	31						1.05														
	32						1.03														
8/15	1	0.65	0	No.2	–	–	1.10	–	–	0.50	–	–	–	–	–	–	St	–	CEMS		I/O-LOAD
	2	0.60																			
	4	0.56																			

C.F. 620

Data Summary Sheet

TEST : No. 2 Fuel Oil Baseline FACILITY : N.A. PAGE : 58

		1	2	3	4	5	6	7	8	9	10	11	12	13	14	15	16	17	18	19	20
DATE & DATA BOOK #	Data Pt. #	FR_{TOT}	FR_{SEC}/FR_{PRI}	PRI FUEL	SEC FUEL	SR_1	SR_2	SR_3	SR_4	PRI FUEL DOPANT	SEC FUEL DOPANT	SEC FUEL INJ	FINAL AIR INJ	PRI ZONE MIXING	SEC FUEL NOZZLE	INJ. ZONE	SAMPLE LOCATION AXIAL	SAMPLE LOCATION RADIAL	SAMPLE TYPE(S)		TEST VARIABLE
C-1		MW	%							$\%N_2$ by wt	$\%N_2$ by wt	in. into boiler	in. into boiler	sec air ax/rad			in. into boiler	in. radius			
8/15	6,20	0.52	0	No.2	–	–	1.10	–	–	0.50	–	–	–	–	–	–	St	–	CEMS		I/O-LOAD
	30	0.52	0	No.2	–	–	1.10	–	–	0.13	–	–	–	–	–	–	St	–	CEMS		I/O-
	31									0.32											$(NH_3)_{PRI}$
	33	0.52	0	No.2	–	–	1.13	–	–	0.50	–	–	–	–	–	–	St	–	CEMS		I/O-
	34						1.16														EA
	35						1.07														
	36						1.05														
	37						1.03														
8/17	1	0.65	0	No.2	–	–	1.07	–	–	–	–	–	–	–	–	–	St	–	CEMS		I/O-
	2,20	0.53																			LOAD
	21	0.53	0	No.2	–	–	1.07	–	–	0.13	–	–	–	–	–	–	St	–	CEMS		I/O-
	22									0.32											$(NH_3)_{PRI}$
	23									0.50											
8/21	1	0.64	0	No.2	–	–	1.10	–	–	–	–	–	–	–	–	–	St	–	CEMS		I/O-
	2																				AIR
	3						0.965	1.10		0.50			84								STAGING
	4												64								
	5									–			64								
	6												84								
	7						0.884			–			84								
	8												64								
	9									0.50			64								
	10												84								
	11						0.857			0.50			84								
	12												64								
	13									–			64								
	14												84								
	15,23	0.52	0	No.2	–	–	1.10	–	–	–	–	–	–	–	–	–	St	–	CEMS		I/O-
	25						1.07														EA
	26						1.05														
	27						1.02														

C.F. 620

NORTH AMERICAN BOILER FACILITY:
NO. 5 (HEAVY) FUEL OIL BASELINE

Data Summary Sheet

TEST: No. 5 Fuel Oil Baseline FACILITY: N.A. PAGE: 59

		1	2	3	4	5	6	7	8	9	10	11	12	13	14	15	16	17	18	19	20
DATE & DATA BOOK #	Data Pt. #	FR_{TOT}	$\frac{FR_{SEC}}{FR_{TOT}}$	PRI FUEL	SEC FUEL	SR_1	SR_2	SR_3	SR_4	PRI FUEL DOPANT	SEC FUEL DOPANT	SEC FUEL INJ	FINAL AIR INJ	PRI ZONE MIXING	SEC FUEL NOZZLE	INS. ZONE	SAMPLE LOCATION AXIAL	RADIAL	SAMPLE TYPE(S)		TEST VARIABLE
C-1		MW	%							% N_2 by wt	% N_2 by wt	in. into boiler	in. into boiler	sec.air $\frac{ax}{rad}$			in. into boiler	in. radius			
11/7	6	0.67	0	No.5	–	–	1.10	–	–	–	–	–	–	–	–	–	St	–	CEMS	, UHC	D
																	105	O	T		
	7	0.62															St	–	CEMS	, UHC	
																	105	O	T		
	8	0.58															St	–	CEMS	, UHC	
																	105	O	T		
	9	0.55															St	–	CEMS	, UHC	
																	105	O	T		
	10	0.50															St	–	CEMS	, UHC	
																	105	O	T		
11/10	E	0.62	0	No.5	–	–	1.10	–	–	–	–	–	–	–	–	–	St	–	CEMS		I/O-LOAD
	F	0.58																			
	G	0.54																			
	H	0.50																			
	61	0.62																			
	64	0.58																			
	67	0.54																			
11/15	73	0.54	0	No.5	–	–	1.13	–	–	–	–	–	–	–	–	–	St	–	CEMS		I/O-EA
	74						1.16														
	75						1.22														
	72						1.05														
	70						1.10														
	80						1.15														
11/17	120-124	0.55	0	No.5	–	–	1.16	–	–	–	–	20-60	84	–	–	–	St	–	CEMS		D
	125-130						1.10					20-60	84				St	–	CEMS		
	131						1.10					–	–				90-100	O	T		
	135						1.16										40-100	O	T		
	139	0.62					1.10										40-100	O	T		
8/16/84	1	0.66	0	No.5	–	–	1.10	–	–	–	–	–	–	–	–	–	St	–	CEMS		I/O-LOAD

C.F. 620

Data Summary Sheet

TEST : No. 5 Fuel Oil Baseline FACILITY : N.A. PAGE : 60

DATE & DATA BOOK #	Data Pt. #	1	2	3	4	5	6	7	8	9	10	11	12	13	14	15	16	17	18	19	20
		FR_{TOT}	$\frac{FR_{SEC}}{FR_{PRI}}$	PRI FUEL	SEC FUEL	SR_1	SR_2	SR_3	SR_4	PRI FUEL DOPANT	SEC FUEL DOPANT	SEC FUEL INJ	FINAL AIR INJ	PRI ZONE MIXING	SEC FUEL NOZZLE	INS. ZONE	SAMPLE LOCATION AXIAL	RADIAL	SAMPLE TYPE(S)		TEST VARIABLE
C-1		MW	%							$\% N_2$ by wt	$\% N_2$ by wt	in. into boiler	in. into boiler	sec air ax/rad			in. into boiler	in. radius			
8/16	2,18	0.54	0	No. 5	–	–	1.10	–	–	–	–	–	–	–	–	–					
	19						1.17										St	–	CEMS		I/O-EA
	20						1.04														
	21						1.01														
	22	0.58	0	No. 5	–	–	1.10	–	–	–	–	–	–	–	–	–					
	23	0.62															St	–	CEMS		I/O-LOAD
	24	0.65																			
8/22	1,8	0.67	0	No. 5	–	–	1.10	–	–	–	–	–	–	–	–	–					
	2						0.95	1.10									St	–	CEMS		I/O-AIR STAGING
	3						0.95						84								
	4						0.89						64								
	5						0.89						64								
	7						0.87						84								
	13	0.53	0	No. 5	–	–	1.10	–	–	–	–	–	64	–	–	–					
	14						1.07						–				St	–	CEMS		I/O-EA
	15						1.04														
	16						1.01														

C.F. 620

NORTH AMERICAN BOILER FACILITY:
NATURAL GAS REBURNING

Data Summary Sheet

TEST: Natural Gas Reburning FACILITY: N.A. PAGE: 61

DATE & DATA BOOK #	Data Pt. #	1 FR_{TOT}	2 FR_{SEC}/FR_{TOT}	3 PRI FUEL	4 SEC FUEL	5 SR_1	6 SR_2	7 SR_3	8 SR_4	9 PRI FUEL DOPANT	10 SEC FUEL DOPANT	11 SEC FUEL INJ	12 FINAL AIR INJ	13 PRI ZONE MIXING	14 SEC FUEL NOZZLE	15 INS. ZONE	16 SAMPLE LOCATION AXIAL	17 SAMPLE LOCATION RADIAL	18 SAMPLE TYPE(S)	19	20 TEST VARIABLE
C-1		MW	%							% N_2 by wt	% N_2 by wt	in. into boiler	in. into boiler	sec air ~~ax~~ rad			in. into boiler	in. radius			
11/9/83	11	0.64	5	No.2	NG	–	1.10	1.04	1.10	–	0	60	84	–	B2N1	–	St	–	CEMS		I/O
	12										0.52										
	13	0.63	10	No.2	NG	–	1.10	1.00	1.11	–	0	60	84	–	B2N1	–	St	–	CEMS		I/O
	14										0.52										
	16	0.62	15	No.2	NG	–	1.10	0.93	1.11	–	0	60	84	–	B2N1	–	St	–	CEMS		I/O –
	15											60	72								τ_R
	17											60	96								
	20											50	74								
	21A											40	64								
	21B											40	88								
	22											70	94								
	23										0.52	60	72								
	24											60	84								
	25											60	96								
	28											50	74								
	29A											40	69								
	29B											40	88								
	30											70	94								
	31										0.26	60	84								I/O –
	32										0.80										$(NH_3)_R$
	33										1.05										
	34	0.61	21	No.2	NG	–	1.10	0.88	1.11	–	0	36	60	–	B2N1	–	St	–	CEMS		I/O
	35										0.52										
11/16	100	0.62	15	No.2	NG	–	1.10	0.94	1.10	–	0	60	84	–	B2N1	–	St	–	CEMS		I/O –
	101										0.52	60									τ_R
	102										0.52	50									
	103										0	50									
	104										0	40									
	105										0.52	40									
	106										0.52	30									

C.F. 620

Data Summary Sheet

TEST: Natural Gas Reburning FACILITY: N.A. PAGE: 62

DATE & DATA BOOK #	Data Pt. #	1	2	3	4	5	6	7	8	9	10	11	12	13	14	15	16	17	18	19	20
		FR_{TOT}	$\frac{FR_{SEC}}{FR_{PRI}}$	PRI FUEL	SEC FUEL	SR_1	SR_2	SR_3	SR_4	PRI FUEL DOPANT	SEC FUEL DOPANT	SEC FUEL INJ	FINAL AIR INJ	PRI ZONE MIXING	SEC FUEL NOZZLE	INS. ZONE	SAMPLE LOCATION AXIAL	SAMPLE LOCATION RADIAL	SAMPLE TYPE(S)		TEST VARIABLE
c-1		MW	%							% N_2 by wt	% N_2 by wt	in. into boiler	in. into boiler	sec air ax/rad			in. into boiler	in. radius			
11/16	107	0.62	15	No.2	NG	-	1.10	0.94	1.10	-	0	30	84	-	B2N1	-	St	-	CEMS		I/o-Tr
	108										0	20									
	109										0.52	20									

Data Summary Sheet

TEST: Natural Gas Reburning FACILITY: N.A. PAGE: 63

DATE & DATA BOOK #	Data Pt. #	1	2	3	4	5	6	7	8	9	10	11	12	13	14	15	16	17	18	19	20
		FR_{TOT}	FR_{SEC}/FR_{PRI}	PRI FUEL	SEC FUEL	SR_1	SR_2	SR_3	SR_4	PRI FUEL DOPANT	SEC FUEL DOPANT	SEC FUEL INJ	FINAL AIR INJ	PRI ZONE MIXING	SEC FUEL NOZZLE	INS. ZONE	SAMPLE LOCATION		SAMPLE TYPE(S)		TEST VARIABLE
																	AXIAL	RADIAL			
C-1		MW	%							$\%N_2$ by wt	$\%N_2$ by wt	in. into boiler	in. into boiler	sec.air ax/rad			in. into boiler	in. radius			
11/10/83	36	0.65	5	No.5	NG	–	1.10	1.04	1.10	–	0	60	84	–	B2N1	–	St	–	CEMS		I/O
	37										0.52										
	38	0.64	10	No.5	NG	–	1.10	0.99	1.10	–	0	60	84	–	B2N1	–	St	–	CEMS		I/O
	39										0.52										
	40	0.63	15	No.5	NG	–	1.10	0.94	1.10	–	0	60	84	–	B2N1	–	St	–	CEMS		I/O-
	41											60	72								I_R
	42											60	96								
	45											50	74								
	46A											40	64								
	46B											40	88								
	47											70	94								
	48										0.52	60	72								
	49											60	84								
	50											60	96								
	53											50	74								
	54A											40	64								
	54B											40	88								
	55											70	94								
	56										0.26	60	84								I/O-
	57										0.78										(NH_3)
	58										1.05										
	59	0.62	20	No.5	NG	–	1.10	0.89	1.11	–	0	60	84	–	B2N1	–	St	–	CEMS		I/O
	60										0.52										
	62	0.65	5	No.5	NG	–	1.10	1.05	1.10	–	0	36	60	–	B2N1	–	St	–	CEMS		I/O
	63										0.52										
	65	0.64	10	No.5	NG	–	1.10	1.00	1.11	–	0	36	60	–	B2N1	–	St	–	CEMS		I/O
	66										0.52										
	68	0.63	15	No.5	NG	–	1.10	0.94	1.10	–	0	36	60	–	B2N1	–	St	–	CEMS		I/O
	69										0.52										
11/15	79	0.63	15	No.5	NG	–	1.10	0.94	1.10	–	0	60	84	–	B2N1	–	St	–	CEMS		I/O

C.F. 620

Data Summary Sheet

TEST : Natural Gas Reburning FACILITY : N.A. PAGE : 64

		1	2	3	4	5	6	7	8	9	10	11	12	13	14	15	16	17	18	19	20
DATE & DATA BOOK #	Data Pt. #	FR_{TOT}	$\frac{FR_{SEC}}{FR_{PRI}}$	PRI FUEL	SEC FUEL	SR_1	SR_2	SR_3	SR_4	PRI FUEL DOPANT	SEC FUEL DOPANT	SEC FUEL INJ	FINAL AIR INJ	PRI ZONE MIXING	SEC FUEL NOZZLE	INS. ZONE	SAMPLE LOCATION AXIAL	RADIAL	SAMPLE TYPE(S)		TEST VARIABLE
C-1		MW	%							$\% N_2$ by wt	$\% N_2$ by wt	in. into boiler	in. into boiler	secair ax/rad			in. into boiler	in. radius			
11/15	81	0.63	15	No.5	NG	-	1.15	0.98	1.15	-	0	60	84	-	B2N1	-	St	-	CEMS		I/O-
	82										0.52	60									SR_{PRI}
	83										0.52	70									
	84										0	70									
	85										0	50									
	86										0.52	50									
	87										0.52	40									
	88										0	40									
	89										0	30									
	90										0.52	30									
	91										0.52	20									
	92										0	20									
	93	0.63	15	No.5	NG	-	1.15	0.98	1.15	-	0	60	84	-	B2N1	-	St	-	CEMS		I/O-
	94								1.19												EA
	95								1.23												
	96								1.12												
	97								1.10												
	98								1.08												
	71	0.62	20	No.5	NG	-	1.10	0.88	1.10	-	0	20	84	-	B2N1	-	St	-	CEMS		I/U

C.F. 620

NORTH AMERICAN BOILER FACILITY:
NO. 2 (DISTILLATE) FUEL OIL REBURNING

Data Summary Sheet

TEST: No. 2 Fuel O:I Reburning FACILITY: N.A. PAGE: 65

		1	2	3	4	5	6	7	8	9	10	11	12	13	14	15	16	17	18	19	20
DATE & DATA BOOK #	Data Pt. #	FR_{TOT}	FR_{SEC}/FR_{TOT}	PRI FUEL	SEC FUEL	SR_1	SR_2	SR_3	SR_4	PRI FUEL DOPANT	SEC FUEL DOPANT	SEC FUEL INJ	FINAL AIR INJ	PRI ZONE MIXING	SEC FUEL NOZZLE	INS. ZONE	SAMPLE LOCATION AXIAL	RADIAL	SAMPLE TYPE(S)		TEST VARIABLE
C-1		MW	%							% N_2 by wt	% N_2 by wt	in. into boiler	in. into boiler	sec.air ax/rad			in. into boiler	in. radius			
8/14/82	3	0.63	5	#2	#2	–	1.10	1.04	1.10	–	–	60	84	–	B2D4.0,45°	–	St	–	CEMS		I/O -
	5	0.65	13					0.96													LOAD
	7	0.61	14					0.95													
	8	0.56	6					1.04													
	9	0.61	14					0.95													
	10	0.65	19					0.89													
	12	0.65	19	#2	#2	–	1.10	0.89	1.10	–	–	60	72	–	B2D4.0,45°	–	St	–	CEMS		I/O -
	13												78								TR
	14												90								
	15											70	84								
	16											60									
	17											50									
	18											40									
	19											30									
	21	0.65	19	#2	#2	–	1.10	0.89	1.10	–	–	60	84	–	B2D4.0,45°	–	St	–	CEMS		I/O -
	22								1.07												EA
	23								1.05												
	24								1.02												
	25								1.13												
	26								1.15												
	33	0.65	19	#2	#2	–	1.03	0.83	1.11	–	–	60	84	–	B2D4.0,45°	–	St	–	CEMS		I/O - SR_2
8/15	3	0.63	5	#2	#2	–	1.10	1.09	1.11	0.50	–	60	84	–	B2D4.0,45°	–	St	–	CEMS		I/O -
	5	0.65	13					0.96													LOAD
	7	0.61	14					0.95													
	8	0.57	6					1.04													
	9	0.65	19					0.89													
	10	0.65	19	#2	#2	–	1.10	0.89	1.11	0.50	–	60	78	–	B2D4.0,45°	–	St	–	CEMS		I/O -
	11												72								TR
	13												90								
	14											70	84								

C.F. 620

Data Summary Sheet

TEST: No. 2 Fuel Oil Reburning FACILITY: N.A. PAGE: 66

Date & Data Book #	Data Pt. #	1 FR$_{TOT}$	2 FR_{SEC}/FR_{TOT}	3 PRI FUEL	4 SEC FUEL	5 SR$_1$	6 SR$_2$	7 SR$_3$	8 SR$_4$	9 PRI FUEL DOPANT	10 SEC FUEL DOPANT	11 SEC FUEL INJ	12 FINAL AIR INJ	13 PRI ZONE MIXING	14 SEC FUEL NOZZLE	15 INJ. ZONE	16 SAMPLE LOCATION AXIAL	17 SAMPLE LOCATION RADIAL	18 SAMPLE TYPE(S)	19	20 TEST VARIABLE
C-1		MW	%							%N_2 by wt	%N_2 by wt	in. into boiler	in. into boiler	sec air ax/rad			in. into boiler	in. radius			
8/15	15	0.65	19	#2	#2	-	1.10	0.89	1.11	0.50	-	60	84	-	B2D9.0, 45°	-	St	-	CEMS		I/o - T_R
	16											50									
	17											40									
	18											30									
	21	0.65	19	#2	#2	-	1.10	0.89	1.10	0.50	-	60	84	-	B2D9.0 45°	-	St	-	CEMS		I/o -
	22								1.14												EA
	23								1.17												
	24								1.08												
	25								1.05												
	26								1.02												
	27	0.65	19	#2	#2	-	1.10	0.89	1.10	0.50	-	60	84	-	B2D9.0 45°	-	St	-	CEMS		I/o -
	28									0.32											(NH_3)[illegible]
	29									0.13											
	38	0.65	19	#2	#2	-	1.03	0.83	1.10	0.50	-	60	84	-	B2D4.0, 45°	-	St	-	CEMS		I/o - SR$_2$
8/21	17	0.64	19	#2	#2	-	1.10	0.89	1.10	0.50	-	82	84	-	B2D4.0 45°	-	St	-	CEMS		I/o -
	18									-											T_R
	19									-		60	84								
	20									0.50											
	21									0.50		20	84								
	22									-											

C.F. 620

NORTH AMERICAN BOILER FACILITY:
NO. 5 (HEAVY) FUEL OIL REBURNING

Data Summary Sheet

TEST: No. 5 Fuel Oil Reburning FACILITY: N.A. PAGE: 67

		1	2	3	4	5	6	7	8	9	10	11	12	13	14	15	16	17	18	19	20
DATE & DATA BOOK #	Data Pt. #	FR_{TOT}	FR_{SEC}/FR_{TOT}	PRI FUEL	SEC FUEL	SR_1	SR_2	SR_3	SR_4	PRI FUEL DOPANT	SEC FUEL DOPANT	SEC FUEL INJ	FINAL AIR INJ	PRI ZONE MIXING	SEC FUEL NOZZLE	INS. ZONE	SAMPLE LOCATION AXIAL	RADIAL	SAMPLE TYPE(S)		TEST VARIABLE
C-1		MW	%							$\%N_2$ by wt	$\%N_2$ by wt	in. into boiler	in. into boiler	sec air ax/rad			in. into boiler	in. radius			
8/14/84	3	0.65	19	#5	#5	—	1.10	0.89	1.07	—	—	60	84	—	BZD4.0,	45° -	St	—	CEMS		I/o-
	4											50	74								τ_R
	5											40	64								
	6								1.10			40	64								
	7											30	54								
	8											40	59½								
	9												74								
	10												84								
	11	0.65	19	#5	#5	—	1.10	0.89	1.10	—	—	40	64	—	BZD4.0,	45° -	St	—	CEMS		I/o-
	12	0.61	14					0.95													LOAD
	13	0.56	6					1.04													
	14	0.65	19	#5	#5	—	1.10	0.89	1.15	—	—	40	64	-	BZD4.0,	45° -	St	-	CEMS		I/o-
	15								1.07												EA
	16								1.05												
	17								1.02												
8/17	3	0.65	19	#2	#5	—	1.07	0.87	1.05	—	—	60	84	—	BZD4.0,	45° -	St	—	CEMS		I/o-
	4											50	74								τ_R
	5											40	64								
	6								1.07			40	64								
	7											30	54								
	8											60	84								
	9											40	84								
	10												74								
	11	0.65	19	#2	#5	—	1.07	0.87	1.13	—	—	40	64	—	BZD4.0,	45° -	St	—	CEMS		I/o-
	12								1.02												EA
	13								1.00												
	14	0.65	19	#2	#5	—	1.07	0.87	1.07	0.50	—	40	64	-	BZD4.0,	45° -	St	-	CEMS		I/o-
	15									0.32											(NH_3)
	16									0.13											
	17	0.65	19	#2	#5	—	1.07	0.87	1.07	—	-	40	64	-	BZD4.0,	45° -	St	—	CEMS		I/o- LOAD

C.F. 620

Data Summary Sheet

TEST: No. 5 Fuel Oil Reburning FACILITY: N.A. PAGE: 68

DATE & DATA BOOK #	Data Pt. #	1 FR_{TOT}	2 FR_{SEC}/FR_{TOT}	3 PRI FUEL	4 SEC FUEL	5 SR_1	6 SR_2	7 SR_3	8 SR_4	9 PRI FUEL DOPANT	10 SEC FUEL DOPANT	11 SEC FUEL INJ	12 FINAL AIR INJ	13 PRI ZONE MIXING	14 SEC FUEL NOZZLE	15 INS. ZONE	16 SAMPLE LOCATION AXIAL	17 SAMPLE LOCATION RADIAL	18 SAMPLE TYPE(S)	19 SAMPLE TYPE(S)	20 TEST VARIABLE
C-1		MW	%							$\%N_2$ by wt	$\%N_2$ by wt	in. into boiler	in. into boiler	sec.air ax/rad			in. into boiler	in. radius			
8/17	18	0.61	14	#2	#5	-	1.07	0.92	1.07	-	-	40	64	-	B2D4.0,45°	-	St	-	CEMS		I/O -
	19	0.56	6					1.01													LOAD
8/22	10	0.66	19	#5	#5	-	1.10	0.89	1.10	-	-	40	64	-	B2D4.0,45°	-	St	-	CEMS		I/O -
	11											60	84								τ_R
	12											50	84								
	20	0.64	20	#2	#5	-	1.10	0.88	1.10	-	-	40	64	-	B2D4.0,45°	-	St	-	CEMS		I/O -
	21											60	84								τ_R
	22											40	84								

C.F. 620

PBS TESTS PERFORMED AFTER
OCTOBER 1, 1984

Data Summary Sheet

Reburning on PBS

PAGE: 1

		1	2	3	4	5	6	7	8	9	10	11	12	13	14	15	16	17	18	19	20
DATE & DATA BOOK #	# Data Pts	FR_{TOT}	FR_{SEC}/FR_{PRI}	PRI FUEL	SEC FUEL	SR_1	SR_2	SR_3	SR_4	PRI FUEL DOPANT	SEC FUEL DOPANT	SEC FUEL INJ	FINAL AIR INJ	PRI ZONE MIXING	SEC FUEL NOZZLE	INS. ZONE	TEST TYPE	TEST DESCRIPTION			
		MW	%							% N_2 by wt	% N_2 by wt	in. into boiler	in. into boiler	sec air ax/rad			I/O or D				
E1																		Firing Arrangements:			
10/23/89	27	0.74	25	NG	NG	0.69	1.11	0.89-1.10	1.10	0.65	0	40	64	0	tee	–	I/O	- Air Staging			
10/24	14	0.74	25	NG	NG	0.68	1.11	0.87-1.08	1.11	0.65	0	40	64	0	none	–	I/O	- Reburning - Biased Reburning			
10/25	12	0.74	25	NG	NG	0.66	1.09	0.88-0.99	1.09	0.65	0	40	76	0	ell	–	I/O				
10/26	8	0.74	25	NG	NG	0.66	1.10	0.80-0.99	1.11	0.65	0	40	76	0	ell	–	I/O				
	7							0.88				40	52-88								
E1											NH_3 (SCFM) ↓	(NH_3) ↓						Thermal De-NO_x			
10/30	8	0.59	0	NG	–	0.67	1.10	–	–	0.65			–	0	–	–	D		–	Temp.	
	7										(0.095)	40-64					I/O				
10/31	10	0.59	0	NG	–	0.67	1.10	–	–	0.65	(0.095)	(40-94)	–	0	–	–	I/O				
	6										(0.006-0.095)	(82)					I/O				
	16										(0.095)	(82)					D		–	CEMS, NH_3	
													[illegible] (0.096)								
11/1	14	0.74	25	NG	NG	0.67	1.10	0.89	1.10	0.65	0	40	64-100	0	B3N9	–	I/O				
	2	0.59	0	NG	–	0.67	1.10	–	–	0.65	(0.095)	(82)	–	0	–	–	D		–	Stack NH_3	
11/2	4	0.74	25	NG	NG	0.67	1.10	0.89	1.10	0.65	0	40	64	0	B3N9	–	D		–	CEMS, NH_3	
	16	0.31	0	NG	–	0.69	1.26	–	–	0.65	(0.095)	(65-90)	–	0	–	–	I/O				
E1																		Air Jet Study			
11/7	14	0.74	25	NG	NG	0.64	1.07	0.86	1.08	0	0	40	64	0	B3N9	–	D		–	CEMS, NO_x	

C.F. 620

Data Summary Sheet

Reburning on PBS

PAGE: 2

DATE & DATA BOOK #	# Data Pts	1	2	3	4	5	6	7	8	9	10	11	12	13	14	15	16	17	18	19	20
		FR_{TOT}	$\frac{FR_{SEC}}{FR_{PRI}}$	PRI FUEL	SEC FUEL	SR_1	SR_2	SR_3	SR_4	PRI FUEL DOPANT	SEC FUEL DOPANT	SEC FUEL INJ	FINAL AIR INJ	PRI ZONE MIXING	SEC FUEL NOZZLE	INS. ZONE	TEST TYPE	TEST DESCRIPTION			
		MW	%							$\% N_2$ by wt	$\% N_2$ by wt	in. into boiler	in. into boiler	sec air $\frac{ax}{rad}$			I/O or D				
E1																					
																		Air	Jet	(confirmed)	
11/8	5	0.59	0	NG	–	0.65	1.08	1.15	–	0,65	0	–	64	0	–	–	D		–	CEMS	: No Re.
11/9	21	0.74	25	NG	NG	0.65	1.09	0.87	1.13	0,0.65	0	40	64	0	B3N9	–	D		–	CEMS	: Rotate
11/12	18	0.66-0.82	12-38	NG	NG	0.65	1.09	0.79-0.98	1.09	0	0	40	64	0	B3N9	–	D		–	CEMS :	Composition
11/15	12	0.74	25	NG	NG	0.65	1.09	0.87	1.12	0	0	40	64	0	B3N9	–	D		–	CEMS:	$\dot{m}_{air\ jet}$
	5	0.66-0.82	12-38					0.78-0.97									D		–	CEMS :	SR_2
11/16	10	0.59	0	NG	–	0.65	0.82	–	1.10	0	0	–	35-70	0	–	–	D		–	CEMS:	T
	5												88				D		–	Temp.	
11/19	1	0.59	0	NG	–	0.87	–	–	1.08	0	0	–	88	0	–	–	D		–	Temp	
	12												0-80				D		–	CEMS:	T
E2																					
11/20	25	0.59-0.78	0-33	NG	NG	0.65	0.88,1.09	0.66-1.10	1.08	0.65	0	40	76	0	B3N9	–	I/O	Firing	Arrangements		
E2																					
														← spokes				Air	Jet	Study	
11/21	5	0.71	20	NG	NG	0.65	1.09	0.91	1.15	0.65	0	40	76	0	B3N9	–	I/O				
														← annulus							
11/28	9	0.74	25	NG	NG	0.65	1.09	0.88	1.15	0.65	0	40	76	0	B3N9	–	I/O				
	7										0,1.0						D		–	CEMS	
11/29	6	0.3-0.44	13-50	NG	NG	0.60	1.05	0.8-1.1	1.15	0.36	0	40	76	0	B3N9	–	I/O	Half	Load	Tests	
	3	0.3	-	NG	–	0.60	1.05	–	–							-	D		–	Temp.	
12/3	12	0.44	50	NG	NG	0.65	1.11	0.74	1.10	0	0	40	76	0	B3N9	–	D		–	CEMS	
12/4	30	0.44	50	NG	NG	0.63	1.09	0.73	1.08	0	0	40,10	52-94	0	B3N9	–	I/O	+D	–	Temp	
	15	0.74	25	NG	NG			0.86													
12/5	20	0.74	25	NG	NG	0.64	1.08	0.87	1.08	0	0	40	52-124	0	B3N9	–	I/O	+ D	–	CEMS	

C.F. 620

DATA SUMMARY SHEET

Reburning in PBS

PAGE: 3

DATE & DATA BOOK #	# DATA PTS.	1	2	3	4	5	6	7	8	9	10	11	12	13	14	15	16	17	18	19	20
		FR_{TOT}	$\frac{FR_{SEC}}{FR_{PRI}}$	PRI. FUEL	SEC. FUEL	SR_1	SR_2	SR_3	SR_4	PRI. FUEL DOPANT	SEC. FUEL DOPANT	SEC. FUEL INJ.	FINAL AIR INJ.	PRI. ZONE MIXING	SEC. FUEL NOZZLE	INJ. ZONE	TEST TYPE	TEST DESCRIPTION			
E-2		MW	%							$\%N_2$ by wt.	$\%N_2$ by wt.	in. into boiler	in. into boiler	Sec Air Ax/Rad			I/O or D				
12/6	25	0.55	87	NG	NG	1.09	1.09	0.59	1.06	0	0	10	52-88	-	B3N9	-	I/O+	D	-	CEMS,	Temp.
F-1																					
12/12	40	0.6-0.72	5-22	NG	#2	0.91	1.02	0.85-1.0	1.12	0	0	10,40	52-88	0	B3,D40,45°	-	I/O	Fuel	Oil	High	Temperature
12/13	25	0.59	0	NG	-	0.[illegible]1	1.00	-	-	0	-	-	-	0	-	-	D		-	CEMS,	Temp
12/13	15	0.59	0	NG	-	0.87	-	-	1.06	0	-	-	76	-	-	-	D		-	CEMS	Temp
12/14	40	0.6-0.72	5-22	NG	#2	0.91	-	0.76-0.8[illegible]	1.11	0	0	10,40	52-88	-	B3,D4.0,45°	-	I/O+	D	-	CEMS	
12/18	15	0.3-0.42	10-43	NG	#2	0.87	1.03	0.7-0.9	1.06	0	0	10	52-76		B3,D4.0,45°	-	I/O+	D	-	Temp.	
12/20	25	0.47	0	#2	-	0.59	0.79	1.07	-	0	-	-	52-118	0	-	-	I/O+	D	-	CEMS	
E-2																					
1/3/85	15	0.30	0	NG	-	0.85	-	-	1.17	1.3	-	-	52-76	-	-	-	I/O+	D	Half Load	Tests	
1/8	25	0.45	48	NG	NG	0.60	1.10	0.74	1.19	1.3,0	0	10	80-100	0	B3N9	-	I/O+	D	-	CEMS	
1/9	35	0.45	49	NG	NG	0.60	1.10	0.74-0.97	1.2	0,1.3	0	10,40	74-100	0	B3N9	-	I/O+	D	-	CEMS,	HCN,NH3
1/11	18	0.45	49	NG	NG	0.61	1.11	0.74	1.20	1.3	0	10	52-100	0	B3N9	-	I/O+	D	-	CEMS,	HCN,NH3
1/22	20	0.45	49	NG	NG	0.59	1.09	0.74	1.19	1.3	0	10	52-100	0	B3N9	-	I/O+	D	-	CEMS,	HCN,NH3
1/23	12	0.45	49	NG	NG	0.60	1.11	0.74	1.20	0	0	10	52-100	0	B3N9	-	I/O+	D	-	CEMS,	HCN,NH3
1/24	30	0.30	0	NG	-	1.08	-	-	-	0	-	-	-	-	-	-	D		-	CEMS,Temp	
1/28	16	0.45	50	NG	NG	1.10	-	0.74	1.20	0	0	10,40	52-88	-	B3N9	-	I/O+	D	-	CEMS,	HCN,NH3
1/29	20	0.37	24	NG	NG	1.09	-	0.88	1.11	0	0	10,40	52-76	-	B3N9	-	I/O+	D	-	CEMS,	HCN,NH3
1/30	5	0.37	24	NG	NG	1.09	-	0.88	1.11	0	0	10	70	-	B3N9	-	D		-	Temp	
1/31	20	0.52	77	NG	NG	1.08	-	0.61	1.08	0	0	10,40	52-94	-	B3N9	-	I/O+	D	-	CEMS,	HCN, NH3
2/5	18	0.45	50	NG	NG	1.09	-	0.73	1.18	0	0-1.0	10	64-76	-	B3N9	-	I/O			+HCN,	NH3
2/6	15	0.45	50	NG	NG	1.06	-	0.71	1.16	0	0	10,40	76	-	B3N9	-	D		-	TEMP	
	10	0.30	0	NG	-	0.59	0.80	-	1.10	1.3	0	-	52-100	0	B3N9	-	I/O+	D	-	CEMS	
2/7	35	0.30	0	NG	-	0.58	1.07	-	-	1.3	-	-	-	0	B3N9	-	D		-	CEMS,	Temp
E-3																					
2/12	10	0.30	0	NG	-	0.61	1.10	-	-	0	-	-	-	0	B3N9	-	D		-	CEMS	
2/13	35	0.45	50	NG	NG	0.62	1.17	0.95	1.86	0	0	40	64	0	B3N9	-	D	Leak	Check		Tests

C.F. 620

DATA SUMMARY SHEET

Reburning in PBS

PAGE: 4

DATE & DATA BOOK #	# DATA PTS	1	2	3	4	5	6	7	8	9	10	11	12	13	14	15	16	17	18	19	20
		FR_{TOT}	FR_{SEC}/FR_{PRI}	PRI. FUEL	SEC. FUEL	SR_1	SR_2	SR_3	SR_4	PRI. FUEL DOPANT	SEC. FUEL DOPANT	SEC. FUEL INJ.	FINAL AIR INJ.	PRI ZONE MIXING	SEC. FUEL NOZZLE	INS. ZONE	TEST TYPE	TEST DESCRIPTION			
E-3		MW	%							$\%N_2$ by wt.	$\%N_2$ by wt.	in. into boiler	in. into boiler	Sec Air Ax/Rad			I/O or D				
2/14	20	0.3, 0.6	0	NG	—	0.6	1.1	1.8	—	0	—	—	52-112	0	—	—	D	Leak		Check	Tests
2/26	10	0.59	0	NG	—	0.60	1.12	—	—	0	—	—	—	0	—	—	D	NO_x		Meter	Tests
2/27	5	0.59	0	NG	—	0.59	1.09	—	—	0.65	—	—	—	∞	—	—	D				
2/28	10	0.59	0	NG	—	0.62	1.13	—	—	0.65	—	—	—	∞	—	—	D				
3/1	10	0.59	0	NG	—	0.62	1.13	—	—	0.65	—	—	—	∞	—	—	D				
3/5	4	0.30	0	NG	—	0.56	0.75	1.05	—	0, 1.3	—	—	64	∞	—	—	D	Half		Load	Tests
3/6	30	0.30	0	NG	—	0.5-1.1	1.0-1.5	—	—	0, 1.3	—	—	—	∞	—	—	I/O				
3/7	10	0.30	0	NG	—	1.0-1.4	—	—	—	0	—	—	—	—	—	—	I/O				
	30	0.30	2-12	NG	NG	0.59	0.88	—	1.26	0, 1.3	0	64	76	∞	B3N9	—	D				
3/11,12	50	0.30	0	NG	—	0.5-1.1	1.1-1.5	—	—	0, 1.3	—	—	—	∞	—	—	I/O				
3/13	24	0.30	0	NG	—	0.6-0.9	0.7-1.0	—	1.1	0, 1.3	—	—	76	∞	—	—	I/O +	D	-	CEMS	
3/25	20	0.38	30	NG	NG	0.81	1.12	0.86	1.2	0, 1.3	0	40	74	∞	B3N9	-	I/O +	D	-	CEMS	
3/26	30	0.33-0.46	12-50	NG	NG	0.86	1.11	0.75-1.0	1.15	0, 1.3	0	40	74	∞	B3N9	—	I/O +	D	-	CEMS	
3/27	30	0.38	30	NG	NG	0.85	1.10	0.85	1.10	0, 1.3	0	40	74, 84	∞	B3N9	—	I/O +	D	-	TEMP,	HCN, NH_3
3/28	25	0.30	0	NG	—	0.84	—	—	1.16	0, 1.3	—	—	61-93	-	—	—	D		-	CEMS,	Temp
4/1	5	0.74	24	NG	NG	0.62	1.13	0.91	1.18	0.65	0	40	76	∞	B3N9	—	I/O				
4/2	10	0.30	0	NG	—	0.84	—	—	1.17	0, 1.3	—	—	61	—	-	—	D		-	HCN,	NH_3
4/10	2	0.38	30	NG	NG	0.86	1.11	0.85	1.16	0, 1.3	0	40	74	∞	B3N9	—	I/O				
E-4																					
4/11	8	0.38	30	NG	NG	0.86	1.11	0.85	1.16	0, 1.3	0	40	74	∞	B3N9	—	I/O	+ soot		measurement	
4/12	4	0.30	0	NG	-	0.86	—	—	1.18	0, 1.3	-	-	61	—	B3N9	—	I/O	+ soot		measurement	
4/17	6	0.74	24	NG	NG	0.60	1.09	0.88	1.12	0.65	0	40	64	∞	B3N9	—	I/O	Tertiary		Gas	Inj
4/18	15	0.74	24	NG	NG	0.61	1.11	0.89	1.13	0.65	0	40	52-106	∞	B3N9	—	I/O				
4/19	7	0.59	0	NG	—	0.60	1.08	—	—	0.65	—	—	—	∞	—	—	D	↓	-	CEMS	
4/22	8	0.3, 0.6	50, 0	NG	NG	0.85, 0.61	1.10	0.74, -	1.1, -	1.3, 0.65	0, -	40, -	81, -	∞	B3N9	—	I/O	NO_x		Meter	Tests
4/23	4	0.59	0	NG	—	0.61	1.10	—	—	0.65	—	—	—	∞	—	—	I/O				
4/25	15	0.59	0	NG	—	0.63	1.12	—	—	0.65	—	—	—	∞	—	—	D		-	CEMS,	NO_2, NO_3
4/26	10	0.74	24	NG	NG	0.63	1.13	0.91	1.09	0.65	0	40	52-112	∞	B3N9	—	I/O		+	NO_2,	NO_3
4/29	15	0.30	0	NG	-	0.80	-	—	1.11	1.3	—	—	52-112	—	—	—	I/O +	D	—	CEMS,	NO_2, NO_3

C.F. 620

DATA SUMMARY SHEET

Reburning in PBS

PAGE: 5

DATE & DATA BOOK #	# DATA PTS.	1	2	3	4	5	6	7	8	9	10	11	12	13	14	15	16	17	18	19	20
		FR_{TOT}	FR_{SEC}/FR_{PRI}	PRI. FUEL	SEC. FUEL	SR_1	SR_2	SR_3	SR_4	PRI. FUEL DOPANT	SEC. FUEL DOPANT	SEC. FUEL INJ.	FINAL AIR INJ.	PRI. ZONE MIXING	SEC. FUEL NOZZLE	INS. ZONE	TEST TYPE	TEST DESCRIPTION			
E-4		MW	%							$\%N_2$ by wt.	$\%N_2$ by wt.	in. into boiler	in. into boiler	sec Air Ax/Rad.			I/O or D				
4/30	25	0.74,0.89	24,48	NG	NG	0.63,0.89	1.1	0.9,0.73	1.1	0.65,1.3	0	40	112	∞	B3N9	–	I/O +	D	–	CEMS, NO_x	, NO_2
5/7	18	0.66-0.81	12-37	NG	NG	1.11	–	0.82-0.89	1.1	0.65	0-2	40	76	–	B3N9	–	I/O				
5/8	25	0.66-0.81	12-37	NG	NG	0.63-0.77	0.75-1.0	0.72-0.9	1.1	0	0	40	76	0	B3N9	–	I/O				
5/9	45	0.66-0.81	12-37	NG	NG	0.61	0.9-1.1	0.8-1.0	1.15	0,0.65	0	40	76	∞	B3N9	–	I/O	Optimization Tests			
5/10	15	0.66-0.81	12-37	NG	NG	0.60	1.11	0.8-1.0	1.15	0.65	0	40	76	∞	B3N9	–	I/O	Vary Final Air Inj.			
E-5																					
5/13	20	0.66	12	NG	NG	1.10	–	0.98	1.14	0-0.65	1.9	40,10	76	–	B3N9	–	I/O	Ammonia Injection			
5/14	15	0.66	12	NG	NG	0.98	1.10	0.99	1.15	0.25	0-20	40,10	76	0	B3N9	–	I/O				
5/15	25	0.69-0.78	9-22	NG	NG	1.10	–	0.98	1.13	0	0-20	40	76	–	B3N9	–	I/O				
5/16	24	0.65-0.8	10-36	NG	NG	1.10	1.10	0.8-1.0	1.1	0	0-25	40	76	–	B3N9	–	I/O				
5/17	34	0.65-0.8	10-36	NG	NG	0.95	1.10	0.8-1.0	1.10	0	0-25	40	76	∞	B3N9	–	I/O			+NH_3	, HCN
5/21	44	0.59	0	NG	–	0.6,0.5	1.0,0.9	–	1.10	0.65	–	46-10	64	∞	B3N9	–	I/O				
5/22	9	0.65-0.8	10-36	NG	NG	0.50	1.10	0.8-1.0	1.11	0.65	0-20	10	76	∞	B3N9	–	I/O				
5/23	20	0.65	10	NG	NG	1.10	–	0.99	1.10	0	0,25	40	76	–	B3N9	–	D		–	CEMS	HCN, NH_3
5/29	20	0.65	10	NG	NG	1.11	–	1.00	1.08	0	0	40	76	–	B3N9	–	D		–	Temp	
5/30	30	0.65	10	NG	NG	1.11	–	1.00	1.13	0	0-40	10,40	76-100	–	B3N9	–	I/O		+	Temp	
6/3	25	0.61-0.8	5-34	NG	NG	1.20	–	0.9-1.15	1.22	0	0-25	40	64	–	B3N9	–	I/O				
6/4	40	0.59	0	NG	–	1.04	–	–	1.10	0	–	20-69	64	–	B3N9	–	I/O		+	Temp	
6/7	50	0.59	0	NG	–	0.60	0.9-1.2	–	1.1	0.65	–	40-90	40-100	∞	B3N9	–	I/O				
6/10	10	0.59	0	NG	–	0.60	1.00	–	1.10	0.65	–	80	80	∞	B3N9	–	D		–	CEMS	, NH_3
6/11	40	0.59	0	NG	–	0.58	1.05	–	1.10	0.65	–	52-100	52-100	∞	B3N9	–	I/O		+	Temp	
6/12	40	0.59	0	NG	–	0.58	0.98	–	1.08	0.65	–	40-100	54-100	∞	B3N9	–	I/O				
6/13	10	0.59	0	NG	–	0.59	0.99	–	1.09	0.65	–	80	80	∞	B3N9	–	I/O		+	NH_3	
6/14	15	0.59	0	NG	–	0.56	0.86-1.1	–	1.04.3	0.65	–	80	80	∞	B3N9	–	I/O				

C.F. 620

RAW DATA SHEETS

PBS FACILITY:

RAW DATA SHEETS

REBURN TEST DATA SHEET
PBS FACILITY

1A. INPUT DATA-- PRIMARY FUELS

DATE :

TEST SERIES # :

INITIALS :

	1	2	3	4	5	6	7	8	9	10	11	12	13	14	15	16	17	18	19	20
DATA PT. #	TIME	MAIN GAS			PRIMARY FUEL				OIL	ATOMIZING AIR			AMMONIA		ADDITIVE		OIL	ADDITIVE		PRI. FIRING RATE
		P	ΔP	FLOW	TYPE	P	T	VALVE SETTING	FLOW	P	ΔP	FLOW	P	ROTOMETER	FLOW	N_2	DOPANT	AMOUNT	N_2	
		psi	in. H_2O	SCFM	#	psi	°F		gph	psi	in. H_2O	SCFM	psi	% scale	SCFM	molar % of Fuel		volume % of fuel	molar % of Fuel	MBtu/Hr

Engineer's Initials :

REBURN TEST DATA SHEET
PBS FACILITY

18. INPUT DATA -- SECONDARY FUELS

DATE: TEST SERIES #: INITIALS:

	1	2	3	4	5	6	7	8	9	10	11	12	13	14	15	16	17	18	19	20
DATA PT #	TIME	SECONDARY NG			SECONDARY OIL				SEC. ATOMIZING AIR FLOW	BOOM & NOZZLE		INJ. LOCATION	AMMONIA ADDITIVE				OIL ADDITIVE			SEC. FIRING RATE
		P	ROTO-METER	FLOW	TYPE	P/T	PUMP SETTING	FLOW					P	ROTO-METER	FLOW	N_2	DOPANT	AMOUNT	N_2	
		psi	% scale	SCFM	#	psi/°F		gph	SCFM			in. into boiler	psi	% scale	SCFM	molar % of fuel		volume % of fuel	molar % of fuel	MBtu/Hr

Engineer's Initials:

REBURN TEST DATA SHEET
PBS FACILITY

3. OUTPUT DATA

DATE: TEST SERIES #: INITIALS:

	1	2	3	4	5	6	7	8	9	10	11	12	13	14	15	16	17	18	19	20
DATA PT. #	TIME	BOILER LOCATION		GASEOUS EMISSIONS							SUCTION PYROMETER				PITOT PROBE					
		AXIAL	RADIAL	O_2	CO_2	CO	UHC	NO	NO @0%O_2		FLOW	T_{LOW}	T_{HIGH}		SCALE	N	$\overline{\sqrt{\Delta P}}$	$\overline{\sqrt{\Delta P}}$	$\sigma_{\sqrt{\Delta P}}$	V
		in. into boiler	in. from ℄	%	%	ppm	ppm	ppm	ppm		SCFM	°F	°F		torr		(without zeroes) $torr^{1/2}$	$torr^{1/2}$		fps

REBURN TEST DATA SHEET
PBS FACILITY

Z. INPUT DATA -- COMBUSTION AIRS

DATE:

TEST SERIES #:

INITIALS:

	1	2	3	4	5	6	7	8	9	10	11	12	13	14	15	16	17	18	19	20
			TOTAL BLOWER AIR			PRIMARY AIR			SECONDARY			SECONDARY			TERTIARY AIR					
DATA PT. #	TIME	$P_{bar.}$	P_1/T_1	ΔP	FLOW	P_1	ΔP	FLOW	P_1/T_1	ΔP	AXIAL FLOW	P_1/T_1	ΔP	RADIAL FLOW	P_1	ΔP	FLOW	TER. AIR INJ. LOCATION	OTHER AIR FLOWS	TOTAL AIR FLOW
		in. Hg	in. H_2O /°F	in H_2O	SCFM	in. H_2O	in. H_2O	SCFM	in. H_2O /°F	in. H_2O	SCFM	in H_2O /°F	in. H_2O	SCFM	in. H_2O	in. H_2O	SCFM	in. into boiler	SCFM	SCFM

REBURN TEST DATA SHEET
PBS FACILITY

4. MONITORING TEMP. AND AIR/FUEL RATIOS

DATE :

TEST SERIES # :

INITIALS :

	1	2	3	4	5	6	7	8	9	10	11	12	13	14	15	16	17	18	19	20
DATA PT. #	TIME	FURNACE TEMPERATURES			Cooling H_2O	DOWTHERM			COOLING		AIR	ADVANCE BIAS AIR			REBURN AMOUNT	TOT. FIRING RATE	STOICHIOMETRY			
		T_1	T_2	T_{st}	T	T	FLOW		P	ROTO-METER	FLOW	P_1	ΔP	FLOW			SR_1	SR_2	SR_3	SR_4
		°F	°F	°F	°F	°F	gpm		psi	% scale	SCFM	psi	in. H_2O	SCFM	% of pri.	MBtu/Hr				

REBURN TEST DATA SHEET
PBS FACILITY

5. WET CHEMISTRY & GC DATA

DATE:　　　　　　TEST SERIES #:　　　　　　INITIALS:

	1	2	3	4	5	6	7	8	9	10	11	12	13	14	15	16	17	18	19	20
DATA PT. #	TIME	INITIAL H_2O	FINAL H_2O	INLET T	OUTLET T	SAMPLE P	INITIAL V	FINAL V	AVE. SAMPLE T	SAMPLE V	SAMPLE TIME	NH_3 SOL.	$[NH_3]$	RPD	HCN SOL.	[HCN]	RPD		GC $[N_2O]$	
		ml	ml	°F	°F	in. Vac.	ACF	ACF	°F	SCF	min.	ppm	ppm	%	ppm	ppm	%		ppm	

NH_3 Electrode Calibration: slope = ___ ; ref. = ___
HCN Electrode Calibration: slope = ___ ; ref. = ___
N_2O GC Calibration:

NORTH AMERICAN BOILER FACILITY:

RAW DATA SHEETS

1A. INPUT DATA -- PRIMARY FUELS

REBURN TEST DATA SHEET
NORTH AMERICAN FACILITY

DATE :

TEST SERIES # :

INITIALS :

	1	2	3	4	5	6	7	8	9	10	11	12	13	14	15	16	17	18	19	20
DATA PT #	TIME	PRIMARY		FUEL	OIL	ATOMIZING			AIR	AMMONIA		ADDITIVE		OIL	ADDITIVE			PRI. AIR FLOW		PRI. FIRING RATE
		TYPE	FLOW	T_1	T_2	P	T	ROTO-METER	FLOW	P	ROTO-METER	FLOW	N_2	DOPANT	AMOUNT	N_2				
		#	gph	°F	°F	psi	°F	% scale	SCFM	psi	% scale	SCFM	molar % of fuel		volume % of fuel	molar % of fuel		SCFM		MBtu/Hr

Engineer's Initials :

REBURN TEST DATA SHEET
NORTH AMERICAN FACILITY

1B. INPUT DATA -- SECONDARY FUELS

DATE: TEST SERIES #: INITIALS:

	1	2	3	4	5	6	7	8	9	10	11	12	13	14	15	16	17	18	19	20
DATA PT #	TIME	SECONDARY NG P	ROTO-METER	FLOW	SECONDARY OIL TYPE	P/T	PUMP SETTING	FLOW	SEC. ATOMIZING AIR FLOW	BOOM & NOZZLE		INJ. LOCATION	AMMONIA P	ROTO-METER	ADDITIVE FLOW	N_2	OIL DOPANT	ADDITIVE AMOUNT	N_2	SEC. FIRING RATE
		psi	% scale	SCFM	#	psi/°F		gph	SCFM			in. into boiler	psi	% scale	SCFM	molar % of fuel		volume % of fuel	molar % of fuel	MBtu/Hr

Engineer's Initials:

REBURN TEST DATA SHEET
NORTH AMERICAN FACILITY

2. INPUT DATA -- AIRS

DATE:

TEST SERIES #:

INITIALS:

	1	2	3	4	5	6	7	8	9	10	11	12	13	14	15	16	17	18	19	20
DATA PT. #	TIME	FINAL			FINAL AIR INJ. LOCATION			TOTAL AIR FLOW	STOICHIOMETRY							TOTAL FIRING RATE	REBURN AMOUNT			
		P_o	ΔP	AIR FLOW		P_{bar}			SR_1	SR_2	SR_3		P_{st}	T_{st}						
		psi	in. H_2O	SCFM	in. into boiler	in. Hg		SCFM					in. H_2O	°F		MBtu/Hr	% of tot.			

REBURN TEST DATA SHEET
NORTH AMERICAN FACILITY

3. OUTPUT DATA

DATE: TEST SERIES #: INITIALS:

	1	2	3	4	5	6	7	8	9	10	11	12	13	14	15	16	17	18	19	20
DATA PT. #	TIME	BOILER LOCATION		GASEOUS EMISSIONS.							SUCTION PYROMETER				PITOT PROBE					
		AXIAL	RADIAL	O_2	CO_2	CO	UHC	NO	NO @0%O_2		FLOW	T_{LOW}	T_{HIGH}		SCALE	N	$\overline{\sqrt{\Delta P}}$	$\overline{\sqrt{\Delta P}}$	$\sigma_{\sqrt{\Delta P}}$	V
		in. into boiler	in. from ℄	%	%	ppm	ppm	ppm	ppm		SCFM	°F	°F		torr		(without factors) $torr^{1/2}$	$torr^{1/2}$		fps